Optimized Metal Recovery from Fly Ash from Municipal Solid Waste Incineration

Inauguraldissertation

der Philosophisch-naturwissenschaftlichen Fakultät
der Universität Bern

vorgelegt von

Gisela Weibel

von Rapperswil BE

Leiter der Arbeit:	PD Dr. Urs Mäder, Institut für Geologie, Universität Bern
Ko-Leiter:	Dr. Urs Eggenberger, Institut für Geologie, Universität Bern
Ko-Leiter:	Dr. Stefan Schlumberger, Zentrum für nachhaltige Abfall- und Ressourcennutzung (ZAR), Zuchwil
Koreferent:	Prof. Dr. Michael Schuster, Technische Universität München

Optimized Metal Recovery from Fly Ash from Municipal Solid Waste Incineration

Inauguraldissertation

der Philosophisch-naturwissenschaftlichen Fakultät
der Universität Bern

vorgelegt von

Gisela Weibel

von Rapperswil BE

Leiter der Arbeit:	PD Dr. Urs Mäder, Institut für Geologie, Universität Bern
Ko-Leiter:	Dr. Urs Eggenberger, Institut für Geologie, Universität Bern
Ko-Leiter:	Dr. Stefan Schlumberger, Zentrum für nachhaltige Abfall- und Ressourcennutzung (ZAR), Zuchwil
Koreferent:	Prof. Dr. Michael Schuster, Technische Universität München

Von der Philosophisch-naturwissenschaftlichen Fakultät angenommen.

Der Dekan

Bern, 09.06.2017 Prof. Dr. G. Colangelo

Die schmutzige Natur des sauberen Menschen liegt in der nachlässigen Art, seinen Abfall zu beseitigen.

Daniel Mühlemann, Naturfotograf

Die vorliegende Arbeit ist ein Beitrag zum Versuch, dies im Detail besser zu machen...

Dank

Zahlreiche Personen haben wesentlich zum Gelingen dieser Arbeit beigetragen – ihnen möchte ich meinen herzlichen Dank aussprechen.

Vorab möchte ich mich bei meinen drei Betreuern Urs Eggenberger, Stefan Schlumberger und Urs Mäder bedanken. Sie haben mir ermöglicht, diese Arbeit durchzuführen und mich stets mit hohem Engagement und grosser Umsicht begleitet. Die vielen konstruktiven Hinweise und wertvollen Anregungen sowie das kollegiale und angenehme Arbeitsklima haben die bestmöglichen Voraussetzungen für das Gedeihen dieser Arbeit geschaffen. Insbesondere Urs Eggenberger gebührt ein tiefer Dank, denn ich durfte mit Einbezug der Masterarbeit sechs tolle und lehrreiche Jahre bei der Fachstelle für Sekundärrohstoffe verbringen. Stefan Schlumberger danke ich für die Bereitstellung von Analysedaten und Literatur; zudem konnte ich von seiner analytischen, zielorientierten Denkweise und seiner Nähe zum grosstechnischen Betrieb enorm profitieren. Urs Mäder möchte ich einen besonderen Dank für die Unterstützung bei den englischen Korrekturen sowie der Aufbauarbeit von wichtigen Versuchseinrichtungen aussprechen.

Im Weiteren gilt mein Dank dem AWEL Zürich und insbesondere Elmar Kuhn und Leo Morf, deren Förderung und finanzielle Unterstützung dieses Projekt erst ermöglicht hat. Ein grosses Dankeschön geht zudem an Bernhard Dettwiler und Oliver Steiner für den regen Austausch und die wertvollen fachlichen Inputs. Danken möchte ich auch Michael Hügi und dem Bundesamt für Umwelt für die Finanzierung des ersten grossen Teilprojektes.

Christine Lemp, Martin Fisch (Institut für Geologie), Ivo Budde, Waldemar Klink und Anna Zappatini (ZAR Zuchwil) danke ich herzlich für die analytische Unterstützung und die konstruktive und kollegiale Stimmung während des gesamten Projekts. Einen grossen Beitrag zum Gelingen dieser Arbeit haben zudem diverse Mitarbeiter des Instituts für Geologie geleistet: Vielen herzlichen Dank Nick Waber, Priska Bähler, Stefan Weissen, Alfons Berger, Thomas Siegenthaler, Thomas Aebi, Stefan Brechbühl und Nadine Lötscher. Sergey Churakov und seiner Forschungsgruppe am Paul-Scherrer Institut und insbesondere Dmitrii Kulik und Wolfgang Hummel danke ich für die grosszügige Unterstützung bei den geochemischen Modellierungen.

Den Betreibern der Kehrichtverbrennungsanlagen KEBAG Zuchwil, KEZO Hinwil, SATOM Monthey, KVA Linth, KHKW Hagenholz Zürich und Energiezentrale Forsthaus danke ich für angenehme Zusammenarbeit und die Mithilfe bei den diversen Probenahmen. Insbesondere danke ich Stefan Ringmann und der KVA Linth für das entgegengebrachte Vertrauen bei der Optimierung des FLUWA-Verfahrens. Herrn Prof. Michael Schuster danke ich für die diversen informativen Treffen sowie für das sorgfältige Durchlesen und das Beurteilen dieser Arbeit.

Danken möchte ich auch meinen Eltern Marlis und Ruedi, welche in mir den Enthusiasmus für die Naturwissenschaften bereits früh geweckt haben und während allen Phasen meiner Studienzeit mit mir mitgefühlt und mitgelitten haben. Ihre Unterstützung in sämtlichen Belangen hat mir die Chance gegeben, meinen Weg zu gehen. Zum Schluss geht ein riesiges Dankeschön an meinen Freund Patrick. Er hat mich nicht nur angespornt und durchgefüttert, sondern mir bei dieser Arbeit auch immer wieder mit klugen Denkanstössen zu entscheidenden Durchbrüchen verholfen. Patrick, ich danke dir von Herzen.

Abstract

Switzerland plays a pioneering role in sustainable waste management with a long tradition of waste incineration and the prohibition to landfill unburnt municipal solid waste since 2000. In recent years, the focus has been laid on further reduction of pollutants from incineration residues because the revised Swiss Waste Ordinance prescribes the recovery of metals from fly ash starting in 2021. Fly ash collected in the heat recovery section and the electrostatic precipitator contains high concentration of aluminosilicates, oxides, soluble salts, heavy metals and toxic organic compounds. Metals are either carried along with the flue gas as particles, forming enriched mineral aggregates or vaporized and condensed as complex chlorides or sulphates in fly ash. An efficient treatment of fly ash promises considerable ecological and economic benefits due to an improved quality for disposal and the recovery of the metals contained. At present acidic fly ash leaching (FLUWA) is the state-of-the-art process, where up to 80% of Zn and minor amounts of Pb and Cu are recovered.

This thesis contributes considerably to a better understanding of fly ash composition and leaching behaviour as a basis for improved metal separation. Detailed analyses of fly ash describing the chemical associations of metals were the basis for nearly 200 leaching experiments of various fly ashes. The achieved data set contains valuable information regarding the binding environment of metals in fly ash and the leaching behaviour covering a wide range of pH-values, redox conditions, liquid to solid ratios, temperatures and leaching times. It could be shown that acidic fly ash leaching under oxidative conditions as well as a secondary leaching step using concentrated sodium chloride solution leads to an almost complete mobilization of Pb, Cu and Cd.

Based on these findings at laboratory scale, an optimization of the acidic fly ash leaching on industrial-scale was tested. It could be shown, that the trends of the chemical processes and metal recovery pointing in the right direction. Difficulties have been experienced in keeping and monitoring stable process conditions at the given system technology.

The results of this thesis may also serve as a decision support for the upcoming implementation aid by the Federal Office for the Environment (FOEN), where the criteria for fly ash treatment and metal recovery efficiency have to be formulated.

List of Abbreviations

APC	Air pollution control
ASR	Automobile shredder residues
AWEL	Amt für Abfall, Wasser, Energie und Luft des Kantons Zürich
BSE	Backscattered electron
EDS	Energy dispersive spectroscopy
Eh	Redox potential (mV)
ESP	Electrostatic precipitator
FLUREC	FLUgaschen RECycling
FLUWA	Saure Flugaschenwäsche (acidic fly ash leaching)
FOEN (BAFU)	Federal Office for the Environment (Bundesamt für Umwelt)
GEM-Selektor	Gibbs free energy minimization program
IC	Ion chromatography
ICP-MS	Inductively coupled plasma mass spectrometry
ICP-OES	Inductively coupled plasma optical emission spectroscopy
INAA	Neutron activation analysis
LS (FF)	Liquid to solid ratio (Flüssig-Fest-Verhältnis)
LM	Light microscope
LOI	Loss on ignition
m	Molal: 1 mol/kg
M	Molar: 1 mol/L
MSW	Municipal solid waste
MSWI	Municipal solid waste incineration
nm	Nanometer, 10^{-9} m
PHREEQC	Geochemical modelling code
pH	Negative logarithm of the hydrogen ion concentration
ppm	Parts per million
PVC	Polyvinyl chloride
SEM	Scanning electron microscope
SelFrag	Selective (electrodynamic) fragmentation
SE	Secondary electrons
SI	Saturation index
TIC	Total inorganic carbon
TOC	Total organic carbon
TC	Total carbon
TD	Total digestion

TVA	Technische Verordnung über Abfälle 1990 (Swiss Waste Ordinance)
VBSA	Association of Swiss Operators of Thermal Waste Processing Plants
VVEA	Abfallverordnung 2016 (revised Swiss Waste Ordinance)
WDS	Wavelength dispersive spectroscopy
wt.% (gew.%)	Weight percentage (Gewichtsprozent)
XRD	X-ray diffraction
XRF	X-ray fluorescence
ZAR	Zentrum für nachhaltige Abfall- und Ressourcennutzung
λ	Wavelength

Sample labelling:

FABER	Fly ash from MSWI plant Bern
WABER	Wood ash from MSWI plant Bern
FAHAG	Fly ash from MSWI plant Hagenholz
FAHIN	Fly ash from MSWI plant Hinwil
FAMON	Fly ash from MSWI plant Monthey
FANIE	Fly ash from MSWI plant Linth/Niederurnen
FAZUC	Fly ash from MSWI plant Zuchwil
FCBER	Acidic leached filter cake from MSWI plant Bern
FCNIE	Acidic leached filter cake from MSWI plant Linth/Niederurnen
FCSAT	Neutrally leached filter cake from MSWI plant Monthey
FCZUC/FKZUC	Acidic leached filter cake from MSWI plant Zuchwil
FKHAG	Acidic leached filter cake from MSWI plant Hagenholz

BCR 176R	Standard reference material
NIST 2701	Standard reference material
Soil N1	Contaminated soil Niederglatt
Soil N2	Contaminated soil Niederglatt
Soil R1	Contaminated soil Rivera
Soil R2	Contaminated soil Rivera
Soil T1	Contaminated soil Thun
Cement	Non-reduced Portland cement from Holcim
Fly ash	Fly ash from MSWI plant Zuchwil

List of Contents

Part A: Introduction

Part B: Research Papers

Part C: Technical Reports

Part D: Summary and Outlook

Part A: Introduction

Chapter 1

Preface

The present thesis deals with a small but important part in the field of waste management – the fly ash from municipal solid waste incineration.

1.1 Context

Switzerland has a long tradition of waste incineration and today combustible waste that cannot be recycled is thermally treated in 30 municipal solid waste incineration (MSWI) plants. The lack of suitable landfill sites and the large environmental impact of direct landfilling of waste resulted in the prohibition to landfill unburnt municipal solid waste in 2000. Treatment of the combustible waste produces approximately 750'000 tons of bottom ash and 75'000 tons of fly ash annually in Switzerland.

In recent years, the focus has been laid on the optimization of the treatment of these incineration residues. During thermal waste treatment, volatile heavy metals accumulate in the fly ash. An efficient treatment of this fly ash promises considerable ecological and economic benefits due to an improved quality for disposal and the recovery of the heavy metals contained. With the acidic fly ash leaching process (FLUWA), a method for the targeted heavy metal separation and recovery is available. The FLUWA process is currently implemented at 12 Swiss MSWI plants and represents the state-of-the-art. With the revised Swiss Waste Ordinance in 2016, the treatment of fly ash and recovery of metals is prescribed from 2021 onwards. Therefore, the investigation and optimization of the FLUWA process is of increasing interest and an industrial solution for direct metal recovery within Switzerland is in development.

1.2 Aim of the thesis

The present thesis provides a detailed description of the chemical and mineralogical composition of fly ash and the leaching processes to improve heavy metal separation and to estimate the limiting factors of metal depletion. The thesis focuses on the following topics:

- Selection of analytical methods that allow an efficient and detailed description of the fly ash and the chemical associations of metals. Special attention is paid on the enclosed phases controlling the metal leaching in fly ash to increase the recovery of mainly Zn, Pb, Cu and Cd. The focus is laid on chemical and mineralogical characterization of fly ash and the corresponding leached residue (filter cake) from six Swiss MSWI plants. The detailed characterization of the fly ash allows additionally the description and understanding of the fly ash formation processes.

- Carrying out selected leaching tests and mechanical separation experiments for a better understanding of the complex phase composition of fly ash. In order to cover the large range of chemical compositions present in fly ash from different plants, a highly heavy metal-rich fly ash and a strongly alkaline fly ash with lower concentration of heavy metals is used for the experiments.

- Optimization of the metal recovery and thus improvement of the final storage quality of the leached filter cake from the FLUWA process. This is achieved by optimization of the leaching conditions (e.g. pH, redox conditions), supplemented by an additional leaching step of the filter cake with concentrated sodium chloride solution before deposition. The hazardous potential for Cr(VI) from leached filter cake and other contaminated materials is determined additionally because of the environmental importance of chromate.

- Based on the findings at laboratory scale, a large-scale optimization of the FLUWA process is performed to complete the thesis.

1.3 Thesis structure

The thesis is organized in four parts:

(A) A background chapter introduces to the main aspects of waste management and focusing on municipal solid waste incineration, the possibilities of fly ash treatment and summarizes the most relevant methods for separation and recovery of heavy metals from fly ash.

(B) The second part contains two research papers that have been published in international journals and a third paper that has been submitted. The papers describe the characterization and leaching optimization of fly ash and the determination of Cr(VI) in leached filter cake, soil and cement.

(C) The third part contains three technical reports which describe the characterization of six fly ashes in detail, findings from numerous leaching experiments, and the results of the large-scale optimization of the FLUWA process.

(D) The fourth part summarizes the main findings of the thesis by discussing general implications for the optimization of the FLUWA process and complemented by an outlook for possible further studies.

Chapter 2

Background

The following information will guide to the main aspects of municipal solid waste incineration, the treatment of fly ash and the separation and recovery of heavy metals from fly ash as a basis for the following research papers and technical reports.

2.1 Municipal solid waste incineration

The concern about environmental aspects of municipal solid waste (MSW) was nonexistent in Switzerland until the second half of the 20th century, even though there has been a significant increase and change in composition, caused by the increasing industrialization. Environmentally friendly waste management was initialized in the 1970s by the improvement of the Law for Protection of Waters (Swiss Confederation, 1972). The Swiss Environmental Protection Law (Swiss Confederation, 1983) formed the basis for a sustainable waste management. The objectives and principles of the guidelines for waste management (FOEN, 1986) have influenced the Swiss waste policy significantly for the last three decades and the pollutant emitted by the industry were reduced significantly. In 1970, the separately collected waste material accounted only for about 20% of incinerated and landfilled MSW (Figure 2-1). The defined principles of the guidelines for waste management for the production of either recyclable materials or residual materials suitable for storage in final repositories resulted in the prohibition to landfill unburnt municipal solid waste in 2000. Nowadays, the Swiss Waste Ordinance (VVEA; Swiss Confederation, 2016) contains threshold values based on the total chemical composition as well as the leaching behaviour for toxic substances that define the general classification into one of five waste deposit categories.

The amount of MSW has tripled in Switzerland since 1970 and has increased twice as fast as the Swiss population (Figure 2-1). In an international comparison Switzerland belongs to the leaders with a waste production of 744 kg per capita in 2014 (or 6.01 Mio. tonnes). Only Denmark produces similar amounts of waste whereas the average amount of MSW in Europe lies at 478 kg per capita (OECD, 2015). The high per capita proportion of MSW in Switzerland is based on the high living standard and the complete and detailed statistical recording. The results of a national MSW composition study performed in 2012 (FOEN, 2014) show a significant increase in biogenic waste (32.2%) compared to the study from 2001/02.

Other important fractions of MSW are paper (13.5%), plastics (11.0%) and other composite goods (12.8%). The increase in the amount of waste has been largely compensated by an improved recycling rate. Switzerland plays a pioneering role in waste recycling and the amount of separately collected MSW has been steadily increased to 50% in recent years (Figure 2-1). In 2015, 3.18 million tonnes of waste generated in Switzerland were recycled and around 2.85 million tonnes were burnt. In other European countries the direct disposal of MSW in landfills is still widespread.

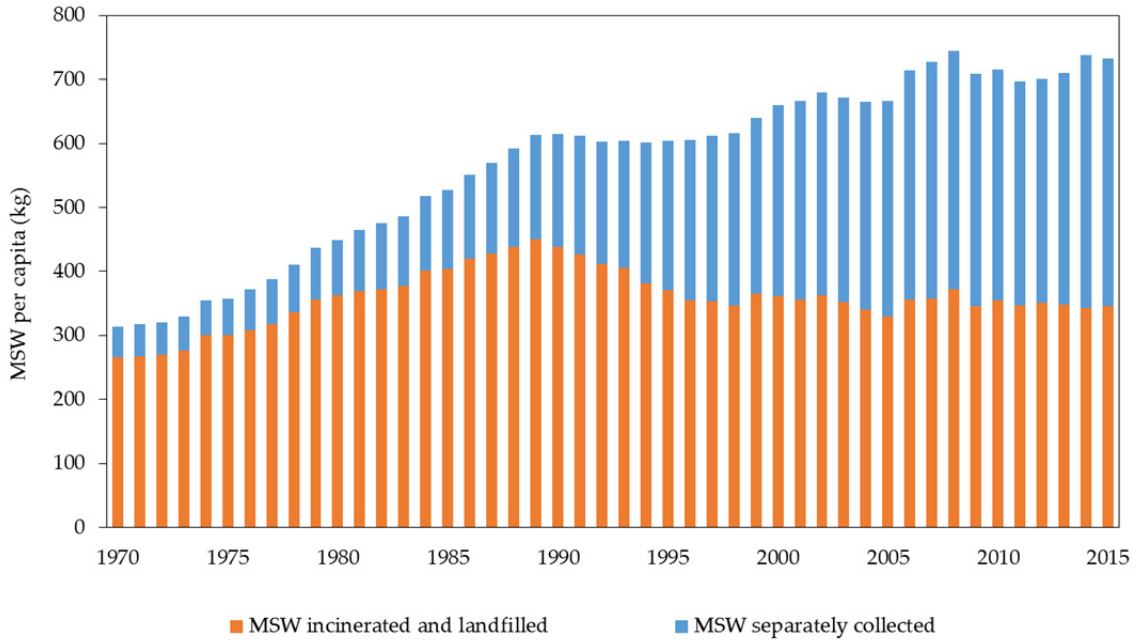

Figure 2-1: *Amount of MSW per capita (kg) produced annually from 1970 to 2015. MSW separately collected includes compost, papier, cardboard, glass, metals, textiles, batteries (since 1993), electrical and electronic devices (since 2001). The data shown do not include waste import (FOEN, 2016).*

Switzerland has a long tradition of waste incineration and already in 1904 the first municipal solid waste incineration (MSWI) plant started operating in Zürich. In 1978, already 73% of the MSW was burnt and today combustible waste that cannot be recycled is thermally treated in 30 MSWI plants. Modern waste incineration has a number of benefits for non-recyclable residues:

- Reduction of the waste mass (75%) and volume (90%).
- Destruction of organic pollutants and inertization of residual waste.
- Use of the enthalpy of the residual waste to produce energy.
- Transfer of some of the residues into recyclable secondary products (especially metals).

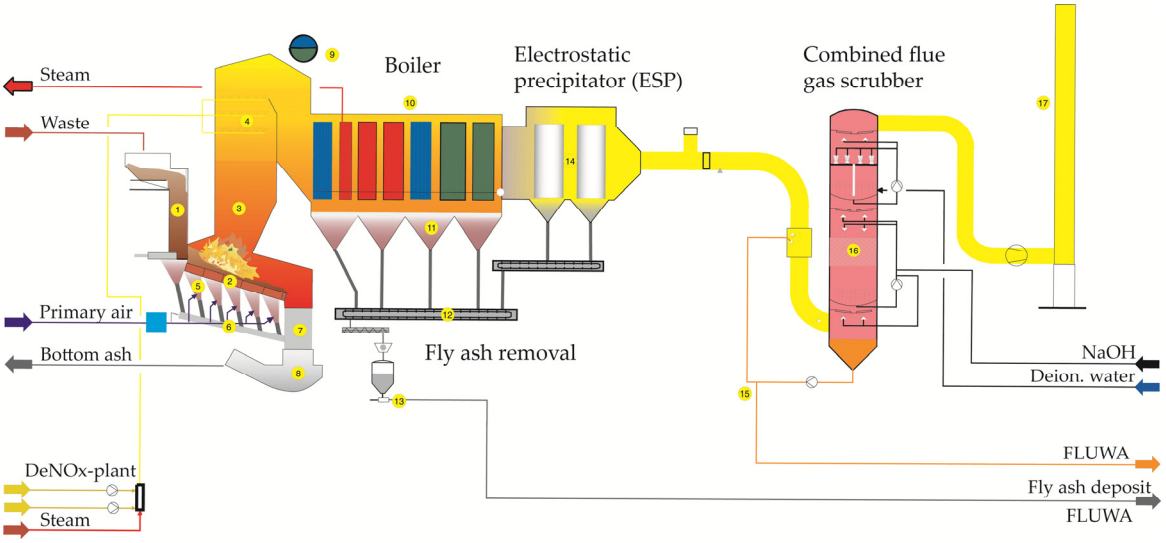

Figure 2-2: *Scheme of the MSWI plant Zuchwil. (1) Feed funnel (2) grate (3) combustion chamber (5) bottom ash (6) ash and slag removal system (7) slag hopper (8) slide de-sludger (10) boiler (11) ash funnels (12) boiler ash removal (13) pneumatic ash removal system (14) electrostatic precipitator (15) scrub water circulation (16) flue gas scrubber (17) chimney (adapted from Hitachi Zosen INOVA).*

In Figure 2-2 the schematic principle of the material flow and the main processes of MSWI are shown. After storage in a waste bunker, the MSW is usually incinerated in a grate-firing furnace; however, there also exist other incineration techniques such as fluidized-bed firing and rotary-kiln system (Brunner, 2010). The firing temperature lies typically between 800-1'000°C where primary air is blown continuously into the bed from the bottom. Volatile compounds along with dust particles are emitted through the flue gas flow and this flue gases are purified using a multi-stage cleaning system. Fly ash particles enriched in heavy metals, salts and organic pollutants are collected at the heat recovery section or removed from the flue gas by fabric filters or electrostatic precipitators. Volatile components are removed from the flue gas in a subsequent dry or wet flue gas cleaning process. Water is injected directly into the flue gas for wet flue gas cleaning where mainly HCl, HF and NH_3 are removed (acidic scrub water). In a second step, NaOH is added to remove sulphur oxides (SO_2, SO_3) as sodium sulphate solution (neutral scrub water). The waste incineration process results in the production of three main residues: bottom ash, fly ash and air pollution control (APC) residues.

2.2 Incineration residues

2.2.1 Bottom ash

Bottom ash makes up the major part of incombustible solid residues remaining after waste incineration (20% of waste input mass). Every year 750'000 tons of bottom ash are produced in Switzerland which consist primarily of non-combustible materials and unburnt organic matter (Sabbas et al., 2003). The bottom ash remaining on the grate is collected at the outlet of the combustion chamber and quenched with water or removed in its dry state. The chemical composition of bottom ash is dependent on the waste input and the elemental partitioning occurring during incineration. The partition coefficient of heavy metals among the residues during combustion has been studied by several authors (Brunner and Mönch, 1986; Verhulst and Buekens, 1996; Morf et al., 2000; Abanades et al., 2002; Morf et al., 2013; Funari et al., 2016). Elements possessing high boiling points (e.g. Si, Ca, Al, Mg, Fe or Ti) are almost not volatilized during incineration and thus end up mainly in the bottom ash (Table 2-1). At the given temperature conditions silicate glass and new minerals are formed, however, due to the short incineration process (ca. 30 minutes) most reactions are not complete and bottom ash does thus not reach a thermodynamic equilibrium state (Eggenberger and Mäder, 2010). The composition of bottom ash is dominated by the mineral fraction (80-90 wt.%), whereas the metals make up only 10-20 wt.%. The mineralogical composition is dominated by glasses and minerals which can be divided into refractory minerals already present in the waste input (e.g. quartz, feldspars, ceramics) and minerals newly-formed during the incineration process or during cooling (e.g. melilites, wollastonite, lime) (Eusden et al., 1999). Nowadays, different techniques of bottom ash treatment are implemented in Switzerland with the objective of metal separation and recycling (ZAV Recycling AG, supersort®technologie, RecuLAB, Selfrag). However, the metal depleted mineral fraction still has to be deposited and further possibilities for recycling (e.g. substitute construction material) are subject to ongoing research.

2.2.2 Fly ash

Every year 75'000 tons of fly ash (2% of the waste input mass) are produced in Switzerland which consist primarily of aluminosilicates, oxides, soluble salts, heavy metals and toxic organic compounds. Ash particles are collected at the heat recovery section (boiler ash, coarse particles) or removed from the flue gas by fabric filters or electrostatic precipitators (ESP ash, fine particles). The mixture of boiler ash and ESP ash is usually combined and referred to as fly ash. Volatile heavy metals such as Zn, Cd and Pb escape with the flue gas and either condense on fly ash particles or are trapped by the air pollution control system. Heavy metal fractionation depends on the composition of MSW, the binding form of the metals and the operating conditions of the incinerator. Metal transfer to the fly ash is favoured by higher furnace temperatures and thus increasing amounts of dust

particles as well as elevated chlorine and sulphur concentration in the flue gas (Jakob et al., 1996; Belevi and Moench, 2000; Morf et al., 2000). Metal concentration in fly ash varies between 10-15% and is dominated by Zn, Al, Fe and Pb (Table 2-1). The concentration of matrix elements (e.g. Ca, Cl) and heavy metals in fly ash of specific MSWI plants are varying strongly within a year depending on waste input and season (Figure 2-3). An elevated industrial waste incineration results in higher concentration of heavy metals and lower concentration of Ca in fly ash compared to fly ash arising from processes where more household waste is incinerated. The elevated concentration of Cl in fly ash (10 wt.%) originates mostly from the combustion of plastics (PVC). Increasing chlorine content forces the vaporisation of heavy metals with higher vapour pressures in form of chloride complexes (Jakob et al., 1996; Verhulst and Buekens, 1996; Morf et al., 2000). Due to the high concentration of organic and inorganic pollutants, fly ash has to be disposed under strict regulations and at great costs or has to be treated properly (see Section 2.3). The high concentration of metals (mainly Zn, Al, Fe, Pb and Cu) in fly ash favours an economically interesting heavy metal separation and recovery (urban mining) beside the benefit of avoiding their deposition. Studies have shown that also strategic elements such as In, Y, Bi, Se and Te show a potential for recovery in the future because they all have transfer coefficients higher or equal to 0.4 to fly ash (Morf et al., 2013).

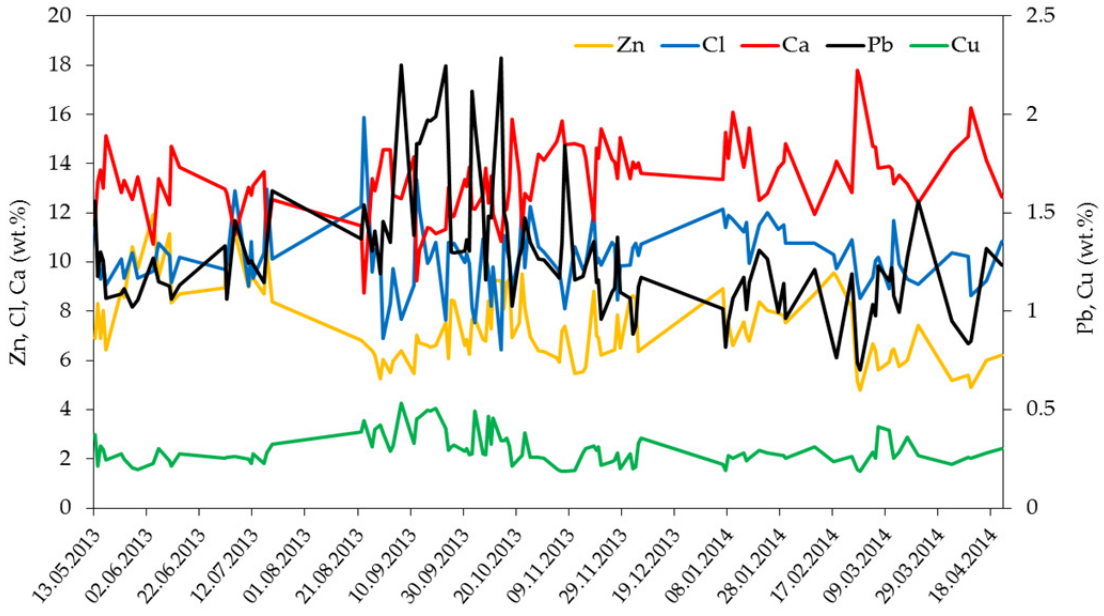

***Figure* 2-3:** *Daily and seasonal variations of Zn, Cl, Ca, Pb and Cu in fly ash from MSWI plant Zuchwil, determined by ED-XRF (Budde, 2015).*

2.2.3 Air pollution control (APC) residues

APC residues include the particulate material captured after reagent injection in the acid gas treatment units prior to discharge of the effluents into the atmosphere (Sabbas et al., 2003). Depending on whether dry or wet flue gas cleaning processes are installed, solid or liquid APC residues are produced. Scrub water from the wet flue gas cleaning is a typical liquid APC residue that can be further used to leach fly ash in order to remove heavy metals because of its acidic property (Section 2.4.1).

Table 2-1: *Concentration ranges for different elements in incineration residues (Chandler et al., 1997).*

	Concentration (mg/kg)			
Element	**Bottom ash**	**Fly ash**	**Dry-/semi dry APC residues**	**Liquid APC residues**
Al	22'000 - 73'000	49'000 - 90'000	120'000 - 83'000	21'000 - 39'000
As	0.1 - 190	37 - 320	18 - 530	41 - 210
Ba	400 - 3'000	330 - 3'100	51 - 14'000	55 - 1'600
Ca	370 - 123'000	74'000 - 130'000	110'000 - 350'000	87'000 - 200′000
Cd	0.3 - 70	50 - 450	140 - 300	150 - 1'400
Cl	800 - 4'200	29'000 - 210'000	62'000 - 380'000	17'000 - 51'000
Cr	23 - 3'200	140 - 1'100	73 - 570	80 - 560
Cu	190 - 8'200	600 - 3'200	16 - 1'700	440 - 2'400
Fe	4'100 - 150'000	12'000 - 44'000	2'600 - 71'000	20'000 - 97'000
Hg	0.02 - 8	0.7 - 30	0.1 - 51	2.2 - 2'300
K	750 - 16'000	22'000 - 62'000	5'900 - 40'000	810 - 8'600
Mg	400 - 26'000	11'000 - 19'000	5'100 - 14'000	19'000 - 170'000
Mn	80 - 2′400	800 - 1′900	200 - 900	5′000 - 12′000
Mo	2 - 280	15 - 150	9 - 29	2 – 44
Na	2'800 - 42'000	15'000 - 57'000	7'600 - 29'000	720 – 3'400
Ni	7 - 4'200	60 - 260	19 - 710	20 – 310
Pb	100 - 13'700	5'300 - 26'000	2'500 - 10'000	3'300 – 22'000
S	1'000 - 5'000	11'000 - 45'000	1'400 - 25'000	2'700 – 6'000
Sb	10 - 43	260 - 1'100	300 - 1'100	80 – 200
Si	91'000 - 308'000	95'000 - 210'000	36'000 - 120'000	78'000
V	20 - 120	29 - 150	8 - 62	25 – 86
Zn	610 - 7'800	7'000 - 70'000	7'000 - 20'000	8'100 – 53'000

2.3 Treatment and use of fly ash

Due to the contamination with organic and inorganic pollutants, an efficient treatment of fly ash is essential. Numerous studies about the treatment and use of incineration residues from the last two decades are known (Wiles, 1996; Van der Sloot, 2001; Ferreira et al., 2003; Sabbas et al., 2003; Quina et al., 2008; Lam, 2010; Zacco, 2014; Margallo et al., 2015). In general, the treatments for fly ash can be grouped into three classes: (1) solidification/stabilization, (2) thermal methods and (3) leaching methods.

2.3.1 Solidification/stabilization (S/S)

Solidification/stabilization (S/S) processes are used to immobilize physically and chemically hazardous components present in fly ash by adding additives and/or binders. The main mechanisms in S/S processes are precipitation, adsorption, macroencapsulation, microencapsulation and/or detoxification (Margallo et al., 2015). Chemical stabilization of fly ash does not reduce the amount but reduces the leachability of heavy metals and therefore decreases the potential danger to the environment. Chemical stabilization of fly ash is performed by using phosphates (Uchida et al., 1996; Eighmy et al., 1997; Sun et al., 2011), chelating agents (Youcai et al., 2002; Xu et al., 2013) or ferrous sulphate solution (Lundtorp et al., 2002; Hu, 2005). Recent studies have further shown that colloidal silica leads to a relatively cheap, highly reactive and non-toxic alternative for fly ash stabilization (Bontempi et al., 2010; Guarienti et al., 2014). The most commonly used binders for solidification are Portland cement (Alba et al., 2001; Polettini et al., 2001) and silicates (Zacco et al., 2012). Most often used in practice is first a chemical stabilization followed by a solidification of the waste material (Derie, 1996; Mangialardi et al., 1999). A disadvantage of the S/S processes is the high binder/ash ratio, which increases the mass for deposition.

2.3.2 Thermal methods

Treatment of fly ash using thermal methods has the advantage of volume reduction and formation of a more homogeneous, denser product that is more resistant to leaching. High temperatures lead to the incorporation of elements of concern into the amorphous structure of silicate glass or newly formed phases. Thermal methods have further the advantage of destroying dioxins and furans when heated above 1'300°C (Sakai and Hiraoka, 2000). Thermal processes can be grouped into vitrification, melting and sintering. Vitrification is performed by melting the fly ash with a glass precursor in order to fix the heavy metals in the glassy matrix (Tadashi, 1996; Haugsten and Gustavson, 2000; Park and Heo, 2002; Kuo et al., 2004). Temperatures usually used are in the range of 1'000-1'500°C. Vitrification is widespread in Japan where the avoidance of dioxins and furans has priority (Jung et al., 2005). Melting is similar to vitrification but no additives are used. The glass formed is not homogeneous and results in a multi-phase product (Quina et al., 2008; Zacco, 2014). During the melting process, heavy metals are volatilized as metal chlorides and concentrated in newly formed secondary fly ash (SFA). Elements such as Zn and Pb are present in high concentration in SFA what allows an economic recovery (Nagib and Inoue, 2000). Using sintering for fly ash treatment, the temperature is increased to around 700–1'100°C until solid phase reactions are achieved (Wang et al., 1998; Mangialardi, 2001). A disadvantage of all thermal methods is the elevated energy costs. In addition, the presence of elevated alkali chlorides, sulphates and high concentration of heavy metals in the fly ash lead to technical problems during thermal treatment

and therefore often combined methods with pre-washing and stabilization steps are used (Derie, 1996; Kim and Kim, 2004; Chiang and Hu, 2010).

2.3.3 Leaching methods

Leaching methods allow the heavy metals in fly ash to be transferred into an aqueous solution. The heavy metals can then be separated and recovered using appropriate methods. The soluble salts in fly ash can be removed by using water as washing reagent (Kirby and Rimstidt, 1994; Wang et al., 2001; Abbas et al., 2003; Zhang and Itoh, 2006; Karlfeldt and Steenari, 2007; Bayuseno and Schmahl, 2011). Washing with water to remove soluble salts is often be used as a first step during fly ash treatment before performing S/S or thermal methods (Derie, 1996; Nzihou and Sharrock, 2002; Mangialardi, 2003; Chimenos et al., 2005). Washing methods using water show low metal extraction efficiency, mainly dependent on the resulting alkaline pH-value of the ash suspension. Leaching solutions other than water are required to efficiently extract heavy metals from fly ash. Various studies using chemical agents to improve heavy metal leaching were investigated (Mizutani et al., 1996; Hong et al., 2000; Nagib and Inoue, 2000; Van Herck and Vandecasteele, 2001; Kim and Hesbach, 2009; Zhu et al., 2009; Karlfeldt Fedje et al., 2010). Acidic fly ash leaching shows the most effective fly ash leaching method for heavy metal separation and recovery (Katsuura et al., 1996; Van der Bruggen et al., 1998; Ludwig et al., 2005; Chiang et al., 2008; Aguiar del Toro et al., 2009; Huang et al., 2011; Yang et al., 2012; Tang and Steenari, 2015). Acidic leaching using scrub water from the wet flue gas cleaning is established on an industrial-scale since the 1990s as described in Section 2.4.1 (Vehlow et al., 1990; Schlumberger et al., 2007; Bühler and Schlumberger, 2010). Other metal separation processes for fly ash known are bioleaching (Bosshard et al., 1996; Krebs et al., 2001) or electrochemical processes (Pedersen, 2002; Ferreira et al., 2005). Common to all described methods is the substantial improvement of quality of the residues for deposition.

Table 2-2: *Treatment methods of fly ash adapted after Quina et al., 2008.*

Stabilization/solidification	Thermal methods	Leaching methods
Stabilization with additives	Vitrification	Washing (aqueous extraction)
Solidification with binders	Melting	Leaching (chemical agents)
Macro-encapsulation	Sintering	Bioleaching

2.3.4 Swiss strategies

With the introduction of principles for waste management in 1986 (FOEN, 1986), more and more care was taken about the quality of incineration residues produced in Switzerland. In contrast to the period before the Swiss Environmental Protection Law (Swiss Confederation, 1983) was installed, fly ash was often spread on forest roads as weed killer (Fahrni, 2010). The Federal Department for the Environment (FOEN) has published a

detailed report with several proposals for fly ash treatment already in 1987 (FOEN, 1987) and several findings obtained from this report were later integrated in the Swiss Waste Ordinance in 1990 (TVA; Swiss Confederation, 1990). Under the control of the FOEN, various novel high temperature processes for the treatment of municipal solid waste and its incineration residues were investigated in the 1990s (e.g. Jakob et al., 1995; Traber et al., 2002). However, the procedure of thermal treatment for the decontamination and inertization of incineration residues has not been established to date in Switzerland.

In Switzerland, acidic fly ash leaching (FLUWA process) has been established since 1997 and offers an effective method for heavy metal separation and recovery (Schlumberger et al., 2007; Bühler and Schlumberger, 2010). The depleted residue (filter cake) has less impact on the environment and can be deposited together with bottom ash on a landfill type C or D according to the new Swiss Waste Ordinance (VVEA; Swiss Confederation, 2016). Nowadays, more than 60% of the fly ash in Switzerland is treated according to the FLUWA process which represents the state-of-the-art (Figure 2-4). The remaining fly ash is directly deposited in underground storage abroad or extracted with water (neutral leaching) to remove water-soluble salts before stabilization/solidification with cement. One MSWI plant is additionally equipped with the FLUREC process (Schlumberger et al., 2007), in which several valuable metals, in particular zinc, can be selectively recovered. Until the year 2021, all fly ash produced in Switzerland has to be treated and the metals have to be recovered according to the state-of-the-art as prescribed in the Swiss Waste Ordinance.

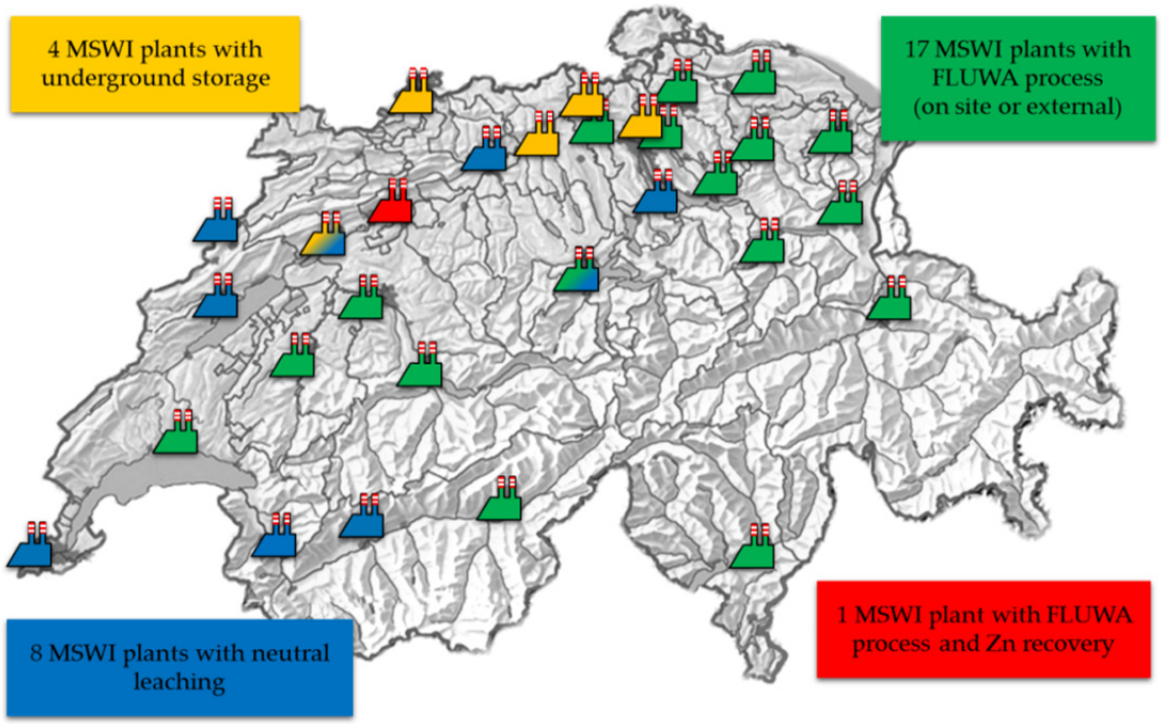

Figure 2-4: *The 30 MSWI plants in Switzerland with their fly ash treatment strategies in 2017.*

2.4 Heavy metal separation and recovery from fly ash

MSWI fly ash comprises a large potential for recyclable metals where the high content of Zn is of particular interest. Treatment of fly ash further contributes positively to the environment due to a reduction of mass and heavy metals to be deposited. The FLUWA process provides the basis for extended methods such as the FLUREC process (Schlumberger et al., 2007) where metals from fly ash are directly recovered.

2.4.1 Acidic fly ash leaching (FLUWA process)

Using scrub waters from the wet flue gas cleaning process for extraction of the heavy metals in fly ash has been first shown in the 3R process by Vehlow et al. (1990). Most often acidic and neutral scrub water is used in the FLUWA process that is purified from mercury by selective ion exchanger. This leads to the removal of >90 wt.% of the mercury entering the incineration process. Within the FLUWA process, the fly ash is leached with acidic scrub water in a multistage cascade (Figure 2-5). The extractability of heavy metals is mainly depending on the alkalinity of the fly ash, acidity of the scrub water, liquid to solid ratio (LS), temperature and leaching time. Depending on the parameters 60-80% Zn, 60-85% Cd and 0-30% Pb and Cu can be extracted by the FLUWA process (Table 2-3). The addition of an oxidizing agent such as hydrogen peroxide (H_2O_2) during fly ash leaching keeps the redox-sensitive metals (mainly Pb, Cu and Cd) in solution, leading to significantly higher depletion factors (Table 2-3, optimized acidic leaching).

Table 2-3: Average metal recovery achieved by the FLUWA process (AWEL, 2013).

	Recovery Acidic leaching (FLUWA)	**Recovery** Optimized acidic leaching (FLUWA + H_2O_2)
	%	%
Pb	0-30	50-90
Cd	60-85	85-95
Cu	0-30	40-80
Zn	60-80	60-80

The addition of an oxidizing agent further converts Fe^{2+} to Fe^{3+} which precipitates as Fe-hydroxide and is accumulated in the remaining filter cake. Removing Fe from the extract solution is important when metal recovery is extended by the FLUREC process that is very sensitive to impurities (Schlumberger et al., 2007). Another process going on during leaching is the formation of gypsum ($CaSO_4 \cdot 2H_2O$) due to the reaction of dissolved calcium (Ca^{2+}) from the fly ash and sulphate (SO_4^{2-}) from scrub water. After ca. 60 minutes of extraction, the suspension is separated by vacuum belt filtration into a metal depleted filter cake and a metal enriched filtrate solution. The metalliferous filtrate is used for di-

rect metal recovery (FLUREC, Schlumberger et al., 2007) or fed to a waste water treatment plant where metal hydroxide sludge precipitation is performed. To transform the dissolved metals into metal hydroxide precipitates, lime is added to the metalliferous filtrate until the ideal pH-value for precipitation of 9.5 is reached. The metal precipitate is then filtrated and pressed into a metal hydroxide sludge with a dry mass of 17-35%, depending of filter system used. This sludge is then exported abroad and the metals are recovered in smelting plants.

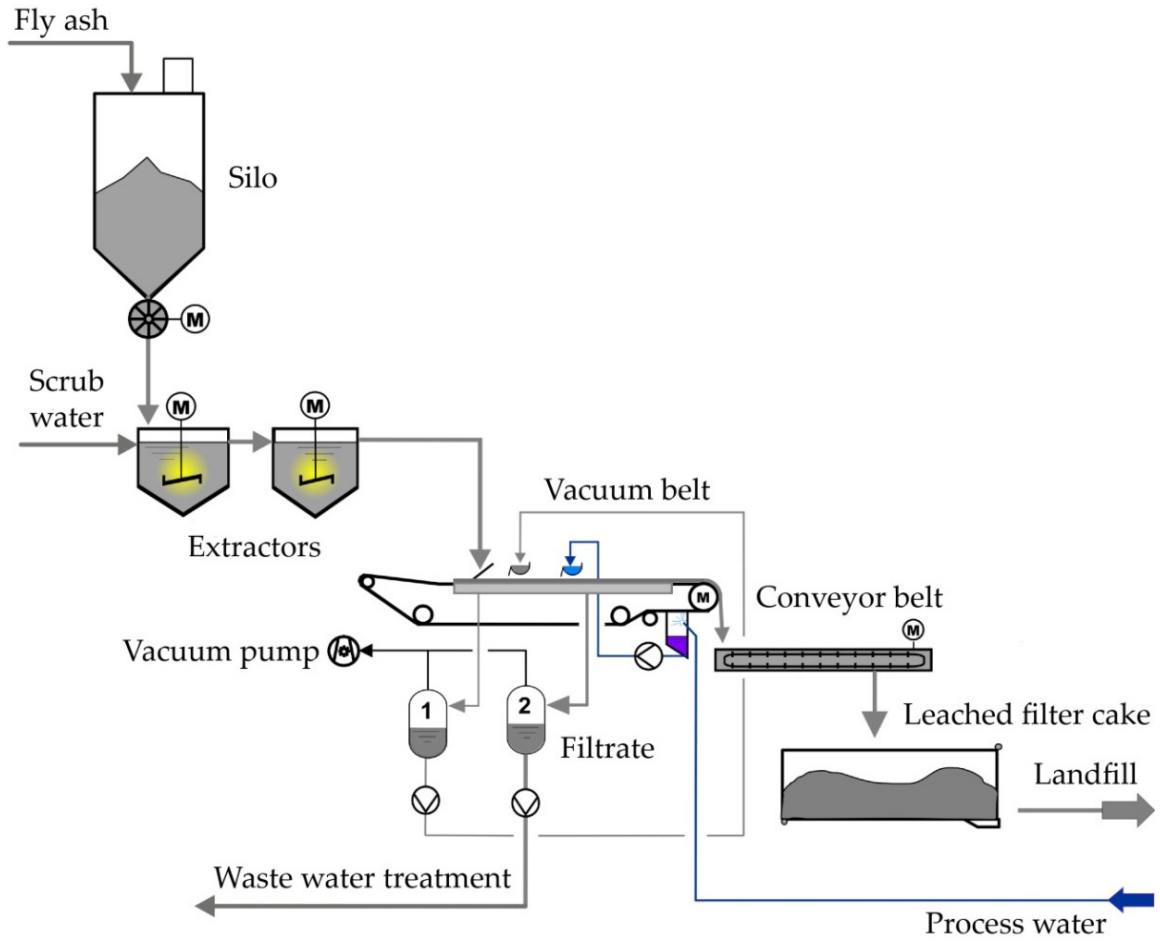

Figure 2-5: *Scheme of the FLUWA process (Bühler and Schlumberger, 2010).*

2.4.2 FLUREC process

The FLUREC process offers a possibility for recovering high-purity zinc (>99.99%) from the heavy-metal enriched filtrate coming directly from the FLUWA process (Schlumberger et al., 2007) (Figure 2-6). The FLUREC process separates Cd, Pb and Cu from the filtrate by a cementation process (reductive separation). Thereby Zn powder is added to the filtrate as reducing agent and metals more noble than Zn are separated as a metallic cementate which is then filtered. Zinc dissolution can be described according to Equation 2-1).

$$Cd^{2+} + Cu^{2+} + Pb^{2+} + 3\ Zn^{0} \rightarrow Cd^{0}\downarrow + Cu^{0}\downarrow + Pb^{0}\downarrow + 3\ Zn^{2+} \quad (2\text{-}1)$$

Due to the high Pb load of 50-70%, the cementate can be sent directly to a Pb smelter where the remaining heavy metals are also recovered in the Pb production process. The Zn in solution is separated selectively from the pre-purified filtrate in a solvent extraction step as described in detail by Schlumberger et al. (2007). For this purpose, the Zn is trapped by a water-insoluble organic complexing phase. The complexation of the Zn is strongly pH dependent and at low pH (pH 2.7-3), 99.5% of the Zn is complexed by the organic phase. In a following washing step, other metals complexed by the organic phase are separated to reduce interferences in the subsequent electrolytic zinc recovery process. The complexed Zn is then transferred to solution again using diluted sulphuric acid where a high-purity zinc sulphate solution is obtained. This solution is then used in a final electrochemical process where Zn is separated from the solution by applying an electrical DC potential and deposition on an aluminium cathode. The recycled Zn metal is sold on the market. The FLUREC process was implemented at MSWI plant Zuchwil in 2012 where about 300 tons of zinc can be recovered annually.

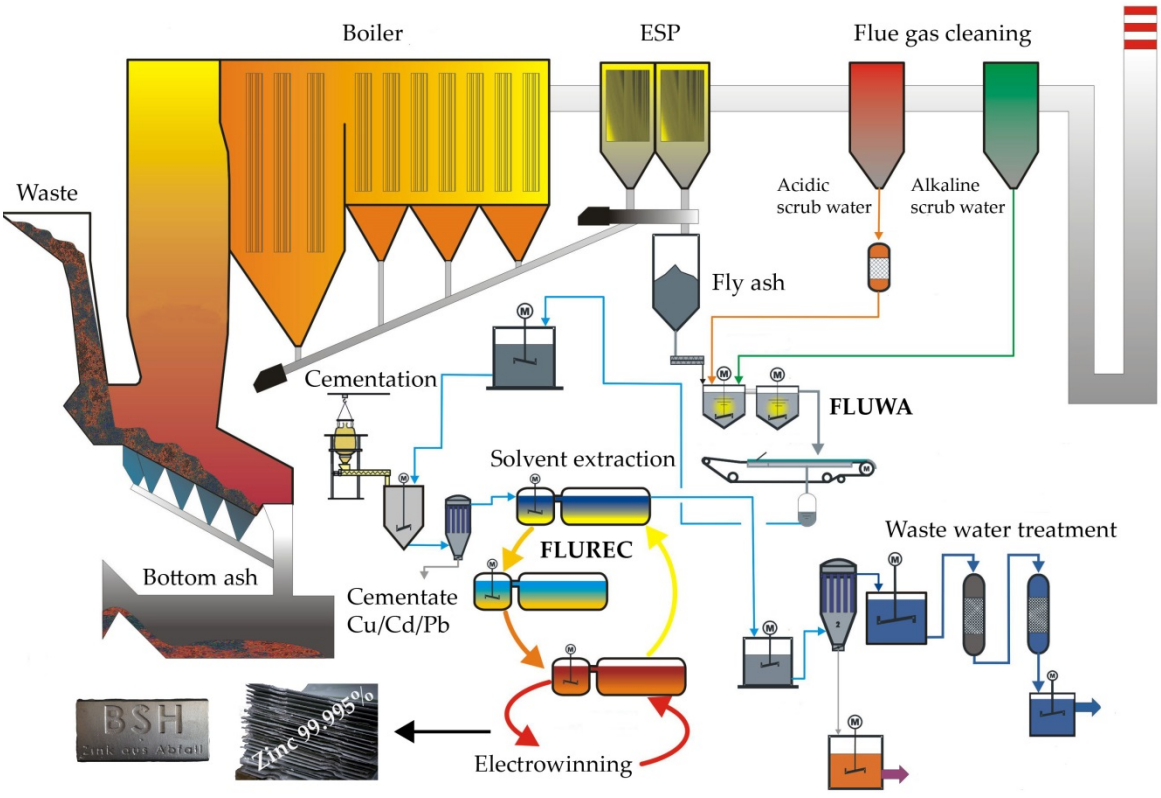

Figure 2-6: *Scheme of the FLUWA and FLUREC process adapted from Bühler and Schlumberger (2010).*

2.4.3 Hydroxide sludge treatment plant with metal recovery (SwissZinc)

The revised Swiss Waste Ordinance prescribes the recovery of metals from fly ash from 2021 onwards. The implementation requires high investments for the plant operators. Therefore, the construction of a central hydroxide sludge treatment plant with integrated metal recovery, similar to the FLUREC process, is planned in Switzerland (SwissZinc). The project under the leadership of the Association of Swiss Operators of Thermal Waste Processing Plants (VBSA) is developing a centralized plant for direct metal recovery within Switzerland. Assuming that all fly ash generated in Switzerland is treated according to the FLUWA process with a recovery of 75% for Zn, about 2'000 tons could be recovered per year (ZAR, 2016). The SwissZinc process will use hydrochloric acid as leaching agent to extract the hydroxide sludge. The following processing of the metal-containing filtrate is carried out analogous to the FLUREC process by a cementation process followed by a solvent extraction and zinc electrowinning. During the first project phase, the technical feasibility of the hydroxide sludge treatment and metal recovery was successfully demonstrated. A preliminary estimate of processing cost for one tonne of moist hydroxide sludge is in the range of CHF 250 per tonne (ZAR, 2016). This is more economically than the previous used recycling paths described above. The final planning and detailed cost estimations for the construction of a central processing plant at MSWI plant Zuchwil are currently being elaborated in a second project phase and form the basis for the decision of implementation expected in 2018.

References

Abanades, S., Flamant, G., Gagnepain, B., Gauthier, D., 2002. Fate of heavy metals during municipal solid waste incineration. Waste Management & Research 20, 55-68.

Abbas, Z., Moghaddam, A.P., Steenari, B.M., 2003. Release of salts from municipal solid waste combustion residues. Waste Management 23, 291-305.

Aguiar del Toro, M., Calmano, W., Ecke, H., 2009. Wet extraction of heavy metals and chloride from MSWI and straw combustion fly ashes. Waste Management 29, 2494-2499.

Alba, N., Vàzquez, E., Gasso, S., Baldasano, J.M., 2001. Stabilization/solidification of MSW incineration residues from facilities with different air pollution control systems. Durability of matrices versus carbonation. Waste Management 21, 313-323.

AWEL, Office for Waste Management, Environmental Protection Agency of Canton Zürich (AWEL Zürich) 2013. Stand der Technik für die Aufbereitung von Rauchgasreinigungsrückständen (RGRR) aus Kehrichtverbrennungsanlagen.

Bayuseno, A.P., Schmahl, W.W., 2011. Characterization of MSWI fly ash through mineralogy and water extraction. Resources, Conservation and Recycling 55, 524-534.

Belevi, H., Moench, H., 2000. Factors determining the element behavior in municipal solid waste incinerators. 1. Field studies. Environmental Science & Technology 34, 2501-2506.

Bontempi, E., Zacco, A., Borgese, L., Gianoncelli, A., Ardesi, R., Depero, L.E., 2010. A new method for municipal solid waste incinerator (MSWI) fly ash inertization, based on colloidal silica. Journal of Environmental Monitoring 12, 2093-2099.

Bosshard, P., Bachofen, R., Brandl, H., 1996. Metal leaching of fly ash from municipal waste incineration by aspergillus niger. Environmental Science & Technology 30, 3066-3070.

Brunner, M., 2010. Trennen durch Verbrennen: Behandlungstechnologien. KVA-Rückstände in der Schweiz - Der Rohstoff mit Mehrwert. Federal Office for the Environment (FOEN), 65-73.

Brunner, P.H., Mönch, H., 1986. The flux of metals through municipal solid waste incinerators. Waste Management & Research 4, 105-119.

Budde, I., 2015. Charakterisierung der elementaren Zusammensetzung von Filteraschen und daraus entstehender Reaktionsprodukte auf einer thermischen Abfallbehandlungsanlage. Aufklärung der möglichen Blei-, Cadmium- und Kupferextraktion aus Filteraschen und Untersuchung möglicher Reaktionsmechanismen, Msc Thesis, Institut für Allgemeine, Anorganische und Theoretische Chemie. Leopold-Franzens-Universität Innsbruck.

Bühler, A., Schlumberger, S., 2010. Schwermetalle aus der Flugasche zurückgewinnen «Saure Flugaschewäsche – FLUWA-Verfahren» ein zukunftsweisendes Verfahren in der Abfallverbrennung. KVA-Rückstände in der Schweiz - Der Rohstoff mit Mehrwert. Federal Office for the Environment (FOEN), 185-192.

Chandler, A.J., Eighmy, T.T., Hartlén, J., Hjelmar, O., Kosson, D., Sawell, S.E., van der Sloot, H.A., Vehlow, J., 1997. Municipal solid waste incinerator residues. International Ash Working Group (IAWG), Elsiever.

Chiang, K.-Y., Hu, Y.-H., 2010. Water washing effects on metals emission reduction during municipal solid waste incinerator (MSWI) fly ash melting process. Waste Management 30, 831-838.

Chiang, K.-Y., Jih, J.-C., Chien, M.-D., 2008. The acid extraction of metals from municipal solid waste incinerator products. Hydrometallurgy 93, 16-22.

Chimenos, J., Fernandez, A., Cervantes, A., Miralles, L., Fernandez, M., Espiell, F., 2005. Optimizing the APC residue washing process to minimize the release of chloride and heavy metals. Waste Management 25, 686-693.

Derie, R., 1996. A new way to stabilize fly ash from municipal incinerators. Waste Management 16, 711-716.

Eggenberger, U., Mäder, U., 2010. Charakterisierung und Alterationsreaktionen von KVA-Schlacken. KVA-Rückstände in der Schweiz - Der Rohstoff mit Mehrwert. Federal Office for the Environment (FOEN), 116-134.

Eighmy, T.T., Crannell , B.S., Butler, L.G., Cartledge, F.K., Emery, E.F., Oblas, D., Krzanowski, J.E., Dykstra Eusden, J., J., Shaw, E.L., Francis, C.A., 1997. Heavy metal stabilization in municipal solid waste combustion dry scrubber residue using soluble phosphate. Environmental Science & Technology 31, 3330-3338.

Eusden, J.D., Eighmy, T.T., Hockert, K., Holland, E., Marsella, K., 1999. Petrogenesis of municipal solid waste combustion bottom ash. Applied Geochemistry 14, 1073-1091.

Fahrni, H.P., 2010. Von der wilden Deponie zu den Verbrennungsrückständen. KVA-Rückstände in der Schweiz - Der Rohstoff mit Mehrwert. Federal Office for the Environment (FOEN), 11-24.

Ferreira, C., Jensen, P., Ottosen, L., Ribeiro, A., 2005. Removal of selected heavy metals from MSW fly ash by the electrodialytic process. Engineering Geology 77, 339-347.

Ferreira, C., Ribeiro, A., Ottosen, L., 2003. Possible applications for municipal solid waste fly ash. Journal of Hazardous Materials B96, 201-216.

FOEN, Federal Office for the Environment, 1986. Leitbild für die Schweizerische Abfallwirtschaft.

FOEN, Federal Office for the Environment, 1987. Behandlung und Verfestigung von Rückständen aus Kehrichtverbrennungsanlagen. Schriftreiche Umweltschutz, BUWAL Bern, Nr 62.

FOEN, Federal Office for the Environment, 2014. Erhebung der Kehricht-zusammensetzung 2012. 1-63.

FOEN, Federal Office for the Environment, 2016. Indicator waste - municipal solid waste, https://www.bafu.admin.ch/bafu/de/home/themen/abfall/zustand/indikatoren/indikator-abfall.pt.html.

Funari, V., Bokhari, S.N., Vigliotti, L., Meisel, T., Braga, R., 2016. The rare earth elements in municipal solid waste incinerators ash and promising tools for their prospecting. Journal of Hazardous Materials 301, 471-479.

Guarienti, M., Gianoncelli, A., Bontempi, E., Moscoso Cardozo, S., Borgese, L., Zizioli, D., Mitola, S., Depero, L.E., Presta, M., 2014. Biosafe inertization of municipal solid waste incinerator residues by COSMOS technology. Journal of Hazardous Materials 279, 311-321.

Haugsten, K.E., Gustavson, B., 2000. Environmental properties of vitrified fly ash from hazardous and municipal waste incineration. Waste Management 20, 167-176.

Hitachi Zosen INOVA, www.hz-inova.com.

Hong, K.J., Tokunaga, S., Kajiuchi, T., 2000. Extraction of heavy metals from MSW incinerator fly ashes by chelating agents. Journal of Hazardous Materials 75, 57-73.

Hu, S.H., 2005. Stabilization of heavy metals in municipal solid waste incineration ash using mixed ferrous/ferric sulfate solution. Journal of Hazardous Materials B123, 158-164.

Huang, K., Inoue, K., Harada, H., Kawakita, H., Ohto, K., 2011. Leaching behavior of heavy metals with hydrochloric acid from fly ash generated in municipal waste incineration plants. Trans. Nonferrous Met. Soc. China 21, 1422-1427.

Jakob, A., Stucki, S., Kuhn, P., 1995. Evaporation of heavy metals during the heat treatment of municipal solid waste incinerator fly ash. Environmental Science & Technology 29, 2429-2436.

Jakob, A., Stucki, S., Struis, R., 1996. Complete heavy metal removal from fly ash by heat treatment: Influence of chlorides an evaporation rates. Environmental Science & Technology 30, 3275-3283.

Jung, C.H., Matsuto, T., Tanaka, N., 2005. Behavior of metals in ash melting and gasification-melting of municipal solid waste (MSW). Waste Management 25, 301-310.

Karlfeldt Fedje, K., Ekberg, C., Skarnemark, G., Steenari, B.M., 2010. Removal of hazardous metals from MSW fly ash - an evaluation of ash leaching methods. Journal of Hazardous Materials 173, 310-317.

Karlfeldt, K., Steenari, B.M., 2007. Assessment of metal mobility in MSW incineration ashes using water as the reagent. Fuel 86, 1983-1993.

Katsuura, H., Inoue, T., Hiraoka, M., Sakai, S., 1996. Full-scale plant study on fly ash treatment by the acid extraction process. Waste Management 16, 491-499.

Kim, A., Hesbach, P., 2009. Comparison of fly ash leaching methods. Fuel 88, 926-937.

Kim, J.-M., Kim, H.-S., 2004. Glass-ceramic produced from a municipal waste incinerator fly ash with high Cl content. Journal of the European Ceramic Society 24, 2373-2382.

Kirby, C.S., Rimstidt, J.D., 1994. Interaction of municipal solid waste ash with water. Environmental Science & Technology 28, 443-451.

Krebs, W., Bachofen, R., Brandl, H., 2001. Growth stimulation of sulfur oxidizing bacteria for optimization of metal leaching efficiency of fly ash from municipal solid waste incineration. Hydrometallurgy 59, 283-290.

Kuo, Y.-M., Lin, T.-C., Tsai, P.-J., 2004. Metal behavior during vitrification of incinerator ash in a coke bed furnace. Journal of Hazardous Materials B109, 79-84.

Lam, C.H.K., Ip, A.W.M., Barford, J.P. McKay, G., 2010. Use of incineration MSW ash: A review. Sustainability 2, 1943-1968.

Ludwig, B., Khanna, P., Prenzel, J., Beese, F., 2005. Heavy metal release from different ashes during serial batch tests using water and acid. Waste Management 25, 1055-1066.

Lundtorp, K., Jensen, D.L., Christensen, T.H., 2002. Stabilization of APC residues from waste incineration with ferrous sulfate on a semi industrial scale. Journal of the Air & Waste Management Association 52, 722-731.

Mangialardi, T., 2001. Sintering of MSW fly ash for reuse as a concrete aggregate. Journal of Hazardous Materials B87, 225-239.

Mangialardi, T., 2003. Disposal of MSWI fly ash through a combined washing-immobilization process. Journal of Hazardous Materials B98, 225-240.

Mangialardi, T., Paolini, A.E., Sirini, P., 1999. Optimization of the solidification/ stabilization process of MSW fly ash in cementitious matrices. Journal of Hazardous Materials B70, 53-70.

Margallo, M., Massoli Taddei, M.B., Hernàndez-Pellon, A., Aldaco, R., Irabien, A., 2015. Environmental sustainability assessment of the management of municipal solid waste incineration residues: a review of the current situation. Clean Techn Environ Policy 17, 1333-1353.

Mizutani, S., Yoshida, T., Sakai, S., Takatsuki, H., 1996. Release of metals from MSWI fly ash and availability in alkaline condition. Waste Management 16, 537-544.

Morf, L.S., Brunner, P.H., Spaun, S., 2000. Effect of operating conditions and input variations on the partitioning of metals in a municipal solid waste incinerator. Waste Management & Research 18, 4-15.

Morf, L.S., Gloor, R., Haag, O., Haupt, M., Skutan, S., Di Lorenzo, F., Böni, D., 2013. Precious metals and rare earth elements in municipal solid waste-sources and fate in a Swiss incineration plant. Waste Management 33, 634-644.

Nagib, S., Inoue, K., 2000. Recovery of lead and zinc from fly ash generated from municipal incineration plants by means of acid and/or alkaline leaching. Hydrometallurgy 56, 269-292.

Nzihou, A., Sharrock, P., 2002. Calcium phosphate stabilization of fly ash with chloride extraction. Waste Management 22, 235-239.

OECD, 2015. Municipal waste, https://data.oecd.org/waste/municipal-waste.htm.

Park, Y.J., Heo, J., 2002. Vitrification of fly ash from municipal solid waste incinerator. Journal of Hazardous Materials B91, 83-93.

Pedersen, A.J., 2002. Evaluation of assisting agents for electrodialytic removal of Cd, Pb, Zn, Cu and Cr from MSWI fly ash. Journal of Hazardous Materials B95, 185-198.

Polettini, A., Pomi, R., Sirini, P., Testa, F., 2001. Properties of portland cement - stabilised MSWI fly ashes. Journal of Hazardous Materials B88, 123-138.

Quina, M.J., Bordado, J.C., Quinta-Ferreira, R.M., 2008. Treatment and use of air pollution control residues from MSW incineration: an overview. Waste Management 28, 2097-2121.

Sabbas, T., Polettini, A., Pomi, R., Astrup, T., Hjelmar, O., Mostbauer, P., Cappai, G., Magel, G., Salhofer, S., Speiser, C., Heuss-Assbichler, S., Klein, R., Lechner, P., 2003. Management of municipal solid waste incineration residues. Waste Management 23, 61-88.

Sakai, S., Hiraoka, M., 2000. Municipal solid waste incinerator residue recycling by thermal processes. Waste Management 20, 249-258.

Schlumberger, S., Schuster, M., Ringmann, S., Koralewska, R., 2007. Recovery of high purity zinc from filter ash produced during the thermal treatment of waste and inerting of residual materials. Waste Management & Research 25, 547-555.

Sun, Y., Zheng, J., Zou, L., Liu, Q., Zhu, P., Qian, G., 2011. Reducing volatilization of heavy metals in phosphate-pretreated municipal solid waste incineration fly ash by forming pyromorphite-like minerals. Waste Management 31, 325-330.

Swiss Confederation, 1972. Allgemeine Gewässerschutzverordnung (AGSchV) vom 19. Juni 1972. AS 1972 967.

Swiss Confederation, 1983. Bundesgesetz über den Umweltschutz (Umweltschutzgesetz, USG). 814.01.

Swiss Confederation, 1990. Technische Verordnung über Abfälle (TVA), 1-36.

Swiss Confederation, 2016. Verordnung über die Vermeidung und die Entsorgung von Abfällen (VVEA), 1-46.

Tadashi, I., 1996. Vitrification of fly ash by swirling-flow furnance. Waste Management 16, 453-460.

Tang, J., Steenari, B.M., 2015. Solvent extraction separation of copper and zinc from MSWI fly ash leachates. Waste Management 44, 147-154.

Traber, D., Mäder, U.K., Eggenberger, U., 2002. Petrology and geochemistry of a municipal solid waste incinerator residue treated at high temperature. Schweizerische mineralogische und petrographische Mitteilungen 82, 1-14.

Uchida, T., Itoh, I., Harada, K., 1996. Immobilization of heavy metals contained in incinerator fly ash by application of soluble phosphaste - treatment and disposal cost redution by combined use of "high specific surface area lime". Waste Management 16, 475-481.

Van der Bruggen, B., Vogels, G., Van Herck, P., Vandecasteele, C., 1998. Simulation of acid washing of municipal solid waste incineration fly ashes in order to remove heavy metals Journal of Hazardous Materials 57, 127-144.

Van der Sloot, H.A.K., D.S., Hjelmar, O., 2001. Characteristics, treatment and utilization of residues from municipal waste incineration. Waste Management 21, 753-765.

Van Herck, P., Vandecasteele, C., 2001. Evaluation of the use of a sequential extraction procedure for the characterization and treatment of metal containing solid waste. Waste Management 21, 685-694.

Vehlow, J., Braun, H., Horch, K., Merz, A., Schneider, J., Stieglitz, L., Vogg, H., 1990. Semi-technical demonstration of the 3-R process. Waste Management & Research 8, 461-472.

Verhulst, D., Buekens, A., 1996. Thermodynamic behavior of metal chlorides and sulfates under the conditions of incineration furnaces. Environmental Science & Technology 30, 50-56.

Wang, K.-S., Chiang, K.-Y., Lin, K.-L., Sun, C.-J., 2001. Effects of a water-extraction process on heavy metal behavior in municipal solid waste incinerator fly ash. Hydrometallurgy 63, 73-81.

Wang, K.-S., Chiang, K.-Y., Perng, J.-K., Sun, C.-J., 1998. The characteristics study on sintering of municipal solid waste incinerator ashes. Journal of Hazardous Materials 59, 201-210.

Wiles, C.C., 1996. Municipal solid waste combustion ash: State-of-the-knowledge. Journal of Hazardous Materials 47, 325-344.

Xu, Y., Chen, Y., Feng, Y., 2013. Stabilization treatment of the heavy metals in fly ash from municipal solid waste incineration using diisopropyl dithiophosphate potassium. Environmental Science & Technology 34, 1411-1419.

Yang, R., Liao, W.-P., Lin, C.-Y., 2012. Feasibility of lead and copper recovery from MSWI fly ash by combining acid leaching and electrodeposition treatment. Environmental Progress & Sustainable Energy 32, 1074-1081.

Youcai, Z., Lijie, S., Guojian, L., 2002. Chemical stabilization of MSW incinerator fly ashes. Journal of Hazardous Materials B95, 47-63.

Zacco, A., Borgese, L., Gianoncelli, A., Struis, R., Depero, L.E., 2014. Review of fly ash inertisation treatments and recycling. Environ Chem Lett 12, 153-175.

Zacco, A., Sacrato, S., Gianoncelli, A., Guerini, L., Tomasoni, G., Ardesi, R., Alberti, M., Bontempi, E., Depero, L.E., 2012. Use of colloidal silica to obtain a new inert from municipal solid waste incinerator (MSWI) fly ash: first results about reuse. Clean Techn Environ Policy 14, 291-297.

ZAR, Zentrum für nachhaltige Abfall- und Ressourcennutzung, 2016. SwissZinc - nationale Anlage zur Verwertung von KVA-Hydroxidschlämme (Project Fact Sheet No. 2), https://zar-ch.ch /fileadmin/user_upload/Contentdokumente/Oeffentliche _Dokumente/Projektblatt_SwissZinc_Nr2.pdf.

Zhang, F.S., Itoh, H., 2006. Extraction of metals from municipal solid waste incinerator fly ash by hydrothermal process. Journal of Hazardous Materials B136, 663-670.

Zhu, F., Takaoka, M., Oshita, K., Takeda, N., 2009. Comparison of two types of municipal solid waste incinerator fly ashes with different alkaline reagents in washing experiments. Waste Management 29, 259-264.

Part B: Research Papers

Chapter 3

Chemical Associations and Mobilization of Heavy Metals in Fly Ash from Municipal Solid Waste Incineration

Gisela Weibel[a], Urs Eggenberger[a], Stefan Schlumberger[b], Urs K. Mäder[a]

[a]*Institute of Geological Sciences, University of Bern, Switzerland*
[b]*Zentrum für nachhaltige Abfall- und Ressourcennutzung (ZAR), Zuchwil, Switzerland*

Waste Management 62 (2017) 147-159

Abstract

This study focusses on chemical and mineralogical characterization of fly ash and leached filter cake and on the determination of parameters influencing metal mobilization by leaching. Three different leaching processes of fly ash from municipal solid waste incineration (MSWI) plants in Switzerland comprise neutral, acidic and optimized acidic (+ oxidizing agent) fly ash leaching have been investigated. Fly ash is characterized by refractory particles (Al-foil, unburnt carbon, quartz, feldspar) and newly formed high-temperature phases (glass, gehlenite, wollastonite) surrounded by characteristic dust rims. Metals are carried along with the flue gas (Fe-oxides, brass) and are enriched in mineral aggregates (quartz, feldspar, wollastonite, glass) or vaporized and condensed as chlorides or sulphates. Parameters controlling the mobilization of neutral and acidic fly ash leaching are pH and redox conditions, liquid to solid ratio, extraction time and temperature. Almost no depletion for Zn, Pb, Cu and Cd is achieved by performing neutral leaching. Acidic fly ash leaching results in depletion factors of 40% for Zn, 53% for Cd, 8% for Pb and 6% for Cu. The extraction of Pb and Cu are mainly limited due to a cementation process and the formation of a $PbCu^0$-alloy-phase and to a minor degree due to secondary precipitation ($PbCl_2$). The addition of hydrogen peroxide during acidic fly ash leaching (optimized acidic leaching) prevents this reduction through oxidation of

ash leaching (optimized acidic leaching) prevents this reduction through oxidation of metallic components and thus significantly higher depletion factors for Pb (57%), Cu (30%) and Cd (92%) are achieved. The elevated metal depletion using acidic leaching in combination with hydrogen peroxide justifies the extra effort not only by reduced metal loads to the environment but also by reduced deposition costs.

3.1 Introduction

The main objectives of thermal treatment of municipal solid waste are mass and volume reduction, destruction of organic contaminants, energy and metal recovery. Two main residues are produced after incineration on grates at 800-1'000°C: bottom ash (20 wt.% of the waste input) and fly ash (2 wt.%). The partition coefficient of metals among the residues during combustion has been studied by several authors (Brunner and Mönch, 1986; Verhulst and Buekens, 1996; Morf et al., 2000; Abanades et al., 2002; Morf et al., 2013; Funari et al., 2016). Heavy metal fractionation depends on the composition of municipal solid waste (MSW), the binding environment of the metals and the operating conditions of the incinerator. Metal transfer to the fly ash is favoured by higher furnace temperatures and thus increasing amounts of dust particles as well as elevated chlorine and sulphur concentration in the flue gas (Jakob et al., 1996; Belevi and Moench, 2000; Morf et al., 2000). Ash particles enriched in heavy metals, salts and organic pollutants are collected at the heat recovery section (boiler ash, coarse particles) or removed from the flue gas by fabric filters or electrostatic precipitators (ESP ash, fine particles). The mixture of boiler and ESP ash is usually combined and referred to as fly ash. Volatile components are removed from the flue gas in a subsequent dry or wet flue gas cleaning process. Water is injected directly into the flue gas in wet flue gas cleaning where mainly HCl, HF and NH_3 are removed (acidic scrub water). In a second step, NaOH is added to remove sulphur oxides (SO_2, SO_3) as sodium sulphate solution (neutral scrub water). These scrub waters can be further used to leach the fly ash in order to remove heavy metals, as first shown in the 3R process (Vehlow et al., 1990). In Switzerland, acidic fly ash leaching (FLUWA process) has been established since 1997 and offers an effective method for heavy metal separation and recovery (Schlumberger et al., 2007). Nowadays, 50% of the fly ashes in Switzerland are treated according to the FLUWA process which represents the state-of-the-art. The other 50% are directly deposited in underground storage abroad or extracted with water (neutral leaching) to remove water-soluble salts before stabilization/solidification with cement (Ferreira et al., 2003; Quina et al., 2008a). Neutral leaching shows low metal extraction efficiency (<5%), mainly dependent on the resulting pH-value of the ash suspension. Within the next five years, all fly ash produced in Switzerland has to be acid leached according to the state-of-the-art as prescribed in the Swiss Waste Ordinance (Swiss Confederation, 2016). Within the FLUWA process, the fly ash is leached with hydrochloric acid (acidic scrub water) in a multistage cascade. The extractability of heavy metals is depending on the alkalinity of the fly ash, acidity of the scrub water, liq-

uid to solid ratio (LS), temperature and extraction time. After ca. 60 minutes of extraction, the suspension is separated by vacuum belt filtration into a metal depleted filter cake and a metal enriched filtrate solution. The filter cake is deposited and the metalliferous filtrate is used for direct metal recovery (FLUREC; Schlumberger et al., 2007) or fed to a waste water treatment plant with metal hydroxide sludge precipitation and subsequent zinc recovery abroad. The extraction of heavy metals from fly ash is mainly dependent on the metal associations and their accessibility. The incorporation of metals in carbonates, oxides, silicates or glasses or its presence in metallic form affects the solubility and dissolution rates of the metals during fly ash leaching. This is evident from the concentrations in the remaining filter cakes (Johnson et al., 1999; Van Herck et al., 2000).

To increase the recoveries of mainly Zn, Pb, Cu and Cd from the fly ash and therefore minimize the metal load to the landfills, the knowledge of the binding forms of heavy metals and the enclosed phases (host particles) controlling the metal leaching in fly ash is essential. Numerous studies related to the characterization of untreated fly ash are known (Eighmy et al., 1995; Sandell et al., 1996; Le Forestier and Libourel, 1998; Thipse et al., 2002; Li et al., 2004; Kutchko and Kim, 2006; Quina et al., 2008b; Mahieux et al., 2010) and a lot of data on the mineralogical composition of leached filter cake are obtained from laboratory experiments (Kirby and Rimstidt, 1994; Eighmy et al., 1995; Liu et al., 2009; Karlfeldt Fedje et al., 2010; Bayuseno and Schmahl, 2011).

The aim of this study is to investigate the industrial scale leaching process from fly ash to improve heavy metal separation and to estimate the limiting factors of depletion. The focus is on chemical and mineralogical characterization of fly ash and the corresponding filter cake from three Swiss MSWI plants. Plant A is performing neutral leaching, plant B acidic leaching and plant C optimized acidic leaching with the addition of an oxidizing agent. The detailed characterization of the fly ash contributes additionally to a better understanding of the ash formation processes.

3.2 Materials and methods

3.2.1 Origin of fly ash and filter cake

The three MSWI plants have similar flue gas cleaning systems built of boiler, electrostatic precipitator (ESP), flue gas scrubber, catalyst and chimney. Fly ash is only composed of boiler- and ESP ash and additional residuals from the flue gas cleaning process are removed separately (e.g. dioxin, mercury). Plant A produces 6.5 t/d fly ash that is neutrally leached using water from the last step of the water treatment process with an initial pH of 7.9-9.5 (process water). Neutral leaching is performed by mixing 0.35 t/h fly ash and 4 m^3/h process water with a pH of 10.8 after 1h of extraction (Table 3-1). Plant B produces 7 t/d fly ash that is treated using the scrub water from the wet flue gas cleaning process. This acidic fly ash leaching (FLUWA process) is performed in a two-stage extraction cascade using 7 t/h fly ash and 10 m^3/h of a mix of acidic and neutral scrub water. The reac-

tion of fly ash and scrub water in the first extraction tank result in a pH of 2.5-3.2 at 60°C after 20 minutes. The second extraction tank is used for reaction stabilization and the pH-value increases to 5.5 at 55°C after 40 minutes. A pH >4 is required in the last extraction tank for smooth vacuum belt filtration. This is achieved by varying the fly ash/scrub water ratio or if necessary by the addition of lime or sodium hydroxide. Plant C produces 8 t/d fly ash and together with the fly ash from another Swiss plant, the mixture is treated by acidic leaching. The acidic fly ash leaching at plant C is performed with the addition of hydrogen peroxide 35% (40 L/t fly ash) in a three-stage extraction cascade (optimized FLUWA process). In a first extraction tank 1 t/h fly ash and 3.5 m^3/h of a mix of acidic and neutral scrub water are extracted and a pH of 4.2 is adjusted after 30 minutes of extraction. The ash slurry is further transferred into a second and third extraction tank to stabilize the reaction before filtration. The metalliferous filtrate is used for direct metal recovery by solvent extraction and zinc electrowinning (FLUREC).

Table 3-1: *Technical details of investigated MSWI plants.*

Parameter	Plant A	Plant B	Plant C
Type of furnace	2x reciprocating grate	1x moving grate and 1x reciprocating grate	4x reciprocating grate
Produced fly ash (t/day)	6.5	7	8
Fly ash leaching type	Neutral leaching	Acidic leaching (FLUWA process)	Optimized acidic leaching (optimized FLUWA process)
Volumes	Fly ash: 0.35 t/h Process water: 4 m^3/h	Fly ash: 7 t/h Scrub water: 10 m^3/h Deion. water: 2.5 m^3/h (filtration)	Fly ash: 1 t/h Scrub water: 3.5 m^3/h H_2O_2 (35%): 40 L/t fly ash Deion. water: 0.7 m^3/h (filtration)
LS ratio	11.4	1.4	3.5
pH process-/scrub water	pH 7.9-9.5	pH <1	pH <1
Extraction time	60 minutes	20 minutes per tank	25 minutes per tank
Mass loss (wt.%)	5	13	32
pH of ash slurry	pH 10.8 (25°C)	Tank 1: pH 2.5-3.2 (60°C) Tank 2: pH 5.5 (55°C)	Tank 1: pH 2.5-3.5 (60°C) Tank 2: pH 4.2 (58°C) Tank 3: pH 4.8 (55°C)

3.2.2 Sampling and sample preparation

Heavy metal concentration in fly ash varies significantly, mainly depending on waste input and season. It has been shown that a sampling of fly ash and filter cake over three weeks (November/December 2013) is necessary for representative samples of each plant. Since there is a time lag between fly ash and filter cake production, still slightly different compositions may be achieved due to simultaneous sampling. Approximately 15 kg of fly ash and leached filter cake were collected from each plant. The fly ash samples were homogenized and split into 1 kg batches for further analyses. Half of the prepared material was dried at 105°C (chemical analysis) and the other half at 40°C (mineralogical analysis).

The fly ashes, present as fine powders (ca. 0.1 mm), were ground to a particle size <0.01 mm in a tungsten-carbide disk mill. The filter cake samples were wet and compacted and thus less homogeneous. Before splitting to 1 kg, the material was therefore crushed with a mortar and two aliquots were dried for several days at 40°C and 105°C, respectively, to constant mass before final grinding.

3.2.3 Chemical analysis

Elemental composition of the fly ashes and filter cakes was determined by energy dispersive X-ray fluorescence analysis (ED-XRF) using a Spectro Xepos spectrometer with matrix adjusted calibration. The measurements were performed on pressed powder pellets (32 mm diameter) using 4.0 g material <0.01 mm and 0.9 g Hoechstwax as binder. For quality control, ten replicates (precision) of fly ash C were measured and accuracy was verified by analyzing the standard reference material BCR 176R (Held et al., 2007). Elements of special interest (Al, Ca, Cd, Cu, Fe, Mg, Na, Pb, Ti, Zn) were further analyzed by inductively coupled plasma optical emission spectroscopy (ICP-OES, Varian 720-ES) after total digestion (TD) with a mixture of nitric acid and hydrofluoric acid in a high pressure microwave system (MLS Ethos Plus). The ED-XRF results of ten replicates show a good reproducibility for fly ash C with relative standard deviations (RSD) <2% for Cu, Zn, Cd, Sb, Pb, Br, Sn, Ba, <5% for Al, Si, S, Cl, Ca, Ti, Mn, Fe, Cr, Sr and <10% for K, Na, Mg. Accuracy for the standard reference material BCR 176R within ±10% for the certified elements Cd, Cu, Fe, Pb, Sb, Zn are achieved by ED-XRF. The results by TD-ICP-OES reveals erroneous quantifications from ED-XRF for Al, Mg and Na due to matrix interferences (metallic Al^0) and low sensitivity of the ED-XRF at low energy (Mg, Na). The results of the TD-ICP-OES analyses were therefore preferred.

The process and scrub water samples were analyzed by ICP-OES with analytical errors of ±5% for all elements except Na, K, Ca, Sb, and S that show ±10% error based on multiple measurements of certified standard solutions (ICP Multi-element Standard CertiPur IV and X, Merck). Moreover, the major anions (F^-, Cl^-, Br^-, and SO_4^{2-}) were analyzed in the scrub and process water by ion chromatography (IC) using a Metrohm 850 Professional IC system (columns: Metrosep A Supp 7 - 250/4.0 and Metrosep C 4-150/4.0). The analytical error based on multiple measurements of certified standard solutions (AccuSPEC Standard SCP Science, Fluka/Sigma-Aldrich) was ±5%.

3.2.4 X-ray diffraction analysis

Fly ash and filter cake samples (dried at 40°C) were mixed with 20 wt.% griceite (internal standard) and ground for 10 minutes (<0.01 mm). Disorientated samples were measured using a PANalytical X'Pert Pro diffractometer (CuKα-radiation) from 5-60° 2Theta at 0.017°/step, an acceleration voltage of 40kV and an electron generating current of 40 mA for 8 h. Identification of mineral phases as well as their structural analyses was done by Rietveld refinement using the PANalytical software "High-Score Plus". The absolute con-

tents of the mineral phases and the amorphous parts were calculated based on the internal standard.

3.2.5 SEM microscopy

The original fly ash and filter cake samples were impregnated with epoxy resin and polished (water-free). The specimens were coated with carbon to avoid surface charging for SEM analyses. A Zeiss EVO-50 XVP electron microscope (SEM) coupled with an EDAX Apollo X energy dispersive system (EDS) was used to perform rapid semi-quantitative chemical spot analyses. An accelerating voltage of 20 kV, high vacuum mode and a spot size of 504 nm were used for backscattered electron (BSE) images. Using an EDS system, interpretation and quantification are limited due to interferences of overlapping peaks such as the location of the major sulfur Kα peak (2.307 keV) and the lead M peak (2.342 keV).

3.2.6 Electron probe microanalysis

The known difficulty with the Pb/S discrimination by EDS was avoided by using a JEOL Model JXA-8200 electron microprobe equipped with five wavelength dispersive X-ray spectrometers (WDS) for select samples.

3.3 Results

3.3.1 Chemical composition

Fly ash

The major constituents in the three fly ash samples are Ca, Cl (>90'000 mg/kg), Na, K, Si, S (>40'000 mg/kg), Zn, Al, Fe, and Mg (>10'000 mg/kg) (Table 3-2). Heavy metals with a high vapour pressure and a low boiling point such as Zn, Pb and Cd are highly enriched in the fly ash as shown in previous studies (Le Forestier and Libourel, 1998; Li et al., 2004; Bayuseno and Schmahl, 2011). A comparison of the three samples shows small differences in concentration of major constituents such as Ca, Cl, Na, K, Si or S and a considerable variability of the heavy metal concentrations among fly ashes. Fly ash B and C have elevated Zn concentrations >40'000 mg/kg compared to fly ash A (26'770 mg/kg). Fly ash C has further a slightly elevated concentration of the highly volatile Pb (12'055 mg/kg) whereas fly ash A has an elevated Cu concentration (3'901 mg/kg) compared to the other two ashes.

Extraction agent and leached filter cake

The process water used for neutral leaching at plant A shows elevated concentrations of Ca (4'118 mg/L) and Cl (8'133 mg/L) (Table 3-2). The scrub waters from the wet flue gas cleaning of plant B and C are heavily enriched in Na (>10'000 mg/L) and Cl (>40'000

mg/L) and show elevated values for Ba (>1'000 mg/L). The sulphur concentration of the scrub water at plant C (8'365 mg/L) is twice the concentration of plant B (4'582 mg/L). During neutral fly ash leaching significant amounts of water soluble phases are dissolved and the remaining filter cake A is depleted in Na (19'200 mg/kg), K (15'480 mg/kg) and Cl (30'040 mg/kg) (Table 3-2). Acidic fly ash leaching (filter cake B and C) shows an even higher dissolution of Na, K and Cl (≤10'000 mg/kg remaining). As a consequence of the mass loss (Table 3-1), most of the remaining elements show higher weight percentages in the filter cake even though they are partly extracted during fly ash leaching.

Table 3-2: *Chemical composition of fly ash and filter cake determined by ED-XRF and process-/scrub water used for fly ash leaching and analyzed by ICP-OES and IC.*

	Fly ash mg/kg			**Filter cake** mg/kg			**Process/Scrub-water** mg/L		
	A	**B**	**C**	**A**	**B**	**C**	**A**	**B**	**C**
Al*	36'300	37'900	31'750	41'300	43'700	35'900	0.2	1	10
Ba	1'711	2'901	1'856	1'875	3'359	2'406	n.d	n.d	n.d
Br	3'563	2'798	3'700	1'293	257	228	151	1'548	1'320
Ca	191'500	168'900	151'150	193'400	199'300	178'700	4'118	138	158
Cd	227	264	355	262	139	39	<0.1	0.1	1
Cl	106'900	97'050	103'010	30'040	8'268	6'834	8'133	44'583	55'780
Cr	650	676	486	707	789	655	n.d	n.d	n.d
Cu	3'901	2'573	2'544	4'292	2'738	2'360	<0.1	0.2	5
Fe	19'120	21'610	20'635	17'420	22'500	25'810	<0.1	0.2	13
K	45'250	45'940	46'930	15'480	8'146	6'208	510	13	228
Mg*	14'025	15'090	13'598	15'151	14'092	9'958	32	22	43
Mn	761	806	762	771	845	699	<0.1	0.1	1
Na*	43'100	46'300	48'800	19'200	10'100	7'390	589	11'836	10'418
Pb	9'540	9'108	12'055	10'400	9'469	6'810	<0.1	0.3	24
Sb	3'037	2'428	2'935	2'997	2'585	3'936	<0.1	1	7
Si	83'100	83'090	69'490	68'810	78'800	77'920	4	38	49
Sn	1'463	1'334	1'644	1'566	1'479	2'251	1	1	7
Sr	542	425	346	618	464	386	n.d	n.d	n.d
Ti	10'120	10'010	8'908	10'230	11'350	11'150	<0.1	0.1	1
Zn	26'770	48'190	65'170	28'940	32'570	25'350	0.1	5	287
S	59'030	47'610	56'750	65'270	79'150	108'700	313	4'582	8'365

*Determined by TD-ICP-OES

3.3.3 Mineralogical composition

Fly ash

XRD Rietveld analyses of the three fly ashes show only minor differences in the main mineralogical composition. The samples contain ca. 40 wt.% crystalline phases and are dominated by the melilith-group mineral gehlenite ($Ca_2Al_2SiO_7$, 13-14 wt.%, Table 3-3, Figure 3-1). Calcite ($CaCO_3$) is readily identified and especially fly ash B has an elevated calcite concentration (5 wt.%). Lime (CaO) in its crystalline form is only found in concentrations <1 wt.%. However, it is assumed that a significant amount of lime is present in a non-crystalline form due to the enormous Ca concentration of fly ashes and the preferred formation of CaO during combustion. Highly soluble sodium and potassium salts such as halite (NaCl) and sylvite (KCl) are frequent in all three fly ashes. Potassium-zinc-chloride (K_2ZnCl_4) occurs in fly ash B and C and the concentrations (6 and 9 wt.%) are in good agreement with previous studies (Eighmy et al., 1995; Bayuseno and Schmahl, 2011). Anhydrite ($CaSO_4$) is the dominant sulphate mineral (7 wt.%) whereas sulphate hemihydrates (e.g. bassanite, $CaSO_4 \cdot 0.5H_2O$) are only rarely present. The quantification of trace minerals (<1 wt.%) is very difficult due to the complexity of the mineralogy and thus possible peak overlaps. The high amount of amorphous content (>50 wt.%) is clearly visible by a background bump between 20-40° 2Theta.

Table 3-3: *Main mineralogy (wt.%) of fly ash and leached filter cake determined by XRD and Rietveld refinement.*

Mineral phase	Abbr.	Formula	Fly ash (wt.%)			Filter cake (wt.%)		
			A	B	C	A	B	C
Silicates								
Quartz	Qz	SiO_2	<1	1	1	1	2	2
Gehlenite	Ge	$Ca_2Al_2SiO_7$	14	13	13	9	4	1
Oxides								
Hematite	He	Fe_2O_3	<1	<1	<1	<1	<1	<1
Lime	Li	CaO	<1	1	1	n.d.	n.d.	n.d.
Carbonates								
Calcite	Ca	$CaCO_3$	2	5	2	5	5	1
Chlorides								
Halite	Ha	NaCl	6	6	6	1	<1	<1
Sylvite	Sy	KCl	2	<1	<1	1	<1	<1
K-Zn-Chloride	Kc	K_2ZnCl_4	n.d.	6	9	n.d.	n.d.	n.d.
Sulphates								
Anhydrite	An	$CaSO_4$	7	7	7	3	6	12
Bassanite	Ba	$CaSO_4 \cdot 0.5H_2O$	<1	n.d.	n.d.	n.d.	n.d.	n.d.
Ettringite	Et	$Ca_6Al_2(OH)_{12}(SO_4)_3 \cdot 26H_2O$	n.d.	n.d.	n.d.	1	6	n.d.
Gypsum	Gy	$CaSO_4 \cdot 2H_2O$	n.d.	n.d.	n.d.	6	7	11
Amorphous portion			67	59	60	71	69	72

Filter cake

Despite the different agents used for fly ash leaching, the mineralogical composition of the filter cakes is rather homogeneous. The neutrally leached filter cake A is depleted in gehlenite (40% dissolved) and soluble chlorides (Table 3-3, Figure 3-1). Acidic leaching causes dissolution of gehlenite of 70% (filter cake B) up to 100% (filter cake C) and the total dissolution of the chlorides halite, sylvite and K_2ZnCl_4. An increased concentration of calcite is determined in filter cake A whereas filter cake B and C have similar concentrations as the untreated fly ash. Half of the anhydrite is removed in filter cake A whereas the anhydrite concentration stays constant (filter cake B) or increases (filter cake C) after acidic leaching. The mineralogical alteration is dominated by the formation of gypsum ($CaSO_4 \cdot 2H_2O$) and concentrations up to 12 wt.% are determined (filter cake C). Filter cake A and B additionally show 1 wt.% and 6 wt.% ettringite ($Ca_6Al_2(OH)_{12}(SO_4)_3 \cdot 26H_2O$). The dissolution of soluble phases leads to an increase of the relative content of insoluble minerals and thus an increase in amorphous phases (ca. 70 wt.%) in the leached filter cakes.

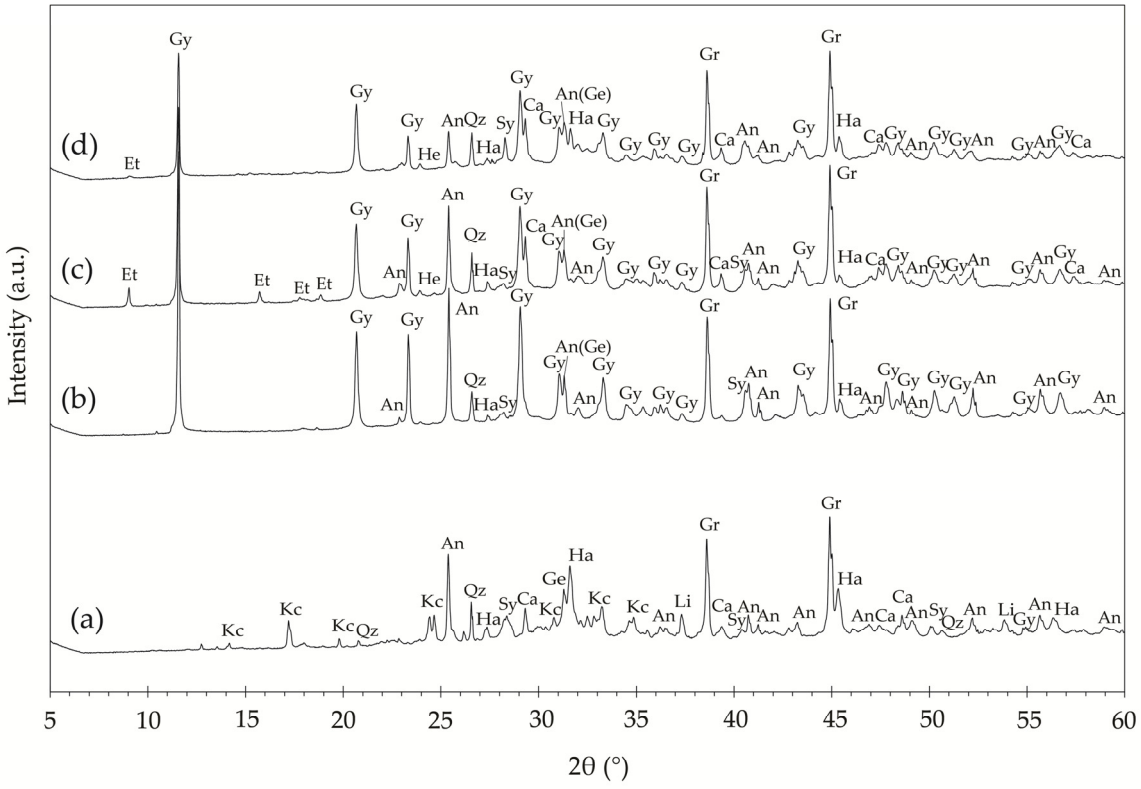

Figure 3-1: *XRD powder patterns of (a) fly ash A, (b) filter cake C, (c) filter cake B and (d) filter cake A. The peaks are labelled: An (anhydrite), Ca (calcite), Et (ettringite), Ge (gehlenite), Gr (griceite, internal standard), Gy (gypsum), Ha (halite), He (hematite), Kc (potassium-zinc-chloride), Li (lime), Sy (sylvite), Qz (quartz).*

3.3.4 Morphology and particle chemistry

Fly ash

Information about morphological features and phase associations as a framework for the data obtained from XRD was achieved by analyzing epoxy-embedded specimens of fly ashes and filter cakes using backscattered electron images (BSE) and energy dispersive X-ray spectroscopy (EDS). Fly ash A is characterized through particles in the range from 20 to 200 μm in diameter with many elongate shapes (Figure 3-2). Fly ash B is characterized by large and well-rounded particles in the range from 100 to 400 μm in diameter and fly ash C has a more bimodal particle distribution with two groups between 20-100 μm and 200-400 μm in diameter (Figure 3-2).

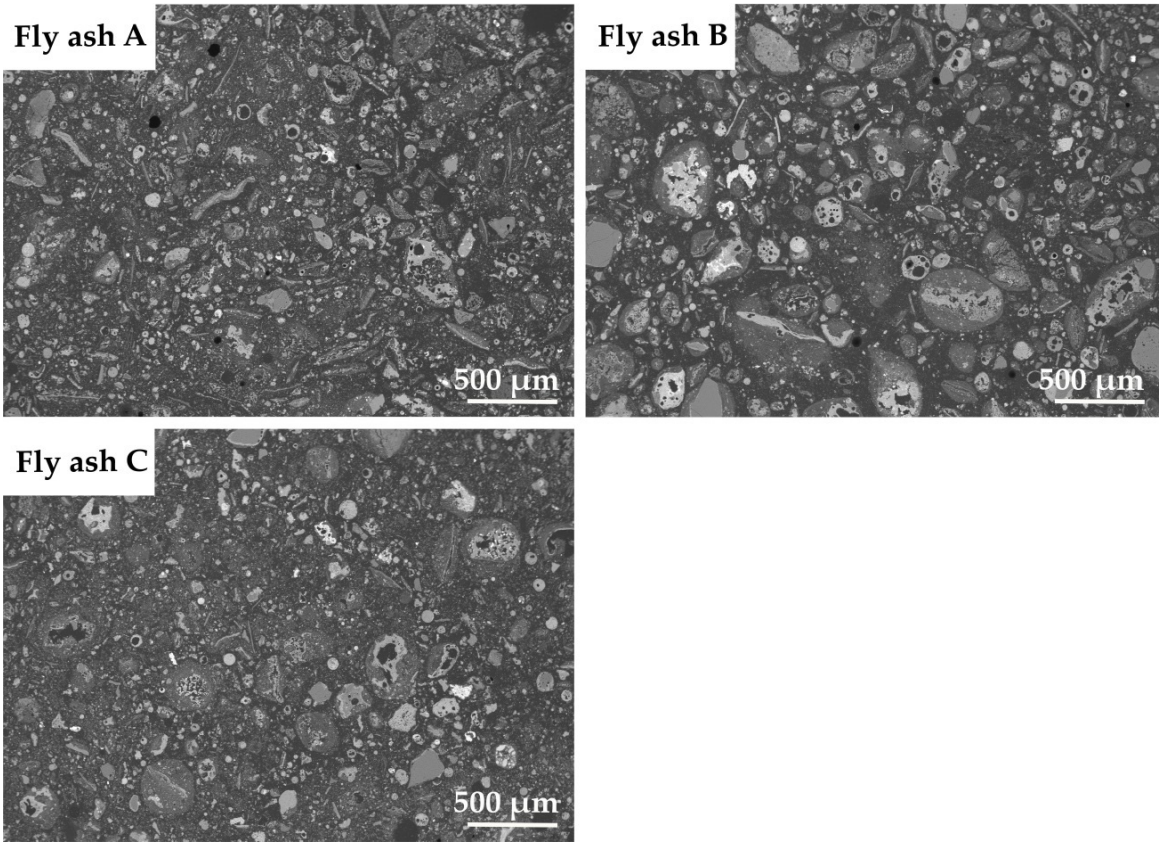

Figure 3-2: *Backscattered electron (BSE) images of epoxy-embedded specimens of the three fly ashes.*

Remaining carbon particles, quartz fragments and hollow glassy cenospheres account for the major part of the larger-size particles. Ca-rich elongated and porous feldspar-type aluminosilicates (Al/Si ratio 1:3) that belong to the plagioclase anorthite ($Ca[Al_2Si_2O_8]$) are very common in fly ash A and C (Table 3-4). Gehlenite ($Ca_2Al_2SiO_7$) is determined as dominant Ca-Al-silicate by XRD (Table 3-3) with an Al/Si ratio of 2:1 and twice the Ca-concentration compared to the Ca-feldspar. Surprisingly, no particles >20 μm with a composition close to gehlenite could be identified by SEM-EDS. Oval particles (>200 μm) of calcite ($CaCO_3$) and lime (CaO) are frequently present together with calcium silicates

close to the composition of wollastonite ($CaSiO_3$, Table 3-4). The wollastonite-like phases appear as rounded dense or porous particles with a size range of 50-100 µm and that have commonly metal-bearing phases incorporated. Beside anhydrite, complex sulphate phases with compositions close to omongwaite ($Na_2Ca_5(SO_4)_6 \cdot 3H_2O$), syngenite ($K_2Ca(SO_4)_2 \cdot (H_2O)$) or gorgeyite ($K_2Ca_5(SO_4)_6 \cdot H_2O$) are frequent in all fly ashes. Beside individual mineral particles there are aggregates of minerals and metals present with quartz or quartz and feldspar in the cores (Figure 3-4). Wollastonite ($CaSiO_3$) and glasses generally surround the core grains. In most cases larger metallic Fe-fragments and finely distributed Cu- and Zn-bearing phases are incorporated within wollastonite and glassy matrix.

A very fine-grained (<1 µm) dust rim is usually accumulated around minerals, phase aggregates or glassy cenospheres (Figure 3-3a). EDS spot analyses of these dust rims show an elevated concentration of volatile elements such as Na, S, Cl and K for the three fly ashes (Figure 3-3a). The dust rims of fly ash B and C additionally contain 10-15% Zn what is related to the high total Zn concentrations. Fly ash B has very thick and compact dust rims around the particles whereas fly ash A and C have less pronounced rims and additionally abundant fine grained dust distributed loosely between larger particles.

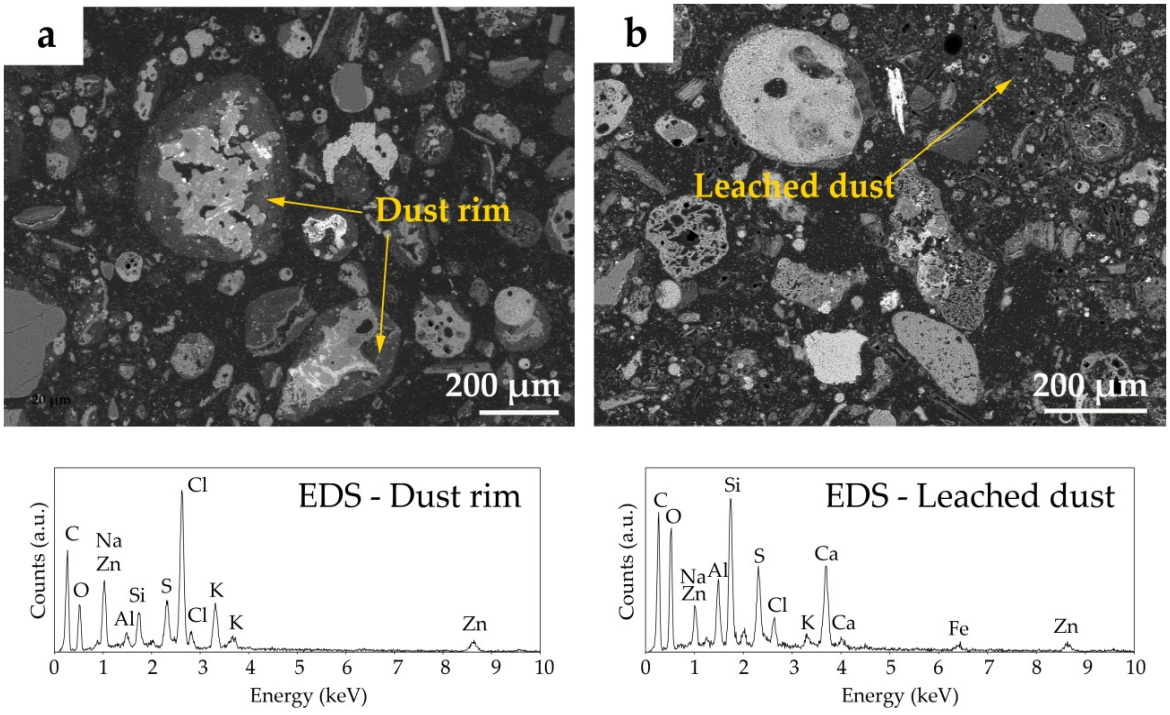

***Figure 3-3**: Backscattered electron (BSE) images of epoxy-embedded specimens of fly ash and filter cake B with EDS spectra of the dust rim before and after leaching. (a) Compact dust rims around larger particles enriched in Na, K, Cl, Si, Al, Zn, and (b) dust re-arranged after leaching and depleted in soluble elements such as Na, K, Cl.*

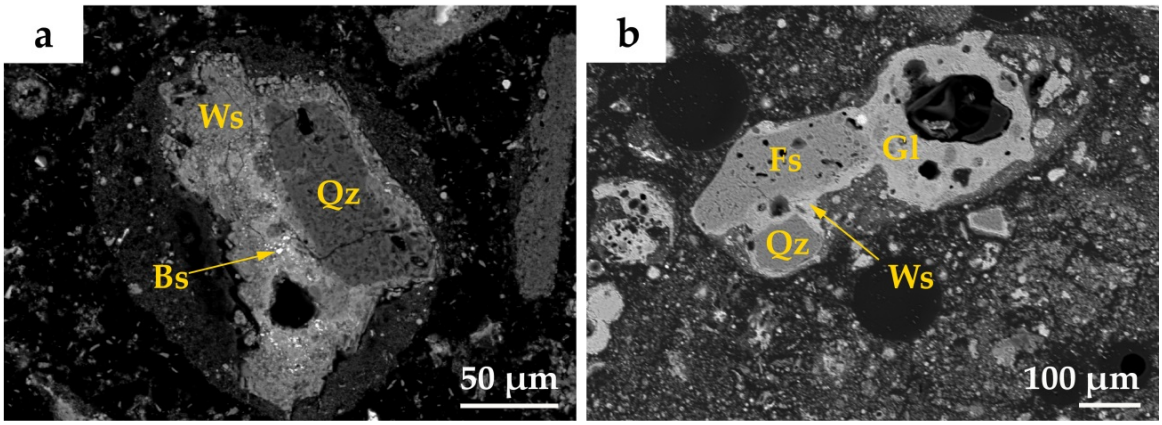

***Figure 3-4**: Backscattered electron (BSE) images of typical phase aggregates in (a) fly ash C and (b) fly ash A: Bs (brass, $Cu_{0.6}Zn_{0.4}$), Fs (feldspar), Gl (glass), Qz (quartz), Ws (wollastonite).*

***Table 3-4**: Main mineral phases (particles >20 µm) and the relative quantities in fly ash and filter cake identified by SEM-EDS (+ rare; ++ frequent; +++ very frequent).*

Main mineral phases		Fly ash			Filter cake		
		A	B	C	A	B	C
Silicates							
Quartz	SiO_2	+	+	++	++	++	++
Anorthite	$Ca[Al_2Si_2O_8]$	++	n.d.	++	+++	++	++
Albite	$Na[AlSi_3O_8]$	+	n.d.	+	+	+	+
Orthoclase	$K[AlSi_3O_8]$	+	n.d.	+	++	+	++
Oxides							
Lime	CaO	+	+	+	n.d.	n.d.	n.d.
Carbonates							
Calcite	$CaCO_3$	+	++	+	+++	++	+
Chlorides							
Halite	NaCl	+	+	+	n.d.	n.d.	n.d.
Sylvite	KCl	++	+	+	n.d.	n.d.	n.d.
Sulphates							
Anhydrite	$CaSO_4$	++	++	++	n.d.	n.d.	n.d.
Gypsum	$CaSO_4{\cdot}2H_2O$	n.d.	n.d.	n.d.	++	++	+++
Syngenite	$K_2Ca_5(SO_4)_6{\cdot}H_2O$	+	+	+	n.d.	n.d.	n.d.
Omongwaite	$Na_2Ca_5(SO_4)_6{\cdot}3H_2O$	++	+	++	n.d.	n.d.	n.d.
Calcium silicates							
Wollastonite	$CaSiO_3$	+	+	++	n.d.	n.d.	n.d.
Monticellite	$CaMgSiO_4$	+	n.d.	+	n.d.	n.d.	n.d.
Glass		++	++	++	+++	+++	+++

Filter cake

The depleted filter cakes are relatively enriched in resistant glasses and refractory minerals such as quartz and feldspars. The neutrally leached filter cake A is enriched in mainly the Ca-rich plagioclase anorthite and contains numerous newly formed calcite particles >20 µm which is consistent with results determined by XRD. The newly formed gypsum is predominantly present in filter cake C as clearly visible large crystals (Figure 3-5). The fine-grained dust rim which covers larger particles in the untreated fly ashes is rearranged after leaching (Figure 3-3b). Large particles have no durst rim anymore and fine dust is present loosely between larger particles or forms clusters up to 200 µm in the filter cakes (Figure 3-5). These nests are intersected by fine gypsum crystals and due to interaction with extracting agent the dust is depleted in soluble components such as Na, S, Cl and Zn and enriched in Ca and Si (Figure 3-3b).

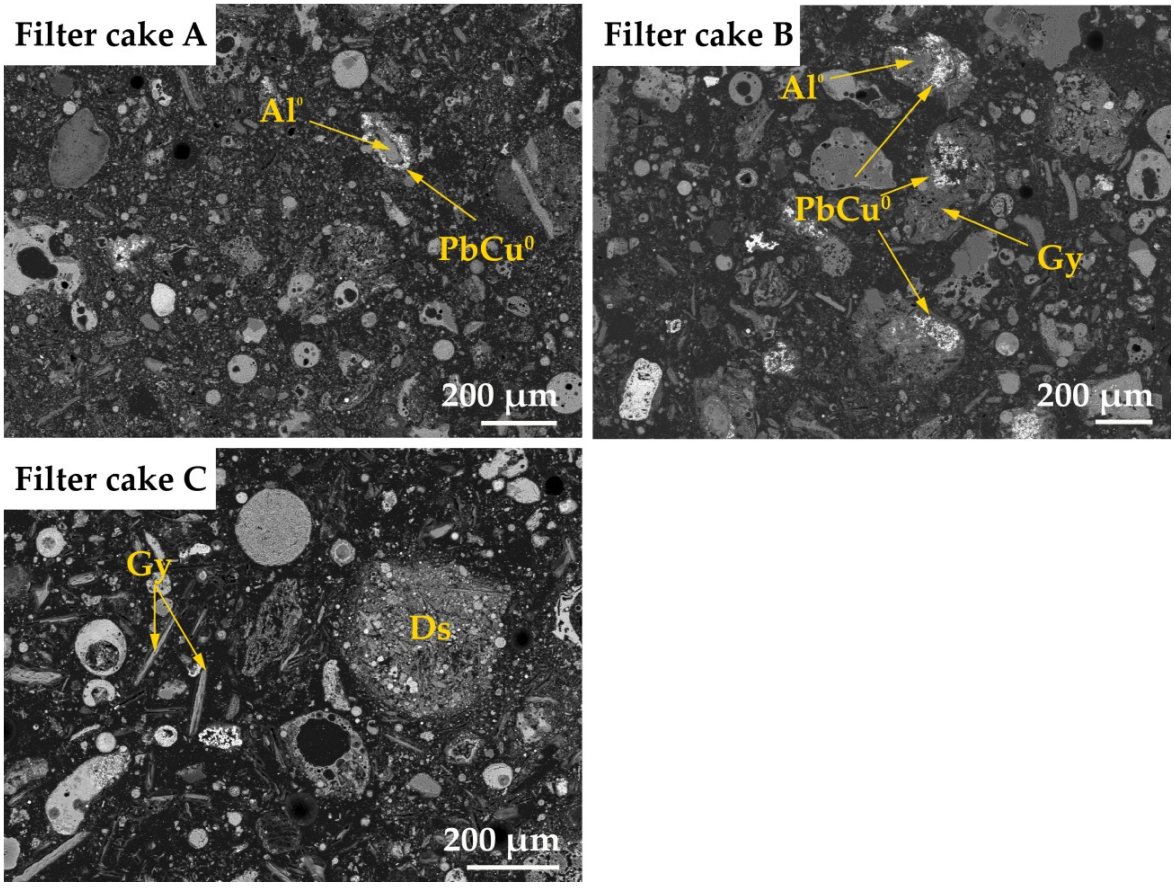

Figure 3-5: *Backscattered electron (BSE) images of the filter cakes A, B and C. (Filter cake A) Cementation phase ($PbCu^0$) around Al^0, (filter cake B) High amount of $PbCu^0$-alloy-phase surrounded by newly formed gypsum (Gy), (filter cake C) large amounts of gypsum crystals and clusters of newly-arranged leached dust (Ds).*

3.3.5 Metal-bearing phases and their associated particles

Fly ash

Fe-bearing phases are the most commonly found metal-containing components in fly ash (Table 3-5). Iron is present as spheres of Fe-oxide mixed with Ca-silicates showing a characteristic segregation texture (Figure 3-6a) and a composition close to hematite (Fe_2O_3) or magnetite (Fe_3O_4). Similar mixed Fe-oxide/alumino-silicate spheres with various textures have also been found in coal fly ashes by Kutchko and Kim (2006). Aluminium is mostly present in its metallic form as large particles up to 400 μm with a composition of 85 wt.% Al and 15 wt.% Si. The alloy brass made of copper and zinc is frequently found in the proportions of 60% Cu and 40% Zn ($Cu_{0.6}Zn_{0.4}$) in fly ash C (Figure 3-6b). Fly ash B and C contain potassium-zinc-chloride (K_2ZnCl_4) which is generally accompanied by halite crystals (Figure 3-6c). It is the only metal-bearing phase that has also been identified by XRD (Table 3-3). In general zinc has the tendency to accumulate within the entire ash matrix, especially observed in fly ash C. This may be the reason why fly ash C contains several Zn-phases whose chemical composition cannot be associated to known mineral phases (Table 3-5). Lead is mostly found as Pb-bearing sulphate showing a Pb:S ratio of 4:1 up to 7:1 with K, Na and Cl as minor elements (Figure 3-6d). The major sulfur Kα peak (2.307 keV) is located very close to the position of the lead M peak (2.342 keV) in EDS analysis and this may cause an erroneous quantification of sulphur. The existence of sulphur (similar Pb:S ratios) was therefore verified using electron probe microanalysis (wavelength-dispersive detector) as has also been shown by Sandell et al. (1996). It seems that Pb in all three fly ashes is predominantly present as sulphates close to the composition of anglesite ($PbSO_4$), palmierite ($(K,Na)_2Pb(SO_4)_2$) or caracolite ($Na_3Pb_2(SO_4)_3Cl$) (Figure 3-6d). Copper is mainly present as brass in all ashes and to a minor extend as tenorite (CuO) or cuprite (Cu_2O; Figure 3-6e) and in its metallic form Cu^0. No Cd-bearing phases were identified by SEM-EDS and a more detailed study or higher resolution techniques are required to get information about phase associations.

Essential for the understanding of the leaching processes is not only the binding form of metals but also the type of particles they are enclosed in (host particles). During extraction, these particles have to be dissolved for mobilization of the metals and their chemistry is therefore of importance. Ca-silicates such as wollastonite ($CaSiO_2$) are the most prominent host particles for zinc. Brass ($Cu_{0.6}Zn_{0.4}$) is often incorporated in such Ca-silicates (Figure 3-6b) or finely distributed within the ash matrix (1-5 μm). Metals together with soluble chlorides (halite, sylvite) are only found in the case of K_2ZnCl_4 in fly ash B and C (Figure 3-6c). Pb-bearing phases are almost entirely associated with sulphates (anhydrite, syngenite) and present as inclusions within the porous sulphate host particle (Figure 3-6d). Metallic Cu^0 and Cu-oxides are associated with Ca-silicate and sulphate host particles (Figure 3-6e). Metal-bearing phases <2 μm that are diffusely distributed in the fly ash and filter cake matrix cannot be identified optically at the given instrumental conditions.

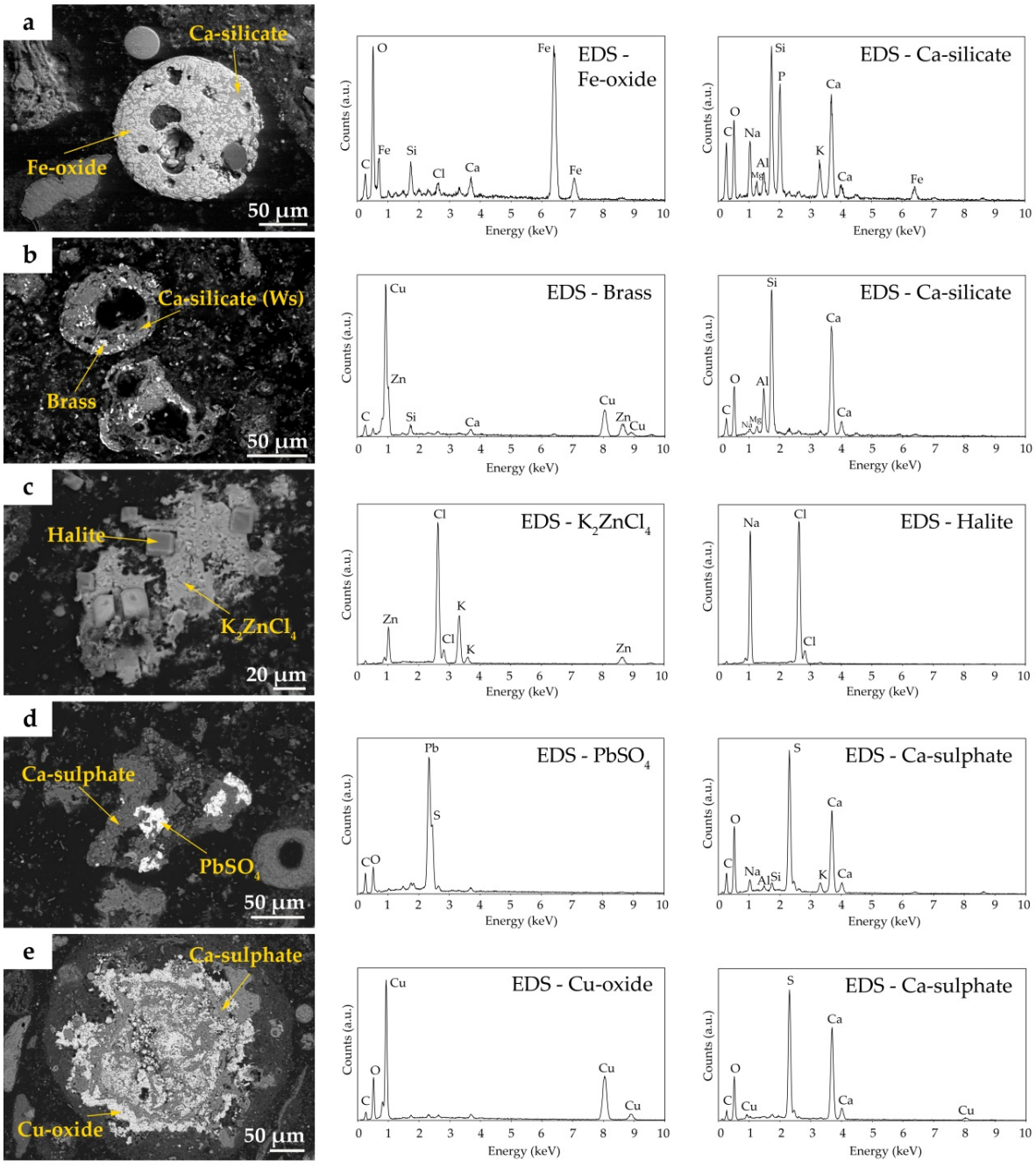

***Figure 3-6**: Backscattered electron (BSE) images with elemental spectra of typical metal-bearing phases and their host particles in fly ash: (a) Fe-oxide rich Ca-Si-sphere in fly ash C, (b) brass incorporated in Ca-silicate particle close to the composition of wollastonite (Ws) in fly ash C, (c) K_2ZnCl_4 together with halite in fly ash C, (d) Pb-bearing sulphate inclusion in Ca-sulphate host particle in fly ash C, and (e) Cu-oxide incorporated in Ca-sulphate in fly ash B.*

Filter cake

Compared to the untreated fly ashes, significantly less metal-bearing phases are identified in the filter cakes. The amount of Fe-spheres is considerably reduced (Table 3-5). Metallic Al^0 as frequently found in the untreated fly ashes is still present in the same amount in filter cake A and B whereas filter cake C does not contain Al^0 anymore. Soluble metal-chlorides such as potassium-zinc-chloride (K_2ZnCl_4) are completely dissolved during leaching as well as the total amount of Pb-bearing sulphates. Brass ($Cu_{0.6}Zn_{0.4}$) incorporated in wollastonite-like Ca-silicates completely disappears after leaching and the few remaining brass particles are incorporated in newly formed gypsum crystals within the filter cake matrix. Due to the loss of soluble chlorides during leaching, Zn-bearing glasses which show a composition close to hemimorphite ($Zn_4Si_2O_7(OH)_2 \cdot 2H_2O$) are found in the filter cakes. The interaction of fly ash and the leaching agent leads to new phase formation at specific conditions. The most prominent secondary formed metal phase in filter cake A and B is an alloy of Pb and Cu with a molar ratio of Pb:Cu of ca. 3.5 accompanied by 10 wt.% Cl (Table 3-5, Figure 3-7). The newly formed $PbCu^0$-alloy-phase is found on the surface of metallic Al^0-particles in filter cake A and B (Figure 3-7a) and in case of filter cake B additionally surrounded by newly formed gypsum (Figure 3-7b). There is evidence for cotunnite ($PbCl_2$) in filter cake B and C because a Pb-bearing phase with up to 20% chlorine is identified by SEM-EDS.

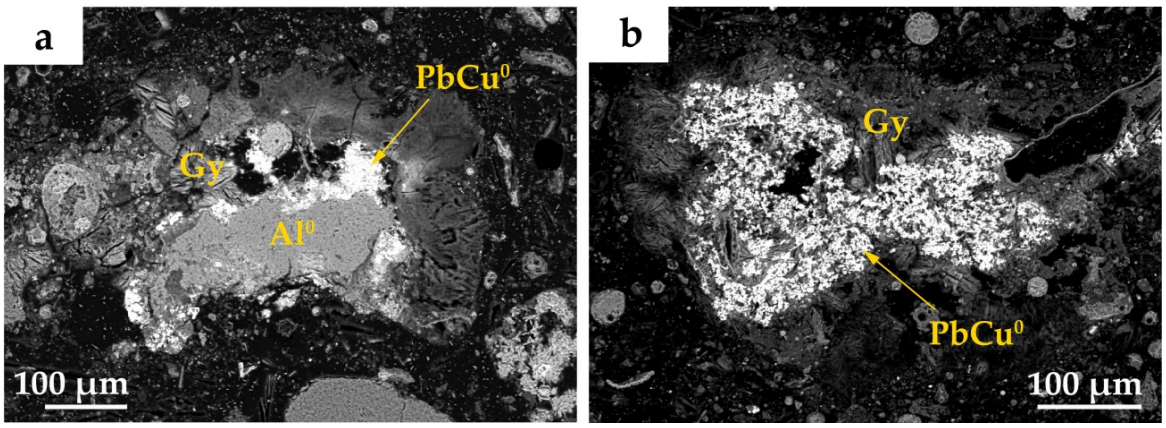

***Figure 3-7**: Backscattered electron (BSE) images of the $PbCu^0$-alloy-phase in filter cake B. (a) On the surface of Al^0, and (b) surrounded by newly formed gypsum (Gy).*

***Table 3-5**: Metal-bearing minerals and alloys in fly ash and filter cake determined by SEM-EDS (+ rare; ++ frequent; +++ very frequent).*

	Metal bearing phases	Formula or elemental distribution	Fly ash			Filter cake		
			A	B	C	A	B	C
Fe	**Oxides**							
	Hematite	Fe_2O_3	+++	+++	+++	++	++	++
	Magnetite	Fe_3O_4	+++	+++	+++	++	++	++
Al	**Metallic**							
	Al^0	Al (85 wt.%), Si (15 wt.%)	++	++	++	++	++	n.d.
Zn	**Silicates**							
	Hemimorphite	$Zn_4Si_2O_7(OH)_2 \cdot 2H_2O$	n.d.	n.d.	n.d.	+	+	+
	Oxides							
	Zincite	ZnO	+	n.d.	n.d.	+	+	+
	Chlorides							
	K-Zn-Chloride	K_2ZnCl_4	n.d.	+	+	n.d.	n.d.	n.d.
	Alloys							
	Brass	$Cu_{0.6}Zn_{0.4}$	+	+	+++	+	+	+
	Other commonly found phase compositions							
	Zn-K-S-phase	Zn (20 wt.%), K (15 wt.%), S (15 wt.%)	n.d.	n.d.	++	n.d.	n.d.	n.d.
	Zn-Ca-Mg-phase	Zn (45 wt.%), Ca (20 wt.%), Mg (5 wt.%)	n.d.	n.d.	+	n.d.	n.d.	n.d.
Pb	**Chlorides**							
	Cotunnite	$PbCl_2$	n.d.	n.d.	n.d.	n.d.	+	+
	Sulphates							
	Anglesite	$PbSO_4$	+	n.d.	+	n.d.	n.d.	n.d.
	Palmierite	$(K,Na)_2Pb(SO_4)_2$	++	+	+++	n.d.	n.d.	n.d.
	Caracolite	$Na_3Pb_2(SO_4)_3Cl$	++	+	+++	n.d.	n.d.	n.d.
	Alloys							
	$PbCu^0$	Pb (50 wt.%), Cu (15 wt.%), Cl (10 wt.%)	n.d.	n.d.	n.d.	++	+++	+
Cu	**Oxides**							
	Tenorite	CuO	+	+	n.d.	+	n.d.	n.d.
	Alloys/metallic							
	Brass	$Cu_{0.6}Zn_{0.4}$	+	+	+++	+	+	+
	$PbCu^0$	Pb (50 wt.%), Cu (15 wt.%), Cl (10 wt.%)	n.d.	n.d.	n.d.	++	+++	+
	Cu^0	Cu (>90 wt.%)	n.d.	n.d.	+	n.d.	n.d.	n.d.

3.4 Discussion

3.4.1 Composition of fly ashes and their formation processes

The waste composition, grate technology, residence time on the grate, oxygen flow and cooling time of the fly ash in the boiler mainly influence the particle morphology. During combustion, melting leads to the formation of glass and silicates which accumulate in the bottom ash or are transported as tiny melt droplets in the combustion flue gas. Hollow glassy cenospheres as a result of degassing and vitrification contribute, together with small dust particles, to the major part of the non-crystalline material (60 wt.%). Elements with a high vapour pressure and a low boiling point (Na, K, Cl, Zn, Pb, Cd) undergo volatilization and are transported together with unburnt carbon and light metallic particles such as brass and aluminium foil in the combustion flue gas. Decomposition of phases and solid-solid reactions occur on the grate and in the combustion chamber and new high-temperature phases are formed. The most abundant feldspar determined in the fly ash is the Ca-rich plagioclase anorthite. This observation is consistent with results from tests of ceramic firing (Cultrone et al., 2001) where plagioclase increases its Ca content with increasing temperature (more anorthite-like composition). Decomposition of carbonates starts at temperatures >700°C and calcite is fully transformed into burnt lime (CaO). During storage of the fly ash lime is reacting with humidity to form portlandite ($Ca(OH)_2$) and with atmospheric CO_2 to calcite (Equation 3-1).

$$CaO + H_2O \rightarrow Ca(OH)_2 \text{ and } Ca(OH)_2 + CO_2 \rightarrow CaCO_3 + H_2O \quad (3\text{-}1)$$

Wollastonite-like phases ($CaSiO_3$) and gehlenite ($Ca_2Al_2SiO_7$) appear at 800°C. Gehlenite starts to form by grain-boundary reaction between CaO, Al_2O_3 and SiO_2 (Cultrone et al., 2001). Lime is reacting with quartz fragments and aluminium from Al-foil particles, melt droplets (glass) or feldspar fragments to form gehlenite in the hot flue gas. The fact that a significant concentration of crystalline gehlenite is detected by XRD but no particles are identified by SEM-EDS indicates that gehlenite occurs very finely distributed as tiny crystals within the ash matrix. The residence time in the combustion chamber seems too short to form larger crystals recognizable by SEM. Wollastonite is preferentially formed at the carbonate-quartz boundary (Equation 3-2).

$$CaCO_3 + SiO_2 \rightarrow CaSiO_3 + CO_2 \quad (3\text{-}2)$$

Such solid-solid reactions between particles transported in the flue gas lead to the formation of complex phase aggregates as shown in Figure 3-4. Small refractory mineral fragments of quartz and feldspar pass the combustion process without showing melting or recrystallization and often act as nuclei for the formation of mineral aggregates with newly formed calcium silicate phases in the hot flue gas. Often associated with high temperature phases are Fe-fragments and brass ($Cu_{0.6}Zn_{0.4}$) that are carried along with the flue gas and trapped in mineral aggregates. Brass has a relatively low melting point of

900-920°C which further decreases with increasing zinc concentration (Deutsches Kupferinstitut, 2007). Despite the low melting point, the constant Cu-Zn ratio indicates that brass is transported as fine solid particle from the waste into the flue gas during combustion without chemical transformation. During flue gas cooling, volatile elements such as Zn, Na, S, Cl, K condensate on the surface of larger particles as shown by a characteristic enriched dust rim in Figure 3-3a. The thick and compact dust rims of fly ash B are a result of larger quantities of fine dust in the flue gas due to a different grate technology (moving grate), higher temperatures or longer residence time on the grate compared to plant A and C. Fine dust particles in the flue gas act as carriers for condensable heavy metals shown by the 10-15 wt.% Zn accumulated in the dust rims of fly ash from plant B and C. Apart from Zn, the chemical composition of this fine dust rim is similar in all fly ashes, indicating that the condensation on dust particles for most elements is independent of waste input and operating conditions. The elevated concentration of Cl in all fly ashes (10 wt.%) originates mostly from the combustion of plastics (PVC). Most of the chlorides are accumulated finely distributed in the ash matrix and in the dust rims (Figure 3-4). An elevated chlorine and alkali metal concentrations in the flue gas provide the basis for the formation of Cl-metal complexes such as potassium-zinc-chloride (K_2ZnCl_4) during cooling of the flue gas or even during storage. Increasing chlorine content forces the vaporisation of heavy metals with higher vapour pressures in form of chloride complexes (Jakob et al., 1996; Verhulst and Buekens, 1996; Morf et al., 2000). Zinc is also bound to silicates due to its high affinity for silicate melts as analyses of bottom ashes have shown (Traber et al., 2002). Lead is predominantly transferred to the gas phase due to its low melting point (327.5°C). The chalcophile association between lead and sulphur is the reason for the abundant occurrence of complex Pb-sulphates in fly ashes.

3.4.2 Phase dissolution and new phase formation during fly ash leaching

Factors controlling heavy metal mobilization during fly ash leaching are pH-value of leaching agent, reaction pH of ash slurry, redox conditions, liquid to solid ratio (LS), temperature and reaction time. Variations of these parameters during plant operation affect mineralogy and depletion factors of heavy metals.

3.4.3 Neutral leaching

The neutral fly ash leaching at plant A is performed using process water (pH 7.9-9.5) and a LS ratio of 11.4. Initially, highly soluble alkali salts (NaCl, KCl) dissolve and only small amounts of chlorides remain in the filter cake (Table 3-3, Figure 3-8). The leaching of these species is availability-controlled and the accessible amount is immediately dissolved with little influence of pH-value (Eighmy et al., 1995; Sabbas et al., 2003; Quina et al., 2009). The interaction of fly ash with extraction agent dissolves the fine dust rims around larger ash particles and the accumulated Na, K and Cl are dissolved (Figure 3-3b). The formation of clusters of such leached dust (Figure 3-5) may be due to filtration or

sample preparation artefacts (epoxy-embedded specimen). A total mass loss of 5 wt.% during leaching is determined using fairly immobile elements Ba, Cr, Sb, Sn and Ti for normalization. These inert elements are not extractable under the present conditions and therefore accumulate in the filter cake. The specific enrichment of all other elements is corrected with the calculated mass loss. A pH-value of 10.8 after 60 minutes of neutral leaching implies a high buffering capacity of fly ash. Calcite ($CaCO_3$) and lime (CaO) contribute significantly to the highly alkaline nature of fly ash. Calcite is able to buffer the system in pure water to a pH-value of 8.42 at 25°C and at equilibrium with the atmosphere (Stumm and Morgan, 1996). The hydration of lime during leaching leads to the formation of portlandite ($Ca(OH)_2$) and this adjusts the pH at a value of 10.8 as has been shown in studies of the leaching behaviour of bottom ash (Comans and Meima, 1994; Johnson et al., 1995; Sabbas et al., 2003; Bayuseno and Schmahl, 2011). Other earth alkali metal hydroxides and aluminosilicates such as anorthite and gehlenite may additionally buffer the solution, although to a minor degree due to slower kinetics compared to carbonates and lime/portlandite. The partial dissolution of gehlenite ($Ca_2Al_2SiO_7$) supports the assumption that very small crystal size enhances its dissolution. The main contribution to calcium originates from the dissolution of calcite, portlandite and sulphates such as syngenite ($K_2Ca_5(SO_4)_6 \cdot H_2O$). The alkaline condition favours the re-precipitation of carbonates as shown by the frequent occurrence of newly-formed calcite particles in filter cake A. Formation of gypsum ($CaSO_4 \cdot 2H_2O$) is mainly the product of anhydrite hydration and rarely new precipitation. Almost no depletion for Fe, Al, Zn, Pb, Cu and Cd is achieved by performing neutral leaching (Figure 3-8). Iron is present in fly ash A at a concentration of 19'120 mg/kg and mainly incorporated in Fe-oxide rich Ca-silicate spheres (Figure 3-6a). The depletion of 13% Fe shows that at least a small portion of Fe has to be bound to partially soluble phases (Figure 3-8). The aluminium concentration in fly ash A is 36'300 mg/kg and a considerable amount is present in metallic form. Alkaline conditions favour the decomposition of metallic particles because the dissolved Cl- activates the surface which is covered with an oxidizing protective coating (Musselman et al., 2000; Saffarzadeh et al., 2011). The formation of 1 wt.% ettringite ($Ca_6Al_2(OH)_{12}(SO_4)_3 \cdot 26H_2O$) is a result of the reaction of Al^0 with dissolved species such as Ca^{2+}, Cl^- and SO_4^{2-}. Fly ash A contains 9'540 mg/kg Pb and the dissolution of soluble Pb-bearing sulphates such as palmierite ($(K,Na)_2Pb(SO_4)_2$) leads to mobilization as Pb^{2+}. The origin of Cu^{2+} is not yet identified because no Cu-bearing phases are found to be dissolved by neutral leaching even though the fly ash contains 3'901 mg/kg Cu. No Pb and Cu are mobilized due to cementation of these metals during fly ash leaching (Figure 3-8, Free, 2013). More noble metal ions can coat the surfaces of less noble metals and this results in reduction of the dissolved metal to the metallic state (contact reduction, Equation 3-3) as has been widely investigated by several authors (Nadkarni et al., 1967; Stefanowicz et al., 1997; Karavasteva, 2005; Demirkıran et al., 2007). The process of copper and lead cementation removes the dissolved Pb^{2+} and Cu^{2+} from the extract solution. Observed $PbCu^0$-alloy-phases on the surface of Al^0 particles illustrate this cementation (Figure 3-7a).

$$3\ Cu^{2+} + 2\ Al^{0} \rightarrow 3\ Cu^{0}\downarrow + 2\ Al^{3+} \quad (3\text{-}3)$$

This $PbCu^{0}$-alloy-phase is always accompanied by 5-10 wt.% chlorine that demonstrates the role of chlorine content as surface activator. As a consequence of the cementation, aluminium is dissolved as Al^{3+} and precipitates as aluminiumhydroxide ($Al(OH)_3$) or ettringite at pH >3.5 (Hartinger, 1991). As a net reaction, Al is not extracted due to these dissolution-precipitation mechanisms. Zinc is present in fly ash A in significantly lower concentration (26'770 mg/kg) compared to fly ash B and C (48'190 mg/kg and 65'170 mg/kg). The low total concentration is mainly the reason why no Zn is accumulated in the dust rim of particles and no soluble Zn-bearing chlorides (e.g. K_2ZnCl_4) are formed during incineration. The absence of such easily accessible Zn is the main reason why no Zn is mobilized by neutral leaching (Figure 3-8). The pH-conditions to dissolve brass ($Cu_{0.6}Zn_{0.4}$) or Zn-silicates are not acidic enough and these phases remain in the filter cake.

3.4.4 Acidic leaching

In contrast to neutral fly ash leaching, acidic leaching is performed at pH conditions between 2.5 and 5.5. The used scrub water (pH <1) from the wet flue gas cleaning process dissolves almost the complete amount of soluble alkali salts (NaCl, KCl, K_2ZnCl_4) at low LS ratio of 1.4 at plant B. This results in a depletion of >80% Na, K and Cl and a mass loss of 13 wt.% in the filter cake (Table 3-1, Figure 3-8). The fly ash is buffering the system from an initial pH-value of 2.5 up to 5.5, induced by the dissolution of lime (CaO). Calcite ($CaCO_3$) is present in significantly higher concentrations in fly ash B (5 wt.%) compared to fly ash A and C (2 wt.%) and due to the lower reaction kinetics compared to lime, calcite is only dissolved partially under the present extraction conditions (Table 3-3). Anhydrite ($CaSO_4$) is not hydrated and remains stable during the entire extraction process whereas more complex sulphates such as syngenite ($K_2Ca_5(SO_4)6{\cdot}H_2O$) are completely dissolved. The dissolved Ca^{2+} originates mainly from the dissolution of carbonates and sulphates and is reacting with sulphur to form 7 wt.% gypsum ($CaSO_4{\cdot}2H_2O$). Gypsum is the solubility controlling phase for calcium in the pH range of 4-8 (Dijkstra et al., 2006). The formation of gypsum is controlled by the availability of sulphur dissolved that mainly originates from the scrub water (4'582 mg/L). Ettringite ($Ca_6Al_2(OH)_{12}(SO_4)_3{\cdot}26H_2O$) is newly formed in almost the same quantity as gypsum (6 wt.%) and the availability of aluminium has to be also high at low pH conditions. The main influence factor on the dissolution of heavy metals during acidic leaching is the high acid concentration in the first extraction tank. The initial pH of 2.5 dissolves the Fe-oxides incorporated in Ca-silicate spheres partially as Fe^{2+} and Fe^{3+}. Fe^{3+}-hydroxide starts precipitating rapidly with increasing extraction time and thus higher pH-value, whereas Fe^{2+}-hydroxide requires pH conditions >7 for precipitation (Hartinger, 1991). The low depletion factor of Fe of 8% after 60 minutes of extraction suggests that most of the dissolved iron was present as Fe^{3+} and subsequently precipitated as amorphous Fe^{3+}-hydroxide at the given pH conditions of 5.5 after 60 minutes of extraction (Equation 3-4).

$$Fe^{3+} + 3\ H_2O \rightarrow Fe(OH)_3\downarrow + 3\ H^+ \quad (3\text{-}4)$$

Lead and copper show concentrations of 9'108 mg/kg and 2'573 mg/kg, respectively, in fly ash B and are only extractable to a very small degree (6-8%) because of its cementation ($PbCu^0$-alloy-phase) observed in filter cake B (Figure 3-5, Figure 3-7). The formation of secondary precipitates such as cotunnite ($PbCl_2$) is the result of the reaction of dissolved Pb^{2+} with Cl^- present in high concentrations in the scrub water.

Zinc is determined in fly ash B at almost twice the concentration (48'190 mg/kg) compared to fly ash A. Highly soluble K_2ZnCl_4 and the accumulated Zn (12 wt.%) in the thick dust rims immediately dissolve and a depletion of 40% Zn is reached by performing acidic leaching (Figure 3-8). Cadmium is chemically related to zinc and 53% are mobilized under the present acidic conditions (Figure 3-8). Limited mixing at a low LS ratio of 1.4 is mainly the reason for the low Zn and Cd depletion of the industrial process of this study compared to other studies (60-85% for Cd, 60-80% for Zn; AWEL, 2013).

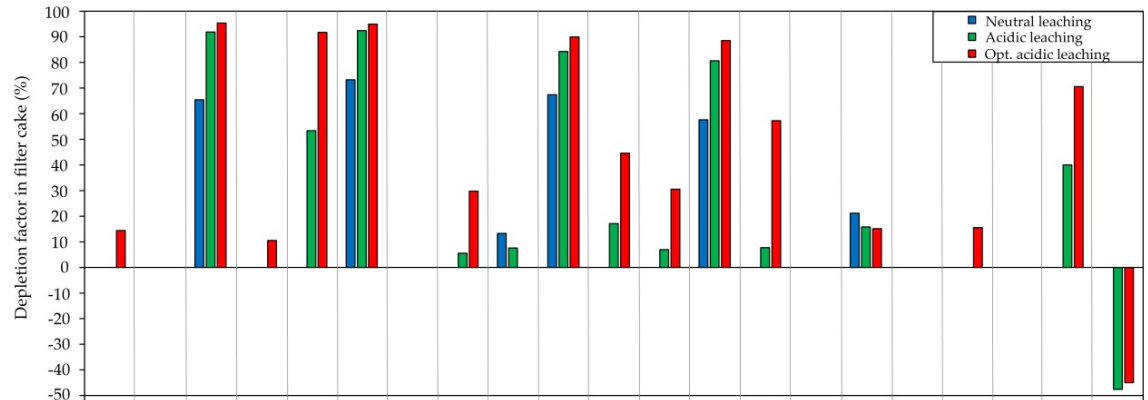

	Al	Ba	Br	Ca	Cd	Cl	Cr	Cu	Fe	K	Mg	Mn	Na	Pb	Sb	Si	Sn	Sr	Ti	Zn	S
Plant A	<5	<5	65	<5	<5	73	<5	<5	13	67	<5	<5	58	<5	<5	21	<5	<5	<5	<5	<5
Plant B	<5	<5	92	<5	53	92	<5	6	8	84	17	7	81	8	<5	16	<5	<5	<5	40	-48
Plant C	14	<5	95	11	92	95	<5	30	5	90	45	31	89	57	<5	15	<5	16	<5	71	-45

***Figure 3-8**: Depletion factors in % of elements of special interest in filter cake after neutral fly ash leaching (plant A), acidic fly ash leaching (plant B) and optimized acidic fly ash leaching with the addition of hydrogen peroxide (plant C). The negative depletion factor for sulphur shows enrichment in the remaining filter cake due to the formation of gypsum ($CaSO_4 \cdot 2H_2O$).*

3.4.5 Optimized acidic leaching

Plant C is performing an optimized acidic fly ash leaching in a three-stage extraction cascade with higher LS ratio, longer extraction time and the addition of hydrogen peroxide (35%) compared to the acidic leaching at plant B. The LS ratio of 3.5 and an extraction time of 25 minutes per tank results in a pH-value of 4.8 after 75 minutes of extraction. An elevated LS ratio and a longer extraction time ensure a more intensive contact of the extraction agent with minerals and metal-bearing particles. This enhances the degree of dissolution of calcite, alkali salts and gehlenite compared to filter cake B resulting in a mass loss of 32 wt.% (Table 3-1). The more acidic conditions and sulphur enriched scrub water (8'365 mg/kg, Table 3-2) results in almost twice the gypsum formation in filter cake C compared to B (Table 3-3). Filter cake C further contains elevated anhydrite content (12 wt.%) compared to the untreated fly ash (7 wt.%) which is explainable with a relative enrichment, neo-formation or the time lag between filter ash and filter cake production. Formation of anhydrite may happen during drying of the filter cake at 40°C where newly formed gypsum is dehydrated. No ettringite is formed in contrast to filter cake B. Possible reasons for this are the lower pH-value (pH 4.8), a more limited Al-availability and the competitive formation of large amounts of gypsum. The total amount of Al^0 is oxidized by the addition of hydrogen peroxide and may precipitate quickly as aluminium-hydroxide and is thus not available for formation of ettringite.

Fly ash C contains 65'170 mg/kg Zn and the filter cake is significantly more depleted in Zn (71%) compared to filter cake B (40%) (Figure 3-8). A lower initial pH-value, higher LS ratio and longer extraction time result in a dissolution of 80% brass because the wollastonite-like host particles are completely dissolved under the present conditions. The addition of hydrogen peroxide (40 L/t fly ash) with a normal potential of 1.736 V at pH-value 0 oxidizes the metallic components in fly ash and no active Al^0-surfaces are available for contact reduction of more noble dissolved metals (Equation 3-5).

$$2\ Al^0 + 3\ H_2O_2 + 6H^+ \rightarrow 2\ Al^{3+} + 6\ H_2O \qquad (3\text{-}5)$$

No $PbCu^0$-alloy-phase is found in filter cake C (Figure 3-5) and the extracted Pb^{2+} and Cu^{2+} remain in solution resulting in a depletion of 57% Pb and 30% Cu in filter cake C (Figure 3-8). Cadmium is almost completely extracted using the optimized fly ash leaching due to the higher LS ratio and oxidizing conditions (92%). The results of this study are comparable to other studies where depletion factors of 50-90% for Pb, 85-95% for Cd, 40-80% for Cu and 60-80% for Zn are achieved by the optimized acidic leaching (AWEL, 2013). The acid leached filter cakes fulfil the threshold values according to the Swiss Waste Ordinance (Swiss Confederation, 2016) and can be deposited like bottom ash in C-type landfills with substantial cost savings.

3.5 Conclusions

The combination of analytical methods allowed a detailed determination of the proportions and morphological characteristics of phases contained in three different fly ashes. The large amount of crystalline phases (ca. 40 wt.%) is remarkable considering the rapid formation and cooling processes taking place during incineration. Fly ash comprises refractory particles (Al-foil, unburnt carbon, quartz, feldspar) and newly formed high-temperature phases (glass, gehlenite, wollastonite) surrounded by a characteristic dust rim. The heavy metal concentrations vary strongly between the fly ashes, depending on the waste input. Metals are either carried along with the flue gas (Fe-oxides, brass) and are enriched in mineral aggregates (quartz, feldspar, wollastonite, glass) or vaporized and condensed as chlorides (K_2ZnCl_4) or sulphates ($PbSO_4$). These metal associations determine the mobilization of metals during subsequent leaching processes. The neutral, acidic and optimized acidic fly ash leaching processes lead to significantly different metal depletion factors with pH being a key-controlling parameter. During acidic leaching, the smaller depletion factors for Zn and Cd at plant B (40% for Zn, 53% for Cd) compared to plant C (71% for Zn, 92% for Cd) are due to a combination of less strong acid attack at a smaller LS ratio, a more extensive precipitation due to a higher equilibrium pH (5.5) and the carryover of soluble Zn in the filter cake after filtration.

The extraction of Pb and Cu are limited by a cementation process and the formation of a $PbCu^0$-alloy-phase and to a minor degree by secondary precipitation ($PbCl_2$). The addition of hydrogen peroxide prevents this reduction by oxidation of metallic components and thus leads to significantly higher metal depletion factors (57% for Pb, 30% for Cu). High LS ratios and the use of hydrogen peroxide are effective means for achieving elevated metal depletion factors. The use of scrub water to extract heavy metals in fly ash is a very economical process due to the synergy between two waste streams. The significant reduction of metal content for fly ash deposition in combination with lower costs for deposition of the leached filter cakes justifies more extensive and more expensive fly ash treatment processes. Viable options with respect to available technology are optimized oxidative conditions during the final stage of fly ash leaching or a secondary leaching step before deposition.

Acknowledgements

The work presented in this paper was financed by the Office for Waste Management, Environmental Protection Agency of Canton Zürich (AWEL Zürich) and the Federal Office for the Environment (FOEN). We thank the MSWI plant operators for providing sample material and information about their fly ash leaching processes. Analytical support by Alfons Berger, Christine Lemp (University of Bern), Ivo Budde and Waldemar Klink (ZAR) is highly acknowledged.

References

Abanades, S., Flamant, G., Gagnepain, B., Gauthier, D., 2002. Fate of heavy metals during municipal solid waste incineration. Waste Management & Research 20, 55-68.

AWEL, Office for Waste Management, Environmental Protection Agency of Canton Zürich (AWEL Zürich) 2013. Stand der Technik für die Aufbereitung von Rauchgasreinigungsrückständen (RGRR) aus Kehrichtverbrennungsanlagen.

Bayuseno, A.P., Schmahl, W.W., 2011. Characterization of MSWI fly ash through mineralogy and water extraction. Resources, Conservation and Recycling 55, 524-534.

Belevi, H., Moench, H., 2000. Factors determining the element behavior in municipal solid waste incinerators. 1. Field studies. Environmental Science & Technology 24, 2501-2506.

Brunner, P.H., Mönch, H., 1986. The flux of metals through municipal solid waste incinerators. Waste Management & Research 4, 105-119.

Comans, R.N.J., Meima, J.A., 1994. Modelling CA-solubility in MSWI bottom ASH leachates. Environmental Aspects of Construction with Waste Materials 60, 103-110.

Cultrone, G., Rodriguez-Navarro, C., Sebastian, E., Cazalla, O., De La Torre, M.J., 2001. Carbonate and silicate phase reactions during ceramic firing. European Journal of Mineralogy 13, 621-634.

Demirkıran, N., Ekmekyapar, A., Künkül, A., Baysar, A., 2007. A kinetic study of copper cementation with zinc in aqueous solutions. International Journal of Mineral Processing 82, 80-85.

Deutsches Kupferinstitut, 2007. Kupfer-Zink-Legierungen (Messing und Sondermessing). 1-30.

Dijkstra, J.J., van der Sloot, H.A., Comans, R.N.J., 2006. The leaching of major and trace elements from MSWI bottom ash as a function of pH and time. Applied Geochemistry 21, 335-351.

Eighmy, T.T., Eusden, J.D., Krzanowski, J.E., Domingo, D.S., Staempfli, D., Martin, J.R., Erickson, P.M., 1995. Comprehensive approach toward understanding element speciation and leaching behavior in municipal solid waste incineration electrostatic precipitator ash. Environmental Science & Technology 29, 629-646.

Ferreira, C., Ribeiro, A., Ottosen, L., 2003. Possible applications for municipal solid waste fly ash. Journal of Hazardous Materials B96, 201-216.

Free, M., 2013. Hydrometallurgy Fundamentals and applications. John Wiley & Sons, Inc., Hoboken, New Jersey.

Funari, V., Bokhari, S.N., Vigliotti, L., Meisel, T., Braga, R., 2016. The rare earth elements in municipal solid waste incinerators ash and promising tools for their prospecting. Journal of Hazardous Materials 301, 471-479.

Hartinger, L., 1991. Handbuch der Abwasser- und Recyclingtechnik. Fachbuchverlag Leipzig.

Held, A., Kramer, G.N., Robouch, P., Wätjen, U., 2007. The Certification of the mass fractions of As, Cd, Co, Cr, Cu, Fe, Hg, Mn, Ni, Pb, Sb, Se, Tl, V and Zn in fly ash BCR-176R. European Commission Directorate-General Joint Research Centre Institute for Reference Materials and Measurements.

Jakob, A., Stucki, S., Struis, R., 1996. Complete heavy metal removal from fly ash by heat treatment: Influence of chlorides an evaporation rates. Environmental Science & Technology 30, 3275-3283.

Johnson, C.A., Brandenberger, S., Baccini, P., 1995. Acid neutralizing capacity of municipal waste incinerator bottom ash. Environmental Science & Technology 29, 142-147.

Johnson, C.A., Kaeppeli, M., Brandenberger, S., Ulrich, A., Baumann, W., 1999. Hydrological and geochemical factors affecting leachate composition in municipal solid waste incinerator bottom ash Part II. The geochemistry of leachate from Landfill Lostorf, Switzerland. J Contam Hydrol 40, 239-259.

Karavasteva, M., 2005. Kinetics and deposit morphology of copper cementation onto zinc, iron and aluminium. Hydrometallurgy 76, 149-152.

Karlfeldt Fedje, K., Ekberg, C., Skarnemark, G., Steenari, B.M., 2010. Removal of hazardous metals from MSW fly ash-an evaluation of ash leaching methods. Journal of Hazardous Materials 173, 310-317.

Kirby, C.S., Rimstidt, J.D., 1994. Interaction of municipal solid waste ash with water. Environmental Science and Technology 28, 443-451.

Kutchko, B., Kim, A., 2006. Fly ash characterization by SEM–EDS. Fuel 85, 2537-2544.

Le Forestier, L., Libourel, G., 1998. Characterization of flue gas residues from municipal solid waste combustors. Environmental Science & Technology 32, 2250-2256.

Li, M., Xiang, J., Hu, S., Sun, L.-S., Su, S., Li, P.-S., Sun, X.-X., 2004. Characterization of solid residues from municipal solid waste incinerator. Fuel 83, 1397-1405.

Liu, Y., Zheng, L., Li, X., Xie, S., 2009. SEM-EDS and XRD characterization of raw and washed MSWI fly ash sintered at different temperatures. Journal of Hazardous Materials 162, 161-173.

Mahieux, P.Y., Aubert, J.E., Cyr, M., Coutand, M., Husson, B., 2010. Quantitative mineralogical composition of complex mineral wastes-contribution of the Rietveld method. Waste Management 30, 378-388.

Morf, L.S., Brunner, P.H., Spaun, S., 2000. Effect of operating conditions and input variations on the partitioning of metals in a municipal solid waste incinerator. Waste Management & Research 18, 4-15.

Morf, L.S., Gloor, R., Haag, O., Haupt, M., Skutan, S., Di Lorenzo, F., Boni, D., 2013. Precious metals and rare earth elements in municipal solid waste-sources and fate in a Swiss incineration plant. Waste Management 33, 634-644.

Musselman, C.N., Staub, W.A., Bidwell, J.N., Carpenter, J.E., Presher, J.R., 2000. Gas generation at a municipal waste combustor ash monofill - Frankling, New Hampshire. Sustainable Construction: Use of incinerator ash, 97-109.

Nadkarni, R.M., Jelden, C.E., Bowles, K.C., Flanders, H.E., Wadsworth, M.E., 1967. A kinetics study of copper precipitation on iron: part I. Transactions of the Metallurgical Society of AIME 239, 581-585.

Quina, M.J., Bordado, J.C., Quinta-Ferreira, R.M., 2008a. Treatment and use of air pollution control residues from MSW incineration: an overview. Waste Management 28, 2097-2121.

Quina, M.J., Bordado, J.C., Quinta-Ferreira, R.M., 2009. The influence of pH on the leaching behaviour of inorganic components from municipal solid waste APC residues. Waste Management 29, 2483-2493.

Quina, M.J., Santos, R.C., Bordado, J.C., Quinta-Ferreira, R.M., 2008b. Characterization of air pollution control residues produced in a municipal solid waste incinerator in Portugal. Journal of Hazardous Materials 152, 853-869.

Sabbas, T., Polettini, A., Pomi, R., Astrup, T., Hjelmar, O., Mostbauer, P., Cappai, G., Magel, G., Salhofer, S., Speiser, C., Heuss-Assbichler, S., Klein, R., Lechner, P., 2003. Management of municipal solid waste incineration residues. Waste Management 23, 61-88.

Saffarzadeh, A., Shimaoka, T., Wei, Y., Gardner, K.H., Musselman, C.N., 2011. Impacts of natural weathering on the transformation/neoformation processes in landfilled MSWI bottom ash: a geoenvironmental perspective. Waste Management 31, 2440-2454.

Sandell, J.F., Dewey, G.R., Sutter, L.L., Willemin, J.A., 1996. Evaluation of lead-bearing phases in municipal waste combustor fly ash. Journal of Environmental Engineering 122, 34-40.

Schlumberger, S., Schuster, M., Ringmann, S., Koralewska, R., 2007. Recovery of high purity zinc from filter ash produced during the thermal treatment of waste and inerting of residual materials. Waste Management & Research 25, 547-555.

Stefanowicz, T., Osinska, M., Napieralska-Zagozda, 1997. Copper recovery by the cementation method. Hydrometallurgy 47, 69-90.

Stumm, W., Morgan, J., 1996. Aquatic chemistry: chemical equilibria and rates in natural waters, 3rd ed. John Wiley & Sons. New York, USA.

Swiss Confederation, 2016. Verordnung über die Vermeidung und die Entsorgung von Abfällen (VVEA). 1-46.

Thipse, S.S., Schoenitz, M., Dreizin, E.L., 2002. Morphology and composition of the fly ash particles produced in incineration of municipal solid waste. Fuel Processing Technology 75, 173-184.

Traber, D., Mäder, U.K., Eggenberger, U., 2002. Petrology and geochemistry of a municipal solid waste incinerator residue treated at high temperature. Schweizerische mineralogische und petrographische Mitteilungen 82, 1-14.

Van Herck, P., Van der Bruggen, B., Vogels, G., Vandecasteele, C., 2000. Application of computer modelling to predict the leaching behaviour of heavy metals from MSWI fly ash and comparison with a sequential extraction method. Waste Management 20, 203-210.

Vehlow, J., Braun, H., Horch, K., Merz, A., Schneider, J., Stieglitz, L., Vogg, H., 1990. Semi-technical demonstration of the 3-R Process. Waste Management & Research 8, 461-472.

Verhulst, D., Buekens, A., 1996. Thermodynamic behavior of metal chlorides and sulfates under the conditions of incineration furnaces. Environmental Science and Technology 30, 50-56.

Chapter 4

Extraction of Heavy Metals from MSWI Fly Ash using Hydrochloric Acid and Sodium Chloride Solution

Gisela Weibel[a], Urs Eggenberger[a], Dmitrii A. Kulik[b], Wolfgang Hummel[b], Stefan Schlumberger[c], Waldemar Klink[c], Martin Fisch[a], Urs K. Mäder[a]

[a]*Institute of Geological Sciences, University of Bern, Switzerland*
[b]*Laboratory for Waste Management, Paul Scherrer Institute, Villigen, Switzerland*
[c]*Zentrum für nachhaltige Abfall- und Ressourcennutzung (ZAR), Zuchwil, Switzerland*

Submitted to Waste Management (Mai 2017)

Based on technical report on behalf of the Office for Waste Management, Environmental Protection Agency of Canton Zürich (AWEL), 06. December 2016.

Abstract

Fly ash from municipal solid waste incineration contains a large potential for recyclable metals such as Zn, Pb, Cu and Cd. The Swiss Waste Ordinance prescribes the treatment of fly ash and recovery of metals to be implemented by 2021. More than 60% of the fly ash in Switzerland is acidic leached according to the FLUWA process, which provides the basis for metal recovery. Treatment of fly ash further contributes positively to the environment due to a reduction of mass and heavy metals to be deposited. The investigation and optimization of the FLUWA process is of increasing interest and an industrial solution for direct metal recovery within Switzerland is in development. With this work, a detailed laboratory study on different filter cakes from fly ash leaching using HCl 5% (represents the FLUWA process) and concentrated sodium chloride solution (300 g/L) is described. This two-step leaching of fly ash shows an efficient combination for the mobilization of a high percentage of heavy metals from fly ash (Pb, Cd ≥90% and Cu, Zn 70-80%). The depletion of these metals is mainly due to the combination of redox reactions

and metal-chloride-complex formation. The study allows the definition of the limits for heavy metal depletion with optimized leaching methods that have a potential for application at industrial scale.

4.1 Introduction

Approximately 75'000 tons of fly ash are generated annually in Switzerland from 30 municipal solid waste incineration (MSWI) plants. Due to the load with organic and inorganic pollutants, treatment of fly ash is essential. Untreated fly ash from Switzerland is currently exported untreated to underground storage, solidified with cement before deposition or acidic leached according to the FLUWA process (Schlumberger et al., 2007; Bühler and Schlumberger, 2010). Nowadays, more than 60% of the fly ash in Switzerland is treated according to the FLUWA process which represents the state-of-the-art. It provides the basis for extended methods such as the FLUREC process (Schlumberger et al., 2007), where metals from fly ash are directly recovered. MSWI fly ash comprises a large potential for recyclable metals such as Zn, Pb, Cu and Cd. Additionally, treatment of fly ash makes an important contribution to the environment due to a reduction of mass and heavy metals to be deposited. The revised Swiss Waste Ordinance (Swiss Confederation, 2016) prescribes the recovery of metals from fly ash to be implemented by 2021. In order to achieve this goal, a centralized plant for metal recovery from fly ash is planned in Switzerland (ZAR, 2016). The metal depletion factor by the FLUWA process is currently in the range of 60-80% for Zn, 0-30% for Pb and Cu and 60-85% for Cd (AWEL, 2013). In a previous study, we described in detail the mineralogical and geochemical composition and the binding forms of the metals contained in a wide variety of fly ash and leached filter cake composition (Weibel et al., 2016). It was also shown that the redox conditions during the FLUWA process are of central importance, for increasing the recovery of redox-sensitive metals (mainly Pb, Cu and Cd). This is achieved by adding an oxidizing agent (hydrogen peroxide, H_2O_2) during fly ash leaching (AWEL, 2013).

An additional optimization process to enhance the metal recovery from fly ash is a subsequent leaching step of the residual filter cake from the FLUWA process. A promising option is the leaching of the filter cake using concentrated sodium chloride solution (NaCl). This process is well known from metallurgical processing where heavy metals are kept in solution by metal-chloride-complexes e.g. for Pb (Raghavan et al., 1998; Raghavan et al., 2000; Turan et al., 2004; Ruşen et al., 2008). The lead-sulphate residues react with Cl-ions, whereby the dissolved Pb forms up to four consecutive chloride-complexes in aqueous solution ($PbCl^+$, $PbCl_2$, $PbCl_3^-$, $PbCl_4^{2-}$). This formation of chloride-complexes significantly increases the solubility of Pb and other chloride-complex-forming metals such as Cu and Cd (Sinadinovic et al., 1997).

The aim of this study is to investigate the mobilization of heavy metals from two different fly ashes by hydrochloric acid (HCl, represents the FLUWA process) and subsequent NaCl-leaching with special attention to Pb and Cu mobilization. Of particular in-

terest are the chemical processes responsible for metal mobilization for each leaching step. The metal mobility is predominantly controlled by the redox potential and the chloride concentration. The factors influencing the redox conditions and the role of the chlorine responsible for metal mobilization are thus investigated. This is achieved by chemical and structural characterization of the leached filter cakes, complemented with the determination of aqueous speciation of heavy metals in filtrates using UV-VIS spectroscopy and thermodynamic modelling.

4.2 Materials and methods

4.2.1 Origin of fly ash and sample preparation

The leaching experiments were performed with fly ash from two MSWI plants in Switzerland (Table 4-1). Both plants are using the FLUWA process and in addition to their own fly ash they also treat fly ash from other MSWI plants. The first fly ash mix contains fly ash from two MSWI plants, both with an elevated portion of industrial waste input (fly ash A). The second mix contains fly ash from three MSWI plants with an elevated portion of household waste input (fly ash B). Approximately 15 kg of each fly ash mix was collected over a period of 3 weeks. The fly ash samples were homogenized, split into 1 kg batches and dried at 105°C for further analyses. The fly ash, present as a fine powder (median grain size ca. 0.1 mm), was ground to a particle size <0.01 mm in a tungsten-carbide disk mill. For the leaching experiments the original fly ash was used

Table 4-1: *Composition of fly ash mixes used in this study, determined by ED-XRF (mg/kg).*

Element (mg/kg)	Fly ash A	Fly ash B
Al*	31'429	47'349
Ba	1'881	1'908
Br	3'847	3'211
Ca	152'700	185'500
Cd	370	275
Cl	103'300	109'900
Cr	468	465
Cu	2'512	1'776
Fe	20'510	20'010
K	46'900	46'750
Mg*	12'262	14'434
Mn	784	671
Ni	123	146
P	4'497	4'708
Na*	48'396	49'604
Pb	11'920	8'114
S	55'430	54'580
Sb	2'976	2'396
Si	81'260	76'920

Ti	9'308	10'660
Zn	65'420	40'510
Sn	1'682	1'335

*Determined by TD-ICP-OES

4.2.2 Leaching Experiments

The leaching experiments were performed in two steps (Table 4-2). In a first step, the fly ashes were leached with HCl 5%. The experiments were performed with a liquid to solid ratio (LS) of 4 at 60°C for 60 minutes which is close to the conditions of the FLUWA process at industrial-scale. The pH-value was adjusted to pH 2.5 with HCl 32% and after 60 minutes increased to pH 3.5 with NaOH 30%, to allow a smooth vacuum filtration. The leached residue (filter cake) was washed with deionized water (washing volume: 50% of the HCl-solution previously used) and the leaching solution (filtrate) and washing water were combined (ca. 2:1 ratio). For each fly ash two different experiments were performed with HCl 5%, a first experiment without the addition of an oxidizing agent and a second with a single dose of 7 L H_2O_2/t fly ash. However, it became evident that the amount of H_2O_2 used was not sufficient to maintain oxidative conditions during the entire leaching period. For this reason, a third experiment was carried out where the redox potential was kept constant at >300 mV by the addition of several dosages of H_2O_2. For fly ash A, 30 L H_2O_2/t FA was required in total and for fly ash B 50 L H_2O_2/t FA.

Table 4-2: *Conditions of HCl- and NaCl-leaching.*

Parameter	HCl-leaching (Step 1)	NaCl-leaching (Step 2)
Concentration	HCl 5%	NaCl 150 g/L and 300 g/L
Liquid to solid ratio (LS)	4	5
Time (min)	60	60
Temperature (°C)	60	25/85
pH-value	2.5 (for filtration pH 3.5)	2.5/3.5/4.5
Oxidizing agent	Hydrogen peroxide 30%	-

The leached filter cake was dried at 50°C for mass balance and used for the second leaching step with concentrated NaCl-solution (300 g/L). Then, 25 g of dried filter cake were added to 125 ml of NaCl-solution at 85°C under constant stirring, and the beaker was sealed with a lid. The pH was adjusted by the addition of HCl 32%. During the entire extraction, the temperature, the pH-value and the redox potential (Ag/AgCl reference system) were monitored. The pH-value was kept temperature-compensated, which is not possible with the redox potential. The redox potential is mainly dependent on the temperature and to a smaller degree on the pH-value and the ionic strength of the extract solution. After 60 minutes, the suspension was filtered and washed with hot deionized water (washing volume: 50% of the used NaCl-solution). The filtrate and washing water were combined (ca. 2:1 ratio) and stabilized for the ICP-OES measurements with HNO_3 (pH 2).

In a first series of NaCl-experiments, different leaching conditions were tested. For this purpose, filter cake A from the HCl-leaching without the addition of H_2O_2 was used (experiment 1, Table 4-3). The pH-value (2.5, 3.5, 4.5), the temperature (25°C, 85°C) and the NaCl-concentration (150 g/L and 300 g/L) were varied for the individual experiments (experiments 1-1 to 1-5, Table 4-4). In order to reproduce the industrial process as close as possible, a LS ratio of 5 was used. In a second series, the remaining filter cakes A from the HCl-leaching (experiments 2 and 3, Table 4-3) and the filter cakes B (experiments 4 to 6, Table 4-3) were leached with NaCl. Multiple determinations were carried out under optimized experimental conditions in order to demonstrate the reproducibility of the experiments (experiments 1-2, 3-1, 4-1 and 6-1, Table 4-3).

Table 4-3: *Experimental setup of acidic fly ash leaching using HCl 5%.*

Nr.	Sample	Leaching conditions	Product
1	Fly ash A	HCl 5%, pH 2.5, 60°C	Filter cake A1
2	Fly ash A	HCl 5%, pH 2.5, 60°C, 7 L H_2O_2/t FA	Filter cake A2
3	Fly ash A	HCl 5%, pH 2.5, 60°C, 30 L H_2O_2/t FA	Filter cake A3
4	Fly ash B	HCl 5%, pH 2.5, 60°C	Filter cake B4
5	Fly ash B	HCl 5%, pH 2.5, 60°C, 7 L H_2O_2/t FA	Filter cake B5
6	Fly ash B	HCl 5%, pH 2.5, 60°C, 50 L H_2O_2/t FA	Filter cake B6

Table 4-4: *Experimental setup of NaCl-leaching of residual filter cakes from HCl-leaching.*

Nr.	Sample	Leaching conditions	Product
1-1	Filter cake A1	NaCl 300 g/L, pH **4.5**, 85°C	Filter cake A1-1
1-2	Filter cake A1	NaCl 300 g/L, pH **3.5**, 85°C	Filter cake A1-2
1-3	Filter cake A1	NaCl 300 g/L, pH **2.5**, 85°C	Filter cake A1-3
1-4	Filter cake A1	NaCl **150 g/L**, pH 3.5, 85°C	Filter cake A1-4
1-5	Filter cake A1	NaCl 300 g/L, pH 3.5, **25°C**	Filter cake A1-5
2-1	Filter cake A2		Filter cake A2-1
3-1	Filter cake A3		Filter cake A3-1
4-1	Filter cake B4	NaCl 300 g/L, pH 3.5, 85°C	Filter cake B4-1
5-1	Filter cake B5		Filter cake B5-1
6-1	Filter cake B6		Filter cake B6-1

4.2.3 Chemical analysis

Elemental composition of the fly ashes and leached filter cakes was determined by energy dispersive X-ray fluorescence analysis (ED-XRF) using a Spectro Xepos spectrometer with matrix adjusted calibration. The measurements were performed on pressed powder pellets (32 mm diameter) using 4.0 g material <0.01 mm and 0.9 g Hoechstwax as binder. Elements of special interest (Al, Ca, Cd, Cu, Fe, Mg, Na, Pb, Ti, Zn) were further analyzed by inductively coupled plasma optical emission spectroscopy (ICP-OES, Varian 720-ES) after total digestion (TD) with a mixture of nitric acid (HNO_3 65%) and hydrofluoric acid (HF 40%) in a high pressure microwave system (MLS Ethos Plus). The results by TD-ICP-

OES revealed erroneous quantifications from ED-XRF for Al, Mg and Na due to matrix interferences (metallic Al^0) and low sensitivity of the ED-XRF at low energy (Mg, Na). The results of the TD-ICP-OES analyses were therefore preferred.

The filtrates were analyzed by ICP-OES using matrix adjusted calibrations because of the highly saline solutions after NaCl-leaching. Analytical errors of ±5% are achieved for all elements except Na, K, Ca, Sb, and S that show ±10% error based on multiple measurements of certified standard solutions (ICP Multi-element Standard CertiPur IV and X, Merck). The major anions (F^-, Cl^-, Br^-, and SO_4^{2-}) were analyzed in the filtrates by ion chromatography (IC) using a Metrohm 850 Professional IC system (columns: Metrosep A Supp 7-250/4.0 and Metrosep C 4-150/4.0). The analytical error, based on multiple measurements of certified standard solutions (AccuSPEC Standard SCP Science, Fluka/Sigma-Aldrich) was ±5%.

4.2.4 SEM microscopy

The leached filter cake samples were impregnated under vacuum with epoxy resin and polished (water-free). The specimens were coated with carbon to avoid surface charging for SEM analyses. A Zeiss EVO-50 XVP electron microscope (SEM) coupled with an EDAX Apollo X energy dispersive system (EDS) was used to perform rapid semi-quantitative chemical spot analyses. An acceleration voltage of 20 kV, high vacuum mode and a spot size of 504 nm were used for backscattered electron (BSE) images.

4.2.5 X-ray diffraction analysis

Precipitates from filtrates were measured using a PANalytical X'Pert Pro diffractometer (CuKα-radiation) from 5 to 60° 2θ at 0.017°/step, an acceleration voltage of 40 kV and an electron generating current of 40 mA for 40 minutes. Identification of crystalline phases was done using the PANalytical software "High-Score Plus".

4.2.6 UV-VIS spectroscopy

Absorption spectra of Pb-chloride-complexes were recorded with a spectrophotometer (Varian Cary 50) at 1 nm intervals from 195-315 nm using a 0.1 cm quartz cell (Hellma 170.700.QS). Solutions were introduced into the cell using a syringe pump. Tests with differently concentrated solutions of Pb and NaCl, stored in a thermostatically controlled water bath at different temperatures (20-25°C) resulted in the same absorption spectra for each solution. All solutions are therefore prepared and measured at room temperature (20°C). A first series of measurements were made with NaCl-solutions (0.001-5.4 mol/L) containing 1000 mg/L Pb (from $PbCl_2$). In a second step, the absorption spectra of the heavy metal enriched filtrate from a recently performed fly ash leaching experiment using concentrated NaCl-solution was recorded (experiment 3-1). The measured absorption spectra were deconvoluted with TOPAS Academic (Coelho, 2016) using Gaussian peaks and a flat background. This allows the determination of the species in solution by using

the characteristic absorption bands of free Pb^{2+} and of the various Pb-chloride-complexes ($PbCl^{+}$, $PbCl_2$, $PbCl_3^{-}$ and $PbCl_4^{2-}$). Values of characteristic absorption bands and FHMW from literature were taken as starting values for peak position (Vierling, 1971; Byrne et al., 1981; Seward, 1984; Hagemann, 1999). Peak areas and background were refined individually by non-linear least squares for each spectrum, whereas position and FWHM parameters of each peak were constrained over all datasets, in order to obtain a universal solution for all spectra (Figure 4-1). Resulting parameters are listed in Table 4-5.

There is a shift of the absorption bands (Figure 4-1) to longer wavelengths with increasing chloride complexation from Pb^{2+} to $PbCl_4^{2-}$. It is further known that the absorption band of the 1:4 Pb-chloride-complex is much narrower and the peak almost twice as high (higher molar absorptivity, ε) compared to the other species (Hagemann, 1999). A strong absorption curve occurs below 220 nm with a shift of the maxima to higher wavelengths with increasing chloride concentration. Several peaks are required for refinement of the chloride absorption band at wavelengths <215 nm.

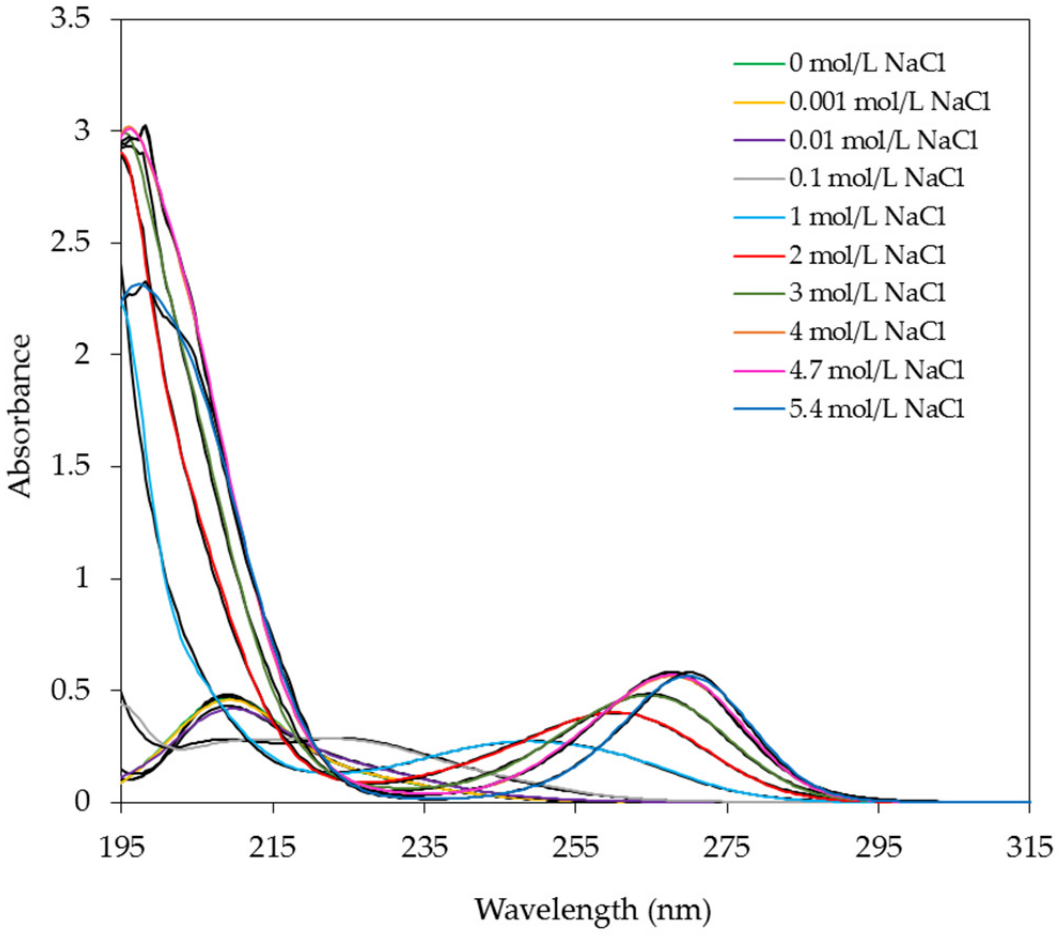

Figure 4-1: *Typical spectra of Pb-chloride-complexes (black lines) at 25°C using 1000 mg/L Pb and different concentrations of NaCl (0, 0.001, 0.01, 0.1, 1, 2, 3, 4, 4.7, 5.3 mol/L NaCl). The characteristic absorption bands for free Pb^{2+} and Pb-chloride-complexes are determined by evaluation of each spectrum using Gaussian peaks (refined absorption spectra shown in colour).*

Table 4-5: *Resulting parameters for characteristic absorption bands of Pb-chloride-complexes after deconvolution of absorption spectra of different NaCl-solutions (0, 0.001, 0.01, 0.1, 1, 2, 3, 4, 4.7, 5.3 mol/L NaCl).*

Species	λ_{max} (nm)	FWHM (1/cm)
Pb^{2+}	208.5	17.9
$PbCl^{+}$	224.7	24.4
$PbCl_2$	244.2	23.7
$PbCl_3^{-}$	260.7	23.4
$PbCl_4^{2-}$	270.6	18.9

4.2.7 Thermodynamic modelling

Thermodynamic modelling was carried out using the method of Gibbs free energy minimization (GEM), implemented in the GEM-Selektor code package (Wagner et al., 2012; Kulik et al., 2013) (http://gems.web.psi.ch). For this study, the PSI/Nagra thermodynamic database 12/07 (Thoenen et al., 2014) was used and enhanced with the thermodynamic data of dissolved species and solids for Pb, Cu, Zn and Cd from IUPAC reviews (Powell et al., 2007; Powell et al., 2009, 2011, 2013) as well as from Robie et al. (1979), Humphreys et al. (1980) and Abdul-Samad et al. (1981) (Appendix 4).

The equilibrium constants of aqueous complex formation and mineral dissolution reactions for 1 bar, 25°C and zero ionic strength were entered into ReacDC records of GEM-Selektor and automatically converted into *G*°-values needed for the GEM input, using the standard thermodynamic data for aqueous ions (master species) Cd^{2+}, Cu^{+}, Cu^{2+}, Pb^{2+}, and Zn^{2+} as well as of water and major ions such as Cl^{-} or CO_3^{2-} from the built-in SUPCRT98 database (Shock et al., 1997). Wherever the complexes of Cd, Cu, Pb and Zn were available from the built-in SUPCRT98 database of GEM-Selektor, they were adopted after replacing the original *G*°-values with those calculated from equilibrium constants from IUPAC compilations.

The activity coefficients of aqueous species were computed with the built-in SIT model (Wagner et al., 2012). The Brønsted-Guggenheim-Scatchard model, also called the SIT (Specific Ion Interaction Theory) model, has been extensively used in IUPAC and NEA TDB evaluations (Grenthe and Puigdomenech, 1997) and in compilation of the Nagra-PSI 01/01 chemical thermodynamic database (Hummel et al., 2002). The molal activity coefficient of an ion of charge z_i in solution is given by Equation 4-1.

$$\log_{10}\gamma_i = -\frac{z_i^2 A_\gamma \sqrt{I}}{1+1.5\sqrt{I}} + \sum_k \varepsilon(i,k)\, m_k \qquad (4\text{-}1)$$

I is the (effective) molal ionic strength, A_γ is the limiting Debye-Hückel law slope, and $\varepsilon(i,k)$ is an interaction coefficient that describes the specific short-range interaction between the ionic species i and k. The summation extends over all species k with molality m_k present in solution. The value of 1.5 in the denominator was empirically selected to minimize the ionic strength dependency of a number of electrolytes at T = 298.15 K. The present notation assumes that interaction coefficients $\varepsilon(i,k)$ do not depend on concentration

and temperature and are symmetric, i.e. $\varepsilon(i,k) \equiv \varepsilon(k,i)$. Interaction coefficients (i,k) for ions of the same sign are assumed to be zero.

The SIT interaction parameters used in this work have been collected from Grenthe et al., 1997 and the IUPAC reviews (Powell et al., 2007; Powell et al., 2009, 2011, 2013). Missing interaction parameters were estimated according to Hummel (2009). Thus, a complete set of SIT interaction parameters have been entered in a phase definition record of GEM-Selektor (Appendix 4). The existence of 1:4 chloride-complexes for Pb, Cu, Zn and Cd, as well as the 1:3 complex for Cu, is controversial because publications reporting experimental work involving these higher complexes at very high ionic strengths are of limited number and the reported constants differ considerably. In the thermodynamic model used in this study the complex $PbCl_4^{2-}$ is included with an equilibrium constant $\log_{10}\beta_4^\circ = 1.46$ for $Pb^{2+} + 4\ Cl^- = PbCl_4^{2-}$, mentioned as a rough estimate but not selected by the IUPAC review (Powell et al., 2009), together with a SIT interaction coefficient $\varepsilon(X^{2-},Na^+) = -0.10$ estimated by Hummel (2009), where X^{2-} is any anion or negatively charged complex with charge -2. Likewise, the complex $CdCl_4^{2-}$ is included with an equilibrium constant $\log_{10}\beta_4^\circ = 1.7$ for $Cd^{2+} + 4\ Cl^- = CdCl_4^{2-}$, mentioned but not selected by the IUPAC review (Powell et al., 2011), together with the same estimated SIT interaction coefficient as used for $PbCl_4^{2-}$. In the case of $ZnCl_4^{2-}$ the IUPAC review (Powell et al., 2013) does not even provide an indicative value for its equilibrium constant. In order to get at least a rough estimate, data have been taken from Fedorov et al. (1979), a study judged as reliable by Powell et al. (2013) and included in their evaluation of 1:1, 1:2 and 1:3 zinc chloride complexation. The equilibrium constant $\log_{10}\beta_4 = -0.70$ for $Zn^{2+} + 4\ Cl^- = ZnCl_4^{2-}$ at $I = 3.0$ M $NaClO_4$, as reported by Fedorov et al. (1979), has been extrapolated to $\log_{10}\beta_4^\circ = -2.0$ with the same estimated SIT interaction coefficient as used for $PbCl_4^{2-}$. In the case of Cu the IUPAC review (Powell et al., 2007) does not recommend any constants for the formation of $CuCl_3^-$ and $CuCl_4^{2-}$. In order to get some rough estimates, data have been taken from Ramette (1986) and Iuliano et al. (1989), two studies judged as reliable by Powell et al. (2007) and included in their evaluation of 1:1 and 1:2 Cu-chloride complexation. In both studies the solubility of sparingly soluble $Cu(IO_3)\cdot xH_2O$ at high ionic strength ($NaClO_4$) in the presence of NaCl was analyzed and the reported copper chloride equilibrium constants are fairly consistent. Ramette (1986), reports $\log_{10}\beta_3 = -0.16$ and $\log_{10}\beta_4 = -1.26$ at 5 M $NaClO_4$, whereas Iuliano et al. (1989) report $\log_{10}\beta_3 = -0.64$ and $\log_{10}\beta_4 = -1.43$ at 6 m (molal) $NaClO_4$. These constants have been extrapolated to zero ionic strength using $\varepsilon(X^-,Na^+) = -0.05$ and $\varepsilon(X^{2-},Na^+) = -0.10$ estimated by (Hummel, 2009), resulting in $\log_{10}\beta_3^\circ = -1.94$ (Ramette, 1986) and -1.80 (Iuliano et al., 1989) and $\log_{10}\beta_4^\circ = -4.22$ (Ramette, 1986) and -4.67 (Iuliano et al., 1989). The unweighted averages $\log_{10}\beta_3^\circ = -1.87$ and $\log_{10}\beta_4^\circ = -4.4$ have been included in the present thermodynamic model.

4.3 Results and discussion

4.3.1 Leaching with HCl 5%

All experiments were performed using HCl 5% for fly ash leaching which is close in composition to the acidic scrub water used in the FLUWA process. Experiments with fly ash and HCl 5% at pH 2.5 and 60°C (experiments 1 and 4, Table 4-3) lead to reducing conditions after 5 minutes of leaching (Eh: -281 mV fly ash A, -580 mV fly ash B, (Table 4-6, Figure 4-7). The oxygen is rapidly consumed by the oxidation of metallic particles contained in the fly ash. At the observed reducing conditions, more noble metal ions in solution react with less noble metal present in the fly ash and form reductive precipitates. This cementation process has been widely investigated by several authors (Nadkarni et al., 1967; Stefanowicz et al., 1997; Karavasteva, 2005; Demirkıran et al., 2007) and was described in detail in our previous study (Weibel et al., 2016). The process of reductive cementation of mainly Cu and Pb removes these metals from the filtrate (Equation 4-2).

$$3\ Cu^{2+} + 2\ Al^{0} \rightarrow 3\ Cu^{0}\downarrow + 2\ Al^{3+} \qquad (4\text{-}2)$$

This process could be clearly identified in filter cakes A and B by scanning electron microscope (SEM), where the cementation form $PbCu^0$-alloys (40-60% Pb, 10-20% Cu), commonly observed in contact with metallic Al^0 particles (Figure 4-2a). Filter cake A also shows the cementation of Pb by Al^0 without the presence of Cu. The cementation phases are always accompanied by approx. 5% Cl, which plays an important role as a surface activator of Al^0. Cadmium is also a metal that can be reductively separated by less noble metallic Al^0, Fe^0 or Zn^0. The leaching of fly ash with HCl 5% (experiments 1 and 4) leads to depletion factors of 71% for Cd and 75% for Zn in fly ash A, and to 60% for Cd and 60% for Zn in fly ash B (Table 4-6, Figure 4-3).

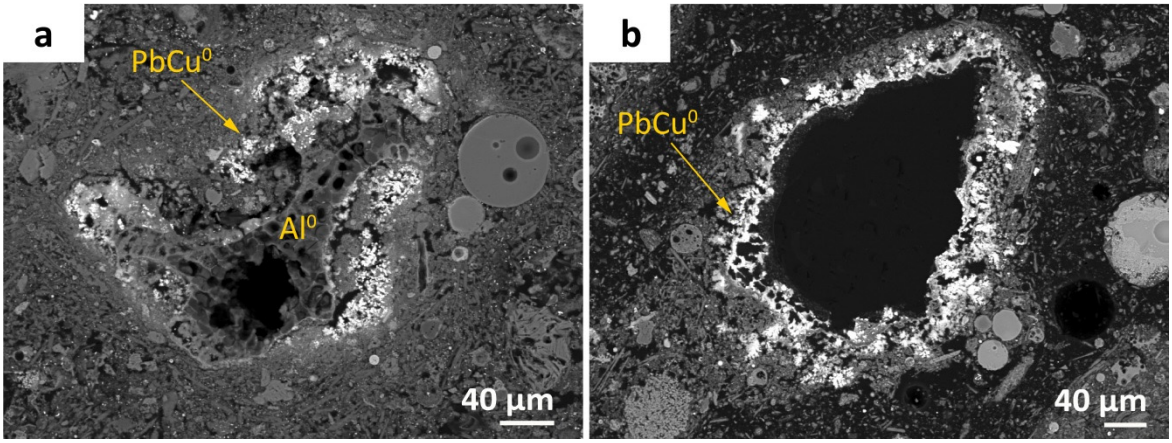

Figure 4-2: *Cementation phases ($PbCu^0$-alloy) in leached filter cake A: (a) without addition of H_2O_2 with Al^0 in the centre, (b) with the addition of 7 L H_2O_2/t fly ash that cannot completely prevent the formation of the $PbCu^0$-alloy, but leads to subsequent oxidation of the Al^0 (central Al^0 is detached).*

Additional experiments with HCl 5% were performed with the use of an oxidizing agent. The addition of H_2O_2 during the HCl-leaching suppresses the cementation because of the oxidation of the predominant part of the metallic components in fly ash (Equation 4-3).

$$2\ Al^0 + 3\ H_2O_2 + 6H^+ \rightarrow 2\ Al^{3+} + 6\ H_2O \quad (4\text{-}3)$$

The dissolved Cu and Pb thus remain in the filtrate and can be recovered (Table 4-6, Figure 4-3). In the experiments with only 7 L H_2O_2/t fly ash there was not enough oxidizing agent to keep oxidizing conditions over the entire leaching period and the redox potential reached values of -220 mV and -300 mV, respectively (experiments 2 and 5). Analyses of filter cake from these experiments show that the cementation process is not suppressed and a cementation phase ($PbCu^0$-alloy) is present in filter cake A and B. In these filter cakes similar stoichiometric ratios of Pb and Cu in the cementation phase are found as in the filter cake without oxidizing agent. However, a pure Pb cementation phase was not found in filter cake A. Since Pb (E^0: -0.13 V), is less noble than Cu (E^0: 0.35 V) it is reductively separated after Cu which explains the 20% recovery for Pb using 7 L H_2O_2/t fly ash. Filter cake B in contrast showed no depletion for Pb and Cu after leaching with 7 L H_2O_2/t fly ash and large amounts of Al^0 were still identified in the leached filter cake. Further experiments showed that a quantity of 30 L H_2O_2/t for fly ash A and 50 L H_2O_2/t for fly ash B was required to maintain the redox potential at values of >300 mV in order to oxidize all metallic components and to suppress the cementation (experiments 3 and 6). At these conditions depletion factors of 62% Pb and 55% Cu in fly ash A, as well as 56% Pb and 18% Cu in fly ash B were achieved (Table 4-6, Figure 4-3).

SEM analyzes showed that the non-mobilizable fraction of Pb was present as metallic PbO in the filter cake. Indications for lead chloride ($PbCl_2$) have also been found, but as shown in earlier studies $PbCl_2$ is present as very fine grained particles and can barely be identified by SEM (Weibel et al., 2016). The fact that fly ash B requires approximately twice the amount of H_2O_2 is due to the large amount of metallic components (e.g. Al^0). In this fly ash the redox potential declined very rapidly after each H_2O_2 addition, as shown in Figure 4-7. The addition of hydrogen peroxide increased Cd recovery to 97% (fly ash A) and 94% (fly ash B). The depletion factor for Zn remained constant at values around 60-70%.

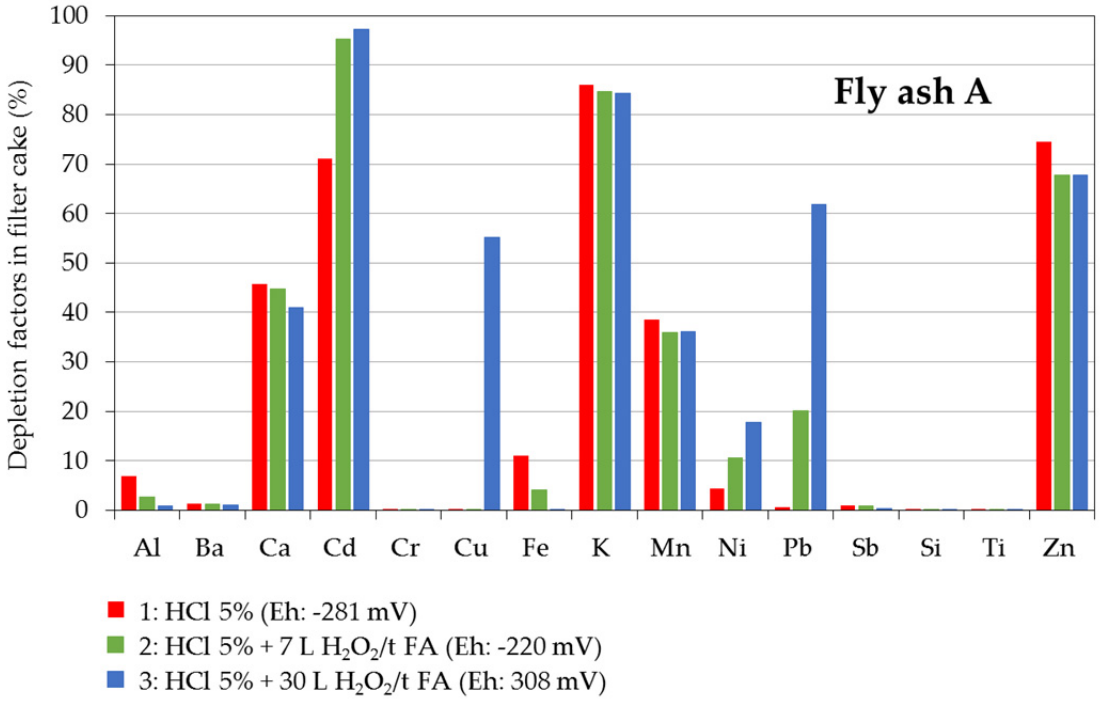

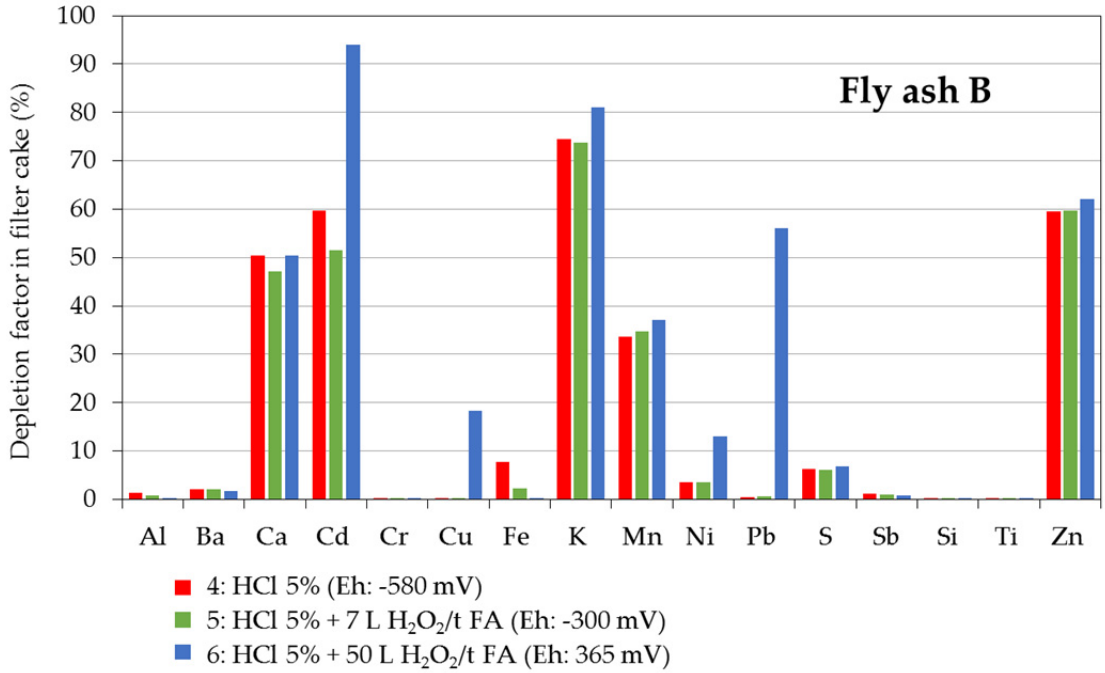

Figure 4-3: *Depletion factor in % of elements of interest in filter cake after leaching with HCl 5% (experiments 1 to 6): (red) without H_2O_2, (green) with the addition of 7L H_2O_2/t fly ash, (blue) with the addition of 30 L H_2O_2/t fly ash (fly ash A) and 50 L H_2O_2/t fly ash (fly ash B).*

4.3.2 Leaching with NaCl-solution

After drying at 50°C, the residual filter cakes from the HCl-experiments were leached in a subsequent step with concentrated NaCl-solution. The evaluation of the optimal leaching conditions with respect to NaCl-concentration, pH-value and temperature was performed using filter cake A (experiments 1-1 to 1-5, Table 4-7). The results show that NaCl-concentration of 300 g/L, a pH-value of 3.5 at 85°C lead to the best metal depletion factors. Therefore, all following experiments were performed under these conditions.

Influence of pH

NaCl-solution (300 g/L) has a pH of 5.7 and when mixed with the acidic leached filter cake from fly ash A, a temperature-independent equilibrium pH of 4.5 is observed. At a temperature of 85°C, 30% Cu and 76% Pb can be depleted from filter cake A by NaCl (experiment 1-1). The efficiency for Cd is increased from 71% to 100% and only Zn cannot be further depleted with NaCl. A more acidic NaCl-leaching (pH 3.5 and 2.5) results in comparable results for Cd and Zn (experiments 1-2 and 1-3). On the other hand, the mobilization of Cu and Pb is increased by approx. 20% under more acidic NaCl-leaching conditions by the addition of HCl 32%. The acidic conditions positively support the dissolution of Cu and Pb. Due to the elevated buffer capacity, considerably higher amounts of HCl 32% had to be used for filter cake B. Due to the elevated metal mobilization at pH 3.5 compared to 4.5, all the following NaCl-leaching experiments were carried out at pH 3.5.

Influence of concentration

It is known that Pb is predominantly present in the acidic leached filter cake as a $PbCu^0$-alloy, PbO and $PbCl_2$. For the mobilization of these solid phases, a high Cl-activity must be present in the leaching agent for the formation of increasingly complexed Pb-chloride-compounds. Experiments with 300 g/L and 150 g/L NaCl show that comparable depleteon factors are achieved for Cd, Cu and Zn at the varied ionic strength (Table 4-7). Only Pb shows significantly lower depletion (59%) compared to tests with twice the chloride concentration (89%). SEM analyses of the filter cake after the extraction with 150 g/L NaCl still show accumulations of the $PbCu^0$-alloy and rarely $PbCl_2$-phases. For the mobilization of the residual Pb, a high NaCl-concentration in the range of 300 g/L is required. Copper is less affine to the formation of chloride-complexes and the mobilization is controlled by the redox conditions (see Section 4.3.1).

Influence of temperature

The NaCl-leaching at 25°C already results in a significant mobilization of 92% Cd, 15% Cu, 59% Pb and 76% Zn (experiment 1-5). At elevated temperature (85°C), the dissolution of the metal phases is increased because both the solubility of $PbCl_2$ as well as the kinetics of the oxidation of the cementation phase ($PbCu^0$-alloy) is enhanced. This leads, especially for Cu and Pb, to significantly higher depletion factors (Cu 36%, Pb 89% at 85°C, Table

4-7). The high NaCl-concentration is crucial for high metal recovery. Just washing the filter cake with water at 85°C is not efficient to mobilize these metals as shown by preliminary tests.

Table 4-6: *Depletion factor in % of Cd, Cu, Pb and Zn in filter cake after leaching with HCl 5% and different amounts of H_2O_2. The last column shows the measured redox potential (mV, Ag/AgCl) of the ash slurry at the end of each experiment.*

Nr.	Sample	Leaching conditions	Cd	Cu	Pb	Zn	Eh
1	Fly ash A	HCl 5%, pH 2.5, 60°C	71	0	1	75	-281
2	Fly ash A	HCl 5%, pH 2.5, 60°C, 7 L H_2O_2/t FA	95	0	20	68	-220
3	Fly ash A	HCl 5%, pH 2.5, 60°C, 30 L H_2O_2/t FA	97	55	62	68	308
4	Fly ash B	HCl 5%, pH 2.5, 60°C	60	0	0	60	-580
5	Fly ash B	HCl 5%, pH 2.5, 60°C, 7 L H_2O_2/t FA	51	0	1	60	-300
6	Fly ash B	HCl 5%, pH 2.5, 60°C, 50 L H_2O_2/t FA	94	18	56	62	365

Table 4-7: *Depletion factor in % of Cd, Cu, Pb and Zn in filter cake after leaching with concentrated NaCl-solution. The results show the method development by varying the NaCl concentration, pH-value and leaching temperature. Filter cake A1 from the previous HCl-leaching is used for all tests.*

Nr.	Sample	Leaching conditions	Cd	Cu	Pb	Zn	Eh
1-1	Filter cake A1	NaCl 300 g/L, pH **4.5**, 85°C	100	30	76	76	210
1-2	Filter cake A1	NaCl 300 g/L, pH **3.5**, 85°C	100	36	89	77	200
1-3	Filter cake A1	NaCl 300 g/L, pH **2.5**, 85°C	100	40	89	77	200
1-4	Filter cake A1	NaCl **150 g/L**, pH 3.5, 85°C	100	40	59	77	210
1-5	Filter cake A1	NaCl 300 g/L, pH 3.5, **25°C**	92	15	59	76	315

Table 4-8: *Depletion factor in % of Cd, Cu, Pb and Zn in filter cake after leaching with concentrated NaCl-solution. Based on the results of the method development (Table 4-7), the following leaching conditions were determined as optimal and all further tests and repeat measurements were carried out under these conditions: NaCl 300 g/L, pH 3.5, 85°C.*

Nr.	Sample	Leaching conditions	Cd	Cu	Pb	Zn	Eh
1-2	Filter cake A1	NaCl 300 g/L, pH 3.5, 85°C	100	36	89	77	200
1-2	Filter cake A1		100	41	88	77	205
1-2	Filter cake A1		100	37	85	77	200
2-1	Filter cake A2		100	67	85	76	422
3-1	Filter cake A3		100	83	99	77	408
3-1	Filter cake A3		100	80	96	79	406
3-1	Filter cake A3		100	81	98	78	413
4-1	Filter cake B4	NaCl 300 g/L, pH 3.5, 85°C	88	0	18	67	-312
4-1	Filter cake B4		91	0	25	66	-312
4-1	Filter cake B4		92	1	32	68	-350
5-1	Filter cake B5		93	9	71	67	212
6-1	Filter cake B6		97	52	84	72	361
6-1	Filter cake B6		98	57	86	72	361
6-1	Filter cake B6		98	57	85	72	389

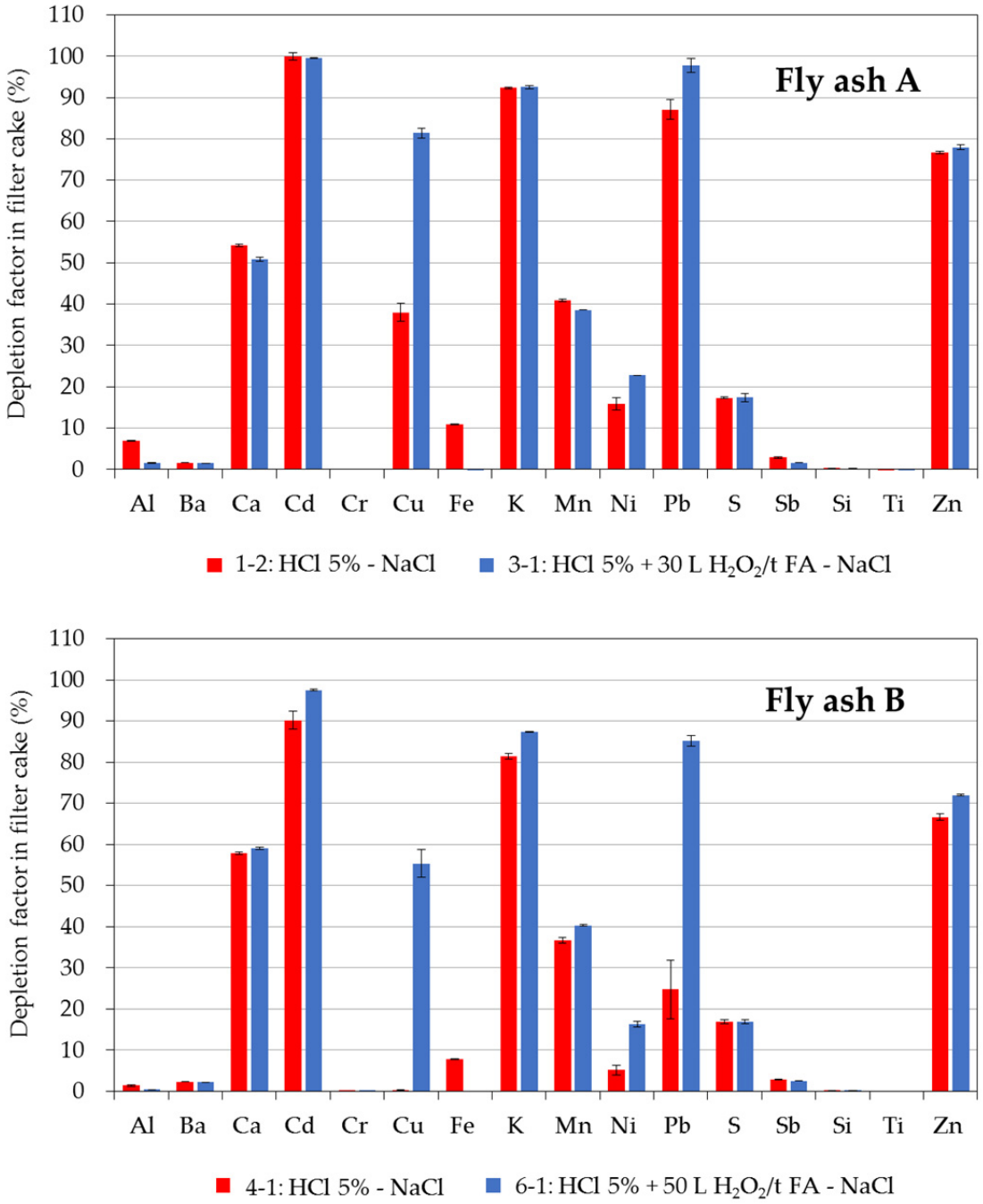

Figure 4-4: *Depletion factors in % of elements of interest in filter cake after NaCl-leaching: (red) NaCl-leaching of the filter cakes from the HCl-leaching without oxidizing agent, (blue) NaCl-leaching of the filter cakes from HCl-leaching with H_2O_2. The results represent mean values from triple determination and the error bars correspond to the standard deviation.*

Influence of redox potential

Leaching of fly ash A with HCl 5% (experiment 1) results in a strongly negative redox potential of -281 mV (Ag/AgCl) at the end of the experiment (Table 4-6, Figure 4-7). The drying of the filter cake at 50°C and the subsequent leaching with concentrated NaCl-solution (Eh-value of the NaCl-solution: 200 mV), however, leads to positive redox potentials during the entire leaching experiment (Eh: >200 mV, Figure 4-7). The values of the redox potential during the NaCl-leaching remain constant with changes in concentration and pH-value at 85°C. A significantly higher redox potential is measured for the same leaching conditions at 25°C, showing the strong influence of the temperature on the redox potential (experiments 1-1 to 1-5, Table 4-7). In addition to the high Cl-concentration and the formation of metal-chloride-complexes, the oxidative conditions during NaCl-leaching are mainly responsible for the large depletion of the redox-sensitive elements Cu and Pb. The drying in the laboratory oven at 50°C activates the surface of the metallic Al^0 particles by oxidation in the oven atmosphere. The metallic particles are then more easily accessible to oxidation during the subsequent NaCl-leaching. This leads to positive redox potentials and the mobilization of the cementation phases ($PbCu^0$-alloy) is promoted. SEM analyses show that the existing cementation phases in filter cake A are completely oxidized by the leaching with NaCl (Figure 4-5). The leaching of filter cake A with concentrated NaCl-solution results in a mean recovery from triple determination of 100% for Cd, 38% for Cu, 87% for Pb and 77% for Zn (Table 4-8, Figure 4-4).

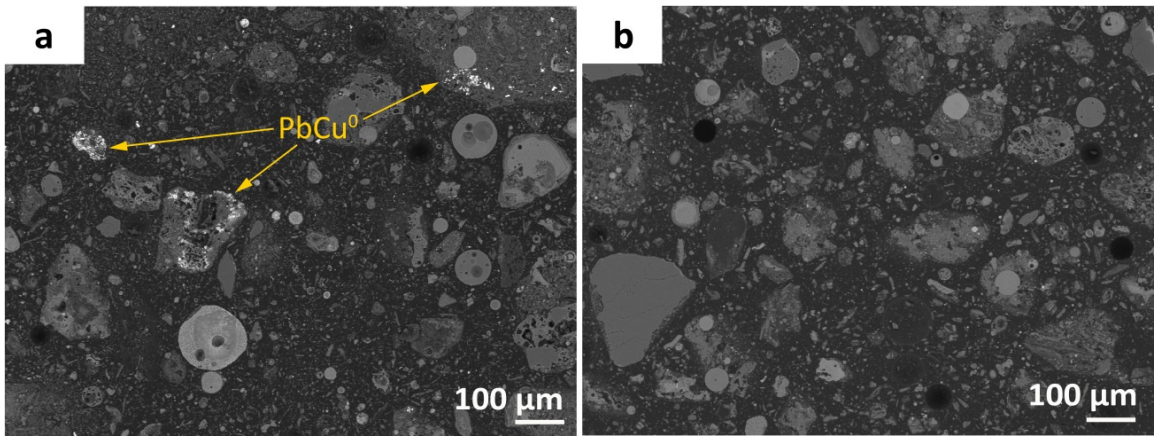

Figure 4-5: *(a) Cementation phase ($PbCu^0$-alloy) in filter cake A after leaching with HCl 5%, (b) complete oxidation and thereby mobilization of the $PbCu^0$-alloy after NaCl-leaching.*

The HCl-leaching of fly ash B (experiment 4) leads to a very negative redox potential of -580 mV, that leads to a doubling of the amount of H_2O_2 required for the oxidation of the metallic components compared to fly ash A (Figure 4-7). Drying of the filter cake in the laboratory oven and subsequent leaching with NaCl alone is not sufficient to keep sustainably oxidizing conditions. The Eh-value becomes negative after 20 minutes during the experiment (Eh: -312 mV, Table 4-8, Figure 4-7). The reducing conditions result in 0% Cu and <35% Pb being depleted (Table 4-8, Figure 4-4). The reason for the poor metal

depletion becomes obvious in the SEM investigations, where cementation phases and metallic Al^0 are still detectable after NaCl-leaching in filter cake B. The drying of the filter cake B in the laboratory oven and the subsequent NaCl-leaching leads only to a partial oxidation of the Al^0. The continuous oxidation of metallic particles during the entire NaCl-leaching is resulting in negative Eh-values (-312 mV, experiment 4-1). The influence of still present metallic Al^0 in the filter cake when performing NaCl-leaching can be very well explained by having a look to the filter cakes from HCl-leaching under partial oxidizing conditions (7 L H_2O_2/t fly ash, experiments 2 and 5). SEM analyses of filter cake B after NaCl-leaching still show large amounts of the $PbCu^0$-alloy, however, with a partial dissolution of the central Al^0 (Figure 4-6). Due to this partial dissolution of Al^0 and thus the elevated oxidizing conditions (fly ash A: 422 mV in experiment 2-1; fly ash B: 212 mV in experiment 5-1, Table 4-8) more Cu can be mobilized during the NaCl-leaching. In contrast, Pb can be depleted with NaCl even under less oxidizing conditions (Eh 200 mV, experiment 1-2).

Keeping oxidative conditions during the HCl-leaching by adding H_2O_2, already leads to a high recovery for Cd, Cu and Pb (experiments 3 and 6). By subsequent drying in the laboratory oven and leaching with NaCl, the redox potential of fly ash A can be maintained at values >400 mV (Figure 4-7), yielding depletion factors of approximately 100% for Cd and Pb and 80% for Cu and Zn (experiment 3-1, Table 4-8, Figure 4-4). In the case of fly ash B, the redox potential during the NaCl-leaching remains at values >350 mV and the recovery for the redox-sensitive elements Cu and Pb is slightly lower compared to fly ash A (Cd 98%, Cu 55%, Pb 85%, Zn 72%, experiment 6-1). This is primarily due to the generally lower metal contents present in fly ash B where relative depletion factors are more difficult to achieve.

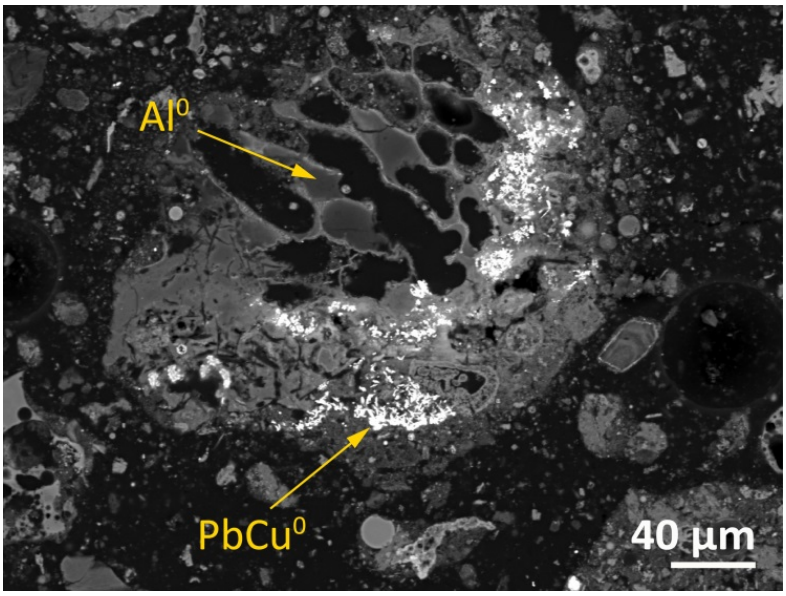

Figure 4-6: *Partially dissolved Al in filter cake A after HCl- (7 L H_2O_2/t fly ash) and NaCl-leaching (experiment 4-1).*

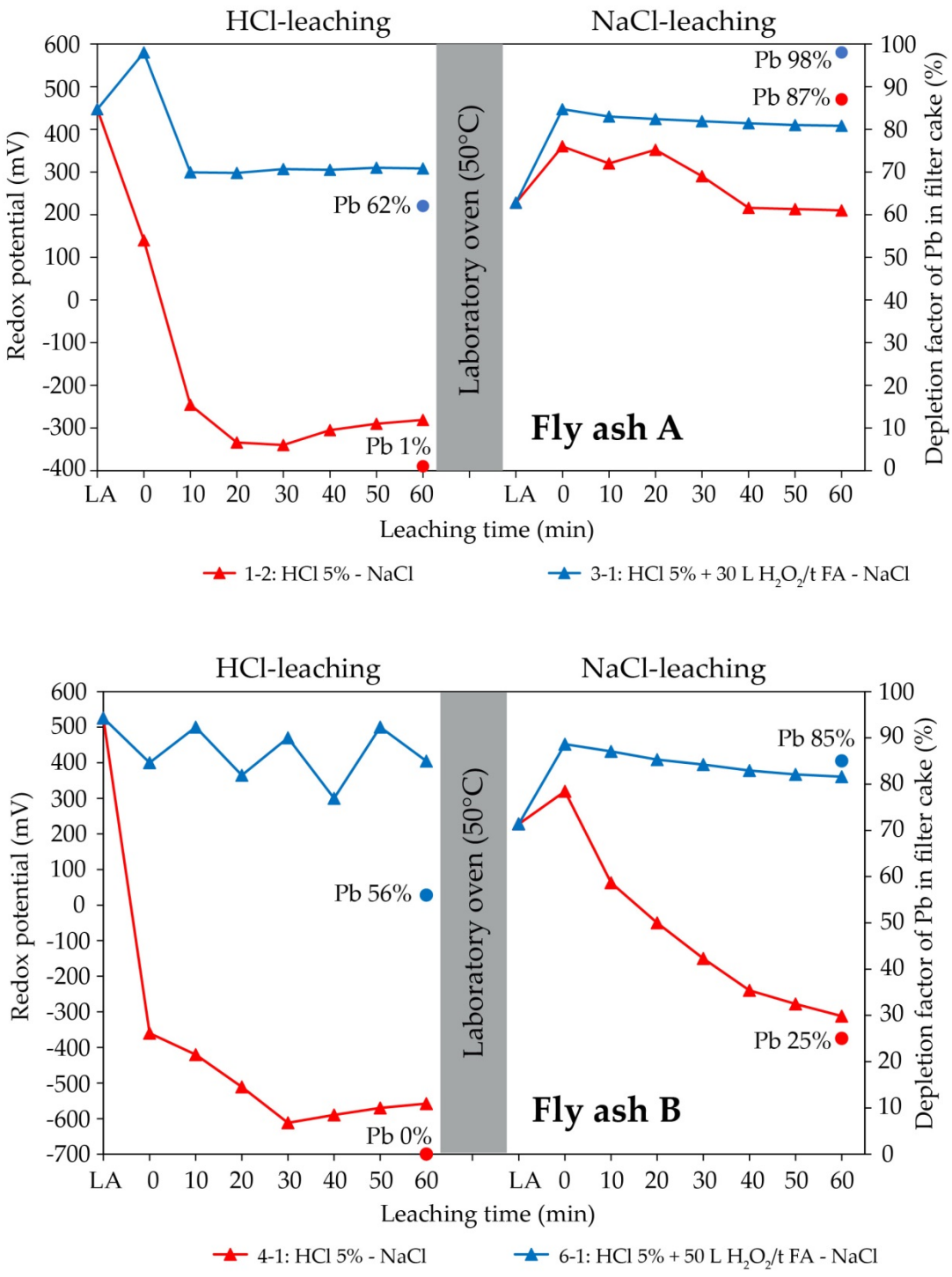

Figure 4-7: *Curve of the Eh-value (Ag/AgCl) without (red) and with (blue) addition of H_2O_2 during HCl-leaching at 60°C and subsequent NaCl-leaching at 85°C. The dots show the depletion factor for Pb after each leaching step. LA = Initial redox potential of the leaching agent at 60°C (HCl-leaching) and 85°C (NaCl-leaching).*

Residual metal in filter cake

As could be shown, an almost complete mobilization of Cd and Pb occurs by a peroxide-supported HCl-leaching, followed by drying of the filter cake and leaching with NaCl-solution (Table 4-8, Figure 4-4). The recovery for Cu, on the other hand, is significantly lower with an average maximum of 81% (fly ash A) and 55% (fly ash B). This is related to the redox conditions and the binding form. Detailed SEM analysis of filter cake A shows that residual Cu is contained primarily in few µm-sized Ca-Al-Si-particles in filter cake A (Figure 4-8) after the entire leaching process (experiment 3-1). The Cu is often finely incorporated in particles and is generally associated with sulphur. Under the given leaching conditions, it is not possible to dissolve these aluminosilicates that clearly limit the mobilization of Cu.

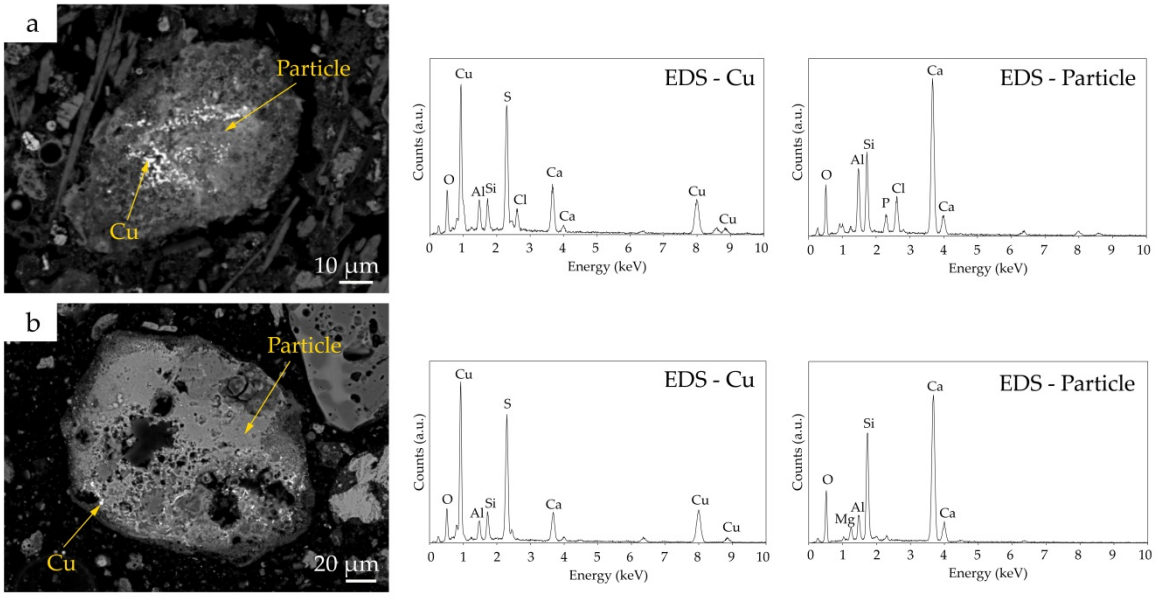

Figure 4-8: *Backscattered electron (BSE) images with elemental spectra of typical Cu-bearing phases and their host particles in filter cake A after leaching with HCl 5% and NaCl 300 g/L: (a, b) Cu associated with sulphur and surrounded by Ca-Al-Si-host particles.*

The mobilization of Zn is also limited by its binding form. The maximum amount of Zn that can be dissolved under the given conditions (70-80% depending on fly ash) is already mobilized during the HCl-leaching. The subsequent treatment with NaCl-solution does not lead to an increase in the recovery of Zn for both fly ashes. The remaining Zn (20-30%), that cannot be mobilized under the chosen conditions in fly ash A, are either bound in glassy particles (Figure 4-9a) or associated with iron (galvanized steel, Figure 4-9b) in the filter cake. The SEM analyses of filter cake B after the entire leaching process do not show remaining metal phases. This is explained by significantly lower metal contents present in fly ash B compared to fly ash A (Table 4-1).

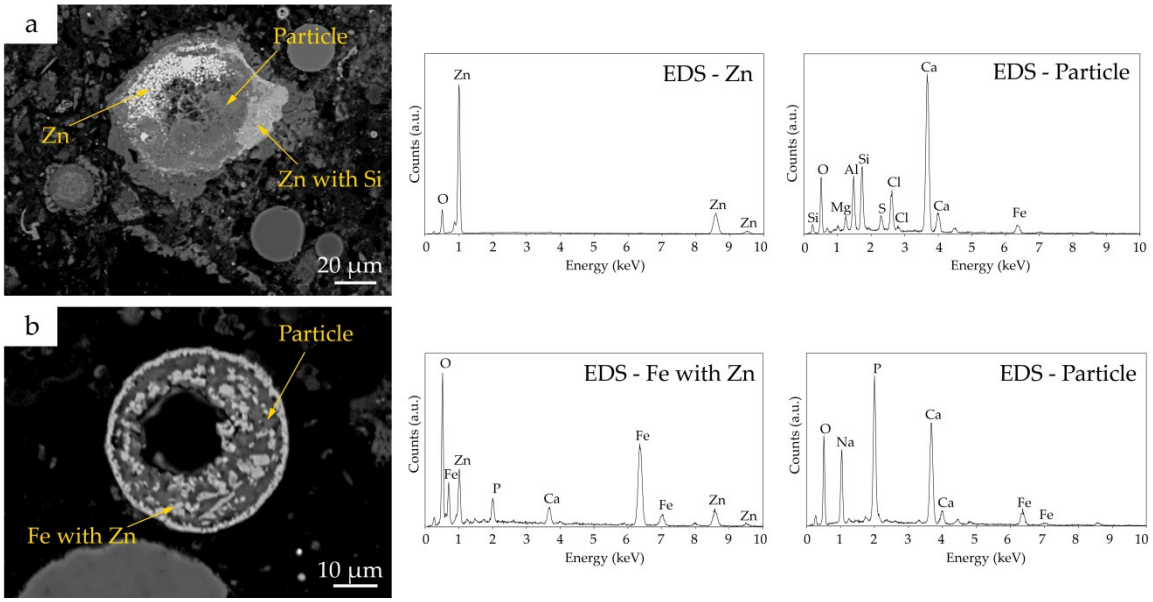

Figure 4-9: *Backscattered electron (BSE) images with elemental spectra of typical Zn-bearing phases and their host particles in filter cake A after leaching with HCl 5% and NaCl 300 g/L: (a) Zn bound in glassy particle, (b) Zn present together with Fe (galvanized steel).*

4.3.3 Metal speciation and saturation of solid phases in leaching solutions

Dissolved species

The speciation of the heavy metals Pb, Cu, Zn and Cd in leaching solution (filtrate) and the degree of saturation with respect to solid phases was calculated using the Gibbs free energy minimization program GEM-Selektor.

The calculated speciation of metal-chloride-complexes is independent of pH in acidic solutions (pH <6) and the distribution of metal-chloride-complexes is dominated by the amount of chloride, independent of the metal concentration present because chloride concentration is around two orders of magnitude higher. Identification of aqueous species in heavy-metal enriched filtrate (solution without washing water) at pH-value adjusted during fly ash leaching reveals the role of chlorine during metal mobilization. As an overall picture, the calculated changes in speciation show that Pb and Cd form strong chloride-complexes in the filtrate using HCl 5% and NaCl 300 g/L whereas Cu and Zn form weaker chloride-complexes (Table 4-10). A correlation of increasing leaching efficiency with increasing metal-chloride-complex formation can be seen comparing depletion factors (Figure 4-3 and Figure 4-4, Table 4-6, Table 4-7, Table 4-8) with aqueous species distributions (Table 4-10), but no general 1:1 correspondence is revealed. Other factors such as redox conditions and precipitation and dissolution kinetics of solids also play important roles in actually achieved depletion factors.

Lead speciation in HCl-filtrates from experiments 1 to 6 (~2.8 mol/L Cl) indicates predominance of the $PbCl_4^{2-}$-complex (~65%), followed by the $PbCl_3^-$-complex (~20%). The neutral $PbCl_2$-complex accounts for ~10% of total species (Table 4-10). Very high chloride concentrations (~5.6 mol/L Cl) as present in the filtrates using 300 g/L NaCl (experiments 1-1 to 6-1) show a shift towards an elevated percentage of the $PbCl_4^{2-}$-complex (~95%) and smaller amounts of the $PbCl_3^-$-complex (~5%) compared to the HCl-filtrates. Using 150 g/L NaCl for leaching (experiment 1-4) results in a Cl-concentration of 111'000 mg/L (3.1 mol/L) in the filtrate and thus comparable species distribution as in the filtrates from the HCl-experiments (82% $PbCl_4^{2-}$, 14.6% $PbCl_3^-$, 2.8% $PbCl_2$, 0.2% $PbCl^+$).

The results for Pb species obtained from modelling (Table 4-10) where compared with UV-VIS spectroscopy results from filtrate of experiment 3-1. Despite the high concentration of other ions (e.g. Ca^{2+}, K^+, SO_4^{2-}) in solution, a distinct absorption spectrum is obtained between 240 and 300 nm (Figure 4-10). The deconvolution of the absorption spectra by Gaussian peaks results in a dominance of highly complexed $PbCl_4^{2-}$ and $PbCl_3^-$ species (Table 4-9). Even without considering the higher molar absorptivity (ε) for $PbCl_4^{2-}$ compared to other species (see Section 4.2.6) the calculated ratio for $PbCl_3^-/PbCl_4^{2-}$ are higher compared to the modelled ones (Table 4-10).

The fact that the 1:4 chloride complex ($PbCl_4^{2-}$, λ_{max} 270.6 nm) is required to describe the absorbance spectrum of the filtrate solution from NaCl-leaching is a strong indication for its existence (see Section 4.2.6) and justifies its inclusion in the present thermodynamic model. The difference in the calculated ratios for $PbCl_3^-/PbCl_4^{2-}$ from UV-VIS spectroscopy data and the thermodynamic model may indicate a slight overestimation of the rather uncertain $PbCl_4^{2-}$ stability constant. However, further investigations would be necessary to clarify this point.

Table 4-9: *Parameters determined for Pb-chloride-complexes in filtrate from NaCl-leaching (experiment 3-1) between 240 and 300 nm.*

Species	λ_{max} (nm)	FWHM (nm)	Peak area	Peak height
$PbCl_2$	244.2	23.7	0.3	0.04
$PbCl_3^-$	260.7	23.4	3.2	0.15
$PbCl_4^{2-}$	270.6	18.9	13.6	0.70

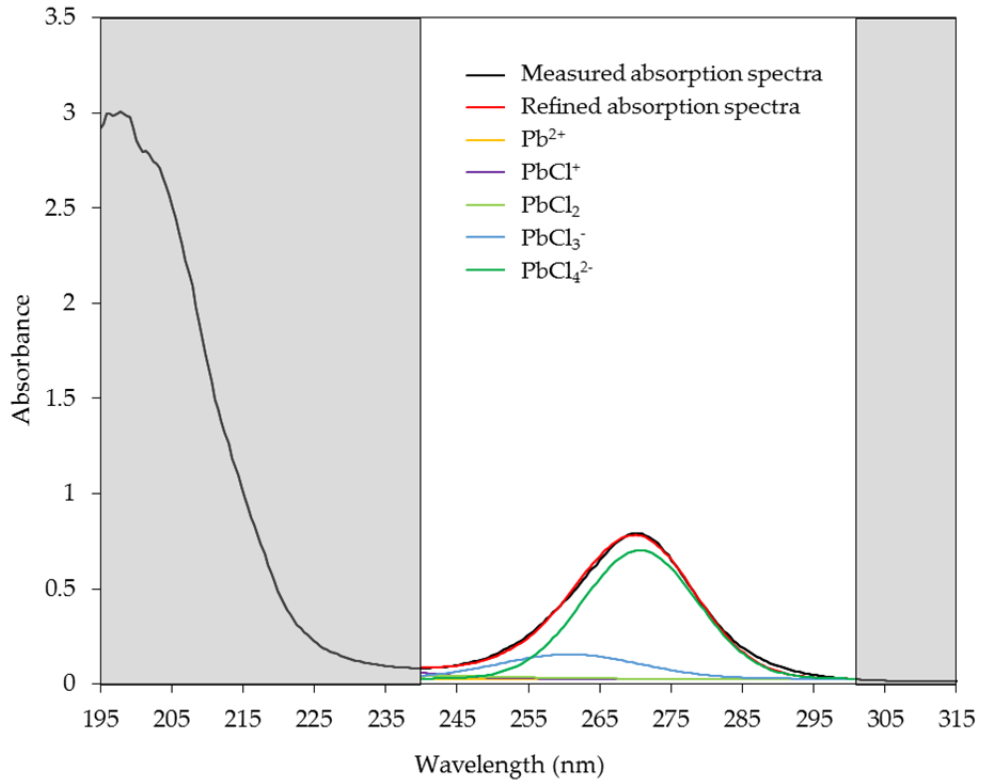

Figure 4-10: *Absorption spectrum of Pb-chloride-complexes at 25°C from filtrate of NaCl-leaching (experiment 3-1). The Pb speciation is derived from the observed spectrum using the characteristic absorption bands (Table 4-5). The peak deconvolution is only shown for the adsorption spectra between 240 and 300 nm. At wavelengths <240 nm the adsorption bands of Pb^{2+} and $PbCl^{+}$ cannot be clearly identified due to other absorbing components present in the filtrate.*

Cadmium shows similar percentage ratios of chloride-complexes as Pb with a dominance of $CdCl_4^{2-}$ and $CdCl_3^{-}$. This corresponds to similar depletion factors reached for Cd and Pb (under oxidizing conditions, Table 4-6 and Table 4-8). A more detailed look reveals that Pb depletion factors are always somewhat lower than Cd depletion factors. This may again indicate that the rather uncertain $PbCl_4^{2-}$ stability constant is slightly overestimated in the present thermodynamic model.

Calculated copper speciation in HCl-filtrates indicates the presence of significant amount of the free ionic form Cu^{2+}. The complexes $CuCl^{+}$ and $CuCl_2$ occur in similar percentages at this ionic strengths (~2.8 mol/L Cl). At higher chloride concentrations, when performing NaCl-leaching (~5.6 mol/L Cl), a shift to higher chloride-complexes is observed. This favorably corresponds to significantly higher depletion factors achieved for Cu (under oxidizing conditions) when higher chloride concentrations were applied in the leaching experiments, e.g. when comparing experiments 3 and 6 (Table 4-6) with experiments 3-1 and 6-1 (Table 4-8).

Zinc is predominantly present as $ZnCl_3^-$ in filtrates from HCl-leaching whereas the 1:4 chloride complex ($ZnCl_4^{2-}$) predominates in filtrates with elevated Cl-concentration (NaCl-leaching). These model results are in agreement with the overall picture that Zn depletion factors are found in between Cd and Cu depletion factors (Figure 4-3 and Figure 4-4). However, no significant increase in Zn depletion factors is observed with higher chloride concentrations as it was found in the case of Cu. This indicates that the rather uncertain $ZnCl_4^{2-}$ stability constant might be slightly overestimated in the present thermodynamic model, as further discussed in the following section considering precipitation of solids.

Table 4-10: *Total amount (mg/L) and proportion of aqueous species (%) of Pb, Cu, Zn and Cd in filtrate (solution without washing water) at pH-value adjusted during HCl- and NaCl-leaching.*

		HCl-leaching				NaCl-leaching					
Nr.		**1**	**3**	**4**	**6**	**1-1**	**1-2**	**1-4**	**3-1**	**4-1**	**6-1**
Leaching pH	-	2.5	2.5	2.5	2.5	4.5	3.5	3.5	3.5	3.5	3.5
Cl	mg/L	90'285	89'732	99'210	85'470	218'985	189'201	111'000	194'481	213'345	214'620
Pb	mg/L	18	2164	10	1'319	3'107	3'635	2'449	1552	484	783
Pb^{+2}	%	0.1	0.0	0.0	0.1	0.0	0.0	0.0	0.0	0.0	0.0
$PbCl^+$	%	1.9	1.4	0.9	2.4	0.0	0.0	0.2	0.0	0.0	0.0
$PbCl_2$	%	11.1	9.4	7.4	12.8	0.2	0.5	2.8	0.3	0.2	0.2
$PbCl_3^-$	%	23.5	21.8	19.6	24.8	4.2	6.5	14.6	5.1	4.4	4.4
$PbCl_4^{2-}$	%	63.4	67.4	72.1	59.9	95.6	93.0	82.3	94.6	95.4	95.4
Cd	mg/L	72	105	46	75	37	37	38	3	27	3
Cd^{+2}	%	0.0	0.0	0.0	0.1	0.0	0.0	0.0	0.0	0.0	0.0
$CdCl^+$	%	2.1	1.5	0.9	2.7	0.0	0.0	0.2	0.0	0.0	0.0
$CdCl_2$	%	14.8	12.3	9.3	17.0	0.2	0.4	3.3	0.2	0.2	0.2
$CdCl_3^-$	%	24.8	23.3	21.4	25.8	4.8	7.4	16.4	5.8	5.0	5.0
$CdCl_4^{2-}$	%	58.3	62.9	68.3	54.4	95.0	92.2	80.1	93.9	94.9	94.8
Cu	mg/L	1	407	1	95	481	586	658	229	1	203
Cu^{+2}	%	17.7	15.1	12.0	19.5	0.1	1.0	8.7	0.4	0.2	0.2
$CuCl^+$	%	41.0	38.6	35.2	42.2	1.9	8.9	36.8	4.0	2.1	2.2
$CuCl_2$	%	39.0	43.7	49.7	35.9	7.5	23.6	43.9	13.4	8.3	8.5
$CuCl_3^-$	%	1.0	1.3	2.0	0.8	42.9	40.3	8.2	43.9	43.3	43.4
$CuCl_4^{2-}$	%	0.1	0.1	0.3	0.1	47.5	26.2	1.8	38.3	46.1	45.6
$CuSO_4$	%	1.2	1.1	0.9	1.5	0.0	0.1	0.6	0.0	0.0	0.0
Zn	mg/L	13'366	13'013	6'826	7'300	429	562	479	2299	1'003	1'395
Zn^{+2}	%	6.2	4.3	2.4	8.0	0.0	0.0	1.1	0.0	0.0	0.0
$ZnCl^+$	%	8.2	6.4	4.5	9.6	0.0	0.2	3.2	0.1	0.0	0.0
$ZnCl_2$	%	17.5	15.4	12.7	18.9	0.6	2.2	13.2	1.1	0.6	0.6
$ZnCl_3^-$	%	64.7	70.0	75.3	60.4	10.8	25.8	60.2	16.7	11.7	11.8
$ZnCl_4^{2-}$	%	3.0	3.6	4.9	2.5	88.6	71.8	22.3	82.2	87.6	87.5
$ZnSO_4$	%	0.4	0.3	0.2	0.7	0.0	0.0	0.1	0.0	0.0	0.0

Precipitates in filtrates

The heavy-metal enriched filtrate from each experiment is usually mixed with washing water for further analysis (ratio 2:1). The washing water arises from the washing of the leached filter cake after filtration of the fly ash slurry. The high reactivity of fly ash and the elevated concentration of heavy metals result in an oversaturation of the filtrates with respect to several solid phases. For solution analysis, immediate measurement or strong dilution of the concentrated solution is therefore mandatory. Leaving the filtrate undisturbed, precipitation starts within hours after filtrate and washing water are mixed. Pseudoboleite ($Pb_5Cu_4Cl_{10}(OH)_8 \cdot 2H_2O$), an indigo blue hydrated chloride hydroxide containing Pb and Cu has been determined by XRD in precipitates of some filtrates (Table 4-11, Figure 4-11). Hence, pseudoboleite as well as other lead copper chloride hydroxides such as cumengite ($Pb_{21}Cu_{20}Cl_{42}(OH)_{40}$) and diaboleite ($CuPb_2Cl_2(OH)_4$), and the copper carbonate hydroxides azurite ($Cu_3(CO_3)_2(OH)_2$) and malachite ($Cu_2(CO_3)(OH)_2$), are included in the present thermodynamic model. The model calculations show that the saturation indices of all these solids strongly depend on pH, which is an obvious result as all solids contain OH^- as constituents, and azurite and malachite in addition CO_3^{2-} whose concentration also directly depends on pH. The filtrates diluted with washing water from the HCl-experiments using H_2O_2 of both fly ashes (experiments 3 and 6, Table 4-3) show a pH-value of 5.4 and are oversaturated with respect to azurite, cumengite, diaboleite, malachite and pseudoboleite (Table 4-11). Similar saturation indices are calculated for the NaCl-leaching experiments 1-1 (pH 5.4) and 1-4 (pH 5.2) (Table 4-11). In all these cases pseudoboleite has been determined by XRD as precipitate but none of the other solids. Filtrates from HCl-leaching experiments at pH <4.5 are strongly undersaturated with respect to all the above solids. Some NaCl-leaching experiments at pH ≤5 still show calculated oversaturation for cumengite and pseudoboleite. No precipitation of any of these solids has been determined by XRD.

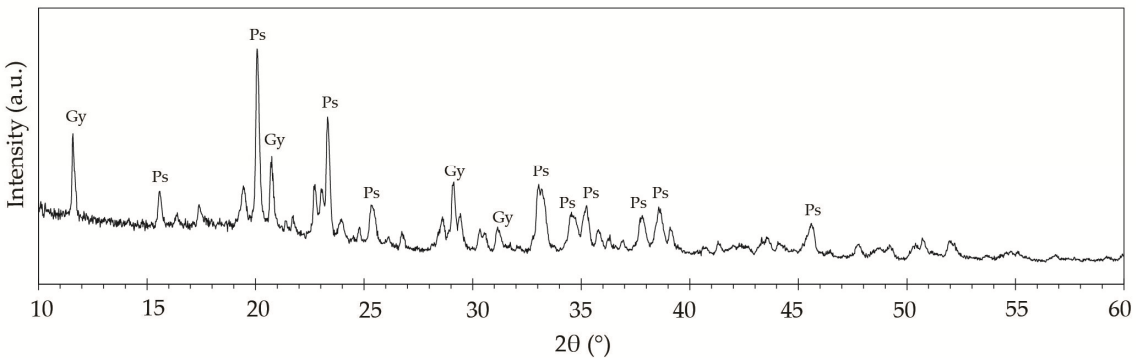

Figure 4-11: *XRD pattern of pseudoboleite (Ps) and gypsum (Gy) precipitated in filtrate 3, 6, 1-1 and 1-4. Only the main peaks of the specific minerals are labelled.*

Saturation indices of solids with different stoichiometries cannot be compared directly as the calculated values depend on the stoichiometry coefficients given in the formula of the solid. However, a ranking of over- and undersaturation of different solids with respect to a certain constituent is possible. For example, the relative oversaturation of the different lead copper chloride hydroxides with respect to lead can be calculated by re-norming the formulae of all solids to one Pb, i.e. by dividing the calculated SI values by the stoichiometry coefficients of Pb in the original formulae.

Re-norming the SI values of experiment 3 (Table 4-11) with respect to one Pb the recalculated SI values are 6.3, 1.0 and 6.6 for cumengite, diaboleite and pseudoboleite, respectively. Re-norming the SI values of experiment 3 with respect to one Cu results in 1.4, 5.0, 2.0, 2.0 and 8.3 for azurite, cumengite, diaboleite, malachite and pseudoboleite, respectively. Similar values are obtained for the other experiments where pseudoboleite has been determined by XRD (experiments 6, 1-1 and 1-4, Table 4-11). In all cases, pseudoboleite is the most oversaturated solid with respect to Pb and Cu. It seems that this most oversaturated solid pseudoboleite overcomes the nucleation barrier first and starts precipitating. Later, when the precipitating pseudoboleite decreases the concentration of dissolved Pb and Cu, the other solids become undersaturated and pseudoboleite remains the only thermodynamically stable solid in these systems. As mentioned, some NaCl-leaching experiments at pH ≤5 still show calculated oversaturation for cumengite and pseudoboleite (experiments 1-2, 1-4 and 6-1, Table 4-11). Re-norming the SI values to one Pb results in 2.2-2.9 for cumengite and 3.2-3.8 for pseudoboleite. It seems that these much lower oversaturations do not allow to overcome nuleation barriers and no precipitate is found by XRD.

The HCl-filtrates are further calculated to be slightly oversaturated with respect to zincite (ZnO), however, only goslarite ($ZnSO_4 \cdot 7H_2O$) is determined structurally as a precipitate in HCl-filtrate 1 and 4. But goslarite is always significantly undersaturated according to the present thermodynamic model and no precipitate would be expected according to these calculations. A first suspicion was that the thermodynamic data of goslarite, taken from Robie et al. (1979), might be in error. A recent experimental determination of the goslarite-bianchite equilibrium, $ZnSO_4 \cdot 7H_2O \Leftrightarrow ZnSO_4 \cdot 6H_2O + H_2O(g)$, by Chou & Seal (2005) resulted in $\Delta G_r° = 9634 \pm 56$ J/mol (uncertainty presumably 1σ). The value $\Delta G_r° = 9698$ J/mol calculated from data listed by Robie et al. (1979) is consistent with the new determination of Chou & Seal (2005) and hence, $\Delta G_f°$ of goslarite given by Robie et al. (1979) is most probably correct. A possible explanation of the discrepancy between structurally determined goslarite in some experiments and its generally calculated significant undersaturation could be slight overestimations of the rather uncertain $ZnCl_4^{2-}$ stability constant estimated in this study and the also uncertain $ZnCl_3^-$ stability constant judged as "provisional" by Powell et al. (2013).

The HCl-filtrates without the addition of H_2O_2 (experiments 1 and 4) show an orange precipitation of amorphous ferrihydrite whereas HCl-filtrates with H_2O_2 (experiments 3 and 6) have no Fe-precipitation. Under oxidizing conditions, Fe is present as Fe^{3+} and immediately precipitates as amorphous Fe^{3+}-hydroxide in the residual filter cake during leaching and is removed from the solution ($Fe^{3+} + 3\ OH^- \rightarrow Fe(OH)_3$). Additionally, the washing step after filtration mobilizes significant amounts of Ca^{2+} and SO_4^{2-} from the residual filter cake and precipitates as gypsum ($CaSO_4 \cdot 2H_2O$) in the filtrate. In all cases the thermodynamic model predicts saturation (Table 4-11, HCl-leaching) or values very close to saturation (Table 4-11, NaCl-leaching).

Table 4-11: *Saturation indices (SI) of mineral phases in filtrates mixed with washing water (ca. 2:1) after fly ash leaching with HCl and NaCl determined by GEM-Selektor. Precipitates in filtrates are determined by XRD. Gy: gypsum, Gs: goslarite, Ps: Pseudoboleite; Ha: Halite, n.d. not determined.*

Mineral name	**Formula**	**HCl-leaching**				**NaCl-leaching**					
Nr.		**1**	**3**	**4**	**6**	**1-1**	**1-2**	**1-4**	**3-1**	**4-1**	**6-1**
Precipitates determined by XRD		Gy, Gs	Ps, Gy	Gy, Gs	Ps, Gy	Ps, Gy	Gy, Ha	Ps, Gy	Gy, Ha	Gy	Gy
Solution pH (filtrate + washing water)		4.2	5.4	4.3	5.4	5.4	4.3	5.2	4.5	4.7	5.0
Anglesite	$PbSO_4$	-2.6	-0.6	-3.1	-0.5	-3.1	-3.1	-0.9	-3.5	-4.0	-3.8
Anhydrite	$CaSO_4$	-0.1	0.1	0.1	0.0	-0.6	-0.7	-0.5	-0.6	-0.7	-0.7
Azurite	$Cu_3(CO_3)_2(OH)_2$	-23	4.1	-22	2.5	6.9	-3.6	2.7	-2.6	-22	0.0
Calcite	$CaCO_3$	-6.0	-3.4	-5.5	-3.5	-3.8	-6.2	-4.7	-5.7	-5.7	-4.8
Cerussite	$PbCO_3$	-7.3	-2.8	-7.5	-2.7	-5.1	-7.4	-3.8	-7.3	-7.7	-6.6
Cotunnite	$PbCl_2$	-2.3	-0.3	-2.7	-0.4	-1.5	-1.4	-0.6	-1.8	-2.2	-2.0
Cumengite	$Pb_{19}Cu_{24}Cl_{42}(OH)_{44}$	-134	119	-133	103	120	43	103	41	-119	56
Diaboleite	$Pb_2CuCl_2(OH)_4$	-14	2.0	-14	1.5	-0.6	-6.3	0.2	-6.3	-13	-5.0
Ferrihydrite	$Fe_{10}O_{14}(OH)_2$	1.2	1.0	1.3	-3.2	-3.3	-0.1	1.3	-4.7	0.0	0.4
Gibbsite	$Al(OH)_3$	0.8	3.6	0.6	3.2	1.9	-0.6	2.3	0.6	-0.3	1.4
Goslarite	$ZnSO_4 \cdot 7H_2O$	-3.5	-3.6	-6.6	-6.0	-4.0	-3.6	-6.4	-6.3	-4.9	-3.5
Gypsum	$CaSO_4 \cdot 2H_2O$	0.1	0.2	0.2	0.2	-0.5	-0.6	-0.3	-0.5	-0.6	-0.6
Halite	NaCl	-2.4	-2.3	-2.2	-2.4	-0.6	-0.6	-1.5	-0.6	-0.7	-0.7
Kaolinite	$Al_2Si_2O_5(OH)_4$	3.9	9.1	3.1	7.9	5.5	1.2	7.1	3.6	1.3	5.0
Laurionite	PbCl(OH)	-3.7	-0.5	-4.0	-0.5	-2.2	-3.3	-1.1	-3.5	-3.9	-3.3
Malachite	$Cu_2(CO_3)(OH)_2$	-14	3.9	-13	2.8	5.6	-1.3	2.9	-0.7	-13	1.1
Pseudoboleite	$Pb_5Cu_4Cl_{10}(OH)_8(H_2O)_2$	-14	33	-14	30	31	17	30	16	-11	19
Tenorite	CuO	-10	-0.9	-9.7	-1.4	0.0	-3.4	-1.4	-3.1	-9.4	-2.2
Zincite	ZnO	0.8	3.3	0.8	3.2	0.7	-1.6	1.3	-0.4	-0.8	0.2

4.4 Conclusion

This detailed laboratory study on different filter cakes from MSWI fly ash explores and defines the limits for heavy metal depletion with optimized leaching methods that have a potential for application at industrial scale.

The leaching of fly ash with HCl 5% and highly concentrated NaCl-solution shows an efficient combination for the mobilization of a high percentage of heavy metals from fly ash. Especially for Pb and Cd a very high depletion factor of ≥90% from both fly ash mixes is achieved. The efficient depletion of Pb is due to the combination of redox reactions and metal-chloride-complex formation. The oxidative leaching conditions using hydrogen peroxide ensure the oxidation of metallic particles in fly ash that supresses the reductive separation of dissolved Pb^{2+} and Cu^{2+} as $PbCu^0$-alloy on the surfaces of less noble metallic particles such as Al^0. This first leaching step using HCl 5% therefore results in a mobilization of 60% Pb. The residues remaining in the filter cake (predominantly Pb^0 and $PbCl_2$) can be effectively depleted with concentrated NaCl-solution in a subsequent leaching step. The Pb-phases in the filter cake react thereby with the Cl-ions from the highly concentrated NaCl-solution. The dissolved Pb^{2+} is forming Pb-chloride-complexes with increased chloride content ($PbCl_3^-$, $PbCl_4^{2-}$), which significantly increases the solubility of the metal. The existence of the 1:4 Pb-chloride-complex ($PbCl_4^{2-}$) in filtrates has been confirmed using UV-VIS spectroscopy.

HCl-leaching without or with insufficient oxidizing agent results in lower metal depletion factors due to the reductive separation and accumulation of cementation phases (e.g. $PbCu^0$-alloy) in the filter cake. This can be monitored by measuring the redox potential. By drying the acidic leached filter cake at 50°C, the metallic residues are activated by surface oxidation. These metallic residues oxidize easily during the subsequent NaCl-leaching, resulting in oxidative conditions already at the beginning of the experiment. The mobilization of Zn is limited to 70-80% by its binding form under the given HCl- and NaCl-leaching conditions.

At an industrial scale, the drying of the fly ash is hardly practical and taking the entire metallic load to a second leaching step seems economically questionable. Therefore, in the first extraction step, the metallic parts should be oxidized by sufficient oxidizing agent. For further optimization of the NaCl-leaching step as a potential supplement to the FLUWA method, further systematic tests with different NaCl-concentrations and extraction temperatures should be carried out in order to achieve economically and ecologically meaningful leaching conditions. A possible Cl-source for leaching offers the reuse of Cl-containing water from the waste water treatment in the FLUWA process.

Acknowledgements

The work presented in this paper was financed by the Office for Waste Management, Environmental Protection Agency of Canton Zürich (AWEL Zürich). We thank the MSWI plant operators for providing sample material and information about their fly ash leaching process. Analytical support by Christine Lemp, Priska Bähler, Wolfgang Zucha (University of Bern), Ivo Budde and Anna Zappatini (ZAR) is highly acknowledged.

References

Abdul-Samad, F.A., Humphreys, D.A., Thomas, J.H., Williams, P.A., 1981. Chemical studies on the stabilities of boleite and pseudoboleite Mineralogical Magazine 44, 101-104.

AWEL, Office for Waste Management, Environmental Protection Agency of Canton Zürich (AWEL Zürich) 2013. Stand der Technik für die Aufbereitung von Rauchgasreinigungsrückständen (RGRR) aus Kehrichtverbrennungsanlagen.

Bühler, A., Schlumberger, S., 2010. Schwermetalle aus der Flugasche zurückgewinnen «Saure Flugaschewäsche – FLUWA-Verfahren» ein zukunftsweisendes Verfahren in der Abfallverbrennung. KVA-Rückstände in der Schweiz - Der Rohstoff mit Mehrwert (Federal Office for the Environment, FOEN), 185-192.

Byrne, R.H., Young, R.W., Miller, W.L., 1981. Lead chloride complexation using ultraviolett molar absorptivity characteristics. Journal of Solution Chemistry 10.

Chou, I.-M., Seal, R.R., 2005. Determination of goslarite–bianchite equilibria by the humidity-buffer technique at 0.1 MPa. Chemical Geology 215, 517-523.

Coelho, A., 2016. TOPAS-Academic V6. Coelho Software, Brisbane.

Demirkıran, N., Ekmekyapar, A., Künkül, A., Baysar, A., 2007. A kinetic study of copper cementation with zinc in aqueous solutions. International Journal of Mineral Processing 82, 80-85.

Fedorov, V.A., Kuznechikhina, M.A., Kan, I.V., 1979. Formation of mixed zinc halide complexes in aqueous solutions. Soviet Journal of Coordination Chemistry, 33-38.

Grenthe, I., Puigdomenech, I., 1997. Modelling in aquatic chemistry. NEA OECD, Paris, 724.

Hagemann, S., 1999. Thermodynamische Eigenschaften des Bleis in Lösungen der ozeanischen Salze, Gemeinsame Naturwissenschaftliche Fakultät. Technische Universität Carolo-Wilhelmina zu Braunschweig.

Hummel, W., 2009. Ionic strength corrections and estimation of SIT ion interaction coefficients, Paul Scherrer Institut.

Hummel, W., Berner, U., Curti, E., Pearson, F.J., Thoenen, T., 2002. Nagra/PSI chemical thermodynamic data base 01/01. Universal Publishers/uPUBLISH.com, USA, also published as Nagra Technical Report NTB 02-16, Wettingen, Switzerland.

Humphreys, D.A., Thomas, J.H., Williams, P.A., 1980. The chemical stability of mendipite, diaboleite, chloroxiphite, and cumengite, and their relationships to other secondary lead(II) minerals. Mineralogical Magazine 43, 901-904.

Iuliano, M., Porto, R., Vasca, E., 1989. Choride complexes of copper(II) and nickel(II) ions in 6m NaClO4. Annali di Chimica by Societa Chimica Italiana 79.

Karavasteva, M., 2005. Kinetics and deposit morphology of copper cementation onto zinc, iron and aluminium. Hydrometallurgy 76, 149-152.

Kulik, D., Wagner, T., Dmytrieva, S.V., Kosakowski, G., Hingerl, F.F., Chudnenko, K.V., Berner, U.R., 2013. GEM-Selektor geochemical modeling package: revised algorithm and GEMS3K nu-merical kernel for coupled simulation codes. Comput. Geosci. 17, 1-24.

Nadkarni, R.M., Jelden, C.E., Bowles, K.C., Flanders, H.E., Wadsworth, M.E., 1967. A kinetics study of copper precipitation on iron: part I. Transactions of the Metallurgical Society of AIME 239, 581-585.

Powell, K.J., Brown, P.L., Byrne, R.H., Gajda, T., Hefter, G., Leuz, A.-K., Sjöberg, S., Wanner, H., 2009. Chemical speciation of environmentally significant metals with inorganic ligands. Part 3: The Pb^{2+} + OH^-, Cl^-, CO_3^{2-}, SO_4^{2-}, and PO_4^{3-}-systems (IUPAC Technical Report). Pure Appl. Chem. 81, 2425-2476.

Powell, K.J., Brown, P.L., Byrne, R.H., Gajda, T., Hefter, G., Leuz, A.-K., Sjöberg, S., Wanner, H., 2011. Chemical speciation of environmentally significant metals with inorganic ligands. Part 4: The Cd^{2+} + OH^-, Cl^-, CO_3^{2-}, SO_4^{2-}, and PO_4^{3-}-systems (IUPAC Technical Report). Pure Appl. Chem. 83, 1163-1214.

Powell, K.J., Brown, P.L., Byrne, R.H., Gajda, T., Hefter, G., Leuz, A.-K., Sjöberg, S., Wanner, H., 2013. Chemical speciation of environmentally significant metals with inorganic ligands. Part 5: The Zn^{2+} + OH^-, Cl^-, CO_3^{2-}, SO_4^{2-}, and PO_4^{3-}-systems (IUPAC Technical Report). Pure Appl. Chem. 85, 2249-2311.

Powell, K.J., Brown, P.L., Byrne, R.H., Gajda, T., Hefter, G., Sjöberg, S., Wanner, H., 2007. Chemical speciation of environmentally significant metals with inorganic ligands: Part 2: The Cu^{2+} + OH^-, Cl^-, CO_3^{2-}, SO_4^{2-}, and PO_4^{3-}-systems (IUPAC Technical Report). Pure Appl. Chem. 79, 895-950.

Raghavan, R., Mohanan, P.K., Patnaik, S.C., 1998. Innovative processing technique to produce zinc concentrate from zinc leach residue with simultaneous recovery of lead and silver. Hydrometallurgy 48, 225-237.

Raghavan, R., Mohanan, P.K., Swarnkar, S.R., 2000. Hydrometallurgical processing of lead-bearing materials for the recovery of lead and silver as lead concentrate and lead metal. Hydrometallurgy 58, 103-116.

Ramette, R.W., 1986. Copper(II) complexes with chloride ion. Inorganic Chemistry 25, 2481-2482.

Robie, R.A., Hemingway, B.S., Fisher, J.R., 1979. Thermodynamic properties of minerals and related substances at 298.15 K and 1 Bar (105 Pascals) pressure and at higher temperatures, U.S. Geological Survey Bulletin, United States Government Printing Office, Washington.

Ruşen, A., Sunkar, A.S., Topkaya, Y.A., 2008. Zinc and lead extraction from Çinkur leach residues by using hydrometallurgical method. Hydrometallurgy 93, 45-50.

Schlumberger, S., Schuster, M., Ringmann, S., Koralewska, R., 2007. Recovery of high purity zinc from filter ash produced during the thermal treatment of waste and inerting of residual materials. Waste Management & Research 25, 547-555.

Seward, T.M., 1984. The formation of lead(II) chloride complexes at 300°C: a spectrophotometric study. Geochimica et Cosmochimica Acta 48, 121-134.

Shock, E.L., Sassani, D.C., Willis, M., Sverjensky, D.A., 1997. Inorganic species in geologic fluids: Correlations among standard molal thermodynamic properties of aqueous ions and hydroxide complexes. Geochimica et Cosmochimica Acta 61, 907-950.

Sinadinovic, D., Kamberovic, Z., Sutic, A., 1997. Leaching kinetics of lead from lead (II) sulphate in aqueous calcium chloride and magnesium chloride solutions. Hydrometallurgy 47, 137-147.

Stefanowicz, T., Osinska, M., Napieralska-Zagozda, 1997. Copper recovery by the cementation method. Hydrometallurgy 47, 69-90.

Swiss Confederation, 2016. Verordnung über die Vermeidung und die Entsorgung von Abfällen (VVEA). 1-46.

Thoenen, T., Hummel, W., Berner, U., Curti, E., 2014. Thd PSI/Nagra chemical thermodynamic database 12/07. PSI Bericht Nr. 14-04 (ISSN 1019-0663), Paul Scherrer Institute, Villigen.

Turan, M.D., Altundogan, H.S., Tümen, F., 2004. Recovery of zinc and lead from zinc plant residue. Hydrometallurgy 75.

Vierling, F., 1971. Étude des équilibres de coordination entre les ions Pb2+ et Cl par spectrophotometrie dans l´ultraviolet. Bull. Soc. chim. France, 25-29.

Wagner, T., Kulik, D., Hingerl, F.F., Dmytrieva, S.V., 2012. GEM-Selektor geochemical modeling package: TSolMod library and data interface for multicomponent phase models. Can. Mineral. 50, 1173-1195.

Weibel, G., Eggenberger, U., Schlumberger, S., Mäder, U.K., 2017. Chemical associations and mobilization of heavy metals in fly ash from municipal solid waste incineration. Waste Management 62, 147-159.

ZAR, Zentrum für nachhaltige Abfall- und Ressourcennutzung, 2016. SwissZinc - nationale Anlage zur Verwertung von KVA-Hydroxidschlämme (Project Fact Sheet No. 2), https://zar-ch.ch /fileadmin/user_upload/Contentdokumente/Oeffentliche _Dokumente/Projektblatt_SwissZinc_Nr2.pdf.

Appendix 4

Table A4-1: *Thermodynamic data of dissolved species and solids of Pb, Cu, Zn and Cd added to the PSI/Nagra thermodynamic database 12/07. The activity coefficients of aqueous species were computed with the SIT interaction parameters (ε).*

Name	Reaction	$\log_{10}K°$	$\Delta G°_f$ (J/mol)	Name	ε
Dissolved species					
$PbOH^+$	$Pb^{2+} + H_2O(l) \rightarrow PbOH^+ + H^+$	-7.46	-218'492	$\varepsilon(PbOH^+, ClO_4^-)$	-0.05
$Pb(OH)_2(aq)$	$Pb^{2+} + 2\,H_2O(l) \rightarrow Pb(OH)_2(aq) + 2\,H^+$	-16.94	-164'381	$\varepsilon(Pb(OH)_2, Na^+, ClO_4^-)$	-0.26
$Pb(OH)_3^-$	$Pb^{2+} + 3\,H_2O(l) \rightarrow Pb(OH)_3^- + 3\,H^+$	-28.03	-338'261	$\varepsilon(Pb(OH)_3^-, Na^+)$	-0.01
$Pb_3(OH)_4^{2+}$	$3\,Pb^{2+} + 4\,H_2O(l) \rightarrow Pb_3(OH)_4^{2+} + 4\,H^+$	-23.01	-889'063	$\varepsilon(Pb_3(OH)_4^{2+}, ClO_4^-)$	-0.50
$Pb_4(OH)_4^{4+}$	$4\,Pb^{2+} + 4\,H_2O(l) \rightarrow Pb_4(OH)_4^{4+} + 4\,H^+$	-20.57	-926'882	$\varepsilon(Pb_4(OH)_4^{4+}, ClO_4^-)$	-0.15
$Pb_6(OH)_8^{6+}$	$6\,Pb^{2+} + 8\,H_2O(l) \rightarrow Pb_6(OH)_8^{4+} + 8\,H^+$	-42.89	-1'795'992	$\varepsilon(Pb_6(OH)_8^{4+}, ClO_4^-)$	-0.63
Pb_2OH^{3+}	$2\,Pb^{2+} + H_2O(l) \rightarrow Pb_2OH^{3+} + H^+$	-7.28	-243'410	$\varepsilon(Pb_2OH^{3+}, ClO_4^-)$	0.27
$PbCl^+$	$Pb^{2+} + Cl^- \rightarrow PbCl^+$	1.50	-163'743	$\varepsilon(PbCl^+, ClO_4^-)$	0.04
$PbCl_2(aq)$	$Pb^{2+} + 2\,Cl^- \rightarrow PbCl_2(aq)$	2.10	-298'458	$\varepsilon(PbCl_2, Na^+, ClO_4^-)$	-0.05
$PbCl_3^-$	$Pb^{2+} + 3\,Cl^- \rightarrow PbCl_3^-$	2.00	-429'177	$\varepsilon(PbCl_3^-, Na^+)$	-0.08
$PbCl_4^{2-}$	$Pb^{2+} + 4\,Cl^- \rightarrow PbCl_4^{2-}$	1.46	-557'385	$\varepsilon(PbCl_4^{2-}, Na^+)$	-0.10
$PbCO_3(aq)$	$Pb^{2+} + CO_3^{2-} \rightarrow PbCO_3(aq)$	6.45	-588'690	$\varepsilon(PbCO_3, Na^+, ClO_4^-)$	-0.51
$Pb(CO_3)_2^{2-}$	$Pb^{2+} + 2CO_3^{2-} \rightarrow Pb(CO_3)_2^{2-}$	10.13	-1'137'678	$\varepsilon(Pb(CO_3)_2^{2-}, Na^+)$	-0.20
$PbHCO_3^+$	$Pb^{2+} + HCO_3^- \rightarrow PbHCO_3^+$	1.86	-621'448	$\varepsilon(PbHCO_3^+, ClO_4^-)$	0.00
$Pb(CO_3)OH^-$	$Pb^{2+} + CO_3^{2-} + OH^- \rightarrow Pb(CO_3)OH^-$	10.90	-771'361	$\varepsilon(Pb(CO_3)OH^-, Na^+)$	0.29
$Pb(CO_3)Cl^-$	$Pb^{2+} + CO_3^{2-} + Cl^- \rightarrow Pb(CO_3)Cl^-$	6.47	-720'094	$\varepsilon(Pb(CO_3)Cl^-, Na^+)$	-0.19
$PbSO_4(aq)$	$Pb^{2+} + SO_4^{2-} \rightarrow PbSO_4(aq)$	2.72	-783'876	$\varepsilon(PbSO_4, Na^+, ClO_4^-)$	0.05
$CdOH^+$	$Cd^{2+} + H_2O(l) \rightarrow CdOH^+ + H^+$	-7.95	-269'459	$\varepsilon(CdOH^+, ClO_4^-)$	0.04
$Cd(OH)_2(aq)$	$Cd^{2+} + 2\,H_2O(l) \rightarrow Cd(OH)_2(aq) + 2\,H^+$	-20.19	-199'593	$\varepsilon(Cd(OH)_2, Na^+, ClO_4^-)$	0.00
$Cd(OH)_3^-$	$Cd^{2+} + 3\,H_2O(l) \rightarrow Cd(OH)_3^- + 3\,H^+$	-33.5	-360'802	$\varepsilon(Cd(OH)_3^-, Na^+)$	-0.05
$Cd(OH)_4^-$	$Cd^{2+} + 4\,H_2O(l) \rightarrow Cd(OH)_4^{2-} + 3\,H^+$	-47.28	-346'697	$\varepsilon(Cd(OH)_4^-, Na^+)$	0.20
Cd_2OH^{3+}	$2\,Cd^{2+} + H_2O(l) \rightarrow Cd_2OH^{3+} + H^+$	-8.73	-374'938	$\varepsilon(Cd_2OH^{3+}, ClO_4^-)$	0.56
$CdCl^+$	$Cd^{2+} + Cl^- \rightarrow CdCl^+$	1.98	-220'247	$\varepsilon(CdCl^+, ClO_4^-)$	0.12
$CdCl_2(aq)$	$Cd^{2+} + 2\,Cl^- \rightarrow CdCl_2(aq)$	2.64	-355'304	$\varepsilon(CdCl_2, Na^+, ClO_4^-)$	0.02
$CdCl_3^-$	$Cd^{2+} + 3\,Cl^- \rightarrow CdCl_3^-$	2.30	-484'654	$\varepsilon(CdCl_3^-, Na^+)$	-0.08
$CdCl_4^{2-}$	$Cd^{2+} + 4\,Cl^- \rightarrow CdCl_4^{2-}$	1.70	-612'519	$\varepsilon(CdCl_4^{2-}, Na^+)$	-0.10
$CdCO_3(aq)$	$Cd^{2+} + CO_3^{2-} \rightarrow CdCO_3(aq)$	4.40	-630'752	$\varepsilon(CdCO_3, Na^+, ClO_4^-)$	0.00
$Cd(CO_3)_2^{2-}$	$Cd^{2+} + 2\,CO_3^{2-} \rightarrow Cd(CO_3)_2^{2-}$	6.20	-1'169'009	$\varepsilon(Cd(CO_3)_2^{2-}, Na^+)$	-0.10
$CdHCO_3^+$	$Cd^{2+} + HCO_3^- \rightarrow CdHCO_3^+$	0.84	-669'390	$\varepsilon(CdHCO_3^+, ClO_4^-)$	0.00
$CdSO_4(aq)$	$Cd^{2+} + SO_4^{2-} \rightarrow CdSO_4(aq)$	2.36	-835'585	$\varepsilon(CdSO_4, Na^+, ClO_4^-)$	0.02
$Cd(SO_4)_2^{2-}$	$Cd^{2+} + 2\,SO_4^{2-} \rightarrow Cd(SO_4)_2^{2-}$	3.32	-1'585'524	$\varepsilon(Cd(SO_4)_2^{2-}, Na^+)$	0.10
$CuOH^+$	$Cu^{2+} + H_2O(l) \rightarrow CuOH^+ + H^+$	-7.95	-126'220	$\varepsilon(CuOH^+, ClO_4^-)$	-0.15
$Cu(OH)_2(aq)$	$Cu^{2+} + 2\,H_2O(l) \rightarrow Cu(OH)_2(aq) + 2\,H^+$	-16.20	-79'129	$\varepsilon(Cu(OH)_2, Na^+, ClO_4^-)$	0.14
$Cu(OH)_3^-$	$Cu^{2+} + 3\,H_2O(l) \rightarrow Cu(OH)_3^- + 3\,H^+$	-26.60	-256'948	$\varepsilon(Cu(OH)_3^-, Na^+)$	0.40
$Cu(OH)_4^-$	$Cu^{2+} + 4\,H_2O(l) \rightarrow Cu(OH)_4^{2-} + 4\,H^+$	-39.74	-181'944	$\varepsilon(Cu(OH)_4^{2-}, Na^+)$	0.19
Cu_2OH^{3+}	$2\,Cu^{2+} + H_2O(l) \rightarrow Cu_2OH^{3+} + H^+$	-6.40	-69'484	$\varepsilon(Cu_2OH^{3+}, ClO_4^-)$	0.54
$Cu_2(OH)_2^{2+}$	$2\,Cu^{2+} + 2\,H_2O(l) \rightarrow Cu_2(OH)_2^{2+} + 2\,H^+$	-15.00	-257'577	$\varepsilon(Cu_2(OH)_2^{2+}, ClO_4^-)$	0.29
$Cu_3(OH)_4^{2+}$	$3\,Cu^{2+} + 4\,H_2O(l) \rightarrow Cu_3(OH)_4^{2+} + 4\,H^+$	-21.10	-760'644	$\varepsilon(Cu_3(OH)_4^{4+}, ClO_4^-)$	0.33
$CuCl^+$	$Cu^{2+} + Cl^- \rightarrow CuCl^+$	0.83	-70'444	$\varepsilon(CuCl^+, ClO_4^-)$	0.30
$CuCl_2(aq)$	$Cu^{2+} + 2\,Cl^- \rightarrow CuCl_2(aq)$	0.60	-200'421	$\varepsilon(CuCl_2, Na^+, ClO_4^-)$	0.14
$CuCl_3^-$	$Cu^{2+} + 3\,Cl^- \rightarrow CuCl_3^-$	-1.87	-317'612	$\varepsilon(CuCl_3^-, Na^+)$	-0.05
$CuCl_4^{2-}$	$Cu^{2+} + 4\,Cl^- \rightarrow CuCl_4^{2-}$	-3.90	-437'315	$\varepsilon(CuCl_4^{2-}, Na^+)$	-0.10
$CuCO_3(aq)$	$Cu^{2+} + HCO_3^- \rightarrow CuCO_3(aq) + H^+$	-3.56	-501'035	$\varepsilon(CuCO_3, Na^+, ClO_4^-)$	-0.01
$Cu(CO_3)_2^{2-}$	$Cu^{2+} + 2\,HCO_3^{2-} \rightarrow Cu(CO_3)_2^{2-} + 2\,H^+$	-10.30	-1'049'503	$\varepsilon(Cu(CO_3)_2^{2-}, Na^+)$	0.34

Name	Reaction	$\log_{10}K°$	$\Delta G°_f$ (J/mol)	Name	ε
$CuHCO_3^+$	$Cu^{2+} + HCO_3^- \rightarrow CuHCO_3^+$	1.84	-531'859	$\varepsilon(CuHCO_3^+, ClO_4^-)$	0.46
$Cu(CO_3)OH^-$	$Cu^{2+} + CO_3^{2-} + OH^- \rightarrow Cu(CO_3)OH^-$	11.21	-683'655	$\varepsilon(Cu(CO_3)OH^-, Na^+)$	0.10
$CuSO_4(aq)$	$Cu^{2+} + SO_4^{2-} \rightarrow CuSO_4(aq)$	2.35	-692'289	$\varepsilon(CuSO_4, Na^+, ClO_4^-)$	0.15
$ZnOH^+$	$Zn^{2+} + H_2O(l) \rightarrow ZnOH^+ + H^+$	-8.96	-333'316	$\varepsilon(ZnOH^+, ClO_4^-)$	0.24
$Zn(OH)_2(aq)$	$Zn^{2+} + 2\ H_2O(l) \rightarrow Zn(OH)_2(aq) + 2\ H^+$	-17.82	-282'743	$\varepsilon(Zn(OH)_2, Na^+, ClO_4^-)$	0.25
$Zn(OH)_3^-$	$Zn^{2+} + 3\ H_2O(l) \rightarrow Zn(OH)_3^- + 3\ H^+$	-28.05	-461'532	$\varepsilon(Zn(OH)_3^-, Na^+)$	0.12
$Zn(OH)_4^{2-}$	$Zn^{2+} + 4\ H_2O(l) \rightarrow Zn(OH)_4^{2-} + 4\ H^+$	-40.41	-390'981	$\varepsilon(Zn(OH)_4^{2-}, Na^+)$	0.25
Zn_2OH^{3+}	$2\ Zn^{2+} + H_2O(l) \rightarrow Zn_2OH^{3+} + H^+$	-7.90	-486'643	$\varepsilon(Zn_2OH^{3+}, ClO_4^-)$	0.86
$ZnCl^+$	$Zn^{2+} + Cl^- \rightarrow ZnCl^+$	0.40	-280'850	$\varepsilon(ZnCl^+, ClO_4^-)$	0.24
$ZnCl_2(aq)$	$Zn^{2+} + 2\ Cl^- \rightarrow ZnCl_2(aq)$	0.69	-413'796	$\varepsilon(ZnCl_2, Na^+, ClO_4^-)$	0.21
$ZnCl_3^-$	$Zn^{2+} + 3\ Cl^- \rightarrow ZnCl_3^-$	0.48	-543'887	$\varepsilon(ZnCl_3^-, Na^+)$	0.17
$ZnCl_4^{2-}$	$Zn^{2+} + 4\ Cl^- \rightarrow ZnCl_4^{2-}$	-2.00	-661'021	$\varepsilon(ZnCl_4^{2-}, Na^+)$	-0.10
$ZnCO_3(aq)$	$Zn^{2+} + CO_3^{2-} \rightarrow ZnCO_3(aq)$	4.75	-702'372	$\varepsilon(ZnCO_3, Na^+, ClO_4^-)$	0.08
$Zn(CO_3)_2^{2-}$	$Zn^{2+} + 2\ CO_3^{2-} \rightarrow Zn(CO_3)_2^{2-}$	5.40	-1'234'064	$\varepsilon(Zn(CO_3)_2^{2-}, Na^+)$	-0.10
$ZnHCO_3^+$	$Zn^{2+} + HCO_3^- \rightarrow ZnHCO_3^+$	1.62	-743'464	$\varepsilon(ZnHCO_3^+, ClO_4^-)$	0.45
$Zn_2CO_3^{2+}$	$2\ Zn^{2+} + CO_3^{2-} \rightarrow Zn_2CO_3^{2+}$	4.04	-698'319	$\varepsilon(Zn_2CO_3^{2+}, ClO_4^-)$	0.00
$ZnSO_4(aq)$	$Zn^{2+} + SO_4^{2-} \rightarrow ZnSO_4(aq)$	2.30	-904'887	$\varepsilon(ZnSO_4, Li^+, ClO_4^-)$	0.27
$Zn(SO_4)_2^{2-}$	$Zn^{2+} + 2\ SO_4^{2-} \rightarrow Zn(SO_4)_2^{2-}$	3.20	-910'002	$\varepsilon(Zn(SO_4)_2^{2-}, Li^+)$	0.38
				$\varepsilon(H^+, ClO_4^-)$	0.14
				$\varepsilon(OH^-, Na^+)$	0.04
				$\varepsilon(Cl^-, Na^+)$	0.03
				$\varepsilon(HCO_3^-, Na^+)$	0.00
				$\varepsilon(CO_3^{2-}, Na^+)$	-0.08
				$\varepsilon(SO_4^{2-}, Na^+)$	-0.12
				$\varepsilon(Pb^+, ClO_4^-)$	0.15
				$\varepsilon(Cd^+, ClO_4^-)$	0.23
				$\varepsilon(Cu^{2+}, ClO_4^-)$	0.32
				$\varepsilon(Zn^{2+}, ClO_4^-)$	0.35
				$\varepsilon(Cl^-, Ca^{2+})$	0.14
				$\varepsilon(Cl^-, Mg^{2+})$	0.19
Solids					
Litharge	$PbO(s)(red) + 2\ H^+ \rightarrow Pb^{2+} + H_2O(l)$	12.62	-189'039		
Massicot	$PbO(s)(yellow) + 2\ H^+ \rightarrow Pb^{2+} + H_2O(l)$	12.90	-187'440		
Cotunnite	$PbCl_2(s) \rightarrow Pb^{2+} + 2Cl^-$	*-4.75*	-313'584		
Laurionite	$PbClOH(s) \rightarrow Pb^{2+} + Cl^- + OH^-$	-13.27	-236'524		
Cerrusite	$PbCO_3(s) \rightarrow Pb^{2+} + CO_3^{2-}$	-13.18	-627'105		
Hydrocerrusite	$Pb_3(CO_3)_2(OH)_2(s) + 2\ H^+ \rightarrow 3\ Pb^{2+} + 2\ H_2O(l) + 2\ CO_3^{2-}$	*-5.82*	-1'699'800		
Phosgenite	$Pb_2(CO_3)Cl_2(s) \rightarrow 2\ Pb^{2+} + CO_3^{2-} + 2\ Cl^-$	-9.93	-895'025		
Anglesite	$PbSO_4(s) \rightarrow Pb^{2+} + SO_4^{2-}$	-7.80	-812'873		
Otavite	$CdCO_3(s) + 2\ H^+ \rightarrow Cd^{2+} + H_2O(l) + CO_2(g)$	6.08	-666'148		
$Cd(OH)_2(s)$	$Cd(OH)_2(s) + 2\ H^+ \rightarrow Cd^{2+} + H_2O(l)$	13.72	-388'197		
Tenorite	$CuO(s) + 2H^+ \rightarrow Cu^{2+} + 2\ H_2O(l)$	7.64	-127'990		
$Cu(OH)_2(s)$	$Cu(OH)_2(s) + 2H^+ \rightarrow Cu^{2+} + 2\ H_2O(l)$	8.67	-268'949		
Malachite	$Cu_2CO_3(OH)_2(s) \rightarrow 2\ Cu^{2+} + CO_3^{2-} + 2\ OH^-$	-33.16	-931'803		
Azurite	$Cu_3(CO_3)_2(OH)_2(s) \rightarrow 3Cu^{2+} + 2CO_3^{2-} + 2\ OH^-$	-44.9	-1'476'798		
Smithsonite	$ZnCO_3(s) \rightarrow Zn^{2+} + CO_3^{2-}$	-10.93	-737'648		
Hydrozincite	$0.2\ Zn_5(CO_3)_2(OH)_6(s) + 2\ H^+ \rightarrow Zn^{2+} + 0.4\ CO_2(g) + 1.6\ H_2O$	9.07	-3'147'019		
ZnO(s)	$ZnO(s) + 2H^+ \rightarrow Zn^{2+} + H_2O(l)$	11.12	-353'263		
ε-$Zn(OH)_2(s)$	ε-$Zn(OH)_2(s) + 2H^+ \rightarrow Zn^{2+} + 2\ H_2O(l)$	11.38	-351'778		
Name	**Formula**		**$\Delta G°_f$ (J/mol)**		
Mendipite	$Pb_3O_2Cl_2$		-740'000 ± 20'000		
Paralaurionite	PbOHCl		-383'700		
Chloroxiphite	$Pb_3CuCl_2O_2(OH)_2$		-1'129'000 ± 20'000		
Cumengit	$Pb_{19}Cu_{24}Cl_{42}(OH)_{44}$		-15'163'000 ± 20'000		
Diaboleite	$Pb_2CuCl_2(OH)_4$		-1'160'000 ± 20'000		
Pseudoboleite	$Pb_5Cu_4Cl_{10}(OH)_8(H_2O)_2$		-3'705'400 ± 55'000		
Goslarite	$ZnSO_4 \cdot 7H_2O$		-2'562'652		
Zinkosite	$ZnSO_4$		-871'530		

Chapter 5

Influence of Sample Matrix on the Alkaline Extraction of Cr(VI) in Soils and Industrial Materials

Gisela Weibel, H. Niklaus Waber, Urs Eggenberger, Urs K. Mäder

Institute of Geological Sciences, University of Bern, Switzerland

Environmental Earth Sciences (2016) 75:548

Abstract

An accurate and efficient determination of the highly toxic Cr(VI) in solid materials is important to determine the total Cr(VI) inventory of contaminated sites and the Cr(VI) release potential from such sites to the environment. Most commonly, total Cr(VI) is extracted from solid materials following a hot alkaline extraction procedure (U.S. EPA method 3060A) where a complete release of water-extractable and sparingly soluble Cr(VI)-phase is achieved. This work presents an evaluation of matrix effects that may occur during the hot alkaline extraction and in the determination of the total Cr(VI) inventory of variably composed contaminated soils and industrial materials (cement, fly ash) and is compared to water-extractable Cr(VI) results. Method validation including multiple extractions and matrix spiking along with chemical and mineralogical characterization showed satisfying results for total Cr(VI) contents for most of the tested materials. However, unreliable results were obtained by applying method 3060A to anoxic soils due to the degradation of organic material and/or reactions with Fe^{2+}-bearing mineral phases. In addition, in certain samples discrepant spike recoveries have also to be attributed to sample heterogeneity. Separation of possible extracted Cr(III) by applying cation-exchange cartridges prior to solution analysis further show that under the hot alkaline extraction conditions only Cr(VI) is present in solution in measurable amounts, whereas Cr(III) gets precipitated as amorphous $Cr(OH)_{3(am)}$. It is concluded that prior to routine application of method 3060A to a new material type, spiking tests are recommended for

the identification of matrix effects. In addition, the mass of extracted solid material should to be well adjusted to the heterogeneity of the Cr(VI) distribution in the material in question.

5.1 Introduction

Chromium is a heavy metal of environmental concern at mining sites, industrial sites and waste deposits. Chromium occurs in two stable oxidation states in solid phases and dissolved in groundwater (Adriano, 1986; Rai et al., 1989). Whereas Cr(III) is only sparingly soluble, Cr(VI) is easily soluble as oxy-anion (mainly as chromate, CrO_4^{2-}), highly toxic and readily bioavailable (Adriano, 1986). The presence and concentration of Cr(VI) in effluents of contaminated sites depend on the site-specific processing of Cr compounds. For example, chromic acid (H_2CrO_4) discharged in metal processing activities (Baral, 2002; Wanner et al., 2012a) may quickly reach the subsoil and groundwater. Similarly, water-soluble dichromate compounds such as sodium dichromate ($Na_2Cr_2O_7$) and potassium dichromate ($K_2Cr_2O_7$) are produced during chromite ore processing (Burke et al., 1991; Farmer et al., 1999). This results in a variety of Cr(VI)-bearing mineral phases with different solubilities and dissolution kinetics in the subsurface of contaminated areas. For example, Burke et al. (1991) and Wanner et al. (2012a) report sparingly soluble crocoite ($PbCrO_4$), jarosite ($KFe_3((SO_4)_x(CrO_4)_{1-x})_2(OH)_6$) and chromatite ($CaCrO_4$) that have formed due to inappropriate handling, poor storage of chromic acid or during chemical manufacturing of chromate. In addition to abandoned industrial sites, present-day sources of Cr(VI) include cement, brick and by-products from municipal solid waste incineration (MSWI fly ash), all produced under oxidizing conditions at very high temperatures (Hills and Johansen, 2007; Leisinger et al., 2014). The strong redox control of the Cr system and the kinetically differently reacting secondary mineral phases with different solubilities renders the behaviour of Cr(VI) compounds in the environment complex and controlled by the site- and material-specific redox conditions (Bartlett and James, 1979; Christensen et al., 1994; Puls et al., 1999; Flury et al., 2009). This makes the estimation of the various Cr(VI) reservoirs and the assessment of the total Cr(VI) inventory and its release potential difficult (Wanner et al., 2012a). The potential of the Cr(VI) release from a contaminated site is often assessed by the amount of Cr(VI) that is extractable with water from the solid material. For example, in Switzerland threshold values for Cr(VI) concentrations in solid material of contaminated sites and waste deposits are defined by aqueous extraction with deionized water according to the Contaminated Sites Ordinance (CSO test) (Swiss Confederation, 1998) or the Technical Ordinance on Waste (TOW test) (Swiss Confederation, 1990, 2013) but no analytical method is prescribed for the determination of the total Cr(VI) inventory in the solid material. Extraction by water over a few hours does neither dissolve less soluble or kinetically slowly reacting Cr(VI)-bearing minerals nor does it capture any Cr(III) minerals that might get oxidized in the subsoil over long time periods (Adriano, 1986; Palmer and Puls, 1994; James, 1996).

The present study focuses on the determination the total Cr(VI) inventory of contaminated and industrial solid materials based on the U.S. EPA method 3060A (U.S. Environmental Protection Agency, 1996a). This method attempts a complete release of Cr(VI) from solid materials by extracting the water-extractable Cr(VI) in readily soluble mineral phases and the fraction of sparingly soluble Cr(VI) mineral phases, but without oxidizing possibly present Cr(III)-phases, under alkaline conditions and at elevated temperature. Up to present, method 3060A has been systematically tested to a limited degree for the effects of compositional differences in the matrix of Cr(VI) contaminated materials (Vitale et al., 1994). In order to extend the data basis and to allow better understanding of matrix effects and the chemical processes during extraction, a validation study of method 3060A was performed using different contaminated soils and industrial materials. Special emphasis is given on the presence of other redox-active compounds in the solid materials such as Fe, Mn, S, and total organic carbon (TOC). The study includes multiple extraction of the test materials, matrix spiking and uncertainty estimation accompanied by chemical and mineralogical characterization of the various solid materials. Additionally, the TOW test was performed to determine the water-extractable Cr(VI) fraction of each test material. The results of this study allow an assessment of the applicability and reliability of EPA method 3060A to a range of Cr(VI)-bearing solid materials of variable matrix compositions.

5.2 Materials and methods

5.2.1 Investigated materials

The solid materials used may be divided into two groups. The first group consists of Cr(VI) contaminated soil samples from three abandoned industrial sites at Niederglatt (ZH), Rivera (TI) and Thun (BE) located in different geological environments in Switzerland. The industrial buildings at Niederglatt (ZH) are located above a fluvial gravel aquifer of the Swiss Molasse Basin. The Cr(VI) contamination of the subsoil is related to chromic acid (H_2CrO_4) that was used in the production of the terpenoid camphor ($C_{10}H_{16}O$) until 1932. The two soil samples were obtained from the unsaturated zone (N1: 0.6-1 m depth) and the transition zone between the unsaturated and saturated zone (N2:1.3-1.9 m depth) from two different cores of a drilling campaign performed in 2010.

The former industrial site at Rivera (TI) is located in an environment of fluvioglacial gravel sediments that consists of crystalline and metamorphic rocks with intercalated lenses of organic-rich swamp and bog deposits (Wanner et al., 2012a). Here, the Cr(VI) contamination stems from the production of chromic acid between 1948 and 1960. In this process, chromite ($FeCr_2O_4$) was oxidized to Na_2CrO_4 and followed by extraction with H_2SO_4 (Wanner et al., 2012a). During the industrial activity chromic acid and H_2SO_4 were spilled and reached the subsoil. Two subsoil samples were obtained from different

cores (R1: 2.6-3.55 m depth and R2: 3.6-4.25 m depth) of a drilling campaign performed in 2009.

The decommissioned industrial complex at Thun (BE) is located above the fluvial gravel aquifer of the Aare river, which is composed of carbonate-rich clastic sediments with subordinate silty layers. The Cr(VI) contamination originates from periodic disposal of chromic acid, which was used for acid cleaning of copper alloy surfaces between 1895 and 1990 (Wanner et al., 2012b). Interaction between the disposed chromic acid residues and the aquifer material led to a cementation of the subsoil in the uppermost metres. The sample used in this study (T1, taken at the surface) was collected from this cemented rock, which forms the hotspot of the contamination.

The second group of materials used in this test series consists of two different industrial materials that are both known to contain some chromium. The first material consists of a non-reduced Portland cement sample (CEM 1 52.5N, VDZ) from Holcim Technology Ldt., Holderbank. The second material is a MSWI fly ash sample from the waste incinerator Zuchwil which is washed on site according to the FLUWA-process (Bühler and Schlumberger, 2010). The extraction tests were complemented using a standard reference material (NIST 2701) (Nagourney et al., 2008) to test the entire extraction and analytical procedure.

5.2.2 Analyses of solid material

Soil samples were dried at 40°C, homogenized and sieved prior to analysis. Alkaline extraction tests were conducted on the grain-size fraction <2 mm. An aliquot of 100 g of dried material of this grain-size fraction was milled to a grain size <2 μm using a disc mill for chemical and mineralogical analyses. The chemical composition of the solid materials were first semi-quantitatively analyzed by wavelength dispersive X-ray fluorescence analysis using a Philipps PW2400 spectrometer and UniQuant® software (Omega Data Systems, 2004). The analytical error for XRF measurements is ~0.2 wt.% (major elements) and ~20-30 mg/kg (Mn, S). The total Cr content, $Cr_{(tot)}$, was determined by ICP-OES (Varian 720-ES) after microwave assisted complete acidic digestions of the solid materials. Mineralogical investigations were performed by powder X-ray diffraction analysis (XRD) using a Panalytical CubiX^3 diffractometer with CuKα-radiation (λ=1.54Å) and the Panalytical Software High Score Plus. The mineralogical characterization is supplemented by scanning electron microscopy (SEM) and optical microscopy. A Zeiss EVO-50 XVP electron microscope coupled with an energy dispersive system (EDS) was used with an accelerating voltage of 20 kV and a spot size of 504 nm for backscattered electron (BSE) images. The total organic carbon (TOC) content was calculated from the total carbon (TC) and the total inorganic carbon (TIC) contents measured by a Stroehlein CS-Mat system on the combusted solid materials. Concentrations of Fe^{2+} were obtained by acidic digestions (mixture of HF 40% and H_2SO_4 98%) of the solid materials in an oxygen-free atmosphere and the digest solutions were analyzed by spectrophotometry (Varian Cary 50) after col-

oured-complex formation with 2,2-bipyridine. Loss on ignition (LOI) was determined by heating the samples to 1'050°C for 1.5 h, except for the fly ash which was heated to 600°C during 1.5 h.

5.2.3 Extraction procedures

Hot alkaline extraction of total Cr(VI) from the solid materials followed the method 3060A procedure (U.S. Environmental Protection Agency, 1996a). For the extraction 2.5 g dry material of a grain size of <2 mm were added to 50 mL of 0.28 mol/L Na_2CO_3/0.5 mol/L NaOH solution in a 250 ml round bottom flask and heated to 90-95°C for 60 minutes under continuous stirring. To prevent oxidation of Cr(III) during extraction, 400 mg $MgCl_2$ and 0.5 ml phosphate buffer (0.5 M K_2HPO_4/0.5 M KH_2PO_4) were added to the suspension. In contrast to the description given by method 3060A, the hot extract solutions were immediately filtered in their hot state in order to minimise any temperature-dependent redox and solubility processes possibly interfering with dissolved Cr. Filtration occurred with a pressure filtration device (0.45 μm) using argon gas. The reagents used were all of analytical grade and solutions were prepared with ultra-pure water. The redox potential (Eh), pH and temperature were monitored (Knick Portamess measurement devices) during the entire extraction process to investigate the different behaviour of the test materials during the hot alkaline extraction. Eh-values were measured using a Hamilton Oxytrode PTI 120 Pt-Ag/AgCl electrode. Measured values were later corrected relative to the standard hydrogen electrode (SHE) (Stumm and Morgan, 1996). The eluate test according to the Technical Ordinance on Waste (TOW test, Swiss Confederation, 1990) is performed by shaking 50 g of homogenized, dry material of a grain size <2 mm in 500 mL of deionized water during 24 hours with an end-over-end shaker. After extraction, the solution is filtered (0.45 μm) prior to Cr(VI) determination. No TOW test was performed for the standard reference material (NIST 2701) due to the limited amount of material available.

5.2.4 Analyses of extracts

Method 3060A gives a detailed description of the extraction procedure but does not prescribe the analytical quantification of Cr(VI) in the extract solutions. Therefore, two analytical methods described in the guidelines (Swiss Confederation, 2013) for the Cr(VI) determination in TOW extract solutions have been chosen for this study: spectrophotometry (U.S. Environmental Protection Agency, 1992) and cation-exchange cartridge separation prior to ICP-OES analysis.

Using spectrophotometry dissolved Cr(VI) is reacted with diphenylcarbazide (DPC) at pH 2 to produce a red-violet coloured Cr-DPC complex. Complexation was performed using a Spectroquant chromate test set (Merck, No. 1.14758) and absorption was measured at 540 nm using a Merck Pharo 100 spectrophotometer. The reported detection limit and analytical error based on multiple measurements of Cr(VI) standard solution

(Merck, No. 1.19780.05) is <0.05 mg/L and ±10% for Cr(VI), respectively. Alternatively, Cr(VI) was determined by Cr(III)-Cr(VI) separation using CHROMAFIX® PS-H^+ (M) cartridges (Macherey Nagel), followed by ICP-OES analysis (Varian 720-ES). The detection limit and analytical error of this method based on multiple measurements of certified standard solutions (Merck ICP Multi-element Standard CertiPur IV and X) is <0.001 mg/L and ±5% for $Cr_{(tot)}$. The application of such cartridges has been successfully applied to moderately mineralised groundwater samples by Ball and McCleskey (2003). The effectiveness of the cartridges was tested using pure Cr(III) and a mixed Cr(III)/Cr(VI) standard solutions prepared from $Cr(NO_3)_3$ and K_2CrO_4. The retention of Cr(III) in the cartridge was excellent for both standards with an average Cr(III) retention of about 99.9%. In contrast to the pure standard solutions, moderately mineralised groundwaters and TOW extract solutions, alkaline extract solutions are of higher ionic strength up to 1.3 mol/L. The high loads of Na^+ from the extraction agent (0.5 mol/L NaOH and 0.28 mol/L Na_2CO_3) and other components that were dissolved from the solid material during extraction may interfere with the separation efficiency of the cartridge. To inspect such possible interferences and to elaborate the optimal ionic strength of the solution, extract solutions from method 3060A were diluted to different degrees and spiked with 100 µg/L Cr(III) prior to cation-exchange separation. The ideal dilution for all samples was found to be ~1:50, at which no measurable Cr(III) passed through the cartridge.

5.2.5 Method validation

The application of method 3060A to solid matrices of different composition and the analysis of the extract solution was evaluated in order to understand the chemical processes that may take place during alkaline extraction of Cr(VI). The soil and industrial samples were extracted in replicates (precision) and the extract solutions were analyzed by ICP-OES with and without prior Cr-species separation. The replicate extractions aimed at detecting possible experimentally induced changes in the Cr-speciation related to the different material matrices and so to assess the general applicability and effectiveness of the method to a variety of solid matrices. The accuracy of method 3060A was determined by multiply extracting and analyzing the standard reference material NIST 2701 (National Institute of Standards & Technology, 2009). An uncertainty estimation of the entire process of the hot alkaline extraction was performed using data obtained from extraction of the standard reference material. To calculate the combined measurement uncertainty, the contribution of precision and accuracy were combined by Gaussian error propagation. Matrix effects that may affect the alkaline Cr(VI) extraction by the dissolution of specific compounds from the extracted substance and which would interfere with the extracted Cr by redox and/or complexation reactions were investigated by spiking the matrix with a known amount of Cr(VI) and/or Cr(III) before extraction. Water-extractable (K_2CrO_4) and water-insoluble ($PbCrO_4$) Cr(VI) spikes were used in order to confirm that all Cr(VI)-phases did dissolve and that no reduction of Cr(VI) took place during extrac-

tion. A quantitative recovery of the water-insoluble $PbCrO_4$ matrix spike would indicate that also sparingly soluble Cr(VI)-phases were dissolved under alkaline conditions. Spiking test were conducted by a standard addition with two different concentrations of water-extractable and water-insoluble Cr(VI) (detailed concentrations in Appendix 5, Table A5-1*Table*). In a first batch, the concentration equal to the total Cr(VI) concentration determined in the non-spiked materials was added to each material. In the second batch, twice the total Cr(VI) concentration was spiked in form of water-extractable and water-insoluble Cr(VI) prior to the hot alkaline extraction. For the potential oxidation of Cr(III), 50 and 100 mg/kg soluble Cr(III), added as $Cr(NO_3)_3$, was spiked to each material.

5.2.6 Geochemical modelling

Speciation and solubility calculations of chromium compounds in the hot alkaline extract solutions were calculated with the geochemical computer code PHREEQC (Parkhurst and Appelo, 2013) with the thermodynamic database WATEQ4 (Ball and Nordstrom, 1991). The latter was expanded observing internal consistency with the thermodynamic data for Cr-bearing aqueous species and mineral phases recommended by Ball and Nordstrom (1998).

5.3 Results and discussion

5.3.1 Sample characterization

For the subsoil materials the total Cr concentrations, $Cr_{(tot)}$, as determined by total digestion range from 1'400-11'000 mg/kg (Table 5-1). Total Cr(VI) concentrations in these soils as determined by hot alkaline extraction range from 40-300 mg/kg and water-extractable Cr(VI) determined by TOW eluates range from 0.2-18.2 mg/kg Cr(VI) for the subsoil materials. Cr(VI)-bearing mineral phases in amounts quantifiable by XRD (i.e. >1 wt.%; Table 5-2) were not observed.

The total Cr concentration in soil material N2 from Niederglatt is ten times higher than for sample N1. In contrast, total Cr(VI) in sample N2 is on average only 2.5 times higher than in sample N1 after multiple hot alkaline extractions of the samples (Table 5-1, Table 5-3). The water-extractable Cr(VI) fraction of both samples are in the same dimension (18.2 mg/kg and 14.9 mg/kg) and elevated compared to the other test materials. At the Niederglatt site the most abundant minerals identified in the samples by XRD are quartz, calcite, dolomite, plagioclase and K-feldspar (Table 5-2). Less frequently found are clay minerals, muscovite and Fe-hydroxides. The bulk chemical analyses by WD-XRF show high SiO_2 concentrations (>50 wt.%), but relatively low in $Fe_{(tot)}$ content (expressed as Fe_2O_3) compared to samples from Rivera and Thun (Table 5-1). Concentrations of Fe^{2+} and total organic carbon (TOC) are generally low, but sample N2 has the highest total manganese, $Mn_{(tot)}$, concentration of 1'520 mg/kg of all other soil samples although it is still lower than that of the NIST standard reference material. Both samples from Nieder-

glatt display lower total sulphur contents ($S_{(tot)}$ <400 mg/kg) than in all other samples (Table 5-1).

Soil sample R1 of the Rivera site has a three times higher $Cr_{(tot)}$ concentration compared to sample R2. Both samples have total Cr(VI) concentrations of <60 mg/kg that are significantly lower than those of the other subsoil samples from contaminated industrial sites (Table 5-1). The concentrations of the water-extractable Cr(VI) are 2.9 mg/kg for R1 and 0.2 mg/kg for R2. The mineralogy of the soil is typical for the Ceneri-Gneiss source rocks of this area and the samples are mainly composed of quartz, plagioclase and K-feldspar and contain substantial amounts of biotite, muscovite and secondary clay minerals such as chlorite (Table 5-2). The Rivera samples differ chemically from those from the other sites in that they have the highest Fe^{2+} contents at comparable $Fe_{(tot)}$ concentrations and elevated total organic carbon concentrations. In contrast, the concentrations of $Mn_{(tot)}$ and total sulphur are intermediate between the other samples (Table 5-1). Previous investigations by Wanner et al. (2012a) showed that the aquifer contains lenses of fine-grained sediments with elevated TOC contents (1-2 wt.%) thus confirming the elevated TOC contents observed in the two present samples.

The soil sample T1 from Thun site shows high concentrations of $Cr_{(tot)}$ as well as of total Cr(VI). However, the water-extractable Cr(VI) is lower (7.8 mg/kg) compared to the Niederglatt samples. The major mineralogy is similar to that from the Niederglatt site with quartz, calcite, plagioclase and K-feldspars being most abundant (Table 5-2). The strong Cr contamination resulted, however, in precipitates of abundant secondary mineral phases in the greenish-brown matrix with amorphous Fe-hydroxides being most prominent. This heavily contaminated subsoil has a high $Fe_{(tot)}$ content of 18.8 wt.% (as Fe_2O_3) of which 0.6 wt.% are present as Fe^{2+}, a high $S_{(tot)}$ concentration (8'370 mg/kg), but low concentrations of $Mn_{(tot)}$ and TOC (Table 5-1).

The industrial materials cement and fly ash contain $Cr_{(tot)}$ concentrations of <1'000 mg/kg, total Cr(VI) concentrations of <50 mg/kg and water extractable Cr(VI) concentrations of <1 mg/kg. They are therefore less charged with Cr compared to the soil materials from the contaminated industrial sites. The cement sample is an ordinary Portland cement (OPC) that consists mainly of the clinker phases alite, belite, ferrite and aluminate together with anhydrite and bassanite. The washed fly ash contains quartz, amorphous calcium silicate hydrates and sulphate minerals (anhydrite, gypsum) which are responsible for the elevated $S_{(tot)}$ concentration. The heavily contaminated standard reference material NIST 2701 contains in addition to the certified $Cr_{(tot)}$ and total Cr(VI) concentrations also strongly elevated concentrations of $Fe_{(tot)}$, Fe^{2+}, $Mn_{(tot)}$, $S_{(tot)}$ and TOC (Table 5-1). Our mineralogical and chemical results for NIST 2701 are in agreement with those of Nagourney et al. (2008) who performed an extensive mineralogical and chemical characterization during the development of this material

***Table 5-1**: Chemical analyses of standard reference material (NIST 2701), soil samples and industrial materials. $Cr_{(tot)}$ and Fe^{2+} are obtained by complete acid digestion, total Cr(VI) by hot alkaline extraction and water-extractable Cr(VI) by TOW-eluate (WE-Cr(VI)) followed by ICP-OES analysis. TOC is analyzed by coulometric techniques and all other data by XRF techniques (powder pellets).*

Sample type		NIST 2701	Soil N1	Soil N2	Soil R1	Soil R2	Soil T1	Cement	Fly ash
LOI	wt.%	14.3	3.3	12.3	4.7	5.8	11.2	1.0	5.8
SiO_2	wt.%	7.7	72.5	50.9	53.0	57.0	41.8	20.9	13.0
CaO	wt.%	11.5	0.6	16.5	2.4	1.6	11.2	62.4	25.4
Al_2O_3	wt.%	10.3	12.6	8.8	18.0	19.1	5.3	4.6	6.3
MgO	wt.%	10.4	1.7	2.5	2.9	3.0	0.7	1.6	0.9
Na_2O	wt.%	0.2	1.0	0.7	1.1	2.0	0.5	0.3	0.5
K_2O	wt.%	0.1	2.2	1.5	3.2	3.0	1.0	0.9	0.7
Fe_2O_3	wt.%	36.7	5.0	4.2	10.8	6.4	18.8	2.7	3.8
Fe^{2+}	wt.%	4.0	0.6	1.3	2.9	3.4	0.6	0.0	0.6
TOC	wt.%	1.9	0.0	0.2	0.4	1.1	0.1	0.2	0.1
$Mn_{(tot)}$	mg/kg	2'220	555	1'520	860	571	198	287	546
$S_{(tot)}$	mg/kg	1'050	366	221	779	840	8'370	17'300	132'425
Cr(tot)	mg/kg	42'500	1'642	10'562	4'516	1'424	7'142	88	708
Total Cr(VI)	mg/kg	401	113	298	58	42	298	45	13
WE Cr(VI)	mg/kg	-	18.2	14.9	2.9	0.2	7.8	0.9	0.8

***Table 5-2**: Estimated mineralogical composition of soils and industrial materials based on XRD, SEM and optical microscopy (xxx: >20 wt.%, xx: 5-20 wt.%, x: <5 wt.%). The XRD powder patterns are shown in Appendix 5, Figure A5-1 and Figure A5-2.*

Phase	NIST 2071	Soil N1	Soil N2	Soil R1	Soil R2	Soil T1	Cement	Fly ash
Quartz	x	xxx	xxx	xxx	xxx	xxx	-	x
Clinker phases***	-	-	-	-	-	-	xxx	-
Calcium silicate hydrate**	-	-	-	-	-	-	-	xx
Plagioclase	-	x	x	xx	xx	x	-	-
K-feldspar	-	x	x	xx	xx	x	-	-
Biotite*	-	-	-	xx	xx	-	-	-
Muscovite*	-	x	-	x	x	-	-	-
Clay mineral	-	x	x	xx	xx	-	-	-
Calcite/Dolomite	xx	-	xx	-	-	xx	-	-
Anhydrite/Bassanite/Gypsum	-	-	-	-	-	-	x	xxx
Chromite	xx	-	-	-	-	-	-	-
Fe-hydroxide*	-	x	x	-	-	x	-	-

* Assignment based on optical microscopy, ** SEM observation, *** Alite, belite, ferrite, aluminate

5.3.2 Cr(VI) analyses of extract solutions

The concentration values of total Cr(VI) in the alkaline extract solutions of the different tested soils measured by the spectrophotometric Cr(VI)-DPC method are higher by 12% (T1), 23% (N2) and 67% (R1) compared to the $Cr_{(tot)}$ concentrations obtained by ICP-OES, except for the standard reference material (NIST 2701, Figure 5-1). These results support earlier findings by Milačič et al. (1992), Huo et al. (1998) and Pettine and Capri (2005) who claimed that the presence of extracted compounds from the samples such as humic substances may seriously affect Cr(VI) concentrations obtained with the Cr(VI)-DPC-method. Such compounds absorb light at the same wavelength as the Cr-DPC complex (540 nm) causing a positive interference and thus in an overestimation of the real Cr(VI) concentration.

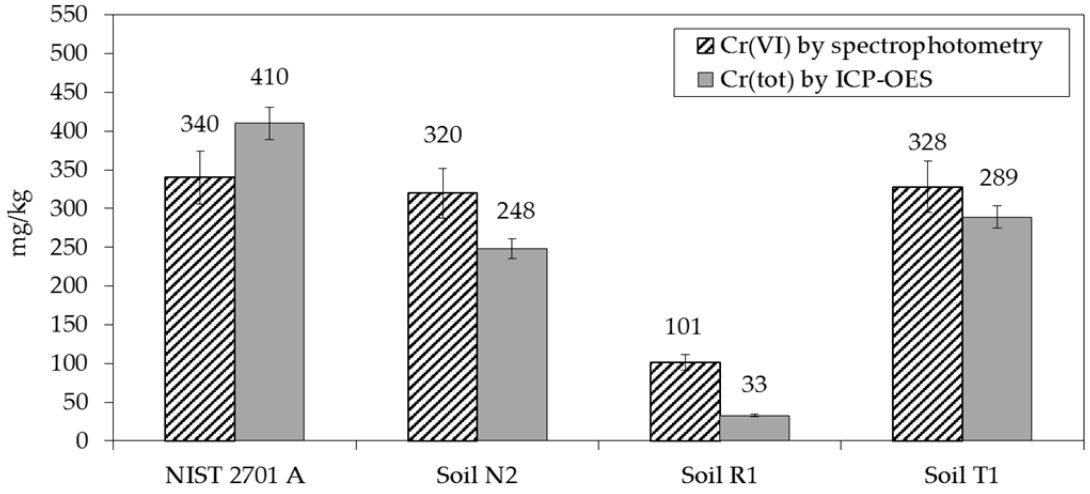

***Figure 5-1**: Total Cr(VI) determined by the spectrophotometric technique (Cr(VI)-DPC method) and $Cr_{(tot)}$ determined by ICP-OES in alkaline extract solutions prepared according to method 3060A. The error bars show the analytical uncertainty for Cr of each method (±10% for spectrophotometry and ±5% for ICP-OES).*

Another issue that interferes with the spectrophotometric Cr(VI)-DPC-method are the high pH conditions of method 3060A extract solutions. The Cr(VI)-DPC-method requires pH of 2 for correct Cr-DPC complex formation. Such pH-value is only attained for solutions with an initial pH between 1 and 9. However, extract solutions from method 3060A have pH-values >10 that interfere with the Cr(VI)-DPC complexation reaction. The observed change from a red-violet to a red-orange colour of the solutions results in a decrease of the extinction intensity at 540 nm that corresponds to the Cr(VI)-DPC complex and thus to an underestimation of the true Cr(VI) concentration. The only option to lower the pH to the required range for correct complex colouration would be a strong dilution of the alkaline extract solution (factor of ≥50). Obviously, such a high dilution factor compromises an already rather high limit of detection (LOD) of 0.05 mg/L Cr(VI) of the spectrophotometric Cr(VI)-DPC-technique. This limits the application of this technique to contaminated materials with Cr(VI) contents of more than 100 mg/kg of solid material.

The subsoil and industrial materials used in this study all have higher total Cr(VI) contents that enabled large dilutions to bring the solutions into the required pH range. In summary, difficulties associated with the pH-value of the alkaline extract solutions, interfering compounds such as humic substances, and possible other yet unknown interferences with the complexation reactants limit the spectrophotometric Cr(VI)-DPC-technique for Cr(VI) quantification in alkaline extract solutions prepared according to method 3060A.

To ensure that no measureable Cr(III) was left in solution after the hot alkaline Cr(VI) extraction, method 3060A extracts were measured by ICP-OES with and without prior Cr-species separation by the application of cation-exchange cartridges. Chromium concentrations obtained for the same solutions with and without the application of cation-exchange cartridges agree within the ±5% uncertainty range of the ICP-OES measurement (Figure 5-2). This indicates that under the strongly reducing extraction conditions of method 3060A only oxidized Cr(VI) was present in the extract solution whereas all Cr(III) was precipitated. Based on the thermodynamic data compiled by Ball and Nordstrom (1998), the equilibrium concentration of the major Cr-species, $Cr(OH)_{3(aq)}$ is ~$5 \cdot 10^{-11}$ mol/L, above which amorphous $Cr(OH)_{3(am)}$ will precipitate under the given extraction conditions (i.e. pH ~10.5, IS ~1.3 M, T = 90°C, Eh_{SHE} ~0 mV; see section identification of chemical processes below). This is considerably lower than that at low ionic strength and ambient temperature, but at similarly high pH-values where the solubility limit of amorphous $Cr(OH)_{3(am)}$ is at ~$1.4 \cdot 10^{-7}$ mol/L of $Cr(OH)_{3(aq)}$. This illustrates that under the applied alkaline extraction conditions, precipitation of amorphous Cr(III)-hydroxide is indeed promoted which would decreases the risk of having Cr(III) in the alkaline extract solution as already pointed out by Rai et al. (1987). Based on this evidence that only Cr(VI) is present in method 3060A extraction, a cation-exchange separation does not appear mandatory for the analyses of the tested subsoil, cement and fly ash samples. Therefore, the validation of method 3060A was performed without the application of cation-exchange cartridges prior to the ICP-OES analyses. Nevertheless, one extract solution of each material type was additionally prepared using cation-exchange cartridges prior to analysis as a control.

Reasonable results of Cr(VI) for the TOW extract solutions are achieved by the Cr(VI)-DPC-method because the pH-value of the solutions were in the range of pH 9. Only the cement sample eluate showed an elevated pH-value of 12.5 and no spectrophotometric Cr(VI) determination was possible. The results of water-extractable Cr(VI) could be confirmed by using cation-exchange cartridges followed by ICP-OES analysis.

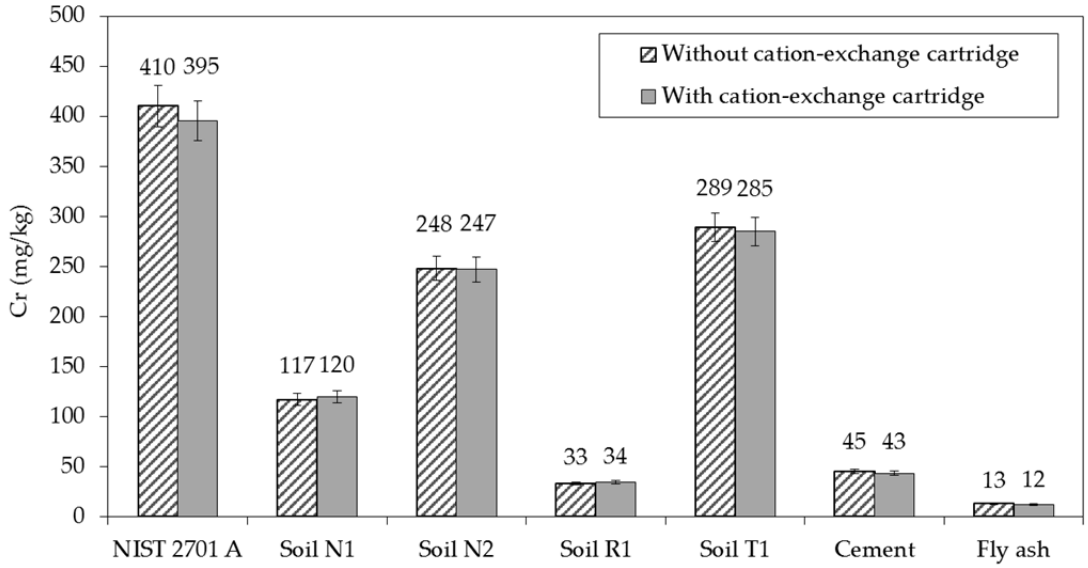

***Figure 5-2**: Cr concentrations measured by ICP-OES with and without prior cation-exchange separation of Cr(III) in alkaline extract solutions prepared by method 3060A. After species separation (hatched bars) only total Cr(VI) is detected whereas without cation-exchange separation (grey bars) possibly present Cr(III) is measured together with the total Cr(VI). The error bars show the analytical uncertainty of ±5% for Cr.*

5.3.3 Method validation

For the replicate alkaline extractions a relative standard deviation (RSD) <10% for the total Cr(VI) concentration was achieved for the standard reference material NIST 2701 and the industrial materials cement and fly ash (Table 5-3). In addition, the subsoil samples N1, N2 and T1 from the Niederglatt and Thun site yielded an RSD between 9% and 13%. In contrast, samples R1 and R2 from the Rivera site yielded large RSD's of 35% and 88% for the replicate extractions. The poor precision obtained for the Rivera samples suggests either a sample heterogeneity due to the small sample size (2.5 g) in spite of exactly the same preparation of the <2 mm grain-size fraction for all samples, and/or a different behaviour of the sample matrix during the hot alkaline extraction compared to all other tested materials (see below). The accuracy of method 3060A was determined by extracting and analyzing the standard reference material NIST 2701 seven times. An average recovery of total Cr(VI) of 73% was achieved for these extractions. This corresponds to the recoveries listed in the certificate of analysis (National Institute of Standards & Technology, 2009) using detection methods such as colorimetry (recovery 69.7%) or ion chromatography (U.S. Environmental Protection Agency, 1996b, recovery 70.5%). In contrast, a 30% higher recovery compared to these analytical methods was reported by the National Institute of Standards and Technology (NIST) using isotope dilution mass spectrometry (U.S. Environmental Protection Agency, 2007) (recovery 100.4%). The value obtained by this latter technique is currently adapted as the certified Cr(VI) value (551.2 mg/kg) in method 3060A extract solutions for the standard reference material. The rather

large differences obtained by different detection techniques highlights the complexity attached to the quantification of Cr(VI) in the hot alkaline extract solutions and this asks for further research. The precision (replicate extraction) and accuracy (recovery of certified value) data obtained from the standard reference material are additionally used to calculate a combined measurement uncertainty of 15% and an expanded uncertainty of 30% for the entire process of total Cr(VI) determination using method 3060A and ICP-OES analysis.

***Table 5-3**: Results of multiple extractions of the test materials: $\bar{x}$ = mean value, s = standard deviation, RSD = relative standard deviation. A mean recovery of 73% (401 mg/kg) for the standard reference material NIST 2701 is determined (certified value: 551.2 mg/kg total Cr(VI)).*

Total Cr(VI) – EPA method 3060A										
Replicate (n)	**1**	**2**	**3**	**4**	**5**	**6**	**7**	**$\bar{x}$**	**s**	**RSD**
	mg/kg	mg/kg	mg/kg	mg/kg	mg/kg	mg/kg	mg/kg	mg/kg	mg/kg	-
NIST 2701	410	384	425	411	375	420	384	401	20	5
Soil N1	117	114	107	101	105	129	101	113	10	9
Soil N2	248	330	324	323	246	318	-	298	40	13
Soil R1	33	40	62	93	65	46	78	58	20	35
Soil R2	112	1	55	40	29	7	50	42	37	88
Soil T1	289	219	297	323	308	307	343	298	39	13
Cement	45	43	47	43	45	-	-	45	2	4
Fly ash	13	12	13	14	15	-	-	13	1	9

For interpretation of the Cr(VI) and Cr(III) spiking results, the mean value of the recoveries from the two spiked concentrations to each material was calculated and the deviation between the single spike recoveries plotted as error bars in (Figure 5-3). Recoveries for the water-extractable and water-insoluble Cr(VI) spikes between 90% and 125% were obtained for all alkaline extracts, except for soil N2 and the two Rivera soil samples. Whereas the water-insoluble spike recovery of sample N2 (76%) from Niederglatt is within the expanded measurement uncertainty of 30% of the method, those for the two Rivera soil samples R1 and R2 show consistently poor and highly diverging spike recoveries for water-extractable Cr(VI) (R1: 0% and 153%; R2: 16% and 6%) and water-insoluble Cr(VI) (R1: 70% and 6%; R2: 43% and 117%). No correlation is established with the large relative standard deviations of 35% and 88% obtained for the total Cr(VI) contents is evident. The recoveries of water-extractable and water-insoluble Cr(VI) spikes of the Rivera samples therefore indicate a dependence on the composition of the extracted material as will be outlined in more detail in the next section.

Addition of soluble Cr(III) spike revealed 2-9% higher Cr concentrations compared to non-spiked solutions for the alkaline solutions of all materials, except for the subsoil

sample Rivera R1 (see below). Some insight into this elevated Cr recovery is gained from the spiked extraction of a non-contaminated blank sample from the Niederglatt site. This sample N3 was spiked with 100 mg/kg of Cr(III) prior to extraction and 10% of this spiked Cr were still found in the solution after extraction. Interestingly, the same amount of spiked Cr was also analyzed in the solution after passing it through a cation-exchange cartridge that removed all Cr(III) from this solution. This indicates that in this extraction some 10% of the added Cr(III) spike were oxidized to Cr(VI) during extraction. Within this context it is important to note that the Cr(III) spike was added to the extract solution at ambient temperature as dissolved $Cr(NO_3)_3$. It thus appears that under the initial oxidizing conditions of the extract solutions at ambient temperature the oxidation of spiked and dissolved Cr(III) is quicker than its precipitation as amorphous Cr(III)-hydroxide. It is concluded that the 2-9% higher Cr concentrations obtained in Cr(III)-spiked alkaline extract solution compared to non-spiked solutions are due to partial oxidation of the added Cr(III) spike during the initial phase of the alkaline extraction process. While the interpretation of partial oxidation of the Cr(III) spike is in agreement with the findings by Vitale et al. (1994), we associate this oxidation to faster reaction kinetics of the Cr(III) oxidation in the solution compared to that of the Cr(III) precipitation from the alkaline extract solution. The present data do not allow to either support or reject the hypothesis by Eary and Rai (1987) who proposed the oxidation of Cr(III) by β-MnO_2 during extraction. However, the similar degree of observed oxidation of spiked Cr(III) in the extract solutions (i.e. 2-9%) of samples with strongly variable $Mn_{(tot)}$ contents (~290-2'220 mg/kg, Table 5-1) seem to argue against the oxidation by MnO_2 as a dominant process. Such oxidation is inhibited during extraction at 90°C by the lowering of the redox potential of the extract solution and the lowering of the solubility of Cr(III), by several orders of magnitude. Soil R1 showed an anomalous mean Cr(III) spike recovery of 62% (Figure 5-3) in contrast to all other samples. This value results from a recovery of 123% of Cr(III) after spiking with 50 mg/L of Cr(III) and a recovery of 2% of Cr(III) after spiking with 100 mg/L of Cr(III). A repeat extraction with 50 mg/L of Cr(III) spike added to sample R1 resulted in an even higher recovery of 144%. This erratic behaviour can hardly be related to chemical reactions taking place during the alkaline extraction. For instance, the extract solution of this sample showed the lowest redox potential (Eh_{SHE}~50 mV, Figure 5-4) just after addition of the spike. Combined with the intermediate $Mn_{(tot)}$ content (860 mg/kg), this extract solution is thus expected to have a Cr(III) oxidation capacity during the initial phase of the extraction that is at least as low as in all other extract solutions. The much lower redox potential during the continuation of the extraction at 90°C compared to all other solutions (Figure 5-4) also argues against an oxidation of Cr(III) during this phase of extraction. Therefore, the observed Cr concentration in the Cr(III)-spiked extract solutions can only be attributed to the presence of a different amount of soil-derived Cr(VI) in this sample aliquot compared to the non-spiked sample aliquot. Such sample heterogeneity is supported by the large standard deviation of multiple extractions of the Rivera samples (Table 5-3). The Rivera R1 sample aliquots thus indicate how sensitive the de-

termination of Cr(VI) in small soil aliquots of 2.5 g is, even if the preparation occurs with great care.

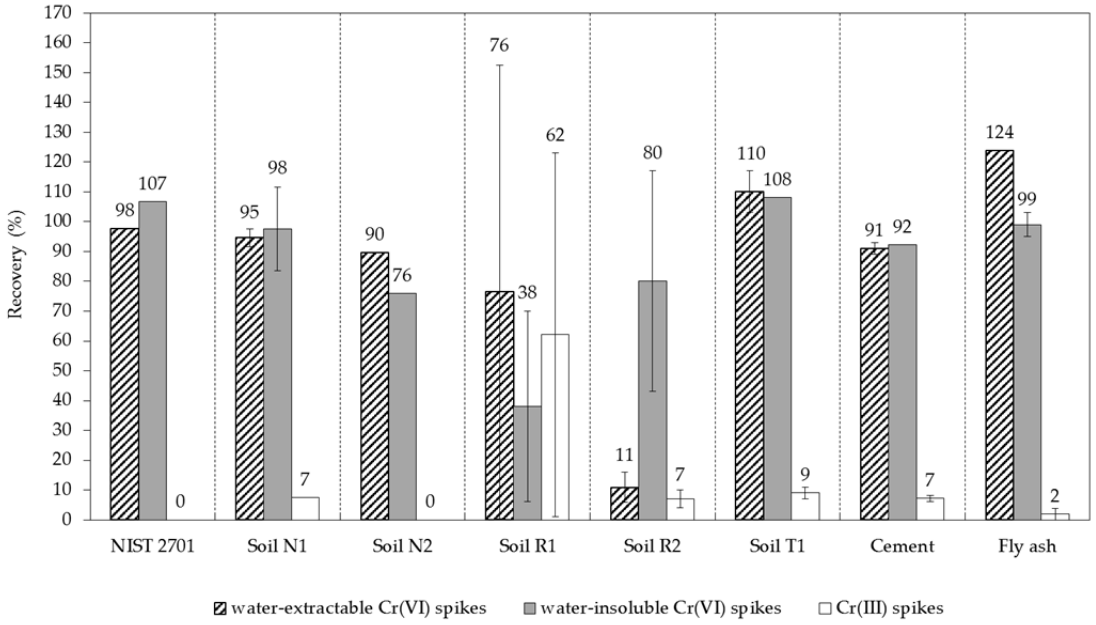

***Figure 5-3**: Recovery of Cr(VI) and Cr(III) spikes from alkaline extract solutions prepared from the various solid materials. Hatched bars indicate the mean (n=2) Cr recovery in % after water-extractable Cr(VI) spiking, grey bars after water-insoluble Cr(VI) spiking and the white bars represent the mean Cr recovery after spiking the alkaline solutions with Cr(III). The error bars show the deviations between spike recoveries of replicate samples performed for each spiking type. The Cr(VI) and Cr(III) spike recoveries for soil N2 and the standard reference material (NIST 2701) are only based on single spike experiments.*

5.3.4 Identification of chemical processes during extraction

The water-extractable Cr(VI) concentration is about one order of magnitude smaller compared to the total Cr(VI) concentration independent of the type and origin of the material (Table 5-1). Water-extractable Cr(VI) does not correlate with the total inventory of Cr(VI) present in a contaminated or newly manufactured solid material. The true Cr(VI) inventory is thus underestimated by simply applying the TOW eluate test. After 24 h of extraction pH-values between 9 and 10 and Eh_{SHE}-values between 360-450 mV have been measured. At these conditions, the dominant Cr species in solution is chromate (CrO_4^{2-}) (Ball and Nordstrom, 1998). No relation between the total Cr(VI) and the water extractable Cr(VI) exists and the measured concentrations of the TOW test do not help to understand the aberrant behaviour of the Rivera soil samples by performing method 3060A.

Some insight into the chemical interaction between the sample matrix and the hot alkaline solution may be obtained from monitoring pH, Eh and temperature during the extraction process and from geochemical modelling. Stable measurements were obtained during monitoring within less than a minute for all samples except for the fly ash sample,

which is composed of highly reactive sulphides, sulphates, oxides, carbonates, salts and silicates.

The target extraction temperature of 90-95°C was reached for all test materials within ~20 minutes (Figure 5-4). The initial solution pH of about 13.2 decreased to a value near 11 during this heating period for all soil samples. Subsequently, pH smoothly decreased to a value near 10.5 without reaching an obvious steady state until the end of the extraction after 80 minutes. Geochemical model calculations indicate that for the pure extract solution (0.5 mol/L NaOH and 0.28 mol/L Na_2CO_3) the temperature increase from 20°C to 90°C results in a decrease of the solution pH from 13.2 to 11.5. Solely the additional decrease by one log unit between 30 and 80 minutes is therefore related to buffering reactions within the solid material. Modelling further reveals that neither the carbonate system (calcite, dolomite) nor the Mg system (Mg added as buffer), nor the Si system (quartz) can reduce the pH to the observed values. It appears that the dissolution of relatively abundant Al-silicates (feldspars, mica, clays) is responsible for the pH reduction. Under the prevailing alkaline conditions, Al released from dissolving Al-silicates is highly soluble and forms $Al(OH)_{4^-(aq)}$ and $Al(OH)_{3(aq)}$ complexes until saturation with amorphous Al-hydroxide ($Al(OH)_{3(am)}$) is reached. For example, the dissolution of about 40 mmol/L of K-feldspar would results in a decrease of the extract solution pH from 11.5 to 10.6 near equilibrium with gibbsite, but not yet with $Al(OH)_{3(am)}$. This latter observation and the still decreasing pH indicate that after 80 minutes the system is not yet at equilibrium and is still kinetically controlled with respect to the interaction with the sample matrix. The only approximately stable high pH conditions for the quartz-feldspar-calcite dominant subsoil samples will, however, not directly interfere with the systematics of the Cr-system. A similar behaviour is also observed for the cement sample, although there the final pH is slightly lower (near 10) and the decreasing trend is more pronounced (Figure 5-4).

In contrast to pH, changes in the redox conditions will directly influence the Cr-system during the alkaline extraction. The initial Eh_{SHE} of extract solutions at 20°C without soil was 330 mV. According to the Nernst equation, an increase of the Eh_{SHE} by about 34 mV would result due to the decrease in pH induced by heating the solution to 90°C. By adding the different soil materials to the extract solution at 20°C this initial Eh_{SHE} is quickly reduced to about 110–130 mV for all materials, except for the Rivera R1 soil samples where a decrease occurred to Eh_{SHE} ~50 mV. Monitoring of the redox potential during the ~20 minutes of heating up to 90°C revealed another pronounced decrease in Eh for all materials, but to a different extent (Figure 5-4). For the standard reference material (NIST 2701) and the soil samples Niederglatt N1 and Thun T1, the decrease in Eh_{SHE} amounts to ~160 mV, whereas a decrease of >300 mV and >500 mV was observed for the Rivera R1 and the cement sample, respectively. The most reducing conditions were attained after 20 to 30 minutes of extraction time independent of the material. The most negative Eh_{SHE}-value was obtained for Rivera R1 sample (-249 mV, corrected for tempera-

ture) and the Portland cement sample (-312 mV), whereas samples from Niederglatt and Thun yielded minimum Eh_{SHE}-values of only about -50 mV.

The strong lowering of the redox potential to Eh_{SHE} ~50 mV of the alkaline extract solution immediately after addition of the Rivera R1 sample at 20°C indicates a high reduction capacity with quickly reacting reducing components in this soil. This is supported by the observation that the initially colourless extract solution changed rapidly to dark-brown colour after getting in contact with the Rivera soils at room temperature. This indicates the release of organic material from these soils, which continues with increasing temperature until an almost black colour was reached after 60 minutes. Analysis of TOC shows that the Rivera materials contain elevated TOC contents (0.5 and 1.1 wt.%) compared to soil material from the Niederglatt and Thun sites (Table 5-1). Elevated TOC contents are consistent with the locally anoxic conditions due to the degradation of organic matter in lenses of organic-rich swamp and bog deposits at this site. Therefore, the different behaviour of the Rivera samples during extraction is associated mainly with the strong reducing potential of these soils because of the presence of organic matter.

Furthermore, it is known that apart from organic-rich sediments also minerals containing reduced sulphur (i.e. sulphides) and/or ferrous iron (e.g. magnetite, biotite, chlorite, hornblende) may function as Cr(VI) reducing agents (Palmer and Puls, 1994; Bishop et al., 2014). In sulphide minerals such as pyrite (FeS_2), both the iron and the sulphide are able to act as electron donors. Materials from Rivera show increased concentrations of biotite and secondary sheet silicates (e.g. chlorites) compared to the other samples (Table 5-2). This is supported by the higher Fe^{2+} concentrations obtained for the Rivera soils (2.9 and 3.4 wt.%) compared to soils from the Niederglatt (0.6 and 1.3 wt.%) and Thun (0.6 wt.%) sites (Table 5-1). Wanner et al. (2012a) tested the Cr(VI) reduction potential of the gravel aquifer material at the Rivera site with a simple batch experiment. They milled a sample of uncontaminated, weathered Ceneri-Gneiss and shook it with K_2CrO_4 solution (10 mg/L) for 10 days. This batch experiment resulted in a Cr(VI) concentration below detection for the spectrophotometer (<0.05 mg/L Cr(VI)). The authors concluded that the entire aquifer material has the potential of operating as a Cr(VI) reducing agent. Although the milling of the Gneiss material possibly produced fresh, reactive and non-oxidized, Fe^{2+}-bearing mineral surfaces and the reactions might occur more slowly with naturally weathered material, this experiment combined with the above Fe^{2+} concentrations are clear evidence that such reactions may occur. The elevated TOC and Fe^{2+} concentrations in the soil material and the observed Cr(VI) reducing potential of the extract solutions of the Rivera samples explain the discrepant behaviour of the Rivera samples, whereas the hot alkaline extraction according to method 3060A worked fine for all other test materials including the standard reference material. Matrix effects and the strong reducing potential of the Rivera soil samples reduce the spiked Cr(VI) with subsequent precipitation of $Cr(OH)_{3(am)}$ as discussed above. This is in agreement with findings by Vitale et al. (1994) who observed low Cr(VI)-spike recoveries by applying method 3060A to anoxic, sulphidic sediments that contained 27 wt.% of organic carbon and 100 mg/kg

sulphides. The results of water-extractable and water-insoluble Cr(VI)-spike recoveries indicate that soils with elevated amounts of reducing minerals (e.g. Fe^{2+}-bearing phases) and/or organic matter will induce matrix effects that interfere with Cr(VI) spikes. A strong negative redox potential as observed for the Rivera samples is, however, not an unambiguous indicator for a low Cr(VI)-spike recovery. This is exemplified by the Portland cement sample (CEM I), which reached an even more negative redox potential of Eh_{SHE} -312 mV during extraction (Figure 5-4), but yielded an excellent Cr(VI)-spike recovery (92%). This suggest that the reduction of Cr(VI) does not primarily depend on the reducing potential of a material, but more on the reducing agents present in such materials. The present data do, however, not allow a more detailed description of the involved processes and further investigations are required for such special types of industrial materials.

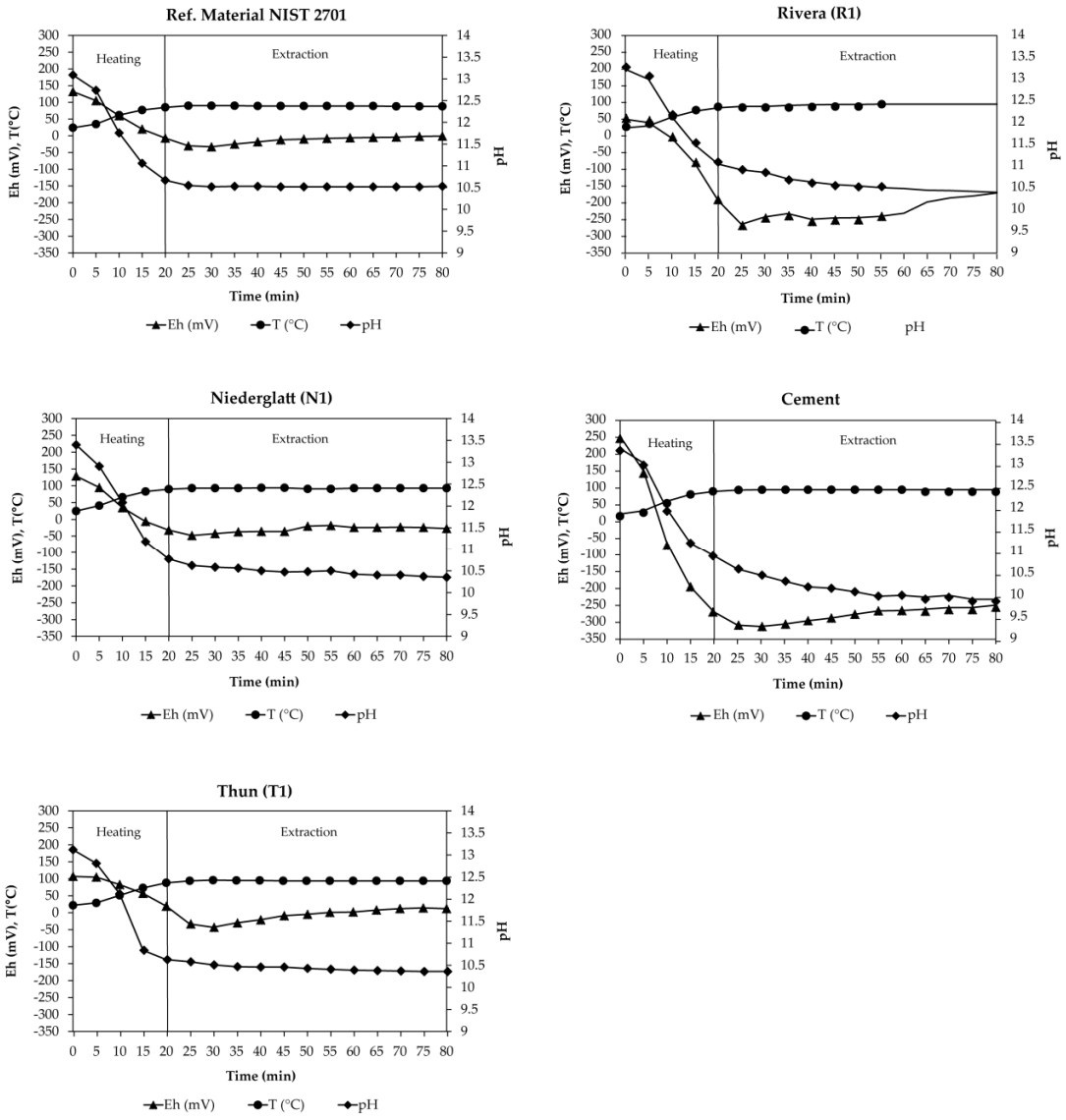

***Figure 5-4**: Variation of the parameters Eh (relative to SHE and corrected for temperature), pH and temperature as a function of extraction time during the alkaline extraction.*

5.4 Conclusion

The results of this study demonstrate that the determination of Cr(VI) in extract solutions from U.S. EPA method 3060A by the spectrophotometric diphenylcarbazide (DPC) method likely leads to discrepant results due to interfering substances arising from the extraction process and due to the high pH conditions (pH >10). Tests under hot alkaline extraction conditions with and without cation-exchange cartridges to remove Cr(III) reveal that only oxidized Cr(VI) is present in the alkaline solution and that dissolved Cr(III) precipitated presumably as amorphous $Cr(OH)_{3(am)}$. A cation-exchange procedure prior to determination of Cr in the extract solution by spectrometric techniques is a priori not indicated. Nevertheless, a redox-sensitive analytical technique is recommended to assure that no Cr(III) is erroneously quantified in samples of unknown matrix composition.

The applicability of method 3060A in combination with ICP-OES analysis was successfully tested and validated for subsoil samples from oxidizing, weathered environments with matrices mainly composed of quartz, calcite, plagioclase and K-feldspar and low contents of Fe^{2+}, TOC and $Mn_{(tot)}$. For such type of soils and including standard reference material (NIST 2701) a good reproducibility of Cr(VI) determinations was obtained and the recovery of Cr(III)- and Cr(VI)-spikes was within the expanded uncertainty of 30% of the method. This indicates that no substantial matrix effects interfered with soil-derived Cr(VI) and Cr(III) during extraction. A similar behaviour was found for a Portland cement (OPC-1) and a MSWI fly ash sample. The poor reproducibility of soil-derived Cr(VI) and the anomalous and heterogeneous Cr(III)- and Cr(VI)-spike recoveries obtained for Rivera subsoil samples is attributed to severe matrix effects during the alkaline extraction and compositional heterogeneity between different sample aliquots. Matrix effects are responsible for the anomalous recovery of Cr(VI) spike in the alkaline extract solutions of the Rivera samples and can be related to differences in the mineralogical and chemical composition, notably the elevated Fe^{2+} and TOC contents. Sample heterogeneity is indicated by the poor reproducibility of soil-derived Cr(VI) in combination with the anomalous recovery of the Cr(III) spike in these alkaline extract solutions. In addition, the comparison of the total Cr(VI) and the water-extractable Cr(VI) concentrations do not show simple dependencies on phase composition.

To circumvent some of the experienced problems related to the application of method 3060A alkaline extraction to differently composed materials it is recommended that a) prior to routine application to a new material type, spiking tests are to be performed for the identification of possible matrix effects, b) that the mass of solid material to be extracted is adjusted to the heterogeneity of the Cr(VI) distribution in the material in question, and c) that the solid material is added to the alkaline extract solution not until the solution has reached 90°C. Point c) requires further confirmation. However, the chemical reactions identified appear to take place during the initial phase of the alkaline extraction during heating from 20°C to 90°C. This seems to support such a modification of method 3060A.

Acknowledgements

We would like to thank the geological consulting companies CSD and Schenker Korner Richter AG for providing sample material and internal information about the various contaminated sites. Holcim Technology Ldt. and KEBAG AG are acknowledged for providing cement and fly ash samples and Bachema AG for technical support (method development). The financial support by Metallwerke Refonda AG and AWEL Zürich is highly appreciated. The constructive comments by two anonymous reviewers greatly helped to improve the manuscript.

References

Adriano, D.C., 1986. Trace elements in the terrestrial environment, 1 ed. Springer-Verlag (New York).

Ball, J.W., McCleskey, R.B., 2003. A new cation-exchange method for accurate field speciation of hexavalent chromium. Talanta 61, 305-313.

Ball, J.W., Nordstrom, D.K., 1991. WATEQ4F—User's manual with revised thermodynamic data base and test cases for calculating speciation of major, trace and redox elements in natural waters. U.S. Geological Survey Open-File Report, 90–129, 185.

Ball, J.W., Nordstrom, D.K., 1998. Critical evaluation and selection of standard state thermodynamic properties for chromium metal and its aqueous ions, hydrolysis species, oxides, and hydroxides. Journal of Chemical & Engineering data, 895-918.

Baral, A., Engelken, R.D., 2002. Chromium-based regulations and greening in metal finishing industries in the USA. Environmental Science & Policy 5, 121-133.

Bartlett, R.J., James, B.R., 1979. Behavior of chromium in soils: III. Oxidation. Journal of Environmental Quality, 31-35.

Bishop, M.E., Glasser, P., Dong, H., Arey, B., Kovarik, L., 2014. Reduction and immobilization of hexavalent chromium by microbially reduced Fe-bearing clay minerals. Geochimica et Cosmochimica Acta 133, 186-203.

Bühler, A., Schlumberger, S., 2010. Schwermetalle aus der Flugasche zurückgewinnen «Saure Flugaschewäsche – FLUWA-Verfahren» ein zukunftsweisendes Verfahren in der Abfallverbrennung. KVA-Rückstände in der Schweiz - Der Rohstoff mit Mehrwert. Federal Office for the Environment (FOEN), 185-192.

Burke, T., Fagliano, J., Goldoft, M., Hazen, R.E., Iglewicz, R., McKee, T., 1991. Chromite ore processing residue in Hudson County, New Jersey. Environmental Health Perspectives 92, 131-137.

Christensen, T.H., Kjeldsen, P., Albrechtsen, H.J., Heron, G.P., Nielsen, H., Bjerg, P.L., Holm, P.E., 1994. Attenuation of landfill leachate pollutants in aquifers. Critical Reviews in Environmental Science and Technology 24, 199-202.

Eary, L.E., Rai, D., 1987. Kinetics of chromium(III) oxidation to chromium(VI) by reaction with manganese dioxide. Environmental Science & Technology 21, 1187-1193.

Farmer, J.G., Graham, M.C., Thomas, R.P., Paterson, E., Campbell, C.D., Geelhoed, J.S., Lumsdon, D.G., Roe, M.J., Conner, A., Fallick, A.E., 1999. Chemistry and potentials for remediative treatment of chromium-contaminated land. Environmental Geochemistry & Health 21, 331-337.

Flury, B., Frommer, J., Eggenberger, U., Mäder, U., Nachtegaal, M., Kretzschmar, R., 2009. Assessment of long-term performance and chromate reduction mechanisms in a field scale permeable reactive barrier. Environmental Science & Technology 43, 6786-6792.

Hills, L., Johansen, V.C., 2007. Hexavalent chromium in cement manufacturing: Literature Review. Portland Cement Association (2983).

Huo, D., Lu, Y., Kingston, H.M.S., 1998. Determination and correction of analytical biases and study on chemical mechanisms in the analysis of Cr(VI) in soil samples using EPA Protocols. Environmental Science & Technology 32, 3418-3423.

James, B.R., 1996. The challenge of remediating chromium-contaminated soil. Environmental Science & Technology 30, 248-251.

Leisinger, S.M., Bhatnagar, A., Lothenbach, B., Johnson, C.A., 2014. Solubility of chromate in a hydrated OPC. Applied Geochemistry 48, 132-140.

Milačič, R., Štupar, J., Kožuh, N., Korošin, J., 1992. Critical evaluation of three analytical techniques for the determination of chromium (VI) in soil extracts. Analyst 117, 125-130.

Nagourney, S.J., Wilson, S.A., Buckley, B., Kingston, H.M.S., Yang, S.-Y., Long, S.E., 2008. Development of a standard reference material for Cr(VI) in contaminated soil. Journal of Analytical Atomic Spectrometry 23, 1550.

National Institute of Standards & Technology, 2009. Certificate of analysis standard reference material 2701. Certificate of Analysis Standard Reference Material 2701.

Omega Data Systems, 2004. UniQuant 5. A unique concept in XRF analysis. User manual.

Palmer, C.D., Puls, R.W., 1994. Natural attenuation of hexavalent chromium in groundwater and soils. EPA Ground Water Issue Paper EPA/540/5-94/505 US Environmental Protection Agency. US Government Printing Office. Washington, DC, USA.

Parkhurst, D.L., Appelo, C.A.J., 2013. Description of Input and examples for PHREEQC Version 3—A computer program for speciation, batch-reaction, one-dimensional transport, and inverse geochemical calculations. U.S. Geological Survey Techniques and Methods Book 6, 497.

Pettine, M., Capri, S., 2005. Removal of humic matter interference in the determination of Cr(VI) in soil extracts by the diphenylcarbazide method. Analytica Chimica Acta 540, 239-246.

Puls, R.W., Paul, C.J., Powell, R.M., 1999. The application of in situ permeable reactive (Zero-valent iron) barrier technology for the remediation of chromate-contaminated groundwater: a field test. Appl Geochem 14, 989-1000.

Rai, D., Eary, L.E., Zachara, J.M., 1989. Environmental chemistry of chromium. Sci. Total Environ 86, 15-23.

Rai, D., Sass, B.M., Moore, D.A., 1987. Chromium (III) hydrolysis constants and solubility of chromium (III) hydroxide. Inorganic Chemistry 26, 345-349.

Stumm, W., Morgan, J., 1996. Aquatic chemistry: chemical equilibria and rates in natural waters, 3rd ed. John Wiley & Sons. New York, USA.

Swiss Confederation, 1990. Technische Verordnung über Abfälle (TVA), 1-36.

Swiss Confederation, 1998. Verordnung über die Sanierung von belasteten Standorten (AltlV), 1-20.

Swiss Confederation, 2013. Analysenmethoden im Abfall- und Altlastenbereich: Umwelt-Vollzug Nr. 1334, 80.

U.S. Environmental Protection Agency, 1992. EPA Method 7196, Hexavalent chromium (colorimetric). US Government Printing Office, Washington, DC, 1-6.

U.S. Environmental Protection Agency, 1996a. EPA Method 3060A, Alkaline digestion for hexavalent chromium. US Government Printing Office, Washington, DC.

U.S. Environmental Protection Agency, 1996b. EPA Method 7199, Determination of hexavalent chromium in drinking water, groundwater and industrial waste water effluents by ion chromatography. US Government Printing Office, Washington, DC December 1996, 1-10.

U.S. Environmental Protection Agency, 2007. EPA Method 6800, Elemental and speciated isotope dilution mass spectrometry. US Government Printing Office, Washington, DC, 1-47.

Vitale, R.J., Mussoline, G.R., Petura, J.C., James, B.R., 1994. Hexavalent chromium extractions from soils: evaluation of an alkaline digestion method. Journal of Environmental Quality 23, 1249-1256.

Wanner, C., Eggenberger, U., Kurz, D., Zink, S., Mäder, U., 2012a. A chromate-contaminated site in southern Switzerland–Part 1: Site characterization and the use of Cr isotopes to delineate fate and transport. Applied Geochemistry 27, 644-654.

Wanner, C., Zink, S., Eggenberger, U., Mader, U., 2012b. Assessing the Cr(VI) reduction efficiency of a permeable reactive barrier using Cr isotope measurements and 2D reactive transport modeling. J Contam Hydrol 131, 54-63.

Appendix 5

Table A5-1: *Cr(VI)- and Cr(III)-spike concentrations and recoveries for each individual sample type subjected to the hot alkaline extraction according to method 3060A.*

Sample	Spike added mg/kg	Total Cr(VI) mg/kg	Recovery %	Mean recovery %
Standard reference material NIST 2701	Without spike	384	-	**-**
Cr(VI) water-extractable	500	873	98	**-**
Cr(VI) water-insoluble	500	918	107	**-**
Cr(III)	100	374	0	**-**
Soil N1	Without spike	127	-	-
Cr(VI) water-extractable	100	219	92	95
	200	322	97	
Cr(VI) water-insoluble	100	212	84	98
	200	355	111	
Cr(III)	50	131	7	7
	100	135	7	
Soil N2	Without spike	248	-	-
Cr(VI) water-extractable	100	338	90	-
Cr(VI) water-insoluble	100	325	76	-
Cr(III)	100	240	0	-
Soil R1	Without spike	40	-	-
Cr(VI) water-extractable	30	38	0	76
	60	132	153	
Cr(VI) water-insoluble	30	61	70	38
	60	44	6	
Cr(III)	50	102	123	62
	100	42	2	
Soil R2	Without spike	1	-	-
Cr(VI) water-extractable	50	9	16	11
	100	7	6	
Cr(VI) water-insoluble	50	23	43	80
	100	119	117	
Cr(III)	50	3	4	7
	100	17	10	
Soil T1	Without spike	219	-	-
Cr(VI) water-extractable	300	570	117	110
	600	837	103	
Cr(VI) water-insoluble	300	546	108	108
	600	871	108	
Cr(III)	50	222	7	9
	100	229	11	
Cement	Without spike	43	-	-
Cr(VI) water-extractable	50	87	89	91
	100	136	93	
Cr(VI) water-insoluble	50	89	93	92
	100	134	92	
Cr(III)	50	47	8	7
	100	49	6	
Fly ash	Without spike	12	-	-
Cr(VI) water-extractable	20	37	124	124
	40	62	124	
Cr(VI) water-insoluble	20	29	95	99
	40	53	103	
Cr(III)	50	14	4	2
	100	11	0	

XRD powder patterns were measured with a Panalytical CubiX³ diffractometer equipped with a Cu X-ray source (40 kV/40 mA), secondary monochromator and automatic divergence slits. The patterns were collected from 4° to 60° 2θ. The estimation of the amounts was performed using RIR and Rietveld refinement (High Score Plus). Even though all peaks were assigned only the major peaks of the relevant phases are marked in Figure and Figure . Sheet silicates are detected by XRD, however, the differentiation between biotite, muscovite, illite and phengite is hardly possible. Therefore, the soils were analyzed by optical microscopy whereby biotite and muscovite are clearly identified.

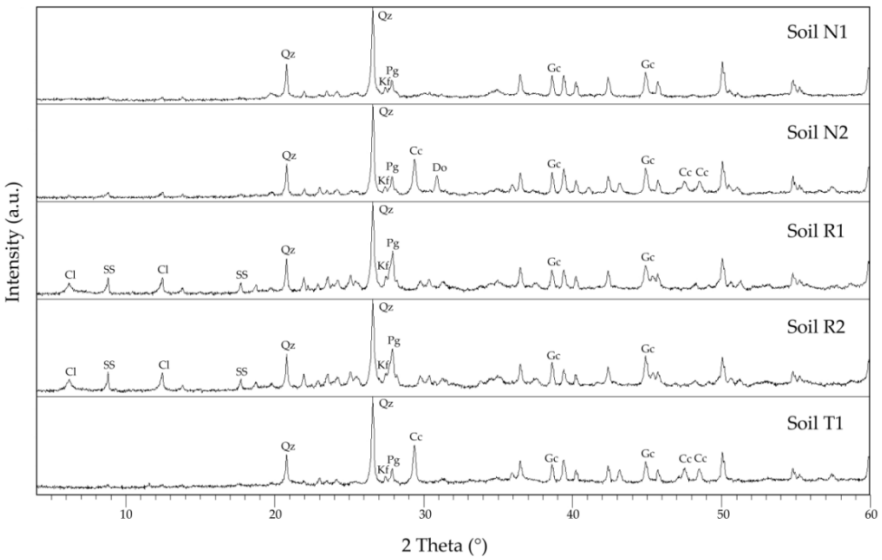

***Figure A5-1**: XRD powder patterns of soil samples: (Qz) quartz; (Kf) K-feldspar; (Pg) plagioclase; (Cc) calcite; (Do) dolomite; (Cl) chlorite; (SS) sheet silicates; (Gc) griceite (internal standard, 10 wt.%).*

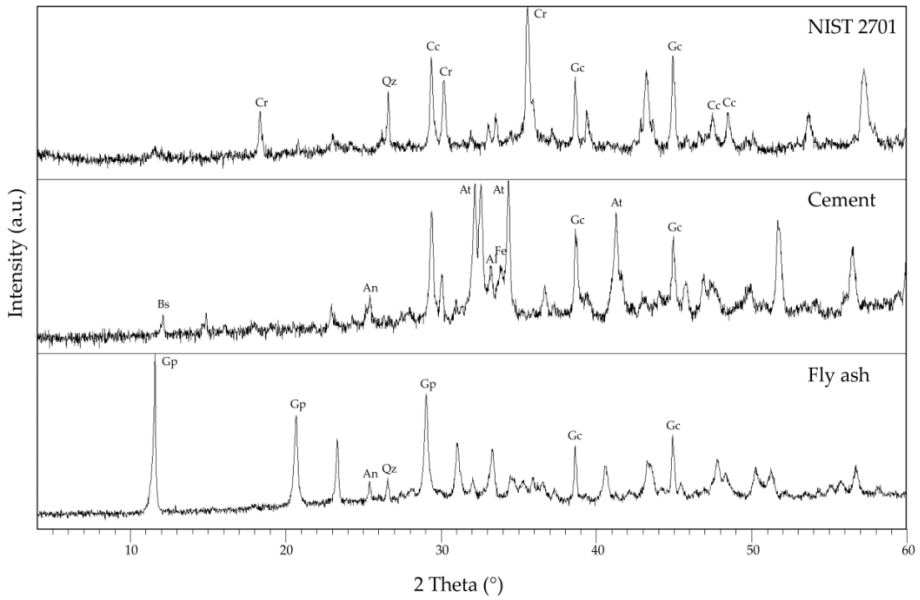

***Figure A5-2**: XRD powder patterns of standard reference material (NIST 2701), cement and fly ash sample: (Qz) quartz; (Cc) calcite; (Cr) chromite; (An) anhydrite; (Bs) bassanite; (Gp) gypsum; (At) alite/belite; (Fe) ferrite; (Al) aluminate; (Gc) griceite (internal standard, 10 wt.%).*

Part C: Technical Reports

Chapter 6

Characterization of Fly Ashes and Leached Filter Cakes from Six Swiss Municipal Solid Waste Incinerators

Gisela Weibel & Urs Eggenberger

Institute of Geological Sciences, University of Bern, Switzerland

On behalf of the Swiss Federal Office for the Environment (FOEN), December 2014 (2nd Version)

6.1 Introduction

6.1.1 Background

The thermal treatment of waste has become indispensable in Switzerland and in recent years the focus has been laid on the treatment optimization of the incineration residues. Bottom ash and fly ash are promising secondary sources of metals which can be reused as economic valuable materials. The chemical and structural composition of the incineration residues is mainly dependent from the waste input and the furnace type. The treatment of fly ash with an acidic leaching agent (FLUWA process, Schlumberger et al., 2007) is used in more than half of the Swiss municipal solid waste incineration (MSWI) plants, it is therefore the state-of-the-art in modern MSWI in Switzerland. The incorporation in mineral phases or glasses affects the mobility of the metals essentially. Prediction about the extractability of an element is only possible under the consideration of the type of chemical binding. In the 1990s, detailed investigations on different treatment processes (mostly thermal processes were performed in the context of a national priority program, Ludwig et al., 2003, SPPU IP Abfall). However, detailed structural and chemical investigations of the metal binding types of fly ash and as a consequence the leaching process optimization are mostly lacking.

In order to extend and deepen studies in this specific area and encounter the difficulties stated above, several preliminary investigations were performed on behalf of the Federal Office for the Environment (FOEN) and the Office for Waste Management of the Environmental Protection Agency of Canton Zürich (AWEL) during the last two years. The focus of a study performed at the Institute of Geological Sciences, University of Bern and the EAWAG Dübendorf in 2013 was placed on the mineralogy, chemistry and the eluate behaviour of untreated and leached fly ash from the two MSWI plants Zuchwil and Hinwil (AWEL, 2013). Based on these first results, a PhD-project has been initiated to investigate the element associations and leaching behaviour of heavy and precious metals in fly ash from municipal solid waste incineration.

6.1.2 Aim of the project

The aim of this project is a detailed characterization of fly ash (FA) and leached filter cake (FC) of six MSWI plants in Switzerland. A defined sampling concept and sample preparation procedure are necessary to produce comparable results of the different MSWI plants. The incorporation of metals in mineral phases or glasses affects essentially the mobility of the metals during fly ash leaching process and in the remaining filter cake. To understand the metal depletion during extraction, the morphology of the particles and the type of chemical binding has to be known. The main mineralogy, the distribution of high concentrated metals, the binding form as well as concentrations from diffusely distributed metals has to be analyzed with standard methods such as X-ray powder diffraction (XRD), inductively coupled plasma optical emission spectrometry (ICP-OES), X-ray fluorescence (XRF) and scanning electron microscopy coupled with an energy dispersive system (SEM-EDS). The results show if there is a dependency of fly ash composition related to the furnace type and the waste input. The results of this study provide the basis for the publication presented in Chapter 3 (Weibel et al., 2016) and the following leaching experiments (Chapter 7).

6.1.3 Investigated waste incinerators

Six MSWI plants in Switzerland were selected for the investigations of this project. A detailed description of each incinerator with important technical parameters is attached in Appendix 6A. The incinerators Zuchwil, Bern and Linth/Niederurnen perform an acidic fly ash leaching (FLUWA process) on site and the fly ash of MSWI plant Hinwil is transported to Zuchwil for treatment. MSWI plant Hagenholz has been started with the FLUWA process in summer 2014 and therefore no leached filter cake was available during the sampling campaign in the end of 2013. MSWI plant Monthey is performing a neutral fly ash leaching and uses instead of acidic scrub water (FLUWA process) cleaned process water. The results of fly ash and filter cake characterization gained from this project are discussed also in connection with the waste combusted during the three months before and after the sampling campaign. The delivered waste is stored and homogenized in the

waste bunker and a capacity of 500 tons per day on average can be combusted in the furnaces. This has the result that dwell times in the bunker occur and the produced combustion residues cannot be attributed directly to the waste input. Nevertheless, interesting shows the question if a correlation between the waste input and the matrix characteristics and/or metal contents of the fly ash is observable in the months around the sampling campaign (detailed sampling weeks see Table 6-8). The plant operators therefore have been provided waste input data categorized in the following groups:

***Table 6-1**: Different categories of waste incinerated.*

Waste type	Description
Municipal waste	Everyday items that are discarded by the public (household waste).
Industrial/commercial waste	Waste which is produced by industrial activities which includes any material that is rendered useless during a manufacturing process such as construction- or plastic waste and bulky goods. Commercial waste consists of waste mainly for the purpose of sport, education or entertainment.
Automobile shredder residues (ASR)	Combustible materials from the car recycling such as car seats, dashboards or isolation materials.
Special waste	Special waste from hospitals and the chemical industry after the regulation on dealings with waste (VeVa).
Sewage sludge	Sewage sludge originates from the process of treatment of waste water and is in most cases combusted in dehydrated form.

SATOM Monthey

This incinerator has burned 175'414 tons of waste with an average municipal waste portion of 60% during the year 2013. This portion is decreasing at the beginning of 2014 with ca. 50% municipal waste input. On the other hand, the commercial waste is increasing from 25% at the end of 2013 to 45% in March 2014. No automobile shredder residues (ASR) are combusted during the months before and after sampling. On average 263 t/d of waste produces 6.5 t/d fly ash. This fly ash is leached with recycled water which comes from the last step of the water treatment process before discharging to the Rhone River. The leaching process produces 11 t/day filter cake which are deposited on a residual-waste landfill in Oulens VD. At the moment Monthey and Hinwil are the only MSWI plants in Switzerland where the bottom ash is discharged dry and not quenched with water.

Table 6-2: *Waste input data from MSWI plant Monthey over the year 2013 and during the three months before and after the sampling campaign (26.11-12.12.2014). The data are obtained from SATOM.*

Waste type	Municipal waste		Industrial/commercial waste		Special waste		Sewage sludge		Total
	t	%	t	%	t	%	t	%	t
2013 total	105'598	60	53'756	31	1'311	0.7	14'749	8	175'414
September 13	8'583	60	4'356	31	109	0.8	1'232	9	14'279
October 13	9'888	56	6'311	36	149	0.8	1'293	7	17'640
November 13	8'690	64	3'631	27	108	0.8	1'107	8	13'537
December 13	8'865	65	3'407	25	115	0.9	1'191	9	13'579
January 14	7'493	54	4'822	35	138	1.0	1'515	11	13'968
February 14	6'736	49	5'463	39	134	1.0	1'547	11	13'880
March 14	7'309	45	7'314	45	134	0.8	1'485	9	16'242

Energiezentrale Forsthaus Bern

MSWI plant Bern has been in operation since March 2013 and total 116'676 tons of waste was burned in 2013. On average 300 t/d of waste is combusted in one furnace (MARTIN GmbH) and the municipal waste makes up ca. 60% and the industrial/commercial part ca. 40%. 1% of the total waste input is special VeVa-waste and sewage sludge is only burned from January to March 2014. 6-7 t/d fly ash is produced which are leached together with the accruing wood ash from the wood chip power plant.

Table 6-3: *Waste input data from MSWI plant Bern over the year 2013 and during the three months before and after the sampling campaign (25.11-12.12.2014). The data are obtained from Energie Wasser Bern (EWB).*

Waste type	Municipal waste		Industrial/commercial waste		Special VeVa-waste		Sewage sludge		Total
	t	%	t	%	t	%	t	%	t
2013 total	75'402	64	39'883	34	1'276	1	352	0	116'913
September 13	5'658	59	3'897	40	71	0.7	0	0	9'626
October 13	6'165	57	4'498	42	63	0.6	0	0	10'726
November 13	5'911	57	4'232	41	141	1.4	0	0	10'284
December 13	5'789	64	3'062	34	98	1.1	27	0	8'976
January 14	5'991	61	3'053	31	74	0.8	648	7	9'766
February 14	5'040	56	3'246	36	97	1.1	624	7	9'007
March 14	5'613	55	4'189	41	87	0.8	355	3	10'244

Linth Niederurnen

A total amount of 113'400 tons of waste was combusted at MSWI plant Linth/Niederurnen during 2013. The industrial waste amount is almost 60% with ca. 3% AS-residues and 1% special hazardous waste. Around 300 tons of waste is incinerated and 7 tons of fly ash is accruing daily. The FLUWA process is performed half-day at 3 d/week and ca. 18 tons leached filter cake is produced daily. MSWI plant Niederurnen has two oven lines, a Stiefel moving-grate and a MARTIN reciprocating grate with a Stiefel water cooling system.

Table 6-4: *Waste input data from MSWI plant Niederurnen over the year 2013 and during the three months before and after the sampling campaign (25.11-03.12.2014). The data are obtained from MSWI plant Linth/Niederurnen.*

Waste type	Municipal waste		Industrial/commerical waste		ASR		Special waste		Total
	t	%	t	%	t	%	t	%	t
2013 total	48'174	42	60'533	53	3'489	3.1	1'205	1.1	113'400
September 13	4'048	41	5'503	55	288	2.9	112	1.1	9'951
October 13	4'504	39	6'515	57	360	3.1	115	1.0	11'494
November 13	3'960	41	5'383	55	285	2.9	118	1.2	9'746
December 13	4'557	51	4'046	45	303	3.4	81	0.9	8'987
January 14	4'859	61	2'761	35	211	2.7	81	1.0	7'912
February 14	4'174	55	3'075	40	325	4.2	80	1.0	7'653
March 14	4'496	53	3'550	42	342	4.0	108	1.3	8'496

Hagenholz Zürich

This plant is a typical city incinerator where the amount of municipal waste is elevated. Total 258'337 tons waste was burned 2013 whereas 64% (164'635 t) are municipal waste, 24% (62'553 t) industrial/commercial waste, 3% AS-residues and special VeVa-waste (8'014 t) and 9% sewage sludge (23'135 t). The incineration residues should contain significant lower metal concentrations due to a municipal waste portion of >60% and the small industrial input compared to incinerators with a high industrial waste input such as MSWI plant Zuchwil or Hinwil.

Table 6-5: *Waste input data from MSWI plant Hagenholz over the year 2013 and during the three months before and after the sampling campaign (21.11-12.12.2014). The data are obtained from Entsorgung & Recycling Zürich (ERZ).*

Waste type	Municipal waste		Commercial waste		ASR and special-waste		Sewage sludge		Total
	t	%	t	%	t	%	t	%	t
2013 total	164'635	64	62'553	24	8'014	3.1	23'135	9.0	258'337
September 13	10'889	64	4'211	25	428	2.5	1'416	8.4	16'944
October 13	13'514	64	5'084	24	504	2.4	1'994	9.5	21'097
November 13	14'146	65	5'181	24	520	2.4	1'790	8.3	21'638
December 13	15'578	66	5'521	23	909	3.8	1'746	7.4	23'754
January 14	15'528	67	5'359	23	692	3.0	1'552	6.7	23'131
February 14	14'225	68	4'835	23	635	3.0	1'171	5.6	20'865
March 14	13'864	60	6'244	27	1'084	4.7	1'740	7.6	22'933

KEZO Hinwil

The MSWI plant Hinwil has three oven lines and a total amount of 194'044 tons of waste were burned in the year 2013. Half of the amount (89'179 t) was municipal waste and the other half (85'672 t) waste from the industry (commercial-, special waste and ASR). Obvious are the high amounts (10-15%) of AS-residues and hazardous waste (VeVa-waste) compared to other incinerators. In addition, 19'194 tons of dehydrated sewage sludge were combusted because it has been prohibited to use it as fertilizer in agriculture in Switzerland since 2006 (FOEN, 2014). Between 550 and 950 tons of waste is incinerated

daily whereas 10.2-13.7 t/d fly ash is produced. The whole fly ash is leached together with the fly ash from Zuchwil at MSWI plant Zuchwil.

Table 6-6: *Waste input data from MSWI plant Hinwil over the year 2013 and during the three months before and after the sampling campaign (29.11-18.12.2014). The data are obtained from KEZO.*

Waste type	Municipal waste		Industrial/commercial waste		ASR and special-waste		Sewage sludge		Total
	t	%	t	%	t	%	t	%	t
2013 total	89'179	46	65'622	34	20'050	10	19'194	10	194'045
September 13	7'980	48	5'409	33	1'753	11	1'454	9	16'596
October 13	8'000	45	5'894	33	2'276	13	1'693	10	17'863
November 13	7'145	43	5'420	33	2'380	15	1'500	9	16'445
December 13	7'089	47	5'246	35	1'231	8	1'550	10	15'116
January 14	6'923	51	3'700	27	1'268	9	1'730	13	13'621
February 14	6'105	51	2'998	25	1'305	11	1'539	13	11'947
March 14	7'166	49	4'497	31	1'352	9	1'655	11	14'670

Emmenspitz Zuchwil

The incinerator Emmenspitz Zuchwil combusted 220'852 tons of waste in 2013. 540-750 tons were combusted daily whereas the industrial/commercial part makes up around 50% of the total waste input, which is a high value compared to conventional municipal incinerators such as MSWI plant Hagenholz. In addition, 3% of sewage sludge, 0.5-1% AS-residues and special waste (VeVA-waste) were combusted simultaneously. ASR waste contains ca. 1% metals and increasing burned ASR amounts result in elevated metal concentrations in the fly ash. Thereby 15-21 t/d fly ash was produced which was leached by the FLUWA process together with the delivered fly ash from MSWI plant Hinwil. The primary waste delivered to MSWI plant Zuchwil in the year 2013 and during the three months prior and after the sampling campaign (September 13 - March 14) is composed in average of the groups summarized in Table 6-7.

Table 6-7: *Waste input data from MSWI plant Zuchwil over the year 2013 and during the three months before and after the sampling campaign (29.11-18.12.2014). The data are obtained from KEBAG AG.*

Waste type	Municipal waste		Industrial/commercial waste		ASR and special-waste		Sewage sludge		Total
	t	%	t	%	t	%	t	%	t
2013 total	110'114	50	101'415	46	1'580	0.7	7'743	3.5	220'852
September 13	8'851	47	9'371	49	214	1.1	502	2.7	18'938
October 13	10'224	48	10'103	47	250	1.2	804	3.8	21'381
November 13	8'831	48	8'905	48	89	0.5	664	3.6	18'489
December 13	9'236	54	7'320	43	57	0.3	526	3.1	17'139
January 14	9'491	56	6'709	40	65	0.4	671	4.0	16'936
February 14	8'051	51	6'970	44	77	0.5	585	3.7	15'683
March 14	9'111	50	8'367	46	80	0.4	552	3.0	18'110

6.2 Materials and methods

6.2.1 Sampling and sample preparation

Fly ash and leached filter cake samples from the six described MSWI plants were taken during three weeks in November/December 2013. The daily sampling over three weeks resulted in 2-3 containers (15 kg) of fly ash and filter cake from each plant. The fly ash was already relatively homogeneous and was prepared for analysis by splitting to 1 kg. Half of the prepared material was dried at 105°C (chemical analysis) and the other half was dried at 40°C (mineralogical analysis). The fly ash has already been collected as fine powder and only needed a final grinding to particle size <0.1 mm (tungsten-carbide disk) for the chemical and mineralogical analyses. The filter cake was wet and compacted and thus less homogeneous. Before splitting to 1 kg, the material was therefore crushed with a mortar and one part was dried at 40°C and the other at 105°C for several days. For the SEM analysis the non-milled samples were used. In addition, a certified reference material (BCR 176R, Held et al., 2007) is used as quality control for each method.

Table 6-8: *Used fly ash (FA) and leached filter cake (FC) samples from the 6 MSWI plants.*

Sample	Description	MSWI plant	Sampling period
FAMON	Fly ash	SATOM Monthey	26.11. - 12.12.13
FCMON	Neutral leached filter cake	SATOM Monthey	26.11. - 12.12.13
FABER	Fly ash	EZ Forsthaus Bern	25.11. - 12.12.13
FCBER	Acidic leached filter cake (Mix from FABER/wood ash (WABER))	EZ Forsthaus Bern	25.11. - 12.12.13
FANIE	Fly ash	Linth Niederurnen	25.11. - 03.12.13
FCNIE	Acid leached filter cake	Linth Niederurnen	25.11. - 03.12.13
FAHAG	Fly ash	Hagenholz Zürich	21.11. - 12.12.13
FAHIN	Fly ash	KEZO Hinwil	29.11. - 18.12.13
FAZUC	Fly ash	Emmenspitz Zuchwil	29.11. - 18.12.13
FCZUC	Acidic leached filter cake mix KEBAG + KEZO	Emmenspitz Zuchwil	29.11. - 18.12.13
BCR 176R	Reference Material	-	-

6.2.2 Chemical and mineralogical analyses

WD-XRF

The X-ray fluorescence technique (XRF) is used in geosciences as a standard method for the chemical analysis of rocks. Each element has a unique X-ray signature that can be identified by measurement of its characteristic X-ray emission energy (ED-XRF) or wavelength (WD-XRF). A major advantage of XRF techniques compared to wet chemical procedures is the direct multielemental analysis of solid samples. The time consuming wet digestion step with toxic acids such as hydrofluoric acid (HF 40%) can be avoided and a considerable decrease in preparation and analysis time is achieved. An often applied preparation method for XRF analysis is fusion and the production of glass tablets using a flux such as lithium tetraborate. The dilution with the flux yields to a constant matrix

composition and reduces analytical problems. However, tests with fly ash and acidic leached filter cake showed that fusion is not a suitable preparation method for fly ash analysis. The high concentrations of heavy metals (presumably Zn) provoke cracking during cooling, especially in the case of the leached filter cake. Moreover, volatile elements such as Cd, Pb or Zn evaporate during the fusion process. An alternative preparation method is the pressure of powder tablets (32 mm diameter, 4 g fly ash material + 0.9 g Hoechstwax as binder). Using this preparation method, a homogenous aliquot is essential and the ash samples have to be ground to a very fine-grained powder. Fly ash is already relatively fine grained and homogenous compared to bottom ash and the powder tablet preparation offers a reliable preparation method. After the XRF analysis, the measured intensities of each element have to be converted into a quantitative value. Uniquant, a program developed by Omega Data (Omega Data Systems, 2004) offers the possibility of quantification of the measured intensity of a fluorescence line by using fundamental physical parameters. It measures a number of channels, which are measuring positions at a defined instrumental setting. The analysis program is optimized for speed, a typical measurement lasts only about 6 minutes. UniQuant achieves this speed by measuring only a number of selected fluorescence lines, instead of scanning the entire spectrum. The analyzed elements are divided into several groups, each of them having an optimized instrumental setting. The method developed is called "semiquantitative" or "standardless" since it is not based on a set of standards and calibration curves. This means that the method does not require a material-dependant standartization and samples prepared in very variable ways are measurable. The chemical analysis of the major and trace elements were performed on pressed powder tablets with a Philipps WD-XRF PW2400 and calculated by UniQuant at the University of Fribourg. The loss on ignition (LOI) was done by drying the fly ash overnight at 105°C and then heating them at 1'050°C in a muffle furnace for 1.5 h.

Total digestions prior to ICP-OES analysis (TD-ICP-OES)

For detailed trace element analysis a Varian 720-ES ICP-OES was used after microwave assisted acid digestion of the fly ash. The sample preparation for ICP-OES and the analyses were performed according to the operation procedure in Appendix 6D.

6.2.3 X-ray powder diffraction analysis (XRD)

The X-ray powder diffraction analysis (XRD) were performed using a Panalytical X'Pert Pro diffractometer with CuKα-radiation (λ=1.541 Å), an acceleration voltage of 40kV and an electron generating current of 40 mA. The measurement step size was 0.0167 °2θ, the scan range 5-60°. 2 g of the milled and dried (40°C) ash samples were mixed with 20 wt.% griceite (internal standard) and pressed into the sample holders. To avoid orientation effects a special textured stamp was used. Identification of mineral phases as well as their structural analyses applying Rietveld refinement was performed using the Panalytical

Software "High Score Plus". The absolute contents of the mineral phases and the amorphous parts were calculated with the help of the internal standard.

6.2.4 Scanning electron microscopy (SEM)

The dried samples were impregnated with epoxy resin, sanded and polished (without water). The samples were coated with carbon to avoid surface charging for SEM analyses. A Zeiss EVO-50 XVP electron microscope (SEM) coupled with an energy dispersive system (EDS) was used to perform spot chemical analyses of solid material. For backscattered electron (BSE) images, the tension of the electron beam was set to 20 kV in the high vacuum mode and a spot size of 504 nm was used. Acquiring secondary electron (SE) images of unconsolidated fly ash specimens, the tension of the electron beam was set to 20 kV with variable pressure of 10 Pa and a spot size of 477 nm.

6.2.5 External analyses

For method comparison all fly ash and filter cake samples were external analyzed by Bachema AG, Schlieren and Actlabs Activation Laboratories Ltd, Anchaster, Ontario. Total digestions prior to ICP-OES (ICP-MS for Cd) were performed by Bachema and neutron activation analyses (INAA) or ICP-OES analyses (element depending) were performed by Actlabs. Furthermore, all samples were analyzed at the laboratory of the Zentrum für nachhaltige Abfall- und Ressourcennutzung (ZAR) Zuchwil using a Spectro Xepos ED-XRF.

6.3 Results and discussion

6.3.1 Chemical composition

The total elemental composition of the fly ash and filter cake from the six MSWI plants were determined by WD-XRF and the results expressed in terms of weight percent of oxide due to the formation under oxidizing conditions (Table A6-1 to A6-3, Appendix 6C). Beside the bulk chemical analyses performed by WD-XRF, microwave assisted total digestions of all fly ash and filter cake samples were produced. Enriched, volatile heavy metals (Zn, Pb, Cu, Cd) and other metals of interest (Al, Fe, Sb) and some high enriched matrix elements (Ca, Mg) are analyzed in the acidic digestions by ICP-OES.

In the course of these investigations the validity of XRF and TD-ICP-OES analysis for the determination of selected elements (Ca, Al, Fe, Zn, Pb, Cu, Sb and Cd) in fly ash was tested by comparing them with data obtained from independent laboratories using different techniques (WD-XRF, ED-XRF, TD-ICP-OES and INAA). In addition, a fly ash standard reference material (BCR 176R) was used as quality control for each analysis method.

WD-XRF analyses

The major constituent in the six fly ash samples is CaO (~22 wt.%) followed by SiO_2 (ca. 10 wt.%), Na_2O (ca. 9 wt.%), K_2O (ca. 6 wt.%) and Al_2O_3 (ca. 4.5 wt.%). In addition, the concentrations of Cl (ca. 106'000 mg/kg), P_2O_5 (ca. 4'200 mg/kg) and SO_3 (ca. 55'000 mg/kg) are strongly elevated in all fly ashes. The LOI was determined at 1'050°C and shows rather high values of ca. 10 wt.% (Table A6-1, Appendix 6C). Tests have shown that beside the H_2O and the CO_2 also significant concentrations of the volatile elements Pb and Zn as well as Cl release from the fly ash during heating to 1'050°C. The used method is evaluated for less reactive rock materials and for future LOI analysis of fly ash, a more moderate program with a maximum temperature of 600-700°C and a slower temperature increase over several hours is required (Li et al., 2004; Bayuseno and Schmahl, 2011). The sum of all constituents (major constituents as oxides) including the LOI provided the total of ca. 90%. Many volatile metals with low melting points are highly enriched in the fly ash such as Pb (327.4°C), Zn (419.5°C) or Cd (321.1°C). The concentration of Pb range from 3'460 mg/kg to 11'600 mg/kg and the concentration of Zn reach values of 21'300 mg/kg to 69'700 mg/kg. The metal concentration depends strongly on the waste input and the combustion conditions (e.g. firing temperature) of the MSWI plants as will be discussed further below when the waste input is involved in the discussion (Section 6.4.3). After acidic leaching (FLUWA process) significant amounts (ca. 30 wt.%) of highly soluble constituents are dissolved and the remaining filter cake therefore depleted in Na_2O (<1 wt.%), K_2O (ca. 1 wt.%) or Cl (<10'000 mg/kg) (Table A6-1, Appendix 6C). On the other hand, the dissolution of these phases leads to an increase of the relative content of less soluble major phases such as SiO_2, CaO, Al_2O_3 or SO_3. The heavy metal depletion is discussed in detail on the basis of the total digestions measured by ICP-OES (see below).

ICP-OES analysis after microwave digestion

FAHAG shows the most elevated Ca-concentration (261'121 mg/kg) and FAKEZ and FAZUC have the lowest Ca-concentration (Table A6-5, Appendix 6C). These results are in accordance with the determined CaO concentrations by WD-XRF. The Ca concentration in the leached filter cake is elevated compared to the fly ash. Reasons for this elevated concentrations are the formation of gypsum ($CaSO_4 \cdot 2H_2O$) and the increasing relative Ca content due to the dissolution of highly soluble components (mainly salts). The second analyzed matrix element magnesium is 10 times less concentrated in the fly ash compared to Ca. The Mg concentrations of all fly ashes are between 14'000 and 15'000 mg/kg, except from FAZUC (12'501 mg/kg).

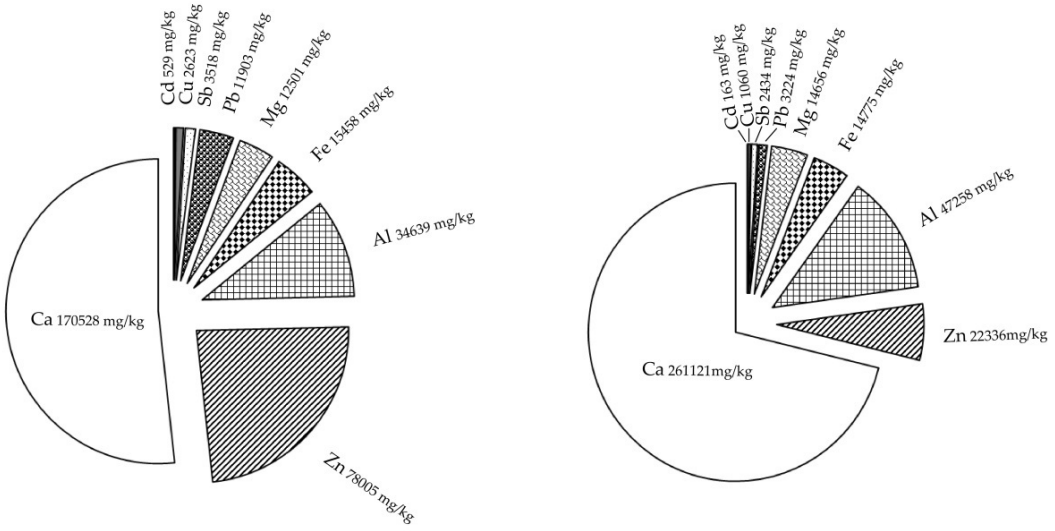

Figure 6-1: *Element distribution in mg/kg of fly ash Zuchwil (FAZUC, left) and fly ash Hagenholz (FAHAG, right).*

The leached filter cakes from Bern and Zuchwil (FCBER and FCZUC) are depleted in Mg with concentrations <10'000 mg/kg (Table A6-5, Appendix 6C). The Pb concentration varies strongly between the different plants. Zinc is heavily enriched and the most dominant heavy metal in fly ash and the only metal which is industrially recycled so far in Switzerland (FLUREC process, Schlumberger et al., 2007). A first group including FANIE, FAHIN and FAZUC shows elevated Zn concentration >50'000 mg/kg. A second group including FAMON, FABER and FAHAG shows significant lower Zn concentration between 20'000 and 30'000 mg/kg. The Zn concentration in all acidic leached filter cakes is strongly reduced compared to the neutral leached filter cake from Monthey (FCMON). The less volatile elements Fe and Al are mostly present in the bottom ash. Nevertheless, due to their high concentration in the waste input a significant concentration is also present in the fly ash. FANIE and FAHIN have Fe concentrations >20'000 mg/kg and all others around 15'000 mg/kg. The Al concentrations of FAHIN and FAZUC (ca. 34'000 mg/kg) are lower compared to all other fly ash which show values >40'000 m/kg. Iron and aluminium are both hardly depleted in the filter cake and therefore relatively enriched due to the leaching of the soluble matrix components. The untreated fly ashes FAZUC and FAHIN have concentrations of the volatile Pb >10'000 mg/kg whereas FAHAG shows a Pb concentration of 3'224 mg/kg. The only filter cake sample which shows a significant Pb reduction is FCZUC which is the mix of leached FAZUC and FAHIN. The fly ash with the highest Cu concentration is FAMON (mg/kg), followed by FANIE, FAHIN and FAZUC (ca. 2'650 mg/kg). FABER and FAHAG show significant lower Cu concentrations <1'500 mg/kg. No obvious depletion is noticeable in the filter cake and intensive research is required to achieve an increasing Cu depletion. The heavily toxic Sb is present in fly ash in concentrations between 2'271 and 3'518 mg/kg and is not extracted during the FLUWA process. The high volatile Cd is in general present in fly ash in low concentration

<600 mg/kg. FAZUC shows twice the concentration of Cd (529 mg/kg) compared to the other fly ashes which have concentrations <300 mg/kg Cd. After acidic leaching, the Cd is effectively depleted in FCBER and FCZUC (≤50 mg/kg). FCNIE shows a depletion of ca. half of the concentration presents in the untreated fly ash (118 mg/kg to 292 mg/kg before) and the neutral leaching performed at MSWI plant Monthey (FCMON) leads to zero Cd depletion.

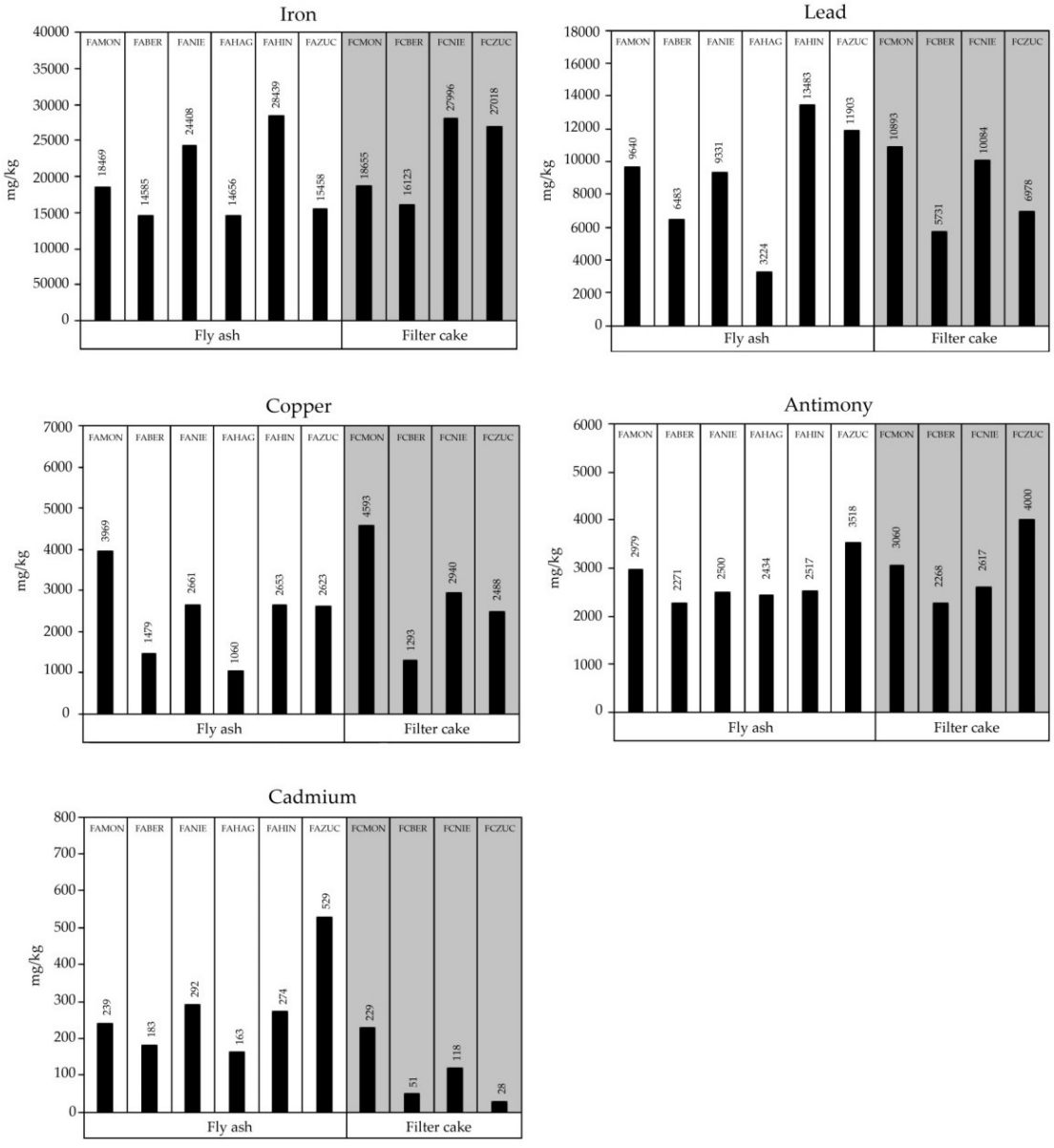

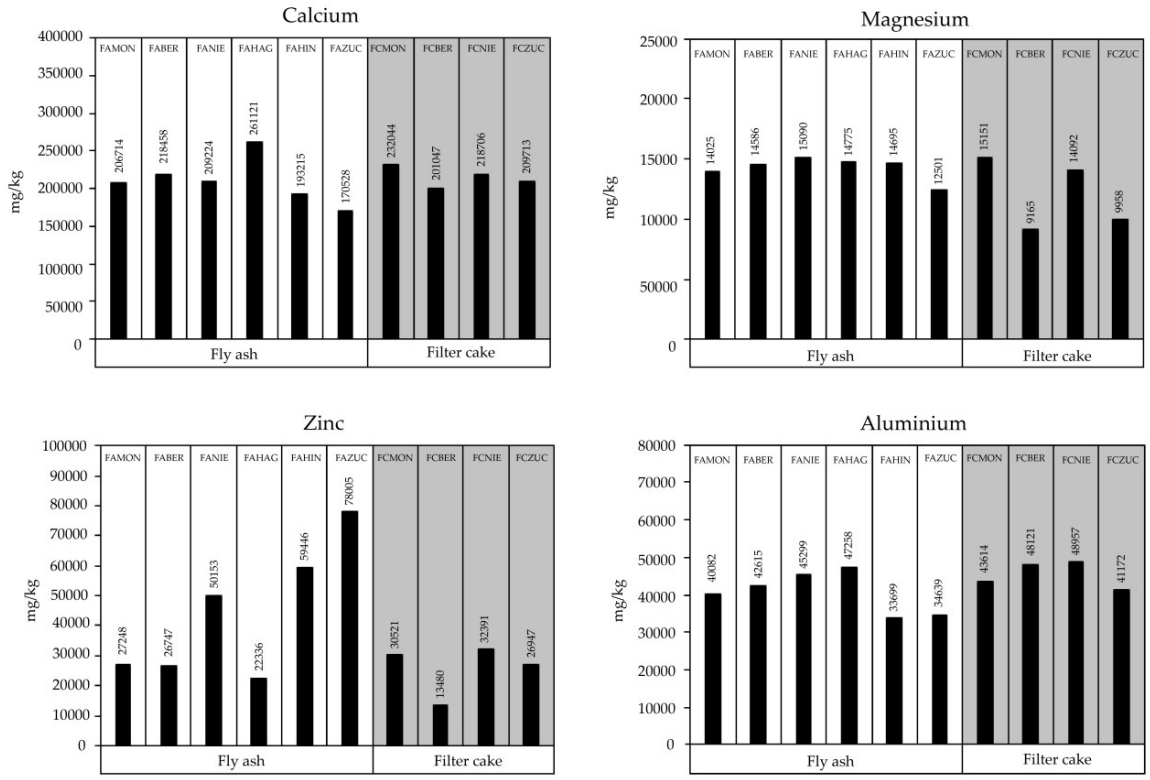

***Figure 6-2**: Concentration (mg/kg) of each specific element determined by TD-ICP-OES in the fly ash (FA) of the different plants (white background) and the acidic (FCBER, FCNIE, FCZUC) or neutral (FCMON) leached filter cakes (FC, grey background).*

6.3.2 Method comparison

The evaluation of a robust analytical procedure for metal determination in fly ash is very important because fly ash has a very challenging matrix because of the high metal and silicate concentration. For routine application a rapid and simple analytical method with an adequate precision and accuracy is important. As described in Section 6.2.2 the major advantage of XRF techniques compared to wet chemical procedures is the multielemental and fast analysis of solid materials without laborious wet digestion steps. An evaluation of the XRF method for analysis of some major and minor elements (Ca, Zn, Fe, Al, Pb, Cu, Sb and Cd) in fly ash was done by comparison with data obtained from independent laboratories using different techniques (Table 6-9).

Table 6-9: *List of laboratories and techniques used for the fly ash analysis comparison with the corresponding expanded measurement uncertainty area for all measured elements.*

Laboratory	Technique	Expanded measurement uncertainty
Institute of Geological Sciences, University of Bern (UniBE)	Total digestion + ICP-OES	10-20%
Bachema AG, Schlieren	Total digestion + ICP-OES (ICP-MS)	12-24%
Actlabs Activation Laboratories Ltd, Ontario	INAA or ICP-OES	-
Institute of Geological Sciences, University of Fribourg (UniFR)	WD-XRF	12-25%
ZAR, Zuchwil	ED-XRF	11-22%

Microwave assisted digestions plus ICP-OES analyses were performed on our own at the Institute of Geological Sciences and parallel at Bachema AG. This method offers a precise technique for element determination in fly ash. After acidic digestion, the whole matrix is dissolved and the element concentrations are exact determinable by ICP-OES after appropriate dilution with deionized water. However, to ensure efficient mobilization of all metals into solution, a strong acid mix (HNO_3/HF) is required due to the presence of high concentrations of Si. The acid mix together with the digestion temperature of 200°C poses a certain risk for the lab technician and is also more time consuming compared to non-destructive methodologies such as XRF or neutron activation analyses (INAA). Wavelength dispersive X-ray fluorescence analyses (WD-XRF) were performed on pressed powder tablets at University of Fribourg and energy dispersive X-ray fluorescence analysis (ED-XRF) at ZAR Zuchwil. Furthermore, all samples were sent to Canada (Activation Laboratories) for INAA-analyses.

The precision and accuracy of each method, except INAA, was checked by analyzing the certified reference material BCR 176R. Good agreements were achieved in general between certified values and data obtained with a recovery range from 90-120%. The destructive TD-ICP-OES technique performed at our institute and Bachema AG show even more precise recoveries of 95-110% compared to the two non-destructive XRF-techniques (90-120%) (Table A6-8, Appendix 6C).

Table 6-10: *Recovery in % of the certified elements in BCR 176R by the different laboratories and analytical techniques.*

BCR 176R certified values (mg/kg)		**Recovery (%)**			
Elements	mg/kg	TD-ICP-OES UniBE	TD-ICP-OES Bachema	WD-XRF UniFR	ED-XRF ZAR
Zn	16'800	95	107	95	100
Fe	13'100	109	111	90	99
Pb	5'000	101	99	94	92
Cu	1'050	106	102	90	95
Sb	850	102	-	121	104
Cd	226	99	93	109	117

All generated results from TD-ICP-OES and XRF for the six fly ashes and the four leached filter cakes give values within the expanded measurement uncertainty. Relative standard deviations (RSD) calculated across the two TD-ICP-OES and the two XRF methods show values for the elements Zn, Pb (Table 6-11) and Cu <8% and in most cases <5%. However, the Actlabs results are on average 27% (Zn) and 12% (Cu) lower compared to all other methods and Pb results generated by Actlabs are all over the used calibration range and therefore useless (Table A6-6 and A6-7, Appendix 6C).

Table 6-11: *Pb concentrations in each fly ash and filter cake analyzed with the different techniques.*

Sample	**TD-ICP-OES UniBE**	**TD-ICP-OES Bachema**	**WD-XRF UniFR**	**ED-XRF ZAR**	**x**	**s**	**RSD (%)**
	mg/kg	mg/kg	mg/kg	mg/kg	mg/kg	-	%
FAMON	9'640	9'560	9'590	9'332	9'530	136	1.4
FCMON	10'893	10'600	11'700	10'220	10'853	628	5.8
FABER	6'483	6'260	6'530	6'311	6'396	131	2.0
FCBER	5'731	5'400	5'430	5'047	5'402	280	5.2
FANIE	9'331	8'950	9'520	9'013	9'204	269	2.9
FCNIE	10'084	9'530	11'200	9'489	10'076	797	7.9
FAHIN	13'483	13'400	13'600	13'090	13'393	218	1.6
FAZUC	11'903	11'400	11'400	11'176	11'470	307	2.7
FCZUC	6'978	6'700	7'000	6'740	6'855	156	2.3
FAHAG	3'224	3'140	3'460	3'220	3'261	138	4.2
BCR 176R	5'028	4'950	4'680	4'617	4'819	201	4.2

The Actlabs results show Ca-concentrations in the range as the other methods (15-26 wt.%) (Figure 6-3). The lowest Ca-values are generated by WD-XRF, followed by the Actlabs results and the TD-ICP-OES. The RSD calculation for Ca across all methods lies between 5% and 15% and is significant higher compared to the elements Zn, Pb and Cu. In addition, the total digestions also generate the highest Fe and Al concentrations whereas the XRF results are significant lower. The opposite distribution is present in the case of Cd and Sb. XRF analysis give the highest concentration, followed by the total digestions and the Actlabs analysis.

The results of this method comparison show that WD-XRF offers a reliable alternative analytical method especially for the determination of Zn, Pb and Cu. These three heavy metals are the most relevant elements for recycling at the moment and of particular interest for the plant operators. Fast analysis of fly ash and filter cake without long and complicated sample preparation are possible directly at the plant. It is recommended not to trust UniQuant-analyses at concentrations <100 ppm (Omega Data Systems, 2004) and the limit of detection of XRF techniques (ca. 5 mg/kg) compared to ICP-OES (0.001 mg/L) is relatively high. However, these facts shows no problem for XRF fly ash analyses due to the high metal concentrations of mostly >1%.

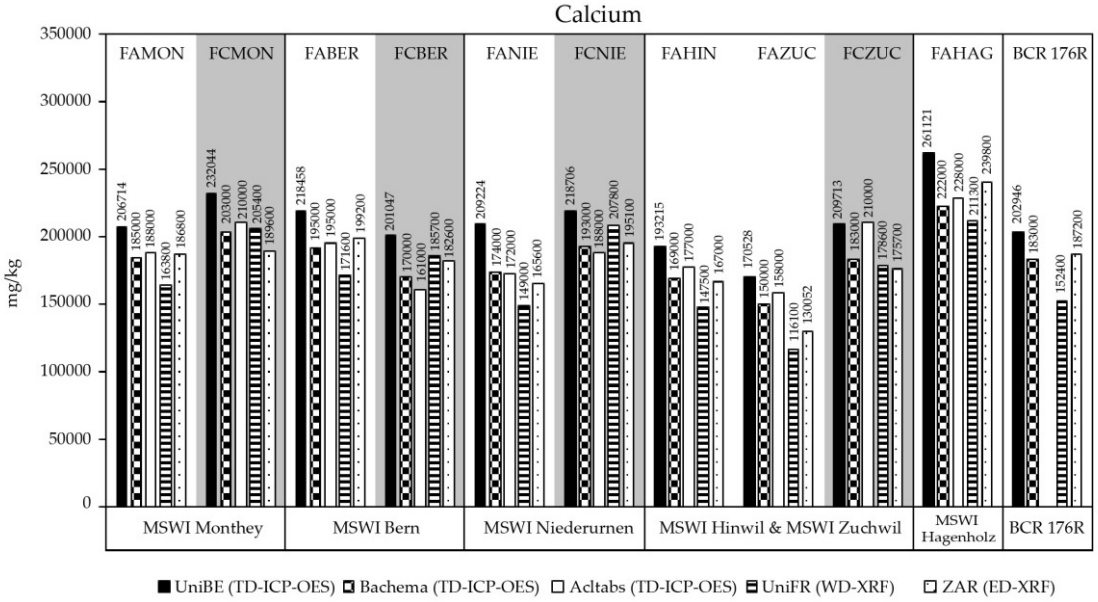

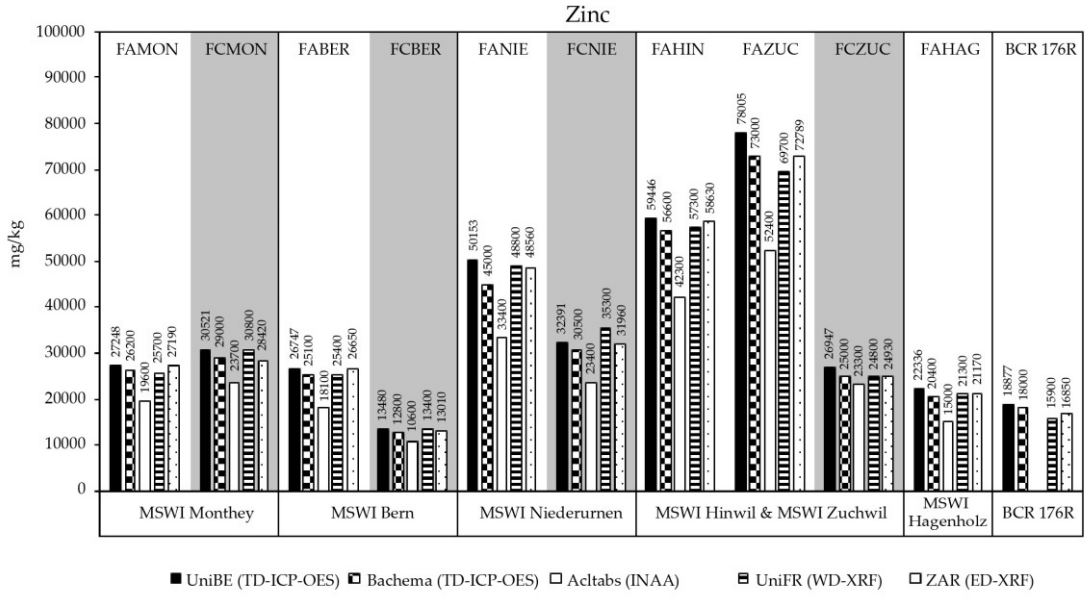

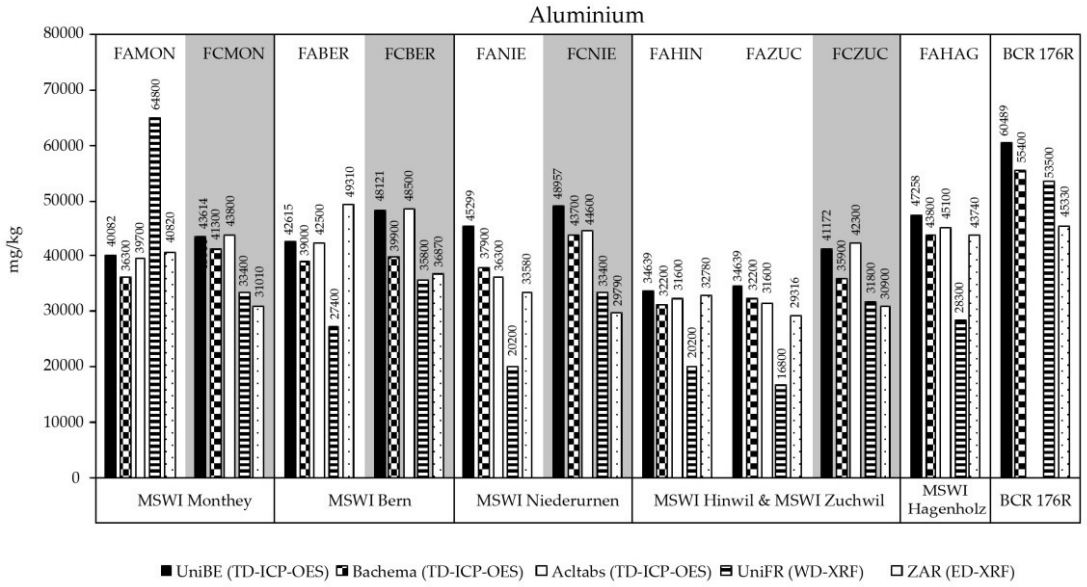
Aluminium
mg/kg
80000
70000
60000
50000
40000
30000
20000
10000
0
FAMON
FCMON
FABER
FCBER
FANIE
FCNIE
FAHIN
FAZUC
FCZUC
FAHAG
BCR 176R
40082
36300
39700
64800
40820
43614
41300
43800
33400
31010
42615
39800
42500
27400
49310
48121
39900
48500
35800
36870
45299
37900
36300
20200
33580
48957
43700
44600
33400
29790
34639
32200
31600
20200
32780
34639
32200
31600
16800
29316
41172
38900
42300
31800
30900
47258
43800
45100
28300
43740
60489
55400
53500
45330
MSWI Monthey
MSWI Bern
MSWI Niederurnen
MSWI Hinwil & MSWI Zuchwil
MSWI Hagenholz
BCR 176R
UniBE (TD-ICP-OES)
Bachema (TD-ICP-OES)
Acltabs (TD-ICP-OES)
UniFR (WD-XRF)
ZAR (ED-XRF)

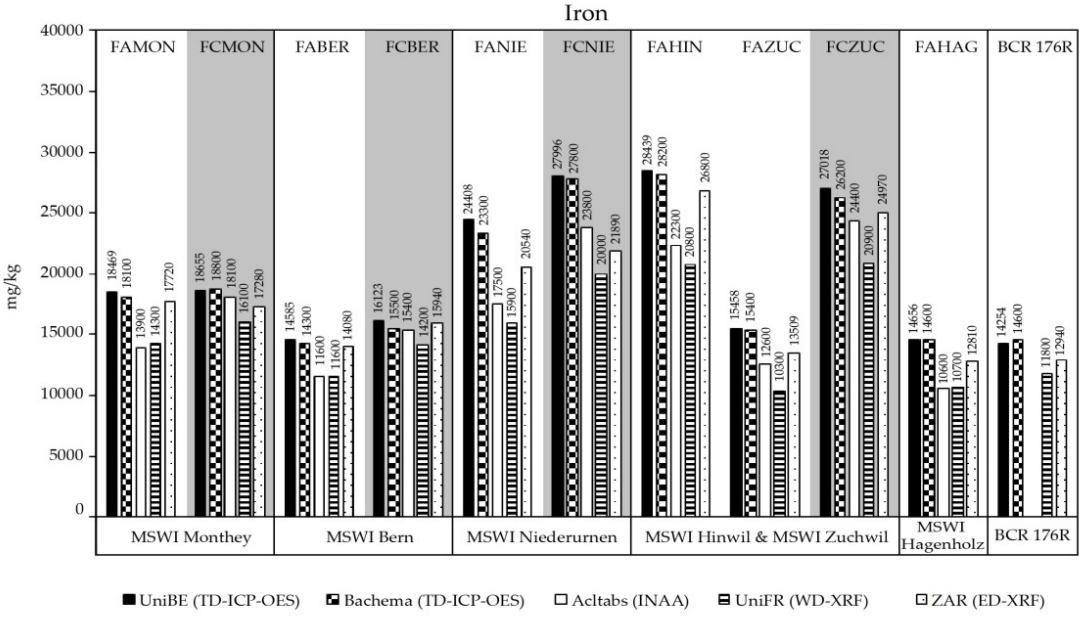
Iron
mg/kg
40000
35000
30000
25000
20000
15000
10000
5000
0
FAMON
FCMON
FABER
FCBER
FANIE
FCNIE
FAHIN
FAZUC
FCZUC
FAHAG
BCR 176R
18469
18100
13900
14300
17720
18655
18800
18100
16100
17280
14585
14300
11600
11600
14080
16123
15500
15400
14200
15940
24408
23300
17500
15900
20540
27996
27800
23800
20000
21890
28439
28200
22300
20800
26800
15458
15400
12600
10300
13509
27018
26200
24400
20980
24970
14656
14600
10600
10700
12810
14254
14600
11800
12940
MSWI Monthey
MSWI Bern
MSWI Niederurnen
MSWI Hinwil & MSWI Zuchwil
MSWI Hagenholz
BCR 176R
UniBE (TD-ICP-OES)
Bachema (TD-ICP-OES)
Acltabs (INAA)
UniFR (WD-XRF)
ZAR (ED-XRF)

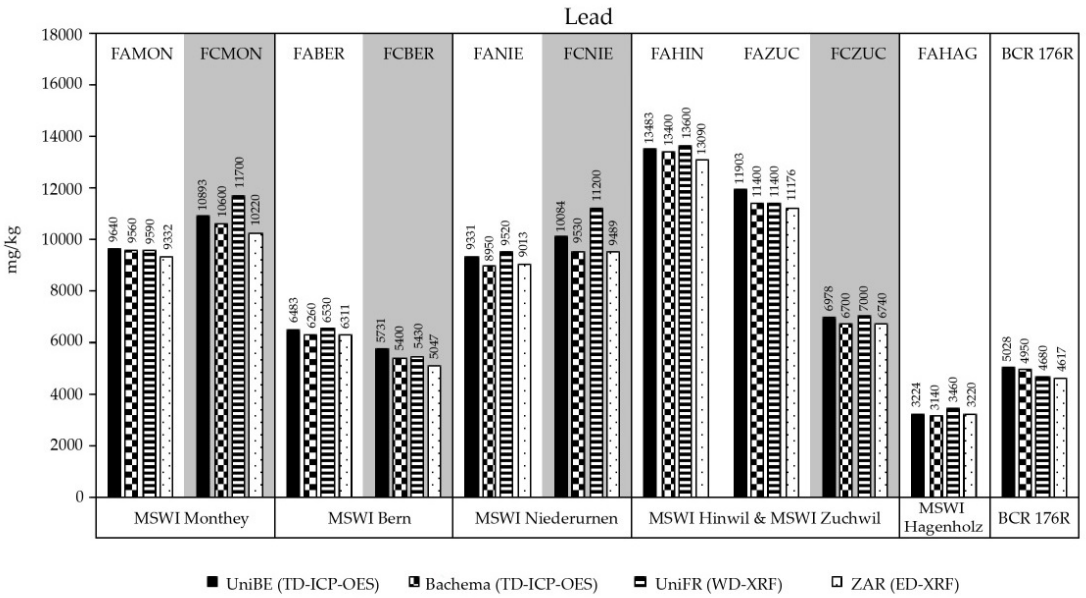
Lead
mg/kg
18000
16000
14000
12000
10000
8000
6000
4000
2000
0
FAMON
FCMON
FABER
FCBER
FANIE
FCNIE
FAHIN
FAZUC
FCZUC
FAHAG
BCR 176R
9640 9560 9590 9332
10893 10600 11700 10220
6483 6260 6530 6311
5731 5400 5430 5047
9331 8950 9520 9013
10084 9530 11200 9489
13483 13400 13600 13090
11903 11400 11400 11176
6978 6700 7000 6740
3224 3140 3460 3220
5028 4950 4680 4617
MSWI Monthey
MSWI Bern
MSWI Niederurnen
MSWI Hinwil & MSWI Zuchwil
MSWI Hagenholz
BCR 176R
UniBE (TD-ICP-OES)
Bachema (TD-ICP-OES)
UniFR (WD-XRF)
ZAR (ED-XRF)

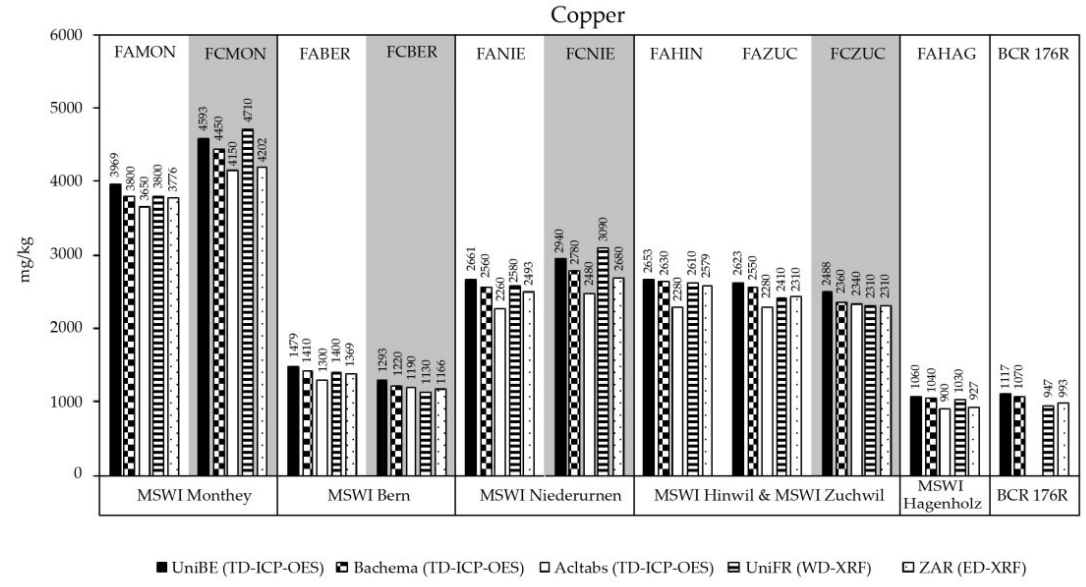
Copper
mg/kg
6000
5000
4000
3000
2000
1000
0
FAMON
FCMON
FABER
FCBER
FANIE
FCNIE
FAHIN
FAZUC
FCZUC
FAHAG
BCR 176R
3969 3800 3650 3800 3776
4593 4450 4150 4710 4202
1479 1410 1300 1400 1369
1293 1220 1190 1130 1166
2661 2560 2260 2580 2493
2940 2780 2480 3090 2680
2653 2630 2280 2610 2579
2623 2550 2280 2410 2310
2488 2360 2340 2310 2310
1060 1040 900 1030 927
1117 1070 947 993
MSWI Monthey
MSWI Bern
MSWI Niederurnen
MSWI Hinwil & MSWI Zuchwil
MSWI Hagenholz
BCR 176R
UniBE (TD-ICP-OES)
Bachema (TD-ICP-OES)
Acltabs (TD-ICP-OES)
UniFR (WD-XRF)
ZAR (ED-XRF)

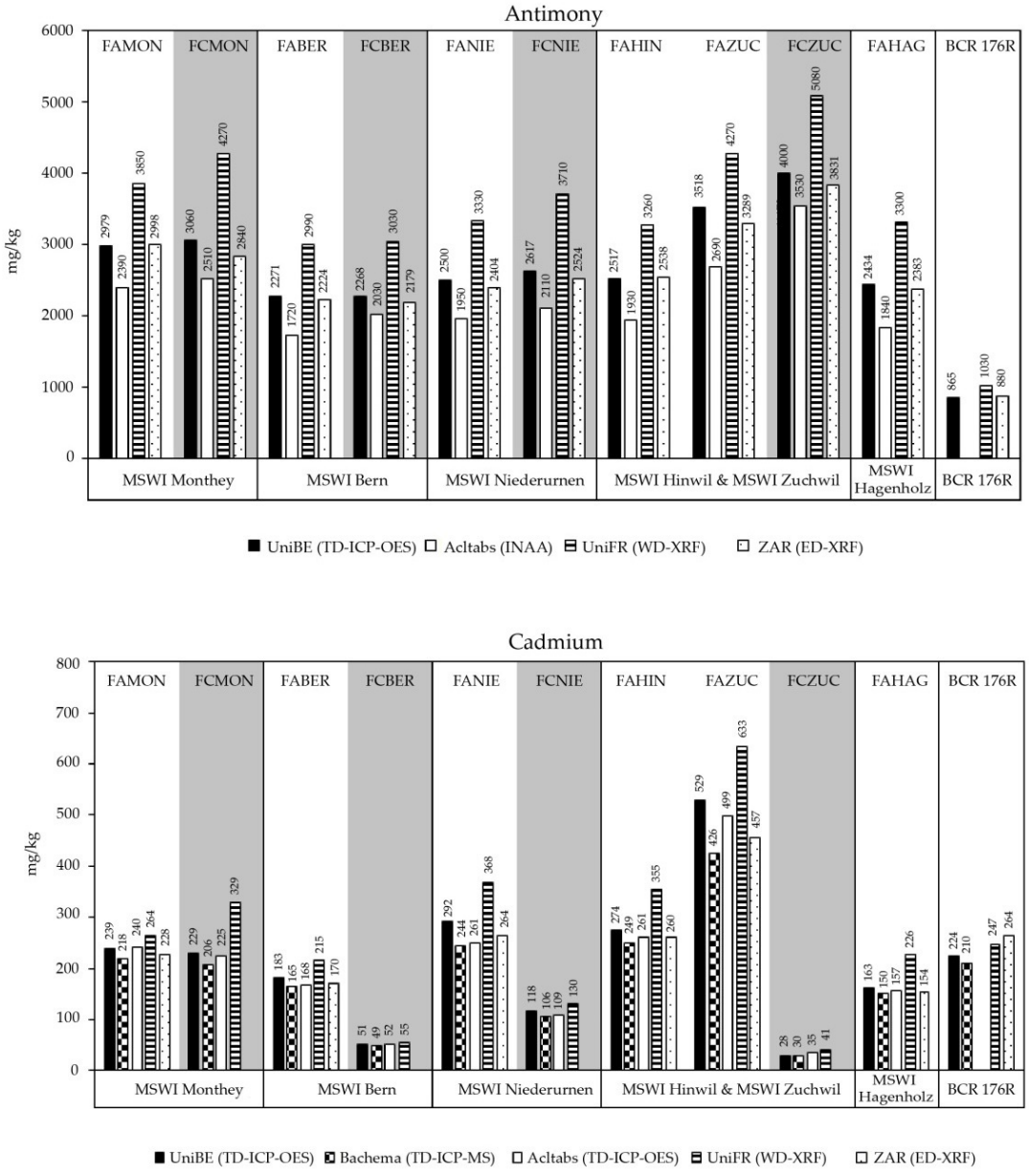

Figure 6-3: *Comparison of concentrations (mg/kg) of some major and trace elements in fly ash (FA, white background) and filter cake (FC, grey background) from the six MSWI plants measured by UniBE (TD-ICP-OES), UniFR (WD-XRF), ZAR Zuchwil (ED-XRF), Bachema (TD-ICP-OES(MS)) and Actlabs (INAA or TD-ICP-OES).*

6.3.3 Mineralogical composition

The quantitative determination of the mineral composition of fly ash is very challenging because of the complexity of the mineralogy as shown in further studies (Kirby and Rimstidt, 1994; Eighmy et al., 1995; Li et al., 2004; Mahieux et al., 2010; Bayuseno and Schmahl, 2011). Several processes are responsible for the complex mineralogy of fly ash

including vaporisation, melting, crystallisation, vitrification, condensation and precipitation, which occur during combustion and treatment of the flue gas (Jakob et al., 1996). Mineralogical analyses were performed to determine major crystalline host phases of metals and phases controlling the leaching chemistry.

Untreated fly ash

XRD Rietveld analyses show that fly ash samples contain ca. 40 wt.% crystalline phases and are dominated by sulphates and chlorides (Table 6-12). The principle minerals present in all fly ashes are highly soluble sodium and potassium salts such as halite (NaCl) and sylvite (KCl). However, potassium-zinc-chloride (K_2ZnCl_4) is identified only in FAZUC, FAHIN and FANIE. Anhydrite ($CaSO_4$) is the dominant sulphate mineral and most abundant in FAHIN. The increased amount of calcite ($CaCO_3$) found in the fly ash is evidence of $CaCO_3$ production through the incorporation of carbon dioxide (CO_2) after cooling. In case the fly ash is directly leached after sampling and not stored for several weeks, only poor crystalline Ca-hydrates are formed but almost no calcite. It is supposed that FAHAG was stored in an open container during three weeks of sampling because an increased calcite amount (8 wt.%) is determined compared to fly ash from other incinerators (2-4 wt.%). Melilite close to gehlenite ($Ca_2Al_2SiO_7$) are the most common newly formed phases during incineration. However, spinel group minerals, which are often associated with melilite, were not identified in any sample. Quartz is identified in all fly ash samples and mostly passed the incineration process without transition (transitory item). The identification of trace minerals (<1%) is very difficult due to the complexity of the mineralogy and thus possible peak overlaps. Identified minor minerals are periclase (MgO), hematite (Fe_2O_3) and mayenite ($Ca_{12}Al_{14}O_{33}$). In addition, hematite (Fe_2O_3) is present in all samples and possibly formed through the oxidation of metallic iron particles.

The amorphous part is determined by the difference between the sum of all crystalline phases and 100%. This results in an amorphous glassy part of ca. 60% for all fly ash samples. This value is rather high and possibly other minor crystalline phases which could not be identified may be involved in this calculated amorphous part. An interesting approach to determine the amorphous phase by Rietveld refinement is shown by Le Bail (1995), in which the amorphous phase is modelled as a nanocrystalline solid where the long range order is lost. This and possibly other methods for the determination of the amorphous part have to be tested for our fly ash matrices in the future. Another procedure to study this amorphous phase is described by Mahieux et al. (2010) who heated the fly ash up to 1'000°C and then slowly cooled to room temperature. The temperature was high enough to melt the amorphous phase and the slow cooling enabled its crystallisation. They concluded that the amorphous phase could be regarded as amorphous gehlenite because the peak of crystalline gehlenite increased significantly in the XRD pattern of the fly ash after the thermal treatment and the hump of the amorphous phase disappeared completely.

Leached filter cake

In comparison to the untreated fly ash, many soluble minerals such as halite and K_2ZnCl_4 are completely dissolved after the acidic leaching (Table 6-12). The only mineral phase remaining in the leached filter cake in almost the same concentrations as in the untreated fly ash is anhydrite (6-11%). However, the neutral leached filter cake FCMON shows half amount of anhydrite (3%) compared to the fly ash. The gehlenite is dissolved completely during acidic leaching whereas during neutral leaching, half of the gehlenite concentration is still present. If well-crystallized gelenites, as known from the ceramic industry, were present a lower solubility would be expected. The complete dissolution of the identified gehlenites is evidence for a very small crystal size where the extract solution has easily access to dissolve them. The dissolution of many soluble phases leads to an increase of the relative content of insoluble minerals and the amorphous phase (>70 wt.%) in the leached filter cake.

The most dominant newly formed mineral phase in all filter cakes is gypsum ($CaSO_4 \cdot 2H_2O$). Except ettringite ($Ca_6Al_2(OH)_{12}(SO_4)_3 \cdot 26H_2O$), which is present FCNIE, all other possible new formed crystalline phases are below detection limit.

Table 6-12: *Mineralogical composition of fly ash (FA) and leached filter cake (FC).*

Mineral phase (wt.%)	Formula	Monthey		Bern			Niederurnen		Hagenholz	Hinwil & Zuchwil		
		FA MON	FC MON	FA BER	WA BER	FC BER	FA NIE	FC NIE	FA HAG	FA HIN	FA ZUC	FC ZUC
Silicates												
Gehlenite	$Ca_2Al_2SiO_7$	13.1	6.7	10.5	10.2	-	11.9	1.0	12	15.1	12.9	-
Quartz	SiO_2	0.5	1.2	2.3	3.6	2.6	0.9	1.4	1.1	1.0	1.5	1.3
Carbonates												
Calcite	$CaCO_3$	2.1	5.7	3.6	15	1.8	4.7	4.9	8.3	2.2	1.5	0.9
Dolomite	$CaMg(CO_3)_2$	-	-	-	-	-	0.7	-	-	0.3	0.5	-
Ankerite	$Ca(Fe,Mg,Mn)(CO_3)_2$	-	-	-	-	-	-	-	-	-	0.1	-
Oxides												
Lime	CaO	0.2	-	0.5	4.3	-	0.9	-	1.5	0.7	0.8	-
Hematite	Fe_2O_3	0.6	0.6	0.5	0.7	0.6	0.6	0.6	0.6	0.7	0.5	0.7
Periclase	MgO	0.4	0.5	0.5	1.5	0.2	0.4	0.4	0.4	-	0.4	0.2
Rutile	TiO_2	-	-	-	0.5	-	-	-	-	-	-	-
Mayenite	$Ca_{12}Al_{14}O_{33}$	1.4	-	-	-	-	1.7	-	-	-	-	-
Chlorides												
Halite	NaCl	5.8	1.4	8.1	-	0.2	6.2	0.3	7.6	5.1	6.4	0.2
Sylvite	KCl	2.2	1.0	2.4	1.8	0.3	0.6	0.2	2.5	0.6	0.5	0.4
K-Zn-Chloride	K_2ZnCl_4	-	-	-	-	-	5.8	-	-	6.2	8.7	-
Sulphates												
Anhydrite	$CaSO_4$	7.2	3.2	6.2	-	6.3	7	6.1	6.2	10.8	7.3	11.7
Bassanite	$Ca[SO_4] \cdot 0.5\ H_2O$	0.4	0.3	0.4	-	-	-	-	0.4	-	-	-
Ettringite	$Ca_6Al_2(OH)_{12}(SO_4)_3 \cdot 26H_2O$	-	-	-	-	-	-	4.8	-	-	-	-
Gypsum	$CaSO_4 \cdot 2H_2O$	-	6.9	-	-	11.3	-	8.1	-	-	-	13.7
Amorphous portion		66.0	71.5	65.1	62.4	76.8	58.7	72.0	59.3	57.5	58.9	71.0

6.3.4 SEM study of fly ash

Scanning electron microscopy (SEM) equipped with an EDS system was used for characterizing the morphology and metal associations in fly ash and leached filter cake. XRD Rietveld method is a useful technique to determine dominant phases controlling the leaching chemistry and the host phases of metals. However, XRD technique is not appropriate for the detection limit of small portions of metal phases present. In this study mostly backscattered electron imaging (BSE) was used to characterize the constituents of fly ash samples. BSE provides visual information based on grey-scale intensity of elements forming components. Information about the particle morphology and chemical composition were generated on the basis of polished, epoxy-resin impregnated specimen of each fly ash and filter cake sample.

Morphology

In a first step, secondary electron (SE) images of unconsolidated fly ash specimens were taken which indicate that the untreated fly ash consist largely of agglomerated particles. Fine-grained ash particles (<1 μm) adhere to the larger ones forming agglomerates of >50 μm (Figure 6-4).

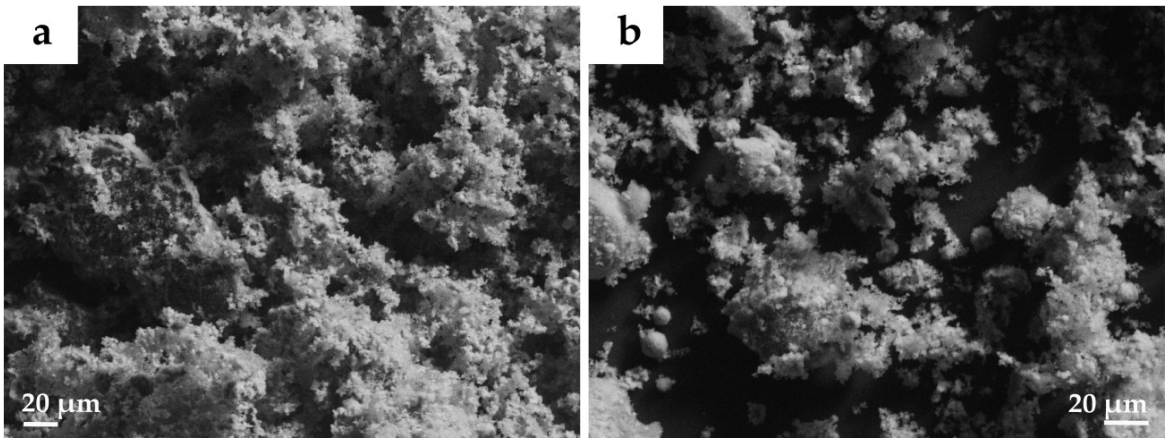

Figure 6-4: *Secondary electron image (SE-mode) of unconsolidated fly ash. (a) FAZUC and (b) FAHAG.*

No information about single particle shapes and metal phases is received with such unconsolidated specimens using the SE-mode. Therefore, epoxy impregnated specimen of each fly ash sample have been produced and analyzed using the BSE-mode. Metal phases are clearly identifiable by BSE because they appear as the brightest particles in the images due to their high atomic mass and atom density.

The morphology of fly ash particles is the result of combustion temperature, the residence time at high temperatures and the cooling rate in the boiler and electrostatic precipitator. The BSE-overview pictures show major differences in particle size and shape (Figure 6-6). Three general particle types are identified in the entire six fly ash specimens (Figure 6-5):

1) Very fine-grained (<1 μm) dust which consists of ash particles usually accumulated around larger aggregates.
2) Larger aggregates or glass particles which are coated with fine grained dust rim. Most regions with elevated heavy metal concentration are associated with these aggregates which are commonly formed during the incineration process.
3) Refractory particles or minerals which pass the incineration process without showing melting or recrystallization. During cooling also the surfaces of newly formed minerals and refractory minerals are agglomerated by the dust particles.

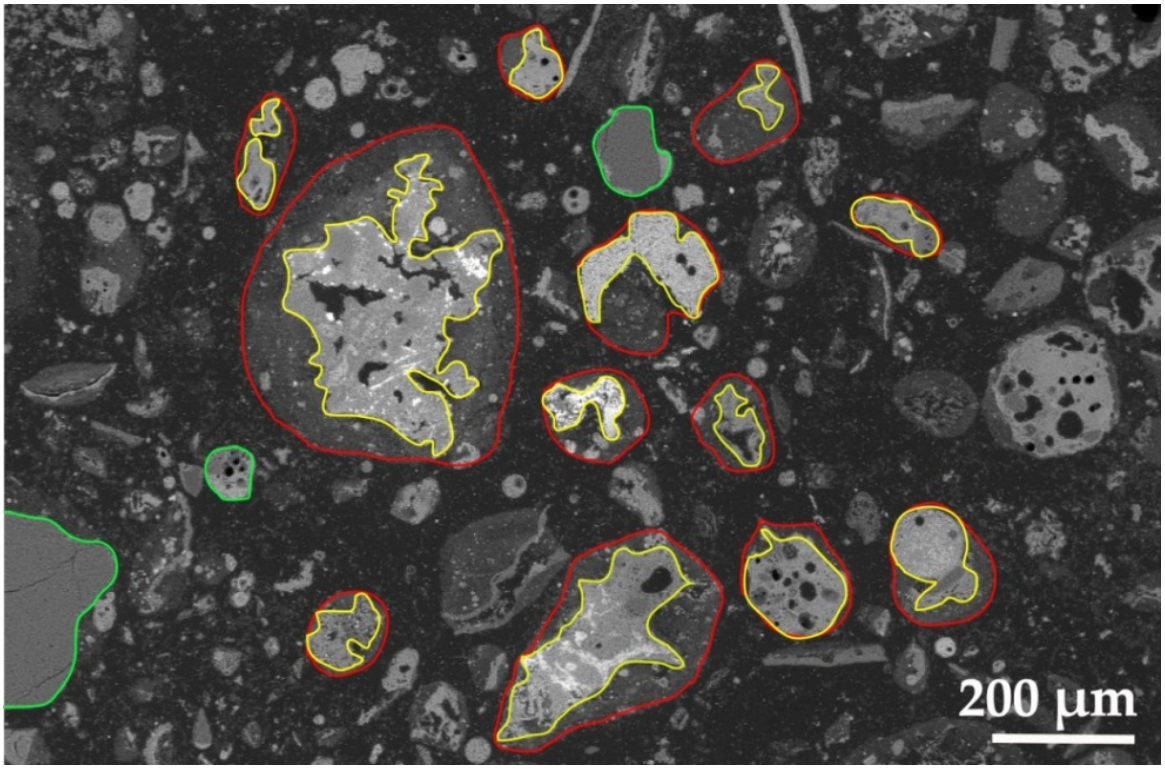

Figure 6-5: *BSE-image of epoxy-resin specimen of FANIE. Beside the epoxy resin ($C_{21}H_{25}ClO_5$) from the sample impregnation (black parts), the fly ash contains three general particle types. Particles composed of aggregates (yellow) and fine grained dust rim (red) building larger particles with higher metal concentration in the aggregates. In green are refractory minerals such as SiO_2.*

The size of particles observed in all fly ashes range from less than 1 μm to larger than 500 μm. During combustion melting and degassing phenomena occur. During the slow cooling rate in the boiler new crystalline phases or aggregates are formed. Therefore, a wide range of particle shapes are identified. Hollow glassy cenospheres, elongated particles, mineral aggregates and other agglomerated particles which include metal phases are observed in all fly ashes. FAMON and FABER have a relatively homogeneous particle size between 50 and 300 μm (Figure 6-6). Obvious in these two fly ashes are the frequent presence of elongated particles. On the other hand FANIE is characterized by large and well-rounded particles of around 100-400 μm in diameter. A thick dust rim covers the larger aggregates, where the boarder of the individual particles is more clearly visible,

compared to all other fly ashes. Only little amount of free dust particles are present within the epoxy resin of FANIE, whereas especially FAZUC has a lot of fine-grained unconsolidated dust particles <1 µm in the matrix. Two main groups of particles were identified in FAZUC, a first with a size between 50 and 100 µm and a second with a size of 200-300 µm. FAHAG and FAHIN show a very heterogeneous grain size distribution up to >500 µm

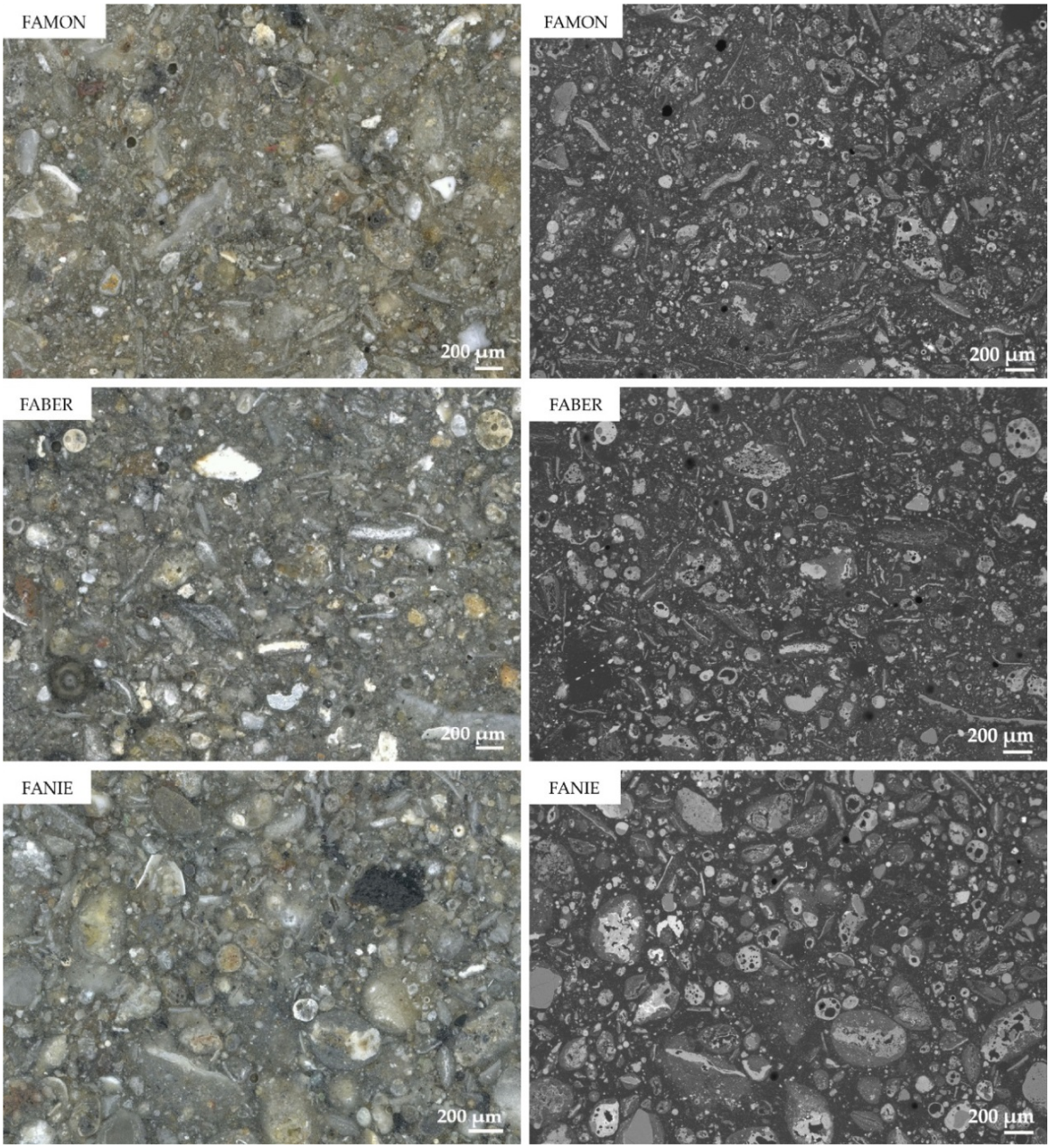

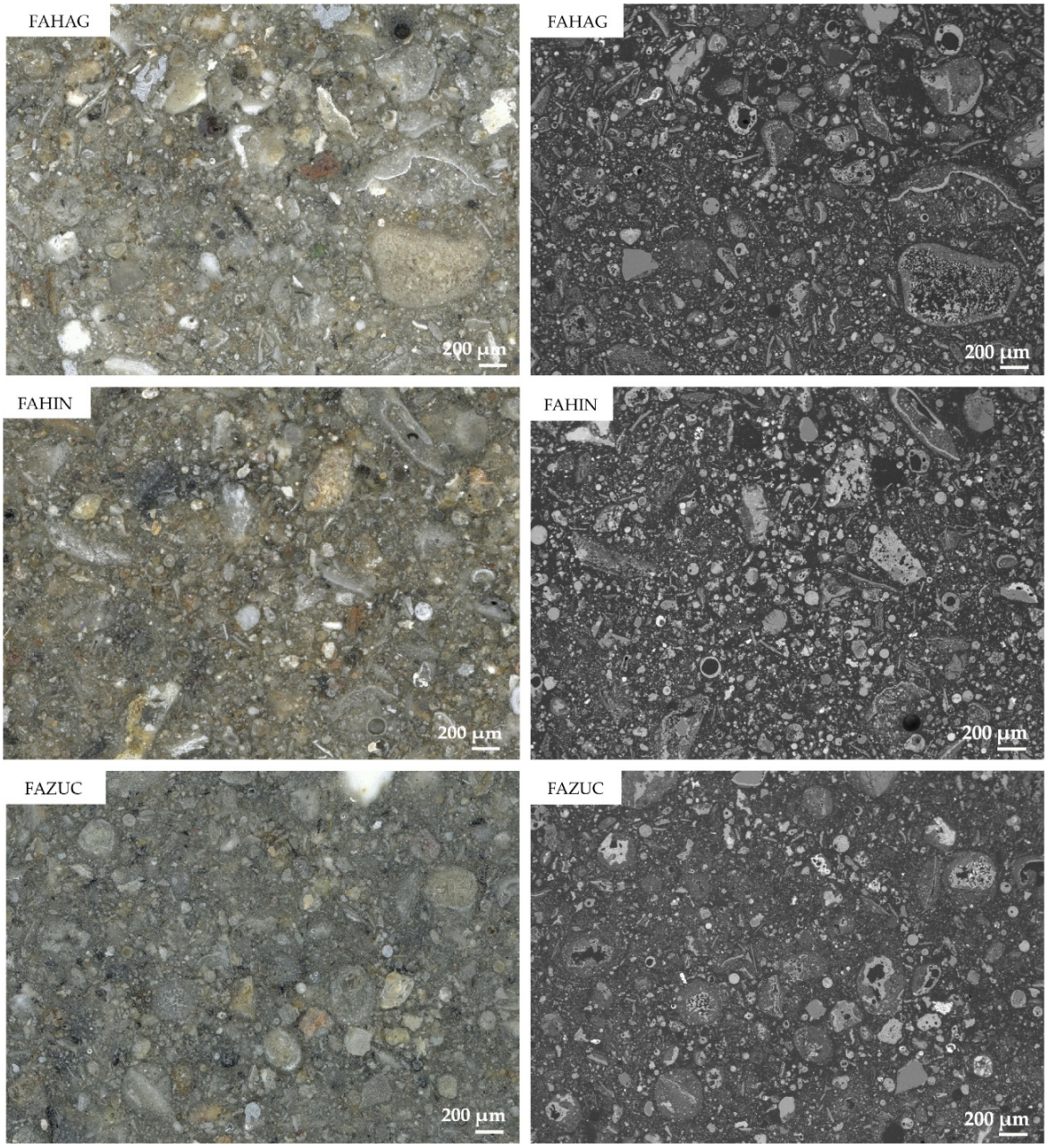

Figure 6-6: *Light microscope images (left) and backscattered electron images (right) of epoxy-resin specimens of the fly ashes from the six MSWI plants.*

It is obvious that SEM and BSE-mode offer a proper tool to characterize phase boundaries, different shapes and especially metal phases, where the light microscope study (LM) offers just diffuse phase boundaries and the variety of shapes is not so clear visible (Figure 6-6). Furthermore, no metals are identifiable except some Al-phases and therefore the light microscope is considered as a not suitable tool for the characterization of fly ash.

Mineral phases

EDS spot analyses on unconsolidated fly ash specimens show elevated concentration of volatile elements such as K, Na, Cl and Zn on the surface of the ash aggregates (Figure 6-7).

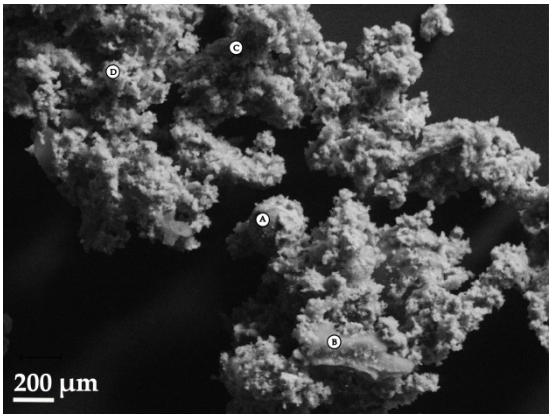

A: O (34 wt.%), Zn (22 wt.%), Fe (14 wt.%), Cl (9 wt.%), K (8 wt.%), S (7 wt.%), Minor* (Si, Al)

B: Cl (26 wt.%), O (26 wt.%), Na (21 wt.%), K (11 wt.%), Minor (S, Ca, Mg, Si, Al)

C: O (59 wt.%), Si (18 wt.%), Al (10 wt.%), Ca (8 wt.%), Minor (Cl, K)

D: O (32 wt.%), Cl (23 wt.%), Na (13 wt.%), Ca (9 wt.%), Zn (8 wt.%), K (8 wt.%), Minor (S, Al, Si)

Figure 6-7: *Secondary electron image and EDS spot analyses on different positions of unconsolidated fly ash (FAZUC). *Minor phases: phases which are present in concentrations <5 wt.%.*

No chemical analyses of single ash particles or metal phases are possible with these specimens and therefore all further analyses are performed using epoxy-resin specimens. Several EDS spot analyses of the fine-grained dust rims which cover larger aggregates show an increased concentration of specific elements. Beside the most frequent element oxygen, volatile elements such as Zn, Na, S, Cl, K as well as Ca, Si and Al are observed in these rims. During combustion at 800-900°C elements with low melting points (e.g. Pb 327.4°C, Cd 321.1°C, Zn 419.5°C) evaporate and condensate together with dust particles on larger aggregate surfaces during cooling in the boiler. The compositions of these dust rims are very homogeneous and their elemental composition is similar for all analyzed fly ashes (Table 6-13).

Table 6-13: *Averaged elemental concentrations of dust rims from all fly ash samples (n=number of measurements) as well as the mean value from all fly ashes and the relative standard deviation (s).*

		FAZUC	**FAHIN**	**FANIE**	**FAHAG**	**FABER**	**FAMON**	**Mean**	**s**
n	-	10	2	4	8	4	7	-	-
O	wt.%	40	41	44	35	40	47	41	4
Na	wt.%	7	15	16	7	10	6	10	4
Al	wt.%	-	-	-	4	-	2	3	1
Si	wt.%	6	6	8	5	6	10	7	2
S	wt.%	8	14	10	8	9	8	10	2
Cl	wt.%	14	15	13	14	14	10	13	2
K	wt.%	8	15	7	9	8	5	9	4
Ca	wt.%	13	5	13	22	16	13	13	5
Zn	wt.%	12	10	14	-	-	-	12	2

As shown with the XRD Rietveld analysis, around 60 wt.% of the fly ash is composed by amorphous phases. Most of this amorphous part is present as glass which is a common product of melting. It is usually rich in Si, Ca and Fe and partial recrystallization of the glass can often be observed. Most often found are hollow glassy cenospheres with the following main elemental glass composition:

Element	wt.%
O	35
Na	6
Mg	4
Al	4
Si	20
P	2
K	1
Ca	17
Fe	6
Ti	6

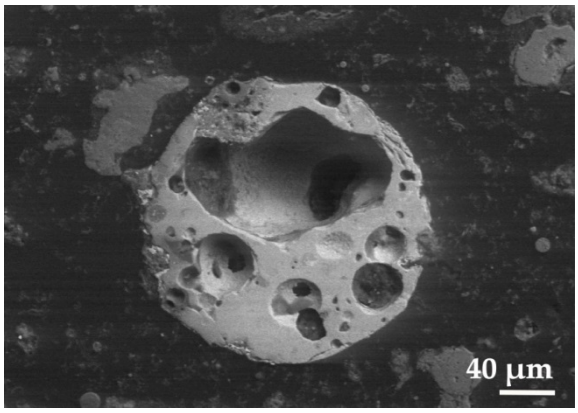

Figure 6-8: *Representative EDS spot analyse of hollow glassy cenospheres as often found in all six fly ashes.*

The crystallized fraction of the fly ash can be subdivided in refractory and newly formed mineral phases. Due to the limited duration of the incineration process (ca. 30 minutes), most of the inorganic components originally present in the waste may go through the combustion without structural change and act as refractory minerals. The most common refractory minerals are quartz and aluminosilicate-endmembers (e.g. orthoclase, albite and anorthite). Quartz appears as dark-grey dense fragments within the ash and the aluminosilicates are present as light grey and porous particles with a rough surface (Figure 6-9). An enormous variety of aluminosilicate particle shapes are observed which reach from spherical and more compact to streak-like and more porous structures.

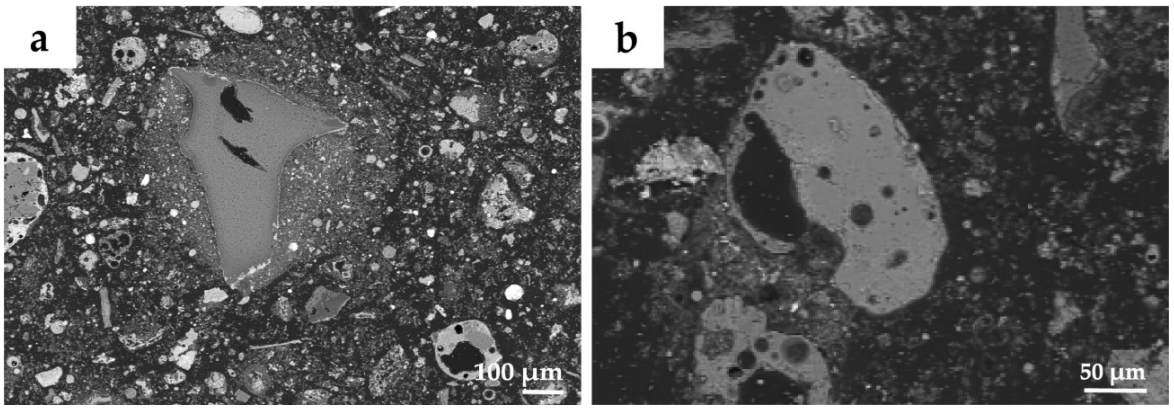

Figure 6-9: *Refractory minerals as often present in fly ash. (a) quartz and (b) aluminosilicate (close to the chemical composition of anorthite).*

The most often identified new formed minerals during combustion are anhydrite and complex sulphate phases which are "contaminated" with Na, K or Cl close to the composition of omongwaite ($Na_2Ca_5(SO_4)_6 \cdot 3H_2O$), syngenite ($K_2Ca(SO_4)_2 \cdot (H_2O)$) or gorgeyite ($K_2Ca_5(SO_4)_6 \cdot H_2O$). These phases mostly contain heavy metals as discussed further down. The most common phases found in the ash matrix beside the sulphates are highly calcium enriched phases (29-71 wt.% Ca) such as CaO and others with low concentration of Si and Cl (<10 wt.%) beside. Especially FABER and FAHAG show numerous Ca-rich elongated particles, showing chemical composition close to that of calcium silicate hydrate phases (C-S-H-phases). In addition, FAHAG contains a phase consisting of Ca and Cl in the same ratio (43 wt.% Ca, 37 wt.% Cl). The most common identified new formed silicate phase by XRD is gehlenite (Table 6-12). However, almost no melilite group compositions are identified by SEM-EDS and only the composition of orthorhombic monticellite ($Ca(Mg,Fe)[SiO_4]$) is found rarely. Monticellite occurs in strongly SiO_2-undersaturated basanitic rocks as a reaction product from impure limestones and in association with melilites (Deer et al., 1996). The gehlenite may be finely dispersed within the matrix or the Si content may be overestimated. The described phases are all present as relatively homogeneous particles within the fly ash.

However, there are also many particles present where different phases are aggregated together during incineration and cooling (Figure 6-10). Most often found are quartz grains surrounded by Ca-Si-phases close to the chemistry of wollastonite ($CaSiO_3$) or gehlenite-related phase compositions. Quartz fragments pass the incineration process without modification and within the hot flue gas, phases such as melilite-group-minerals or Ca-silicates condensed at the quartz surface (lighter grey). These newly formed phases mostly contain fine distributed metals such as brass ($Cu_{0.6}Zn_{0.4}$) or Fe-oxide. The particles are mostly coated with the above described fine grained dust rims.

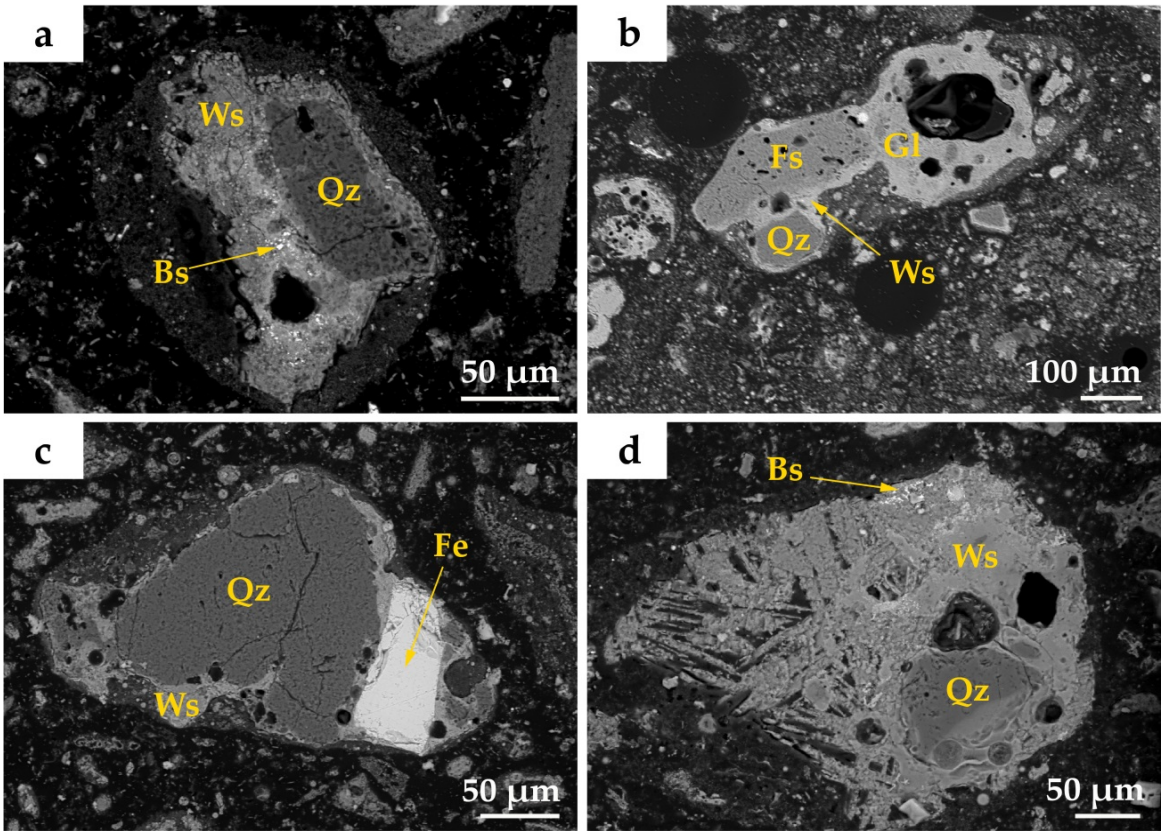

Figure 6-10: *Backscattered electron images of typical phase aggregates in (a) FAZUC, (b) FAMON, (c) FAHAG and (d) FABER: Bs (brass, $Cu_{0.6}Zn_{0.4}$), Fe (Fe-oxide), Fs (feldspar), Gl (glass), Qz (quartz), Ws (wollastonite).*

Lead phases

Lead has a melting point of 327.4°C and therefore most Pb present in the waste is transferred to the gas phase during combustion. Lead inclusions with high amounts of Pb (30-90 wt.%) in particles of various composition were therefore found in five out of six sampled fly ashes. In all cases the identified Pb inclusions were located mainly on the interior of the particles and appear as the brightest phase in the images due to the high atomic number (207.2 g/mol) in the BSE-images. The chemical composition determined by EDS allowed the identification of two different lead-bearing phases (Table 6-14). Lead is often associated to sulphur in the inclusions, with a mass fractions of 10-15 wt.%. In FAZUC and less often FAMON pure anglesite ($PbSO_4$) was identified which is a rather insoluble Pb species in water (Phase A). Pure lead sulphate was determined rarely because it is mostly associated with low quantities of Cl, K, Ca, Na, and Si (<10%). The presence of these elements can result in the formation of more complex Pb-bearing sulphate phases such as the highly water soluble palmierite ($(K,Na)_2Pb(SO_4)_2$) or caracolite $Na_3Pb_2(SO_4)_3Cl$) (Phase B). The lead inclusions of FANIE, FAHIN and FABER have a similar complex Pb-bearing sulphate composition with Cl, K, Ca, Na and Si. Most of the Pb inclusions of FAMON have Pb:S ratios of 4:1 with subordinate K, Ca, Na and Si rates which is similar to the Pb inclusion composition from other plants. Metallic Pb^0 was

identified rarely which is explainable by the fact that most of the present Pb is molten and evaporized at incineration temperatures of 800-900°C. No Pb-bearing phases have been identified in FAHAG.

Table 6-14: *The two most often identified Pb-bearing phases present in the different fly ashes.*

Pb-phases	Description	Phase identified in fly ash
Phase A	Anglesite ($PbSO_4$)	FAZUC, FAMON
Phase B	Complex Pb-bearing sulphate phases (palmierite ($(K,Na)_2Pb(SO_4)_2$) or caracolite ($Na_3Pb_2(SO_4)_3Cl$).	FAZUC, FAHIN, FANIE, FAMON, FABER

The matrix composition of the aggregates containing the Pb (host particles) of all studied fly ashes includes the elements O, S, Si, K, Ca, Na and Zn. Complex sulphate phases with compositions similar to omongwaite ($Na_2Ca_5(SO_4)_6 \cdot 3H_2O$), syngenite ($K_2Ca(SO_4)_2 \cdot (H_2O)$) or gorgeyite ($K_2Ca_5(SO_4)_6 \cdot H_2O$) are often identified in all fly ashes and these phases are identified as main phase enclosing the Pb. In addition, FAZUC and FAHIN show significant amounts of Zn in the matrix of most host particles (~15%). The fact that most Pb inclusions are surrounded by particle aggregates makes leaching of these phases very challenging. However, SEM images show that many of these host particles appear to be porous (Figure 6-11). This porosity can be of particular importance during extraction experiments because the existence of pores may allow a leaching medium to contact the Pb-containing phases within the interior matrix of a particle.

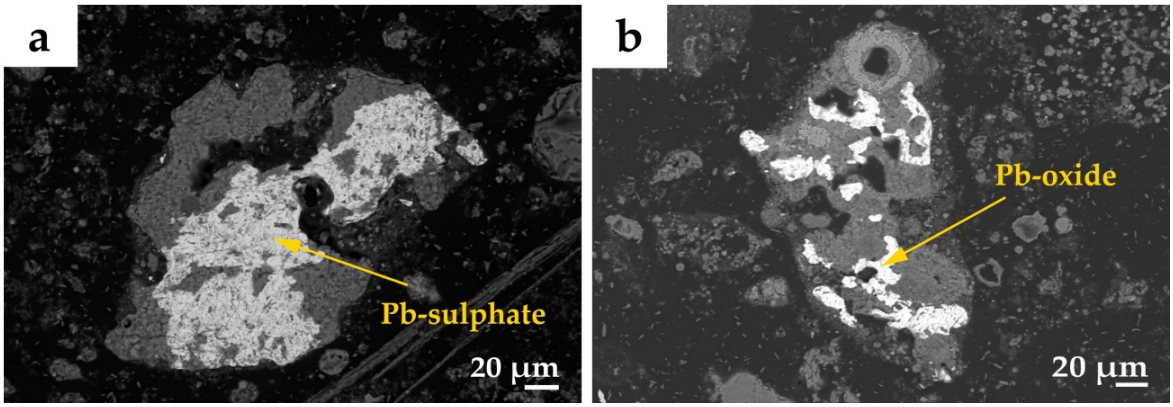

Figure 6-11: *Backscattered electron images of typical Pb-bearing phases: (a) Pb-sulphate in FAZUC and (b) Pb-oxide in FAMON.*

Zinc phases

Phases with high amounts of Zn (11-90 wt.%) were found in all six fly ashes (Table 6-15). Zinc is rarely found as clear inclusions and more present distributed in particles with no clear boundaries. Compared to the Pb inclusions, much more different Zn-bearing phases were identified. The phase most often identified is brass ($Cu_{0.6}Zn_{0.4}$), an alloy made of copper and zinc (Phase A). Brass appears as very bright phase and it is distributed in very small inclusions all over the particles and within the matrix (Figure 6-12a). Howev-

er, no Cu-phase is found in FAHIN and therefore no brass was identified in this fly ash. A second Zn-phase (Phase B) is identified in FAZUC and FAHIN which consists beside Zn (20 wt.%) significant amounts of S (15 wt.%) and K (15 wt.%). In addition, FAZUC shows a third Zn-phase (Zn 45 wt.%) with major Ca (20 wt.%) and Mg (5 wt.%) concentration and minor concentration of S, Cl, Si and Al. Zn concentration between 11 and 27 wt.% is also found in Pb-bearing particles in FAZUC and FANIE. This Zn is diffusely distributed in the surrounding dust rim and not clearly visible as an individual phase (Phase D). During combustion Zn and other volatile elements such as Pb and Cd are evaporated and during cooling they accumulate on particle surfaces. The only Zn-bearing phase identified by XRD was K_2ZnCl_4 (Table 6-12b) but this phase was only found in FAZUC and FAHIN, the two fly ashes with the highest Zn amounts (Phase E) (Figure 6-12b). Furthermore, a Zn-silicate close to the chemistry of hemimorphite ($Zn_4Si_2O_7(OH)_2 \cdot 2H_2O$) was found in FANIE and FABER (Phase F). The study of FAHAG and FAMON showed some metallic Zn^0 with Zn amounts around 90 wt.% (Phase G).

Table 6-15: *The identified Zn-bearing phases in the different fly ashes.*

Zn-phases	Description	Phase identified in fly ash
Phase A	Brass ($Cu_{0.6}Zn_{0.4}$)	FAZUC, FANIE, FABER, FAHAG, FAMON
Phase B	Zn-phase (20 wt.%) with S (15 wt.%) and K (15 wt.%)	FAZUC, FAHIN
Phase C	Zn-phase (45 wt.%) with Ca (20 wt.%) and Mg (5 wt.%)	FAZUC
Phase D	Zn (11-27 wt.%) diffusely distributed in dust rim	FAZUC, FANIE
Phase E	Potassium-zinc-chloride (K_2ZnCl_4)	FAHIN
Phase F	Hemimorphite ($Zn_4Si_2O_7(OH)_2 \cdot 2H_2O$)	FANIE, FABER
Phase G	Metallic zinc (Zn^0) and ZnO	FAHAG, FAMON

As already described, the Zn-phases are less surrounded by aggregated particles compared to the Pb-phases. Nevertheless, the Zn-phases frequently occur in combination with host particles. Four different particles are identified which occur together with Zn. Except FAHAG, all fly ashes show a Ca- or Si-rich phase such as anhydrite, syngenite or omongwaite. This phase is similar to the main Pb-bearing phase as discussed above. A second Zn-host-phase which was identified in all fly ashes except FAHIN shows elevated Ca (4-40 wt.%) and Si (11-34 wt.%) contents close to the chemistry of wollastonite ($CaSiO_3$). The identified K_2ZnCl_4 in FAHIN is accompanied with halite and sylvite. A fourth very Ca-rich particle (32-66 wt.%) is identified together with Zn mainly in FAHAG and subordinate in FAZUC and FAMON. Brass is often associated with this Ca-rich particle whereas other Zn-phases are more often present in combination with sulphate or Ca-silicate host particles.

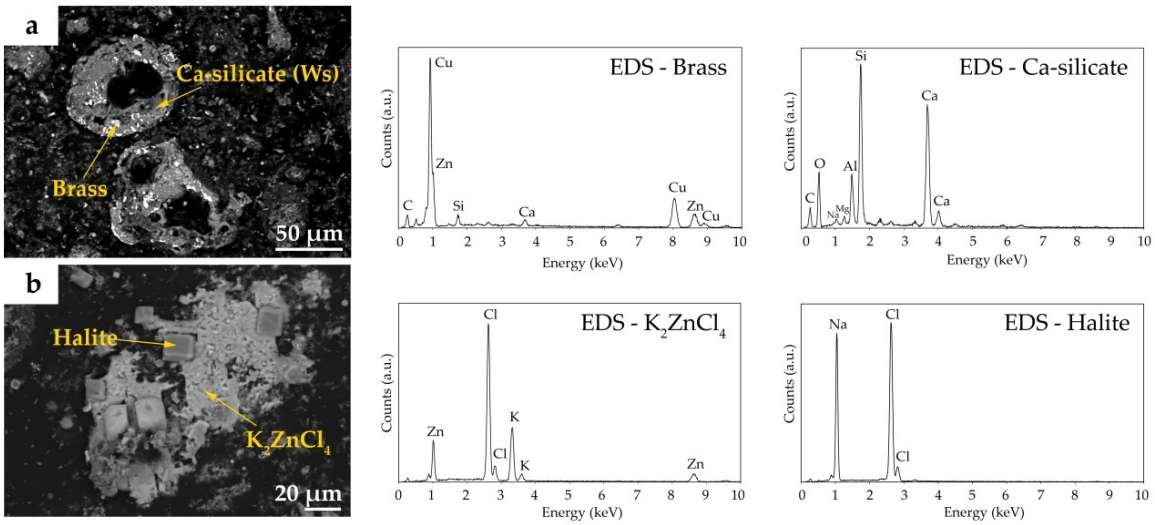

Figure 6-12: *Backscattered electron images with elemental spectra of typical Zn-bearing phases and their host particles in fly ash: (a) brass incorporated in Ca-silicate particle close to the composition of wollastonite (Ws) in FAZUC, (b) K_2ZnCl_4 together with halite in FAHIN.*

Copper phases

Copper is not found in clear inclusions and more distributed diffuse with no clear boundaries. Phases with high amounts of Cu (10-90 wt.%) were found in in five out of six sampled fly ashes (Table 6-16). The alloy brass (Phase A) is the most Cu-bearing phase and distributed very fine over the particles as described above. Additional three Cu-bearing phases were identified during the SEM-EDS study. Copper sulphide (chalcocite, Phase B), copper oxide (tenorite, Phase C) and metallic Cu^0 with Cu amounts around 90 wt.% (Phase D). No Cu-phases were identified in FAHIN so far.

Table 6-16: *The four identified Cu-bearing phases in the different fly ashes.*

Cu-phase	Description	Phase identified in fly ash
Phase A	Brass ($Cu_{0.6}Zn_{0.4}$)	FAZUC, FANIE, FABER, FAHAG, FAMON
Phase B	Chalcocite (Cu_2S)	FAZUC, FAMON
Phase D	Tenorite (CuO)	FANIE
Phase C	Metallic copper (Cu^0)	FAZUC, FAHAG

The rarely identified Cu-phases beside the brass are mostly accompanied with similar particles as the Zn-phases, mainly sulphates (omongwaite, syngenite) and Ca-silicates (wollastonite).

Iron phases

Iron is present in the analyzed fly ashes between 14'585 mg/kg (FABER) and 28'439 mg/kg (FAHIN) (see Section 6.3.1). During the SEM-EDS study Fe-phases are the most often found metals in all fly ash and clearly identifiable due to the matt-grey appearance (Figure 6-13). However, the significance of recovery is not so high in the case of iron due to the lower atomic mass compared to Pb, Zn or Cu. Therefore, less attention was given to identify Fe-phases during the SEM study and investigations were focused on FAZUC. The iron oxide shows various textures both on the surface and interior of particles. Often found are iron spheres which consist of iron oxide mixed with Ca-Si-phases (Figure 6-13). Furthermore, other iron-bearing Ca-Si-rich particles are observable where the iron oxide is located on the surface of the grain or where the Ca-Si-grain and the iron oxide phase are grown simultaneously. Additionally, iron oxide particles surrounded of less iron rich phases are observed regularly.

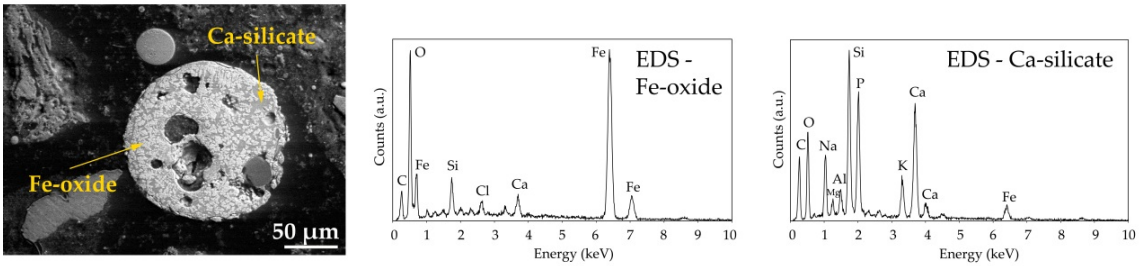

Figure 6-13: *Backscattered electron images with elemental spectra of Fe-oxide rich Ca-Si-sphere in FAZUC.*

Aluminium phases

Aluminium is the only metal which is visible under the reflected light microscope (Figure 6-14a). This is due to the metallic occurrence in form of 85 wt.% Al and 15 wt.% Si. Aluminium foil particles may pass the incineration process without significant modification.

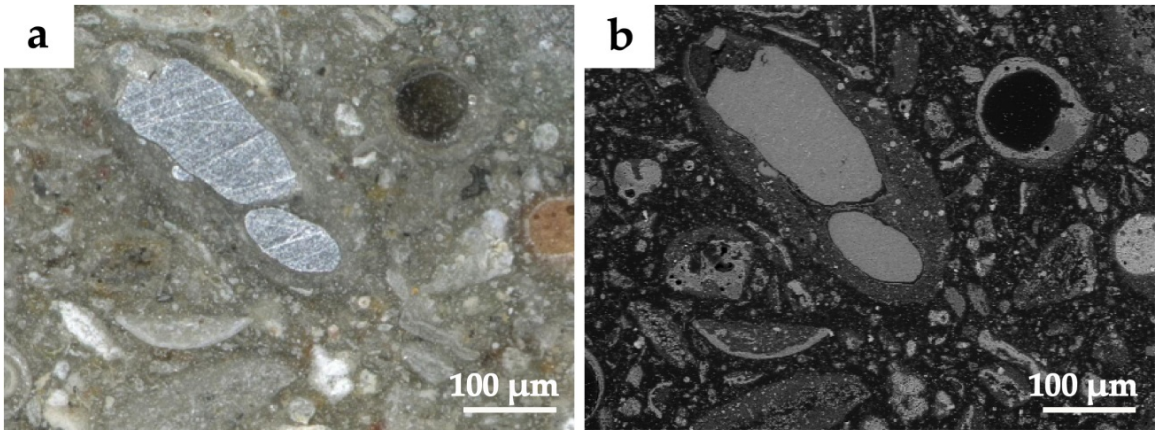

Figure 6-14: *(a) Light microscope image and (b) backscattered electron image of an Al^0-particle in FAHAG.*

Efflorescences

Despite the storage under nitrogen atmosphere, efflorescences have been formed at the surface of the polished fly ash specimens after six months (Figure 6-15). The precipitated white mineral has a characteristic shape and is distributed all over the surface. EDS analysis indicates that the white mineral is K_2ZnCl_4. Such efflorescences are especially visible on specimens of FAZUC and FAHIN which have significant higher Zn-concentrations compared to other fly ashes. Another identified newly precipitated phase shows beside significant Zn- and Cl-concentrations also 7-10 wt.% sulphur. In addition other chlorides such as halite and sylvite appear as cubic crystals at the surface. It is assumed that these efflorescences could be the result of ash alteration reactions with residual water within the fly ash.

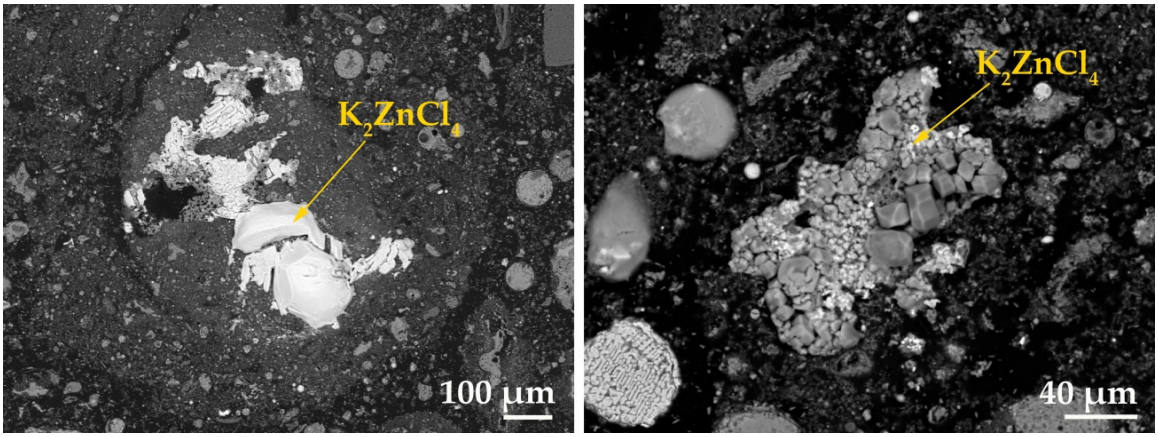

Figure 6-15: *Backscattered electron images of K_2ZnCl_4-efflorescences in FAZUC.*

6.3.5 SEM study of leached filter cake

Morphology

The particle morphology changed significantly through the leaching process and matrix composition and constituents of metal-bearing phases are altered and hydrated significantly. Several phases are dissolved and others are newly formed through the interaction between fly ash and scrub water (FLUWA process) or through neutral leaching (FCMON).

Three general particle types were identified in the fly ash as described in Section 6.3.4). A very fine-grained dust rim which covers larger metal-bearing particles or aggregates is very characteristic for untreated fly ash. After the fly ash leaching these rims are disappeared almost completely and the larger particles are not coated anymore. An example is given in Figure 6-16 where the dust rim of the aggregates in fly ash (a) disappears almost completely after acidic leaching in the filter cake (b). Leached dust that is depleted in soluble elements such as Na, K and Cl is distributed loosely between larger particles in the filter cake (Figure 6-16b).

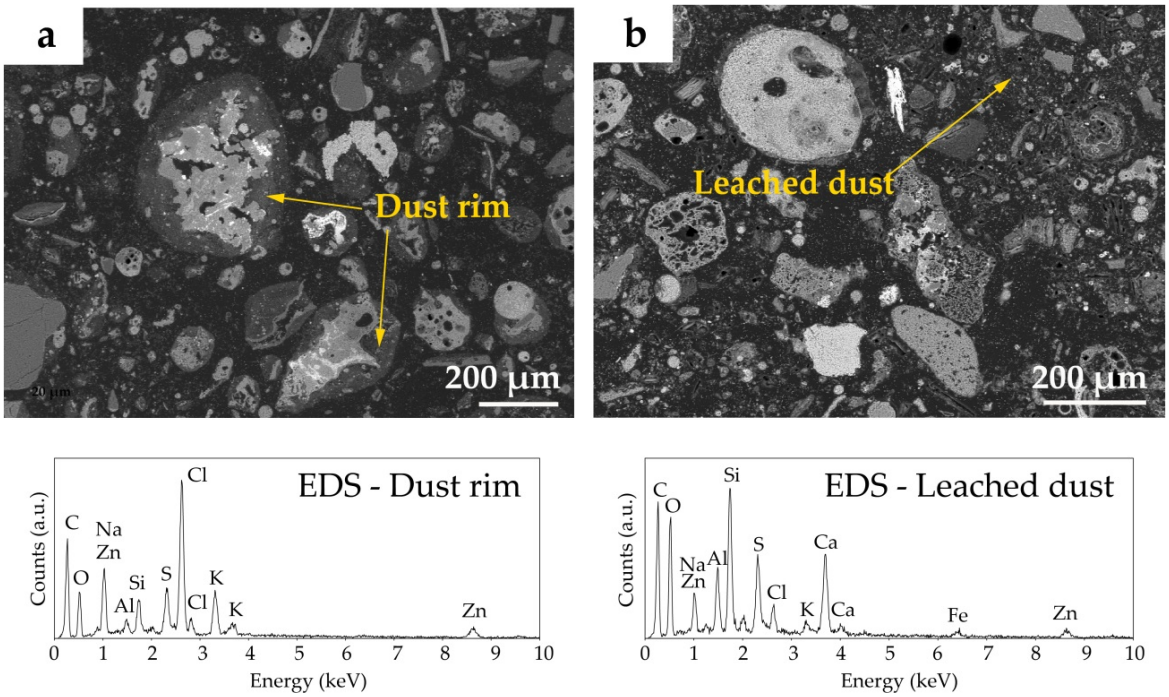

Figure 6-16: *Backscattered electron images of epoxy-embedded specimens of FANIE and FCNIE with EDS spectra of the dust rim before and after leaching. (a) Compact dust rims around larger particles enriched in Na, K, Cl, Si, Al, Zn, and (b) dust re-arranged after leaching and depleted in soluble elements such as Na, K, Cl.*

The overview pictures of the epoxy-resin specimens show significant smaller grain sizes in all leached filter cakes compared to the untreated fly ash (Figure 6-17). There are more fine-grained particles distributed in the epoxy matrix and the grain boundaries are less clearly visible. FCNIE shows an enrichment of insoluble refractory minerals (large, light grey grains) and less fine-grained particles are aggregated in the matrix.

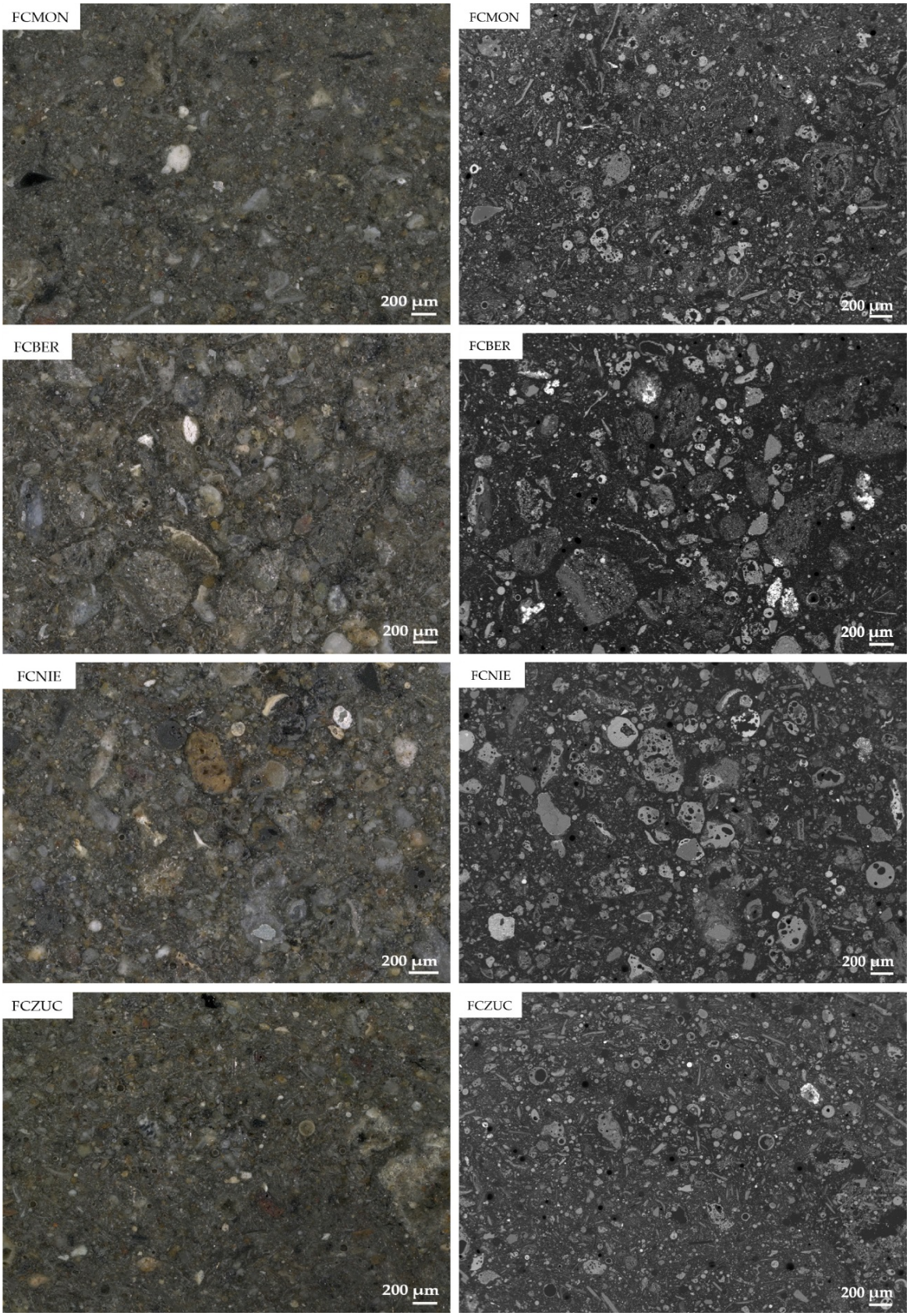

Figure 6-17: *Light microscope images (left) and backscattered electron images (right) of epoxy-resin specimens of the leached filter cakes from the six MSWI plants.*

Mineral phases

The mineralogical composition of the fly ash changes through dissolution and formation of secondary minerals after acidic or neutral leaching. Important reactions during leaching beside dissolution and precipitation are oxidation, carbonation, neutralization of pH or sorption (Bayuseno and Schmahl, 2011). There is an increase of the amorphous part from ca. 60 wt.% to ca. 70 wt.% after the fly ash leaching. Soluble mineral phases such as halite, sylvite or K_2ZnCl_4 are completely dissolved after leaching meanwhile the relative content of insoluble minerals increases (Table 6-12). The mass loss of ca. 30 wt.% is related to dissolution of sulphate and chloride minerals and therefore insoluble phases such as quartz and aluminosilicate-endmembers (orthoclase, albit, anorthite) are more frequent identified during the SEM study in the filter cakes The hydrated fly ash results in a large abundance of gypsum ($CaSO_4 \cdot 2H_2O$) which is the most dominant newly formed secondary mineral phase in filter cakes (Figure 6-18). The FLUWA process, as used at the MSWI plants Zuchwil, Niederurnen and Bern uses both acidic and alkaline scrub water as extraction reagent (see Section 6.1.3). The dissolved calcium (Ca^{2+}) from the fly ash reacts with the sulphate (SO_4^{2-}) from the alkaline scrub water to $CaSO_4 \cdot 2H_2O$, which precipitates as sparingly soluble gypsum. The prominent crystals observed in all filter cakes show the precipitated gypsum (Figure 6-18).

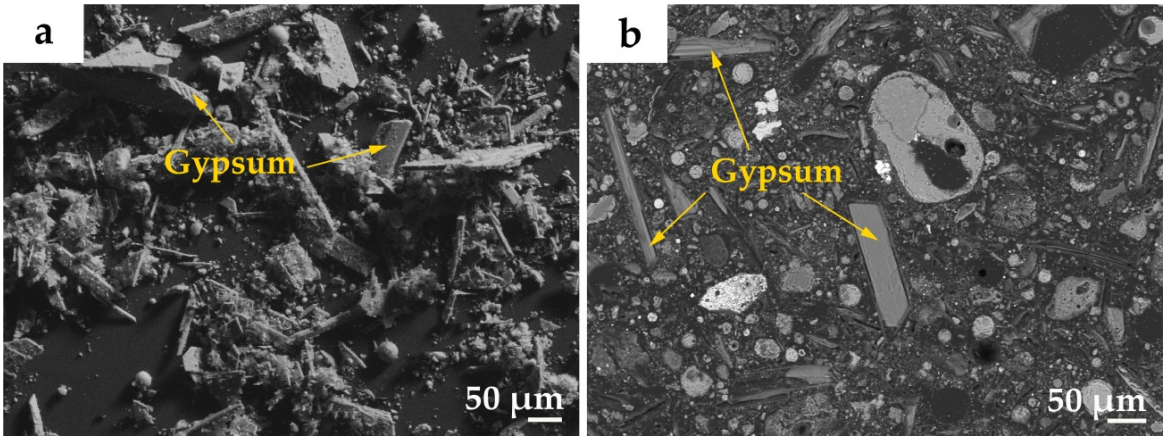

Figure 6-18*: Newly formed gypsum ($CaSO_4 \cdot 2H_2O$) in filter cakes: (a) Secondary electron image of unconsolidated acidic leached filter cake (FCZUC), (b) backscattered electron image of epoxy-embedded specimen of acidic leached filter cake (FCNIE).*

Lead phases

Compared to the untreated fly ash, the identified Pb-bearing particles in the analyzed filter cakes show lower Pb-content (<73 wt.%). In general, three different Pb-bearing phases were identified during the SEM study in all four filter cakes (Table 6-17).

Table 6-17: *The three identified Pb-bearing phases present in the different filter cakes.*

Pb-phase	Description	Phase identified in filter cake
Phase A	Cotunnite ($PbCl_2$)	FCNIE, FCBER, FCMON, (FCZUC)
Phase B	Pb phase with significant Ca concentration (11-33 wt.%)	FCNIE, FCMON
Phase C	$PbCu^0$-alloy-phase	FCZUC, FCNIE, FCBER, FCMON

The most common element along with Pb in untreated fly ash is sulphur with a mass fraction of 10-15 wt.%. However, almost no sulphur was identified in combination with Pb in the leached filter cake. Complex Pb-bearing phases such as palmierite or caracolite are highly water soluble and therefore washed out during leaching. Identified in all four filter cakes are Pb-phases which contain a significant amount of chlorine such as $PbCl_2$. Especially in FCZUC (mix of fly ash from Zuchwil and Hinwil) shows a phase close to the chemistry of cotunnite ($PbCl_2$) (Phase A). Furthermore, FCNIE and FCMON contains a Pb-phase which is rich in Ca (11-33 wt.%) (Phase B). Another very prominent Pb-phase mainly found in FCNIE, FCBER and FCMON is a combination of Pb with Cu and minor amounts of chlorine on the surface of metallic Al^0 (Phase C, Figure 6-19). This $PbCu^0$-alloy-phase was also found in filter cakes from MSWI plant Zuchwil, however, significantly less frequent. No metallic Pb^0 was found in any of the analyzed filter cakes.

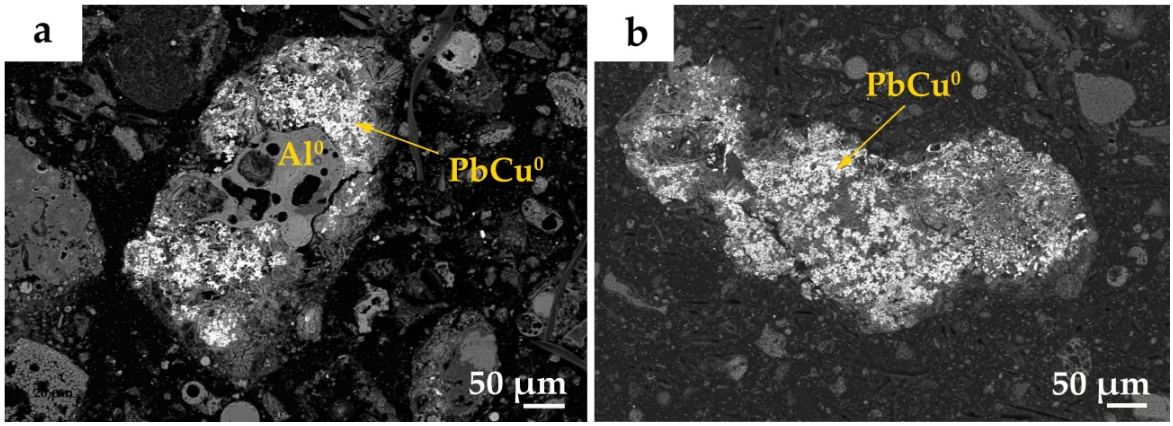

Figure 6-19: *Backscattered electron images of the $PbCu^0$-alloy-phase in FCNIE (a) and FCBER (b).*

Zinc phases

Compared to the untreated fly ash, significant less Zn-bearing phases were found in the leached filter cake (Table 6-18). Water-soluble Zn-phases such as K_2ZnCl_4 are efficiently removed during the FLUWA process. Found phases are Zn-silicates close to the chemistry of hemimorphite ($Zn_4Si_2O_7(OH)_2 \cdot 2H_2O$, Phase A) in FCZUC, FCNIE and FCMON, followed by a Ca-rich Zn-phase (11-44 wt.%) which was identified in FCZUC, FCNIE and FCBER (Phase B). Additionally found, however less frequent, are ZnO (Phase D) and brass (Phase C) in FCZUC, FCNIE and FCMON.

Table 6-18: *The identified Zn-bearing phases in the different filter cakes.*

Zn-phases	Description	Phase identified in filter cake
Phase A	Hemimorphite ($Zn_4Si_2O_7(OH)_2 \cdot 2H_2O$)	FCZUC, FANIE, FCMON
Phase B	Highly Ca-bearing (15-35 wt.%) Zn-phase	FCZUC, FCNIE, FCBER
Phase C	Zincite (ZnO)	FCZUC, FCNIE, FCMON
Phase D	Brass ($Cu_{0.6}Zn_{0.4}$)	FCZUC, FCNIE, FCMON

Copper phases

Copper is mostly found together with Pb as $PbCu^0$-alloy phase in all filter cakes as already discussed above (Table 6-19). In addition, Cu is present in high concentrations (>55 wt.%) together with Zn as brass. There are several other Cu-phases present in the filter cake which cannot be systematically allocated to a specific group.

Table 6-19: *The three identified Cu-bearing phases present in the different filter cakes.*

Cu-phases	Description	Phase identified in filter cake
Phase A	$PbCu^0$-alloy-phase	FCZUC, FCNIE, FCBER, FCMON
Phase B	Brass ($Cu_{0.6}Zn_{0.4}$)	FCZUG, FCNIE, FCMON

6.3.6 Summary SEM-EDS study

Fly ash

Three particle groups were identified in polished epoxy-resin specimens of the fly ash during the SEM-EDS study. A first very fine-grained phase which consists of dust particles enriched in volatile elements (Zn, Na, S, Cl, K) accumulated as dust rim. This dust rim coats all larger, metal-containing particles which represent the second group. A third particle group are the refractory materials such as quartz and aluminosilicates which pass the incineration process without modification. Each fly ash has his characteristic particle association and in general the particle size varies between 50 and 400 μm.

Hollow glassy cenospheres are a common product of melting and degassing processes and such glasses make up the major part of the amorphous phase in the larger size particles of the fly ash. The crystalline fraction can be subdivided in refractory and newly formed mineral phases. Beside quartz a large number of different refractory aluminosilicates are observed which reach from more compact to streak-like and porous particle shapes. The most often new formed minerals are anhydrite and complex sulphate phases with compositions close to the chemistry of omongwaite syngenite or gorgeyite, frequently associated with metals. Beside the particles with defined composition, very characteristic for all fly ashes are phase aggregates of different composition. The refractory mineral quartz often builds the core of such an aggregate and during cooling melilite-group minerals (gehlenite, akermanite) or Ca-silicates condenses at its surface and other metal phases may be incorporated in these newly formed aggregates. Two very prominent Pb

phases are identified in the fly ash. Lead sulphate generally with low quantities of Cl, K, Ca, Na and Si (<10 wt.%) and more complex Pb-containing sulphates with composition close to highly water soluble palmierite or caracolite. Compared to Pb, a much larger variety of Zn-phases are identified by SEM-EDS. Brass ($Cu_{0.6}Zn_{0.4}$) is mostly fine dispersed all over the particles and within the ash matrix. All additionally identified Zn-phases are listed in the table below. Of special interest is the observation of K_2ZnCl_4-efflorescences which are precipitated at the surface of the polished specimens after six months of storage even under nitrogen atmosphere. Copper is found beside brass along with sulphur (Cu_2S), oxygen (CuO) or in its metallic form (Cu^0).

Table 6-20: *The main identified metal phases in the fly ashes from six MSWI plants.*

Pb-phases	**Description**	**Phase identified in fly ash**
Phase A	Anglesite ($PbSO_4$)	FAZUC, FAMON
Phase B	Complex Pb-bearing sulphate phases (palmierite ($(K,Na)_2Pb(SO_4)_2$) or caracolite ($Na_3Pb_2(SO_4)_3Cl$).	FAZUC, FAHIN, FANIE, FAMON, FABER
Zn-phases		
Phase A	Brass ($Cu_{0.6}Zn_{0.4}$)	FAZUC, FANIE, FABER, FAHAG, FAMON
Phase B	Zn-phase (20 wt.%) with S (15 wt.%) and K (15 wt.%)	FAZUC, FAHIN
Phase C	Zn-phase (45 wt.%) with Ca (20 wt.%) and Mg (5 wt.%)	FAZUC
Phase D	Zn (11-27 wt.%) diffusely distributed in dust rim	FAZUC, FANIE
Phase E	Potassium-zinc-chloride (K_2ZnCl_4)	FAHIN
Phase F	Hemimorphite ($Zn_4Si_2O_7(OH)_2 \cdot 2H_2O$)	FANIE, FABER
Phase G	Metallic zinc (Zn^0) and ZnO	FAHAG, FAMON
Cu-phases		
Phase A	Brass ($Cu_{0.6}Zn_{0.4}$)	FAZUC, FANIE, FABER, FAHAG, FAMON
Phase B	Chalcocite (Cu_2S)	FAZUC, FAMON
Phase D	Tenorite (CuO)	FANIE
Phase C	Metallic copper (Cu^0)	FAZUC, FAHAG
Fe-Phases		
Phase A	Fe-spheres	FAZUC, FAHIN, FANIE, FABER, FAHAG, FAMON
Phase B	Fe-oxide (FeO)	FAZUC, FAHIN, FANIE, FABER, FAHAG, FAMON
Al-Phase		
Phase A	Metallic Al^0 with 85 wt.% Al, 15 wt.% Si	FAZUC, FAHIN, FANIE, FABER, FAHAG, FAMON

Filter cake

The particle morphology changed significantly after the leaching process and matrix composition and constituents of metal-bearing phases are altered and hydrated. After the fly ash leaching the fine-grained dust rim, which covers larger particles or aggregates in fly ash is disappeared almost completely.

The mass loss of ca. 30 wt.% after leaching is related to the release of very soluble sulphate and chloride minerals in water (halite, sylvite, K_2ZnCl_4) and therefore insoluble phases such as quartz and aluminosilicates are more frequent identified in the filter cake. The mineralogical alteration is dominated by the formation of gypsum. Identified in all four filter cakes are Pb-phases which contain a significant amount of chlorine such as cotunnite. Another very prominent Pb-phase found in all filter cakes is a $PbCu^0$-alloy with a minor amount of chlorine often on the surface of metallic Al^0. No metallic Pb^0 was found in any of the analyzed filter cake. Compared to the untreated fly ash, significant less Zn-phases were found in the leached filter cakes. Water-soluble Zn-phases such as K_2ZnCl_4 are almost completely removed during the FLUWA process whereas Zn-silicates close to the composition of hemimorphite are more often found in the filter cakes. Copper is mostly found associated with Pb or Zn (brass) in all filter cakes.

Table 6-21: *The main identified metal phases in leached filter cakes.*

Pb-phases	**Description**	**Phase identified in filter cake**
Phase A	Cotunnite ($PbCl_2$)	FCNIE, FCBER, FCMON, (FCZUC)
Phase B	Pb phase with significant Ca concentration (11-33 wt.%)	FCNIE, FCMON
Phase C	$PbCu^0$-alloy-phase	FCZUC, FCNIE, FCBER, FCMON
Zn-phases		
Phase A	Hemimorphite ($Zn_4Si_2O_7(OH)_2 \cdot 2H_2O$)	FCZUC, FANIE, FCMON
Phase B	Highly Ca-bearing (15-35 wt.%) Zn-phase	FCZUC, FCNIE, FCBER
Phase C	Zincite (ZnO)	FCZUC, FCNIE, FCMON
Phase D	Brass ($Cu_{0.6}Zn_{0.4}$)	FCZUC, FCNIE, FCMON
Cu-phases		
Phase A	$PbCu^0$-alloy-phase	FCZUC, FCNIE, FCBER, FCMON
Phase B	Brass ($Cu_{0.6}Zn_{0.4}$)	FCZUG, FCNIE, FCMON

Advantages and limitations of the SEM-EDS method for fly ash characterization

The big advantage of the SEM technique using the backscattered mode (BSE) is the generation of visual information based on grey-scale intensity between chemical phases. Therefore, metal phases with high atomic mass and density appear as the brightest objects and are identifiable easily in polished epoxy-resin preparations. The percentage and

spatial distribution of elements in alloys, particles or minerals can be determined using energy dispersive X-ray spectroscopy (EDS). This combination of imaging technique and EDS detector offers a promising method for ongoing analyses of filter cake from different leaching experiments. Compared to electron probe micro-analyses (EPMA) less standartization is required and particle analyses are generated quickly from particle to particle (50-400 μm). The EDS spot analyses have to be considered as semi-quantitative analyses with errors between 5 and 15% which has to be considered if mineral phases are described based on these measurements. With a large number of measurements groups of metal- and mineral phases and general trends during leaching are recognized. To get more information about phase or elemental distributions, element mapping offers a possibility to generate pictures of different phases. To get more information about phase distributions and statistical data about grain size and shape varieties, image analysis (e.g. Image SXM) would be an option. Image analysis can help to test the representativeness of the generated BSE-pictures and therefore the validity of single pictures may be verified with this technique.

6.4 Summary and interpretation

6.4.1 Dissolution and mineral formation processing during fly ash leaching

The chemical and mineralogical composition of the fly ash changed through dissolution and formation of secondary minerals after acidic or neutral leaching. This leads to significant changes in the particle morphology and chemical composition:

- The analyses of the leached filter cakes show significant metal depletions in the case of Zn and Cd and less depletion for Pb and Cu after the FLUWA process and general smaller depletion factors after neutral leaching.
- Grain size reduction from average sizes of 100-200 μm in the fly ash to 50 μm in the filter cakes is obvious.
- Most of fine-grained, unconsolidated ash particles <1 μm of the fly ash matrix are dissolved or aggregated to larger particles after leaching.
- Leaching and re-arrangement of fine-grained, volatile element-containing dust rim which covers larger metal-bearing aggregates in untreated fly ash.
- Soluble mineral phases such as halite, sylvite or K_2ZnCl_4 are completely dissolved after leaching.
- Acidic leaching by the FLUWA process causes dissolution of the melilite-group minerals (akermanite-gehlenite) which were formed during the combustion process in the boiler. The complete dissolution and the fact that no melilite phases have been identified by SEM-EDS, indicate a small crystal size and a fine distribution within the ash matrix. Such dissolving processes lead to decreasing concentrations of Na_2O, K_2O and chlorine.

- A mass loss of ca. 30 wt.% is related to the release of chloride and partially sulphate minerals after leaching and therefore insoluble phases such as SiO_2, CaO, Al_2O_3 or SO_3 and the amorphous part are relatively enriched in the filter cake.
- The hydrated fly ash results in an enrichment of Ca (except filter cake from Bern) due to the new formation of gypsum which is the most dominant newly formed secondary mineral phase in all filter cakes.

6.4.2 Binding forms and metal depletion

Metals of interest show generally different binding forms which control the leachability. Metal associations are primary identified for Pb, Zn and Cu. In general, FCZUC is significantly more depleted in the redox-sensitive elements Cu, Pb and Cd compared to other filter cakes. This is due to the hydrogen peroxide (H_2O_2) dosage during the FLUWA process which forces the oxidation of metallic phases and therefore supresses the reductive separation of redox-sensitive elements (cementation). During the cementation relative noble ions are reduced to zero valence and bond to surface of less noble metal. A common cementation occurs between Cu-ions and metallic Al^0. The added H_2O_2 immediately oxidizes the Al^0 to Al^{3+} and avoids this reaction ($3\ Cu^{2+} + 2\ Al^0 \rightarrow 3\ Cu^0\downarrow + 2\ Al^{3+}$).

Al: Aluminium present in its metallic form shows an initial composition of 85 wt.% Al and 15 wt.% Si because Al-foil particles pass the incineration process without modification. Fly ash is in general depleted in freely available Al which is the reason why only minor amount of aluminosilicates are present.

Zn: Zinc is present in fly ash in concentrations between 2 wt.% (FAHAG) and 7.5 wt.% (FAZUC). The neutral leaching, as performed at MSWI plant Monthey, extracts no Zn and a relatively increased concentration is measured in the filter cake. The Zn-phase most often identified is brass ($Cu_{0.6}Zn_{0.4}$), which is distributed fine-grained in the fly ash. Brass is also identified in the leached filter cake, however, in significantly smaller amounts. Due to its small particle size, brass may dissolve during the acidic leaching. K_2ZnCl_4 is highly soluble and completely removed in the filter cake whereas the highly insoluble Zn-silicate phases close to the chemistry of hemimorphite are frequently present. New found in the filter cake is a secondary formed Ca-bearing Zn-phase (15-35 wt.% Ca). Important for metal depletion experiments are not only the type of metal phases but also the type of particles they are associated (host particles). Zn-bearing phases in fly ashes are mainly associated with complex sulphate phases (omongwaite and syngenite).

Fe: Due to the highly oxidative conditions during combustion, most metals are present as oxides and especially iron is often identified as Fe-oxide. These Fe-oxides are mostly present as iron spheres which are incorporated in Ca-Si-phases. During the

FLUWA process, the pH is adjusted to 4.4 and therefore Fe is completely transformed into Fe^{3+} and precipitates as Fe^{3+}-hydroxide.

Pb: Lead is mostly found in clear inclusions together with sulphur. Highly water-soluble Pb-bearing sulphates such as palmierite or caracolite are the main identified Pb-bearing phases in the fly ash. Lead is removed much more efficient with the addition of H_2O_2 compared to the conventional FLUWA process as shown by the Pb depletion in the filter cake from Zuchwil. After fly ash leaching none of these Pb-bearing sulphate phases are identified so far. However, Pb-chlorides with compositions close to cotunnite are present in the filter cake which may precipitate by adding hydrochloric acid during the FLUWA process. Another very prominent secondary formed Pb-phase in all filter cakes, except FCZUC, is a $PbCu^0$-alloy-phase. This phase is part of the cementation process during leaching as described above. Using H_2O_2 during the FLUWA process, as performed at MSWI plant Zuchwil, prevents this cementation and no $PbCu^0$-alloy is reductively separated. The host particle of Pb-bearing phases is of great interest because the leaching of such metals is dependent from the solubility and porosity of these surrounding particles. As the Zn-bearing phases, also most of the Pb-bearing phases are associated with water-soluble complex sulphate phases with similar compositions to omongwaite and syngenite.

Cu: Copper is not found in clear inclusions and more distributed diffuse with no clear boundaries. The alloy brass is the most copper-bearing phase in fly ash and distributed very fine over the particles as described in the Zn phase Section above. Additional three Cu-bearing phases were identified during the SEM-EDS study. Chalcocite, tenorite, CuO and metallic Cu^0 with Cu amounts around 90 wt.%. In FAHIN, no Cu-phases were identified so far. In the leached filter cake, Cu is mostly found together with Pb as $PbCu^0$-alloy-phase.

Sb: Antimony shows no depletion after the FLUWA process and the Sb concentration is relatively increased in the filter cake compared to the untreated fly ash. No Sb-bearing phases were identified by SEM-EDS and further analyses are required for this specific element.

Cd: The present Cd (<600 mg/kg) is washed out nearly complete during the FLUWA process and due to the low concentration, almost no Cd-phases are identified in fly ash and filter cake by SEM-EDS. Therefore, it is assumed that Cd is predominantly adsorbed at the ash particle surfaces.

6.4.3 Influence of waste type on fly ash composition

The waste input types from the six MSWI plants differ significantly. As shown in Section 6.1.3, MSWI plant Zuchwil has a higher amount of industrial waste compared to other plants. Almost 50% originates from industrial sources such as construction or plastic waste. The elevated concentration of Cl (127'800 mg/kg) in the fly ash may originate from the combustion of plastics (e.g. PVC). Increasing chlorine content forces the vaporisation of heavy metals with higher saturation vapour pressure in form of chlorides (Jakob et al., 1996). This is one reason why the concentration of the heavy metals Zn, Pb and Cd as well as the concentration of Na, K, Br and Sb are significantly higher in FAZUC compared to other plants. The elevated chlorine and alkali metal concentrations which are mobilized during combustion provide the basis for the formation of K_2ZnCl_4 as identified by XRD and SEM-EDS. The mobilization of antimony may also be connected to this process where plastic waste is enriched with flame inhibitors.

MSWI plant Hinwil has an average industrial waste portion of 34% during 2013 and compared to MSWI plant Zuchwil a high input of automobile shredder residues (ASR), special waste (10%) and sewage sludge (10%). Therefore, an elevated heavy metal mobilization is observed due to high plastic content. Despite the significantly higher portion of sewage sludge combustion, phosphorus concentration of FAHIN is in the same concentration range (0.1-0.2 wt.% P) as in FAZUC. Furthermore, Pb and Fe concentrations are 50% higher compared to the average concentration of all six fly ashes (ca. 13'000 mg/kg Pb and ca. 28'500 mg/kg Fe). Analyses taken over several years show in general double Fe-concentrations in FAHIN compared to FAZUC. Iron can only be transported to the flue gas as particles due to the high melting point (1'538°C) and vapour pressure. One explanation for the elevated Fe-concentration may be that the dry bottom ash discharge performed at MSWI plant Hinwil (dust from the abrasion through the dry mechanical treatment carries rusty particles to the flue gas).

Fly ash from MSWI plant Linth/Niederurnen has a high Zn-concentration in the same range as fly ash from Zuchwil and Hinwil plants (>45'000 mg/kg Zn). The morphology of FANIE is significantly different from all others as noticed during the SEM study. An increasing amount of large, well-rounded particles (>300 μm) is observable where a thick layer of dust rim particles (<1 μm) covers the aggregates. In this plant some conditions must be different. During the limited residence time at temperatures between 800 and 900 °C thermodynamic equilibrium of minerals is not achieved, but partial melting and degassing and secondary minerals are formed, what results in the formation of the characteristic morphology of each fly ash. The observed differences may be the result of the elevated calorific values (10'000-12'000 kJ/kg) producing surface temperatures up to 1'100°C. Higher temperatures significantly change the particle shape and size due to melting and degassing processes. In addition grate technology may also influence the element and phase distribution. MSWI plant Linth/Niederurnen is operating with two furnace lines, a Stiefel moving-grate and a MARTIN reciprocating grate with Stiefel water

cooling system. All other incinerators have either MARTIN reciprocating grates (Monthey, Bern, Hagenholz and Hinwil) or von Roll grates (Zuchwil). The grate technology may have a significant effect on the morphology of the incineration residues and this is probably the reason for the ash particle size and shape differences observed in this study.

MSWI plant Monthey is the second incinerator beside Hinwil that performs a dry bottom ash discharge in Switzerland. However, the Fe-concentration is not elevated as shown in FAHIN. Attention should be drawn to the high Cu-concentration which is 60% higher compared to the mean value of all six fly ashes. One possible Cu-source is waste from the chemical industry of Monthey which are combusted periodically.

MSWI plant Bern has a high municipal solid waste portion of ca. 60% and therefore the metal concentrations are fairly reduced compared to plants with higher industrial waste input. Especially copper is 65% lower compared to the average Cu-concentration of all other fly ash. On the other hand elevated Si-values are observable (84'100 mg/kg Si) from street dust combustion which is consistent with the frequent occurrence of quartz phases found by SEM analyses.

The main combusted material at MSWI plant Hagenholz is municipal waste from Zürich city (on average 64% in 2013). Therefore, the fly ash contains a significant lower metal concentrations compared to incinerators with a high industrial waste input such as Zuchwil or Hinwil. Zinc, lead and copper concentrations are 50-60% lower compared to the mean values of all other fly ashes. However, for Ca, Al and Cr the highest concentrations of all ashes are measured which may be explained by the high municipal waste input. However, the source of the high Cr concentrations remains unclear (refractory minerals from the oven?).

Differences in metal concentration in fly ash from different incinerators show an interesting variability. However, these metal concentrations are just a snap-shot over three weeks and are not representative for fly ashes over a whole year. How strong metal concentrations in fly ash can variable over a year is shown in Figure 2-3.

6.5 Conclusion and outlook

6.5.1 Advantages and limitations of analytical methods used

ICP-OES and XRF: It has been shown during this project that robust procedures for heavy metal determination in fly ash and leached filter cake by total digestions prior to ICP-OES analyses and XRF are available. Wavelength-dispersive X-ray fluorescence (WD-XRF) offers a reliable and fast method especially for the determination of Zn, Pb and Cu.

X-ray powder diffraction: Analyses by X-ray powder diffraction offers good results for the main mineralogy of the crystalline part of the fly ash (ca. 50 wt.%). However, almost all metal-bearing minerals are only present in concentrations <1 wt.% and therefore not detectable in the silicate, chloride and sulphate dominated ash matrix. Water-leaching experiments where the soluble salts are dissolved and other enrichment steps can help to concentrate metal-bearing crystalline phases.

SEM-EDS: Especially the backscattered mode (BSE) offers a fast and powerful tool to determine binding forms of metals of interest such as Zn, Pb, Cu or Fe. The metals are bond to a wide range of refractory and secondary formed minerals and the fly ash matrix is therefore enormously diverse. This phase variety represents a challenge to define groups of metal-bearing phases with similar chemical composition. Furthermore, no quantitative statements about the element concentrations and distributions are possible by just analyzing several ash particles by SEM-EDS. Element mapping offers a solution for quantification, however, adequate information about the element distribution is only possible by running an element mapping for several hours in a relatively small area.

6.5.2 Upcoming investigations

For a better understanding of the ongoing fly ash forming processes during the combustion and later during cooling in the boiler a more detailed literature study is required. Interesting experiments about the chlorine influence on evaporation rates of heavy metals were performed by Jakob et al. (1996), Jiao et al. (2011) or Yang et al. (2014). Furthermore, Morf et al. (2000) described the effect of operating conditions and input variations on the partitioning of metals in a MSW incinerator.

The generated data of this project serve as a basis for the different leaching experiments planned for the next project (Chapter 7). In addition, the results of this study act as basis for a more detailed description of the chemical processes going on during neutral and acidic fly ash leaching (Chapter 3, Weibel et al., 2016).

References

AWEL, Amt für Abfall, Wasser, Energie und Luft des Kantons Zürich, 2013. Charakterisierung von Filteraschen und Filterkuchen aus unterschiedlichen Extraktionen. Technischer Bericht.

Bayuseno, A.P., Schmahl, W.W., 2011. Characterization of MSWI fly ash through mineralogy and water extraction. Resources, Conservation and Recycling 55, 524-534.

Deer, W.A., Howie, R.A., Zussman, J., 1996. An introduction to the rock-forming minerals. Prentice Hall.

Eighmy, T.T., Eusden, J.D., Krzanowski, J.E., Domingo, D.S., Staempfli, D., Martin, J.R., Erickson, P.M., 1995. Comprehensive approach toward understanding element speciation and leaching behavior in municipal solid waste incineration electrostatic precipitator ash. Environmental Science & Technology 29, 629-646.

FOEN, Federal Office for the Environment, 2014. Verordnung zur Reduktion von Risiken beim Umgang mit bestimmten besonders gefährlichen Stoffen , Zubereitungen und Gegenständen (Chemikalien-Risikoreduktions-Verordnung, ChemRRV) #814.81.

Held, A., Kramer, G.N., Robouch, P., Wätjen, U., 2007. The Certification of the mass fractions of As, Cd, Co, Cr, Cu, Fe, Hg, Mn, Ni, Pb, Sb, Se, Tl, V and Zn in fly ash BCR-176R. European Commission Directorate-General Joint Research Centre Institute for Reference Materials and Measurements.

Jakob, A., Stucki, S., Struis, R.P.W.J., 1996. Complete heavy metal removal from fly ash by heat treatment: Influence of chlorides an evaporation rates. Environmental Science & Technology 30, 3275-3283.

Jiao, F., Cheng, Y., Zhang, L., Yamada, N., Sato, A., Ninomiya, Y., 2011. Effects of HCl, SO_2 and H_2O in flue gas on the condensation behavior of Pb and Cd vapors in the cooling section of municipal solid waste incineration. Proceedings of the Combustion Institute 33, 2787-2793.

Kirby, C.S., Rimstidt, J.D., 1994. Interaction of municipal solid waste ash with water. Environmental Science & Technology 28, 443-451.

Le Bail, A., 1995. Modelling the silica glass structure by the Rietveld method. Journal of Non-Crystalline Solids 183, 39-42.

Li, M., Xiang, J., Hu, S., Sun, L.-S., Su, S., Li, P.-S., Sun, X.-X., 2004. Characterization of solid residues from municipal solid waste incinerator. Fuel 83, 1397-1405.

Ludwig, C., Hellweg, S., Stucki, S., 2003. Municipal Solid Waste Management. Strategies and technologies for sustainable solutions. Springer-Verlag (New York).

Mahieux, P.Y., Aubert, J.E., Cyr, M., Coutand, M., Husson, B., 2010. Quantitative mineralogical composition of complex mineral wastes-contribution of the rietveld method. Waste Management 30, 378-388.

Morf, L.S., Brunner, P.H., Spaun, S., 2000. Effect of operating conditions and input variations on the partitioning of metals in a municipal solid waste incinerator. Waste Management & Research 18, 4-15.

Omega Data Systems, 2004. UniQuant 5. A unique concept in XRF analysis. User manual.

Schlumberger, S., Schuster, M., Ringmann, S., Koralewska, R., 2007. Recovery of high purity zinc from filter ash produced during the thermal treatment of waste and inerting of residual materials. Waste Management & Research 25, 547-555.

Yang, S., Saffarzadeh, A., Shimaoka, T., Kawano, T., 2014. Existence of Cl in municipal solid waste incineration bottom ash and dechlorination effect of thermal treatment. Journal of Hazardous Materials 267, 214-220.

Appendix 6A: MSWI plants

SATOM Monthey

General information	
Plant	SATOM Monthey
Adress	Zone Industrielle Boeuferrant 1870 Monthey
Operator	Société pour le traitement des ordures du haut bassin
Number of communes	95
Number of inhabitants	250'000
Accountable manager	Edi Blatter
Sampling weeks	KW 48, 49 and 50

(www.vbsa.ch)

Plant details	
Type of furnance	MARTIN reciprocating grate
Construction year	2003/1996
Amount of furnance lines	2
Max. capacity (t/day waste)	240-300 t/day per line
Waste incinerated 2013 (t)	175‘414
Part municipal waste (%)	60
Part industrial waste (%)	40 (commercial waste, hospital and chemical industrial waste, oil and sewage sludge)
Fly ash (t/day)	4.32-8.64
Leached fly ash (t/day)	15.1

	Min.	Max.	Average
Waste input (t/day)	260	268	263
Firing temperature (°C)	737	888	852
Air amount (m^3)	35'645	40'560	38'247
Atmosphere/O_2 (%)	5.2	9.6	6.3

Energiezentrale Forsthaus Bern

General information	
Plant	Energiezentrale Forsthaus Bern
Adress	Murtenstrasse 100, 3008 Bern
Operator	Energie Wasser Bern
Catchment area	Bern
Number of communes	38
Number of inhabitants	310'000
Accountable manager	Thomas Bücherer
Contact person FLUWA	Peter Siegenthaler
Sampling weeks	KW 48, 49 and 50

(www.vbsa.ch)

Plant details	
Type of furnance	MARTIN reciprocating grate
Construction year	2012
Amount of furnance lines	1
Max. capacity (t/day waste)	400
Waste incinerated 2013 (t)	116'676
Part municipal waste (%)	60
Part industrial waste (%)	40 (commerical waste, VeVa-waste, sewage sludge)
Hazardous waste (%)	0.4%
Fly ash (t/day)	6-7 fly ash, 1.5-2.5 wood ash
Leached fly ash (t/day)	12-15

	Min.	Max.	Average
Waste input (t/day)	0.22	587	300

Linth Niederurnen

General information	
Plant	Linth Niederurnen
Adress	Im Fennen 1a, 8867 Niederurnen
Operator	ZKL / Zweckverband für die Kehrichtbeseitigung im Linthgebiet
Catchment area	Canton Glarus, parts of canton St. Gallen, Schwyz and Graubünden
Number of communes	52
Number of inhabitants	230'000
Accountable manager	Walter Furgler/Stefan Ringmann
Contact person FLUWA	Stefan Ringmann
Sampling weeks	KW 48 and 49

(www.vbsa.ch)

Plant details	
Type of furnance	Stiefel moving-grate, MARTIN reciprocating grate with Stiefel water cooling system
Construction year	1999-2001
Amount of furnance lines	2
Max. capacity (t/day waste)	300-315
Waste incinerated 2012 (t)	113'400
Part municipal waste (%)	40
Part industrial waste (%)	60 (commerical waste, ASR, VeVa-waste, sewage sludge)
Fly ash (t/day)	7,2
Leached fly ash (t/h)	FLUWA operation on three days of the week with 4 t/h

	Min.	Max.	Average
Waste input (t/day)	300	315	307
Firing temperature (°C)	-	-	1050
Air amount (m^3)	42'000	45'000	43'500
Athmosphere/O_2 (%)	8	10	9
Operating time FLUWA (h/day)	4	5	4,5

Hagenholz Zürich

General information	
Plant	Hagenholz Zürich
Adress	Hagenholzstrasse 110, 8050 Zürich
Operator	ERZ Entsorgung + Recycling Zürich
Catchment area	Zürich city
Accountable manager	Christoph Zemp (Geschäftsbereichsleiter) Thomas Huber (Leiter Produktion)
Contact person FLUWA	Thomas Huber
Sampling weeks	KW 48, 49 and 50

(www.vbsa.ch)

Plant details	
Type of furnance	MARTIN reciprocating grate
Construction year	2008/2010
Amount of furnance lines	2
Max. capacity (t/day waste)	2x58 t/h steam (total ca. 700 t waste/day)
Waste incinerated 2013 (t)	258'337
Part municipal waste (%)	64
Part industrial waste (%)	37 (commerical waste, ASR, VeVa-waste, sewage sludge)
Fly ash (t/day)	15 (two lines)
Leached fly ash (t/day)	Ca. 40-50 (24 h FLUWA)
	Average
Waste input (t/day)	700 (two lines)
Firing temperature (°C)	850-900
Athmosphere/O_2 (%)	9-9.5
Operating time FLUWA (h/day)	Monday to thursday (24h)

KEZO Hinwil

General information	
Plant	KEZO Hinwil
Adress	Wildbachstrasse 2, 8340 Hinwil
Operator	Zweckverband Kehrichtverwertung Zürcher Oberland KEZO
Number of communes	38
Accountable manager	Daniel Böni
Sampling weeks	KW 48, 49, 50 at MSWI Zuchwil

(www.vbsa.ch)

Plant details	
Type of furnance	MARTIN reciprocating grate
Construction year	1976/1976/1995
Amount of furnance lines	3
Max. capacity (t/day waste)	600 (all three lines)
Waste incinerated 2013 (t)	194'044
Part municipal waste (%)	46
Part industrial waste (%)	54 (commerical waste, ASR, VeVa-waste, sewage sludge)
Fly ash (t/day)	11.4

	Min.	Max.	Average
Waste input (t/day)	550	950	750
Firing temperature (°C)	700	900	850
Air amount (m^3)	150'000	200'000	170'000
Athmosphere/O_2 (%)	10.2	13.7	11.4

Emmenspitz Zuchwil

General information	
Plant	Emmenspitz Zuchwil
Adress	Emmenspitz, 4528 Zuchwil
Operator	KEBAG, Kehrichtbeseitigungs AG
Number of communes	188
Number of inhabitants	483'000
Accountable manager	Markus Juchli
Contact person FLUWA	Urs Obi
Sampling weeks	KW 48, 49, 50

(www.vbsa.ch)

Plant details		
Type of furnance	Von Roll reciprocating grate	
Construction year	1990-1993 (line 4 2002)	
Amount of furnance lines	4	
Max. capacity (t/day waste)	250 t/day pro line	
Waste incinerated 2013 (t)	220'852	
Part municipal waste (%)	48	
Part industrial waste (%)	52 (commerical waste, ASR, VeVa-waste, sewage sludge)	
Fly ash (t/day)	15-21	
Leached fly ash (t/h)	15-19 (wet, dry substance 60%)	
	Min.	Max.
Waste input (t/day)	540	750
Firing temperature (°C)	790	860
Air amount (m^3)	42'000	55'000
Athmosphere/O_2 (%)	8	10
Operating time FLUWA (h/day)	20	22

Appendix 6B: List of identified mineral phases and alloys

Mineral	Chemical formula
Silicates	
Aluminosilicates	$Ca(Al_2Si_2O_8)$–$Na(AlSi_3O_8)$, $K(AlSi_3O_8)$–$Na(AlSi_3O_8)$
Melilite	$Ca_2Al_2SiO_7$–$Ca_2MgSi_2O_7$
Monticellite	$CaMgSiO_4$–$CaFeSiO_4$
Quarz	SiO_2
Wollastonite	$CaSiO_3$
Hemimorphite	$Zn_4Si_2O_7(OH)_2 \cdot 2H_2O$
Carbonates	
Ankerite	$Ca(Fe,Mg,Mn)(CO_3)_2$
Calcite	$CaCO_3$
Dolomite	$CaMg\ (CO_3)_2$
Oxides	
Lime	CaO
Hematite	Fe_2O_3
Mayenite	$Ca_{12}Al_{14}O_{33}$
Periclase	MgO
Rutile	TiO_2
Zincite	ZnO
Tenorite	CuO
Chlorides	
Halite	NaCl
Sylvite	KCl
K-Zn-Chloride	K_2ZnCl_4
Cotunnite	$PbCl_2$
Sulphates	
Anhydrite	$CaSO_4$
Bassanite	$Ca[SO_4] \cdot 0.5\ H_2O$
Ettringite	$Ca_6Al_2(OH)_{12}(SO_4)_3 \cdot 26H_2O$
Gypsum	$CaSO_4 \cdot 2H_2O$
Anglesite	$PbSO_4$
Palmierite	$(K,Na)_2Pb(SO_4)_2$
Caracolite	$Na_3Pb_2(SO_4)_3Cl$
Omongwaite	$Na_2Ca_5(SO_4)_6 \cdot 3H_2O$
Syngenite	$K_2Ca(SO_4)_2 \cdot (H_2O)$
Gorgeyite	$K_2Ca_5(SO_4)_6 \cdot H_2O$
Sulfides	
Chalcocite	Cu_2S
Alloys	
Al^0	Al (85 wt.%), Si (15 wt.%)
Cu^0	Cu (>90 wt.%)
Brass	$Cu_{0.6}Zn_{0.4}$
$PbCu^0$	Pb (50 wt.%), Cu (15 wt.%), Cl (10 wt.%)

Appendix 6C: Chemical data

WD-XRF (UniQuant)

Table A6-1: *Major element composition in oxides of fly ash and filter cake from the six MSWI plants, measured on powder tablets by WD-XRF. Values in wt.%. Sample WABER is the wood ash from MSWI plant Bern which is acidic leached together with FABER.*

Sample	LOI	SiO_2	CaO	Al_2O_3	MgO	Na_2O	K_2O	Fe_2O_3	TiO_2	MnO	SO_3	P_2O_5
FAMON	9.7	9.5	22.9	4.6	1.4	8.7	6.1	2.0	1.1	0.07	6.2	0.6
FCMON	11.8	11.2	28.7	6.3	1.9	1.9	2.1	2.3	1.4	0.08	8.1	0.7
FABER	12.7	12.2	24.0	5.2	1.7	7.6	5.3	1.7	1.3	0.07	4.6	0.4
WABER	15.4	9.6	36.4	2.9	4.5	1.1	11.0	1.9	1.4	0.69	2.9	1.4
FCBER	7.6	15.7	26.0	6.8	0.9	0.6	1.4	2.0	1.8	0.13	12.2	1.0
FANIE	10.3	10.4	20.8	3.8	1.1	9.7	6.1	2.3	1.2	0.08	5.5	0.5
FCNIE	8.4	13.1	29.1	6.3	1.3	1.0	1.1	2.9	1.5	0.09	10.1	0.6
FAHAG	9.7	9.3	29.6	5.3	1.6	8.4	5.1	1.5	1.5	0.06	4.7	0.7
FAHIN	10.4	9.3	20.6	3.8	1.3	8.0	5.1	3.0	1.1	0.08	6.6	0.5
FAZUC	13.2	7.1	16.2	3.2	1.0	10.5	6.9	1.5	1.0	0.06	5.4	0.5
FCZUC	9.8	12.1	25.0	6.0	0.8	0.6	0.8	3.0	1.3	0.07	13.0	0.7
BCR 176R	-	18.1	21.3	10.1	2.1	5.8	4.0	1.69	1.49	0.085	4.2	0.7

Table A6-2: *Major element composition of fly ash and filter cake from the six MSWI plants, measured on powder tablets by WD-XRF. Values in mg/kg.*

Sample	Ca	Na	K	Mg	Si	Zn	Al	Fe	Pb	Cu	Sb	Cd
FAMON	163'800	64'800	50'900	8'580	44'300	25'700	24'200	14'300	9'590	3'800	3'850	264
FCMON	205'400	14'400	17'100	11'500	52'200	30'800	33'400	16'100	11'700	4'710	4'270	329
FABER	171'600	56'100	43'700	10'200	57'000	25'400	27'400	11'600	6'530	1'400	2'990	215
WABER	260'100	8'290	91'300	26'900	45'100	8'350	15'300	13'400	4'240	423	94	56
FCBER	171'600	56'100	43'700	10'200	57'000	13'400	27'400	11'600	5'430	1'130	3'030	55
FANIE	149'000	71'800	50'400	6'900	48'600	48'800	20'200	15'900	9'520	2'580	3'330	368
FCNIE	207'800	7'320	9'370	7'820	61'100	35'300	33'400	20'000	11'200	3'090	3'710	130
FAHAG	211'300	62'600	42'200	9'850	43'300	21'300	28'300	10'700	3'460	1'030	3'300	226
FAHIN	147'500	59'200	42'500	8'120	43'400	57'300	20'200	20'800	13'600	2'610	3'260	355
FAZUC	116'100	77'800	56'900	6'070	33'400	69'700	16'800	10'300	11'400	2'410	4'270	633
FCZUC	178'600	4'310	6'580	4'910	56'400	24'800	31'800	20'900	7'000	2'310	5'080	41
BCR 176R	152'400	43'200	33'300	12'700	84'600	15'900	53'500	11'800	4'680	947	1'030	247

Table A6-3: *Trace element composition of fly ash and filter cake from the six MSWI plants, measured on powder tablets by WD-XRF. Values in mg/kg.*

Sample	Ti	Cl	Ba	Sn	Mn	Cr	Sr	Zr	Rb	V	Bi	Ni	Co	Y
FAMON	6'790	107'100	2'010	1'950	573	796	619	167	127	101	60	90	18	10
FCMON	8'170	34'300	2'370	2'270	632	910	771	201	58	85	97	97	35	13
FABER	7'860	107'200	2'370	1'520	558	437	459	150	128	115	41	28	22	15
WABER	8'620	22'700	4'620	89	5'310	441	852	132	286	100	23	50	9	11
FCBER	7'860	7'770	3'060	1'650	558	521	406	183	45	118	41	35	13	12
FANIE	7'140	102'200	3'800	1'990	596	937	534	284	137	90	202	94	39	7
FCNIE	9'120	10'000	4'520	2'220	702	1'110	616	370	29	117	215	129	42	9
FAHAG	8'980	100'100	2'100	1'130	497	1'230	538	238	89	100	50	94	20	13
FAHIN	6'400	92'800	2'880	2'070	630	678	486	261	134	63	148	94	42	9
FAZUC	5'780	127'800	1'820	2'500	499	487	340	150	180	83	187	68	25	8
FCZUC	7'800	7'710	3'020	3'130	510	822	457	287	39	100	246	106	39	9
BCR 176R	8'960	69'900	5'980	1'680	657	814	451	231	104	106	47	91	40	14

TD-ICP-OES Bachema

Table A6-4: *Trace element composition of fly ash and filter cake measured by Bachema AG using ICP-OES analysis (Cd: ICP-MS) after microwave assisted digestions. Values in mg/kg.*

Element	Ca	Na	K	Si	Zn	Al	Fe	Pb	Cu	Cd
Method	ICP-OES	ICP-OES	ICP-OES	ICP-OES	ICP-OES	ICP-OES	ICP-OES	ICP-OES	ICP-OES	ICP-MS
FAMON	185'000	43'100	45'000	69'900	26'200	36'300	18'100	9'560	3'800	218
FCMON	203'000	19'200	18'600	80'000	29'000	41'300	18'800	10'600	4'450	206
FABER	192'000	40'100	37'700	84'100	25'100	39'000	14'300	6'260	1'410	165
FCBER	170'000	7'640	11'100	102'000	12'800	39'900	15'500	5'400	1'220	49
FANIE	174'000	46'300	40'200	76'600	45'000	37'900	23'300	8'950	2'560	244
FCNIE	193'000	10'100	8'440	88'700	30'500	43'700	27'800	9'530	2'780	106
FAHAG	222'000	42'500	35'000	68'100	20'400	43'800	14'600	3'140	1'040	150
FAHIN	169'000	40'400	37'300	73'600	56'600	31'300	28'200	13'400	2'630	249
FAZUC	150'000	57'200	54'200	60'300	73'000	32'200	15'400	11'400	2'550	426
FCZUC	183'000	7'390	6'820	81'800	25'000	35'900	26'200	6'700	2'360	30
BCR 176R	183'000	34'400	33'800	104'000	18'000	55'400	14'600	4'950	1'070	210

TD-ICP-OES UniBE

Table A6-5: *Element composition of fly ash and filter caks from the six MSWI plants, measured at University of Bern by ICP-OES after microwave assisted acid digestions. Values in mg/kg.*

		Ca	Mg	Zn	Al	Fe	Pb	Cu	Sb	Cd
FAMON	ICP-OES 1	196'903	13'382	25'942	38'441	17'956	9'572	4'030	3'023	238
	ICP-OES 2	213'887	14'671	28'295	41'846	18'979	9'902	4'040	3'059	245
	ICP-OES 3	209'351	14'022	27'506	39'959	18'473	9'445	3'838	2'856	234
	MW	206'714	14'025	27'248	40'082	18'469	9'640	3'969	2'979	239
	SD	8'794	644	1'198	1'706	512	236	114	108	6
	RSD %	4	5	4	4	3	2	3	4	2
FCMON	ICP-OES 1	239'603	15'725	31'534	45'675	19'651	10'477	4'451	2'918	220
	ICP-OES 2	222'897	14'550	29'294	41'584	17'856	11'187	4'705	3'157	235
	ICP-OES 3	233'632	15'178	30'737	43'582	18'459	11'016	4'623	3'106	230
	MW	232'044	15'151	30'521	43'614	18'655	10'893	4'593	3'060	229
	SD	8'465	588	1'135	2'045	913	371	129	126	8
	RSD %	4	4	4	5	5	3	3	4	3
FABER	ICP-OES 1	220'975	14'713	27'070	43'343	14'641	6'427	1'479	2'246	181
	ICP-OES 2	219'185	14'726	26'898	42'739	14'802	6'539	1'491	2'318	185
	ICP-OES 3	215'216	14'319	26'274	41'762	14'311	6'482	1'466	2'250	183
	MW	218'458	14'586	26'747	42'615	14'585	6'483	1'479	2'271	183
	SD	2'948	232	419	798	250	56	12	40	2
	RSD %	1	2	2	2	2	1	1	2	1
WABER	ICP-OES 1	260'591	23'863	8'192	25'411	12'725	3'532	418	0	13
	ICP-OES 2	257'671	23'732	8'097	24'981	12'605	3'556	400	0	12
	ICP-OES 3	285'317	26'042	8'880	28'481	13'904	3'738	417	0	14
	MW	267'860	24'546	8'390	26'291	13'078	3'609	412	0	13
	SD	15'188	1'298	428	1'909	718	113	10	0	1
	RSD %	6	5	5	7	6	3	2	0	11
FCBER	ICP-OES 1	209'501	9'566	14'030	50'180	16'739	5'737	1'284	2'195	50
	ICP-OES 2	186'636	8'465	12'531	44'771	15'017	5'824	1'321	2'352	53
	ICP-OES 3	207'005	9'465	13'879	49'411	16'613	5'632	1'274	2'257	50
	MW	201'047	9'165	13'480	48'121	16'123	5'731	1'293	2'268	51
	SD	12'543	609	825	2'927	960	96	25	79	2
	RSD %	6	7	6	6	6	2	2	4	3
FANIE	ICP-OES 1	207'137	14'985	49'129	44'536	23'891	9'541	2'679	2'548	296
	ICP-OES 2	214'218	15'338	51'652	45'499	25'429	9'380	2'719	2'502	293
	ICP-OES 3	206'317	14'948	49'679	45'861	23'904	9'072	2'584	2'451	286
	MW	209'224	15'090	50'153	45'299	24'408	9'331	2'661	2'500	292
	SD	4'345	215	1'327	685	885	238	69	48	5
	RSD %	2	1	3	2	4	3	3	2	2
FCNIE	ICP-OES 1	221'731	14'121	32'765	49'163	28'098	10'105	2'934	2'670	118
	ICP-OES 2	218'545	14'285	32'326	47'794	28'642	10'255	2'922	2'602	120
	ICP-OES 3	215'841	13'871	32'081	49'913	27'250	9'892	2'965	2'578	115
	MW	218'706	14'092	32'391	48'957	27'996	10'084	2'940	2'617	118
	SD	2'948	209	347	1'074	701	182	22	48	2
	RSD %	1	2	1	2	3	2	1	2	2
FAHAG	ICP-OES 1	260'661	14'895	22'315	46'953	14'474	3'042	998	2'349	155
	ICP-OES 2	271'054	15'355	23'211	48'844	15'582	3'400	1'127	2'567	172
	ICP-OES 3	251'647	14'075	21'483	45'977	13'912	3'232	1'056	2'385	163
	MW	261'121	14'775	22'336	47'258	14'656	3'224	1'060	2'434	163
	SD	9'712	648	864	1'458	850	179	65	117	9
	RSD %	4	4	4	3	6	6	6	5	5

		Ca	Mg	Zn	Al	Fe	Pb	Cu	Sb	Cd
FAHIN	ICP-OES 1	195'971	14'794	59'738	33'592	28'471	12'969	2'556	2'466	264
	ICP-OES 2	191'439	14'493	58'865	33'456	27'828	13'857	2'738	2'535	280
	ICP-OES 3	192'234	14'796	59'733	34'048	29'017	13'625	2'665	2'552	277
	MW	193'215	14'695	59'446	33'699	28'439	13'483	2'653	2'517	274
	SD	2'420	175	503	310	595	461	92	45	9
	RSD %	1	1	1	1	2	3	4	2	3
FAZUC	ICP-OES 1	169'145	12'360	76'816	33'640	15'287	11'942	2'651	3'547	534
	ICP-OES 2	178'391	13'219	81'774	37'068	16'336	11'946	2'620	3'540	532
	ICP-OES 3	164'050	11'926	75'424	33'209	14'751	11'821	2'599	3'469	522
	MW	170'528	12'501	78'005	34'639	15'458	11'903	2'623	3'518	529
	SD	7'270	658	3'338	2'115	806	71	26	43	6
	RSD %	4	5	4	6	5	1	1	1	1
FCZUC	ICP-OES 1	212'777	10'066	27'539	41'867	27'606	7'033	2'482	4'086	28
	ICP-OES 2	194'957	9'376	25'117	38'949	25'613	6'890	2'474	3'926	29
	ICP-OES 3	221'405	10'431	28'186	42'699	27'836	7'011	2'509	3'987	28
	MW	209'713	9'958	26'947	41'172	27'018	6'978	2'488	4'000	28
	SD	13'487	536	1'618	1'969	1'222	77	18	80	0
	RSD %	6	5	6	5	5	1	1	2	1
BCR 176R	ICP-OES 1	209'610	17'176	19'445	62'631	14'766	4'868	1'091	825	216
	ICP-OES 2	200'936	16'587	18'722	59'794	14'090	5'030	1'118	873	226
	ICP-OES 3	198'291	16'241	18'464	59'040	13'907	5'187	1'142	898	230
	MW	202'946	16'668	18'877	60'489	14'254	5'028	1'117	865	224
	Cert. value	-	-	16'800	-	13'100	5'000	1'050	850	226
	Wf %	-	-	112	-	109	101	106	102	99
	SD	5'921	473	509	1'894	452	159	25	37	7
	RSD %	3	3	3	3	3	3	2	4	3

Actlabs Analysis

Table A6-6: *Major element composition of fly ash and filter cake from the six MSWI plants, measured by Actlabs using INAA or ICP-OES.*

Element	Ca	Al	Mg	Na	K	Fe	Ti	S	P
Method	TD-ICP	TD-ICP	TD-ICP	INAA	TD-ICP	INAA	TD-ICP	TD-ICP	TD-ICP
Detection Limit	0.01	0.01	0.01	0.01	0.01	0.01	0.01	0.01	0.001
Unit	wt.%	wt.%	wt.%	wt.%	wt.%	wt.%	wt.%	wt.%	wt.%
FAMON	18.8	3.97	1.28	3.46	2.46	1.39	0.21	5.13	0.151
FCMON	21	4.38	1.4	1.6	1.87	1.81	0.14	5.54	0.151
FABER	19.5	4.25	1.26	2.98	2.8	1.16	0.28	3.88	0.078
WABER	25.3	2.85	2.25	0.69	3.12	0.92	0.03	2.28	0.546
FCBER	16.1	4.85	0.84	0.67	1.17	1.54	0.17	6.27	0.181
FANIE	17.2	3.63	1.18	3.64	2.84	1.75	0.47	5.11	0.128
FCNIE	18.8	4.46	1.23	0.83	0.83	2.38	0.54	5.81	0.079
FAHAG	22.8	4.51	1.29	3.18	2.86	1.06	0.18	3.61	0.107
FAZUC	15.8	3.16	1.08	4.27	2.71	1.26	0.24	6.24	0.111
FAHIN	17.7	3.22	1.32	3.18	2.46	2.23	0.34	6.02	0.189
FCZUC	21	4.23	0.97	0.71	0.76	2.44	0.23	11	0.198

Table A6-7: *Trace element composition of fly ass and filter cake from the six MSWI plants, measured by Actlabs using INAA or ICP-OES. Values in mg/kg or µg/kg.*

Element	**Mn**	**V**	**Cr**	**Co**	**Ni**	**Cu**	**Zn**	**Br**	**Rb**
Analysis Method	TD-ICP	TD-ICP	INAA	INAA	INAA/ TD-ICP	TD-ICP	INAA/ TD-ICP	INAA	INAA
Detection Limit	1	2	2	1	1	1	1	0.5	15
Unit	mg/kg	mg/kg	mg/kg	mg/kg	mg/kg	mg/kg	mg/kg	mg/kg	mg/kg
FAMON	729	24	560	39	152	3'650	19'600	1'980	<15
FCMON	693	23	620	37	175	4'150	23'700	785	<15
FABER	571	24	309	25	69	1'300	18'100	1'170	<15
WABER	4'370	21	268	11	67	317	5'660	43	186
FCBER	944	20	419	19	78	1'190	10'600	81	<15
FANIE	682	27	685	43	138	2'260	33'400	1'560	<15
FCNIE	803	35	797	42	179	2'480	23'400	148	<15
FAHAG	581	17	788	36	141	900	15'000	1'220	<15
FAZUC	630	15	411	61	126	2'280	52'400	2'920	<15
FAHIN	712	30	522	44	150	2'280	42'300	1'440	130
FCZUC	609	25	690	45	147	2'340	23'300	195	<15

Element	**Sr**	**Y**	**Cd**	**Sn**	**Sb**	**Ba**	**Pb**	**Bi**	**Hg**
Analysis Method	TD-ICP	TD-ICP	TD-ICP	TD-MS	INAA	INAA	TD-ICP	TD-MS	INAA
Detection Limit	1	1	0.3	1	0.1	50	3	0.1	1
Unit	mg/kg	mg/kg	mg/kg	mg/kg	mg/kg	mg/kg	mg/kg	mg/kg	mg/kg
FAMON	556	10	240	160	2'390	1'430	>5000	49	<1
FCMON	632	10	225	144	2'510	1'690	>5000	69	<1
FABER	391	13	168	49	1'720	650	>5000	42	<1
WABER	643	7	20	3	57	2'250	3'190	13	<1
FCBER	281	10	52	113	2'030	940	4'860	53	59
FANIE	379	9	251	>200	1'950	< 50	>5000	132	<1
FCNIE	402	11	109	>200	2'110	1'420	>5000	167	<1
FAHAG	425	14	157	50	1'840	900	2'800	52	<1
FAZUC	298	7	499	>200	2'690	1'160	> 5000	158	<1
FAHIN	404	9	261	>200	1'930	1'860	>5000	113	<1
FCZUC	381	11	35	>200	3'530	1'770	>5000	204	<1

Element	**Au**	**Ag**	**Mo**	**As**	**Be**	**Cs**	**Ge**	**Ga**	**In**
Analysis Method	INAA	INAA/ TD-ICP	TD-ICP	INAA	TD-ICP	INAA	TD-MS	TD-MS	TD-MS
Detection Limit	2	0.3	1	0.5	1	1	0.1	0.1	0.2
Unit	µg/kg	mg/kg	mg/kg	mg/kg	mg/kg	mg/kg	mg/kg	mg/kg	mg/kg
FAMON	921	48.2	7	77.3	<1	<1	0.8	13.6	1.7
FCMON	1600	56.4	7	75.6	<1	<1	0.6	15.7	1.9
FABER	354	45.4	4	46.9	<1	<1	1	14.3	1.2
WABER	29	2.1	2	39.0	<1	<1	0.1	5.1	<0.2
FCBER	474	43.4	7	60.5	<1	<1	0.3	16.8	1.3
FANIE	605	46.2	16	55.9	<1	<1	0.4	14.8	2.2
FCNIE	455	53.6	21	51.3	<1	<1	0.5	17.3	2.5
FAHAG	610	39.4	6	32.5	<1	<1	0.4	10.9	1.6
FAZUC	841	72.9	8	79.4	<1	<1	0.8	19.6	4.8
FAHIN	610	70.7	16	71.4	<1	<1	0.8	13.4	2.8
FCZUC	1560	111	18	124	<1	<1	0.5	21.2	4

Element	**Re**	**Ir**	**Li**	**Nb**	**Se**	**Ta**	**Te**	**Th**	**Tl**	**Hf**
Analysis Method	TD-MS	INAA	TD-MS	TD-MS	INAA/ TD-ICP-MS	INAA	TD-MS	INAA	TD-MS	INAA
Detection Limit	0.001	5	0.5	0.1	0.1	0.5	0.1	0.2	0.1	1
Unit	mg/kg	µg/kg	mg/kg	mg/kg	mg/kg	mg/kg	mg/kg	mg/kg	mg/kg	mg/kg
FAMON	0.027	<5	44.4	0.1	<0.1	<0.5	<0.1	<0.2	2.4	<1
FCMON	0.012	<5	35.7	0.1	8	<0.5	0.1	<0.2	1.9	<1
FABER	0.014	<5	44.3	0.2	<0.1	<0.5	<0.1	4.1	1.5	<1
WABER	0.007	<5	17.6	< 0.1	<0.1	<0.5	<0.1	4.3	0.9	1
FCBER	0.004	<5	22.5	0.1	<0.1	<0.5	<0.1	<0.2	0.9	<1
FANIE	0.066	<5	62.2	0.3	<0.1	<0.5	<0.1	2.8	1.9	4
FCNIE	0.011	<5	35.9	0.5	<0.1	<0.5	<0.1	<0.2	1.4	10
FAHAG	0.443	<5	38.3	0.2	<0.1	<0.5	<0.1	<0.2	1.4	<1
FAZUC	0.029	<5	73.4	0.1	<0.1	<0.5	<0.1	<0.2	3.2	<1
FAHIN	0.038	<5	61.4	0.2	17	<0.5	0.1	<0.2	2.4	<1
FCZUC	0.007	<5	24.7	<0.1	10	<0.5	<0.1	<0.2	1.0	<1

Element	**La**	**Eu**	**Tb**	**Yb**	**Lu**	**Sc**	**Nd**	**Sm**	**La**
Analysis Method	INAA	INAA	INAA	INAA	INAA	INAA	INAA	INAA	INAA
Detection Limit	0.5	0.2	0.5	0.2	0.05	0.1	5	0.1	0.5
Unit	mg/kg	mg/kg	mg/kg	mg/kg	mg/kg	mg/kg	mg/kg	mg/kg	mg/kg
FAMON	25.3	<0.2	<0.5	<0.2	<0.05	1.7	<5	1.4	25.3
FCMON	22.8	<0.2	<0.5	<0.2	<0.05	2.3	<5	1.4	22.8
FABER	12.9	<0.2	<0.5	<0.2	<0.05	2.3	<5	1.5	12.9
WABER	8.8	0.3	<0.5	<0.2	<0.05	2.2	<5	1.5	8.8
FCBER	15.3	<0.2	<0.5	<0.2	<0.05	2.8	<5	2.0	15.3
FANIE	11.1	<0.2	<0.5	<0.2	<0.05	1.9	<5	1.2	11.1
FCNIE	13.3	<0.2	<0.5	<0.2	<0.05	2	<5	1.5	13.3
FAHAG	11.2	<0.2	<0.5	<0.2	<0.05	1.6	<5	1.2	11.2
FAZUC	7.8	<0.2	<0.5	<0.2	<0.05	1.5	<5	1.0	7.8
FAHIN	9.7	<0.2	<0.5	<0.2	<0.05	2.2	<5	1.4	9.7
FCZUC	14.0	<0.2	<0.5	<0.2	<0.05	3	<5	1.7	14

Method comparison

Table A6-8: *Comparison of some major and trace element compositions of the fly ashes and filer cakes from the six MSWI plants measured by UniBE (TD-ICP-OES), UniFR (WD-XRF), Bachema (TD-ICP-OES(MS)), ZAR Zuchwil (ED-XRF) and Actlabs (INAA or TD-ICP-OES). Values in mg/kg.*

	Method	Lab	mg/kg							
			Ca	Zn	Al	Fe	Pb	Cu	Sb	Cd
FAMON	ICP-OES	UniBE	206'714	27'248	40'082	18'469	9'640	3'969	2'979	239
	WD-XRF	UniFR	163'800	25'700	64'800	14'300	9'590	3'800	3'850	264
	ICP-OES	Bachema	185'000	26'200	36'300	18'100	9'560	3'800	-	218
	ED-XRF	ZAR	186'800	27'190	40'820	17'720	9'332	3'776	2'998	228
	INAA or ICP-OES	Actlabs	188'000	19'600	39'700	13'900	5'000	3'650	2'390	240
FCMON	ICP-OES	UniBE	232'044	30'521	43'614	18'655	10'893	4'593	3'060	229
	WD-XRF	UniFR	205'400	30'800	33'400	16'100	11'700	4'710	4'270	329
	ICP-OES	Bachema	203'000	29'000	41'300	18'800	10'600	4'450	-	206
	ED-XRF	ZAR	189'600	28'420	31'010	17'280	10'220	4'202	2'840	-
	INAA or ICP-OES	Actlabs	210'000	23'700	43'800	18'100	5'000	4'150	2'510	225
FABER	ICP-OES	UniBE	218'458	26'747	42'615	14'585	6'483	1'479	2'271	183
	WD-XRF	UniFR	171'600	25'400	27'400	11'600	6'530	1'400	2'990	215
	ICP-OES	Bachema	192'000	25'100	39'000	14'300	6'260	1'410	-	165
	ED-XRF	ZAR	199'200	26'650	49'310	14'080	6'311	1'369	2'224	170
	INAA or ICP-OES	Actlabs	195'000	18'100	42'500	11'600	5'000	1'300	1'720	168
FCBER	ICP-OES	UniBE	201'047	13'480	48'121	16'123	5'731	1'293	2'268	51
	WD-XRF	UniFR	185'700	13'400	35'800	14'200	5'430	1'130	3'030	55
	ICP-OES	Bachema	170'000	12'800	39'900	15'500	5'400	1'220	-	49
	ED-XRF	ZAR	175'700	24'930	30'900	24'970	6'740	2'310	3'831	-
	INAA or ICP-OES	Actlabs	161'000	10'600	48'500	15'400	4'860	1'190	2'030	52
FANIE	ICP-OES	UniBE	209'224	50'153	45'299	24'408	9'331	2'661	2'500	292
	WD-XRF	UniFR	149'000	48'800	20'200	15'900	9'520	2'580	3'330	368
	ICP-OES	Bachema	174'000	45'000	37'900	23'300	8'950	2'560	-	244
	ED-XRF	ZAR	165'600	48'560	33'580	20'540	9'013	2'493	2'404	264
	INAA or ICP-OES	Actlabs	172'000	33'400	36'300	17'500	5'000	2'260	1'950	251
FCNIE	ICP-OES	UniBE	218'706	32'391	48'957	27'996	10'084	2'940	2'617	118
	WD-XRF	UniFR	207'800	35'300	33'400	20'000	11'200	3'090	3'710	130
	ICP-OES	Bachema	193'000	30'500	43'700	27'800	9'530	2'780	-	106
	ED-XRF	ZAR	195'100	31'960	29'790	21'890	9'489	2'680	2'524	-
	INAA or ICP-OES	Actlabs	188'000	23'400	44'600	23'800	5'000	2'480	2'110	109
FAHAG	ICP-OES	UniBE	261'121	22'336	47'258	14'656	3'224	1'060	2'434	163
	WD-XRF	UniFR	211'300	21'300	28'300	10'700	3'460	1'030	3'300	226
	ICP-OES	Bachema	222'000	20'400	43'800	14'600	3'140	1'040	-	150
	ED-XRF	ZAR	239'800	21'170	43'740	12'810	3'220	927	2'383	154
	INAA or ICP-OES	Actlabs	228'000	15'000	45'100	10'600	2'800	900	1'840	157
FAHIN	ICP-OES	UniBE	193'215	59'446	33'699	28'439	13'483	2'653	2'517	274
	WD-XRF	UniFR	147'500	57'300	20'200	20'800	13'600	2'610	3'260	355
	ICP-OES	Bachema	169'000	56'600	31'300	28'200	13'400	2'630	-	249
	ED-XRF	ZAR	167'000	58'630	32'780	26'800	13'090	2'579	2'538	260
	INAA or ICP-OES	Actlabs	177'000	42'300	32'200	22'300	5'000	2'280	1'930	261
FAZUC	ICP-OES	UniBE	170'528	78'005	34'639	15'458	11'903	2'623	3'518	529
	WD-XRF	UniFR	116'100	69'700	16'800	10'300	11'400	2'410	4'270	633
	ICP-OES	Bachema	150'000	73'000	32'200	15'400	11'400	2'550	3'289	426
	ED-XRF	ZAR	130'052	72'789	29'316	13'509	11'176	2'437	11'176	456
	INAA or ICP-OES	Actlabs	158'000	52'400	31'600	12'600	5'000	2'280	2'690	499
FCZUC	ICP-OES	UniBE	209'713	26'947	41'172	27'018	6'978	2'488	4'000	28
	WD-XRF	UniFR	178'600	24'800	31'800	20'900	7'000	2'310	5'080	41
	ICP-OES	Bachema	183'000	25'000	35'900	26'200	6'700	2'360	-	30
	ED-XRF	ZAR	175'700	24'930	30'900	24'970	6'740	2'310	3'831	-
	INAA or ICP-OES	Actlabs	210'000	23'300	42'300	24'400	5'000	2'340	3'530	35

	Method	Lab	Ca	Zn	Al	Fe	Pb	Cu	Sb	Cd
BCR 176R	Certified value		-	16'800	-	13'100	5'000	1'050	850	226
	ICP-OES	UniBE	202'946	18'877	60'489	14'254	5'028	1'117	865	224
	Wf %		**-**	**112**	**-**	**109**	**101**	**106**	**102**	**99**
	WD-XRF	Fribourg	152'400	15'900	53'500	11'800	4'680	947	1'030	247
	Wf %		**-**	**95**	**-**	**90**	**94**	**90**	**121**	**109**
	ED-XRF	ZAR	187'200	16'850	45'330	12'940	4'617	993	880	264
	Wf %		**-**	**100**	**-**	**99**	**92**	**95**	**104**	**117**
	ICP-OES	Bachema	183'000	18'000	55'400	14'600	4'950	1'070	-	210
	Wf %		**-**	**107**	**-**	**111**	**99**	**102**	**-**	**93**

Appendix 6D: Method for total digestion of fly ash

Method development

To optimize the total acidic microwave digestion of fly ash, tests with different acid mixtures were performed. Beside fly ash from MSWI plant Zuchwil (FAZUC) and Hinwil (FAHIN), the NIST-standard reference material 1633a (Trace elements in coal fly ash) was used.

Table A6-9: *Different acid mixtures used for method development.*

Digestion Nr.	Description
1	8 ml HNO_3 65% + 5 ml HCl 30% + 2 ml HF 40% (10 ml sat. boric acid)
2	10 ml HNO_3 65% + 4 ml HF 40% (20 ml sat. boric acid)
3	8 ml HNO_3 65% + 2 ml HF 40% (10 ml sat. boric acid)
4	8 ml HNO_3 65% + 1 ml HF 40% (5 ml sat. boric acid)
5	10 ml HNO_3 65% + 1 ml HF 40% (5 ml sat. boric acid)
6	12 ml HNO_3 65% + 2 ml HF 40% (10 ml sat. boric acid)

Table A6-10: *Results of total acidic digestion of fly ash, measured by ICP-OES in mg/kg. bd: below detection limit.*

Name	Digestion Nr.	Al	Ca	Cd	Cu	Fe	Mg	Pb	Zn	Sb
FAZUC 1	1	42'246	167'012	418	2'923	16'851	11'519	9'760	53'774	3'246
FAHIN 1	1	38'262	175'709	260	2'430	26'882	13'548	9'758	44'265	2'395
FAZUC 2	2	39'052	153'180	384	2'649	16'914	10'248	8'932	51'666	3'034
FAHIN 2	2	41'488	190'389	279	2'537	29'123	14'640	10'277	48'398	2'545
FAZUC 3	3	43'412	166'683	408	2'902	19'276	11'015	9'343	56'644	3'222
FAHIN 3	3	40'597	183'781	285	2'578	28827	15'185	10'379	46'946	2'586
FAZUC 4	4	40'384	162'895	429	2'964	19'450	11'564	9'800	55'860	3'233
FAHIN 4	4	38'878	182'233	262	2'358	27'179	13'440	9'438	46'165	2'418
FAZUC 5	5	40'191	159'652	405	2'718	17'700	10'536	9'175	53'964	3'104
FAHIN 5	5	37713	178'461	265	2'346	26'433	13'601	9'560	45'339	2'440
FAZUC 6	6	40'060	155'992	406	2'742	15'227	10'473	9'228	52'028	3'137
FAHIN 6	6	37'567	176'353	278	2'483	27'193	14'362	10'114	44'616	2'538
Reference material 1633a	2	143'619	11'928	6	101	92'325	4'053	107	78	224
Reference material 1633a	3	131'044	10'377	bd	91	90'674	4'002	28	90	bd
Reference material 1633a	5	105'896	10'520	bd	92	94'707	3'246	9	98	bd
Reference material 1633a: certified values		143'000	11'100	1	118	94'000	4'550	72	220	7

Method description

1. Equipment

- Teflon digestion vessels
- Analytical balance (precision ± 0.01 mg)
- Pipettes
- MLS Ethos Plus
- Volumetric flasks, plastic, 100 ml
- Wash bottle with Milli-Q-water

2. Chemicals

Table A6-11: *Used chemicals for total digestion.*

Name	Formula	Producer	Nr.	CAS-Nr.
Nitric acid suprapur 65%	HNO_3	Merck	1.00441.1000	7697-37-2
Hydrofluoric acid suprapur 40%	HF	Merck	1.00335.0500	7664-39-3
Boric acid suprapur	H_3BO_3	Merck	1.00765.0500	10043-35-3

3. Reagents

Boric acid solution: 46.5 g boric acid was diluted in 1 litre Milli-Q water at 20°C. 5 ml of this saturated boric acid solution is added per each used millilitre of HF.

4. Procedure

4.1 Sample pre-treatment:

- The solid materials were dried at 105 °C and milled with a tungsten carbide mill.

4.2 Microwave digestions

- 0.2-0.25 g material is weighted into a teflon vessel.
- 8 ml HNO_3 (65%) and 2 ml HF (40%) are added to the samples and the vessels sealed.
- The samples are digested in the microwave oven after MLS application E700 (Figure A6-1).
- Furthermore, 10 ml saturated boric acid is added to the vessel and digested after MLS application E700/2 (Figure A6-2).
- The digests are then transferred to 100 ml volumetric flasks.
- The teflon vessels are cleaned with 4 ml Milli-q water and 6 ml HNO_3 65% after MLS-application E700/2.
- The solution from the cleaning step is added to the volumetric flask and filled up to the mark with Milli-Q water.

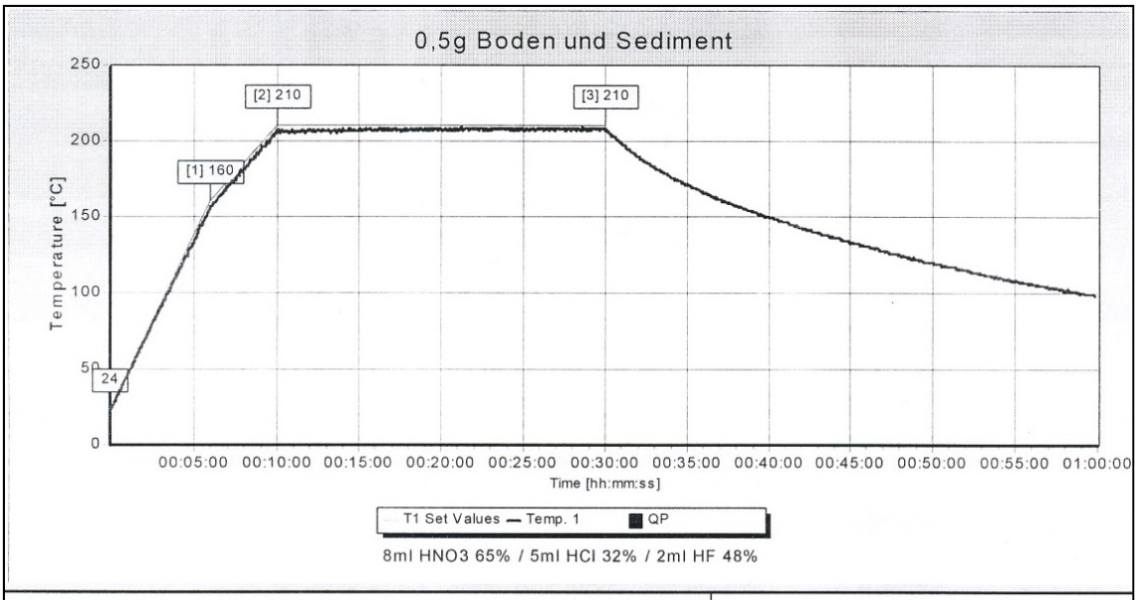

MW-Programm:

Schritt 1:	00:06:00	1000 Watt	T1: 160°C
Schritt 2:	00:04:00	1000 Watt	T1: 210°C
Schritt 3:	00:20:00	700 Watt	T1: 210°C
Vent:	00:25:00		

Einstellungen:

TWIST Control:	an
Rotor Control:	aus
Magnetrührung:	100%

Figure A6-1: *MLS-application E700 for total digestions.*

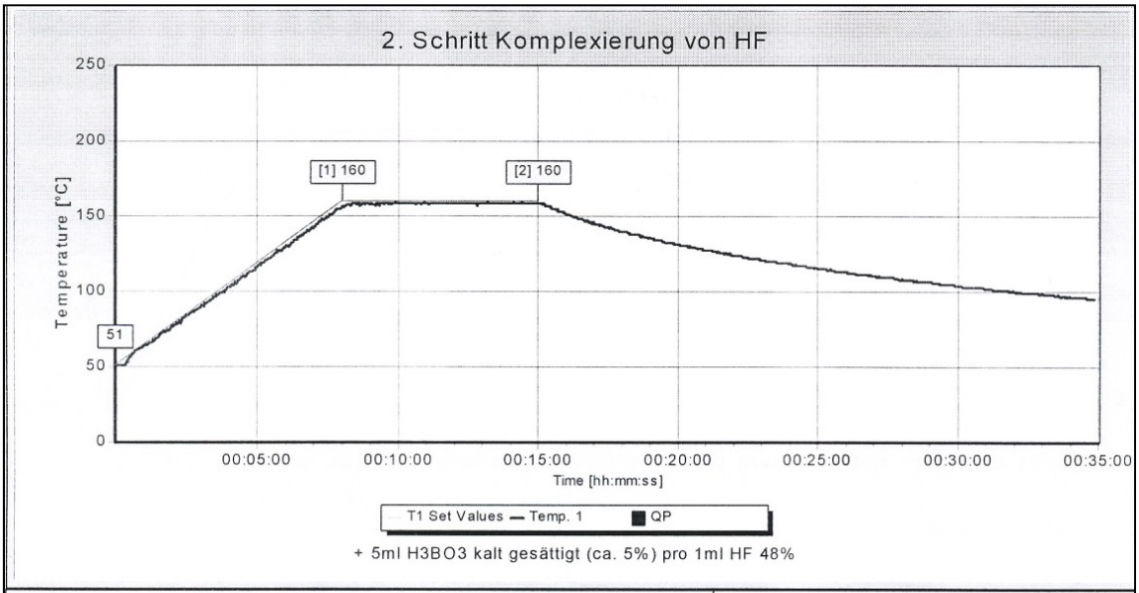

MW-Programm:

Schritt 1:	00:08:00	1000 Watt	T1: 160°C
Schritt 2:	00:07:00	1000 Watt	T1: 160°C
Vent:	00:20:00		

Einstellungen:

TWIST Control:	an
Rotor Control:	aus
Magnetrührung:	100%

Figure A6-2: *MLS-application E700/2 for HF complexation.*

Chapter 7

Extraktionsmethoden und Feststoff-charakterisierung für die Optimierung der Metallabreicherung von Flug-aschen

Gisela Weibel[a], Urs Eggenberger[a], Stefan Schlumberger[b]

[a]*Institut für Geologie, Universität Bern, Schweiz*
[b]*Zentrum für nachhaltige Abfall- und Ressourcennutzung (ZAR), Zuchwil, Schweiz*

Im Auftrag des Amts für Abfall, Wasser, Energie und Luft des Kantons Zürich (AWEL), 04. April 2016 (zweite Version[1)])

7.1 Zusammenfassung

Die Rückgewinnung von Schwermetallen aus Flugaschen der thermischen Abfallverwertung ist ein konkretes Ziel der aktuellen Abfallpolitik. Für die erfolgreiche Optimierung ist es von zentraler Bedeutung, die chemischen Prozesse während der sauren Flugascheextraktion (FLUWA-Verfahren) zu verstehen und die Bindungsverhältnisse der enthaltenen Metalle zu kennen. Um das komplexe Phasensystem von Flugaschen zu beschreiben und die grosse Vielfalt der metallhaltigen Phasen selektiv zu reduzieren, wurden spezifische Extraktions- und mechanische Separationsversuche mit zwei unterschiedlichen Flugaschen durchgeführt. Dabei wurde die stark schwermetallhaltige Flugasche der KVA Emmenspitz Zuchwil (FAZUC) und die stark alkalische und eher schwermetallarme Flugasche der KVA Hagenholz Zürich (FAHAG) verwendet. Es wurden Versuche mit unterschiedlichen Extraktionsmitteln (deionisiertes Wasser, Salzsäure, Schwefelsäure,

[1)] Überarbeitete Version ohne Teil „Laborversuche zur sauren Flugaschenwäsche (FLUWA-Laborversuch) aus Msc I. Budde.

Phosphorsäure, Natronlauge, Ammoniumchlorid und Natriumchlorid), Extraktionszeiten und Temperaturen durchgeführt und die Rückstände chemisch und mineralogisch charakterisiert. Der Fokus wurde dabei auf die relevanten Schwermetalle Zn, Pb, Cu und Cd gelegt und ausgewählte Filterkuchen wurden zusätzlich noch auf wertvolle und seltene Elemente wie Ag, In und Y untersucht. Das Potential einer Anreicherung von Metallen über partikuläre Separation wurde zudem in mehreren Siebversuchen und Magnetseparationen eruiert.

Bei der FAHAG dominiert bei der Extraktion das Karbonatsystem und zeigt dadurch eine deutlich höhere Pufferkapazität verglichen zur FAZUC. Während sich bei der FAZUC mit H_2O ein pH-Wert im neutralen Bereich (pH 6.5) einstellt, erreicht die FAHAG einen pH-Wert >12. Es zeigte sich, dass der Grad der Metallabreicherung vorwiegend pH gesteuert ist und die Art der verwendeten Säure sich kaum auf die Mobilisierung auswirkt. Bei gleicher Säurestärke zeigen Salzsäure (HCl), Schwefelsäure (H_2SO_4) und Phosphorsäure (H_3PO_4) sehr ähnliche Resultate. Um vernünftige Extraktionsausbeuten bei FAHAG zu erreichen, müssen grosse Mengen Säure eingesetzt werden um die Karbonate zu eliminieren und der pH-Wert der Extraktionslösung nachhaltig zu senken. Dies führt zu starker Gasentwicklung (CO_2) und erschwert die Flugascheextraktion erheblich.

Das Vorgehen und die Prozesse bei der HCl-Extraktion im Labor kommen dem FLUWA-Verfahren auf der Anlage sehr nahe. Es zeigte sich, dass ohne den Einsatz von Wasserstoffperoxid 30% (H_2O_2) grosse Mengen von metallhaltigen Zementierungsphasen im gewaschenen Filterkuchen vorliegen ($PbCu^0$-Legierung um Al^0-Partikel). Weiter wurde im Filterkuchen Bleichlorid ($PbCl_2$) identifiziert wobei die Menge sich mit zunehmender Extraktionszeit stark erhöhte. Die Zeit abhängigen Versuche mit HCl zeigen weiter, dass ab einer Extraktionsdauer von 3 h die Zementierungsphasen ($PbCu^0$) bei der FAZUC rückgelöst werden. Das Nachwaschen des Filterkuchens mit saurem Waschwasser (pH 1 und 2) nach der Extraktion mit HCl 5% zeigte keine zusätzliche Lösung von Metallen verglichen zum neutralen Nachwaschen. Dies kann durchaus positiv gewertet werden, da eine spätere Metallmobilisierung auf der Deponie nicht zu erwarten ist. Die starke Gipsbildung bei der Extraktion mit H_2SO_4 scheint nur untergeordnet einen Einfluss auf die Mobilisierbarkeit der Metalle zu haben, da bei gleicher Säurestärke sehr ähnliche Extraktionsausbeuten erreicht werden wie mit HCl.

Die Versuche mit H_2SO_4 lösen Pb welches anschliessend mit dem Sulfat zu Bleisulfat ($PbSO_4$) reagiert und sich im Filterkuchen anreichert. Durch die Bildung von $PbSO_4$ wird die Zementierung von Pb mit Cu zu $PbCu^0$ verhindert. Für einen grosstechnischen Einsatz von Schwefelsäure bei einer zentralen Aufbereitung der Flugaschen spricht der tiefere Preis (zweiprotonige Säure, 98 prozentig) und die geringeren Abwasserfrachten im Vergleich zur Salzsäure. Hingegen sind die Deponiekosten des Filterkuchens durch die starke Gipsbildung höher und eine Gipsverwertung wäre kaum möglich.

Die Nachbehandlung der Filterkuchens aus den HCl- und H_2SO_4-Versuchen mit NaCl-Lösung (300 g/L) führt bei FAZUC zur Mobilisierung grosser Mengen Pb und Cu,

wie sie sonst nur durch den Einsatz von H_2O_2 erreicht werden können. Durch die Interaktion des Filterkuchens mit hoch-saliner Lösung bei einer Temperatur von 85°C kann das vorhandene Pb ($PbCl_2$ und $PbSO_4$) als $PbCl_3^-$ und $PbCl_4^{2-}$ mobilisiert werden.

Die näher betrachteten seltenen und wertvollen Elemente (Ag, Bi, Ga, Ge, In, Rb, Se, Te, Y, Zr) liegen in relativ geringen Konzentrationen in den Flugaschen vor (<100 mg/kg). Die diversen Extraktionsversuche bewirkten generell nur sehr geringe Abreicherungen, welche teilweise innerhalb der Messunsicherheit liegen.

Physikalische Separationsversuche wurden mittels Frantz-Magnetseparator und mittels Siebturm durchgeführt. Für die Magnetseparationsversuche wurde die Flugasche in Wasser dispergiert und mit einer Quetschpumpe über mehrere Stunden durch das Magnetfeld geleitet. Die Analysen der Rückstände aus der Magnetseparation zeigen primär eine starke Anreicherung an Fe. Seltene und wertvolle Elemente scheinen sich hingegen nicht signifikant angereichert zu haben. Der grosse apparative und zeitliche Aufwand für die Magnetseparation mittels Frantz-Separator scheint sich nicht auszubezahlen, da die Resultate sehr ähnlich ausfallen wie bei der Verwendung von starken Permanentmagneten, welche in die Aschesuspension gehalten wurden.

Siebversuche mit 5 unterschiedlichen Sieben (63, 125, 250, 500 und 1'000 μm) zeigen, dass die Flugaschen bei niedriger Amplitude bis zu 5 Stunden gesiebt werden müssen, bis sich ein Massengleichgewicht bei den verwendeten Fraktionen einstellt. Die Siebfraktionen zeigen erhöhte Metallkonzentrationen in den Fraktionen >1'000 μm. Diese Fraktion stellt aber nur <1% der gesamten Masse dar, mehr als 70% verteilen sich auf die Korngrössen 125-500 μm. Es zeigt sich somit, dass mit der Siebung der Asche keine signifikante Anreicherung erreicht werden kann.

Die gewonnenen Erkenntnisse bilden eine gute Grundlage für theoretische Betrachtungen (geochemische Modellierung) und zeigen dass die weiteren Untersuchungen auf den Prozess der Zementierung und die Nachbehandlung der Filterkuchen mittels NaCl-Lösung konzentriert werden sollten, um die anstehenden Werkversuche möglichst vielversprechend zu planen

7.2 Projektbeschreibung und Zielsetzung

Bei der thermischen Abfallverwertung reichern sich unter den Verbrennungsbedingungen flüchtige Schwermetalle bzw. Schwermetallverbindungen in den Flugaschen an. Der nachhaltigen Aufbereitung dieser Verbrennungsrückstände muss deshalb aus ökologischen und ökonomischen Überlegungen ein hoher Stellenwert beigemessen werden. Mit der sauren Flugaschenwäsche (FLUWA-Verfahren, Vehlow et al., 1990; Schlumberger et al., 2007) steht ein Verfahren zur gezielten Schwermetallabtrennung und Rückgewinnung zur Verfügung. Mit dem FLUWA-Verfahren werden derzeit mehr als die Hälfte der Flugaschen in der Schweiz aufbereitet und daher wird dieses Verfahren zum Stand der Technik gezählt. Mit der neuen Abfallverordnung (VVEA; Bundesamt für Umwelt, 2016)

wird zudem gefordert, dass nach einer 5-jährigen Übergangsfrist alle in der Schweiz anfallenden Flugaschen behandelt und die Metalle rückgewonnen werden müssen.

Die Ziele der FLUWA sind auf der einen Seite, die Schwermetallkonzentration der Flugasche zu reduzieren, um eine möglichst ökologisch unbedenkliche Deponierung der entstandenen Rückstände zu ermöglichen und auf der anderen Seite, die abgetrennten Schwermetalle als Wertstoffe zurückzugewinnen. Als Ausbeute wird der prozentuale Anteil der extrahierten Schwermetalle in Bezug auf den initialen Totalgehalt bezeichnet. Die technisch mögliche Ausbeute ist abhängig vom Element, dem verwendeten Eluenten und der chemische Bindungsform. Für die Interpretation der Extraktionsausbeuten kommt deshalb der chemischen Bindungsform eine entscheidende Bedeutung zu. Im Jahr 2013 wurden im Auftrag des Amts für Abfall, Wasser, Energie und Luft des Kantons Zürich (AWEL) diverse Untersuchungen zur Mineralogie, Chemie und dem Eluatverhalten von unbehandelten und behandelten Flugaschen der KVA Emmenspitz Zuchwil und KEZO Hinwil am Institut für Geologie der Universität Bern (IfG) und an der EAWAG Dübendorf durchgeführt. Im Zentrum der Untersuchungen am IfG stand die Fragestellung in welcher Form die Schwermetalle Zn, Pb, Cu und Sb vorwiegend gebunden sind und wie sich die Elementverteilungen und Mineralphasen vor und nach der Aschenwäsche ändern. Aufbauend auf den Resultaten dieser ersten internen Studie wurden nun diverse Fragestellungen vertieft betrachtet.

In einem ersten Teilprojekt welches vom Bundesamt für Umwelt (BAFU) in Auftrag gegeben wurde, wurden Flugaschen (FA) und gewaschene Filterkuchen (FK) aus sechs ausgewählten Schweizer Kehrichtverbrennungsanlagen detailliert mineralogisch und chemisch charakterisiert (Kapitel 6). Um das komplexe Phasensystem der Flugaschen besser zu verstehen und die grosse Vielfalt der metallhaltigen Phasen selektiv zu reduzieren, werden im hier beschriebenen zweiten Teilprojekt spezifische Extraktions- und mechanische Separationsversuche durchgeführt. Um ein möglichst breites Spektrum von Aschezusammensetzungen abzudecken wurden zwei Aschen detailliert betrachtet: die stark schwermetallhaltige Flugasche der KVA Emmenspitz Zuchwil (FAZUC) und die stark alkalische und eher Schwermetall-arme Flugasche von Hagenholz (FAHAG). Der Fokus wurde dabei auf die relevanten Schwermetalle Zn, Pb, Cu und Cd gelegt und ausgewählte Filterkuchen wurden zusätzlich noch auf wertvolle und seltene Elemente wie Ag, In und Y untersucht. Es wurden kombinierte Versuche mit unterschiedlichen Extraktionsmitteln und Feststoffanalysen durchgeführt, um weitere Informationen über das Phasensystem und die Bindungsverhältnisse der interessierten Metalle zu erhalten. Neben den nasschemischen Extraktionsversuchen wurden ergänzend physikalische Separationsversuche (Siebversuche, Magnetseparation) durchgeführt um zu sehen ob eine Anreicherung von Metallen über partikuläre Separation möglich ist.

7.3 Materialien und Methoden

7.3.1 Probenmaterial

Für die Extraktions- und Separationsversuche wurde Flugasche der KVA Hagenholz (FAHAG) sowie ein Mix (1:1) der Flugaschen der KVA Emmenspitz Zuchwil und KEZO Hinwil (FAZUC) verwendet (Tabelle 7-1). Die Aschen von Zuchwil und Hinwil werden gemeinsam in Zuchwil mittels FLUWA-Verfahren behandelt und weisen durch den erhöhten industriellen Abfallinput höhere Schwermetallkonzentrationen auf, verglichen zur städtischen Anlage Hagenholz.

***Tabelle 7-1**: Verwendete Flugaschen.*

Name	Beschreibung	KVA	Probenahme
FAHAG	Flugasche	Hagenholz Zürich	21.11. - 12.12.2013
FAZUC	Flugasche Mix aus KEBAG und KEZO 1:1	Emmenspitz Zuchwil/ KEZO Hinwil	29.11. - 18.12.2013

7.3.2 Versuchsmatrix

***Tabelle 7-2:** Extraktionsversuche zur Aufklärung der Bindungsverhältnisse.*

Extraktions-mittel	Konz.	Flüssig-Fest-Verh. (FF)	Zeit	T (°C)	Vor-/Nachbehandlung des FK	Anzahl Versuche
Deionisiertes H_2O	-	2/10/ 20/400	10/30 min/ 1 h/3 h/6 h	RT/40/ 60/80	gemahlen/ungemahlen	13
Salzsäure (tech)	5%/10%	4	10/30 min/ 1 h/3 h/6 h	RT/40/ 60/80	gemahlen/ungemahlen Vorwaschen mit H_2O Nachwaschen mit anges. H_2O (pH <3.5)	13
Schwefelsäure (p.a)	6.6%/ 13.9%	4	1h	RT/40/ 80	Vorwaschen mit HCl 5%	5
Phosphorsäure (tech)	15%	4	1h	80	Vorwaschen mit HCl 5%	1
Natronlauge	10%/ 20%	15	1h	RT/80	Vorwaschen mit H_2O Nachwaschen mit anges. H_2O (pH <3.5)	4
Ammoniumchlorid	15 g/L	4	1h	80	-	1
Natriumchlorid	300 g/L	5	1h	85	Vorwaschen mit HCl oder H_2SO_4	2

***Tabelle 7-3:** Mechanische Separationsversuche.*

Methode	Details
Siebversuche	Siebgrössen: 63, 125, 250, 500, 1'000 µm Siebdauer: 5 h Amplitude: 20%
Korngrössenverteilung	Mastersizer 2000
Magnetseparation	Abtrennung in Lösung mittels Frantz LB-1 Magnetseparator

7.3.3 Durchführung der Extraktionsversuche

Jeweils 50 g FAZUC und FAHAG wurden bei den HCl-, H_2SO_4-, H_3PO_4- und NH_4Cl-Versuchen eingesetzt. Dabei wurde 200 mL Extraktionslösung in einem 400 mL Becherglas vorgelegt und die Asche anschliessend vorsichtig zugegeben. Für die H_2O- und NaOH-Versuche wurde ein kleinerer Ansatz mit je 20 g Asche gewählt und für die NaCl-Versuche 10 g Asche. Bei allen Versuchen wurden Strömungsbrecher eingebracht und mit einem Stativrührer stark gerührt. Zudem wurden während dem gesamten Extraktionsprozess der pH-Wert und die Temperatur erfasst. Nach dem Ablauf der Extraktionszeit wurde das Gemisch heiss abfiltriert und mit deionisiertem Wasser, aufgeteilt in vier Portionen, nachgewaschen (Menge für jeweilige Versuch siehe Extraktionsprotokolle im Anhang 7A). Das Filtrat (FL) wurde anschliessend mit dem Waschwasser vermengt und sofort mit 1% HNO_3 verdünnt (Verhinderung nachträglicher Ausfällungen). Der Filterkuchen wurde samt Filter in eine Kristallisierschale gegeben und bei 50°C bis zur Gewichtskonstanz getrocknet. Für die XRF und XRD Analysen wurde eine Teilprobe des Filterkuchens mit einer Scheibenschwingmühle gemahlen. Alle Details der Extraktionen inklusive aufgetretene sofortige Ausfällungen oder Probleme beim Abfiltrieren können den diversen Extraktionsprotokollen im Anhang 7A entnommen werden.

7.3.4 Korngrössenverteilung

Die Korngrössenverteilung der ungemahlenen und gemahlenen Ausgangsaschen wurde mittels Mastersizer 2000 analysiert. Die Lösung um die Asche in Schwebe zu halten wurde wie folgt hergestellt: 250 mL Wasser, 1.75 g Natriumcarbonat, 8.25 g Natriummetahexaphosphat. Als Ansatz wurde 2 g Asche zu 30 mL verdünnter Schwebe-Lösung (10 mL Lösung + 20 mL Wasser) gegeben und über Nacht überkopfgeschüttelt.

7.3.5 Magnetseparation

Die Flugasche wird in einem Flüssig-Fest-Verhältnis (FF) von 10 mit deionisierten Wasser angerührt. Die Suspension wird mit einem Stativrührer bei etwa 300 rpm durchmischt. Die Lösung wird über eine Ismatec Quetschpumpe zum Glaseinsatz des Frantz LB-1 Magnetseparators transportiert. Magnetseparationparameter: Vibrationsstärke 5-6, Stromstärke D-C Ampere 4-5, Neigung 35°, Gefälle 10°. Der untere Magnet verläuft von der Mitte gegen oben ans Ende des Glaseinsatzes. Die magnetische sowie nicht magnetische Fraktion wird in zwei mit deionisiertem Wasser gefüllten Behältern aufgefangen. Das Niveau des Wassers entspricht dabei der Höhe des Einlasses des Glaseinsatzes.

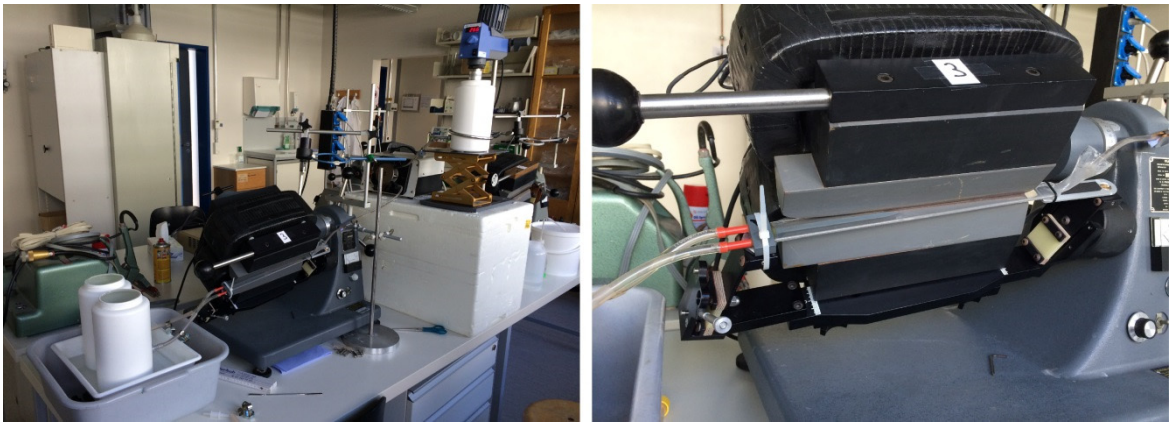

Abbildung 7-1: *Frantz LB-1 Magnetseparator mit Stativrüher und Quetschpumpe zur Förderung der Aschesuspension.*

7.3.6 Siebversuche

Eine Menge von 150 g der FAZUC und FAHAG wurden während 5 h bei einer tiefen Amplitude von 20% gesiebt und stündlich ausgewogen. Folgende Siebe wurden dafür verwendet: 63, 125, 250, 500, 1'000 µm.

7.4 Analytik

7.4.1 ICP-OES

Die ICP-OES Analysen wurden mittels Varian 720-ES an den verdünnten Filtraten durchgeführt. Dabei wurde die Analyse auf die Elemente Na, Ca, K, Zn, Mg, S, Al, Si, Fe, Pb, Sb, Mn, Cd, Ti, Cr und Cu beschränkt. Um allfällige Matrixeffekte während der Messung zu erkennen, wurden vorgängig Standardlösungen in den diversen Extraktionsmittel sowie gespikte Probelösungen gemessen. Für die sauren Extrakte mit HCl, H_2SO_4 und H_3PO_4, NH_4Cl sowie NaCl konnten keine Matrixeffekte eruiert werden. Hingegen musste für die Analysen der basischen NaOH-Extrakte die gesamte Kalibrierung auf die vorhandene Matrix angepasst werden. Zudem wurden die basischen Lösungen mittels konz. HNO_3 auf pH 2 eingestellt. Die Kalibrierung wurde mittels Sigma Multielement-Standard 6 durchgeführt und die Analysen mittels Checkstandards überprüft (Merck IV und Merck X Multielementstandards).

7.4.2 IC

In den wässrigen Filtraten wurden zusätzlich die Parameter NH_4, Sr, F, Cl, Br, NO_3 und SO_4 mittels eines Metrohm 850 Professional Ionenchromatographen bestimmt.

7.4.3 ED-XRF

Wie bei den ICP-OES Analysen wurde die Feststoffanalytik auf eine gewisse Auswahl an relevanten Elementen beschränkt. Dabei wurden die Elemente Ca, K, Zn, S, Al, Si, Fe, Pb, Sb, Mn, Ti, Cu mittels Röntgenfluoreszenzanalyse auf einen Spectron, Xepos ED-XRF beim Zentrum für nachhaltige Abfall- und Ressourcennutzung (ZAR) in Zuchwil bestimmt. Dazu wurden 4.00 g der gemahlenen Ausgangsasche/Filterkuchen mit 0.90 g Bindemittel (Hoechst Wachs) vermengt und zu einer Pulverpille gepresst. Die Elemente Al, Na und Mg sind mittels XRF nicht quantifizierbar und die Konzentrationen dieser Elemente in den Ausgangsaschen wurden deshalb zusätzlich mittels Totalaufschlüssen und anschliessender ICP-OES-Messung bestimmt. Natrium und Magnesium sind schwer zu quantifizieren mittels XRF aufgrund ihrer leichten molaren Massen und beim Aluminium sind die vielen metallischen Anteile Grund für die auftretenden Probleme (Matrixeffekt).

7.4.4 XRD

Die kristallinen Phasen der getrockneten und gemahlenen Ausgangsaschen und Filterkuchen wurden mittels Röntgendiffraktion (XRD) bestimmt. Dabei wurde 20 gew.% Griceite (LiF) als interner Standard beigemischt und die Proben hochauflösend von 4-60° 2Thetha auf einem XPertPro MPD von Panalytical gemessen. Die relativen Anteile der kristallinen Phase (inkl. LiF) wurden mittels Rietfeldverfeinerung bestimmt, die absoluten Gehalte der Mineralphasen und die amorphen Anteile wurden über den „Sollwert" des internen Standards berechnet. Diese Technik dient v.a. der Bestimmung der dominierenden Phasenunterschiede vor und nach den Extraktionen.

7.4.5 REM

Eine Auswahl getrockneter Filterkuchen wurden mit Epoxidharz imprägniert, angeschliffen, poliert (ohne Wasser) und mittels Kohlenstoff bedampft. Ein Zeiss EVO-50 XVP Rasterelektronenmikroskop (REM) gekoppelt mit einem energiedispersiven System (EDS) wurde für die Spotanalysen der Aschepartikel eingesetzt. Die imprägnierten Präparate wurden ausschliesslich mittels BSE-Detektor (Materialkontrast) analysiert. Streupräparate der magnetischen Fracht wurden zudem mittels SE-Detektor (Sekundarelektronen, Topografie) untersucht.

7.5 Extraktionsversuche

Die Festphasencharakterisierung von sechs Flugaschen hat gezeigt, welche enorme Vielfalt an metallhaltigen Phasen vorliegen kann und wie komplex das Phasensystem ist (Kapitel 3 und 6). Um das Verständnis dieses Phasensystems zu vertiefen und entscheidend in der Aufklärung der Bindungsverhältnisse voranzukommen, wurden unterschiedliche An- und Abreicherungsversuche mit den Flugaschen FAZUC und FAHAG durchgeführt. Laborversuche bringen den Vorteil, dass in einem definierten und überwachten System die Lösungs- und Neubildungsprozesse gut beschrieben und mit einer Massenbilanz überprüft werden können. Es wurden Versuche mit unterschiedlichen Extraktionsmitteln, Konzentrationen, Flüssig-Fest-Verhältnissen, Extraktionszeiten sowie Temperaturen durchgeführt und das metallhaltige Filtrat anschliessend mittels ICP-OES und teilweise Ionenchromatographie analysiert (Tabelle 7-2). Anhand der Resultate der Filtrat-Analysen wurde entschieden, bei welchen Versuchsansätzen eine detaillierte Festphasencharakterisierung (XRF, XRD, REM) der Filterkuchen durchgeführt wird. Folgende Extraktionsmittel wurden eingesetzt: Deionisiertes Wasser, Salzsäure, Schwefelsäure, Phosphorsäure, Natronlauge, Ammoniumchlorid und Natriumchlorid. Die detaillierten Versuchsansätze geordnet nach Extraktionsmittel und die erhaltenen Resultate sind in den folgenden Kapiteln ausführlich beschrieben. Um die Bezeichnung der Versuche etwas zu erleichtern, wurde ein einheitliches Benennungssystem eingeführt:

Aschetyp/Extraktionsmittel mit Konzentration (%)/FF-Verhältnis/Zeit (min)/Temperatur (°C)
z.B. ZUC HCl 5/4/60/80

7.5.1 H_2O-Extraktion

Die Extraktion mit deionisiertem Wasser dient primär der Auswaschung grosser Teile löslicher Salze und der damit verbundenen Anreicherung von weniger löslichen Phasen. Weiter dienen H_2O-Extraktionen zur besseren Beschreibung der Phasensysteme, wobei die ablaufenden chemischen Reaktionen sowie das Löslichkeitsverhalten und die Temperaturabhängigkeiten der Phasen und Metalle mittels des Modellierprogramms Phreeqc (Parkhurst and Appelo, 2013) aufgezeigt werden können. Es ist zudem interessant zu sehen, wie gross der prozentuale Anteil an wasserlöslichen, metallhaltigen Phasen in den beiden Flugaschen ist.

Versuchsansätze

Die in Tabelle 7-4 aufgelisteten Versuchsansätze mit deionisiertem Wasser wurden für die FAZUC und FAHAG durchgeführt. Je 20 g Asche wurde pro Versuch eingesetzt. Nach dem Abfiltrieren der Aschesuspension wurde der Filterkuchen noch mit 10 mL deionisiertem Wasser nachgewaschen. Um aufzuzeigen wie viel Substanz sich noch durch das Nachwaschen mobilisieren lässt, wurde bei Versuch 13 der Filterkuchen mit insgesamt 600 mL Wasser nachgewaschen. Die detaillierten Versuchsprotokolle sind im Anhang 7A angefügt.

Tabelle 7-4: *Versuchsansätze der H_2O-Extraktionen. Jeweils 20 g Flugasche wurde eingesetzt.*

Nr.	Bezeichnung	FF	Zeit	Temperatur	Vorbehandlung	Nachwaschen FK
Flüssig-Fest Variation						
1	H_2O/2/10/RT	**2**	10 min	RT (20°C)	-	10 mL H_2O
2	H_2O/10/10/RT	**10**	10 min	RT	-	10 mL H_2O
3	H_2O/20/10/RT	**20**	10 min	RT	-	10 mL H_2O
4	H_2O/400/10/RT	**400**	10 min	RT	-	10 mL H_2O
Oberflächeneinfluss						
5	H_2O/ 10/10/RT g	10	10 min	RT	**gemahlen**	10 mL H_2O
Zeitabhängigkeit						
6	H_2O/10/30/RT	10	**30 min**	RT	**-**	10 mL H_2O
7	H_2O/10/60/RT	10	**60 min**	RT	**-**	10 mL H_2O
8	H_2O/10/3 h/RT	10	**3 h**	RT	**-**	10 mL H_2O
9	H_2O/10/8.5 h/RT	10	**6 h**	RT	**-**	10 mL H_2O
Temperaturabhängigkeit						
10	H_2O/10/10/40	10	10 min	**40°C**	-	10 mL H_2O
11	H_2O/10/10/60	10	10 min	**60°C**	-	10 mL H_2O
12	H_2O/10/10/80	10	10 min	**80°C**	-	10 mL H_2O
Nachwaschen der Probe						
13	H_2O/ 10/10/RT nw	10	10 min	RT	-	600 mL H_2O

Massenverlust und Massenbilanz

Durch den Extraktionsprozess wurden viele lösliche Komponenten aus der Asche entfernt und im Filtrat angereichert. Die analysierten Filtrate entsprechen der Extraktionslösung plus Waschwasser (Anhang 7B). Anhand der ICP-OES Analysen der Filtrate wurde eine Auswahl für die Festphasencharakterisierung getroffen. Die ausgewählten Filterkuchen wurden mittels ED-XRF (Anhang 7B), XRD und REM-EDS charakterisiert.

Durch das Extrahieren leicht löslicher Komponenten sind die gemessenen Gehalte im Feststoff mittels XRF relativ angereichert. Der Faktor dieser Anreicherung lässt sich mit zwei verschiedenen Varianten berechnen. (1) Über das Gewicht (Gewicht FA/FK) oder (2) über inerte Elemente wie Ba, Cr, Sb, Sn oder Ti (Konz. FK/FA). Diese Elemente lassen sich mit den vorhandenen Extraktionsbedingungen nicht abreichern und sind deshalb relativ angereichert im Filterkuchen. Die Aufkonzentrierung der einzelnen Proben und somit der Massenverlust ergibt für Variante 1 und 2 sehr ähnliche Werte (Tabelle 7-5). Die detaillierten Gewichte vor und nach den Extraktionen für alle Experimente den Extraktionsprotokollen entnommen werden (Anhang 7A).

Tabelle 7-5: *Faktor der Aufkonzentrierung der gewaschenen Filterkuchen gerechnet über das Gewicht und inerte Elemente.*

Nr.	Bezeichnung	Ba	Cr	Sb	Sn	Ti	(2) x	(1) Gew. FK
		mg/kg	mg/kg	mg/kg	mg/kg	mg/kg		g
Konzentration im FK								
2	ZUC H_2O/10/10/RT	2'610	681	3'339	2'284	11'620	-	14.69
4	ZUC H_2O/400/10/RT	2'638	781	3'597	2'558	13'120	-	12.22
9	ZUC H_2O/10/8.5 h/RT	2'342	589	2'914	2'059	10'610	-	15.91
12	ZUC H_2O/10/10/80	2'328	596	2'990	2'050	10'640	-	16.02
2	HAG H_2O/10/10/RT	2'007	1'104	2'686	986	14'560	-	15.91
4	HAG H_2O/400/10/RT	1'930	1'247	2'961	1'112	15'960	-	13.88
Faktor der Aufkonzentrierung im FK								
2	ZUC H_2O/10/10/RT	1.4	1.5	1.1	1.4	1.2	**1.3**	**1.4**
4	ZUC H_2O/400/10/RT	1.4	1.7	1.2	1.5	1.4	**1.4**	**1.6**
9	ZUC H_2O/10/8.5 h/RT	1.2	1.3	1.0	1.2	1.1	**1.2**	**1.3**
12	ZUC H_2O/10/10/80	1.2	1.3	1.0	1.2	1.1	**1.2**	**1.2**
2	HAG H_2O/10/10/RT	1.1	2.4	0.9	0.6	1.6	**1.3**	**1.3**
4	HAG H_2O/400/10/RT	1.0	2.7	1.0	0.7	1.7	**1.4**	**1.4**

Abhängig von der Extraktionstemperatur wurde unterschiedlich viel Lösung verdampft und die übrigbleibenden Volumina und gemessenen Konzentrationen unterscheiden sich erheblich (Aufkonzentrierung, Anhang 7B). Um die Versuche untereinander zu vergleichen und Aussagen zu den Extraktionsausbeuten der diversen Metalle zu machen, wurde die absolut extrahierte Menge jedes Elements berechnet. Dabei wurde folgender Ansatz gewählt:

Absolut extrahierte Menge eines Elements (mg) in Filtrat oder Filterkuchen dividiert durch absolute Menge (mg) des Elements in der eingesetzten Flugasche.

(A) Berechnung der Extraktionsausbeute über das Filtrat (FL):

$$\text{Ausbeute (\%)} = 100 \cdot \left(\frac{\frac{c_{FL\ (mg/L)} \cdot V_{FL(mL)}}{1000}}{\frac{c_{FA(mg/kg)} \cdot m_{FA\ (g)}}{1000}}\right)$$

(B) Berechnung der Extraktionsausbeute über den Filterkuchen (FK):

$$\text{Ausbeute (\%)} = 100 \cdot \left(1 - \frac{\frac{c_{FK}\left(\frac{mg}{kg}\right) \cdot m_{FK(mL)}}{1000}}{\frac{c_{FA}\left(\frac{mg}{kg}\right) \cdot m_{FA\ (g)}}{1000}}\right)$$

c: gemessene Konzentration im Filtrat (FL) in mg/L und in der Flugasche (FA) in mg/kg.
m: Masse der Flugasche und des Filterkuchens (FK) in g.
V: Volumen des Filtrats in mL.

Die Extraktionsausbeuten der Experimente dieser Studie entsprechen den Ausbeuten gerechnet über das Filtrat, da nicht alle Filterkuchen analysiert wurden.

Flüssig-Fest-Variation (Versuche 1-4)

Folgende Erkenntnisse können aus den H_2O-Versuchen mit unterschiedlichen Flüssig-Fest-Verhältnissen (FF) gewonnen werden (Abbildung 7-2). Der pH Wert der beiden Aschen in Wasser variiert stark. Während sich bei FAZUC ein pH-Wert im neutralen Bereich (pH 6.5) einstellt, erreicht FAHAG pH >12. Die alkalinen Bedingungen führen dazu, dass der Filterkuchen HAG 2-3x mehr Kalzit ($CaCO_3$) enthält verglichen zum Filterkuchen ZUC (FKZUC). Der Filterkuchen ZUC hingegen zeigt eine signifikante Menge an Gips ($CaSO_2 \cdot 2H_2O$) und die doppelte Menge Anhydrit ($CaSO_2$) verglichen zum Filterkuchen HAG (FKHAG).

FAZUC:

- Bereits ab einem FF von 10 ist die maximal mobilisierbare Chloridmenge (90%) erreicht.
- Beim Sulfat hingegen ist eine kontinuierliche Abreicherung mit zunehmendem FF erkennbar, welche bei FF 400 >80% erreicht. Die Mobilisierung ist löslichkeitskontrolliert und bei stark erhöhtem FF wird kein Gips mehr im Filterkuchen nachgewiesen.
- Na, K und Ca zeigen eine konstante Zunahme der Extraktionsausbeute mit zunehmendem FF. Mg bleibt hingegen bei allen Versuchen konstant tief bei 6%. Bei Ca wird deutlich dass die Mobilisierung bis zu einem FF von 20 stark löslichkeitskontrolliert ist (vergleichbare Konzentrationen).
- Cd und Zn sind die zwei einzigen Metalle welche zu gewissen Anteilen wasserlöslich gebunden vorliegen. Dabei ist eine zunehmende Extraktionsausbeute von FF 2 zu FF 20 erkennbar mit einer maximal löslichen Menge von 15% für Zn und 63% für Cd. Auffällig ist die starke Abnahme bei FF 400 zu nahezu 0% in Lösung, allerding bei einem pH-Wert von ~10.
- Pb zeigt noch eine Abreicherung von 3% und alle anderen Metalle sind durch eine Wasserextraktion unter den gewählten Bedingungen nicht mobilisierbar.
- Der Massenverlust während der Extraktion beträgt bei FF 2 17% und nimmt bei einem erhöhten FF von 400 auf 39% zu.

FAHAG:

- Die H_2O-Extraktion der FAHAG ergibt im Wesentlichen ähnliche Resultate wie FAZUC für die Hauptelemente Cl, SO_4, Na, K, Ca und Mg.
- Verglichen zu FAZUC gibt es mit zunehmendem FF keine signifikanten Phasenveränderung bei FAHAG. Dies ist mit dem stabilen pH-Wert zu begründen.
- Bei den Metallen hingegen sind kleinere Abweichungen zu FAZUC erkennbar. Weder Zn noch Cd können mittels Wasserextraktion in der Hagenholzasche abgereichert werden.
- Jedoch kann verglichen zur FAZUC bis zu 20% Pb mittels simpler Wasserextraktion mobilisiert werden. Diese Pb-Abreicherung hängt mit den amphoteren Eigenschaften dieses Elements zusammen. Während Pb im sauren Bereich gelöst als Pb^{2+} vorliegt, kann es bei der vorhandenen basischer Umgebung (pH >12) während der Extraktion der Hagenholzasche als $[PbOH_3]^-$ in Lösung vorkommen (Takeno, 2005; Holleman and Wiberg, 2007). Der Massenverlust während der Extraktion ist verglichen zu FAZUC etwas tiefer mit Werten von 15% bei FF 2 und 31% bei FF 400. FAHAG weist prozentual weniger Phasen auf, die mittels Wasserextraktion mobilisierbar sind.

Generell stellt sich bei FAHAG ein deutlich höherer pH-Wert ein, was die Mobilisierung von Pb und Zn als lösliche Hydroxide und Cd als Karbonat wesentlich steuert. Die Metallmobilisierbarkeit ist pH-abhängig und Metalle die mittels Wasserextraktion in signifikanten Mengen extrahiert werden konnten sind Zn (bis 14%) und Cd (bis 63%) für die FAZUC und Pb (bis 20%) für die FAHAG. Weiter kann gesagt werden, dass ein FF von 10 genügt um die wasserlöslichen Komponenten grösstenteils zu mobilisieren, was sich mit früheren Erkenntnissen deckt (Abbas et al., 2003; Karlfeldt and Steenari, 2007). Einzig das Sulfat zeigt deutlich höhere Extraktionsausbeuten mit zunehmendem FF und die gesamte Gipsmenge ist gelöst.

Tabelle 7-6: *Zusammensetzung der Ausgangsaschen bestimmt mittels ED-XRF.*

Element	**FAZUC** mg/kg	**FAHAG** mg/kg
Al	31'750	47'258
Ca	152'700	242'900
Cd[2)]	443	202
Cl	103'300	91'530
Cr	468	948
Cu	2'512	992
Fe	20'510	14'570
K	46'900	37'100
Mg	13'598	14'775
Na	48'800	42'500
Pb	11'920	3'445
Sb	2'976	2'461
Si	81'260	80'730
SO_4	166'048	132'377
Zn	65'420	21'250

[2)] Im Verlauf der weiteren Untersuchungen wurde festgestellt, dass die verwendeten Konzentrationen für Cd zu hoch sind (ED-XRF, Turboquant). Neue Berechnungen mittels matrixangepasster Kalibrierung (ED-XRF, FA_v14) ergeben tiefere Cd-Werte (FAZUC: 370 mg/kg, FAHAG: 158 mg/kg), welche u.a. in den Publikationen (Kapitel 3 und 4) verwendet wurden.

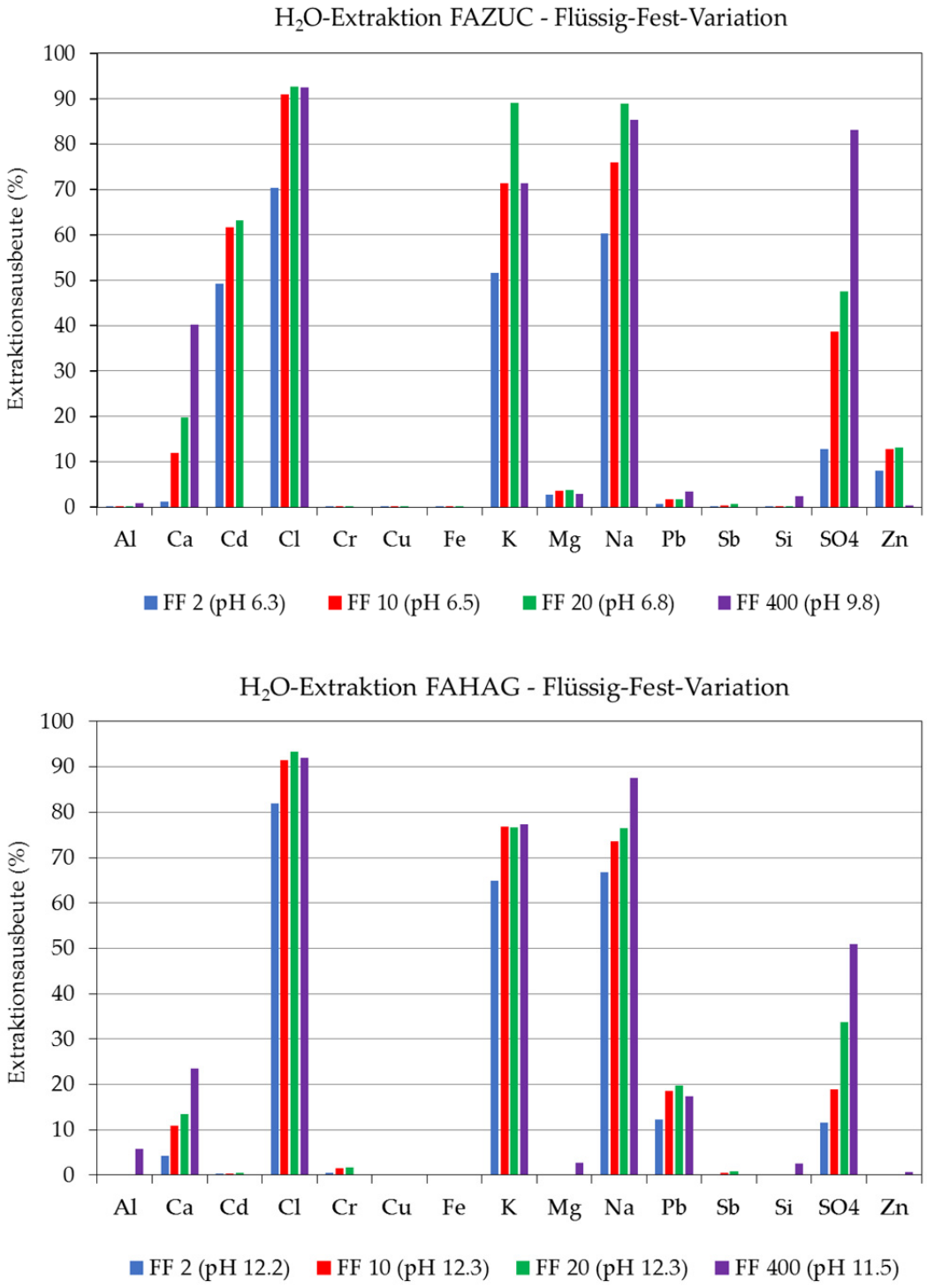

***Abbildung 7-2**: Extraktionsausbeuten (%) unterschiedlicher Flüssig-Fest-Verhältnisse der FAZUC und FAHAG.*

Oberflächeneinfluss (Versuch 5)

Das Mahlen der Flugaschen in einer Scheibenschwingmühle führte zu identischen Extraktionsausbeuten wie beim Einsatz von nicht gemahlener Asche (Abbildung 7-3). Korngrössenverteilanalysen (siehe Kapitel 7.6.3) zeigen, dass es durch das Mahlen der

Probe zu einer deutlichen Verschiebung gegen eine kleinere Korngrösse kommt. BET-Analysen zur Bestimmung der reaktiven Oberfläche zeigen keine signifikanten Unterschiede zwischen den gemahlenen und ungemahlenen Proben (FAZUC: ungemahlen 2.925 m²/g, gemahlen 3.105 m²/g; FAHAG: ungemahlen 3.272 m²/g, gemahlen 3.412 m²/g). Die Korngrösse wird klener aber die dem Wasser zugängliche Oberfläche wird nicht vergrössert (viele poröse Partikel).

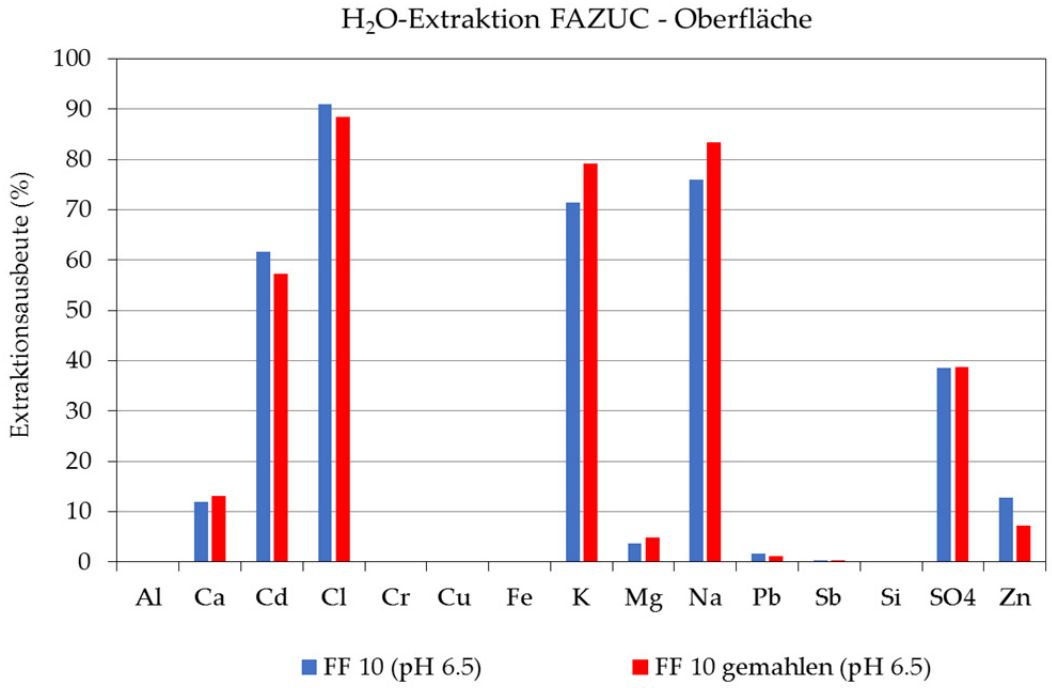

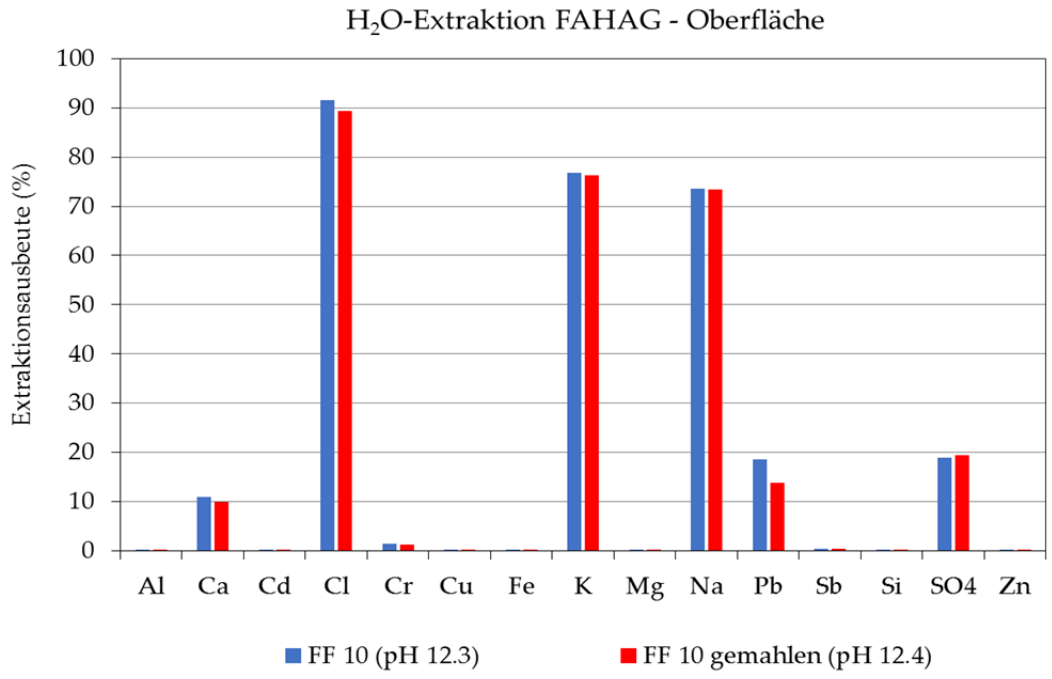

Abbildung 7-3: *Extraktionsausbeuten (%) der gemahlenen/ungemahlenen FAZUC und FAHAG.*

Zeitabhängigkeit (Versuche 6-9)

Die Wahl von unterschiedlichen Extraktionszeiten zwischen 10 Minuten und 8.5 Stunden zeigt im Wesentlichen nur geringe Unterschiede und bestätigt die Erkenntnisse aus den Oberflächenversuchen, dass die Kinetik unter diesen Bedingungen nicht entscheidend ist (Abbildung 7-5). Im Detail sind aber folgende Erkenntnisse zu gewinnen:

FAZUC:

- Stabile Extraktionsausbeuten für Cl und K sowie eine leichte Zunahme des Na in Lösung mit zunehmender Extraktionszeit.
- SO_4, Ca, Zn, Pb und Cd zeigen alle eine abgestufte Ausbeuteverringerung mit zunehmender Extraktionszeit. Eine längere Extraktionszeit führt zu einer sehr starken Gipsausfällung, wodurch der Lösung Ca und SO_4 entzogen werden. Die Abnahme der Metalle steht primär im Zusammenhang mit der pH-Zunahme von 6.5 nach 10 Minuten, zu 10.6 nach 8.5 Stunden. Durch diese pH-Verschiebung verringert sich die Löslichkeit dieser Phasen da sich Metallhydroxide bilden welche sich als Ausfällungen im Filterkuchen anreichern. Ca-Si-Körner welche neu gebildete, fiederartige Zn-Ränder aufweisen sind mittels REM deutlich erkennbar (Abbildung 7-4).

FAHAG:

- Der pH Wert bei der FAHAG zeigt keine Verschiebung über die 6 Stunden Extraktionszeit (pH 12.4). Trotz des konstanten pH-Wertes verringert sich die Ausbeute von SO_4, Ca oder Pb.
- Ca-Sulfate scheinen sich bei längerer Reaktionszeit in geringen Mengen zu bilden, Cd wird zunehmendem pH-Wert fixiert und Pb dürfte bei längerer Aufenthaltszeit und stabilem pH-Wert eher adsorbiert werden.

Die Menge an Filterkuchen beider Aschen nimmt mit zunehmender Extraktionszeit zu (Gipsbildung bei FAHAG): FAZUC +6% und FAHAG +2%.

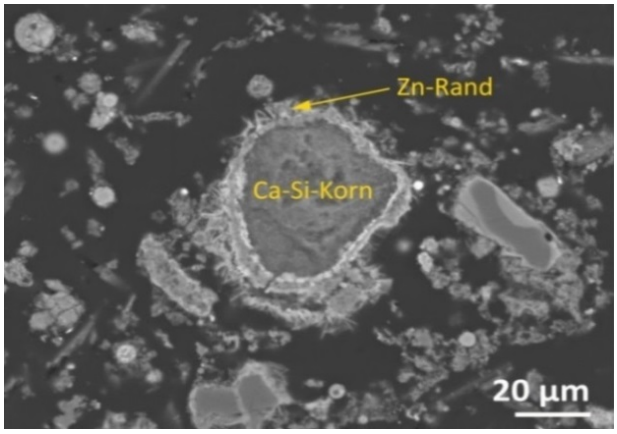

Abbildung 7-4: *Ca-Si-Korn umgeben von neu gebildeten, fiederartige Zn-Ränder in FKZUC nach einer Extraktionsdauer von 8.5 h mit H_2O.*

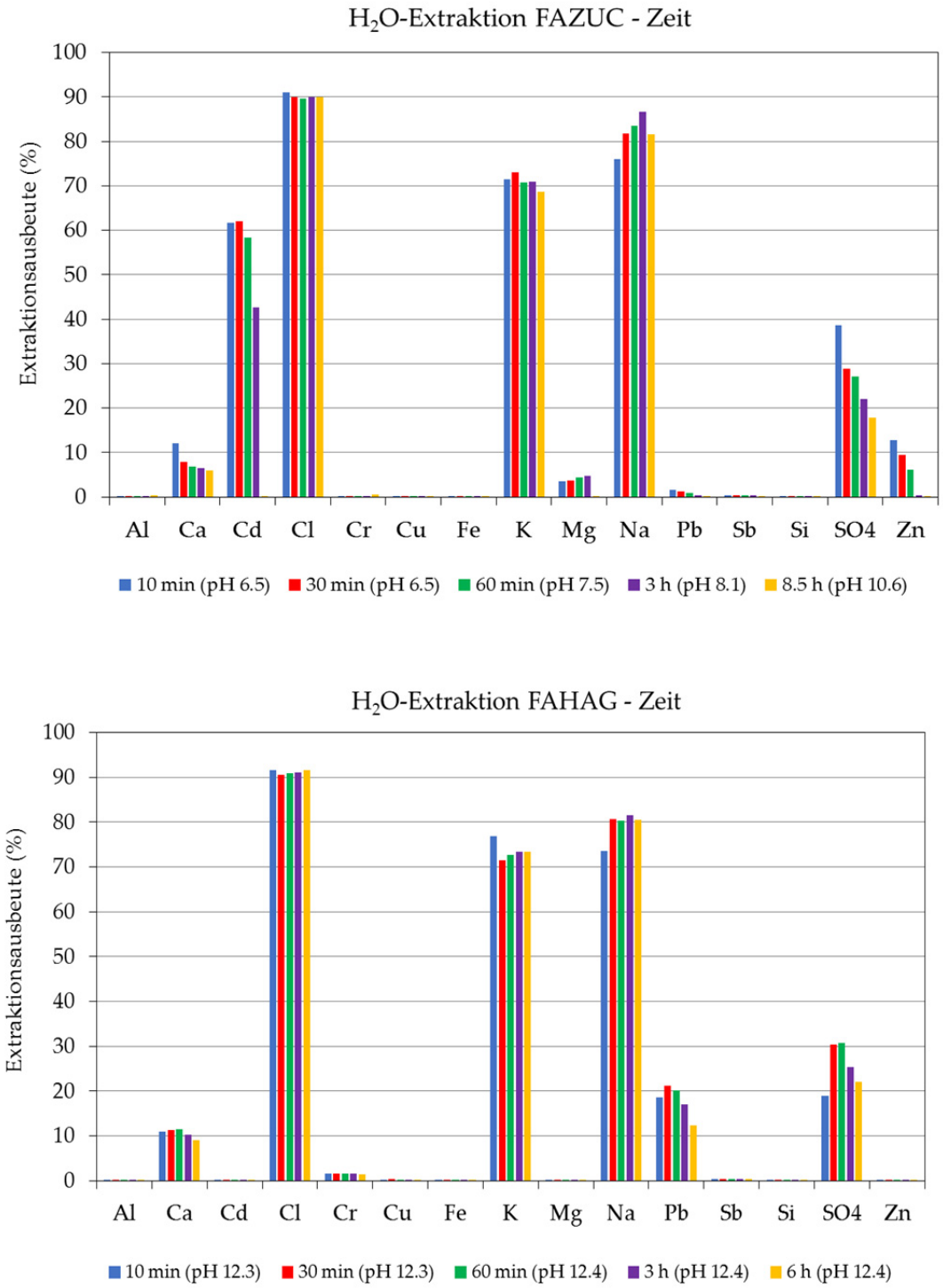

Abbildung 7-5: *Extraktionsausbeuten (%) der zeitabhängigen H2O-Extraktionen der FAZUC und FAHAG.*

Temperaturabhängigkeit (Versuche 10-12)

Temperaturvariationen zeigen für beide Aschen ein ähnliches Lösungsverhalten der Elemente wie diejenigen der zeitabhängigen Versuche (Abbildung 7-7).

FAZUC:

- Mit zunehmender Temperatur verschiebt sich der pH-Wert, vergleichbar wie bei zunehmender Extraktionszeit, auf Werte >10. Da die Löslichkeit diverser Metalle stark pH-abhängig ist, zeigen sich ähnliche Verhalten wie bei den zeitabhängigen Versuchen.
- Beim SO_4 spielt zusätzlich die temperaturabhängige Löslichkeit einer Rolle. Wie Modellrechnungen mit Phreeqc (Parkhurst and Appelo, 2013) zeigen, sinkt mit zunehmender Extraktionstemperatur von Raumtemperatur (RT, 20°C) bis 80°C die Gleichgewichtskonzentration von SO_4 in der Lösung (Abbildung 7-6).

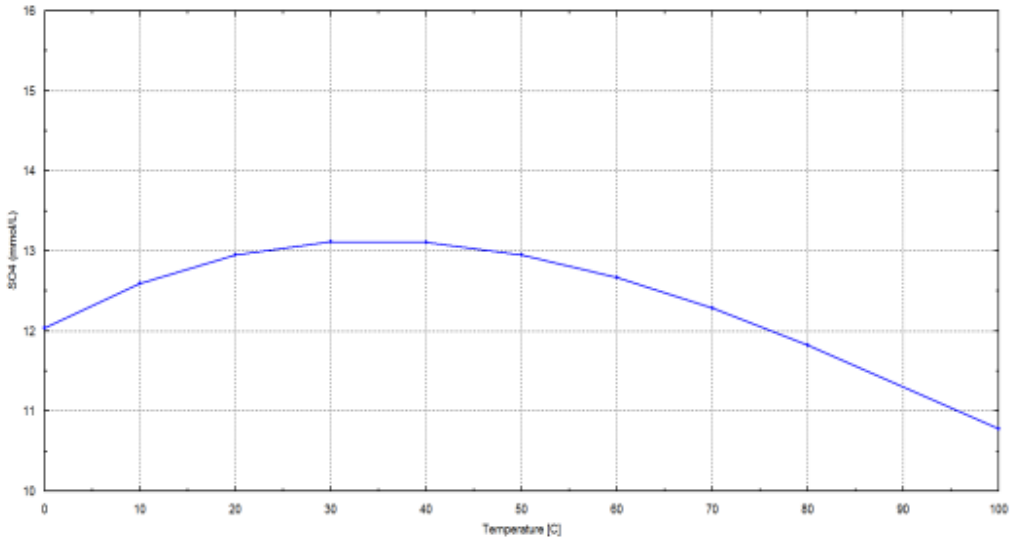

Abbildung 7-6: *Temperaturabhängige Gipslöslichkeit (0-100°C) mit Phreeqc modelliert.*

FAHAG:

- Die Phasen der Flugasche Hagenholz zeigen ebenfalls ein identisches Verhalten sowohl bei zunehmender Temperatur wie auch bei zunehmender Extraktionszeit. Die Ausbeuten von SO_4, Ca und Pb verringern sich mit zunehmender Temperatur.

Mit zunehmender Temperatur nimmt die Masse der Filterkuchen durch Gipsausfällung ebenfalls zu: FAZUC +6%, FAHAG +5%.

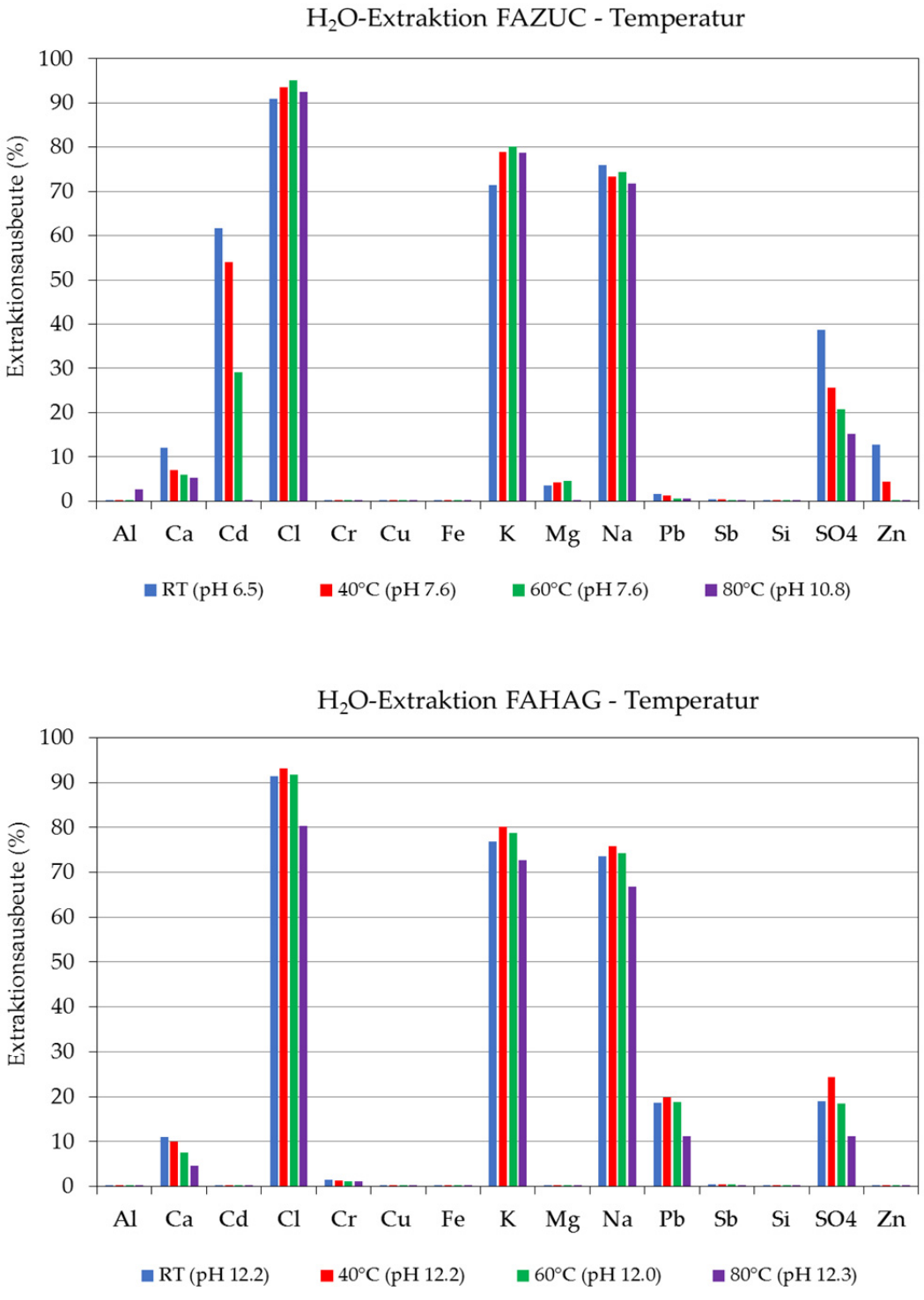

Abbildung 7-7: *Extraktionsausbeuten (%) der temperaturabhängigen H_2O-Extraktionen der FAZUC und FAHAG.*

Nachwaschen des Filterkuchens (Versuch 13)

Die Filterkuchen wurden nach den H_2O-Extraktionen mit einer möglichst geringen Menge Wasser nachgewaschen (10 mL). Um zu testen ob diese Nachwaschmenge genügt, resp. welche Mengen beim weiteren Nachwaschen noch zusätzlich mobilisiert werden können, wurde FKZUC nach einer 10 minütigen Extraktion bei einem FF von 10 und Raumtemperatur mit zusätzlich 4x 50 mL plus am Ende nochmals 400 mL deionisiertem Wasser nachgewaschen (Abbildung 7-8). Die Resultate zeigen, dass bereits nach einem Nachwaschen mit 10 mL beinahe die gesamte mobilisierbare Fracht ausgewaschen wurde. Die nachträglichen Waschschritte bringen nur noch wenige Prozent mit sich.

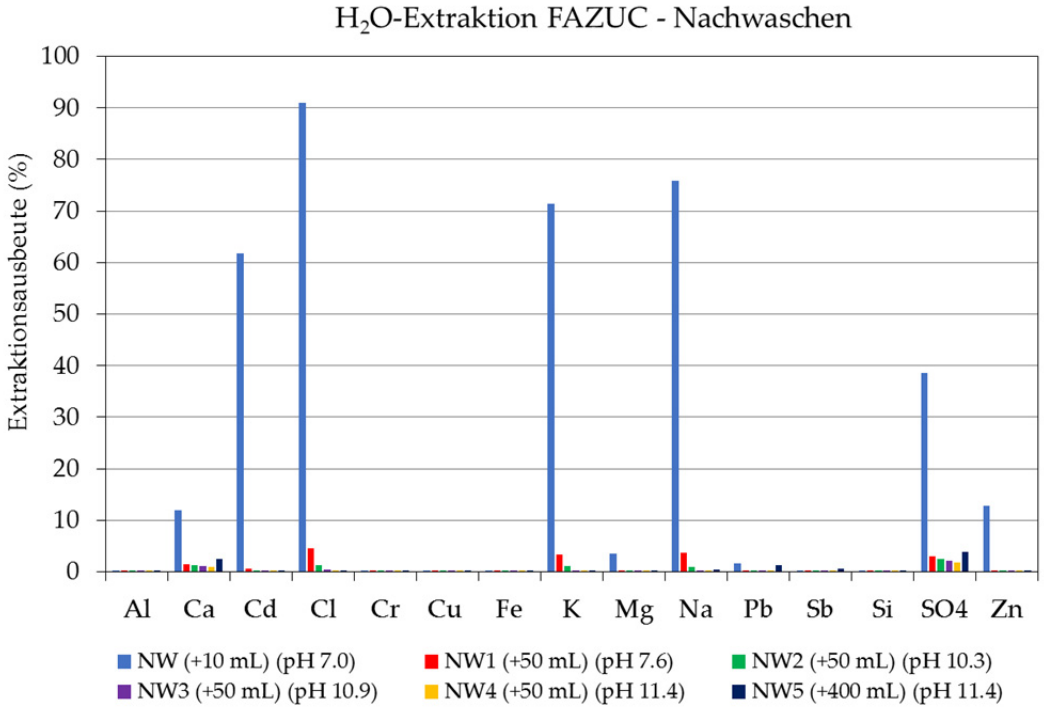

Abbildung 7-8: *Extraktionsausbeuten (%) des Nachwaschversuches des Filterkuchens FKZUC.*

7.5.2 HCl-Extraktion und Titrationsversuche

Die Extraktion mit HCl 5% kommt dem FLUWA-Verfahren relativ nahe und die Analysen der Filterkuchen erscheinen besonders interessant im Hinblick auf die Extraktionsausbeuten und Bindungsverhältnisse der Metalle Zn, Pb, Cu und Cd. Üblicherweise wird bei Laborversuchen, die zur Optimierung des FLUWA-Prozesses dienen, zusätzlich Sulfat zugegeben um den Einfluss der Sulfatfracht vom Quenchwasser auf der Anlage miteinzubeziehen und der pH-Wert auf 4.4 angepasst. Mit den folgenden Versuchen wird jedoch versucht, das System möglichst einfach zu halten um Phasenveränderungen direkt auf die Asche zurückführen zu können und es wurde deshalb auf die Zugabe von Sulfat und eine pH-Anpassung verzichtet. Um den Einfluss der Säure auf die Hauptmineralogie (Pufferung) und Metallmobilisierung im Detail zu studieren, wurden die Flugaschen zusätzlich mittels HCl 5% titriert.

Versuchsübersicht

Die in Tabelle 7-7 aufgeführten Versuchsansätze wurden für die FAZUC und FAHAG durchgeführt. Je 50 g Asche wurde pro Versuch eingesetzt und der Filterkuchen mit 4x 25 mL deionisiertem Wasser nachgewaschen (ausser Versuch 17 und 18 mit angesäuertem Wasser). Die detaillierten Versuchsprotokolle sind im Anhang 7A angefügt.

Tabelle 7-7: *Versuchsansätze der HCl-Extraktionen. Jeweils 50 g Flugasche wurde eingesetzt.*

Nr.	Bezeichnung	HCl	FF	Zeit	Temp.	Vorbehandlung	Nachwaschen FK
Konzentrationsabhängigkeit							
14	HCl 3/4/60/RT	**3%**	4	60 min	RT	**-**	100 mL H_2O
15	HCl 5/4/60/RT	**5%**	4	60 min	RT	**-**	100 mL H_2O
16	HCl 10/4/60/RT	**10%**	4	60 min	RT	**-**	100 mL H_2O
Saures Nachwaschen							
17	HCl 5/4/60/RT WW pH 2	5%	4	60 min	RT	-	**100 mL H_2O (pH 2)**
18	HCl 5/4/60/RT WW pH 1	5%	4	60 min	RT	-	**100 mL H_2O (pH 1)**
Oberflächeneinfluss							
19	HCl 5/4/60/RT g	5%	4	60 min	RT	**gemahlen**	100 mL H_2O
Vorwaschen							
20/21	HCl 5/4/60/RT vw H_2O	5%	4	60 min	RT	**H_2O/10/10/RT**	100 mL H_2O
Zeitabhängigkeit							
22	HCl 5/4/10/RT	5%	4	**30 min**	RT	**-**	100 mL H_2O
23	HCl 5/4/30/RT	5%	4	**60 min**	RT	**-**	100 mL H_2O
24	HCl 5/4/3 h/RT	5%	4	**3 h**	RT	**-**	100 mL H_2O
25	HCl 5/4/6 h/RT	5%	4	**6 h**	RT	**-**	100 mL H_2O
Temperaturabhängigkeit							
26	HCl 5/4/60/40	5%	4	60 min	**40°C**	-	100 mL H_2O
27	HCl 5/4/60/60	5%	4	60 min	**60°C**	-	100 mL H_2O
28	HCl 5/4/60/80	5%	4	60 min	**80°C**	-	100 mL H_2O

Massenverlust und Massenbilanz

Wie bei den H_2O-Versuchen wurden anhand der ICP-OES Resultate der Filtrate eine Auswahl für die Festphasencharakterisierung getroffen. Die ausgewählten Filterkuchen wurden mittels XRF (Anhang 7B), XRD und REM-EDS charakterisiert. Der Massenverlust und somit der Faktor der Aufkonzentrierung der Filterkuchen wurde ebenfalls wie bei den H_2O-Extrakten über das Gewicht und über inerte Elemente bestimmt (Tabelle 7-8). Es wurden gute Übereinstimmungen über die beiden gerechneten Varianten gefunden, einzig der Filterkuchen mit HCl 10% (Versuch 16) ergibt gerechnet über das Gewicht ein viel grösserer Faktor der Aufkonzentrierung (2.1) verglichen zum Mittelwert der inerten Elemente (1.4). Die detaillierten Gewichte vor und nach den Extraktionen für alle Experimente können den Extraktionsprotokollen entnommen werden (Anhang 7A).

Tabelle 7-8: *Faktor der Aufkonzentrierung der Filterkuchen gerechnet über das Gewicht und inerte Elemente.*

Nr.	Bezeichnung	Ba	Cr	Sb	Sn	Ti	(2) x	(1) Gew. FK
		mg/kg	mg/kg	mg/kg	mg/kg	mg/kg		g
Konzentration im FK								
15	ZUC HCl 5/4/60/RT	2'616	713	5'152	2'418	13'740	-	34.2
16	ZUC HCl 10/4/60/RT	3'851	787	2'959	1'221	20'600	-	23.3
21	ZUC HCl 5/4/60/RT vw H_2O	3'082	857	5'685	2'774	15'440	-	40.3
25	ZUC HCl 5/4/6 h/RT	2'668	733	5'059	2'447	14'250	-	34.0
26	ZUC HCl 5/4/60/40	2'622	719	5'394	2'468	13'920	-	33.4
28	ZUC HCl 5/4/60/80	2'535	692	5'027	2'306	14'390	-	34.8
15	HAG HCl 5/4/60/RT	2'174	1'389	3'100	1'086	17'410	-	35.9
16	HAG HCl 10/4/60/RT	2'374	1'452	4'468	1'261	24'100	-	30.3
26	HAG HCl 5/4/60/40	2'168	1'369	3'256	1'108	17'850	-	35.8
Faktor der Aufkonzentrierung im FK								
15	ZUC HCl 5/4/60/RT	1.4	1.5	1.7	1.4	1.5	**1.5**	**1.5**
16	ZUC HCl 10/4/60/RT	2.0	1.7	1.0	0.7	2.2	**1.5**	**2.1**
21	ZUC HCl 5/4/60/RT vw H_2O	1.6	1.8	1.9	1.6	1.7	**1.7**	**1.7**
25	ZUC HCl 5/4/6 h/RT	1.4	1.6	1.7	1.5	1.5	**1.5**	**1.5**
26	ZUC HCl 5/4/60/40	1.4	1.5	1.8	1.5	1.5	**1.5**	**1.5**
28	ZUC HCl 5/4/60/80	1.3	1.5	1.7	1.4	1.5	**1.5**	**1.4**
15	HAG HCl 5/4/60/RT	1.3	1.5	1.3	1.4	1.4	**1.4**	**1.4**
16	HAG HCl 10/4/60/RT	1.4	1.5	1.8	1.6	1.9	**1.7**	**1.6**
26	HAG HCl 5/4/60/40	1.3	1.4	1.3	1.4	1.4	**1.4**	**1.4**

Für alle Extraktionen wurden die Extraktionsausbeuten der diversen Elemente über das Filtrat gerechnet sowie zusätzlich über den Feststoff, falls analysiert (Vorgehen siehe H_2O-Versuche). Es wurde eine gute Übereinstimmung der beiden kalkulierten Abreicherungen für alle überprüften Elemente erreicht.

Konzentrationsabhängigkeit (Versuche 14-16)

Folgende Erkenntnisse können aus den HCl-Versuchen mit unterschiedlichen Konzentrationen gewonnen werden (Abbildung 7-10).

FAZUC:

- Mit zunehmender Säurestärke werden deutlich mehr Schwermetalle aus der Asche extrahiert. Mittels HCl 5% wird dabei eine Extraktionsausbeute für Zn und Cd von >60% erreicht, während dem die Ausbeuten für Pb und Cu <5% betragen. Mit zunehmender Säurestärke (HCl 10%, pH 0.6) steigen die Ausbeuten für Pb und Cu rasant auf Werte >40% an, währenddessen Zn und Cd auf Werte >70% ansteigen.
- In allen Filterkuchen werden grosse Mengen Zementierungsphasen identifiziert ($PbCu^0$-Legierung, Abbildung 7-9). Dabei handelt es sich um die reduktive Abscheidung von Pb und Cu auf weniger edlen metallischen Oberflächen. In den

meisten Fällen wurde diese $PbCu^0$-Legierung auf der Oberfläche von Al^0-Folie Partikeln gefunden.

- Durch die Extraktion von FAZUC mit HCl 5% ist die gesamte mögliche Gipsbildung bereits abgeschlossen. Zudem ist das gesamte Karbonat gelöst. Bei erhöhter Säurekonzentration werden keine signifikanten Veränderungen der dominierenden, kristallinen Phasen beobachtet.
- Mit zunehmender Säurekonzentration wird ein grösserer Massenverlust erreicht, da mehr Asche in Lösung gebracht wird. Ähnlich wie bei den Wasserextraktionen, zeigt die FAZUC einen 20-30% höheren Massenverlust in Bezug auf die FAHAG. FAZUC zeigt 28% bei HCl 3% und 53 bei HCl 10%, FAHAG hingegen nur 22% mit HCl 3% und 40% mit HCl 10%.
- Das Filtrat nach der Extraktion mit HCl 10% war eine dunkle Emulsion. Erst durch das filtrieren mittels 0.45 µm Filter entstand eine klare Lösung.

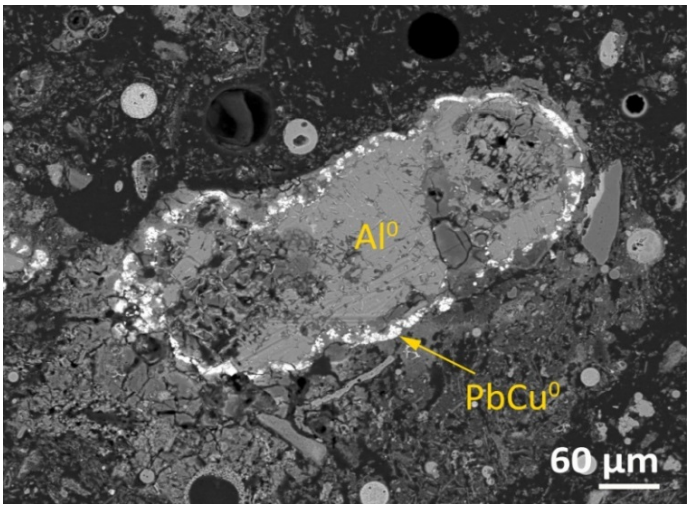

Abbildung 7-9: *Zementierungsphase ($PbCu^0$-Legierung) in Filterkuchen nach der Extraktion mit Salzsäure.*

FAHAG:

- Die Zn-Konzentration der FAHAG ist 3x tiefer verglichen zur FAZUC. Auch die Zn-Ausbeute von 8% ist viel tiefer verglichen zu FAZUC, währenddessen sich Cd in ähnlich hohen Abreicherungsbereichen bewegt (53%). Für Pb und Cu wird 0% Abreicherung erreicht.
- Mit zunehmender Säurekonzentration (HCl 10%) wird eine starke Abreicherung von Zn erreicht (65%). Hingegen bleibt das Pb und Cu auch unter diesen Bedingungen nicht mobilisierbar. Dies ist mit dem relativ hohen pH-Wert von 3.2 verglichen zu FAZUC (pH 0.6) zu erklären. Es müssen Phasen im FKHAG vorhanden sein, die das System zu puffern vermögen und der pH-Wert auch mit HCl 10% vergleichsweise hoch bleibt (Karbonatsystem).

- Die Extraktion mit HCl 5% führt bei FAHAG zu einer starken Gipsbildung. Durch den Einsatz von HCl 10% wird diese Neubildung noch um einen Faktor 2-3 erhöht. Kalzit wird mit HCl 10% in der Hagenholzasche komplett aufgelöst.
- Al und Fe zeigen bei beiden Aschen unterhalb von pH-Wert 1 eine ausgeprägte Mobilisierung.

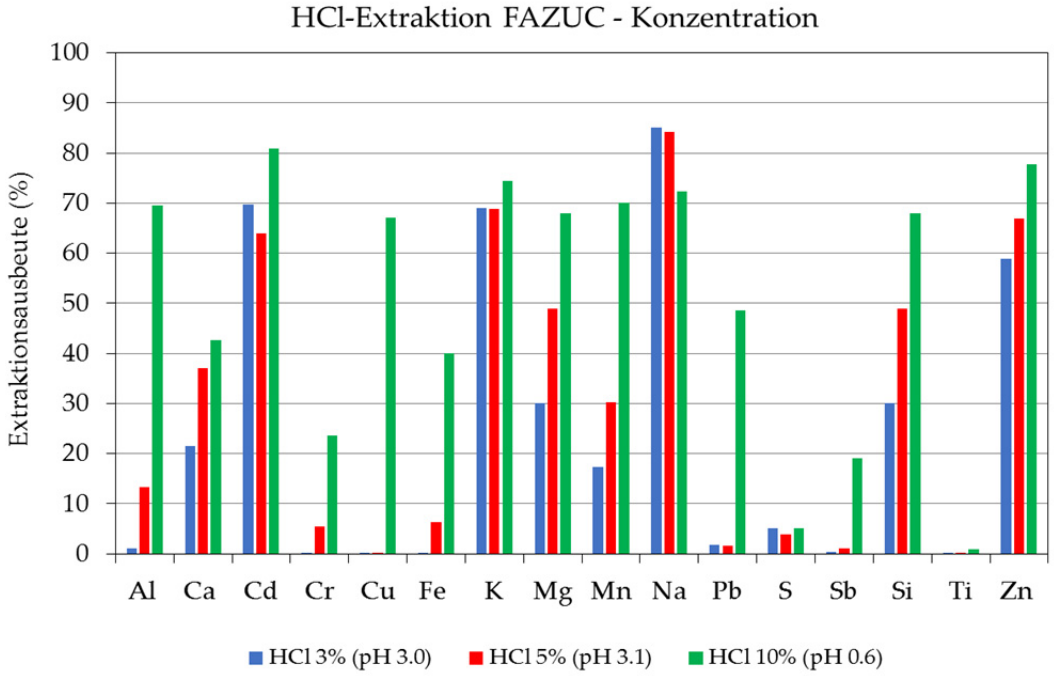

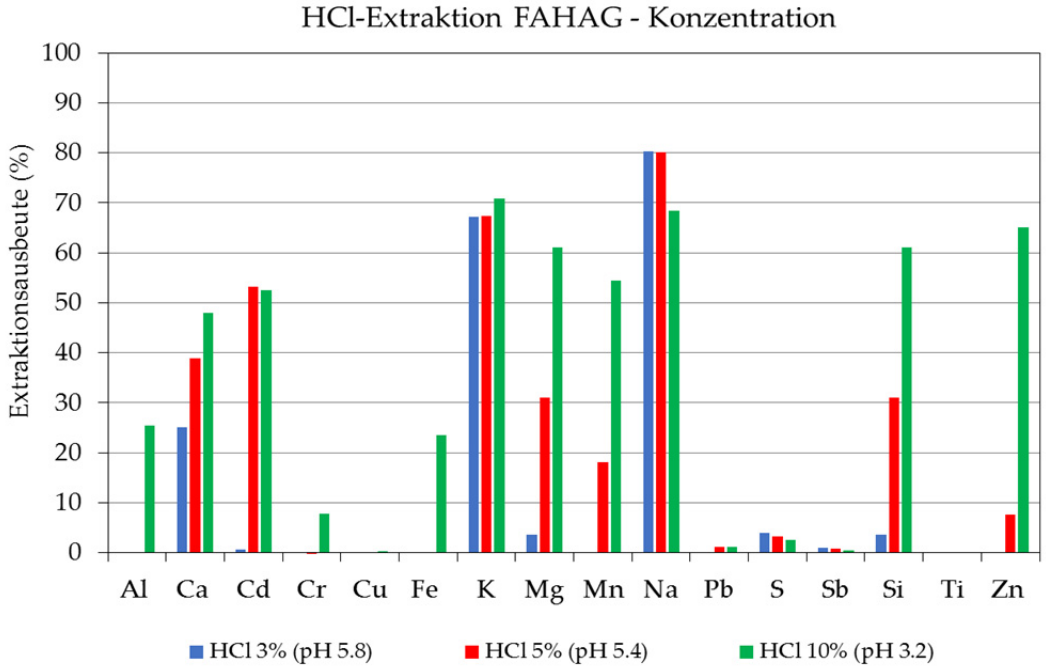

Abbildung 7-10: *Extraktionsausbeuten (%) unterschiedlicher HCl-Konzentrationen der FAZUC und FAHAG.*

Saures Nachwaschen (Versuch 17-18)

Nebst dem Nachwaschen des Filterkuchens mit 100 mL deionisiertem Wasser (ca. pH 6), wurden je zwei Versuche durchgeführt bei denen das Waschwasser mit HCl 32% auf pH 2 resp. pH 1 eingestellt wurde (Abbildung 7-11). Dabei wurden folgende Resultate erreicht:

FAZUC:

- Trotz dem Ansäuern des Waschwassers wurde nach dem Waschen des Filterkuchens ein konstanter pH-Wert von 3.5 gemessen. Dieser Wert entspricht dem pH-Wert der im nicht-angesäuerten Waschwasser gemessen wurde. Die Matrix der Asche puffert das System stark und erhöht den pH-Wert der Lösung nach der Zugabe des angesäuerten Wassers. Daher erstaunt es auch nicht, dass für alle Elemente keine Verbesserung der Ausbeute erreicht werden kann.

FAHAG:

- Die FAHAG puffert den pH-Wert des sauren Waschwassers sogar auf einen Wert von 5. Beim Waschen mit neutralem Wasser wird ein pH-Wert von nahezu 6 erreicht.

Beide Aschen vermögen die Säure der Nachwäsche stark zu puffern, wenn auch auf unterschiedlichem Niveau. Die aufwändige Nachwäsche bewirkt lediglich bei Zn in der FAHAG eine erhöhte Mobilisierung.

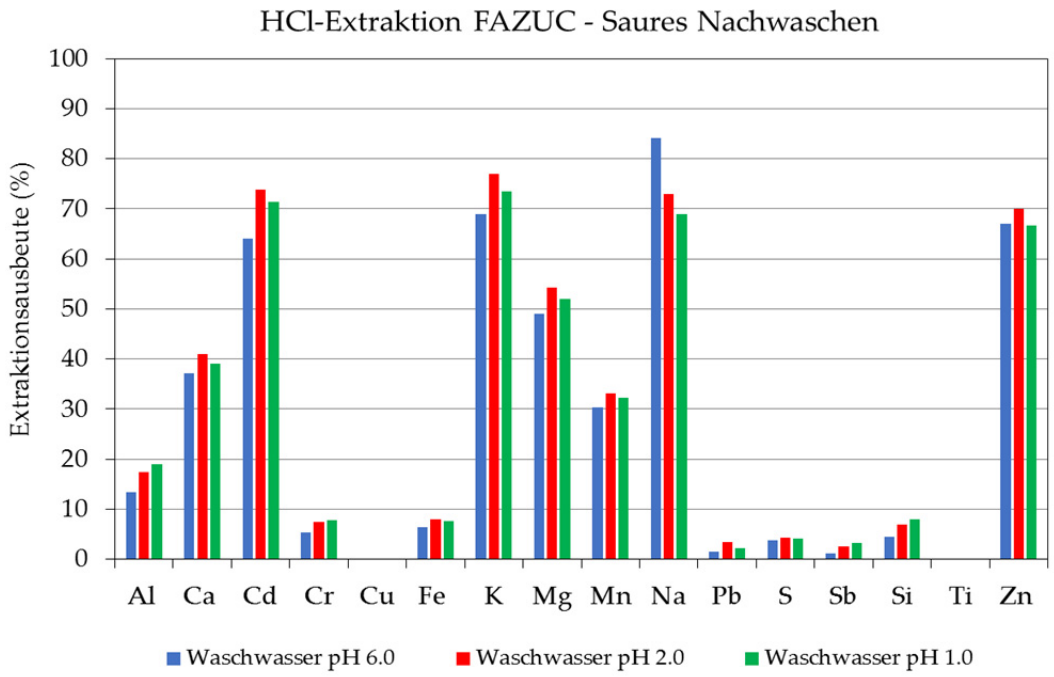

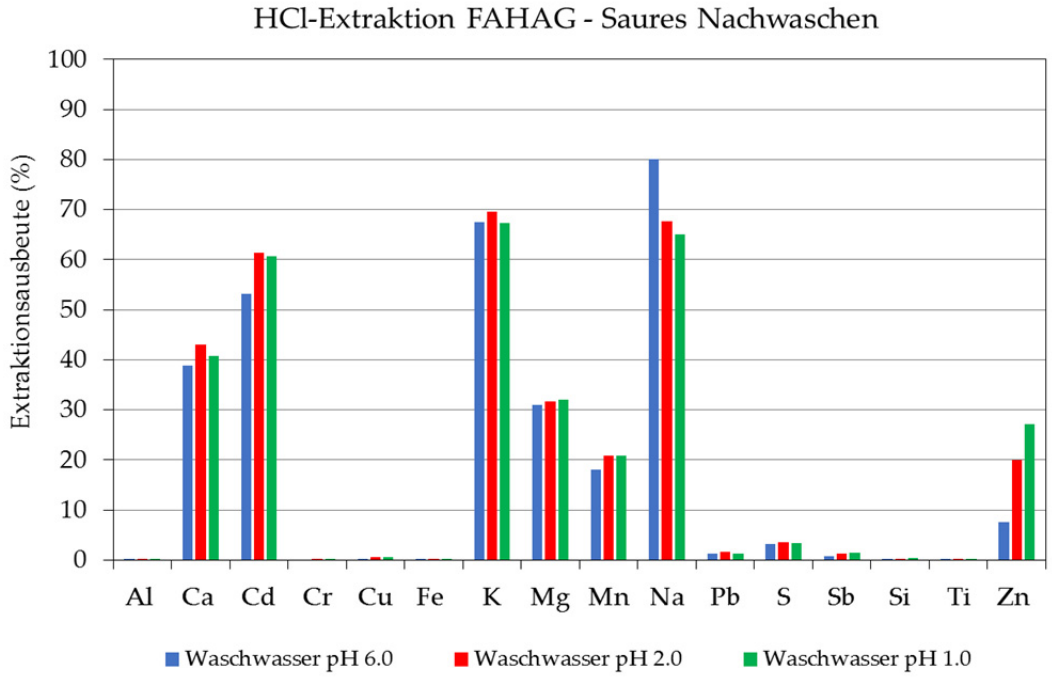

Abbildung 7-11: *Extraktionsausbeuten (%) bei Extraktion mit HCl 5% und saurem Nachwaschen der FAZUC und FAHAG.*

Oberflächeneinfluss (Versuch 19)

Wie bei den H_2O-Versuchen sind keine signifikanten Ausbeute-Unterschiede erkennbar zwischen dem Extrahieren von gemahlener und nicht-gemahlener Flugasche (Abbildung 7-12). Es scheint als ob die Vergrösserung der Oberfläche durch das Malen keinen Einfluss auf die Metallverfügbarkeit hat (die Kinetik ist nicht der limitierende Faktor und es treten keine verstärkten Adsorptionseffekte auf).

Vorwaschen mit H_2O (Versuch 20-21)

Mittels H_2O-Vorwaschschritt erhofft man sich eine grosse Menge löslicher Salze bereits im Vorwaschschritt zu mobilisieren um beim zweiten Waschschritt mit HCl 5% die Metalle besser extrahieren zu können. Die Resultate für FAZUC zeigen, dass die Extraktionsausbeuten verglichen zur HCl 5% Extraktion ohne Vorwaschschritt teilweise sogar tiefer liegen bei der Kombination Wasser/HCl 5% (z.B. Zn) (Abbildung 7-12). Dies hängt mit dem höheren pH-Wert von 4.5 zusammen, da durch das Waschen mit Wasser das Karbonat aktiviert wurde (verstärkte Pufferung). Im Fall des Pb bei FAHAG entspricht der erhöhte Wert derjenigen Fracht, welche mit Wasser extrahierbar ist (siehe H_2O-Versuche) und die anschliessende HCl-Extraktion bringt keine signifikante Verbesserung mehr mit sich.

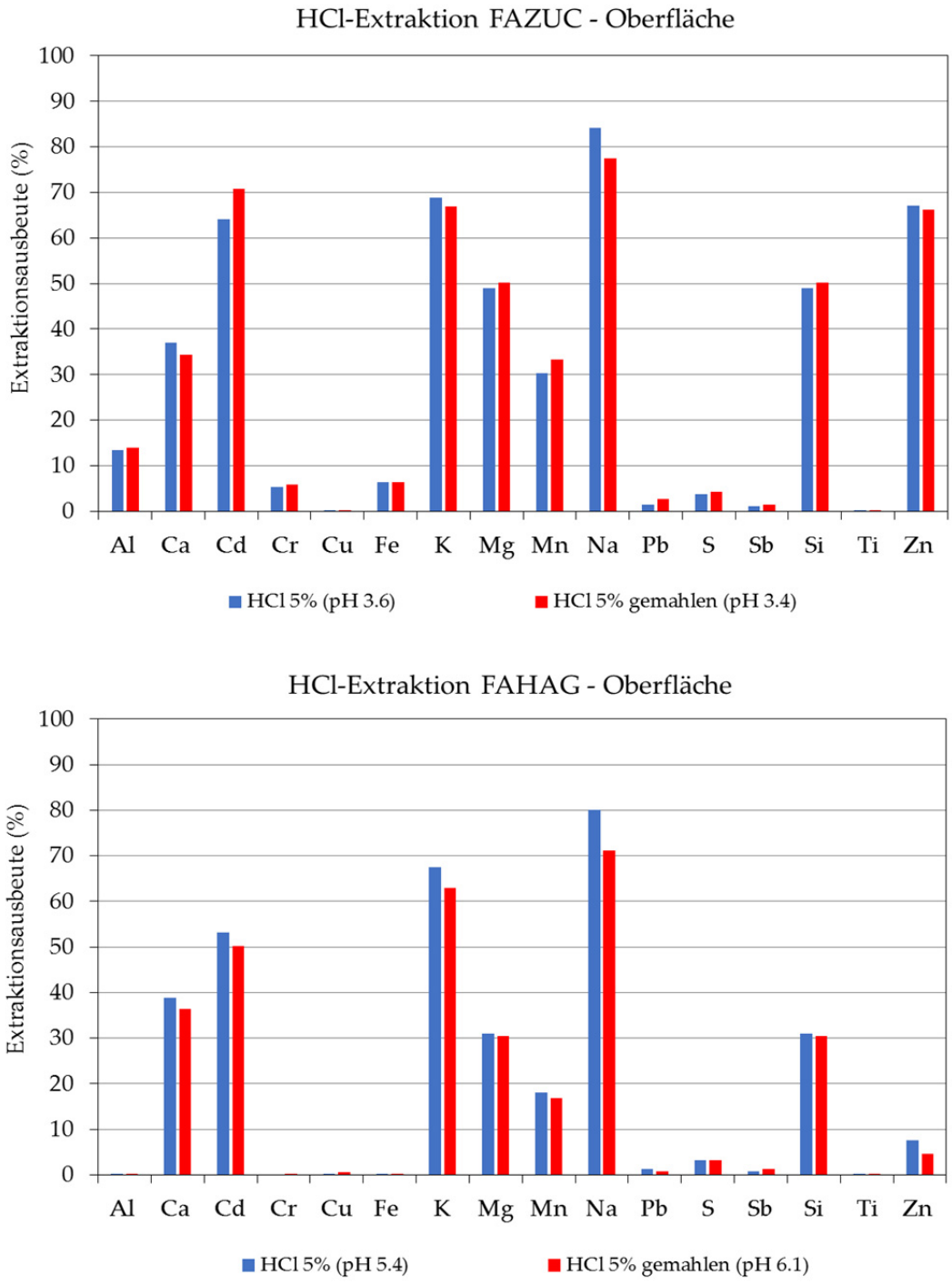

Abbildung 7-12: *Extraktionsausbeuten (%) der gemahlenen/ungemahlenen FAZUC und FAHAG.*

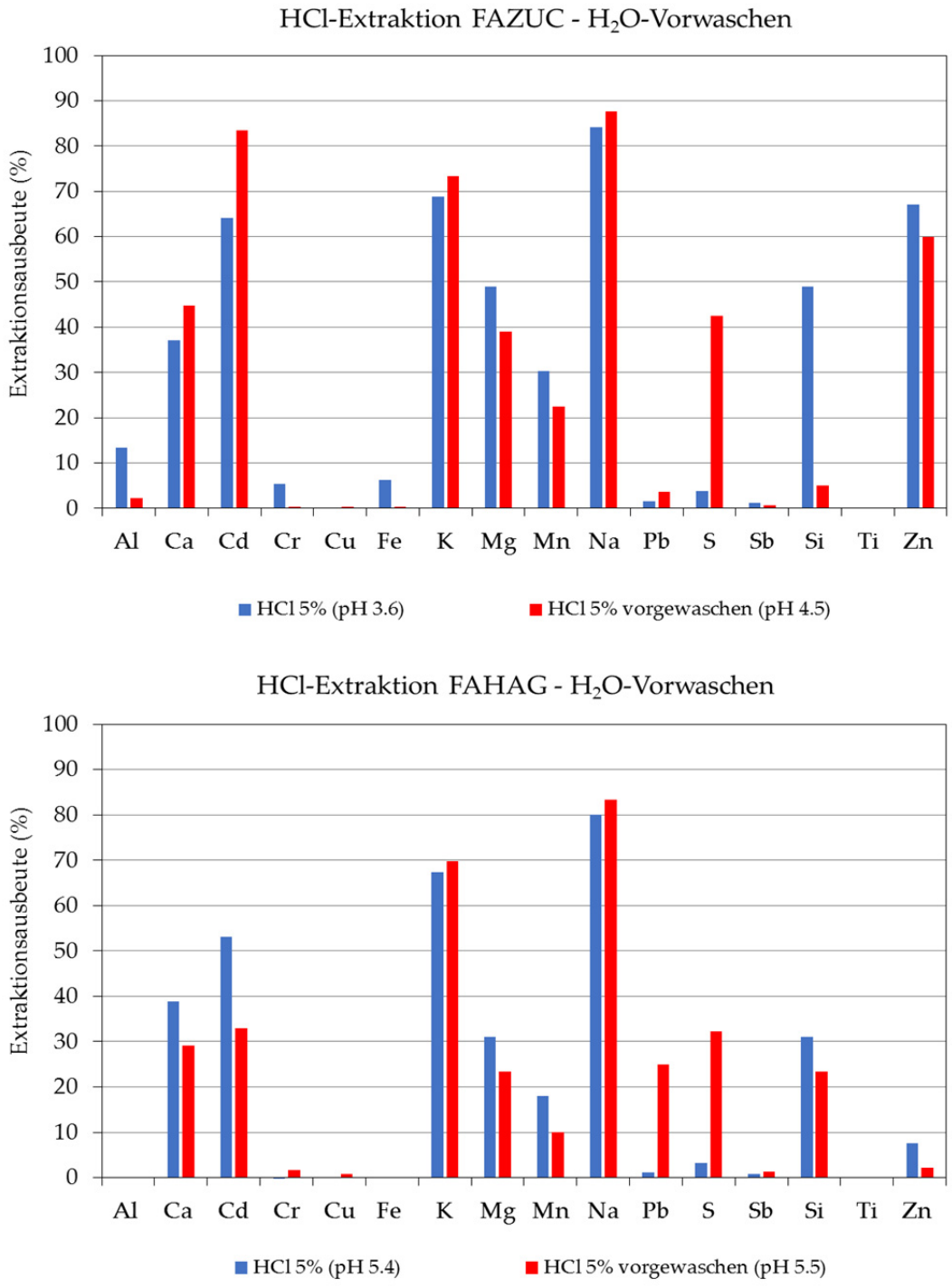

Abbildung 7-13: *Extraktionsausbeuten (%) beim Vorwaschen mit H_2O und anschliessender HCl 5% Extraktion für die FAZUC und FAHAG.*

Zeitabhängigkeit (Versuche 22-25)

Die Wahl unterschiedlicher Extraktionszeiten zwischen 10 Minuten und 6 Stunden zeigen folgende Erkenntnisse (Abbildung 7-15):

FAZUC:

- Der pH-Wert bleibt über die gesamte Extraktionsdauer annähernd stabil (von 3.6 zu 4.0).
- Nach 3 h kommt es zur Rücklösung von Pb, welche nach 6 h noch verstärkt erkennbar ist. Zudem befindet sich ca. 60% des Cu nach 6 h in Lösung. Dieses Rücklösen könnte im Zusammenhang mit ablaufenden Redoxprozessen stehen, da auch das Fe nach 6 h Extraktion deutlich abnimmt. Nach dieser Zeit sind mittels REM keine Zementierungsphasen ($PbCu^0$-Legierung) mehr im Filterkuchen zu erkennen. Hingegen wird häufiger $PbCl_2$ gefunden, welches sich durch die Interaktion mit der HCl nach längerer Extraktionszeit bildet.
- Zn, Al, Si und Fe zeigen mit zunehmender Extraktionszeit kleinere Ausbeuten.

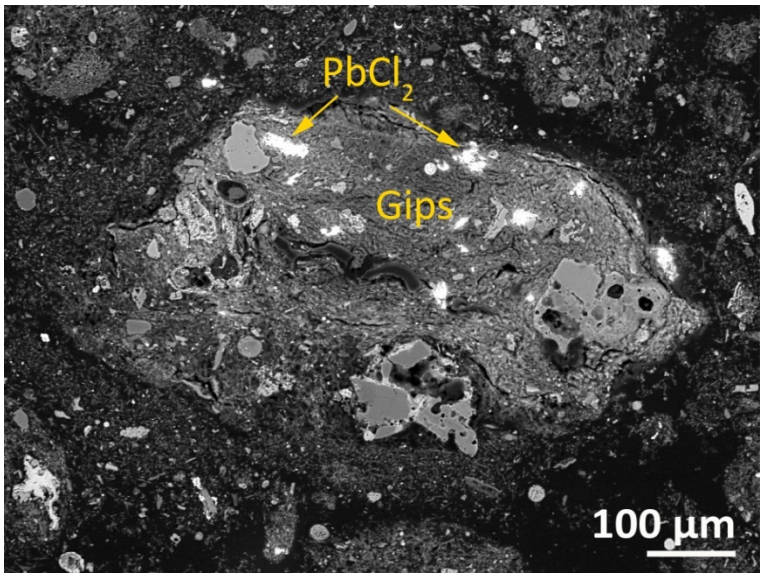

Abbildung 7-14: *Bleichlorid ($PbCl_2$) in Filterkuchen FKHAG nach der 6-stündigen Extraktion mit Salzsäure.*

FAHAG:

- Der pH erhöht sich von 5.6 auf 7.9 nach 6 h.
- Es sind keine Rücklösungen von Metallen wie bei FAZUC erkennbar. Mittels REM sind jedoch deutlich weniger Zementierungsphasen erkennbar, dafür mehr $PbCl_2$ in Gippsaggregaten (Abbildung 7-14).
- Zn, Cd und Mn werden mit zunehmender Extraktionsdauer aus der Lösung entfernt.

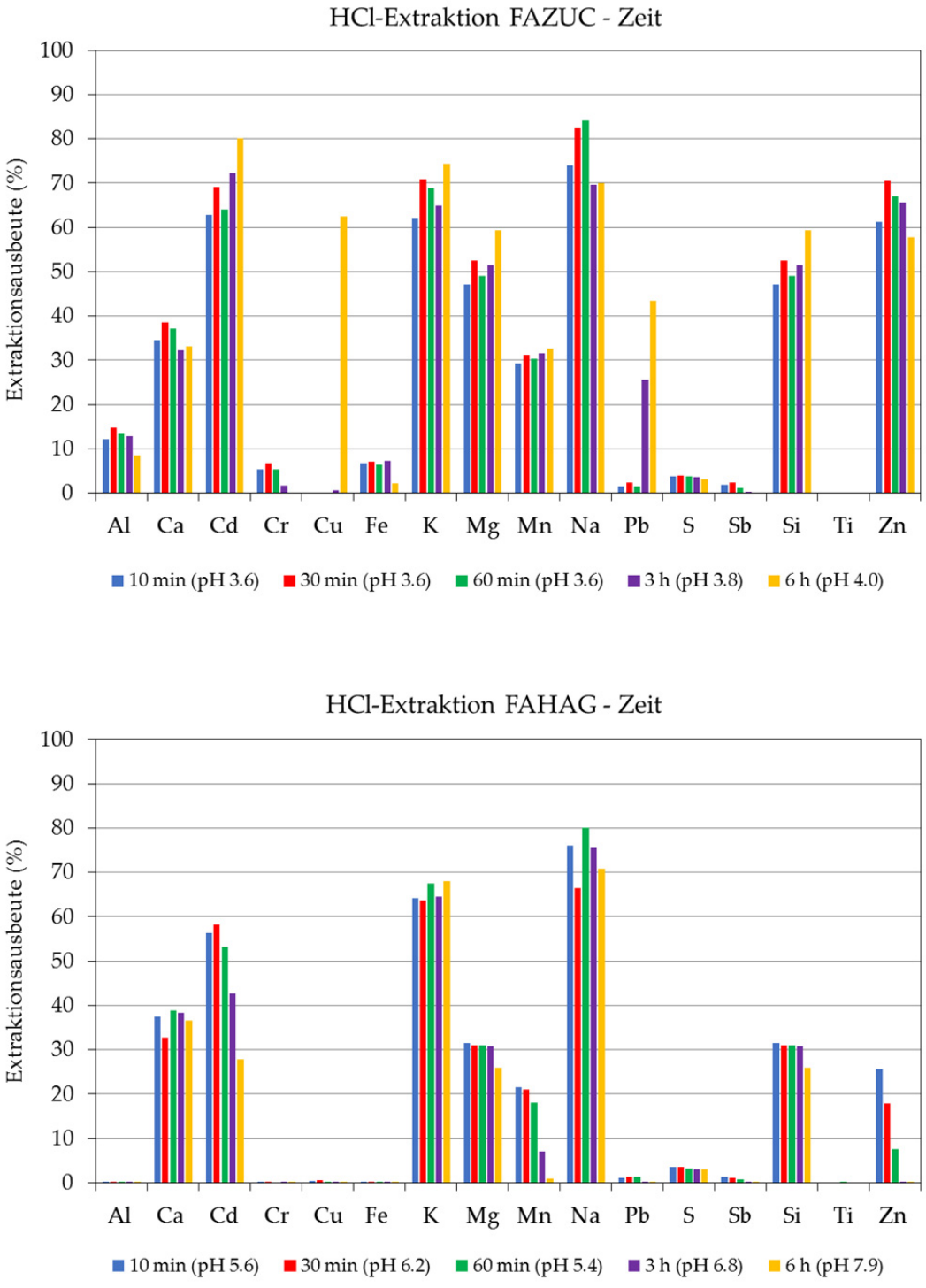

Abbildung 7-15: *Extraktionsausbeuten (%) der zeitabhängigen HCl-Extraktionen der FAZUC und FAHAG.*

Temperaturabhängigkeit (Versuche 26-28)

Temperaturvariationen zeigen für beide Aschen ein ähnliches Lösungsverhalten der Elemente wie die zeitabhängigen Versuche. Dieser Zusammenhang wurde bereits bei den H_2O-Extrakten festgestellt (Abbildung 7-16).

FAZUC:

- Der pH verschiebt sich von RT (20°C) zu 80°C um eine Einheit (von 3.6 zu 4.5).
- Sehr ähnliches Verhalten der Elemente wie bei den Zeitvariationen mit einer Pb-Rücklösung ab 60°C.

FAHAG:

- Geringe pH-Zunahme von 5.4 bei RT auf 5.8 bei 80°C.

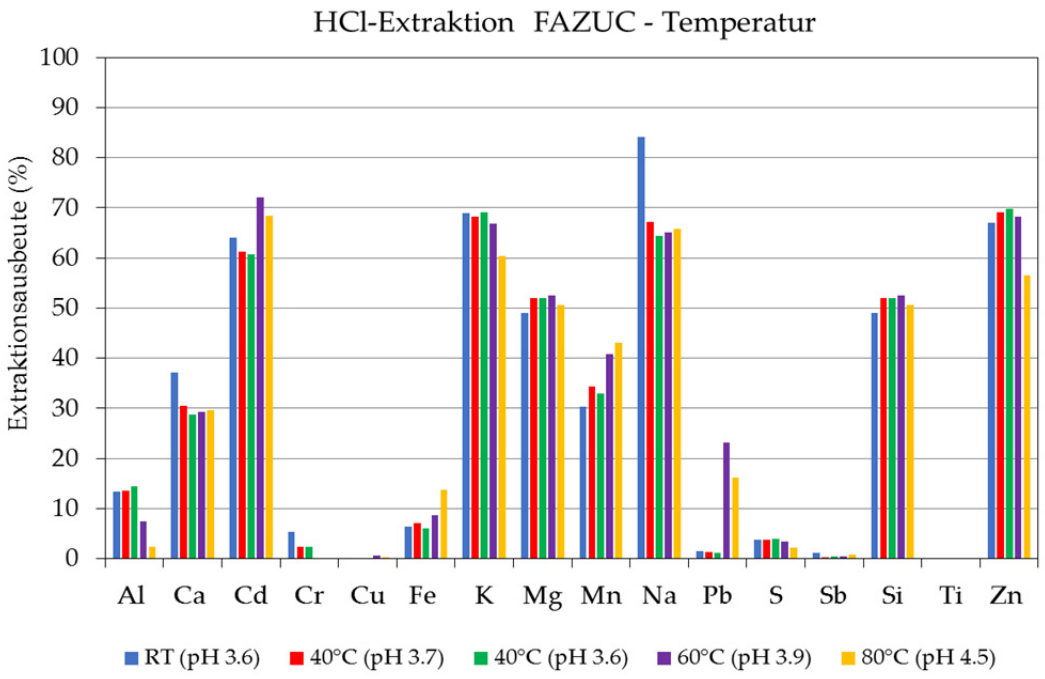

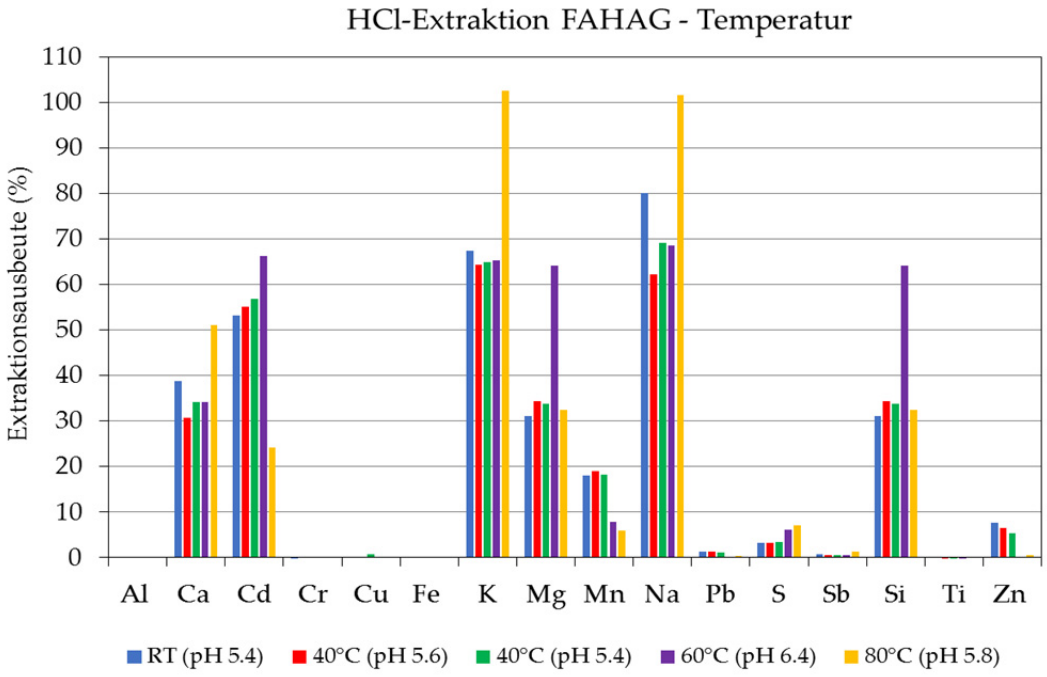

Abbildung 7-16: *Extraktionsausbeuten (%) der temperaturabhängigen HCl-Extraktionen der FAZUC und FAHAG.*

Titrationsversuche mit konstanter Säurezugabe

Die Titrationsversuche dienen dazu, das Verhalten der Flugaschen gegenüber zunehmender Säurekonzentration in Bezug auf Pufferkapazität/Säureverbrauch und deren Reaktivität zu verstehen. Besonders die FAHAG zeigt bei allen Extraktionsversuchen eine ausgeprägte Pufferung, welche die Metallmobilisierung stark erschwert. Die Aschen wurden in Wasser vorgelegt und mittels HCl (1 mol/L) in 40 Schritten titriert (785 DMP Titrino, Metrohm). Dabei wurden verschiedene vorgelegte Volumina, FF-Verhältnisse, Säuremengen und Reaktionszeiten getestet (Tabelle 7-9).

Tabelle 7-9: *Versuchsansätze für die Titrationen der Flugaschen.*

Versuch	Probe	S (g)	L (mL)	FF	Schritte (mL)	Total Säure (1 mol/L) (mL)	Reaktionszeit (min)	pH Start	pH Ende
V1	FAHAG	2	20	10	1	40	1	12.2	0.49
V2	FAHAG	4	40	10	1	40	1	12.2	1.60
V3	FAHAG	4	40	10	1	40	5	12.3	2.29
V4	FAHAG	2	20	10	1	40	5	12.4	0.57
V5	FAZUC	2	20	10	1	40	5	7.0	0.49
V6	FAHAG	2	20	10	1	40	10	12.3	0.57
V7	FAHAG	2	40	20	1	40	5	12.1	0.75

Als optimale Kombination stellte sich eine vorgelegte Menge Asche von 2 g sowie 20 mL H_2O (FF 10) heraus, welche in 40 Schritten von je 1 mL HCl (1 mol/L) und einer Reaktionszeit von 10 Minuten zwischen den Zugaben titriert wurde (V6). Bei den Versuchen V2 und V3 war die Säurestärke zu gering, da der doppelte Ansatz genommen wurde und nur 1 mL Säure pro Schritt zugegeben wurde (Abbildung 7-17). Zudem ist offensichtlich, dass bei V1 die Reaktionszeit von 1 Minute zu kurz und somit die Kinetik zu langsam war. Die Titration der FAZUC startete bei einem deutlich tieferen pH-Wert von 7.0 verglichen zu FAHAG (pH >12). Bereits nach 33 mL Säure war der pH-Wert auf <0.5 gesunken und die Titration wurde beendet. Es ist offensichtlich, dass FAZUC eine viel geringere Pufferkapazität aufweist, was sich bei der Ausbeute als positiv erweist. Der pH-Wert pendelt sich bei der Extraktion viel tiefer ein verglichen zur FAHAG was die Metallmobilisierung erhöht und eine nachhaltige pH-Anpassungen erlaubt.

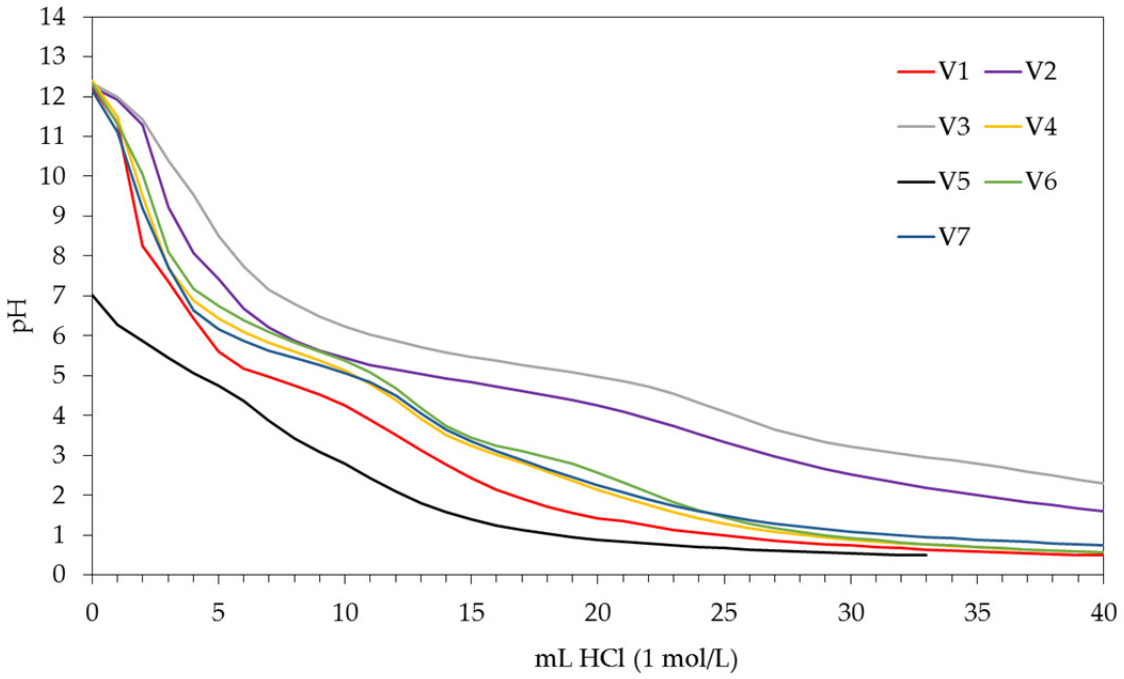

Abbildung 7-17: *Titrationskurven (HCl 1 mol/L) verschiedener Ansätze der FAHAG (V1, 2, 3, 4, 6, 7) und FAZUC (V5).*

Um das Pufferverhalten und die beteiligten Reaktionen von FAHAG besser zu verstehen, wurde die Titrationskurve (V6) in 4 Bereiche (Plateaus) unterteilt. Dazu wurden 4 verschiedene Ansätze bis zu einem definierten End-pH titriert (Tabelle 7-10). Die Filterkuchen der einzelnen Ansätze wurden anschliessend mineralogisch charakterisiert und die Lösungen mittels ICP-OES analysiert.

Tabelle 7-10: *Versuchsansätze für die Titrationen der einzelnen Bereiche (Plateaus).*

Bereich	Probe	S (g)	L (mL)	FF	Schritte (mL)	Total Säure (1 mol/L) (mL)	Reaktionszeit (min)	pH Start	pH Ende
Blank	FAHAG	2	20	10	1	-	10	12.1	12.1
1	FAHAG	2	20	10	1	4	10	12.4	7.3
2	FAHAG	2	20	10	1	12	10	12.4	4.9
3	FAHAG	2	20	10	1	15	10	12.1	3.5
4	FAHAG	2	20	10	1	22	10	12.1	2.1
5	FAHAG	2	20	10	1	40	10	12.3	0.6

Durch das Mischen der Asche mit H_2O (Blank) kommt es zur Lösung der Salze (Halit, Sylvin) und Mobilisierung von 70% Na und K sowie 25% S. Neu identifiziert im Filterkuchen sind grössere Mengen Ettringit. Weiter sind in den einzelnen Bereichen folgende Phasenveränderungen und Metallmobilisierungen gut erkennbar (Abbildung 7-18).

1. Mit den ersten 4 mL Säurezugabe sinkt der pH von >12 auf 7.3 was zur teilweisen Mobilisierung von Ca und Cd führt. Gut lösliche Ca-Phasen (Belit) und Karbonat sind jedoch noch im Filterkuchen vorhanden.

2. Zwischen 4 und 12 mL Säurezugabe wird ein erstes Plateau erreicht. Der Kalzit puffert den pH-Wert und verhindert eine weitere starke pH-Absenkung. Dadurch wird der Kalzit verbraucht, was sich im kleineren Gehalt im Filterkuchen und dem zunehmenden Ca-Gehalt im Filtrat zeigt (41% mobilisiert). Zudem beginnt die Gipsbildung. Cd und Zn sind bereits bei einem pH-Wert von 4.9 um 59% (Cd) resp. 43% (Zn) abgereichert.

3. Nachdem das Karbonat aufgebraucht ist, verringert sich die Pufferwirkung stark und der pH-Wert sinkt wieder schneller mit fortlaufender Säurezugabe. Grosse Mengen Gips sind im Filterkuchen erkennbar. Gips ist die löslichkeitskontrollierende Phase für Ca und S, was die konstanten Mengen in Lösung erklärt.

4. Mit der weiteren Säurezugabe (15-22 mL) ist ein zweites Plateau erkennbar und der pH-Wert sinkt auf 2.1. Dabei werden Ca- und Mg-reiche Alumosilikate/Gläser wie Gehlenit gelöst. Dies ist an der erhöhten Mobilisierung von Al (42%), Mg (56%) und Si (27%) zu erkennen. Die Lösung der Silikate führt wegen den sehr tiefen pH-Werten zur Bildung von Si-Gel.

Asche	Blank	1	2	3	4	Minerale im FK
-	-	4	12	15	22	Säuremenge (mL)
-	12.1	7.3	4.9	3.6	2.1	pH
						Halit
						Sylvin
						Anhydrit
						Bassanit
						Gips
						Ettringit
						Brownmillerit (Belit)
						Kalzit
						Gehlenit
						Siderit
						Quarz
						Hämatit
						Spinel
						Abreicherung (%)
			1	8	42	Aluminium
	1	1	3	3	2	Barium
	7	19	41	48	61	Kalzium
		26	59	58	60	Cadmium
	2	2	1	10	16	Chrom
			10	17	10	Kupfer
				2	12	Eisen
	74	69	68	70	75	Kalium
		3	26	40	56	Magnesium
		2	14	21	30	Mangan
	69	64	65	66	71	Natrium
	4		7	22	20	Blei
	25	20	17	19	26	Schwefel
		4	5	8	15	Antimon
		1	7	13	27	Silizium
					2	Titan
		2	43	49	57	Zink

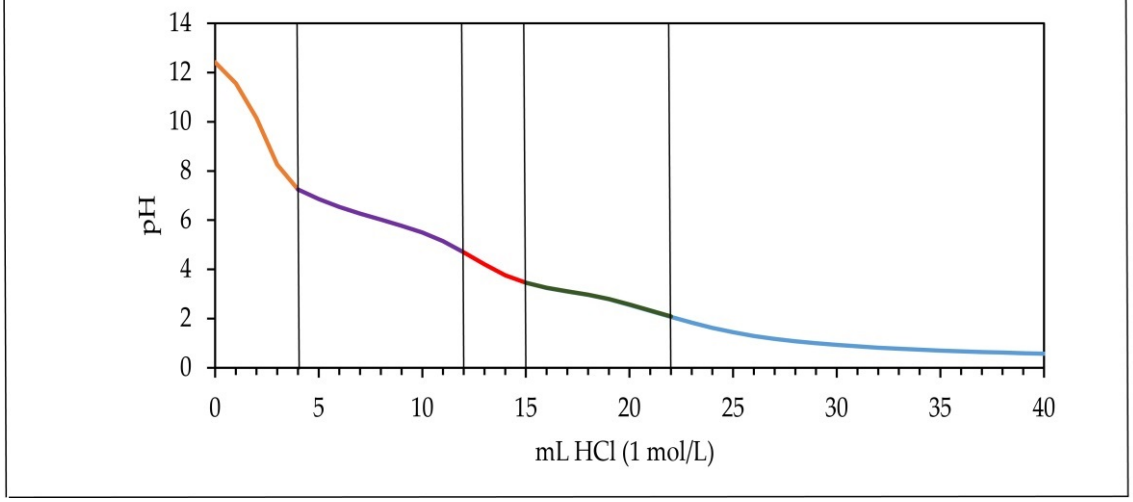

Abbildung 7-18: *Stabile Mineralphasen im FKHAG und Abreicherung (%) diverser Elemente während den unterschiedlichen Titrationsstufen der FAHAG.*

7.5.3 H_2SO_4-Extraktion

Die Extraktionen mit H_2SO_4 wurden primär durchgeführt um die Abhängigkeit der Metallextrahierbarkeit von der Art der Säure, der Säurestärke und dem pH-Wert zu erklären. Zudem kann durch den hohen Schwefeleintrag der Einfluss des Sulfatsystems auf die Metallextrahierbarkeit untersucht werden.

Versuchsübersicht

Folgende Versuchsansätze wurden für die FAZUC und FAHAG durchgeführt. Je 50 g Asche wurde pro Versuch eingesetzt und der Filterkuchen mit 4x 25 mL deionisiertem Wasser nachgewaschen. Die detaillierten Versuchsprotokolle sind im Anhang 7A angefügt.

Tabelle 7-11: *Versuchsansätze der H_2SO_4-Extraktionen. Jeweils 50 g Flugasche wurde eingesetzt.*

Nr.	Bezeichnung	H_2SO_4	FF	Zeit	Temp.	Vorbehandlung	Nachwaschen
Konzentrationsabhängigkeit							
29	H_2SO_4 6.6/4/60/RT	**6.6%**	4	60 min	RT	**-**	100 mL H_2O
30	H_2SO_4 13.9/4/60/RT	**13.9%**	4	60 min	RT	**-**	100 mL H_2O
Vorwaschen							
31	H_2SO_4 6.6/4/60/RT vw HCl 5%	6.6%	4	60 min	RT	**HCl 5/4/60/RT**	100 mL H_2O
Temperaturabhängigkeit							
32	H_2SO_4 6.6/4/60/40	6.6%	4	60 min	**40°C**	-	100 mL H_2O
33	H_2SO_4 6.6/4/60/80	6.6%	4	60 min	**80°C**	-	100 mL H_2O

Massenverlust und Massenbilanz

Anhand der ICP-OES Resultate der Filtrate wurde eine Auswahl für die Festphasencharakterisierung getroffen. Die ausgewählten Filterkuchen wurden mittels XRF (Anhang 7B) und XRD charakterisiert.

Der Massenverlust und somit der Faktor der Aufkonzentrierung der Filterkuchen wurde ebenfalls, wie bei den vorgängigen Extrakten, über das Gewicht und über die inerten Elemente bestimmt (Tabelle 7-12). Die detaillierten Gewichte vor und nach den Extraktionen aller Experimente können in den Extraktionsprotokollen entnommen werden (Anhang 7A).

Tabelle 7-12: *Faktor der Aufkonzentrierung der Filterkuchen gerechnet über das Gewicht und über inerte Elemente.*

Nr.	Bezeichnung	Ba	Cr	Sb	Sn	Ti	(2) x	(1) Gew. FK
		mg/kg	mg/kg	mg/kg	mg/kg	mg/kg		g
Konzentration im FK								
29	ZUC H_2SO_4 6.6/4/60/RT	1'952	468	3'767	1'781	10'290		46.2
30	ZUC H_2SO_4 13.9/4/60/RT	1'904	401	2'387	1'409	11'250		46.1
31	ZUC H_2SO_4 6.6/4/60/RT vw HCl 5%	2'550	602	5'161	2'146	14'740		40.7
35	ZUC NaOH 10/15/60/RT	2'768	728	3'594	2'281	12'390		13.4
36	ZUC NaOH 10/15/60/80	2'898	771	3'535	2'045	12'640		12.4
29	HAG H_2SO_4 6.6/4/60/RT	1'437	824	2'175	699	11'180		55.8
33	HAG H_2SO_4 6.6/4/60/RT vw HCl 5%	1'891	1'099	3'295	970	16'900		47.8
34	HAG NaOH 10/15/60/RT	1'880	1'099	2'545	893	14'050		16.3
35	HAG NaOH 10/15/60/80	1'953	1'179	2'507	896	13'710		15.4
Faktor der Aufkonzentrierung im FK								
29	ZUC H_2SO_4 6.6/4/60/RT	1.0	1.0	1.3	1.1	1.1	**1.1**	**1.1**
30	ZUC H_2SO_4 13.9/4/60/RT	1.0	0.9	0.8	0.8	1.2	**0.9**	**1.1**
31	ZUC H_2SO_4 6.6/4/60/RT vw HCl 5%	1.4	1.3	1.7	1.3	1.6	**1.4**	**1.7**
35	ZUC NaOH 10/15/60/RT	1.5	1.6	1.2	1.4	1.3	**1.4**	**1.5**
36	ZUC NaOH 10/15/60/80	1.5	1.6	1.2	1.2	1.4	**1.4**	**1.6**
29	HAG H_2SO_4 6.6/4/60/RT	0.9	0.9	0.9	0.9	0.9	**0.9**	**0.9**
33	HAG H_2SO_4 6.6/4/60/RT vw HCl 5%	1.1	1.2	1.3	1.2	1.4	**1.2**	**1.5**
35	HAG NaOH 10/15/60/RT	1.1	1.2	1.0	1.1	1.1	**1.1**	**1.2**
36	HAG NaOH 10/15/60/80	1.2	1.2	1.0	1.1	1.1	**1.1**	**1.3**

Für alle Extraktionen wurden die Extraktionsausbeuten der diversen Elemente über das Filtrat gerechnet sowie zusätzlich über den Feststoff, falls analysiert (Vorgehen siehe H_2O-Versuche). Es wurde eine gute Übereinstimmung der beiden kalkulierten Abreicherungen für alle überprüften Elemente erreicht.

Konzentrationsabhängigkeit (Versuche 29-30)

Folgende Erkenntnisse wurden aus den H_2SO_4-Versuchen mit unterschiedlichen Konzentrationen gewonnen (Abbildung 7-19):

FAZUC:

- Mit zunehmender Säurestärke können mehr Metalle extrahiert werden, ähnlich wie dies auch bei erhöhter HCl-Konzentration beobachtet wurde (pH-Senkung von pH 3.9 bei 6.6% auf pH 0.7 bei 13.9% H_2SO_4).
- Verglichen zur Extraktion mit HCl 10% (entspricht der Säurestärke von 13.9% H_2SO_4) wird aber deutlich weniger Pb und Cu mobilisiert.
- Durch den Schwefeleintrag des Extraktionsmittels kommt es zur starken Gipsbildung ($CaSO_4 \cdot 2H_2O$), was auch den tiefen Ca-Wert in Lösung erklärt. Die Gipsbildung ist auch für das hohe Gewicht der Filterkuchen verantwortlich (nur 8% Massenverlust nach Extraktion).

- Die tiefen Pb und Cu Ausbeuten bei H_2SO_4 13.9% verglichen zur HCl 10% stehen mit dem Sulfatsystem im Zusammenhang (Bildung von $PbSO_4$).
- Das Filtrat nach der Extraktion mit H_2SO_4 13.9% war eine dunkle Emulsion wie bei der HCl 10% (zusätzlicher Filtrationsschritt durch 0.45 µm nötig). Zudem bereitete das H_2O-Nachwaschen Schwierigkeiten und erst durch den Einsatz einer sehr starken Vakuumpumpe konnte das Filtrat vom Filterkuchen abgetrennt werden.

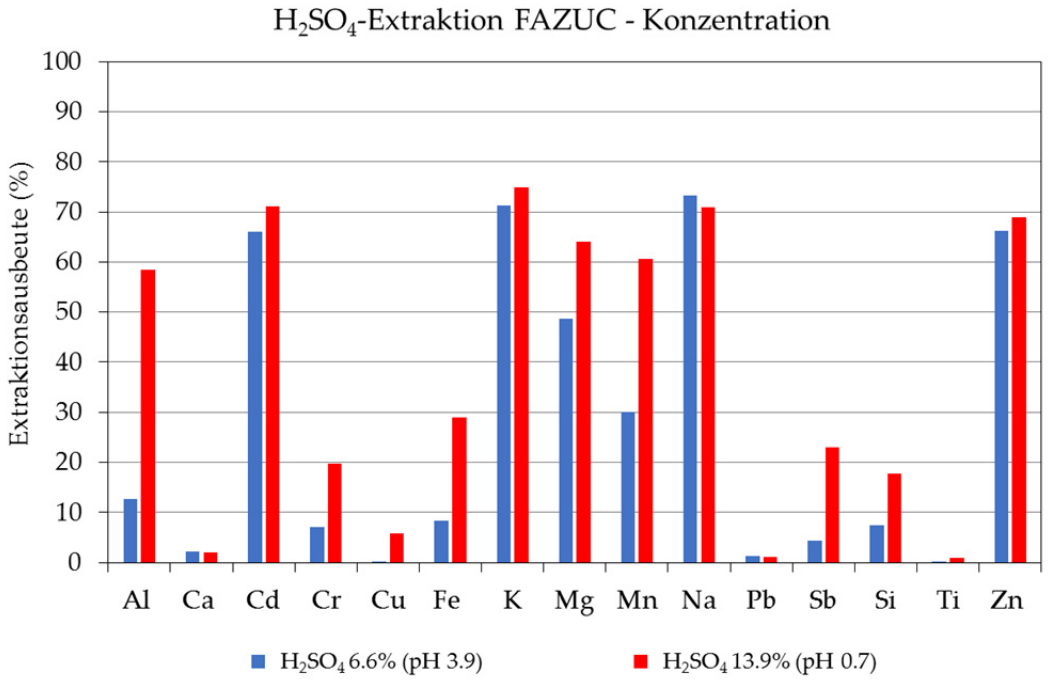

Abbildung 7-19: *Extraktionsausbeuten (%) der konzentrationsabhängigen H_2SO_4-Extraktionen der FAZUC.*

FAHAG:

- Die Extraktion der FAHAG mit H_2SO_4 13.9% musste abgebrochen werden, da sich die Lösung weder mit einer sehr starken Vakuumpumpe noch mittels Zentrifugieren vom Filterkuchen separieren lies. Die Aschematrix veränderte sich stark und blähte sich richtiggehend auf (wahrscheinlich sehr grosse Gipsbildung durch den hohen Ca-Gehalt dieser Asche und des hineingebrachten Schwefels).
- Die enorme Gipsbildung ist auch dafür verantwortlich, dass die Filterkuchen um rund 10% schwerer ausfallen als die Ausgangsasche (50 g Asche eingesetzt, Filterkuchen 56 g).

Gleiche Säurestärke (Versuche 15 und 29)

Der Vergleich zwischen der HCl- und H_2SO_4-Extraktion mit gleicher Säurestärke zeigt für beide Flugaschen annähernd identische Extraktionsausbeuten (Abbildung 7-20). Dies ist mit dem ähnlichen pH-Bereich zu erklären indem man sich während der Extraktion be-

findet (Abbildung 7-20). Es scheint als ob die Säurestärke und damit das pH-Fenster massgeblich für die sich einstellenden Extraktionsausbeuten verantwortlich ist und die starke Gipsbildung bei der Extraktion mit Schwefelsäure und andere Matrixeinflüsse, verursacht durch das Extraktionsmittel, keine signifikante Rolle bei der Element-Mobilisierung spielen.

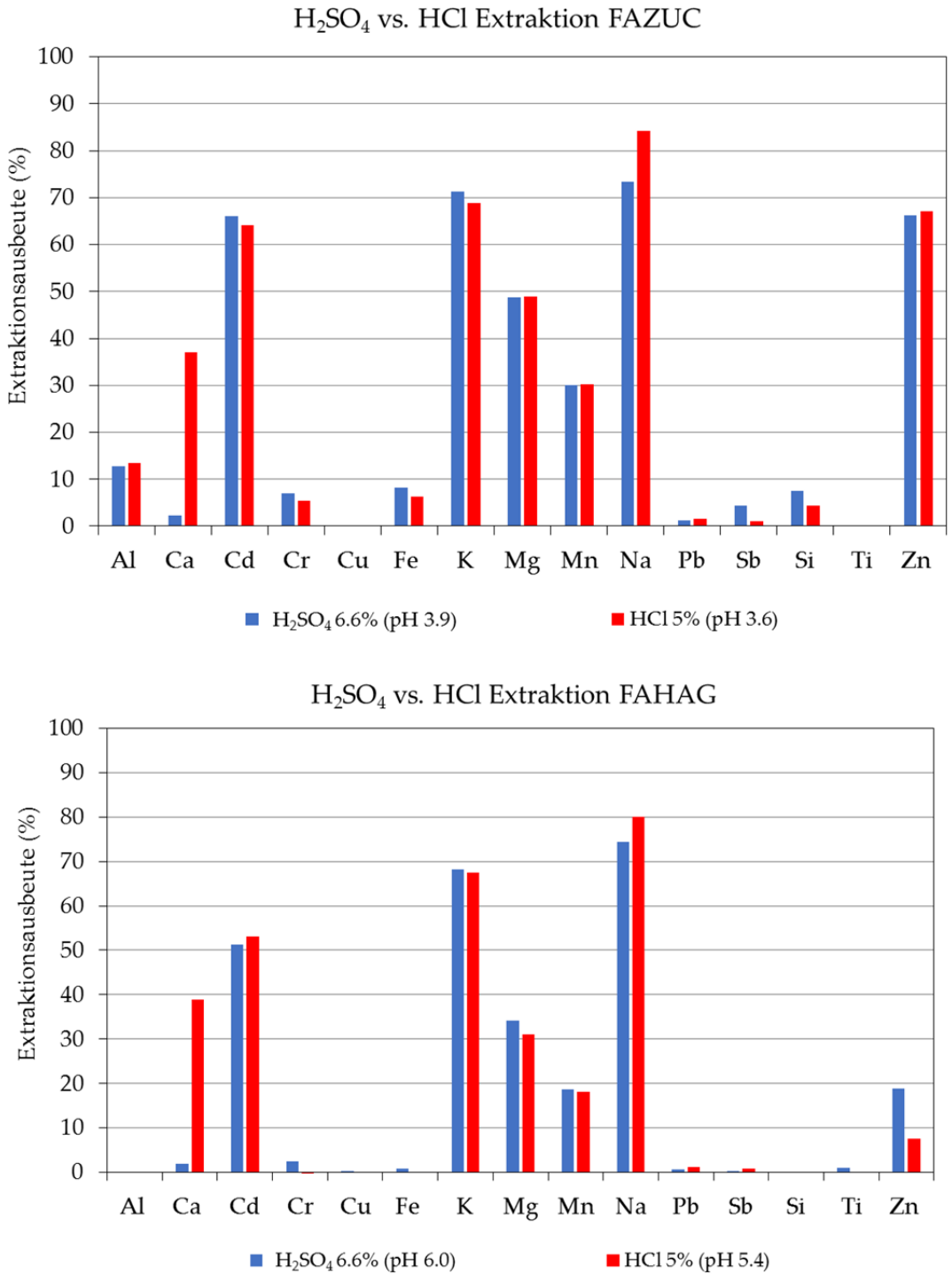

Abbildung 7-20: *Extraktionsausbeuten (%) beim Einsatz von HCl und H_2SO_4 gleicher Säurestärke bei der FAZUC und FAHAG.*

Vorwaschen mit HCl 5% (Versuch 31)

FAZUC:

- Die Vorbehandlung mit HCl 5% gefolgt von der Extraktion mit H_2SO_4 6.6% führt zu deutlich erhöhten Ausbeuten von Zn (82%), Al (53%), Fe (26%), Cd (80%) und Cu (37%) (Abbildung 7-21). Dies ist mit der pH-Absenkung von 3.6 bei der HCl auf pH 1.6 bei der anschliessenden H_2SO_4-Extraktion zu erklären. Versuche einer internen Vorstudie zeigten ähnliche Resultate beim kombinierten Einsatz von HCl und H_2SO_4. Der Ansatz 2x mit HCl 5% zu extrahieren zeige jedoch keine weitere Metallabreicherung beim zweiten Durchgang. Dies hängt mit dem pH-Wert zusammen, welcher sich auch beim 2. Durchgang auf einen Wert von ca. 4 einstellt.
- Eine Steigerung der Ausbeute lässt sich somit erst bei der Kombination von unterschiedlichen Säuren erreichen, wobei es zentral ist, dass beim 2. Durchgang der pH-Wert signifikant gesenkt werden kann.
- Das Nachwaschen am Ende der H_2SO_4-Extraktion bereitete einige Probleme und erst durch Zentrifugieren konnte der Filterkuchen vom Waschwasser abgetrennt werden. Aus diesem Grund wäre es empfehlenswert, diese Versuchsserie 2-3x zu wiederholen.

FAHAG:

- Die zweistufige Extraktion mit HCl 5% und H_2SO_4 6.6% zeigt auch für die FAHAG verbesserte Metall-Ausbeuten im Vergleich zur einstufigen H_2SO_4-Extraktion, jedoch auf einem tieferen Niveau verglichen zur FAZUC.
- Gründe für die tieferen Metall-Ausbeuten sind einerseits die bis zu 3x tieferen Metallkonzentrationen in der Ausgangsasche und andererseits die Unterschiede des pH-Wertes der Extraktlösungen. Bei der FAHAG befindet man sich in einem höheren pH-Bereich, verglichen zur FAZUC (pH 6.0 mit HCl 5%, pH 3.7 mit anschliessender H_2SO_4).
- Verbesserte Ausbeuten werden v.a. für Zn, Fe und Cd erreicht.

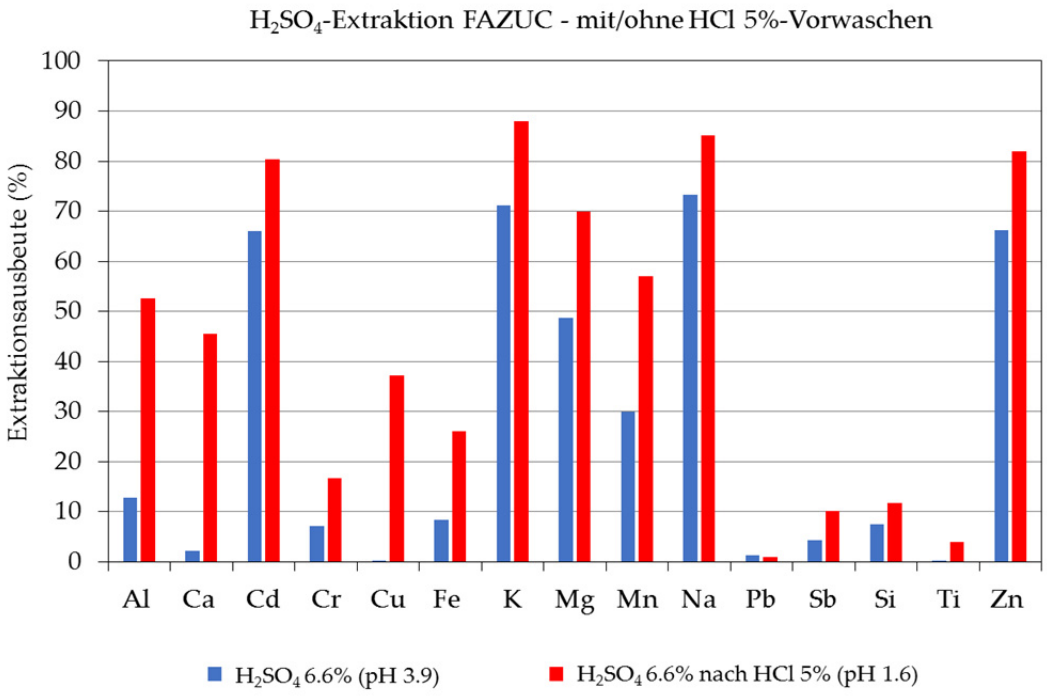

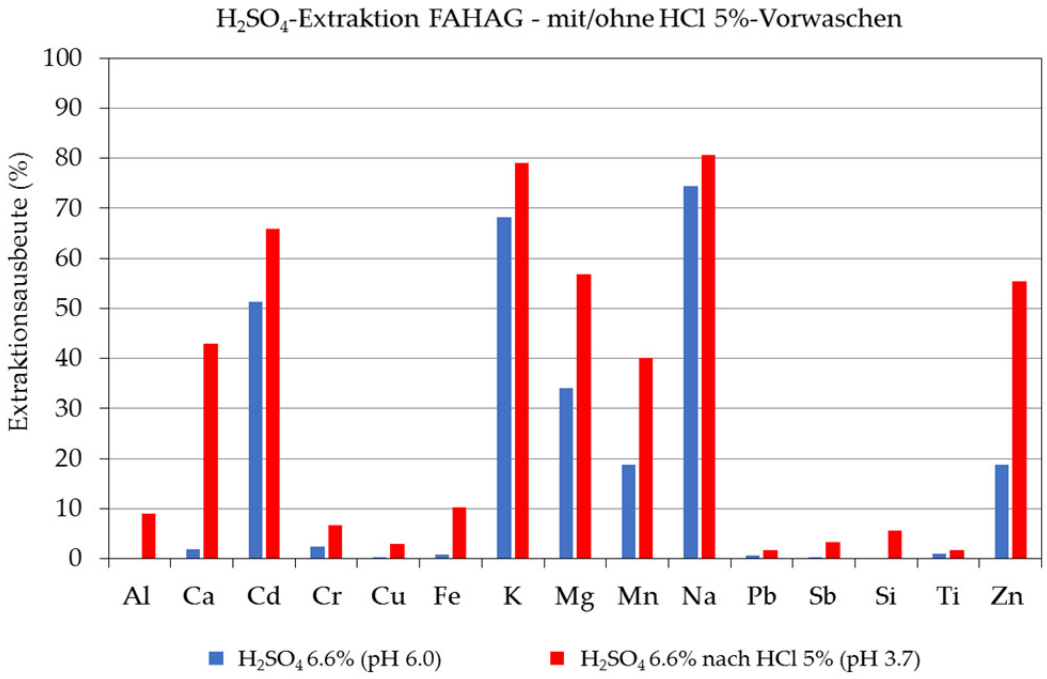

Abbildung 7-21: *Extraktionsausbeuten (%) bei der Extraktion mit H_2SO_4 6.6% und der zweistufigen Extraktion mittels HCl 5% und H_2SO_4 6.6% der FAZUC und FAHAG.*

Temperaturabhängigkeit (Versuche 32-33)

Die temperaturabhängigen H_2SO_4-Versuche zeigen ein ähnliches Bild wie die HCl-Versuche bei 40 und 80°C (Abbildung 7-22). Einzig die Pb-Rücklösung ab 60°C die mit HCl beobachtet werden kann, zeigt sich bei den Versuchen mit H_2SO_2 nicht (Bildung des gering wasserlöslichen $PbSO_4$).

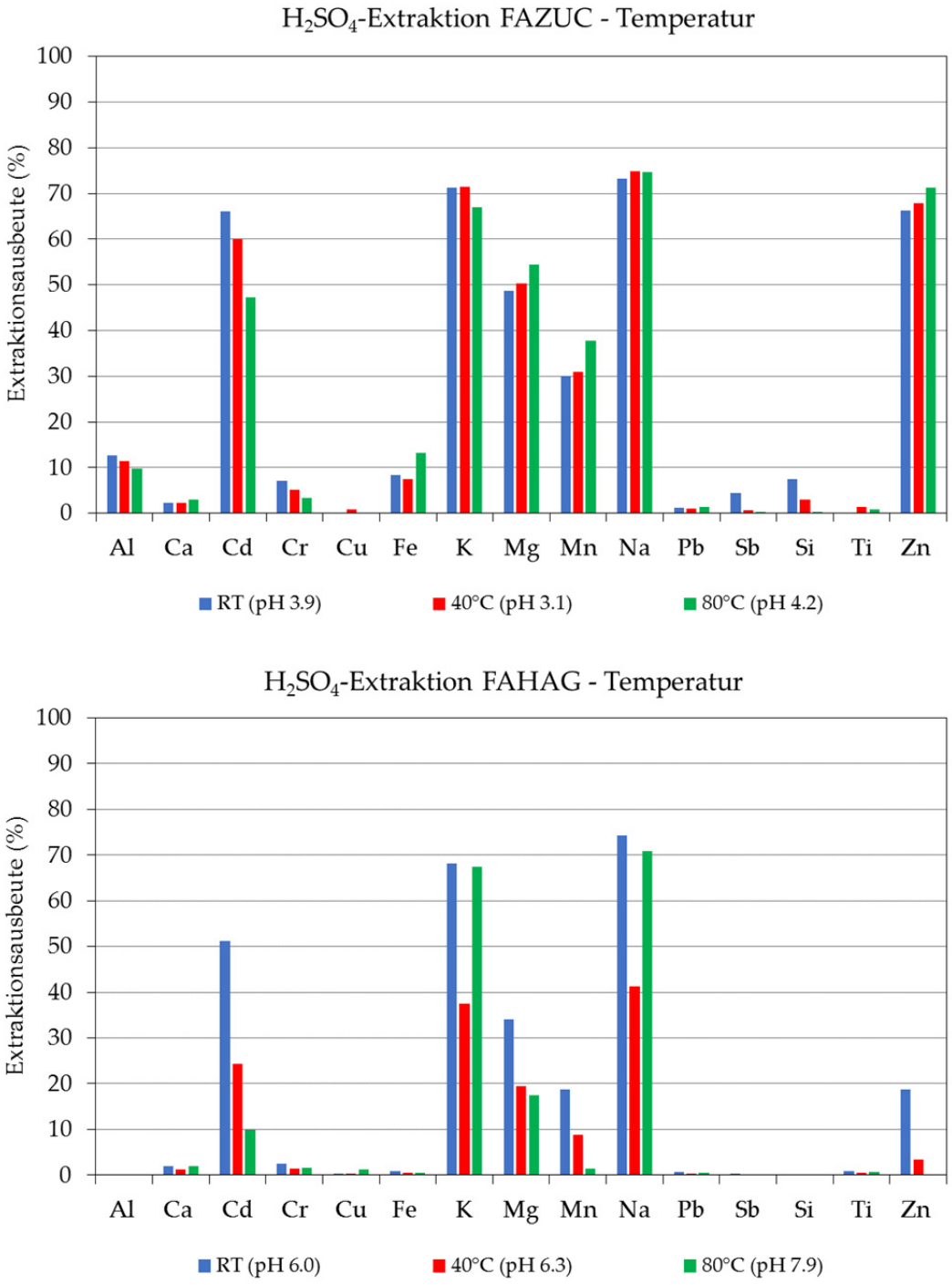

Abbildung 7-22: *Extraktionsausbeuten (%) der temperaturabhängigen H_2SO_4-Extraktionen der FAZUC und FAHAG.*

7.5.4 H_3PO_4-Extraktion

Die Extraktion beider Flugaschen mit H_3PO_4 15% in einem zweiten Schritt nach der Extraktion mit HCl 5%, zeigt ähnliche Tendenzen wie die zweistufige Extraktion mittels H_2SO_4 (Abbildung 7-23). Der pH-Wert wird in der zweiten Stufe deutlich gesenkt und dadurch die Metallabreicherung erhöht. Der Filterkuchen konnte nur durch Zentrifugation von der Lösung getrennt werden und zudem entstand im Filtrat ein milchiger Niederschlag.

Tabelle 7-13: *Versuchsansatz der H_3PO_4-Extraktion. Es wurde 50 g Flugasche eingesetzt.*

Nr.	Bezeichnung	H_3PO_4	FF	Zeit	Temp.	Vorbehandlung	Nachwaschen FK
34	H_3PO_4/4/60/RT vw HCl 5%	15%	4	60 min	RT	HCl 5/4/60/RT	100 mL H_2O

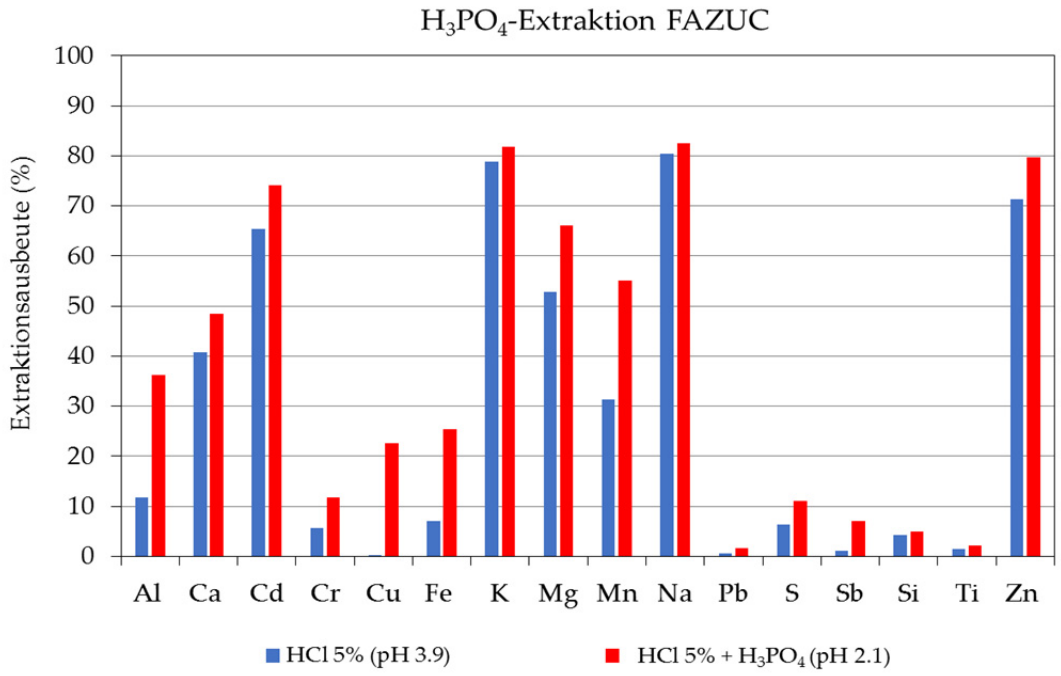

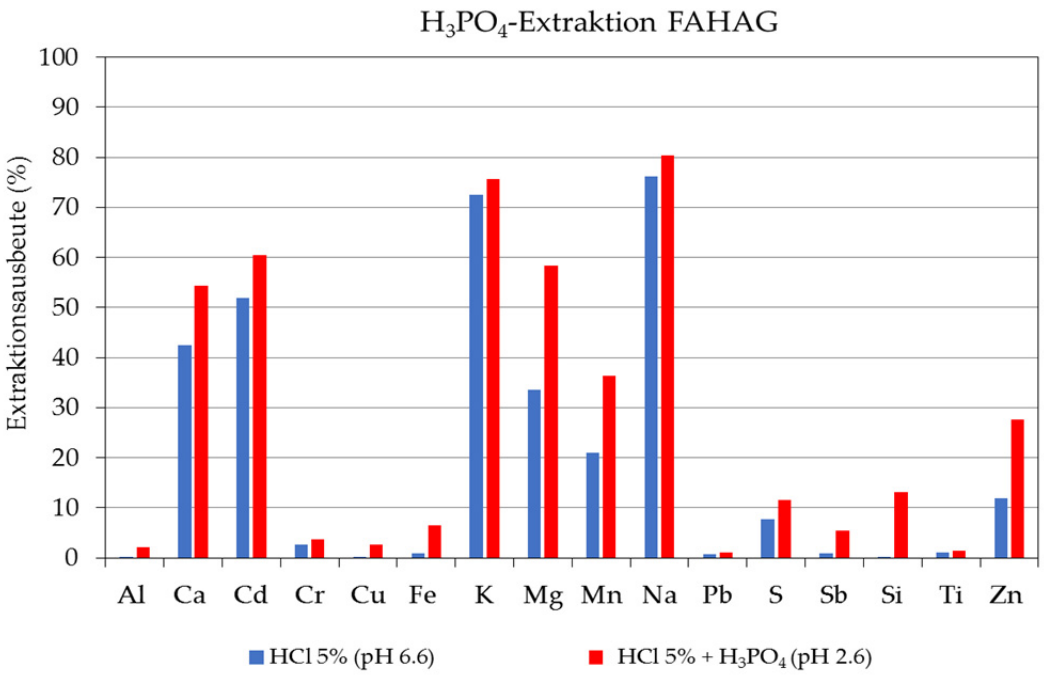

Abbildung 7-23: *Extraktionsausbeuten (%) der kombinierten HCl 5% und H_3PO_4-Extraktionen der FAZUC und FAHAG.*

7.5.5 NaOH-Extraktion

Extraktionsversuche im basischen Milieu wurden gewählt, um Erkenntnisse über das Verhalten der Aschen bei hohen pH-Werten (pH >12) zu erhalten (Hydroxidstabilitäten). Eine saure Umgebung vermag die FAHAG jeweils stärker zu puffern, was zu stark erhöhten pH-Werten in den Extraktionslösungen führt, verglichen zur FAZUC. Mit der Extraktion in basischer Umgebung befinden sich beide Aschen im gleichen pH-Bereich (pH 14) und die Prozesse können direkt verglichen werden (welche Reaktionen sind pH, welche Eh gesteuert?). Zudem erhofft man sich durch die Extraktion mit NaOH die amphoteren Metalle Zn und Pb selektiv zu extrahieren. Erste Analysen der basisch extrahierten Filterkuchen in einer internen Vorstudie zeigten zudem interessante Phasenneubildungen (Hydroxide) mittels XRD und das Aufkommen diverser identifizierbarer Cu-Phasen mittels REM.

Versuchsübersicht

Die in Tabelle 7-14 aufgelisteten Versuchsansätze wurden für die FAHAG sowie die FAZUC durchgeführt. Je 20 g Flugasche wurde pro Versuch eingesetzt und der Filterkuchen mit 4x 25 mL deionisiertem Wasser nachgewaschen. Der Wert des Flüssig-Fest-Verhältnisse wurde der Literatur entnommen (Nagib and Inoue, 2000). Der Versuch mit höher konzentrierter NaOH (20%) zu extrahieren scheiterte, da die Aschesuspension nicht mehr filtrierbar war. Die gemessenen Konzentrationen der Filtrate sind im Anhang

7B zusammen mit den H_2SO_4-Konzentrationen aufgelistet. Die detaillierten Versuchsprotokolle sind im Anhang 7A angefügt.

Tabelle 7-14: *Versuchsansätze der NaOH-Extraktionen. Jeweils 20 g Flugasche wurde eingesetzt.*

Nr.	Bezeichnung	NaOH	FF	Zeit	Temp.	Vor-behandlung	Nachwaschen
35	NaOH 10/15/60/RT	**10%**	15	60 min	RT	**-**	150 mL H_2O
36	NaOH 10/15/60/80	10%	15	60 min	**80°C**	-	150 mL H_2O
37	NaOH 10/15/60/RT vw H_2O	10%	15	60 min	RT	**H_2O/10/10/RT**	150 mL H_2O
38	NaOH 10/15/60/RT WW pH <3.5	10%	15	60 min	RT	-	**150 mL H_2O (pH <3.5)**

FAZUC:

- Mit NaOH 10% konnten 41% Zn und 26% Pb extrahiert werden (Abbildung 7-24).
- Mit zunehmender Temperatur konnte die Pb-Ausbeute auf 75% gesteigert werden.
- Das Vorwaschen mit H_2O ergibt tiefere Metall-Ausbeuten als das direkte Extrahieren mit NaOH.
- Alle Filtrate zeigen einen milchigen Niederschlag, welcher auch bei der Studie von Nagib and Inoue (2000) festgestellt wurde und als $Zn(OH)_2$ und $3PbO{\cdot}H_2O$ identifiziert wurde. Durch den Einsatz von HCl 2-5% anstelle von H_2O zum Nachwaschen des Filterkuchens konnte die Ausfällung verhindert werden.
- Das Nachwaschen mit HCl-angesäuertem Wasser (pH 0.5) in unseren Ansätzen führte dazu, dass nach den ersten 25 mL eine grosse Menge Portlandit und Ca-Zn-Hydroxid-Hydrat ausfielen (pH 13). Die anschliessenden 3x 25 mL Waschwasser führten zu klaren Lösungen und einer pH-Absenkung auf einen Wert von 12. Der Niederschlag löste sich beim Verdünnen mit HNO_3 1% komplett auf.

FAHAG:

- Mit NaOH 10% konnten 33% Zn und lediglich 6% Pb extrahiert werden.
- Mit einer Temperatur von 80°C konnte eine Ausbeute von 58% Zn und 48% Pb erreicht werden.
- Ähnlich wie bei der FAZUC entstand ein milchiges Filtrat und bei den ersten 25 mL des sauren Nachwaschens eine starke Ausfällung von Halit, Calcit und Sylvin.

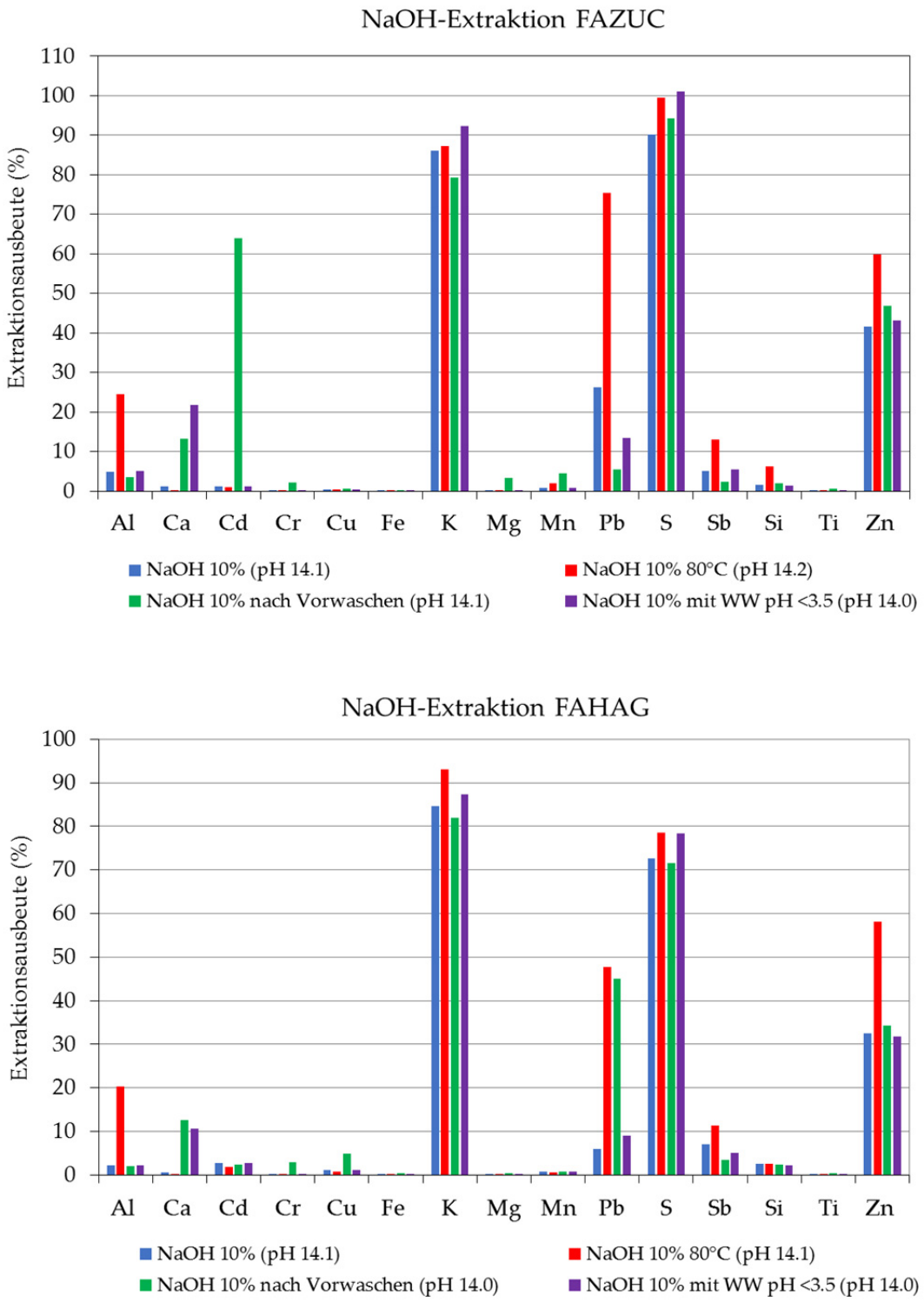

Abbildung 7-24: *Extraktionsausbeuten (%) der NaOH-Extraktionen der FAZUC und FAHAG.*

7.5.6 NH_4Cl-Extraktion

Die Extraktion mit NH_4Cl 15 g/L zeige nur sehr geringe Ausbeuten (siehe Anhang 7B) und es entstand eine starke Ausfällung im Filtrat welche viel Zn, Cl, K und Ca enthält. Die Resultate deuten darauf hin, dass:

- Nicht viel Metalle adsorbiert vorliegen und Oberflächen nicht reaktiv sind. Dies erstaunt nicht, da die Oberflächen der Aschepartikel hohe Temperaturen durchlebt haben und die Atome genügend Zeit hatten geeignete Bindungspartner zu suchen und sich auszurichten.
- Die extrahierten Alkalimetalle (Na, K) wurden durch das Wasser der NH_4Cl-Lösung mobilisiert.

Tabelle 7-15: *Versuchsansatz der NH_4Cl-Extraktion. Es wurde 50 g Flugasche eingesetzt.*

Nr.	Bezeichnung	NH_4Cl	FF	Zeit	Temp.	Nachwaschen FK
39	NH_4Cl/4/60/80	15 g/L	4	60 min	80°C	100 mL H_2O

7.5.7 Nachwaschen mit NaCl-Lösung

Die Filterkuchen FKZUC und FKHAG der HCl- (Versuch 15) und H_2SO_4- (Versuch 29) Versuche wurden nachträglich noch während 60 Minuten mit 300 g/L (5.1 mol/L) NaCl-Lösung (FF 5) bei 85°C und pH 4 nachgewaschen. Dadurch erhofft man sich v.a. eine Mobilisierung des Pb als Chlorid. Mittels REM-EDS wurde $PbCl_2$ in den Filterkuchen der HCl-Versuche nachgewiesen und durch das Extrahieren dieser Filterkuchen mit konzentrierter NaCl-Lösung könnte dieses Pb als $PbCl_3^-$ oder $PbCl_4^{2-}$ mobilisiert werden. Die Spezies $PbCl_3^-$ und $PbCl_4^{2-}$ treten in hoch-saliner Umgebung auf (>5 mol/L Cl), wie dies mittels Raman-Spektroskopie gezeigt werden konnte (GRS, 2012). Das Pb in den Filterkuchen der H_2SO_4-Versuchen liegt hauptsächlich gebunden als $PbSO_4$ vor könnte daher ebenfalls als Pb-Chlorid mobilisiert werden.

Versuchsansätze

Die in Tabelle 7-16 aufgelisteten Versuchsansätze wurden für die FAZUC sowie FAHAG durchgeführt. Je 10 g des Filterkuchens aus der HCl- und H_2SO_4-Extraktion wurde pro Versuch eingesetzt.

Tabelle 7-16: *Versuchsansätze der NaCl-Extraktionen. Jeweils 10 g Flugasche wurde eingesetzt.*

Nr.	Bezeichnung	NaCl	FF	Zeit	Temp.	pH	Vorbehandlung	Nach-waschen
40	NaCl/5/60/85 vw HCl 5%	300 g/L	5	60 min	85°C	4	HCl 5/4/60/RT	50 mL H_2O 85°C
41	NaCl/5/60/85 vw H_2SO_4 6.6%	300 g/L	5	60 min	85°C	4	H_2SO_4 6.6/4/60/RT	50 mL H_2O 85°C

FAZUC:

- Erste Resultate zeigen, dass das Extrahieren mit stark konzentrierter NaCl-Lösung grosse Mengen Pb mobilisiert (Abbildung 7-25). Mit dem Nachbehandeln des Filterkuchens aus dem HCl-Versuch (Versuch 40) wird eine Extraktionsausbeute von 59% erreicht. Das Nachbehandeln des Filterkuchens des H_2SO_4-Versuchs (Versuch 41) führt zur Pb-Abreicherung von 67%.
- Die Extraktion mit NaCl führt weiter zur Mobilisierung von 45% (Versuch 40) resp. 16% (Versuch 41) Cu. Eine bläuliche Ausfällung entstand im Filtrat der beiden Versuche, was einen Hinweis auf Kupferchlorid ist ($CuCl_2 \cdot 2H_2O$).
- Die Ausbeuten für Cd und Zn erhöhten sich ebenfalls noch etwas auf Werte >70%.

FAHAG:

- Aufgrund der starken Pufferkapazität musste der pH-Wert während der Extraktion konstant nachjustiert werden. Bei der Zugabe der Säure gab es grosse Schaumentwicklung und der pH-Wert stieg sofort wieder an und pendelte sich konstant auf 5.6 ein.
- Die generell tieferen Metallkonzentrationen und der höhere pH-Wert führen dazu, dass weder Pb noch Cu durch das Nachbehandeln mittels NaCl mobilisiert werden können. Einzig Zn zeigt erhöhte Ausbeuten von 40% (Versuch 40) resp. 50% (Versuch 41).
- Um das Potential der NaCl-Extraktion für FAHAG besser abschätzen zu können, müssen in einem weiteren Schritt die für die Pufferung zuständigen Komponenten (CaO, $CaCO_3$ etc.) durch die Zugabe von Säure komplett eliminiert werden. Dies erlaubt anschliessend das Einstellen des pH-Wertes auf 4.

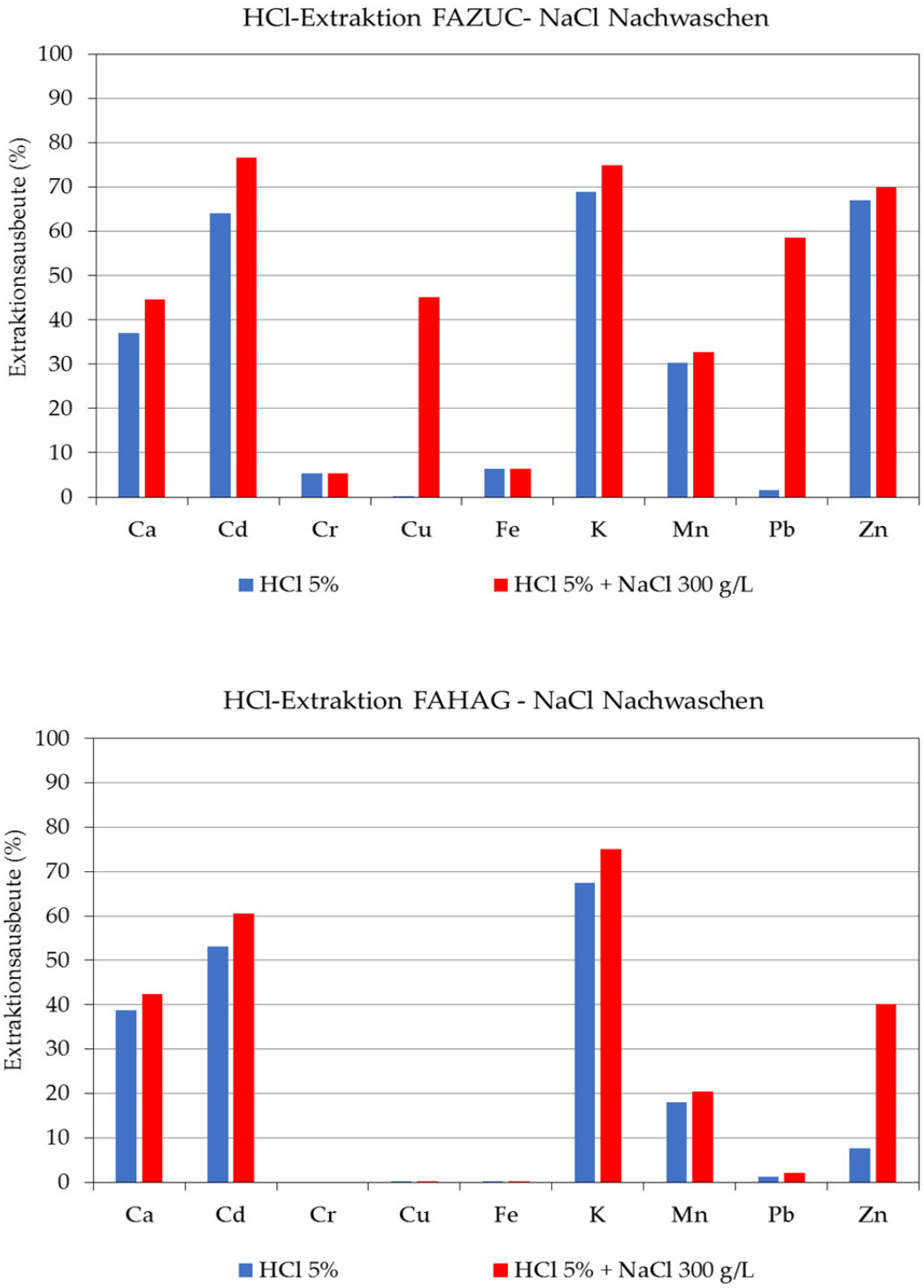

Abbildung 7-25: *Extraktionsausbeuten (%) der NaCl-Extraktionen der FAZUC und FAHAG. Vorgewaschen mit HCl 5% und jeweils Nachgewaschen mit NaCl 300 g/L.*

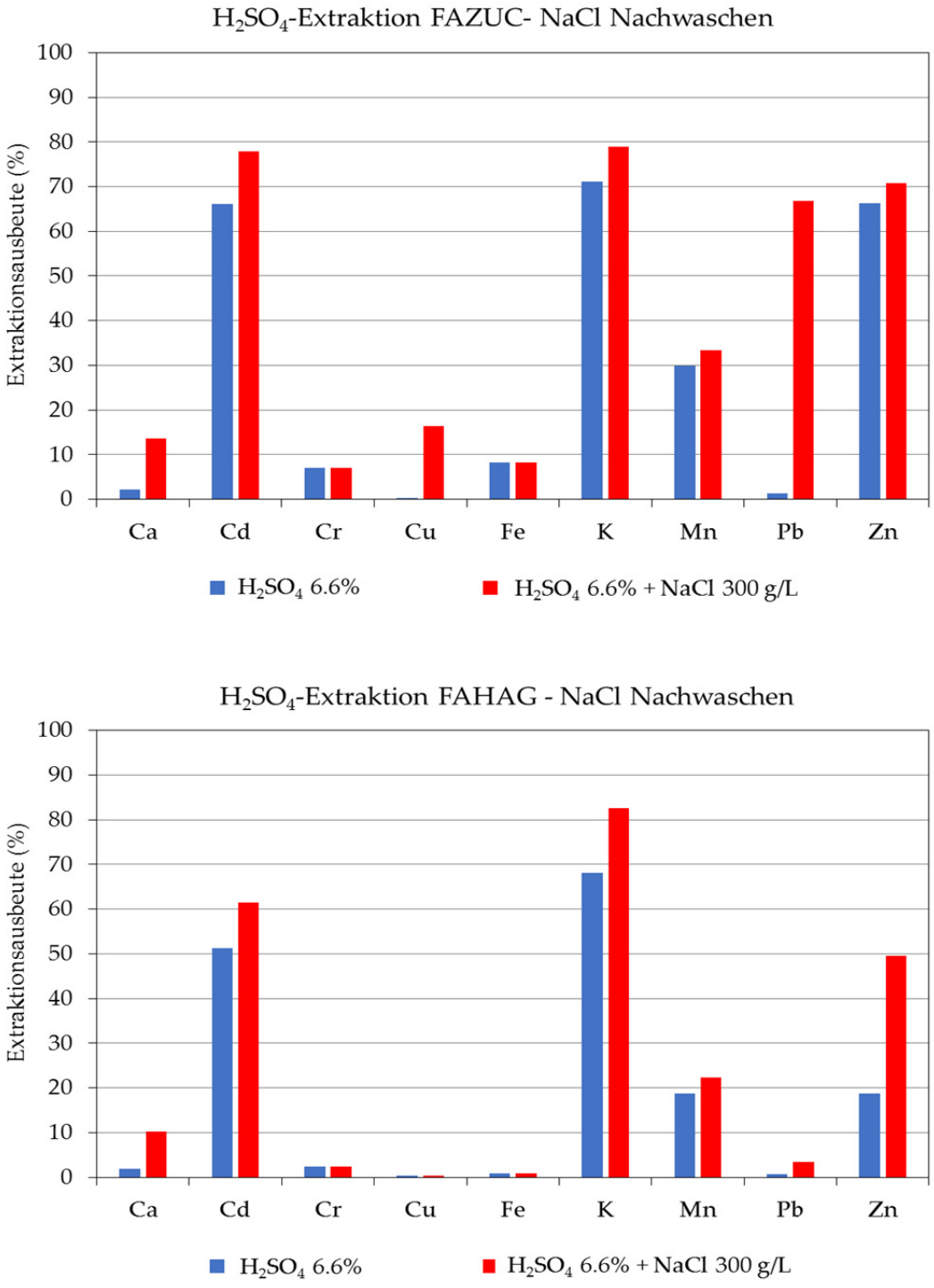

Abbildung 7-26: *Extraktionsausbeuten (%) der NaCl-Extraktionen der FAZUC und FAHAG. Vorgewaschen mit H_2SO_4 6.6% und jeweils Nachgewaschen mit NaCl 300 g/L.*

7.5.8 Erkenntnisse aus den Extraktionsversuchen

Die Studie deckt zwei extreme Vertreter von Flugaschetypen ab. Bei der alkalischen und eher schwermetallarmen FAHAG dominiert bei der Extraktion das Karbonatsystem und zeigt dadurch eine deutlich höhere Pufferkapazität verglichen zur schwermetallreichen FAZUC. Während sich bei FAZUC mit H_2O ein pH-Wert im neutralen Bereich (pH 6.5) einstellt, erreicht FAHAG pH >12. Durch die Extraktion mit HCl wird bei der FAZUC der gesamte Kalzit gelöst, bei FAHAG hingegen liegt noch 50-60% vom initialen Kalzit im Filterkuchen vor. Dies führt zu einer deutlich tieferen Metallabreicherung. Die Art der verwendeten Säure wirkt sich auf die Mobilisierung allerdings kaum aus, bei gleicher Säurestärke zeigen HCl, H_2SO_4 und H_3PO_4 sehr ähnliche Resultate.

Die HCl-Extraktionen im Labor kommen dem FLUWA-Verfahren auf der Anlage sehr nahe. Es zeigte sich, dass ohne den Einsatz von H_2O_2 grosse Mengen von Metall-haltigen Zementierungsphasen im Filterkuchen vorliegen ($PbCu^0$-Legierung) welche hauptsächlich dafür verantwortlich sind, dass kaum Pb und Cu abgereichert werden. Weiter wurde im Filterkuchen $PbCl_2$ identifiziert wobei die Menge sich mit zunehmender Extraktionszeit stark erhöhte. Die zeitabhängigen Versuche mit HCl zeigen weiter, dass ab einer Extraktionsdauer von 3 h die Zementierungsphasen ($PbCu^0$) bei der FAZUC rückgelöst werden. Das Nachwaschen des Filterkuchens mit saurem Waschwasser (pH 1 und 2) nach der Extraktion mit HCl 5% zeigte keine zusätzliche Lösung von Metallen verglichen zum neutralen Nachwaschen. Dies kann durchaus positiv gewertet werden, da eine spätere Metall-Mobilisierung auf der Deponie nicht zu erwarten ist.

Die starke Gipsbildung bei der Extraktion mit H_2SO_4 scheint nur untergeordnet einen Einfluss auf die Mobilisierbarkeit der Metalle zu haben, da bei gleicher Säurestärke sehr ähnliche Extraktionsausbeuten erreicht werden wie mit HCl. Die Versuche mit H_2SO_4 lösen Pb welches anschliessend mit dem SO_4 zu $PbSO_4$ reagiert und sich im Filterkuchen ansammelt. Durch die Bildung von $PbSO_4$ wird die Zementierung von Pb mit Cu zu $PbCu^0$ verhindert. Für einen grosstechnischen Einsatz von H_2SO_4 bei einer zentralen Aufbereitung der Flugaschen spricht der tiefere Preis (zweiprotonige Säure, 98 prozentig) und die geringeren Abwasserfrachten verglichen zur Salzsäure. Hingegen sind die Deponiekosten des Filterkuchens durch die starke Gipsbildung höher und eine Gipsverwertung wäre kaum möglich.

Die Nachbehandlung der Filterkuchen aus den HCl- und H_2SO_4-Versuchen mit NaCl-Lösung (300 g/L) führt bei FAZUC zur Mobilisierung grosser Mengen Pb und Cu, wie sie sonst nur durch den Einsatz von H_2O_2 erreicht werden können. Durch die Interaktion des Filterkuchens mit hoch-saliner Lösung bei einer Temperatur von 85°C kann das vorhandene Pb ($PbCl_2$ und $PbSO_4$) als $PbCl_3^-$ und $PbCl_4^{2-}$ mobilisiert werden. Für die Identifikation der chemischen Prozesse und vorhandenen Pb-Chlorid Spezies müssen weitere Versuchsserien durchgeführt werden und die Resultate durch geochemische Modellierungen unterstützt werden.

7.6 Mechanische Separationsversuche

7.6.1 Magnetseparation

Mit dem Frantz-Magnetseparator (siehe Kapitel 7.3.5) konnte eine magnetische Fraktion von <10% abgetrennt werden, welche mikroskopisch und chemisch mittels ICP-MS (Actlabs, CAN, Anhang 7B) charakterisiert wurde.

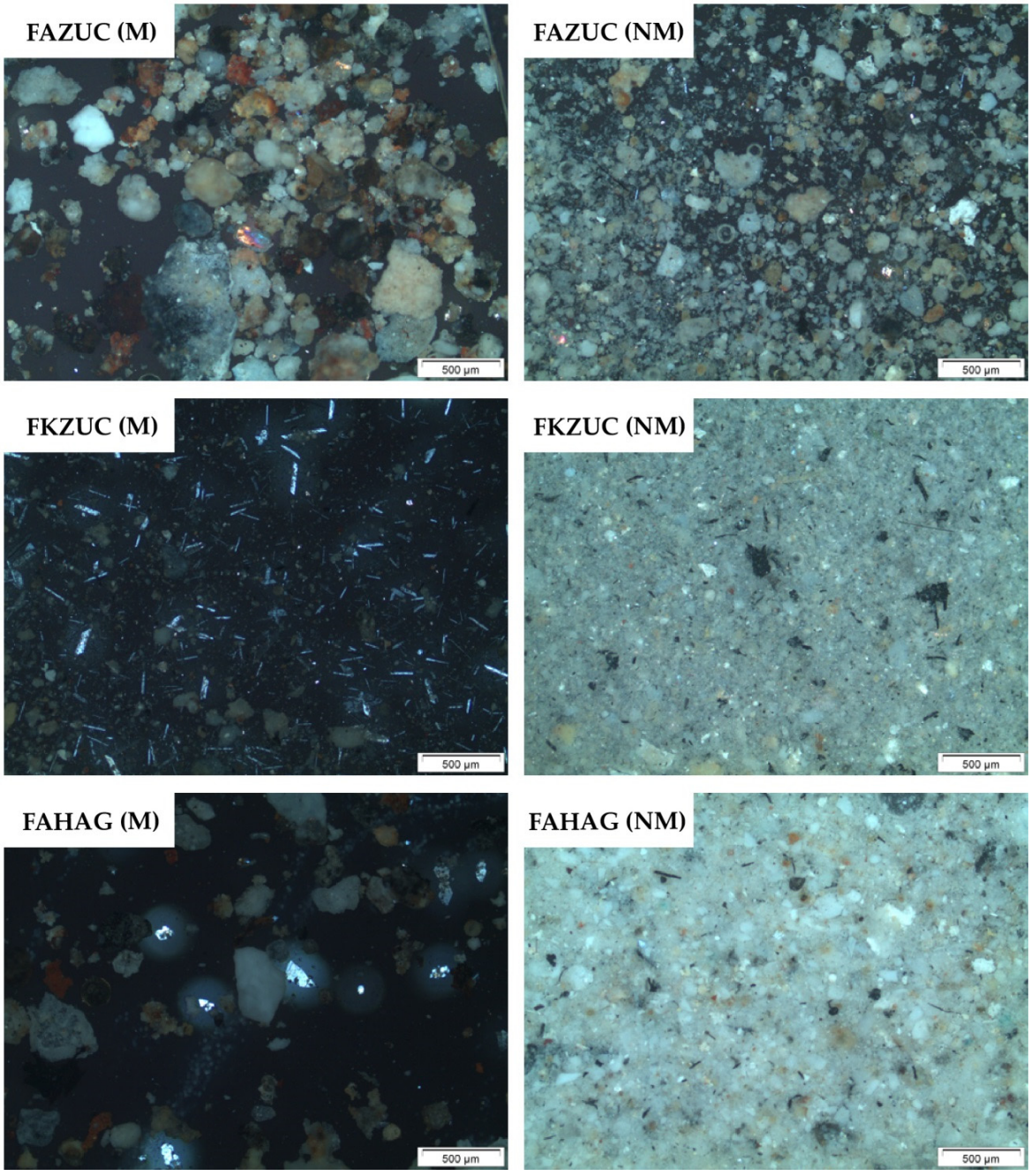

Abbildung 7-27: *Magnetische (M) und nicht-magnetische (NM) Fraktionen unter dem Auflichtmikroskop.*

Die Analysen der Rückstände aus der Magnetseparation zeigen primär eine starke Anreicherung an Fe (Tabelle 7-17). Seltene und wertvolle Elemente scheinen sich hingegen nicht signifikant angereichert zu haben (siehe auch Kapitel 7.7). Der grosse apparative und zeitliche Aufwand für die Magnetseparation mittels Frantz-Separator scheint sich nicht auszubezahlen, da die Resultate sehr ähnlich ausfallen wie mittels starkem Permanentmagneten der in die Aschesuspension gehalten wurde.

Tabelle 7-17: *Chemische Analyse ausgewählter Elemente der Ausgangsasche (FAZUC) und der separierten Konzentrate mittels Frantz Magnetseparator (FAZUC F) und mittels Eintauchen eines Permanentmagneten in die Aschesuspension (FAZUC M). Die Tabelle mit dem kompletten Datensatz ist im Anhang 7B angefügt.*

Bezeichnung	**Ag**	**Al**	**Bi**	**Cd**	**Ce**	**Co**	**Cr**	**Cu**	**Fe**	**Ga**	**Gd**	**Ge**
	mg/kg	gew.%	mg/kg	mg/kg	mg/kg	mg/kg	mg/kg	mg/kg	gew.%	mg/kg	mg/kg	mg/kg
FAZUC	59.1	2.81	123	305	15.6	39.1	250	2'130	1.39	5.4	0.9	0.1
FAZUC F	62.4	4.28	109	147	41.3	231	1'420	2'370	13	<0.1	2.4	<0.1
FAZUC M	38.6	4.75	62.7	114	42	189	1'280	2'020	13.5	0.7	2.2	<0.1
Element	**In**	**Mn**	**Mo**	**Nd**	**Ni**	**Rb**	**Sb**	**Se**	**Sr**	**Te**	**V**	**Y**
	mg/kg	mg/kg	mg/kg	mg/kg	mg/kg	mg/kg	mg/kg	mg/kg	mg/kg	mg/kg	mg/kg	mg/kg
FAZUC	2.2	670	13.9	8	133	64.7	392	5.4	211	0.2	13	4.8
FAZUC F	1.6	2'000	76	39.2	1'010	18.3	286	12	335	16	50	13.8
FAZUC M	0.7	2'260	80.3	45.8	1'080	13.3	83.3	0.3	364	0.9	57	13.6

7.6.2 Siebversuche

Bestimmung der optimalen Siebdauer

Es ist offensichtlich, dass v.a. die unbehandelten Flugaschen mehrere Stunden bei tiefer Amplitude gesiebt werden müssen, damit sich ein Gleichgeweicht einpendelt.

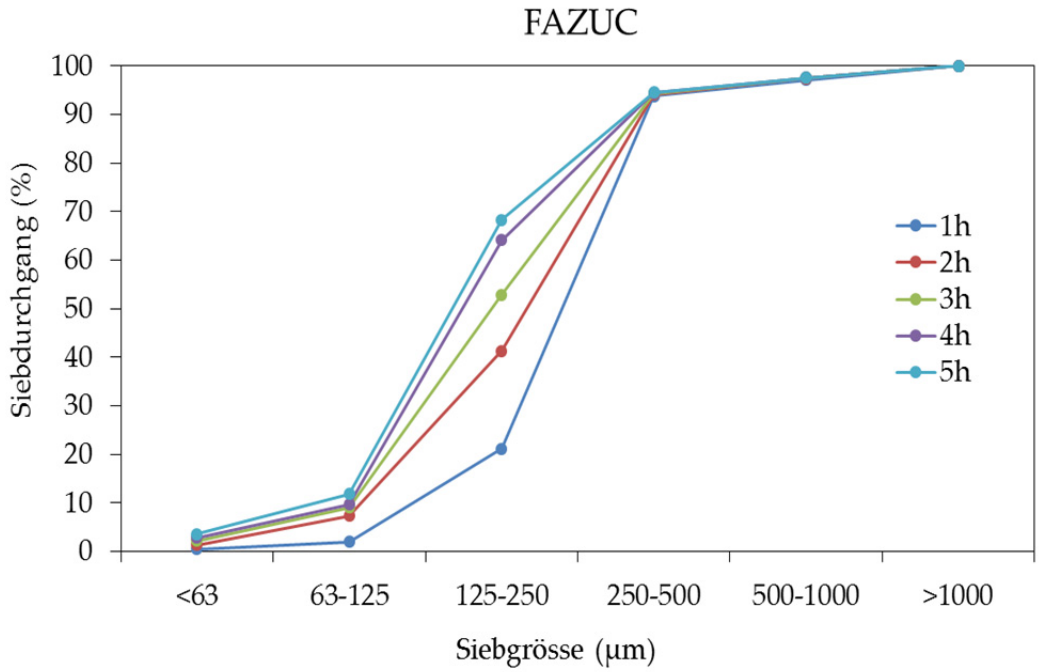

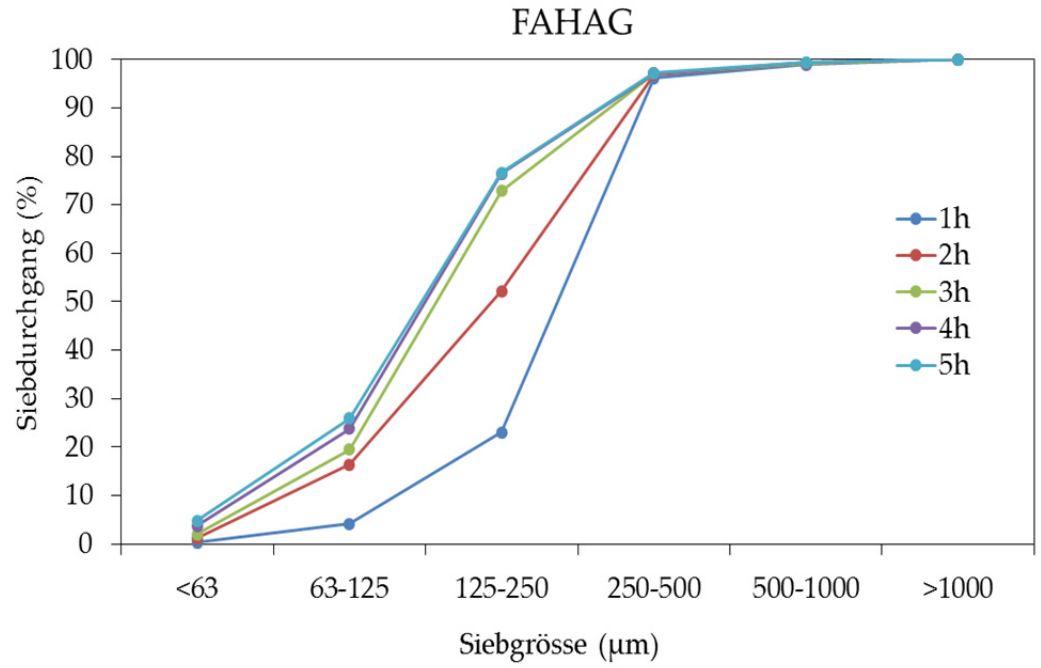

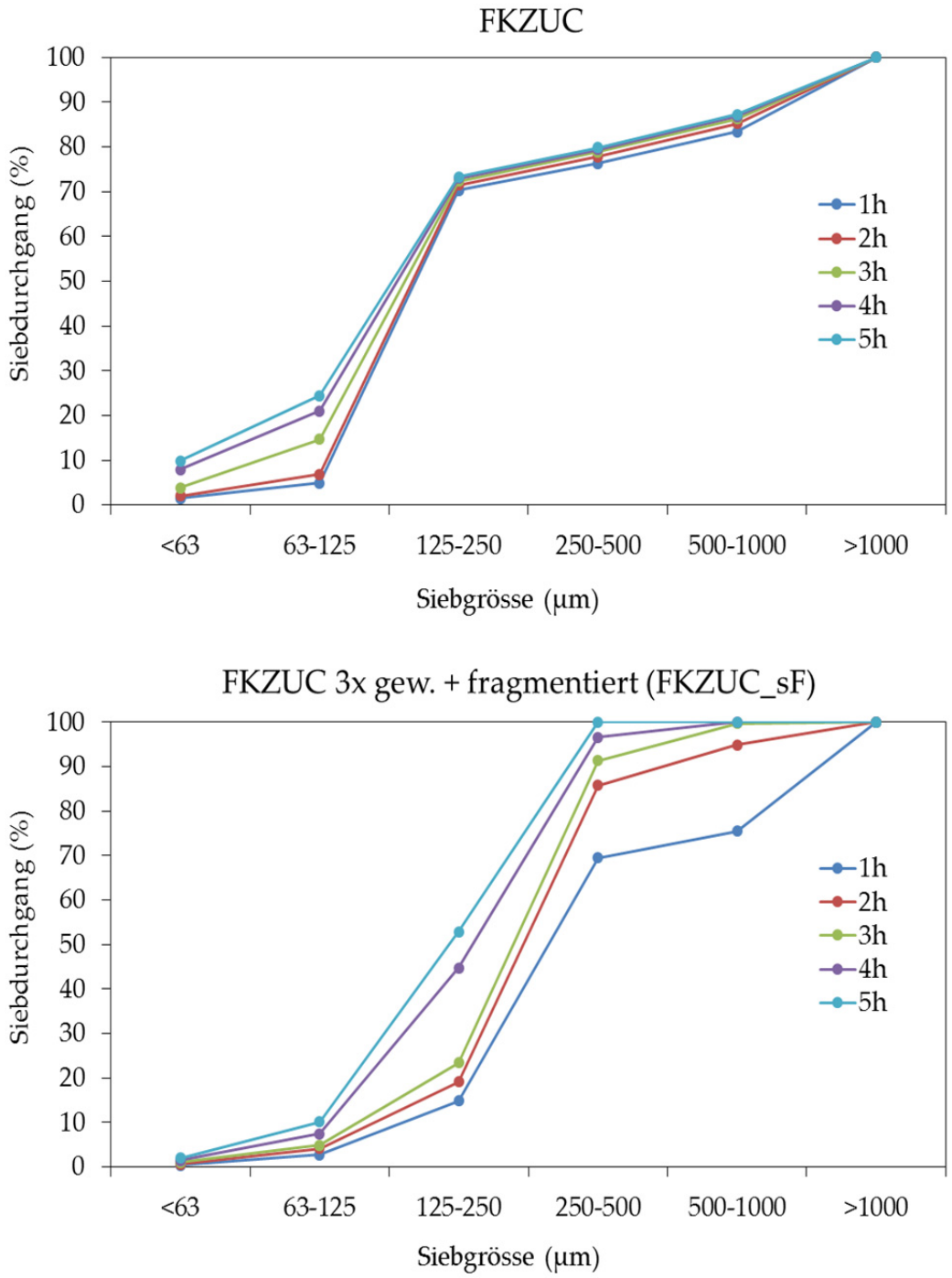

Abbildung 7-28: *Siebkurven von 1-5 h für die FAZUC und FAHAG sowie den Filterkuchen FKZUC und den fragmentierten Filterkuchen FKZUC_sF.*

Chemische Analysen der Siebfraktionen

Die Verschiedenen Siebfraktionen wurden mittels Säuretotalaufschluss in Lösung gebracht und mit ICP-OES analysiert.

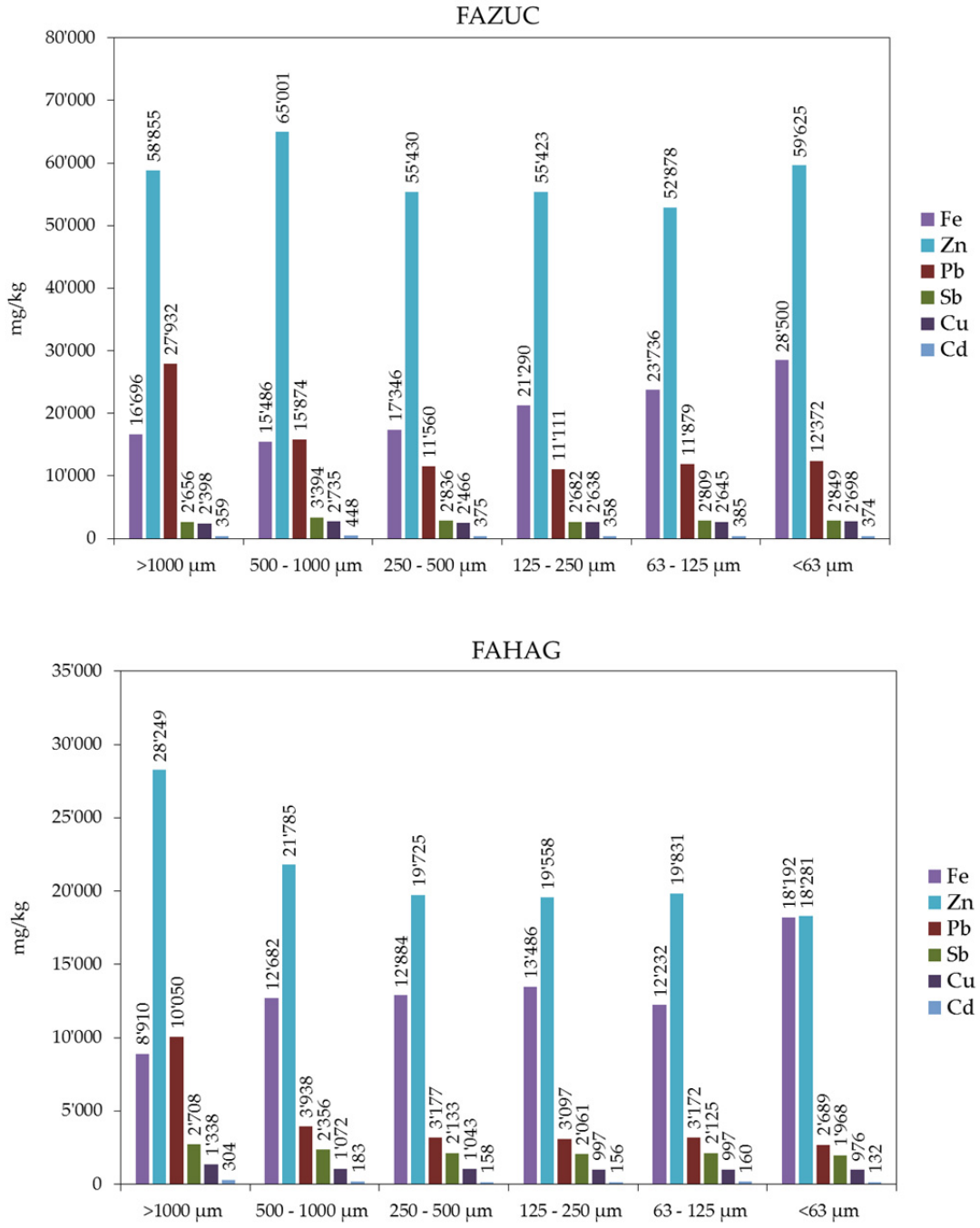

Abbildung 7-29: *Metallgehalte der einzelnen Siebfraktionen der FAZUC und FAHAG.*

Abbildung 7-30: *Blei- und Zinkgehalte der einzelnen Siebfraktionen.*

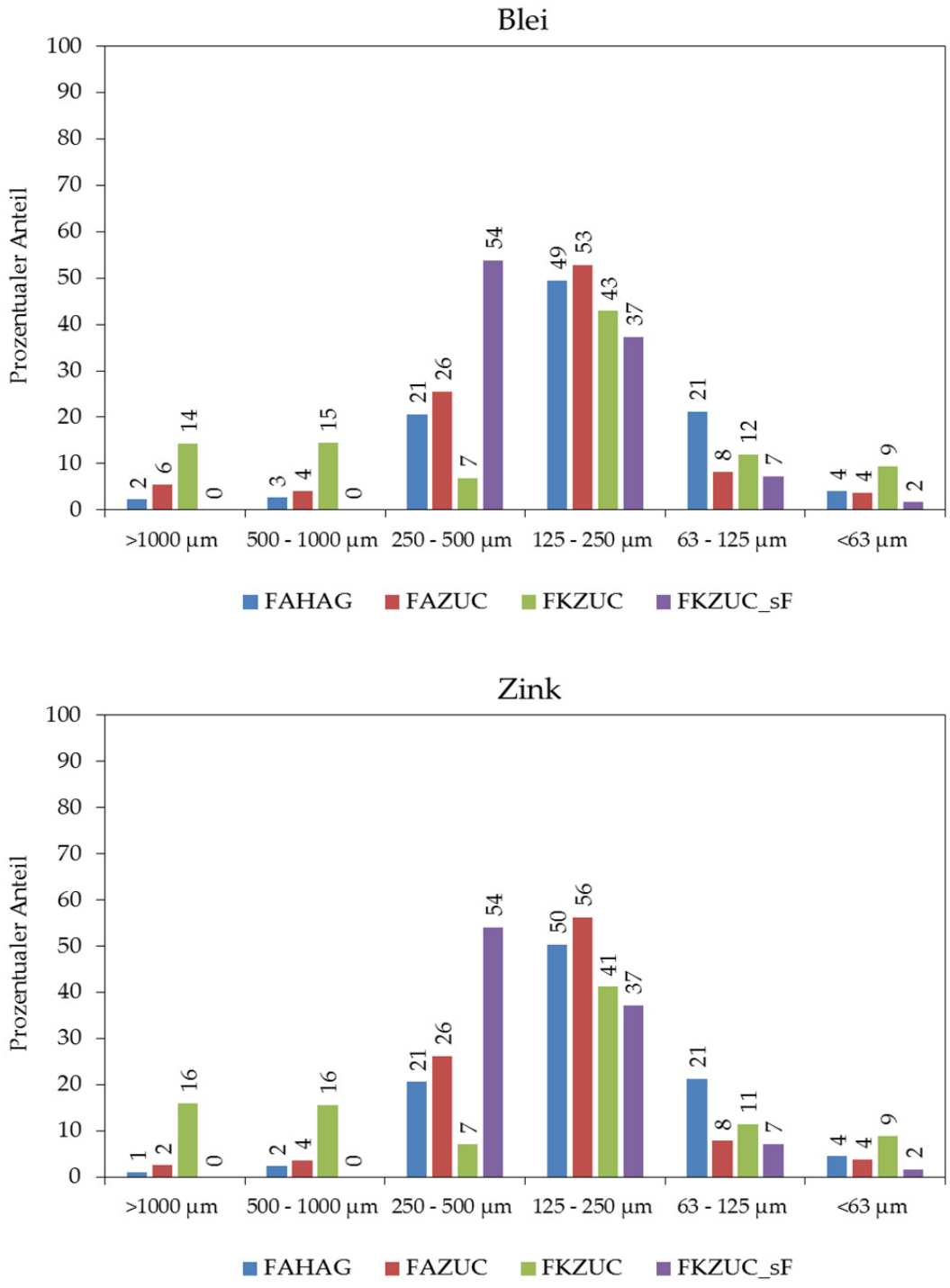

Abbildung 7-31: *Prozentuale Anteile der Metalle Pb und Zn verteilt innerhalb der Korngrössenfraktionen.*

7.6.3 Korngrössenverteilung

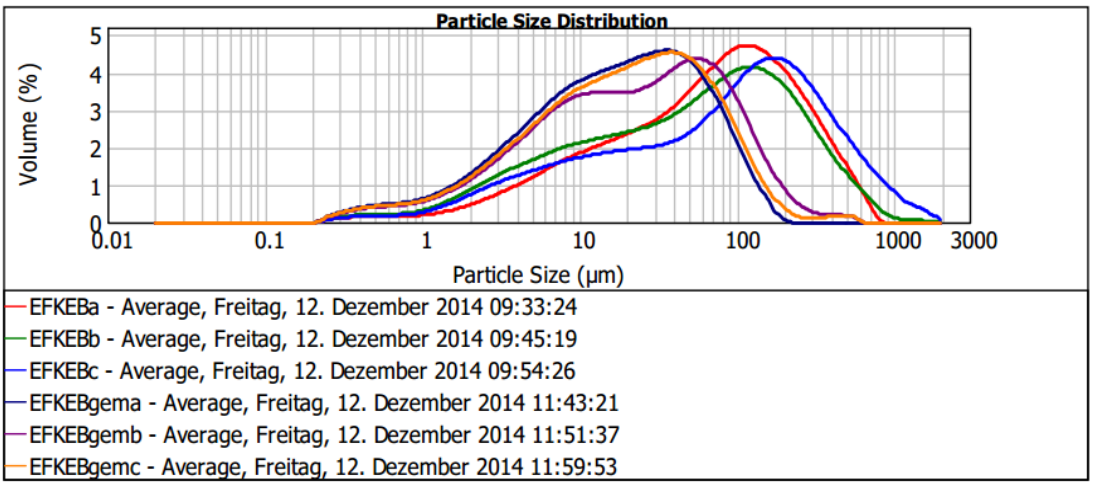

Abbildung 7-32: *Korngrössenverteilung der FAZUC gemahlen und ungemahlen.*

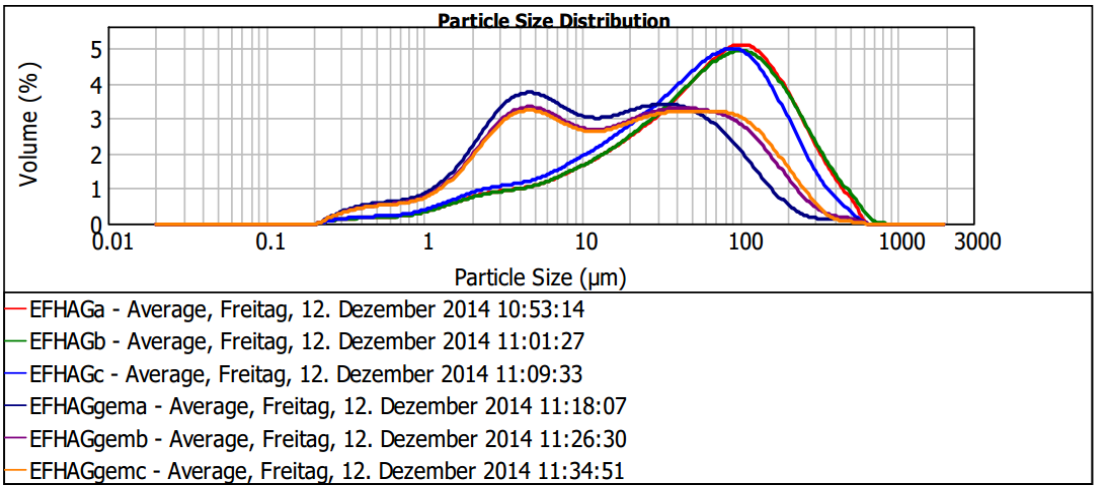

Abbildung 7-33: *Korngrössenverteilung der FAHAG gemahlen und ungemahlen.*

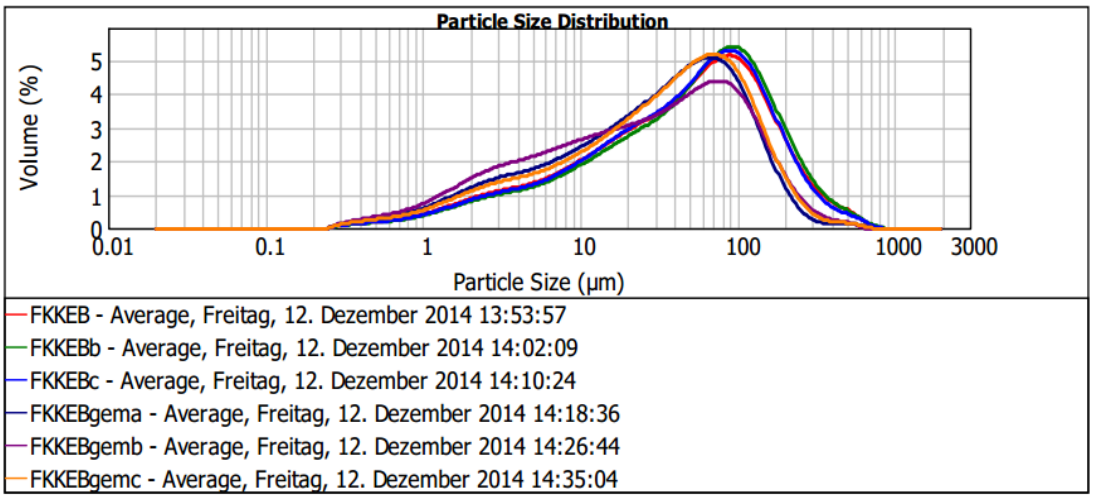

Abbildung 7-34: *Korngrössenverteilung der FCZUC gemahlen und ungemahlen.*

7.7 Seltene und wertvolle Elemente

Nebst den Hauptmetallen (Al, Fe, Zn, Pb, Cu, Cd) wurden zusätzlich noch seltene und wertvolle Elemente untersucht die in den Flugaschen relativ zur Schlacke angereichet sind (Transferkoeffizient >10%, Morf et al., 2013). Dafür wurden die FAZUC und FAHAG sowie ausgewählte Filterkuchen aus den Extraktionsexperimenten und zwei Konzentrate aus den mechanischen Anreicherungsversuchen (FAZUC F, M) von Actlabs, CAN mittels ICP-MS analysiert (Code: Ultratrace 4, Anhang 7B). Durch den Massenverlust während der Extraktion sind die gemessenen Konzentrationen in den Filterkuchen relativ angereichert. Um die Filterkuchen mit den Ausgangsaschen vergleichen zu können, wurden die gemessenen Werte durch den Faktor der Aufkonzentrierung dividiert (siehe Kapitel Massenverlust und Massenbilanz des jeweiligen Extraktionsmittels). Die Rohdaten mit allen analysierten Elementen sind im Anhang 7B angefügt.

Generell liegen die ausgewählten Elemente in beiden Aschen in relativ geringen Konzentrationen vor (<100 mg/kg). Die diversen Extraktionsversuche bewirkten nur sehr geringe Abreicherungen, welche teilweise innerhalb der Messunsicherheit liegen. Die mechanische Separation mittels Frantz-Magnetseparator zeigt keine signifikante Aufkonzentrierung seltener und wertvoller Elemente.

Tabelle 7-18: *Konzentrationen (mg/kg) seltener und wertvoller Elemente in Flugaschen, Filterkuchen und magnetischen Separaten. Die Konzentrationen der Filterkuchen wurden aufgrund des Massenverlustes korrigiert.*

Nr.	Bezeichnung	Ag	Bi	Ga	Ge	In	Rb	Se	Te	Y	Zr
-	FAZUC	59	123	5.4	0.1	2.2	65	5.4	0.2	4.8	42
-	FAHAG	33	40	0.1	0.1	1.0	45	2.9	0.3	7.5	52
2	ZUC H_2O/10/10/RT	62	140	7.8	0.1	2.2	13	4.8	0.2	5.7	52
15	ZUC HCl 5/4/60/RT	65	100	9.1	0.1	2.3	20	5.1	0.2	2.9	28
25	ZUC HCl 5/4/6 h/RT	28	91	9.2	0.1	1.6	23	5.1	0.2	2.6	32
29	ZUC H_2SO_4 6.6/4/60/RT	60	114	8.7	0.1	2.0	21	5.1	0.2	3.9	44
31	ZUC H_2SO_4 6.6/4/60/RT vw HCl 5%	51	82	4.8	0.1	1.4	7.9	4.1	0.1	1.8	51
36	ZUC NaOH 10/15/60/80	61	142	0.1	0.1	2.3	4.3	0.2	0.1	5.9	71
2	HAG H_2O/10/10/RT	31	47	0.1	0.1	1.0	8	3.0	0.4	9.0	68
15	HAG HCl 5/4/60/RT	34	21	3.7	0.1	0.9	15	2.9	0.3	6.8	53
29	HAG H_2SO_4 6.6/4/60/RT	33	41	4.5	0.1	0.9	17	2.8	0.1	6.6	74
31	HAG H_2SO_4 6.6/4/60/RT vw HCl 5%	29	45	5.1	0.1	0.8	8.8	2.9	0.1	6.1	12
36	HAG NaOH 10/15/60/80	36	60	0.1	0.1	1.0	3.1	0.1	0.1	9.3	68
-	FAZUC F	62	109	0.1	0.1	1.6	18	1.2	1.6	14	15
-	FAZUC M	39	63	0.7	0.1	0.7	13	0.3	0.9	14	42

7.8 Ausblick

Mit dem vorliegenden Bericht wird ein breites Spektrum an chemischen und physikalischen Versuchen zur Optimierung der Schwermetallextraktion von Flugaschen abgedeckt und die Resultate dienen als Grundlage für geochemische Modellierungen, um die Prozesse und Phasensysteme auch theoretisch abzustützen. Dabei werden ablaufende chemische Reaktionen sowie das Puffer- und Löslichkeitsverhalten und die Temperaturabhängigkeit der (metallhaltigen) Phasen abgebildet und auf ein Optimierungspotential diskutiert. Die direkte Messung des Redoxpotentials ist bei den vorliegenden Lösungen kaum möglich. Obwohl in der Literatur (Van Herck et al., 2000) der Einfluss des Redoxpotentials nur untergeordnete Bedeutung zugeschrieben wird, soll dies mit den thermodynamischen Berechnungen betrachtet werden. Diese Grundlagen bieten zudem die Möglichkeit das Langzeit-Verhalten unterschiedlich abgereicherten Filterkuchen über 100-1'000 Jahre abzuschätzen und zu vergleichen. Auf der technisch-analytischen Seite gilt es noch diverse Fragen zu klären, bzw. sind in Bearbeitung, um die anstehenden Werkversuche möglichst gut abgestützt zu realisieren. Metallisches Al^0 ist hauptsächlich verantwortlich für den Zementierungsprozess (Reduktive Abscheidung von Cu, Pb). Die Quantifizierung dieses Al^0 in den Flugaschen und Filterkuchen wird z.Z. in Zusammenarbeit mit der FHNW in Muttenz durchgeführt. Dabei werden Epoxy-Präparate der Aschen mittels μXRF Mapping quantitativ erfasst. Die Resultate dieser Studie zeigen, dass grosstechnisch für die Optimierung des FLUWA-Verfahrens im Wesentlichen der pH/Säureverbrauch und die Redoxbedingungen die bestimmenden Parameter sind. Folgende Ansätze sind dabei grosstechnisch möglich:

- Tieferer pH-Wert, z.B. pH <1/1.5/2.0/2.5 für 30 Minuten, dann Einstellen des Filtrations-pH-Wertes, z.B. 3.0/3.5/4.0.
- Effizienzsteigerung der Oxidation (Peroxiddosierung, Sauerstoffzugabe).
- Messung/Kontrolle/Optimierung des Redox-Potentials.

Zudem zeigt das nachträgliche Extrahieren der Filterkuchen aus den HCl- und H_2SO_4-Versuchen mit NaCl-Lösung vielversprechende Extraktionsausbeuten für Pb und Cu. Das Waschen der Filterkuchen mit stark Chlorid-haltiger Lösung könnte grosstechnisch realistisch sein, was durch den Einsatz von NaCl und Rückführung von Cl-haltigem Wasser nach der Abwasserbehandlung im Kreislauf realisiert werden könnte. Dieser Ansatz scheint vielversprechend und wird deshalb weiterverfolgt. Anhand von zusätzlichen Laborversuchen mit anschliessender Charakterisierung der Filterkuchen (XRF, XRD, REM) und Filtrate (ICP-OES, UV/VIS Spektroskopie) sowie unterstützenden Modellierungen sollen die chemischen Prozesse erkannt und die Chlorid-Spezies identifiziert werden (Kapitel 4). Ende 2016 sind 1-2 grosstechnische Versuche geplant, wobei die Erkenntnisse aus den neuen Laborversuchen helfen werden die Rahmenbedingungen zu definieren (Kapitel 8).

Referenzen

Abbas, Z., Moghaddam, A.P., Steenari, B.M., 2003. Release of salts from municipal solid waste combustion residues. Waste Management 23, 291-305.

GRS, Gesellschaft für Anlagen- und Reaktorsicherheit, 2012. Entwicklung eines thermodynamischen Modells für Zink, Blei und Cadmium in salinaren Lösungen.

Holleman, A.F., Wiberg, E., 2007. Lehrbuch der Anorganischen Chemie, 102 ed.

Karlfeldt, K., Steenari, B.M., 2007. Assessment of metal mobility in MSW incineration ashes using water as the reagent. Fuel 86, 1983-1993.

Morf, L.S., Gloor, R., Haag, O., Haupt, M., Skutan, S., Di Lorenzo, F., Böni, D., 2013. Precious metals and rare earth elements in municipal solid waste-sources and fate in a Swiss incineration plant. Waste Management 33, 634-644.

Nagib, S., Inoue, K., 2000. Recovery of lead and zinc from fly ash generated from municipal incineration plants by means of acid and/or alkaline leaching. Hydrometallurgy 56, 269-292.

Parkhurst, D.L., Appelo, C.A.J., 2013. Description of Input and Examples for PHREEQC Version 3 — A computer program for speciation, batch-reaction, one-dimensional transport, and inverse geochemical calculations. U.S. Geological Survey Techniques and Methods Book 6, 497.

Schlumberger, S., Schuster, M., Ringmann, S., Koralewska, R., 2007. Recovery of high purity zinc from filter ash produced during the thermal treatment of waste and inerting of residual materials. Waste Management & Research 25, 547-555.

Bundesamt für Umwelt, 2016. Verordnung über die Vermeidung und die Entsorgung von Abfällen (VVEA). 1-46.

Takeno, N., 2005. Atlas of Eh-pH diagrams intercomparison of thermodynamic databases. National Institute of Advanced Industrial Science and Technology Tokyo, 285.

Van Herck, P., Van der Bruggen, B., Vogels, G., Vandecasteele, C., 2000. Application of computer modelling to predict the leaching behaviour of heavy metals from MSWI fly ash and comparison with a sequential extraction method. Waste Management 20, 203-210.

Vehlow, J., Braun, H., Horch, K., Merz, A., Schneider, J., Stieglitz, L., Vogg, H., 1990. Semi-technical demonstration of the 3-R Process. Waste Management & Research 8, 461-472.

Anhang 7A: Extraktionsprotokolle

Tabelle A7-1: *H_2O-Versuche FAZUC.*

		Flüssig-Fest-Variation				Oberfläche	Zeitabhängigkeit				Temperaturabhängigkeit			Nachwaschen*
Nr.		1	2	3	4	5	6	7	8	9	10	11	12	13
Bezeichnung		ZUC	ZUC	ZUC	ZUC	ZUC	ZUC	ZUC	ZUC	ZUC	ZUC	ZUC	ZUC	ZUC
Feststoffanalytik		H_2O/2/10/RT	H_2O/10/10/RT	H_2O/20/10/RT	H_2O/400/10/RT	H_2O/10/10/RT g	H_2O/10/30/RT	H_2O/10/60/RT	H_2O/10/3h/RT	H_2O/10/8.5h/RT	H_2O/10/10/40	H_2O/10/10/60	H_2O/10/10/80	H_2O/10/10/RT nw
			x		x					x			x	
Versuchsbedingungen														
Aufbereitung/Nachbehandlun						**gemahlen**								Nachgewaschen
Flüssig-Fest-Verhältnis		**2**	**10**	**20**	**400**	10	10	10	10	10	10	10	10	10
Asche	g	20	20	20	20	20	20	20	20	20	20	20	20	20
Wasser	ml	40	200	400	8000	200	200	200	200	200	200	200	200	200
Grösse Becherglas	mL	100	400	1000	Plastikkübel	400	400	400	400	400	400	400	400	400
Zeit	min/h	10 min	10 min	10 min	10 min	10 min	**30 min**	**60 min**	**3h**	**8.5**	10 min	10 min	10 min	10 min
Temperatur	°C	RT	RT	RT	RT	RT	RT	RT	RT	RT	**40°**	**60°**	**80°**	RT
Massenbilanz														
Einwage FA	g	20.01	20.09	20.08	20.01	20.01	20.02	20.01	20.05	20.01	20.08	20.07	20.04	20.00
Gewicht Filter	g	0.20	0.23	0.17	0.37	0.19	0.19	0.19	0.20	0.20	0.19	0.18	0.18	0.37
Tara Schale	g	65.08	58.03	69.50	70.10	75.26	67.68	60.47	59.30	52.95	67.68	66.11	59.31	67.42
Brutto FK nass	g		97.66	92.23	100.55	97.66	91.06	83.80	83.73	78.74	90.14	89.78	83.11	88.06
Brutto FK trocken (50°C)	g	81.86	72.94	83.77	82.69	90.19	83.06	76.04	75.36	69.06	83.30	82.15	75.51	81.22
Netto FK trocken	g	16.58	14.69	14.09	12.22	14.74	15.19	15.38	15.86	15.91	15.43	15.86	16.02	13.43
Wassergehalt FK	g		24.72	8.46	17.86	7.47	8.00	7.76	8.37	9.68	6.84	7.63	7.60	6.84
Volumen														
Filterlösung	mL	30	190	385	8000	190	186	188	178	156	185	172	140	193
Waschwasser (10 mL)	mL	5	10	10	0	11	11	10	11	11	15	10	9	600
FL+WW (mL)	mL	35	200	395	8000	198	196	196	188	166	200	180	144	793
pH & Leitfähigkeit														
Filterlösung (FL)	pH		6.33	6.8		6.33	6.28	7.31	8.2	10.61	7.86	8	10.62	
	LF (mS)		32.6	18.68		32.6	32.6	32.5	33.3	35.8	35.3	45.5	45.5	
Waschwasser (WW)	pH		6.85	7.06		6.85	6.49	8.25	8.03	10.43	8.6	8.26	10.72	
	LF (mS)		24.4	13.25		24.4	21.4	26.7	30	32.2	24.2	30.6	23.8	
FL + WW	pH	6.33	6.48	6.79	9.83	6.48	6.5	7.51	8.11	10.64	7.62	7.61	10.83	6.95
	LF (mS)	107.6	32.2	18.6	1.471	32.2	32.2	32.3	33.1	35.7	33.8	35.2	44.6	34

***Nachwaschen des Filterkuchens:**

Waschvolumen mL	LF	übriges V	Ausfällung	Bezeichnung
50	8.73	48	x	WW 1
50	4.22	48	-	WW 2
50	2.73	48	-	WW 3
50	2.66	49	-	WW 4
400	1.065	395	-	WW 5

Tabelle A7-2: *H_2O-Versuche FAHAG.*

		Flüssig-Fest-Variation				Oberfläche	Zeitabhängigkeit				Temperaturabhängigkeit		
Nr.		1	2	3	4	5	6	7	8	9	10	11	12
Bezeichnung		HAG H_2O/2/10/RT	HAG H_2O/10/10/RT	HAG H_2O/20/10/RT	HAG H_2O/400/10/RT	HAG H_2O/10/10/RT g	HAG H_2O/10/30/RT	HAG H_2O/10/60/RT	HAG H_2O/10/3h/RT	HAG H_2O/10/6h/RT	HAG H_2O/10/10/40	HAG H_2O/10/10/60	HAG H_2O/10/10/80
Feststoffanalytik			x		x								
Versuchsbedingungen													
Aufbereitung						**gemahlen**							
Flüssig-Fest-Verhältnis		**2**	**10**	**20**	**400**	10	10	10	10	10	10	10	10
Asche	g	20	20	20	20	20	20	20	20	20	20	20	20
Wasser	ml	40	200	400	8000	200	200	200	200	200	200	200	200
Grösse Becherglas	mL	100	400	1000	Plastikkübel	400	400	400	400	400	400	400	400
Zeit	min/h	10 min	10 min	10 min	10 min	10 min	**30 min**	**1h**	**3h**	**6h**	10 min	10 min	10 min
Temperatur	°C	RT	RT	RT	RT	RT	RT	RT	RT	RT	**40°**	**60°**	**80°**
Massenbilanz													
Einwage FA	g	20.01	20.01	20.07	20.07	20.03	20.01	20.06	20.03	20.01	20.08	20.00	20.05
Gewicht Filter	g	0.19	0.20	0.20	0.37	0.19	0.20	0.19	0.19	0.19	0.21	0.20	0.21
Tara Schale	g	60.47	64.16	59.85	66.48	66.18	69.50	67.42	59.58	67.56	72.24	58.41	82.95
Brutto FK nass	g	85.07			87.63	88.34	92.68	88.52	81.21	90.61	94.57	82.26	114.25
Brutto FK trocken (50°C)	g	77.70	80.27	75.88	80.73	82.21	85.44	83.46	75.88	84.09	88.64	75.18	100.08
Netto FK	g	17.05	15.91	15.83	13.88	15.85	15.74	15.85	16.11	16.34	16.19	16.58	16.92
Wassergehalt FK	g	7.37			6.90	6.13	7.24	5.06	5.33	6.52	5.93	7.07	14.17
Volumen													
Filterlösung	mL	34	190	395	8000	195	192	196	190	183	190	182	108
Waschwasser (10 mL)	mL	11	20	15	0	15	85	100	11	9	10	11	10
FL+WW (mL)	mL	42	210	410	8000	210	200	204	198	192	198	193	118
pH & Leitfähigkeit													
Filterlösung (FL)	pH	12.17					12.32	12.26	12.34	12.44	12.06	11.9	11.09
	LF (mS)	86.2					36	35.5	35.4	45	40.4	37.2	45.1
Waschwasser (WW)	pH	12.2					12.27	12.35	12.32	12.39	12.09	12.1	12.3
	LF (mS)	53.4					29.7	26.9	26.2	29.3	16.6	27.1	30.5
FL + WW	pH	12.24	12.33	12.32	11.51	12.35	12.27	12.37	12.37	12.42	12.17	12	12.3
	LF (mS)	98.7	34	18.45	1.594	24.6	12.38	35	34.9	35.7	37.7	36.3	38.6

Tabelle A7-3: *HCl-Versuche FAZUC.*

		Konzentrationsabhängigkeit			Saures Nachwaschen		Oberfläche	Vorwaschen		Zeitabhängigkeit				Temperaturabhängigkeit		
Nr.		14	15	16	17	18	19	21	21	22	23	24	25	26	27	28
Bezeichnung		ZUC HC13/4/60/RT	ZUC HCl 5/4/60/RT	ZUC HCl 10/4/60/RT	ZUC HC15/4/60/RT WW pH 2	ZUC HC15/4/60/RT WW pH 1	ZUC HC15/4/60/RT g	ZUC H_2O/10/10/RT	ZUC HCl 5/4/60/RT vw H2O	ZUC HCl 5/4/10/RT	ZUC HC15/4/30/RT	ZUC HCl 5/4/3h/RT	ZUC HC15/4/6h/RT	ZUC HC15/4/60/40	ZUC HCl 5/4/60/60	ZUC HC15/4/60/80
Feststoffanalytik			x	x					x				x	x		x
Versuchsbedingungen																
Aufbereitung, Zugabe							**gemahlen**	**Vorwaschschritt**	**Vorwaschen H_2O**							
Konzentration		**3**	**5**	**10**	5	5	5	-	5	5	5	5	5	5	5	5
Flüssig-Fest-Verhältnis		4	4	4	4	4	4	10	4	4	4	4	4	4	4	4
Asche	g	50	50	50	50	50	50	70	50	50	50	50	50	50	50	50
Wasser	ml	200	200	200	200	200	400	700	400	200	200	200	200	200	200	200
Grösse Becherglas	mL	400	400	400	400	400	400	1000	400	500	500	500	500	500	500	500
Zeit	min/h	1h	1h	1h	1h	1h	1h	10.00	1h	**10 min**	**30 min**	**3h**	**6h**	1h	1h	1h
Temperatur	°C	RT	RT	RT	RT	RT	RT	RT	RT	RT	RT	RT	RT	**40**	**60**	**80**
Massenbilanz																
Einwage FA	g	50.00	50.00	50.02	50.01	50.03	50.02	70.03	50.03	50.00	50.08	50.01	50.01	50.00	50.02	50.01
Gewicht Filter	g	0.20	0.38	0.20	0.37	0.38	0.37	0.49	0.36	0.36	0.37	0.37	0.38	0.36	0.37	0.36
Tara Schale	g	59.40	75.24	64.16	67.69	52.94	73.66	89.53	59.40	67.68	72.24	58.29	57.70	59.31	67.56	82.95
Brutto FK nass	g	118.59	140.60	113.93	131.61	118.71	134.97	163.65	121.17	141.72	133.48	126.08	117.53	117.09	129.09	144.70
Brutto FK trocken (50°C)	g	95.82	109.80	87.68	101.50	86.22	107.50	140.89	100.05	102.47	106.21	93.12	92.05	93.06	101.97	118.16
Netto FK	g	36.23	34.18	23.31	33.45	32.90	33.47	50.87	40.29	34.43	33.60	34.47	33.97	33.39	34.05	34.84
Wassergehalt FK	g	22.77	30.80	26.25	30.11	32.50	27.47	22.76	21.12	39.25	27.27	32.96	25.48	24.02	27.12	26.54
Monitoring																
Start	pH	3	2.55	0.1			2.4		2.9	2.19	1.76				0.42/2.62	2.68
	Temp	33	38	46			37		39	38	38				60/73	80
10 min	pH	4.28	3.08	0.1			3.03		3.5		2.94				3.24	3.23
	Temp	29	31	39			29		37		33				63	75
30 min	pH	4.73	3.33	0.1			3.2		3.87						3.51	4.19
	Temp	24	24	23			25		30						57	78
Ende	pH	5.19	3.48	0.1			3.38		4.43	2.93	3.24				3.67	4.4
	Temp	23	23	23			22		30	32	26				59	80
Volumen																
Filterlösung	mL	170	150	166	155	155	157	665	166	110	162	140	135	142	130	54
Art und Menge des WW	mL	100 H_2O	100 H_2O	100 H_2O	**100 H_2O pH 2**	**100 H_2O pH 1**	100 H_2O	10 H_2O	100 H_2O	100 H_2O	100 H_2O	100 H_2O	100 H_2O	100 H_2O	100 H_2O	100 H_2O
Waschwasser	mL	102	104	104	112	104	95	12	104	135	102	108	100	110	98	100
FL+WW (mL)	mL	272	254	268	277	269	255	677	265	240	260	243	235	250	225	154
pH & Leitfähigkeit																
Filterlösung (FL)	pH	2.85	3.43	0.52	3.16	3.18	3.25	5.03	4.09	3.04	3.14	3.79	3.78	3.27	3.98	3.57
	LF (mS)	106.3	128	194.5			128	34.6	953	128.1	129.1	131.9	135	139.5	169.1	223
Waschwasser (WW)	pH	4.92	3.97	1.01	3.51	3.36	3.81	5.3	4.87	3.78	3.9	4.1	4.02	3.9	3.68	4.7
	LF (mS)	39.8	65.5	105.5			58.5	34	37.4	86.1	55.5	67.9	73.8	66.1	68.2	110.4
FL + WW	pH	3	3.10	0.6	3.29	3.26	3.4	5.28	4.5	3.64	3.6	3.82	4.01	3.62	3.88	4.51
	LF (mS)	84.8	106.6	167.9			104.3	34.5	76	106.3	105.8	108.7	113.7	112.8	129.5	147.9
Bemerkungen				dunkle Emulsion nach Filtration						mühsam zu filtrieren, gelartig						

Tabelle A7-4: *HCl-Versuche FAHAG.*

		Konzentrationsabhängigkeit			Saures Nachwaschen		Oberfläche	Vorwaschen		Zeitabhängigkeit				Temperaturabhängigkeit		
Nr.		14	15	16	17	18	19	20	21	22	23	24	25	26	27	28
Bezeichnung		HAG HCl 3/4/60/RT	HAG HCl 5/4/60/RT	HAG HCl 10/4/60/RT	HAG HCl 5/4/60/RT WW pH 2	HAG HCl 5/4/60/RT WW pH1	HAG HCl 5/4/60/RT g	HAG H_2O/10/10/RT	HAG HCl 5/4/60/RT vw H2O	HAG HCl 5/4/10/RT	HAG HCl 5/4/30/RT	HAG HCl 5/4/3h/RT	HAG HCl 5/4/6h/RT	HAG HCl 5/4/60/40	HAG HCl 5/4/60/60	HAG HCl 5/4/60/80
Feststoffanalytik			x	x										x		
Versuchsbedingungen																
Aufbereitung, Zugabe							**gemahlen**	**Vorwaschschritt**	**Vorwaschen**							
Konzentration		**3**	**5**	**10**	5	5	5	-	5	5	5	5	5	5	5	5
Flüssig-Fest-Verhältnis		4	4	4	4	4	4	10	4	4	4	4	4	4	4	4
Asche	g	50	50	50	50	50	50	70	50	50	50	50	50	50	50	50
Wasser	ml	200	200	400	200	200	400	700	400	200	200	200	200	200	200	200
Grösse Becherglas	mL	400	400	400	400	400	400	1000	400	500	500	500	500	500	500	500
Zeit	min/h	1h	1h	1h	1h	1h	1h	10.00	1h	**10 min**	**30 min**	**3h**	**6h**	1h	1h	1h
Temperatur	°C	RT	RT	RT	RT	RT	RT	RT	RT	RT	RT	RT	RT	**40**	**60**	**80**
Massenbilanz																
Einwage FA	g	50.01	50.01	50.07	50.02	50.03	50.01	70.03	50.06	50.00	50.03	50.03	50.01	50.03	50.06	50.03
Gewicht Filter	g	0.39	0.20	0.18	0.38	0.38	0.20	0.51	0.36	0.37	0.36	0.37	0.37	0.38	0.38	0.37
Tara Schale	g	82.95	58.41	66.48	73.66	66.48	72.24	89.29	58.40	65.08	73.66	59.86	66.08	59.58	52.95	75.73
Brutto FK nass	g	154.55	130.34	139.88	140.96	134.42	139.88	169.37	130.84	138.16	144.19	128.55	137.54	124.58	118.57	145.95
Brutto FK trocken (50°C)	g	122.41	94.47	96.99	108.74	101.53	107.25	145.26	99.73	101.17	109.57	96.08	102.50	95.71	89.31	113.29
Netto FK	g	39.08	35.87	30.32	34.71	34.67	34.81	55.45	40.97	35.72	35.55	35.85	36.04	35.75	35.99	37.19
Wassergehalt FK	g	32.13	35.86	42.89	32.21	32.89	32.63	24.12	31.11	36.99	34.62	32.47	35.05	28.87	29.26	32.66
Monitoring																
Start	pH	6.3	4.0	2.1			4.69		3.3	4.1	4.15				4.3	5.97
	Temp	28	37	53			33		36	38	38				79	80
10 min	pH	8.1	5.7	2.3			5.99		5.1		5.7				6.54	6.38
	Temp	26	35	47			30		31		33				65	80
30 min	pH	9.4	6.5	2.8			6.5		5.81						6.87	6.88
	Temp	25	29	27			27		27						60	80
Ende	pH	9.9	6.9	2.9			6.9		6.74	5.65	6.57				7.28	6.78
	Temp	23	25	23			24		23	33	26				60	82
Volumen																
Filterlösung	mL	150	150	132	146	147	152	670	150	150	151	150	147	152	120	76
Art und Menge des WW	mL	100 H_2O	100 H_2O	100 H_2O	**100 H_2O pH 2**	**100 H_2O pH 1**	100 H_2O	10 H_2O	100 H_2O	100 H_2O	100 H_2O	100 H_2O	100 H_2O	100 H_2O	100 H_2O	100 H_2O
Waschwasser	mL	116	105	102	112	113	104	13	105	105	106	107	104	105	106	104
FL+WW (mL)	mL	265	255	232	258	260	255	680	255	255	255	257	251	255	228	278
pH & Leitfähigkeit																
Filterlösung (FL)	pH	5.3	4.31	2.97	4.48	4.5	5.5	12.41	5.61	5.63	6.17	6.26	6.71	4.5	5.13	5.05
	LF (mS)	108.2	137	166			133.9	37.6	101.2	144.9	136.5	137.7	139.6	143.9	185.1	216
Waschwasser (WW)	pH	6.09	5.95	3.57	4.47	5	6.08	12.2	5.25		6.29	5.53	7.25	5.3	5.71	5
	LF (mS)	53.6	68.4	121.2			60.9	36.8	46		64.9	65.2	66.1	63.4	82.1	103.5
FL + WW	pH	5.84	5.42	3.17	4.73	4.57	6.06	12.36	5.5	5.64	6.19	6.76	7.89	5.4	6.35	5.81
	LF (mS)	85	110.4	150.2			106.7	37.5	80.3	112.4	109	110.1	112.4	114.4	132.2	144.4
Bemerkungen											pH Meter sehr träge (nach Versuchsserie neue KCl)					

Tabelle A7-5: *H_2SO_4, H_2PO_4, NaOH, NH_4Cl-Versuche FAZUC.*

Ziel		Schwefelsäure						Phosphorsäure				Natronlauge				Ammoniumchlorid
		Konzentrationsabhängigkeit		Vorwaschen		Temperaturabhängigkeit		Konzentrationsabhängigkeit		Temperatur	Vor-Nachwaschen					
Nr.		29	30	31	31	32	33	34	34	35	36	37	37	38	39	
Bezeichnung		ZUC H_2SO_4 6.6/4/60/RT	ZUC H_2SO_4 13.9/4/60/RT	ZUC HCl 5/4/60/RT	ZUC H_2SO_4 6.6/4/60/RT vw HCl 5%	ZUC H_2SO_4 6.6/4/60/40	ZUC H_2SO_4 6.6/4/60/80	ZUC HCl 5/4/60/RT	ZUC H_3PO_4/4/60/RT vw HCl 5%	ZUC NaOH 10/15/60/RT	ZUC NaOH 10/15/60/80	ZUC H_2O/10/10/RT	ZUC NaOH 10/15/60/RT vw H_2O	ZUC NaOH 10/15/60/RT WW pH<3.5	ZUC NH_4Cl/4/60/80	
Feststoffanalytik		x	x		x				x	x	x					
Versuchsbedingungen																
Aufbereitung, Zugabe				**Vorwaschschritt**	**Vorwaschen HCl**			**Vorwaschschritt**	**Vorwaschen HCl 5%**			**Vorwaschschritt**	**Vorwaschen H2O**			
Konzentration		**6.6**	**13.9**	5	6.6	6.6	6.6	5	15	**10**	10	-	10	10	15g/L	
Flüssig-Fest-Verhältnis		4	4	4	4	4	4	4	4	15	15	10	15	15	4	
Asche	g	50	50	70	40	50	50	80	50	20	20	50	20	20	50	
Wasser	ml	200	200	280	160	200	200	320	200	300	300	500	300	300	200	
Grösse Becherglas	mL	400	400	400	400	400	400	400	400	400	400	1L	400	400	400	
Zeit	m:n/h	1h	1h	1h	1h	1h	1h	1h	1h	1h	1h	10 min	1h	1h	1h	
Temperatur	°C	RT	RT	RT	RT	**40**	**80**	RT	80	RT	**80**	RT	RT	RT	RT	
Massenbilanz																
Einwage FA	g	50.00	50.02	70.01	40.06	50.02	50.06	80.06	49.91	20.06	20.07	50.05	20.05	20.02	50.03	
Gewich Filter	g	0.36	0.37	0.35	0.35	0.20	0.35	0.39	0.36	0.35	0.37	0.37	0.36	0.36	0.36	
Tara Schale	g	70.09	67.56	57.70	24.36	75.73	59.31	66.18		72.25	69.39	58.03	69.51	67.42	59.54	
Brutto FK nass	g	153.19	167.36	150.10	122.10	149.01	133.09	161.72	587.13	92.62	94.05	110.42	98.05	87.70	121.42	
Brutto FK trocken (50°C)	g	116.68	114.00	101.65	65.43	121.41	106.16	116.77	540.51	86.02	82.14	93.88	87.71	79.96	101.47	
Netto FK	g	46.23	46.07	43.59	40.72	45.48	46.50	50.20	540.15	13.43	12.37	35.49	17.84	12.18	41.58	
Wassergehalt FK	g	36.50	53.36	48.46	56.67	27.60	26.92	44.95	46.62	6.60	11.91	16.53	10.34	7.75	19.95	
Monitoring																
Start	pH	1.1	0.42		0.51	2.1	2.32		1.46	12.6			12.8		6.38	
	Temp	35	38		27	55	95		85	25					80	
10 min	pH	3.04	0.62		0.84	3.21	2.73		1.77	12.65					6.5	
	Temp	32	38		30	46	93		82	24					80	
30 min	pH	3.42	0.64		1.08	3.44	3.12			12.7						
	Temp	25	28		25	40	78			23						
Ende	pH	3.51	0.66		1.27	3.61	3.2		1.92	12.74			12.96		6.37	
	Temp	23	22		25	43	80		79	23					80	
Volumen																
Filterlösung	mL	128	110	210	76	138	58	250	6.2	290	182	480	280	288	78	
Art und Menge des WW	mL	100 H_2O	100 H_2O	140 H_2O	80 H_2O	100 H_2O	100 H_2O	160 H_2O	100 H_2O	150 H_2O	150 H_2O	10 H_2O	150 H_2O	150 H_2O	100 H_2O	
Waschwasser	mL	116	116	155	67	99	102	174	82	149	150	11	150	159	98	
FL+WW (mL)	mL	244	224	365	143	244	160	425	88	435	325	490	425	-	175	
pH & Leitfähigkeit																
Filterlösung (FL)	pH	3.56	0.56	3.36	1.4	3.73	3.83	3.55	1.6	14.12	14.23		14.06	14	7.32	
Waschwasser (WW)	pH	4.12	0.93	4.05	1.91	4.23	4.22	4.52	2.12	12.21	13.45		13.31		7.81	
FL + WW	pH	3.85	0.77	3.58	1.6	4.15	4.14	3.87	2.06	14.02	14		13.88		7.62	
Bemerkungen			ganze Suspension nach ablitrieren: Schlecht rieselbar	Nachwaschen schwierig, nur durch Zerstören der Filterkuchen möglich		Schwierig klein bei Filtrieren		mühlig mit Niederschlag		WW klar, gut filtrierbar					FL hat weisser Niederschlag, der nach Stunden löst	

Tabelle A7-6: *H_2SO_4, H_2PO_4, NaOH, NH_4Cl-Versuche FAHAG.*

		Schwefelsäure				Phosphorsäure			Natronlauge			Ammoniumchlorid
Ziel		Konzentrationsabhängigkeit	Vorwaschen		Temperaturabhängigkeit			Konzentrationsabhängigkeit	Temperatur	Vor-Nachwaschen		
Nr.		29	31		32	33	34	34	35	36	37	38	39	
Bezeichnung		HAG H_2SO_4 6.6/4/60/RT	HAG HCl 5/4/60/RT	HAG H_2SO_4 6.6/4/60/RT vw HCl 5%	HAG H_2SO_4 6.6/4/60/40	HAG H_2SO_4 6.6/4/60/80	HAG HCl 5/4/60/RT	HAG H_3PO_4/4/60/RT vw HCl 5%	HAG NaOH 10/15/60/RT	HAG NaOH 10/15/60/80	HAG H_2O/10/10/RT	HAG NaOH 10/15/60/RT vw H_2O	HAG NaOH 10/15/60/RT WW pH<3.5	HAG NH_4Cl/4/60/80
Feststoffanalytik		x	x				x	x	x	x				
Versuchsbedingungen														
Aufbereitung, Zugabe			**Vorwaschschritt**	**Vorwaschen HCl**			**Vorwaschschritt**	**Vorwaschen HCl 5%**			**Vorwaschschri**	**Vorwaschen H_2O**		
Konzentration		**6.6**	5	6.6	6.6	6.6	5	15	**10**	10	-	10	10	15 g/L
Flüssig-Fest-Verhältnis		4	4	4	4	4	4	4	15	15	10	15	15	4
Asche	g	50	70	40	50	50	80	50	20	20	50	20	20	50
Wasser	ml	200	280	160	200	200	320	200	300	300	500	300	300	200
Grösse Becherglas	mL	400	400	400	400	400	400	400	400	400	1L	400	400	400
Zeit	min/h	1h	1h	1h	1h	1h	1h	1h	1h	1h	10 min	1h	1h	1h
Temperatur	°C	RT	RT	RT	**40**	**80**	RT	RT	RT	**80**	RT	RT	RT	80
Massenbilanz														
Einwage FA	g	50.02	70.01	40.01	50.06	50.04	80.09	50.05	20.02	20.05	50.06	20.03	20.01	50.06
Gewicht Filter	g	0.63	0.37	0.38	0.37	0.37	0.37	0.38	0.36	0.37	0.37	0.37	0.36	0.36
Tara S-chale	g	75.26	59.57	59.40	72.65	58.41	59.85		82.96	65.08	66.11	58.29	64.16	60.47
Brutto FK nass	g	174.88	162.14	152.02	169.14	145.83	170.94	602.50	110.32	106.12	121.57	89.96	91.87	124.87
Brutto FK trocken (50°C)	g	131.65	107.76	106.50	129.13	115.97	114.50	552.16	99.58	80.85	105.72	77.88	79.80	103.40
Netto FK	g	55.76	47.82	46.72	56.10	57.19	54.28	551.78	16.27	15.40	39.24	19.23	15.27	42.58
Wassergehalt FK	g	43.24	54.38	45.52	40.01	29.86	56.44	50.34	10.74	25.27	15.86	12.07	12.08	21.47
Monitoring														
	pH	4.43		0.93	4.3	3.62		2.18	12.43	durchgehend pH >12		durchgehend pH >12	durchgehend pH >12	8.27
Start	Temp	35		34	55	95		90	24					80
	pH	5.48		3.06	5.55	6.38		2.37	12.47					8.7
10 min	Temp	30		30	43	80		80	22					80
	pH	6		3.37	5.93	6.89			12.21					
30 min	Temp	20		25	40	76			23					
	pH	6.32		3.55		7.29		2.62	12.18					8.5
Ende	Temp	20		20		80		80	24					80
Volumen														
Filterlösung	mL	112	210	86	128	62	245	28	280	168	480	285	285	80
Art und Menge des WW	mL	100 H_2O	140 H_2O	80 H_2O	100 H_2O	100 H_2O	160 H_2O	100 H_2O	150 H_2O	150 H_2O	10 H_2O	150 H_2O	150 H_2O	100 H_2O
Waschwasser	mL	122	146	88	108	94	168	100	150	142	10	148	145	102
FL+WW (mL)	mL	234	360	174	134	154	410	130	430	310	490	425	-	160
pH & Leitfähigkeit														
Filterlösung (FL)	pH	5.94	5.67	3.62	5.95	6.9	6.59	2.62	14.11	14.08		14	14	10.11
Waschwasser (WW)	pH	6.07	5.42	3.7	5.66	7.4	6.54	2.96	13.4	13.57		13.28		10.44
FL + WW	pH	6.04	5.58	3.71	6.27	7.89	6.65	2.78		13.96		13.87		10.34
Bemerkungen								FL milchig weiss		WW klar, gut filtrierbar				

Tabelle A7-7: *NaCl-Versuche FAZUC.*

		Salzsäure		Natriumchlorid	
Nr.		**15**	**29**	**40**	**41**
Bezeichnung		ZUC HCl 5/4/60/RT	ZUC H_2SO_4 6.6/4/60/RT	ZUC NaCl/5/60/85 vw HCl 5%	ZUC NaCl/5/60/85 vw H_2SO_4 6.6%
Versuchsbedingungen					
Extraktionsmittel		**HCl**	**H_2SO_4**	**NaCl**	**NaCl**
Konzentration		5	6.6	300g/L	300g/L
Flüssig-Fest-Verhältnis		4	4	5	5
Asche	g	50	50	10	10
Extraktionsmittel	ml	200	200	50	50
Grösse Becherglas	mL	400	400	100	100
Zeit	min/h	1h	1h	1h	1h
Temperatur	°C	RT	RT	85	85
Massenbilanz					
Einwage FA	g	50.00	50.00	10.00	10.00
Gewicht Filter	g	0.38	0.36		
Tara Schale	g	75.24	70.09	72.34	79.92
Brutto FK nass	g	140.60	153.19		
Brutto FK trocken (50°C)	g	109.80	116.68	81.18	88.96
Netto FK	g	34.18	46.23	8.84	9.04
Wassergehalt FK	g	30.80	36.50		
Monitoring					
Start	pH	2.55	1.1	5.1	5.0
	Temp	38	35	85	85
10 min	pH	3.08	3.04	pH eingestellt auf 4.0	pH eingestellt auf 4.0
	Temp	31	32		
30 min	pH	3.33	3.42		
	Temp	24	25		
Ende	pH	3.48	3.51	4.1	4.1
	Temp	23	23	85	85
Volumen					
Filterlösung	mL	150	128	30	36
Art und Menge des WW	mL	100 H_2O	100 H_2O	50 H_2O 85°C	50 H_2O 85°C
Waschwasser	mL	104	116	50	50
FL+WW (mL)	mL	254	244	80	86
pH & Leitfähigkeit					
Filterlösung (FL)	pH	3.43	3.56		
	LF (mS)	128			
Waschwasser (WW)	pH	3.97	4.12		
	LF (mS)	65.5			
FL + WW	pH	3.10	3.85		
	LF (mS)	106.6			

Tabelle A7-8: *NaCl-Versuche FAZUC.*

		Salzsäure		Natriumchlorid	
Nr.		**15**	**29**	**40**	**41**
Bezeichnung		HAG HCl 5/4/60/RT	HAG H_2SO_4 6.6/4/60/RT	HAG NaCl/5/60/85 vw HCl 5%	HAG NaCl/5/60/85 vw H_2SO_4 6.6%
Versuchsbedingungen					
Extraktionsmittel		**HCl**	**H_2SO_4**	**NaCl**	**NaCl**
Konzentration		5	6.6	300g/L	300g/L
Flüssig-Fest-Verhältnis		4	4	5	5
Asche	g	50	50	10	10
Extraktionsmittel	ml	200	200	50	50
Grösse Becherglas	mL	400	400	100	100
Zeit	min/h	1h	1h	1h	1h
Temperatur	°C	RT	RT	85	85
Massenbilanz					
Einwage FA	g	50.01	50.02	10.01	10.00
Gewicht Filter	g	0.20	0.63		
Tara Schale	g	58.41	75.26	78.60	66.85
Brutto FK nass	g	130.34	174.88		
Brutto FK trocken (50°C)	g	94.47	131.65	88.88	76.43
Netto FK	g	35.87	55.76	10.28	9.58
Wassergehalt FK	g	35.86	43.24		
Monitoring					
Start	pH	4.0	4.43	7.1	7
	Temp	37	35	85	85
10 min	pH	5.7	5.48	pH schwierig einzustellen (Pufferung auf 5.6)	pH schwierig einzustellen (Pufferung auf 5.6)
	Temp	35	30		
30 min	pH	6.5	6		
	Temp	29	20		
Ende	pH	6.9	6.32	5.6	5.6
	Temp	25	20	85	85
Volumen					
Filterlösung	mL	150	112	30	24
Art und Menge des WW	mL	100 H_2O	100 H_2O	50 H_2O 85°C	50 H_2O 85°C
Waschwasser	mL	105	122	50	50
FL+WW (mL)	mL	255	234	80	74
pH & Leitfähigkeit					
Filterlösung (FL)	pH	4.31	5.94		
	LF (mS)	137			
Waschwasser (WW)	pH	5.95	6.07		
	LF (mS)	68.4			
FL + WW	pH	5.42	6.04		
	LF (mS)	110.4			

Anhang 7B: Chemische Analysen der Filterkuchen und Filtrate

Tabelle A7-9: *H_2O-Versuche.*

Nr.	Bezeichnung	V (mL)	pH	Al	Ca	Cd	Cr	Cu	ICP-OES Fe	K	Mg	Na	Pb	Sb	Si	Zn	Br	Ca	Cl	F	K	IC Mg	Na	Ti	NH_4	NO_3	SO_4	Sr
				mg/L	mg/L	mg/L	mg/L	mg/L	mg/L	mg/L	mg/L	mg/L	mg/L	mg/L	mg/L	mg/L	mg/L	mg/L	mg/L	mg/L	mg/L	mg/L	mg/L	mg/kg	mg/L	mg/L	mg/L	mg/L
1	ZUC H_2O/2/10/RT	35	6.33	0.72	980	125	<0.05	1.5	<0.05	138'255	216	167'996	42	<1.0	20	2'975	1259	1'017	41'571	17	17'684	247	17'989	<100	5.8	12'053	<100
2	ZUC H_2O/10/10/RT	200	6.48	<0.05	1'016	26	<0.05	0.11	<0.05	2'965	46	3'580	13	<1.0	16	961	280	858	9'068	11	4'259	60	4'226	<71	5.7	5'028	<71
3	ZUC H_2O/20/10/RT	395	6.79	<0.05	1'525	14	<0.05	0.19	<0.05	2'116	26	3'472	11	<1.0	5.5	433	146	1'176	4'852	9.4	2'207	28	2'197	<26	5.5	3'996	<26
4	ZUC H_2O/400/10/RT	8000	9.83	0.63	154	<0.05	<0.05	<0.05	<0.05	84	<1.00	104	<1.0	<1.0	<5.00	0	7.8	143	239	3.1	113	1.0	113	<1.0	6.7	345	<1.0
5	ZUC H_2O/ 10/10/RT g	198	6.48	<0.05	2'022	26	<0.05	0.22	<0.05	3'754	67	4'109	14	<1.0	10	474	279	1'722	9'224	10	4'231	69	4'230	<21	6.6	6'501	<21
6	ZUC H_2O/10/30/RT	196	6.5	0.05	1'221	28	<0.05	0.20	<0.05	3'497	52	40'718	15	<1.0	11	637	313	-	9'488	12	-	-	-	-	<8	4'879	-
7	ZUC H_2O/10/60/RT	196	7.51	<0.05	1'060	26	<0.05	0.11	<0.05	3'388	60	41'550	10	<1.0	8.9	409	311	-	9'443	12	-	-	-	-	<8	4'605	-
8	ZUC H_2O/10/3h/RT	188	8.11	<0.05	1'042	20	<0.05	<0.05	<0.05	3'543	69	44'982	4.2	<1.0	<5.0	28	324	-	9'897	11	-	-	-	-	<8	3'881	-
9	ZUC H_2O/10/8.5h/RT	166	10.64	16	1'107	<0.05	0	<0.05	<0.05	3'876	<1.0	47'990	<1.0	<1.0	<5.0	0.32	359	-	11'208	12	-	-	-	-	<8	3'564	-
10	ZUC H_2O/10/10/40	200	7.62	0.05	1'081	24	<0.05	0.18	<0.05	3'696	58	3'574	16	<1.0	10	293	300	1'024	9'662	11	4'374	60	4'300	<10	5.1	4'270	<10
11	ZUC H_2O/10/10/60	180	7.61	0.17	1'017	14	<0.05	0.05	<0.05	4'174	70	4'029	8.3	<1.0	<5.0	8.5	336	964	10'911	10	4'969	73	4'909	<10	5.0	3'842	<10
12	ZUC H_2O/10/10/80	144	10.83	121	1'133	<0.05	0.19	<0.05	0.06	5'125	<1.0	4'864	10	<1.0	<5.0	0.9	424	1'111	13'275	9	6'022	<10	5'968	<10	4.7	3'498	<10
13	ZUC H_2O WW1	48	7.59	0.49	911	1.0	<0.05	<0.05	<0.05	663	6.7	740	1.0	<1.0	<5.0	25	60	866	1'963	8.7	810	<10	785	<10	<1.6	2'107	<10
13	ZUC H_2O WW2	48	10.33	1.2	829	<0.05	<0.05	<0.05	<0.05	204	0.9	186	<1.0	<1.0	<5.0	1.4	17	754	588	8.4	214	<10	204	<10	<1.6	1'724	<10
13	ZUC H_2O WW3	48	10.89	6.5	681	<0.05	<0.05	<0.05	<0.05	57	<1.0	53	1.6	<1.0	<5.0	0.3	5.8	624	162	7.4	66	<10	52	<10	<1.6	1'461	<10
13	ZUC H_2O WW4	49	11.36	2.0	620	<0.05	<0.05	<0.05	<0.05	40	<1.0	37	2.8	<1.0	<5.0	0.5	4.4	558	120	6.6	47	<10	35	<10	4.5	1'234	<10
13	ZUC H_2O WW5	395	11.36	2.6	192	<0.05	0.05	<0.05	0.05	3.5	<1.0	10	7.7	<1.0	<5.0	1.4	<1.6	176	8.1	4.0	<10	<10	<10	<10	4.1	320	<10
1	HAG H_2O/2/10/RT	42	12.24	0.2	4'856	0.3	2.2	0.61	0.05	11'467	<1.0	13'511	201	<1.0	<5.0	16	770	4'381	35'675	7.2	13'873	<100	15'108	<100	<1.6	7'276	<100
2	HAG H_2O/10/10/RT	210	12.33	<0.05	2'528	<0.05	1.3	0.15	<0.05	2'715	<1.0	2'976	61	<1.0	<5.0	4.2	165	2'557	7'977	7.5	3'211	<45	3'445	<45	<1.6	2'388	<45
3	HAG H_2O/20/10/RT	410	12.32	<0.05	1'588	<0.05	0.7	0.06	<0.05	1'388	<1.0	1'586	33	<1.0	<5.0	2.2	86	1'525	4'167	10	1'646	<19	1'764	<19	<1.6	2'175	<19
4	HAG H_2O/400/10/RT	8000	11.51	6.9	142	<0.05	0.1	<0.05	<0.05	72	<1.0	158	1.5	<1.0	<5.0	0.3	4.6	131	210	3.8	85	<1.0	93	<1.0	<1.6	169	<1.0
5	HAG H_2O/10/10/RT g	210	12.35	0.10	2'289	<0.05	1.2	<0.05	<0.05	2'696	<1.0	2'975	46	<1.0	<5.0	3.0	149	2'170	7'792	5.9	3'089	<41	3'330	<41	5.3	2'451	<41
6	HAG H_2O/10/30/RT	200	12.27	0.09	2'760	<0.05	1.5	0.28	<0.05	2'654	<1.0	34'292	73	<1.0	<5.0	5.3	210	-	8'287	8.0	-	-	-	-	<8	4'018	-
7	HAG H_2O/10/60/RT	204	12.37	0.12	2'715	<0.05	1.5	0.12	<0.05	2'641	<1.0	33'473	68	<1.0	<5.0	5.2	208	-	8'161	<8	-	-	-	-	<8	3'986	-
8	HAG H_2O/10/3h/RT	198	12.37	0.15	2'500	<0.05	1.5	<0.05	<0.05	2'748	<1.0	35'031	59	<1.0	<5.0	4.2	212	-	8'411	<8	-	-	-	-	<8	3'386	-
9	HAG H_2O/10/6h/RT	192	12.42	0.06	2'279	<0.05	1.4	<0.05	<0.05	2'834	<1.0	35'594	44	<1.0	<5.0	3.3	217	-	8'734	<8	-	-	-	-	<8	3'037	-
10	HAG H_2O/10/10/40	198	12.17	0.43	2'459	<0.05	1.2	0.19	<0.05	3'002	<1.0	3'252	69	<1.0	<5.0	6.2	172	2'307	8'609	6.6	3'409	<50	3'649	<50	<1.6	3'244	<50
11	HAG H_2O/10/10/60	193	12.00	0.34	1'905	<0.05	1.0	0.13	0.07	3'028	<1.0	3'270	67	<1.0	<5.0	6.5	174	1'803	8'699	5.8	3'451	<50	3'691	<50	<1.6	2'523	<50
12	HAG H_2O/10/10/80	118	12.3	0.68	1'878	<0.05	1.9	0.12	0.07	4'573	<1.0	4'815	65	<1.0	<5.0	7.4	253	1'427	12'450	5.3	5'016	<83	5'355	<83	<1.6	2'496	<83

Nr.	Bezeichnung	Gewicht FK g	Ba mg/kg	Br mg/kg	Ca mg/kg	Cd mg/kg	Cl mg/kg	Cr mg/kg	Cu mg/kg	Fe mg/kg	K mg/kg	Mn mg/kg	Pb mg/kg	Sb mg/kg	Si mg/kg	Sn mg/kg	Ti mg/kg	Zn mg/kg	P mg/kg	S mg/kg
-	FAZUC	20.00	1'881	3'847	152'700	443	103'300	468	2'512	20'510	46'900	784	11'920	2'976	81'260	1'682	9'308	65'420	4'497	55'430
-	FAHAG	20.00	1'680	2'231	242'900	202	91'530	948	992	14'570	37'100	649	3'445	2'461	80'730	802	12'420	21'250	5'905	44'190
2	ZUC H_2O/10/10/RT	14.73	2'610	417	181'000	173	10'580	681	3'283	29'290	7'820	1'015	13'300	3'339	76'150	2'284	11'620	69'980	6'818	46'140
4	ZUC H_2O/400/10/RT	12.22	2'638	191	160'900	582	5'278	781	3'801	36'490	7'500	1'241	14'920	3'597	88'570	2'558	13'120	98'560	7'616	25'210
9	ZUC H_2O/10/8.5h/RT	15.91	2'342	249	177'100	525	7'940	589	3'061	27'390	6'692	962	12'020	2'914	65'400	2'059	10'610	78'060	5'856	58'810
12	ZUC H_2O/10/10/80	16.02	2'328	218	177'400	539	5'598	596	3'069	28'410	6'668	974	12'280	2'990	66'390	2'050	10'640	79'860	5'847	59'940
2	HAG H_2O/10/10/RT	15.91	2'007	90	257'600	231	5'608	1'104	1'230	15'000	1'332	879	2'132	2'686	84'610	986	14'560	24'190	7'920	32'960
4	HAG H_2O/400/10/RT	13.88	1'930	66	248'400	256	4'565	1'247	1'415	16'840	1'799	961	3'123	2'961	98'500	1'112	15'960	28'010	8'804	25'650

Tabelle A7-10: *HCl-Versuche.*

Nr.	Bezeichnung	V (mL)	pH	ICP-OES Al	Ca	Cd	Cr	Cu	Fe	K	Mg	Mn	Na	Pb	S	Sb	Si	Ti	Zn
				mg/L	mg/L	mg/L	mg/L	mg/L	mg/L	mg/L	mg/L	mg/L	mg/L	mg/L	mg/L	mg/L	mg/L	mg/L	mg/L
14	ZUC HCl 3/4/60/RT	272	3.0	60	6'055	57	0.1	1.1	1.0	5'956	751	25	7'627	39	527	1.8	174	<0.05	7'079
15	ZUC HCl 5/4/60/RT	254	3.1	836	11'141	56	5.0	0.2	255	6'358	1'310	47	8'087	36	412	6.6	705	<0.05	8'630
16	ZUC HCl 10/4/60/RT	268	0.6	4'120	12'144	67	21	314	1'529	6'509	1'724	103	6'593	1'082	528	106	1'533	15	9'493
17	ZUC HCl 5/4/60/RT WW pH 2	277	3.3	994	11'304	59	6.3	0.3	295	6'523	1'332	47	6'422	75	426	14.1	1'016	0	8'256
18	ZUC HCl 5/4/60/RT WW pH 1	269	3.3	1'122	11'087	59	6.8	0.3	293	6'412	1'316	47	6'246	48	426	18.4	1'205	1	8'106
19	ZUC HCl 5/4/60/RT g	255	3.4	865	10'279	61	5.4	0.4	256	6'149	1'339	51	7'405	62	460	8.7	868	0.05	8'483
20	ZUC H_2O/10/10/RT	677	5.3	0.1	1'705	32	<0.1	0.7	0.1	3'375	53	3.3	4'183	20	2'308	<1	21	<0.05	1'292
21	ZUC HCl 5/4/60/RT vw H2O	265	4.5	182	13'491	17	<0.1	0.7	16	451	1'245	38	594	61	326	2.2	128	<0.05	6'951
22	ZUC HCl 5/4/10/RT	240	3.6	804	10'965	58	5.2	0.3	289	6'064	1'335	48	7'532	37	432	12	846	0.6	8'353
23	ZUC HCl 5/4/30/RT	260	3.6	902	11'303	59	6.0	0.4	282	6'384	1'374	47	7'732	54	426	13	1'069	0.08	8'879
24	ZUC HCl 5/4/3h/RT	243	3.8	841	10'112	66	1.7	3.5	306	6'257	1'442	51	6'986	629	407	1.6	230	0.10	8'841
25	ZUC HCl 5/4/6h/RT	235	4.0	573	10'787	76	0.1	334	96	7'420	1'719	54	7'275	1'103	366	<1	45	<0.05	8'047
26	ZUC HCl 5/4/60/40	250	3.6	912	8'800	54	2.2	0.3	247	6'485	1'412	52	6'285	29	440	2.2	385	<0.05	9'139
27	ZUC HCl 5/4/60/60	225	3.9	526	9'961	71	<0.1	3.7	398	6'974	1'586	71	7'053	616	427	2.9	47	<0.05	9'925
28	ZUC HCl 5/4/60/80	154	4.5	253	14'689	98	<0.1	2.9	910	9'198	2'236	110	10'428	626	398	7.7	54	<0.05	11'995
14	HAG HCl 3/4/60/RT	265	5.8	0.2	11'523	0.2	0.3	<0.05	0.02	4'707	101	<0.05	6'432	<1.00	322	4.5	7.3	<0.05	1.0
15	HAG HCl 5/4/60/RT	255	5.4	0.4	18'491	21	0.0	0.3	0.07	4'905	898	23	6'671	8.3	275	3.7	4.9	<0.05	317
16	HAG HCl 10/4/60/RT	232	3.2	2'583	25'147	23	16	0.7	738	5'669	1'942	76	6'267	9.0	240	2.2	216	2.5	2'977
17	HAG HCl 5/4/60/RT WW pH 2	258	4.7	5.7	20'220	24	0.1	1.3	2.88	5'007	908	26	5'575	10.6	299	6.3	34.2	0	823
18	HAG HCl 5/4/60/RT WW pH 1	260	4.6	9.1	19'009	24	0.2	1.0	5.26	4'806	908	26	5'319	8.0	286	6.7	58.1	0	1'112
19	HAG HCl 5/4/60/RT g	255	6.1	0.1	17'365	20	<0.1	1.1	<0.05	4'573	883	21	5'928	5	281	6.3	5.5	<0.05	194
20	HAG H_2O/10/10/RT	680	12.4	0.1	2'786	0.05	1.7	0.5	<0.05	2'552	0.1	<0.05	3'424	88	1'362	<1	<5	<0.05	5.9
21	HAG HCl 5/4/60/RT vw H2O	255	5.5	0.1	17'501	16	<0.1	0.7	<0.05	264	857	16	527	<1	259	5.5	5.5	0.0	101
22	HAG HCl 5/4/10/RT	255	5.6	0.2	17'866	22	<0.1	0.6	<0.05	4'665	911	28	6'329	7.1	309	5.8	51	0.0	1'061
23	HAG HCl 5/4/30/RT	255	6.2	0.1	15'604	23	<0.1	1.0	<0.05	4'629	897	27	5'532	8.3	299	5.3	10.4	0.0	748
24	HAG HCl 5/4/3h/RT	257	6.8	1.0	18'113	17	<0.1	<0.05	0.06	4'652	886	8.9	6'239	<1	265	<1	<5	0.0	3.8
25	HAG HCl 5/4/6h/RT	251	7.9	2.6	17'687	11	<0.1	<0.05	<0.05	5'027	763	1.2	5'997	<1	262	<1	<5	0.0	0.6
26	HAG HCl 5/4/60/40	255	5.4	0.5	16'262	23	<0.1	1.2	<0.05	4'727	979	23	5'760	7.0	293	2.9	<5	0.0	226
27	HAG HCl 5/4/60/60	228	6.4	0.8	18'241	29	<0.1	0.2	0.05	5'307	2'076	11	6'396	1.1	591	2.9	<5	0.0	4.7
28	HAG HCl 5/4/60/80	278	5.8	1.3	22'293	8.8	<0.1	0.2	0.11	6'841	864	7.0	7'767	1.7	568	5.7	<5	<0.05	17

Nr.	Bezeichnung	Gewicht FK	Ba	Br	Ca	Cd	Cl	Cr	Cu	Fe	K	Mn	Pb	Sb	Si	Sn	Ti	Zn	P	S
		g	mg/kg	mg/kg	mg/kg	mg/kg	mg/kg	mg/kg	mg/kg	mg/kg	mg/kg	mg/kg	mg/kg	mg/kg	mg/kg	mg/kg	mg/kg	mg/kg	mg/kg	mg/kg
-	FAZUC	50.00	1'881	3'847	152'700	443	103'300	468	2'512	20'510	46'900	784	11'920	2'976	81'260	1'682	9'308	65'420	4'497	55'430
-	FAHAG	50.00	1'680	2'231	242'900	202	91'530	948	992	14'570	37'100	649	3'445	2'461	80'730	802	12'420	21'250	5'905	44'190
15	ZUC HCl 5/4/60/RT	34.18	2'616	190	150'800	147	9'220	713	3'941	31'340	11'950	814	18'640	5'152	92'250	2'418	13'740	24'670	7'658	87'390
16	ZUC HCl 10/4/60/RT	23.31	3'851	245	175'900	41	14'560	787	1'474	26'440	5'566	530	12'750	2'959	58'480	1'221	20'600	12'490	2'745	128'400
21	ZUC HCl 5/4/60/RT vw H_2O	40.29	3'082	84	144'500	70	5'028	857	4'364	36'970	7'713	1'059	19'710	5'685	109'900	2'774	15'440	37'210	9'470	58'830
25	ZUC HCl 5/4/6h/RT	33.97	2'668	169	145'900	34	7'797	733	1'715	33'330	12'640	807	12'050	5'059	100'800	2'447	14'250	24'150	7'621	84'500
26	ZUC HCl 5/4/60/40	33.39	2'622	140	149'400	199	5'817	719	3'978	30'090	11'980	775	19'480	5'394	95'320	2'468	13'920	22'740	7'746	90'510
28	ZUC HCl 5/4/60/80	34.84	2'535	251	145'100	107	15'120	692	3'830	26'740	12'440	636	15'740	5'027	100'100	2'306	14'390	20'620	7'562	84'230
15	HAG HCl 5/4/60/RT	35.87	2'174	134	179'500	79	11'800	1'389	1'473	18'830	10'770	846	4'353	3'100	94'120	1'086	17'410	28'480	9'538	55'910
16	HAG HCl 10/4/60/RT	30.32	2'374	231	124'500	98	36'570	1'452	1'969	17'120	13'220	675	6'138	4'468	134'200	1'261	24'100	9'915	10'490	61'700
26	HAG HCl 5/4/60/40	35.75	2'168	124	176'100	80	12'130	1'369	1'483	19'290	10'890	854	4'328	3'256	97'730	1'108	17'850	29'950	9'474	56'330

Tabelle A7-11: *H_2SO_4, H_2PO_4, NaOH, NH_4Cl-Versuche.*

Nr.	Bezeichnung	V (mL)	pH	Al	Ca	Cd	Cr	Cu	Fe	K	Mg	Mn	Na	Pb	Si	S	Sb	Si	Ti	Zn
				mg/L	mg/L	mg/L	mg/L	mg/L	mg/L	mg/L	mg/L	mg/L	mg/L	mg/L	mg/kg	mg/L	mg/L	mg/L	mg/L	mg/L
29	ZUC H_2SO_4 6.6/4/60/RT	244	4	829	693	60	7	1	348	6'844	1'358	48	7'331	30	81'260	7'987	27	1'237	1	8'880
30	ZUC H_2SO_4 13.9/4/60/RT	224	1	4'147	651	70	21	33	1'322	7'837	1'945	106	7'726	29	80'730	30'799	152	3'201	20	10'069
31	ZUC HCl 5/4/60/RT	365	4	842	13'039	58	<5	<0.5	347	7'365	1'472	50	7'658	17	696	696	6	661	<25	9'342
31	ZUC H_2SO_4 6.6/4/60/RT vw HCl 5%	143	2	5'531	628	25	24	419	1'583	1'287	829	83	743	8	14'313	8'106	119	2'742	103	2'220
32	ZUC H_2SO_4 6.6/4/60/40	244	4	739	682	54	<5	4	311	6'858	1'400	50	7'481	25	8'106	4	496	<25	9'107	
33	ZUC H_2SO_4 6.6/4/60/80	160	4	971	1'384	65	<5	1	843	9'809	2'311	93	11'385	49	13'254	3	61	<25	14'562	
34	ZUC HCl 5/4/60/RT	425	4	698	11'707	54	<5	<0.5	273	6'960	1'353	46	7'382	13	669	6	654	<25	8'787	
34	ZUC H_3PO_4/4/60/RT vw HCl 5%	88	2	7'029	10'601	35	26	509	3'404	1'250	1'629	169	951	117	2'339	160	502	64	4'917	
35	ZUC NaOH 10/15/60/RT	435	14	73	81	<0.25	<0.01	<0.5	<0.5	1'904	<0.25	<0.25	-	144	2'391	7	58	<0.25	1'280	
36	ZUC NaOH 10/15/60/80	325	14	478	17	<0.25	<0.01	<0.5	<0.5	2'518	<0.25	1	-	553	3'392	24	312	<0.25	2'413	
37	ZUC H_2O/10/10/RT	490	-	<1	1'972	28	<1	1	<5	3'619	45	3	3'603	18	2'339	0	23	<5	1'283	
37	ZUC NaOH 10/15/60/RT vw H_2O	425	14	75	64	<0.25	<0.01	<0.5	<0.5	111	<0.25	<0.25	-	31	1'950	4	95	<0.25	1'201	
38	ZUC NaOH 10/15/60/RT WW pH <3.5	159	-	3	4'152	<0.25	<0.01	<0.5	<0.5	204	<0.25	<0.25	-	186	358	<5	<5	<0.25	68	
39	ZUC NH_4Cl/4/60/RT	175	-	<5	2'511	57	<1	1	<5	8'668	418	5	9'780	13	637	0	7	<5	579	
29	HAG H_2SO_4 6.6/4/60/RT	234	6	<5	971	22	<5	1	<25	5'402	1'076	26	6'751	<5	2'952	1	29	<25	855	
31	HAG HCl 5/4/60/RT	360	6	2	19'964	20	<5	<0.5	32	5'140	971	27	6'189	<5	686	4	5	<25	511	
31	HAG H_2SO_4 6.6/4/60/RT vw HCl 5%	174	4	1'440	613	10	13	9	445	980	1'143	40	827	11	4'792	21	1'542	<25	3'071	
32	HAG H_2SO_4 6.6/4/60/40	134	6	<5	1'146	18	<5	1	<25	5'201	1'074	21	6'548	<5	1'765	1	12	<25	271	
33	HAG H_2SO_4 6.6/4/60/80	154	8	<5	1'524	6	<5	4	<25	8'129	841	3	9'767	<5	1'587	0	5	<25	9	
34	HAG HCl 5/4/60/RT	410	7	<5	20'156	20	<5	<0.5	<25	5'247	969	26	6'325	<5	673	4	7	<25	496	
34	HAG H_3PO_4/4/60/RT vw HCl 5%	130	3	576	16'311	10	<5	14	467	659	2'070	57	994	<5	938	64	6'024	<25	1'885	
35	HAG NaOH 10/15/60/RT	430	-	47	68	<0.25	<0.01	<0.5	<0.5	1'461	<0.25	<0.25	-	9	1'494	8	98	<0.25	321	
36	HAG NaOH 10/15/60/80	310	14	619	33	<0.25	<0.01	<0.5	<0.5	2'228	<0.25	<0.25	-	106	2'239	18	137	<0.25	796	
37	HAG H_2O/10/10/RT	490	-	<1	3'034	<0.05	2	0	<5	2'983	<5	<0.05	7'582	77	4'237	<0.1	<1	<5	6	
37	HAG NaOH 10/15/60/RT vw H_2O	425	14	57	54	<0.25	1	3	<0.5	69	<0.25	<0.25	-	48	1'098	<5	111	<0.25	434	
38	HAG NaOH 10/15/60/RT WW pH <3.5	145	-	3	3'504	<0.25	<0.01	<0.5	<0.5	224	<0.25	<0.25	-	27	298	0	<5	<0.25	31	
39	HAG NH_4Cl/4/60/RT	160	10	21	7'404	0	<1	<0.1	<5	8'407	<5	<0.05	8'783	<1	404	2	2	<5	1	

Nr.	Bezeichnung	Gewicht FK	Ba	Br	Ca	Cd	Cl	Cr	Cu	Fe	K	Mn	Pb	Si	Sn	Ti	Zn	P	S
		g	mg/kg	mg/kg	mg/kg	mg/kg	mg/kg	mg/kg	mg/kg	mg/kg	mg/kg	mg/kg	mg/kg	mg/kg	mg/kg	mg/kg	mg/kg	mg/kg	mg/kg
-	FAZUC	50.00	1'881	3'847	152'700	443	103'300	468	2'512	20'510	46'900	784	11'920	2'976	81'260	1'682	9'308	65'420	4'497	55'430
-	FAHAG	50.00	1'680	2'231	242'900	202	91'530	948	992	14'570	37'100	649	3'445	2'461	80'730	802	12'420	21'250	5'905	44'190
29	ZUC H_2SO_4 6.6/4/60/RT	46.23	1'952	227	171'300	93	3'704	468	3'025	20'600	9'142	577	14'350	3'767	55'320	1'781	10'290	18'260	5'069	116'300
30	ZUC H_2SO_4 13.9/4/60/RT	46.07	1'904	445	178'200	68	6'794	401	2'974	16'460	7'390	368	14'810	2'387	41'420	1'409	11'250	12'640	2'392	142'200
31	ZUC H_2SO_4 6.6/4/60/RT vw HCl 5%	40.72	2'550	89	157'000	36	1'583	602	2'484	24'040	4'509	546	21'540	5'161	92'000	2'146	14'740	14'710	3'313	117'000
34	ZUC H_3PO_4/4/60/RT vw HCl 5%	-	2'528	100	129'700	68	2'303	622	3'211	22'650	7'569	597	20'390	5'407	104'500	2'244	15'840	13'020	60'240	66'740
35	ZUC NaOH 10/15/60/RT	13.43	2'768	200	236'700	611	6'184	728	3'517	27'700	2'410	1'129	7'544	3'594	79'630	2'281	12'390	45'330	6'130	4'821
36	ZUC NaOH 10/15/60/80	12.37	2'898	57	264'800	628	2'805	771	3'512	28'230	340	1'166	4'716	3'535	84'520	2'045	12'640	27'580	6'045	5'729
29	HAG H_2SO_4 6.6/4/60/RT	55.76	1'437	149	198'400	52	4'125	824	1'008	12'060	8'348	514	2'832	2'175	56'360	699	11'180	15'230	5'329	104'400
31	HAG H_2SO_4 6.6/4/60/RT vw HCl 5%	46.72	1'891	35	165'900	39	1'489	1'099	1'440	16'030	5'657	587	4'643	3'295	80'660	970	16'900	10'730	7'901	101'600
34	HAG H_3PO_4/4/60/RT vw HCl 5%	-	1'972	30	139'200	53	2'314	1'193	1'574	17'040	10'200	706	4'796	3'255	69'910	967	19'160	21'580	81'660	40'350
35	HAG NaOH 10/15/60/RT	16.27	1'880	121	292'600	207	5'929	1'099	1'206	13'970	< 10	862	3'113	2'545	75'330	893	14'050	14'020	6'336	5'585
36	HAG NaOH 10/15/60/80	15.40	1'953	28	308'300	223	2'546	1'179	1'239	14'260	< 10	878	1'193	2'507	80'910	896	13'710	8'381	7'265	5'153

Tabelle A7-12: *NaCl-Versuche***.**

Nr.	Bezeichnung	V (mL)	ICP-OES												IC											
			Al	Ca	Cd	Cr	Cu	Fe	K	Mg	Mn	Pb	Zn	Na	NH_4	K	Ca	Mg	F	Cl	Br	NO_3	SO_4
			mg/L	mg/L	mg/L	mg/L	mg/L	mg/L	mg/L	mg/L	mg/L	mg/L	mg/L	mg/L	mg/L	mg/L	mg/L	mg/L	mg/L	mg/L	mg/L	mg/L	mg/L
15	ZUC HCl 5/4/60/RT	254	836	11'141	56	5	0	255	6'358	1'310	47	36	8'630	8'407	<100	7'971	11'275	1'298	570	55'701	631	86'615	1'260
40	ZUC NaCl/5/60/85 vw HCl 5%	80	0	1'005	10	0	207	1	516	73	4	1'242	344	64'735	<100	566	2'370	<100	<16	100'500	<16	<16	4'466
29	ZUC H_2SO_4 6.6/4/60/RT	244	829	693	60	7	1	348	6'844	1'358	48	30	8'880	8'559	<100	8'009	676	1'315	616	19'750	640	8'663	24'957
41	ZUC NaCl/5/60/85 vw H_2SO_4 6.6%	86	0	2'182	7	0	51	0	454	85	3	983	374	64'130	<100	541.0	2'423	104	<16	100'483	25	<16	3'825
15	HAG HCl 5/4/60/RT	255	0	18'491	21	0	0	0	4'905	898	23	8	317										
40	HAG NaCl/5/60/85 vw HCl 5%	80	0	1'497	3	0	0	0	492	265	3	5	1'203										
29	HAG H_2SO_4 6.6/4/60/RT	234	<5	971	22	<5	1	<25	5'402	1'076	26	<5	855										
41	HAG NaCl/5/60/85 vw H_2SO_4 6.6%	74	0	2'480	3	0	0	1	650	196	3	12	793										

Nr.	Bezeichnung	Gewicht FK	Ba	Br	Ca	Cd	Cl	Cr	Cu	Fe	K	Mn	Pb	Sb	Si	Sn	Ti	Zn	P	S
		g	mg/kg	mg/kg	mg/kg	mg/kg	mg/kg	mg/kg	mg/kg	mg/kg	mg/kg	mg/kg	mg/kg	mg/kg	mg/kg	mg/kg	mg/kg	mg/kg	mg/kg	mg/kg
-	FAZUC	50.00	1'881	3'847	152'700	443	103'300	468	2'512	20'510	46'900	784	11'920	2'976	81'260	1'682	9'308	65'420	4'497	55'430
15	ZUC HCl 5/4/60/RT	34.18	2'616	190	150'800	147	9'220	713	3'941	31'340	11'950	814	18'640	5'152	92'250	2'418	13'740	24'670	7'658	87'390
40	ZUC NaCl/5/60/85 vw HCl 5%	8.84	2'903	38	136'300	33	15'180	816	1'584	25'780	4'621	661	4'237	4'180	85'960	2'675	15'360	20'270	9'972	77'210
29	ZUC H_2SO_4 6.6/4/60/RT	46.23	1'952	227	171'300	93	3'704	468	3'025	20'600	9'142	577	14'350	3'767	55'320	1'781	10'290	18'260	5'069	116'300
41	ZUC NaCl/5/60/85 vw H_2SO_4 6.6%	12.05	2'120	28	157'500	19	9'435	585	2'183	17'710	3'614	511	2'524	2'890	54'410	1'916	10'630	14'110	6'547	107'800
-	FAHAG	50.00	1'680	2'231	242'900	202	91'530	948	992	14'570	37'100	649	3'445	2'461	80'730	802	12'420	21'250	5'905	44'190
15	HAG HCl 5/4/60/RT	35.87	2'174	134	179'500	79	11'800	1'389	1'473	18'830	10'770	846	4'353	3'100	94'120	1'086	17'410	28'480	9'538	55'910
40	HAG NaCl/5/60/85 vw HCl 5%	10.28	1'953	22	164'100	38	17'900	1'362	1'182	14'410	4'155	503	3'479	2'799	72'180	1'008	15'130	12'610	10'030	79'200
29	HAG H_2SO_4 6.6/4/60/RT	55.76	1'437	149	198'400	52	4'125	824	1'008	12'060	8'348	514	2'832	2'175	56'360	699	11'180	15'230	5'329	104'400
41	HAG NaCl/5/60/85 vw H_2SO_4 6.6%	9.58	1'412	16	176'900	25	15'290	928	789	10'190	3'191	355	2'319	1'952	49'010	690	10'730	7'516	6'690	104'100

Tabelle A7-13: *Actlabs Analysen.*

Element		Ag	Al	As	B	Ba	Be	Bi	Ca	Cd	Ce	Co	Cr	Cs	Cu	Dy	Er	Eu	Fe	Ga	Gd	Ge	Hf	Hg	Ho	In	K	La	Li
Einheit		ppm	%	ppm	ppm	ppm	ppm	ppm	%	ppm	ppm	ppm	ppm	ppm	ppm	ppm	ppm	ppm	%	ppm	ppm	ppm	ppm	ppb	ppm	ppm	%	ppm	ppm
Detektionslimit		0.05	0.01	0.1	1	1	0.1	0.02	0.01	0.1	0.1	0.1	0.5	0.05	0.2	0.1	0.1	0.05	0.01	0.1	0.1	0.1	0.1	10	0.1	0.1	0.01	0.1	0.5
Methode		TD-MS	TD-MS	TD-MS	TD-MS	TD-MS	TD-MS	TD-MS	TD-MS	TD-MS	TD-MS	TD-MS	TD-MS	TD-MS	TD-MS	TD-MS	TD-MS	TD-MS	TD-MS	TD-MS	TD-MS	TD-MS	TD-MS	TD-MS	TD-MS	TD-MS	TD-MS	TD-MS	TD-MS
-	FAZUC	59	2.8	29	80	80	0.5	123	11	305	16	39	250	7.4	2'130	0.9	0.4	0.2	14	5.4	0.9	0.1	2.3	240	0.1	2.2	2.7	6.1	56
2	ZUC H_2O /80/80/RT	84	4.2	32	10	58	0.8	190	15	123	24	59	315	18	2'890	1.4	0.7	0.3	15	11	1.3	<0.1	3.2	30	0.2	3.0	0.8	9.2	34
14	ZUC HC15/4/60/RT	96	3.9	39	10	32	0.7	147	80	103	15	46	376	3.6	3'180	0.7	0.4	0.2	16	13	0.8	<0.1	1.6	130	0.1	3.3	1.0	6.3	20
25	ZUC HC15/4/60h/RT	41	4.0	36	10	26	0.7	134	8.9	22	14	40	374	4.1	1'330	0.7	0.3	0.2	18	14	0.7	<0.1	2.1	90	<0.1	2.4	1.0	5.8	20
29	ZUC H_2SO_4 6.6/4/60/RT	65	2.7	34	14	23	0.5	123	11	65	14	38	306	2.7	2'260	0.8	0.4	0.2	13	9.4	0.9	<0.1	2.4	270	0.1	2.2	0.8	5.8	19
31	ZUC H_2SO_4 6.6/4/60/RT vw HC15%	88	19	23	40	15	0.4	141	8.4	24	14	36	482	18	1'820	0.5	0.3	0.2	12	8.2	0.7	<0.1	5.5	460	<0.1	2.4	0.4	5.8	15
36	ZUC NaOH 10/15/60/80	99	3.3	4.6	4.0	1'120	0.8	230	22	485	28	55	542	0.4	2'590	1.6	0.9	0.4	2.6	<0.1	1.8	<0.1	5.4	<40	0.3	3.7	0.4	12	29
-	FA ZUC F	62	4.3	27	2.0	460	1.8	109	10	147	41	231	1'420	15	2'370	3.3	1.3	0.6	13	<0.1	2.4	<0.1	0.6	340	0.4	1.6	0.9	18	55
-	FA ZUC M	39	4.8	14	2.0	1'22	1.3	63	12	114	42	189	1'280	0.8	2'920	3.5	1.3	0.6	14	0.7	2.2	<0.1	1.0	350	0.4	0.7	0.7	20	40
-	FAHAG	33	4.0	33	2.0	141	0.5	40	15	126	14	36	424	3.5	864	0.7	0.4	0.3	0.6	<0.1	2.0	<0.1	2.4	40	0.1	1.0	3.3	6.5	28
2	HAG H_2O /80/80/RT	40	5.3	8.3	10	188	0.7	59	20	166	23	41	355	0.7	1'010	1.1	0.6	0.4	0.8	<0.1	2.5	<0.1	3.7	<40	0.2	1.2	0.6	10	22
14	HAG HC15/4/60/RT	48	5.8	10	<1	83	0.7	29	12	56	16	37	507	2.0	1'080	0.9	0.5	0.3	1.0	5.1	2.1	<0.1	3.5	30	0.1	1.3	1.1	9.4	21
25	HAG HC15/4/60h/RT	50	5.9	10	<1	45	0.8	48	12	118	19	55	447	2.1	1'230	1.0	0.6	0.4	1.0	7.3	2.2	<0.1	3.0	40	0.2	1.4	1.1	8.5	27
29	HAG H_2SO_4 6.6/4/60/RT	29	3.5	5.3	7.7	33	0.4	37	12	38	12	27	651	1.5	783	0.7	0.4	0.2	0.8	4.0	1.4	<0.1	3.9	160	<0.1	0.8	0.7	5.9	16
31	HAG H_2SO_4 6.6/4/60/RT vw HC15%	43	4.4	10	4.0	20	0.6	66	11	26	19	30	653	1.4	1'060	1.0	0.5	0.4	0.8	7.4	2.6	<0.1	0.8	240	0.1	1.1	0.5	8.7	15
36	HAG NaOH 10/15/60/80	47	4.1	1.9	2.0	789	0.7	78	24	171	24	30	619	0.2	651	1.2	0.7	0.4	1.0	<0.1	2.6	<0.1	3.4	<40	0.2	1.3	0.3	11	17

Element		Lu	Mg	Mn	Mo	Na	Nb	Nd	Ni	P b	Pr	Rb	Re	Sb	Se	Sm	Sn	Sr	T a	Tb	T e	Th	Tl	T m	U	V	W	Y	Yb	Zn	Zr
Einheit		ppm	%	ppm	ppm	%	ppm	ppm	ppm	ppm	ppm	ppm	ppm	ppm	ppm	ppm	ppm	ppm	ppm	ppm	ppm	ppm	ppm	ppm	ppm	ppm	ppm	ppm	ppm	ppm	ppm
Detektionslimit		0.1	0.01	1	0.05	0.01	0.1	0.1	0.5	0.5	0.1	0.2	0.001	0.1	0.1	0.1	1	0.2	0.1	0.1	0.1	0.1	0.05	0.1	1	0.1	0.1	0.1	0.1	0.2	1
Methode		TD-MS	TD-MS	TD-MS	TD-MS	TD-MS	TD-MS	TD-MS	TD-MS	TD-MS	TD-MS	TD-MS	TD-MS	TD-MS	TD-MS	TD-MS	TD-MS	TD-MS	TD-MS	TD-MS	TD-MS	TD-MS	TD-MS	TD-MS	TD-MS	TD-MS	TD-MS	TD-MS	TD-MS	TD-MS	TD-MS
-	FAZUC	<0.1	0.8	670	14	<3	<0.1	8.0	133	>5000	17	6.5	0.0	392	5.4	10	>200	211	<0.1	0.1	0.2	2.1	2.1	<0.1	2.1	13	3.3	4.8	0.4	>10000	42
2	ZUC H_2O /80/80/RT	<0.1	1.2	903	17	0.9	<0.1	1.3	187	>5000	2.4	1.7	0.0	347	6.6	1.6	>200	266	<0.1	0.2	0.3	2.9	0.9	0.1	1.7	15	5.6	7.7	0.6	>10000	71
14	ZUC HC15/4/60/RT	<0.1	0.6	641	2.4	0.7	<0.1	7.1	187	>5000	1.5	3.0	0.0	347	7.4	1.2	>200	169	<0.1	0.1	0.3	2.6	2.6	<0.1	1.7	12	2.4	4.3	0.4	>10000	41
25	ZUC HC15/4/60h/RT	<0.1	0.5	625	2.4	0.6	<0.1	7.0	174	>5000	1.4	3.4	0.0	344	7.5	0.7	>200	145	<0.1	0.1	0.3	2.4	2.7	<0.1	1.7	14	2.5	3.9	0.4	>10000	47
29	ZUC H_2SO_4 6.6/4/60/RT	<0.1	0.3	498	14	0.6	<0.1	7.0	134	>5000	1.5	2.3	0.0	309	5.5	1.1	>200	194	<0.1	0.1	0.2	2.0	1.5	<0.1	1.1	10	2.8	4.2	0.4	>10000	48
31	ZUC H_2SO_4 6.6/4/60/RT vw HC15%	<0.1	0.3	353	11	0.3	<0.1	7.0	155	>5000	1.5	1.4	0.0	80	7.1	0.8	>200	142	<0.1	0.1	0.1	2.1	1.4	<0.1	1.1	<1	5.7	3.1	0.2	>10000	88
36	ZUC NaOH 10/15/60/80	0.1	1.3	1'160	2.8	1.1	<0.1	1.5	220	>5000	3.2	7.0	0.0	324	0.3	2.0	128	397	<0.1	0.3	<0.1	4.3	3.3	0.1	1.5	9.0	0.8	10	0.8	>10000	114
-	FA ZUC F	0.2	1.4	2'000	7.6	1.1	<0.1	3.9	1'010	>5000	6.3	1.8	0.0	286	1.2	3.8	>200	335	<0.1	0.5	1.6	4.8	0.9	0.2	2.8	50	6.8	14	1.3	>10000	15
-	FA ZUC M	0.2	1.4	2'260	8.0	1.0	<0.1	4.6	1'080	4'840	7.2	1.3	0.0	83	0.3	8.1	>200	364	<0.1	0.5	0.9	4.6	0.7	0.2	2.6	57	6.7	14	1.2	>10000	42
-	FAHAG	<0.1	0.9	562	7.7	>3	<0.1	5.6	144	2'620	1.3	4.5	0.5	179	2.9	0.7	24	254	<0.1	0.2	0.3	2.4	1.1	<0.1	1.5	<1	1.6	7.5	0.5	>10000	52
2	HAG H_2O /80/80/RT	<0.1	1.2	723	7.7	0.9	<0.1	9.3	178	2'370	2.3	1.1	0.3	197	3.8	1.2	18	304	<0.1	0.3	0.5	3.8	0.9	<0.1	3.7	4.0	2.3	11	0.7	>10000	86
14	HAG HC15/4/60/RT	<0.1	0.9	653	10	0.9	<0.1	7.3	179	3'870	1.7	2.1	0.3	276	4.1	1.1	101	201	<0.1	0.2	0.4	3.4	0.9	<0.1	2.3	4.0	4.4	10	0.6	>10000	74
25	HAG HC15/4/60h/RT	<0.1	0.9	788	10	0.9	<0.1	8.6	202	3'870	2.0	2.2	0.4	240	3.9	1.2	100	203	<0.1	0.3	0.3	3.3	1.0	<0.1	3.3	<1	4.5	11	0.7	>10000	72
29	HAG H_2SO_4 6.6/4/60/RT	<0.1	0.5	373	6.9	0.7	<0.1	5.6	108	2'230	1.3	1.6	0.2	250	2.5	0.8	66	190	<0.1	0.2	0.1	2.2	0.7	<0.1	4.5	<1	1.0	5.9	0.4	>10000	66
31	HAG H_2SO_4 6.6/4/60/RT vw HC15%	<0.1	0.4	369	9.4	0.4	<0.1	9.2	141	3'380	2.1	1.3	0.4	229	4.2	1.3	38	175	<0.1	0.3	<0.1	2.7	0.7	<0.1	1.9	<1	1.9	8.9	0.5	8'470	18
36	HAG NaOH 10/15/60/80	<0.1	1.2	760	2.5	1.4	<0.1	1.2	168	7'600	2.6	4.0	0.3	222	<0.1	1.7	20	366	<0.1	0.3	0.1	3.9	1.3	<0.1	1.7	3.0	0.7	12	0.8	5'840	88

Chapter 8

FLUWA-Verfahren – Vom Labor in den Industriemassstab

Gisela Weibel[a], Urs Eggenberger[a], Stefan Ringmann[b]

[a]*Institut für Geologie, Baltzerstrasse 1+3, 3012 Bern, Schweiz*
[b]*KVA Linth, Im Fennen 1A, 8867 Niederurnen, Schweiz*

8.1 Einleitung

In der Schweiz fallen jährlich ca. 72'000 Tonnen Flugaschen (FA) aus den 30 Kehrichtverbrennungsanlagen (KVA) an. Diese Flugaschen werden derzeit entweder unbehandelt in Untertagedeponien exportiert, mit Zement verfestigt und deponiert oder einer sauren Wäsche nach dem FLUWA-Verfahren (Schlumberger et al., 2007; Bühler und Schlumberger, 2010) unterzogen. Das FLUWA-Verfahren wird gegenwärtig von 12 KVA's durchgeführt und entspricht dem Stand der Technik. Fünf weitere Anlagen lassen ihre Flugasche extern in einer KVA aufbereiten. Mit dem FLUWA-Verfahren werden mit saurem Quenchwasser aus der Rauchgasreinigung Salze und Metalle aus den Flugaschen herausgelöst. Die Aschensuspension wird anschliessend mit einem Vakuumbandfilter in ein schwermetallhaltiges Filtrat und einen schwermetallarmen Filterkuchen aufgetrennt. Die Schwermetalle im Filtrat werden durch die Zugabe von Kalkmilch gefällt und der entstehende Hydroxidschlamm kann im Ausland aufbereitet und v.a. metallisches Zink zurückgewonnen werden. Mit der neuen Abfallverordnung (Bundesamt für Umwelt, 2016) wird das Ziel der Schliessung von Stoffkreisläufen verfolgt. Damit müssen nach einer 5-jährigen Übergangsfrist alle in der Schweiz anfallenden Flugaschen behandelt und die Metalle zurückgewonnen werden. Mit dem FLUREC-Verfahren (Schlumberger et al., 2007) steht seit 2012 bei der KEBAG Zuchwil ein Verfahren zur Verfügung, das eine elektrolytische Metallrückgewinnung ermöglicht. Mit dem vorgegebenen Ziel der Metallrückgewinnung aus allen Flugaschen wird im Rahmen des Projektes SwissZinc eine zentrale Rückgewinnung evaluiert. Angestrebt wird eine Aufbereitungs- und Metallrückgewinnungsanlage für Hydroxidschlämme analog dem FLUREC-Prozess. Aufgrund der hohen Konzentrationen bzw. der Toxikologie steht v.a. die Rückgewinnung

der Metalle Zn, Pb, Cu und Cd im Vordergrund. Die Extraktionsausbeuten des FLUWA-Verfahrens für diese Metalle bewegen sich zurzeit im Bereich von 60-80% für Zn, 0-30% für Pb und Cu sowie 60-85% für Cd. Der Kanton Solothurn hat seit 2007 in der Betriebsbewilligung der KEBAG Zuchwil geregelt, dass der gewaschene Filterkuchen eine maximale Pb-Konzentration von 6'000 mg/kg nicht überschreiten darf. Dies entspricht einer geforderten Ausbeute von 50-70% Pb. Diese Vorgabe wird durch eine optimierte verfahrenstechnische Anordnung der FLUWA erreicht und mit der Zugabe von Wasserstoffperoxid 30% (H_2O_2). Die grosstechnisch erreichbaren Extraktionsausbeuten liegen im Bereich von 50-90% für Pb, 40-80% für Cu und 85-95% für Cd.

Um eine möglichst effiziente Metallentfrachtung der Flugaschen zu erreichen und damit schwermetallreiche Hydroxidschlämme für die anschliessende Metallrückgewinnung zu erhalten, sollte die Flugascheaufbereitung mittels FLUWA oder einem analogen Verfahren optimal betrieben werden. Der vorliegende Bericht zeigt das Bestreben an der KVA Linth auf (Abbildung 8-1), wo zwischen November 2016 und April 2017 diverse Versuche zur verfahrenstechnischen Optimierung des FLUWA-Betriebs durchgeführt wurden. Die Versuche wurden durch das Institut für Geologie der Universität Bern begleitet und die im Labor gewonnenen Erkenntnisse der laufenden Dissertation (G. Weibel) dienten als Grundlage für die grosstechnischen Versuche (siehe Kaptiel 7). Diese Arbeiten erfolgten in engem Austausch mit dem Zentrum für nachhaltige Abfall- und Ressourcennutzung in Zuchwil (S. Schlumberger, W. Klink), wo bereits zahlreiche Versuche in diese Richtung durchgeführt wurden.

Abbildung 8-1: *KVA-Linth (31.03.2017).*

8.2 FLUWA-Betrieb KVA Linth

8.2.1 Ausgangslage FLUWA 2016

Vor der Optimierung des FLUWA-Verfahrens der KVA Linth wurde die Ausganslage 2016 aufgenommen. Dabei wurden im November 2016 zwei Probenahmen (Vorgehen Probenahme und Analytik, siehe Kapitel 8.4) von Flugasche und gewaschenem Filterkuchen durchgeführt und die elementspezifischen Extraktionsausbeuten berechnet (Tabelle 8-4). Im Weiteren wurden die Parameter Flugasche- und Quenchwassermenge, pH-Wert, Redoxpotential und Temperatur der Asche-Suspension sowie Verweilzeit pro Extraktionsbehälter aufgenommen (Tabelle 8-1).

Tabelle 8-1: *Durchschnittliche technische Daten des FLUWA-Betriebs der KVA Linth 2016. Detaillierte Werte der FLUWA einzelner Tage sind im Anhang 8 angefügt (Monitoring Leitparameter).*

Parameter	Technische Daten
Extraktionsbehälter	2 (Nutzvolumen pro Behälter 3 m^3)
Durchsatz Flugasche	3.5 bis 5 t/h
Menge Quenchwasser (QW)	QW sauer (HCl 5%): ca. 6 m^3/h QW basisch (Na_2SO_4-Lösung): ca. 4 m^3/h
Waschwassermengen Vakuumbandfilter	Deion. Wasser: ca. 2.5 m^3/h
Verweilzeit	15 Minuten pro Behälter
Bedingungen Extraktionsbehälter	Behälter 1: pH 4.7, Eh -500 mV, Temp. 58°C Behälter 2: pH 5.1, Eh -550 mV, Temp. 58°C

8.2.2 Behandlung von Fremdasche

Im Jahr 2016 wurde nebst der eigenen Flugasche (Flugasche Linth) bei der KVA Linth auch Fremdasche (Fremdasche A) mit dem FLUWA-Verfahren behandelt. Die Flugasche Linth und Fremdasche A werden in getrennten Silos gelagert und einzeln aufbereitet. Die im November 2016 beprobte Flugasche und gewaschener Filterkuchen entsprechen deshalb Mischproben aus Flugasche Linth und Fremdasche A (45% Linth, 55% Fremdasche A, Tabelle 8-2).

Zusätzlich zur eigenen Flugasche Linth und Fremdasche A, wird seit Januar 2017 Flugasche einer weiteren KVA bei der KVA Linth mit dem FLUWA-Verfahren behandelt (Fremdasche B). Bei den Probenahmen über eine Woche verteilt, entsteht somit ein Flugasche-Mix mit unterschiedlichen Anteilen der diversen Flugaschen (durchschnittlich 35% Linth, 40% Fremdasche A, 25% Fremdasche B). Neben den abfallinputbedingten Konzentrationsschwankungen, führte das Beimischen von Fremdasche B zu durchschnittlich etwas tieferen Metallkonzentrationen (Tabelle 8-2).

Tabelle 8-2: *Zusammensetzung des Flugasche-Mix in der jeweiligen Kalenderwoche (mg/kg).*

	Ausgangslage 2016		**Januar - März 2017**				
Asche	*Flugasche Linth (45%), Fremdasche A (55%)*		*Flugasche Linth (35%), Fremdasche A (40%), Fremdasche B (25%)*				
Element	**KW 45/46/ 2016**	**KW 48/ 2016**	**KW 2/ 2017**	**KW 7/ 2017**	**KW 8/ 2017**	**KW 9/ 2017**	**KW 10/ 2017**
Al	32'997	27'650	30'730	27'570	32'760	27'600	26'890
Ba	2'149	2'449	1'967	1'959	2'259	2'072	2'018
Ca	148'533	140'000	164'500	158'900	163'700	147'800	141'300
Cd	309	380	304	223	246	292	340
Cl	87'353	113'600	128'200	160'100	124'600	108'700	110'600
Cr	601	572	556	411	446	557	595
Cu	2'857	2'839	1'990	1'853	2'113	2'003	2'181
Fe	24'147	21'050	15'920	12'790	16'640	15'770	16'460
K	47'240	54'430	52'820	43'290	49'300	61'320	62'630
Mn	804	888	894	721	772	1'007	1'019
P	3'502	3'779	4'081	3'583	3'875	3'994	3'806
Pb	11'040	11'120	7'352	7'543	7'031	10'470	11'540
S	52'617	62'630	49'060	58'190	47'330	74'560	69'780
Sb	3'469	2'632	1'968	2'365	2'854	2'297	2'004
Si	73'947	67'540	69'150	61'900	68'670	60'410	60'000
Sn	1'484	1'622	1'253	1'319	1'384	1'248	1'296
Ti	9'415	8'475	9'480	8'176	9'739	8'572	8'268
Zn	55'323	49'980	37'610	32'830	40'840	37'210	39'800

8.3 Vorgehen Optimierung FLUWA

Basierend auf den Erkenntnissen der Laborversuche wurde versucht, mechanische und chemische Optimierungen des FLUWA-Betriebs der KVA Linth vorzunehmen. Im Labor hat sich gezeigt, dass sich die Optimierung mechanischer Parameter wie die Erhöhung des Flüssig-Fest-Verhältnisses (FF) sowie die Anpassung der Temperatur und Verweilzeit der Aschesuspension im Extraktionsprozess positiv auf die elementspezifischen Extraktionsausbeuten auswirken (siehe Kapitel 7). Chemische Parameter zur Steigerung der Metallausbeuten der FLUWA beinhalten die Anpassung des pH-Wertes sowie den Einsatz eines Oxidationsmittels während der Flugascheextraktion (Kapitel 3, 4 und 7). Die Versuche zur Optimierung der FLUWA bei der KVA Linth werden in zwei Teile unterteilt:

- Optimierung FLUWA Teil 1: In einer ersten Phase wurde versucht, das Flüssig-Fest-Verhältnis und die Verweilzeit der Aschesuspension im Extraktionsprozess zu erhöhen sowie den pH-Wert der Suspension zu senken. Die Anpassungen wurden basierend auf den Laborversuchen aus Kapitel 7 in den Kalenderwochen 48/2016 bis 10/2017 vorgenommen.

- Optimierung FLUWA Teil 2: Basierend auf weiteren Versuchsserien im Labor (Kapitel 8.6), wurde in einem eintägigen Testlauf am 31. März 2017 der Einsatz von Oxidationsmittel (H_2O_2 und Luft) während dem FLUWA-Betrieb getestet.

Um die Effizienz der Optimierungsschritte des FLUWA-Verfahrens zu beurteilen, wurden folgende Leitparameter zwischen November 2016 und März 2017 täglich erfasst (Resultate siehe Anhang 8).

- Flugaschenmenge (t/h)
- Mengen Quenchwasser sauer und basisch (m^3/h)
- pH-Werte der Aschesuspension in den Extraktionsbehältern
- Redoxpotential (mV) der Aschesuspension in den Extraktionsbehältern
- Temperatur (°C) der Aschesuspension in den Extraktionsbehältern
- Verweildauer (min) der Flugasche im jeweiligen Extraktionsbehälter

Das Monitoring diente sowohl für die Beurteilung der Optimierungsschritte, wie auch als Grundlage für die Planung der Probenahme. Nach jedem Optimierungsschritt wurde bei stabilem Betrieb eine einwöchige Probenahme durchgeführt und die Stoffströme Flugasche, Quenchwasser und gewaschener Filterkuchen analysiert.

8.4 Probenahme und Analytik

Während der ersten Optimierungsphase wurde bei stabilen Prozessbedingungen einwöchige Probenahmen der Stoffströme Flugasche, Quenchwasser und Filterkuchen durchgeführt. Dabei wurden von den einzelnen Stoffströmen jeweils 3x täglich Stichproben während einer Woche durch den Anlagenbetreiber entnommen. Durch das batchweise Behandeln von eigener und fremder Flugasche entsprechen die Wochenproben von Flugasche und Filterkuchen Mischungen unterschiedlicher Flugaschen. Während dem Testlauf mit dem Einsatz von H_2O_2 und Luft (Optimierung Teil 2) wurde nach den Veränderungen der Extraktionsbedingungen 1 h bis zur Probenahme des Filterkuchens abgewartet, um repräsentative Proben zu gewährleisten.

Eine Teilprobe der Flugaschen und gewaschenen Filterkuchen wurde im Labor bei 105°C bis zur Gewichtskonstanz getrocknet und die Proben mit einer Scheibenschwingmühle gemahlen. Für die Laborversuche wurde originale, nicht getrocknete und nicht gemahlene Flugasche verwendet.

8.4.1 ED-XRF

Die Feststoffanalytik wurde mittels Röntgenfluoreszenzanalyse auf einem Spectron, Xepos ED-XRF beim ZAR in Zuchwil durchgeführt. Die Elemente Al, Ca, Cd, Cu, Fe, K, Mn, Pb, S, Sb, Si, Ti und Zn wurde mit matrixangepasster Kalibrierung für Flugasche und gewaschener Filterkuchen bestimmt. Die Elemente Ba, Br, Cl, Cr, Ni, Pb und Sn wurden

weiter mit der Turboquant Methode bestimmt. Für die Messung der Proben wurden 4.00 g der gemahlenen Ausgangsasche/Filterkuchen mit 0.90 g Bindemittel (Hoechst Wachs) vermengt und zu einer Pulverpille gepresst. Proben aus KW 48/2016 und KW 2/2017 wurden zusätzlich mit Totalaufschlüssen und anschliessender ICP-OES-Messung bestimmt (TA-ICP-OES). Die Messung von Al mit ED-XRF ergeben ähnliche Resultate wie mit TA-ICP-OES, trotz der bekannten grossen analytischen Unsicherheit von ED-XRF für Al aufgrund der vielen metallischen Anteile in der Flugasche. Die Messresultate sind im Anhang 8 angefügt.

8.4.2 ICP-OES

Die ICP-OES Analysen wurden mit einem Varian 720-ES an den verdünnten Filtraten und Totalaufschlüssen durchgeführt. Dabei wurden die Elemente Al, Ba, Ca, Cd, Co, Cr, Cu, Fe, K, Mg, Mn, Na, Ni, P, Pb, S, Sb, Si, Ti und Zn gemessen. Die Kalibrierung wurde mittels Sigma Multielement-Standard 6 durchgeführt und die Analysen mit einem Checkstandards überprüft (Merck IV und Merck X Multielementstandards). Die Messresultate sind im Anhang 8 angefügt.

8.4.3 IC

In den wässrigen Filtraten wurden zusätzlich die Parameter NH_4, Sr, F, Cl, Br, NO_3 und SO_4 mittels eines Metrohm 850 Professional Ionenchromatographen bestimmt.

8.4.4 Massenverlust und Massenbilanz

Durch die Mobilisierung der säurelöslichen Bestandteile der Flugasche ist die Masse des gewaschenen Filteruchens geringer. Dieser Massenverlust lässt sich gravimetrisch über das Gewicht der Flugasche und des Filterkuchens oder durch analytische Berechnung der inerten Elemente wie Ba, Ti, Cr, Sb, P oder Sn bestimmen. Als inerte Elemente werden dabei diejenigen bezeichnet, die unter den vorliegenden Extraktionsbedingungen kaum abgereichert werden und sich deshalb im Filterkuchen relativ zur Gesamtmasse anreichern. Da bei den meisten grosstechnischen FLUWA-Verfahren die Erfassung der notwendigen Massenströme schwierig ist, bieten inerte Elemente eine gute Möglichkeit für die Berechnung des Massenverlustes und somit der Extraktionsausbeuten (Tabelle 8-3).

Die Mittelwerte der Aufkonzentrierung der jeweiligen Kalenderwochen mit der entsprechenden Flugaschezusammensetzung zeigen für die Ausgangslage 2016 und den ersten Teil der Optimierung einen Massenverlust beim FLUWA-Verfahren der KVA Linth von 29% resp. 27%. Bei den Filterkuchen der Optimierung Teil 2 werden höhere Aufkonzentrierungen bestimmt, was in einem durchschnittlichen Massenverlust von 44% resultiert. Die unterschiedliche Flugaschezusammensetzung und ein etwas höheres Flüssig-Fest-Verhältnis erklären diesen Unterschied.

***Tabelle 8-3**: Faktor der Aufkonzentrierung der gemessenen Elemente im Filterkuchen bestimmt über die-inerten Elemente.*

Element	Methode	Ba	Ti	Cr	Sb	P	Sn	MW
Ausgangslage 2016: *Flugasche Linth (45%), Fremdasche A (55%)*								
FK - KW 45/46/2016	ED-XRF	1.20	1.22	1.24	1.26	1.47	1.28	1.28
FK - KW 48/2016	ED-XRF	1.14	1.25	1.19	1.33	1.26	1.09	1.21
FK - KW 48/2016	TA-ICP-OES	1.28	1.40	1.30	1.34	1.30	-	1.32
Mittelwert der Aufkonzentrierung								1.29
Optimierung Teil 1: *Flugasche Linth (35%), Fremdasche A (40%), Fremdasche B (25%)*								
FK - KW 2/2017	ED-XRF	1.23	1.20	1.28	1.26	1.45	1.21	1.27
FK - KW 2/2017	TA-ICP-OES	1.32	1.30	1.26	1.27	1.29	-	1.29
FK - KW 7/2017	ED-XRF	1.28	1.32	1.43	1.37	1.57	1.21	1.36
FK - KW 8/2017	ED-XRF	1.20	1.09	1.33	1.04	1.36	1.09	1.18
FK - KW 9/2017	ED-XRF	1.15	1.26	1.36	1.43	1.55	1.30	1.34
FK - KW 10/2017	ED-XRF	1.26	1.35	1.24	1.50	1.46	1.18	1.33
Mittelwert der Aufkonzentrierung								1.27
Optimierung Teil 2: *FK 1-2 bis 1-3 Fremdasche A, FK 2-1 bis 2-3 Flugasche Linth*								
FK 1-1	ED-XRF	1.20	1.35	1.37	1.23	1.51	1.09	1.29
FK 1-2	ED-XRF	1.25	1.54	1.55	1.53	1.71	1.31	1.48
FK 1-3	ED-XRF	1.28	1.52	1.48	1.40	1.67	1.13	1.41
FK 2-1	ED-XRF	1.19	1.34	1.46	1.21	1.65	1.29	1.35
FK 2-2	ED-XRF	1.23	1.38	1.52	1.51	1.72	1.59	1.49
FK 2-3	ED-XRF	1.34	1.56	1.50	1.63	1.82	1.64	1.58
Mittelwert der Aufkonzentrierung								1.44

Bei Laborversuchen ist die Erfassung der Gewichte und Volumen gut möglich und eine Massenbilanz kann erstellt werden. Für die Bestimmung der elementspezifischen Extraktionsausbeuten wird dabei die absolut extrahierte Menge eines Elements (mg) im Filtrat oder Filterkuchen dividiert durch absolute Menge (mg) des Elements in der eingesetzten Flugasche gerechnet.

(A) Berechnung der Extraktionsausbeute über das Filtrat (FL):

$$\text{Ausbeute (\%)} = 100 \cdot \left(\frac{\frac{c_{FL\ (mg/L)} \cdot V_{FL(mL)}}{1000}}{\frac{c_{FA(mg/kg)} \cdot m_{FA\ (g)}}{1000}}\right)$$

(B) Berechnung der Extraktionsausbeute über den Filterkuchen (FK):

$$\text{Ausbeute (\%)} = 100 \cdot \left(1 - \frac{\frac{c_{FK}\left(\frac{mg}{kg}\right) \cdot m_{FK(mL)}}{1000}}{\frac{c_{FA}\left(\frac{mg}{kg}\right) \cdot m_{FA\ (g)}}{1000}}\right)$$

c: gemessene Konzentration im Filtrat (FL) in mg/L und in der Flugasche (FA) in mg/kg.

m: Masse der Flugasche und des Filterkuchens (FK) in g.

V: Volumen des Filtrats in mL.

8.5 Optimierung FLUWA Teil 1

Basierend auf den Erkenntnissen der Laborversuche zur Optimierung des FLUWA-Verfahrens (Kapitel 7) wurde in einer ersten Optimierungsphase (Kalenderwochen 48/2016 bis 10/2017) versucht, die Parameter Flüssig-Fest-Verhältnis, Verweilzeit der Aschensuspension im Extraktionsprozess und Senkung des pH-Wertes der Suspension im Industriemassstab umzusetzen.

8.5.1 Flüssig-Fest-Verhältnis

Aus Laborversuchen ist bekannt, dass die Extraktion von Flugasche mit zunehmendem Flüssig-Fest-Verhältnis zu höhere Metallausbeuten führt (Kapitel 7). Mehr Extraktionslösung führt zu einem intensiveren Kontakt zwischen Flüssigkeit und Feststoff und zu einem weniger stark konzentrierten Filtrat, welches anteilig als Restfeuchte bei der Vakuumbandfiltration im gewaschenen Filterkuchen zurückbleibt. Eine erhöhte Menge Extraktionslösung wird durch eine erhöhte Dosierung von Quenchwasser oder anteilsweise Wasser erreicht, was zur Senkung der Leitfähigkeit der Lösung führt. Mit der vorhandenen Kapazität bei der KVA Linth, die durch den Filtrat-Sedimentationsbehälter limitiert wird, konnte bei einer täglichen FLUWA-Betriebszeit von 7-9 h nur mit einem ungünstigen Flüssig-Fest-Verhältnis von 2.0 gefahren werden (siehe Monitoring Leitparameter im Anhang 8). Mit der Inbetriebnahme des neuen Kerzenfilters per Ende April 2017 wird diese Limitierung aufgehoben, was längere Betriebszeiten der FLUWA bei erhöhtem Flüssig-Fest-Verhältnis erlauben wird (15 h/Tag).

8.5.2 Verweilzeit

Im März 2017 (KW 8/2017) wurde die dritte Extraktionsstufe in Betrieb genommen. Dabei wurde der gleiche Rührwerktyp wie in Behälter 2 verwendet und somit die Herstellung des Betriebszustands 2001-2007 erreicht. Dies führt zu 1/3 längerer Verweilzeit (15 min im letzten Behälter) und damit zu einer Extraktionsdauer von ca. 45 Minuten. Die längere Verweilzeit durch den dritten Behälter führt zu erhöhten pH-Werten in der Aschesuspension aufgrund der längeren Interaktionszeit von Flugasche (hohe Pufferkapazität) und Quenchwasser.

Die längere Reaktionszeit kann zu erhöhten Metallextraktionsausbeuten führen, jedoch steigt mit erhöhtem pH-Wert am Ende des FLUWA-Prozesses (pH >4.5) auch die Wahrscheinlichkeit für Metall-Hydroxidausfällungen, insbesondere für Cu (siehe Kapitel 8.7.5). Im Zuge des Einbaus von Behälter 3, wurden zusätzliche pH-Messstellen in den Behältern 2 und 3 (jeweils Ablauf-pH) eingebaut (Messstelle Ablauf Behälter 1 bereits vorhanden).

8.5.3 pH-Wert

Bei einer Menge von 5 t Flugasche und 10 m^3 Quenchwasser (6 m^3 saures QW, 4 m^3 basisches QW; FF=2) pro Stunde stellt sich ein pH-Wert von 3.8-4.5 im ersten Extraktionsbehälter ein, abhängig von der behandelten Flugasche und des Säuregehalts des Quenchwassers. Mit zunehmender Extraktionszeit steigt der pH-Wert im zweiten Extraktionsbehälter der KVA Linth, hauptsächlich aufgrund der Alkalinität der Flugasche, auf Werte von 4.5-5.3 (siehe Monitoring Leitparameter im Anhang 8). Laborversuche haben gezeigt, dass die Extraktion bei tieferem pH-Wert zu deutlich höheren Metallausbeuten führt (Kapitel 7). Seit Februar 2017 (KW 5/2017) wird deshalb durch vorgängige Zugabe von HCl 32% das Quenchwasser weiter angesäuert. Die HCl 32% wird dabei in die beiden Stapeltanks für saures Quenchwasser via Druckleitung zugegeben. Seit KW 5/2017 kann damit der pH-Wert der Aschesuspension im ersten Extraktionsbehälter auf pH 2.5 eingestellt werden. Durch die Pufferung der Flugasche werden im zweiten und dritten Behälter pH-Werte von ca. 3.5 resp. 3.8 erreicht.

8.5.4 Extraktionsausbeuten

Verglichen mit den Proben für die Bestimmung der FLUWA-Ausgangslage 2016, wurden zu Beginn der Optimierungsphase 1 (KW 2-8/2017) tiefere Extraktionsausbeuten für Cd, Cu, Pb und Zn erreicht (Tabelle 8-4). Dies hängt hauptsächlich mit dem tieferen Fest-Flüssig-Verhältnis und dem Umstand, dass seit Januar 2017 zusätzliche Fremdasche B behandelt wird zusammen. Die durchschnittliche wöchentliche Flugaschezusammensetzung hat sich durch die Zugabe von Fremdasche B zu tieferen Schwermetallkonzentrationen hin entwickelt (Tabelle 8-2). Weniger Metalle in der Ausgangsasche führen zu tieferen Extraktionsausbeuten (siehe Kapitel 7). Die Senkung des pH-Wertes auf 2.5 seit KW 7/2017 führte dagegen zu leicht erhöhten Extraktionsausbeuten von Zn (Tabelle 8-4). Die Inbetriebnahme des dritten Extraktionsbehälters (B3) und somit die längere Interaktionszeit von Flugasche und Quenchwasser von 30 auf 45 Minuten, führte zu erhöhten Extraktionsausbeuten für Cd, Cu, Pb und Zn im Vergleich zum FLUWA-Betrieb mit nur zwei Behältern.

Trotz des tieferen pH-Wertes in Behälter 3 (pH-Wert 3.8), durch das Ansäuern des Quenchwassers mit HCl 32%, wird im Filtrat nach der Vakuumbandfiltration ein pH-Wert von >5 gemessen. Dies führt v.a. für Cu zur Hydroxidausfällung (ab pH 4.0-4.5) und somit zu einer tiefen Extraktionsausbeute. Die redox-sensitiven Elemente Pb, Cu und Cd werden weiter durch unedleres metallisches Al^0, Zn^0 oder Fe^0 aus der Flugasche reduktiv abgeschieden und gelangen in den Rückstand (gewaschener Filterkuchen). Diese elektrochemische Separation wird in Kapitel 3, basierend auf Analysen mittels Rasterelektronenmikroskop im Filterkuchen der KVA Linth, detailliert beschrieben.

Tabelle 8-4: *Extraktionsausbeuten (%) für Cd, Cu, Pb und Zn des FLUWA-Verfahrens Ende 2016 (Ausgangslage 2016) und nach den jeweiligen Optimierungsschritten in den entsprechenden Kalenderwochen 2017 (Optimierung Teil 1). Die Betriebsbedingungen entsprechen wöchentlichen Mittelwerten, die täglich erfassten Werte sind im Anhang 8 angefügt (Monitoring Leitparameter). B1: Extraktionsbehälter 1, B2: Extraktionsbehälter 2, B3: Extraktionsbehälter 3.*

Bezeichnung	FF-Verhältnis	Verweilzeit (min)	pH-Werte	Cd	Cu	Pb	Zn
Ausgangslage 2016: *Flugasche Linth (45%), Fremdasche A (55%)*							
KW 45/46/2016	3	30	-	62	15	22	55
KW 48/2016	2.9	30	B1: 4.7	71	11	15	46
Optimierung Teil 1: *Flugasche Linth (35%), Fremdasche A (40%), Fremdasche B (25%)*							
KW 2/2017	2.0	30	B1: pH 3.5 / B2: pH 4.8	55	0	7	38
KW 7/2017	2.0	30	B1: pH 2.6 / B2: pH 3.8	52	7	12	49
KW 8/2017	2.0	30	B1: pH 2.6 / B2: pH 3.8	49	0	6	43
KW 9/2017	2.0	45	B1: pH 2.5 / B2: pH 3.6 / B3: 3.7	53	23	11	60
KW 10/2017	2.0	45	B1: pH 2.6 / B2: pH 3.6 / B3: 3.8	61	18	17	55

8.6 Optimierung FLUWA Teil 2: Laborversuche H_2O_2/Luft

Wie in Kapitel 3 und 4 beschrieben, sind die Redoxverhältnisse während des FLUWA-Verfahrens von zentraler Bedeutung. Während der Extraktion wird der Sauerstoff rasch durch die Oxidation der metallischen Partikel in den Flugaschen verbraucht und die reduzierenden Bedingungen führen während der Extraktion zur Zementierungsreaktion (Gleichung 8-1) von gelöstem Pb^{2+}, Cu^{2+} und Cd^{2+} an der Oberfläche unedlerer Metalle (Al^0, Zn^0 oder Fe^0). Die Analyse des Filterkuchens der KVA Linth mittels Rasterelektronenmikroskop (REM) zeigt deutlich die Zementierungsphasen in Form einer $PbCu^0$-Legierung, welche meist auf metallischen Al^0-Partikeln beobachtet wurde (Kapitel 3).

$$3\ Cu^{2+} + 2\ Al^0 \rightarrow 3\ Cu^0\downarrow + 2\ Al^{3+} \qquad (8\text{-}1)$$

Durch die Zugabe eines Oxidationsmittels wie Wasserstoffperoxid 30% wird die Zementierung unterdrückt und der überwiegende Teil der metallischen Komponenten in den Flugaschen oxidiert. Dies führt dazu, dass das gelöste Cu und Pb im Filtrat verbleibt und so zurückgewonnen werden kann. Die Flugaschen der KEBAG Zuchwil und KEZO Hinwill werden in Zuchwil mittels FLUWA-Verfahren unter Einsatz von 40 L H_2O_2/t FA behandelt.

Mit Laborversuchen unter Einsatz von Oxidationsmittel (H_2O_2, Luft) kann die technisch mögliche Extraktionsausbeute für Pb, Cu und Cd in Flugasche der KVA Linth ermittelt werden. Die optimalen Bedingungen können anschliessend aus den Laborversuchen abgeleitet werden und dienen als Grundlage für den Versuch im Industriemassstab. Der Vergleich der Extraktionsausbeuten der Laborversuche und der Werkversuche gibt Aufschlüsse bezüglich Effizienz und Optimierung der Betriebsbedingungen. In zwei Serien wurden deshalb Extraktionsexperimente mit Flugasche und Quenchwasser (QW)

der KW 48/2016 (Flugasche Linth (45%), Fremdasche A (55%)) und KW 2/2017 (Flugasche Linth (35%), Fremdasche A (40%), Fremdasche B (25%)) durchgeführt. Ziel war es die optimale Menge und Art der Zugabe von H_2O_2 und Luft zu finden, um die maximal mögliche Menge Pb, Cu und Cd mobilisieren zu können.

8.6.1 Versuchsansätze

Für die Versuche wurde jeweils Quenchwasser (Mix von 60% saurem QW, 40% basischem QW) im Becherglas bei 40°C vorgelegt und die Flugasche zugegeben. Es wurde versucht, den kontinuierlichen FLUWA-Prozess über die zwei (Serie 1) resp. drei Extraktionsbehälter (Serie 2) so gut wie möglich im Batchversuch abzubilden (erste 15 min: Extraktionsbehälter 1, zweite 15 min: Extraktionsbehälter 2, dritte 15 min: Extraktionsbehälter 3). Die Lösung wurde mit einem Stativrührer durchmischt und der pH-Wert wurde während den ersten 15 Minuten (Behälter 1) mit HCl 32% auf pH 3.5 eingestellt. Die in der Suspension ablaufenden Reaktionen sind exotherm und die Temperatur steigt dabei auf ca. 60°C an. Während der restlichen Extraktionszeit wird mittels Heizplatte die Temperatur auf 60°C geregelt.

Mit diversen Versuchen wurde in der ersten Versuchsserie die Zugabe von unterschiedlichen Mengen H_2O_2 (30%) getestet. Dabei wurde das H_2O_2 während den ersten 15 Minuten der Extraktion (Behälter 1) kontinuierlich mittels Schlauchquetschpumpe zugegeben. Die Luftzugabe erfolgte über eine Fritte mit konstantem Fluss von 0.3 L/min (Überwachung mit Flowmeter, Abbildung 8-2). Nach 30 Minuten wurde die Flugaschelösung über eine Nutsche abfiltriert und das Filtrat sofort 1:10 verdünnt, um Ausfällungen zu verhindern. Das Redoxpotential (Ag/AgCl-Bezugssystem) und der pH-Wert wurden während der gesamten Extraktionsdauer überwacht und alle 5 Minuten festgehalten (Abbildung 8-3). Der pH-Wert wurde temperaturkompensiert festgehalten, was beim Redoxpotential nicht möglich ist. Das Redoxpotential ist abhängig von der Temperatur, dem pH-Wert und der Ionenstärke. Da alle Versuche bei den gleichen Bedingungen durchgeführt wurden (FF 2.5, pH 3.5, 60°C), werden die gemessenen Redoxpotentiale untereinander verglichen.

Versuchsserie 2 wurde auf den Erkenntnissen der vorgängigen Versuche aufgebaut und die Extraktionsausbeuten mittels Massenbilanz ermittelt. Dazu wurde die Konzentration der relevanten Elemente in den gewaschenen Filterkuchen (getrocknet bei 105°C) und Filtraten mittels ED-XRF und ICP-OES bestimmt. Die Extraktionsdauer wurde für alle Experimente der Serie 2 auf 45 Minuten erhöht (Einbezug von Behälter 3). Die detaillierten Versuchsansätze sind in Tabelle 8-5 und Tabelle 8-6 aufgeführt.

Tabelle 8-5: *Versuchsansätze der Serie 1 mit Flugasche und Quenchwasser der KW 48/2016 (Flugasche Linth (45%), Fremdasche A (55%)).*

Versuchs-Nr.	Menge FA	Menge QW	FF	pH	Zeit (min)	Temp. (°C)	H_2O_2 (L/t FA)	Luft (L/min)	Luftzugabe
1	10	25	2.5	3.5	30	60	-	-	
2	10	25	2.5	3.5	30	60	25	-	
3	10	25	2.5	3.5	30	60	40	-	
4	10	25	2.5	3.5	30	60	50	-	
5	100	250	2.5	3.5	30	60	-	0.3	Behälter 1+2
6	100	250	2.5	3.5	30	60	25	0.3	Behälter 1+2
7	100	250	2.5	3.5	30	60	40	0.3	Behälter 1+2
8	100	250	2.5	3.5	30	60	25	0.3 (O_2)	Behälter 1+2

Tabelle 8-6: *Versuchsansätze der Serie 2 mit Flugasche und Quenchwasser der KW 2/2017 (Flugasche Linth (35%), Fremdasche A (40%), Fremdasche B (25%)).*

Versuchs-Nr.	Menge FA	Menge QW	FF	pH	Zeit (min)	Temp. (°C)	H_2O_2 (L/t FA)	Luft (L/min)	Luftzugabe
Mengen Peroxid									
1	100	250	2.5	3.5	45	60	-	-	-
2	100	250	2.5	3.5	45	60	50 (initial)	-	-
3	100	250	2.5	3.5	45	60	50	-	-
4	100	250	2.5	3.5	45	60	60	-	-
5	100	250	2.5	3.5	45	60	70	-	-
Einstellung auf bestimmten Eh									
6	100	250	2.5	3.5	45	60	90 (Eh +300 mV)	-	-
7	100	250	2.5	3.5	45	60	34 (Eh +100 mV	-	-
8	100	250	2.5	3.5	45	60	32 (Eh 0 mV)	-	-
9	100	250	2.5	3.5	45	60	30 (Eh -200 mV)	-	-
Lufteindüsung									
10	100	250	2.5	3.5	45	60	-	0.3	Behälter 1+2
11	100	250	2.5	3.5	45	60	50	0.3	Behälter 1+2
12	100	250	2.5	3.5	45	60	50	0.3	Behälter 1
13	100	250	2.5	3.5	45	60	50	0.3	Behälter 2
14	100	250	2.5	3.5	45	60	50	0.3	Behälter 1+2 (30°C)

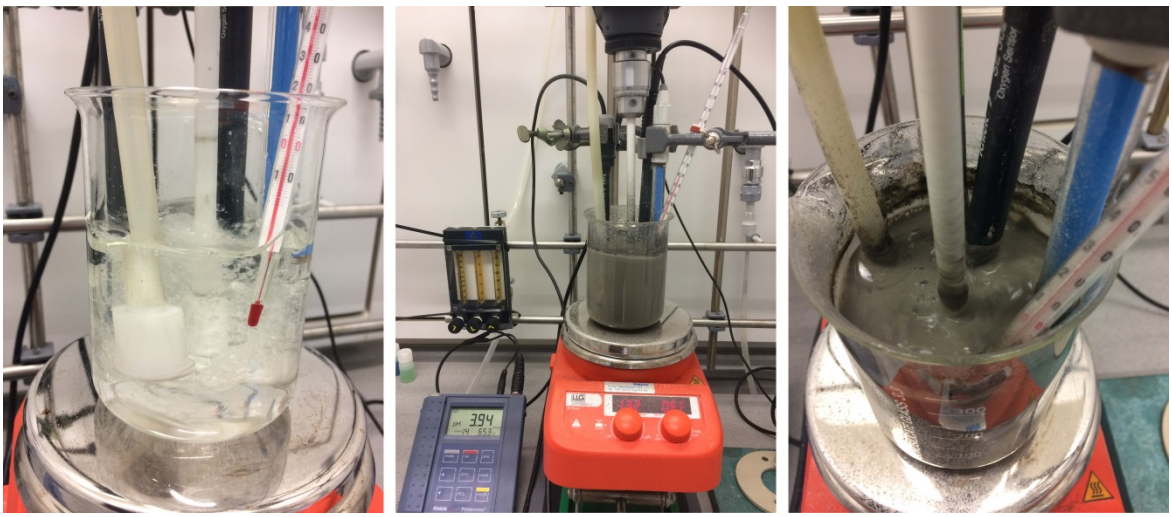

Abbildung 8-2: *Versuchseinrichtung mit Lufteindüsung und pH, Eh-Monitoring.*

Berechnung Lufteindüsung:

Die Menge Luft wurde über die Menge Sauerstoff berechnet, welche 40 L H_2O_2/t Flugasche entspricht. Diese Menge H_2O_2 entspricht dem Erfahrungswert der KVA Linth aus diversen Laborversuchen. Da die Reaktivität von Luft deutlich geringer ist verglichen zu H_2O_2, gibt die Berechnung nur eine grobe Abschätzung der benötigen Luftmenge. Die folgende Berechnung basiert auf der Annahme eines FLUWA-Durchlaufs von 4 Tonnen Flugasche (FA) pro Stunde:

- 40 L H_2O_2 30%/t FA · 1.11 g/cm^3 = 44 kg H_2O_2 30%/t FA
- 44 kg H_2O_2 30% = 13.2 kg H_2O_2 100% (M: 34 g/mol)
- In Luft umrechnen = 12.4 kg O_2 · 4.8 = 59.6 kg Luft/t FA (20.95 vol.% O_2)
- Dichte Luft: 1.2041 kg/m^3
- 1 kg Luft / 1.2041 kg/m^3 = 0.830 m^3 Luft
- 59.6 kg Luft/t FA = 49.5 m^3 Luft/t FA
- FLUWA-Durchlauf: 4 t FA/h = <u>198 m^3/h Luft (3.3 m^3/min)</u>

8.6.2 Resultate und Diskussion

Erste Resultate zeigen, dass für die Flugasche aus KW 48/2016 der KVA Linth eine Menge von 50 L H_2O_2/t Flugasche erforderlich ist, um positive Eh-Werte über die gesamte Extraktionsdauer von 30 Minuten zu halten (Abbildung 8-3). Beim Einsatz von 40 L H_2O_2/t FA resp. 25 L H_2O_2/t FA sank das Redoxpotential rasch nach dem Ende der H_2O_2-Zugabe nach 15 Minuten Extraktion und es stellten sich bis zum Ende der Extraktion negative Eh-Werte ein (-50 bis -400 mV).

Der Einsatz von Luft ohne zusätzliches H_2O_2 führte zu keinem signifikanten Anstieg des Redoxpotentials und die Eh-Werte bleiben im stark negativen Bereich (-350 bis -500 mV). Der Einsatz von H_2O_2 in Kombination mit Luft, zeigt einen minimalen Trend zu positiveren Eh-Werten verglichen zu den Versuchen ohne Luft. Es scheint dass die Lösung bei einem tiefen Flüssig-Fest-Verhältnis von 2.5 nicht genügend Zeit und Kontaktfläche hat damit der Sauerstoff in die Lösung übergehen kann. Am Ende jeder Extraktion wurde ein Aliquot des Filtrates entnommen und die Konzentration der extrahierten Elemente mittels ICP-OES bestimmt (siehe Anhang 8).

Um das Potential der Luftaufnahme der Lösung zu testen, wurde mit zwei unterschiedlichen Düsen versucht O_2-freies Wasser mit Luftsauerstoff zu sättigen. Dabei wurden die für die Extraktionsversuche verwendete Laborfritte und eine sehr feine Spritzpistolendüse verwendet. Es zeigte sich, dass mit der feinen Düse das Wasser in kürzerer Zeit gesättigt werden konnte. Der Einsatz einer feinen Spritzpistolendüse für die Lufteindüsung bei den Extraktionsexperimenten wurde jedoch schnell abgebrochen, da durch den erhöhten Druck das gesamte zugegebene H_2O_2 ausgetrieben wurde und sich rasch reduzierende Bedingungen einstellten. Mit dem Einsatz von reinem Sauerstoff (O_2) können während der gesamten Extraktionsdauer oxidative Extraktionsbedingungen gehalten werden (270 mV nach 30 Minuten). Das zeigt, dass die Eindüsung bei genügender O_2-

Verfügbarkeit sehr effektiv wirken kann. Der limitierende Faktor ist deshalb der Austausch des Sauerstoffs aus der Luft mit der Extraktionslösung.

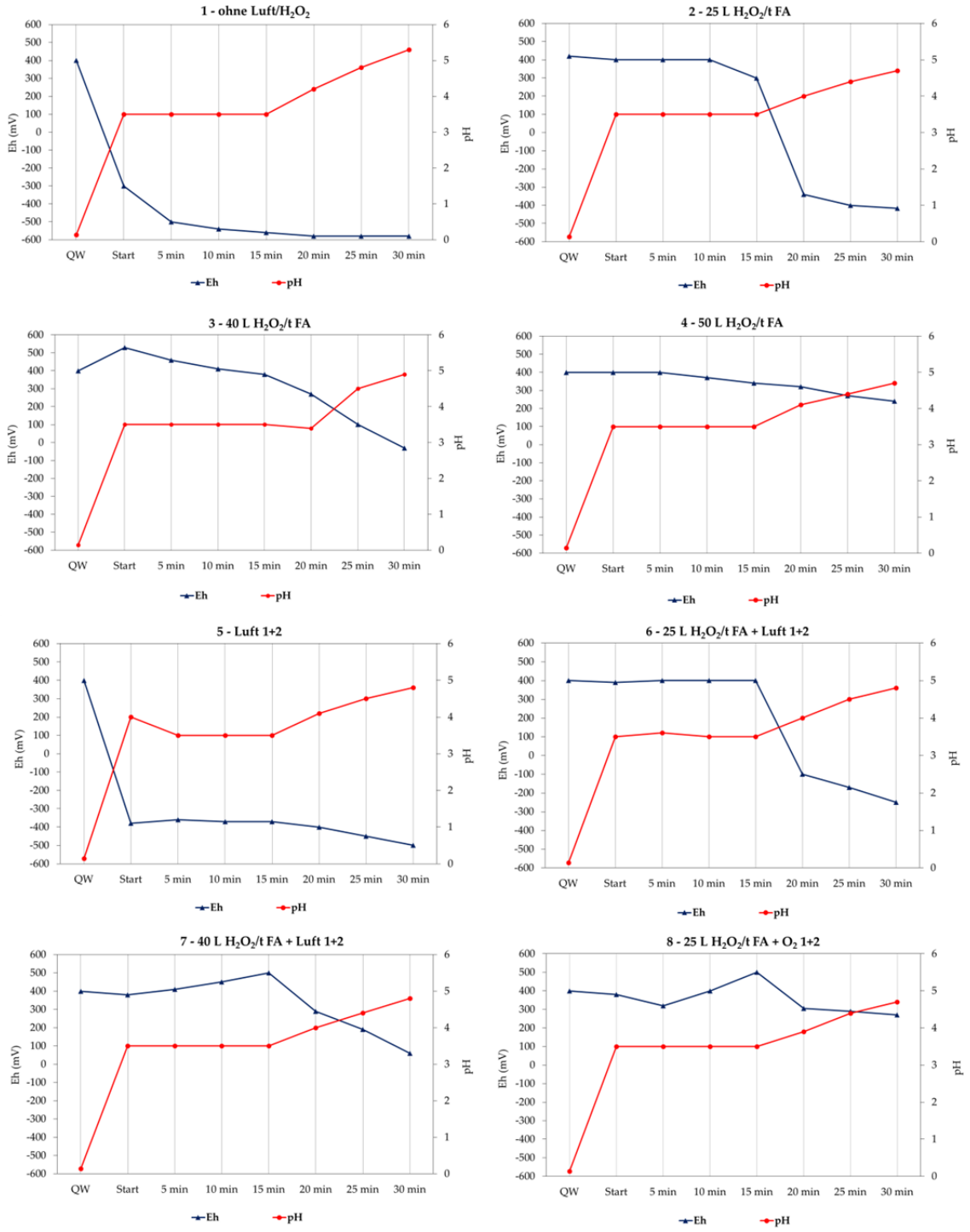

Abbildung 8-3: *Verlauf des pH-Wertes (rot) und Redoxpotentials (blau) während den Extraktionsversuchen der Serie 1 mit Flugasche und Quenchwasser der KW 48/2016.*

In der zweiten Versuchsserie mit Flugasche der KW 2/2017 wurde versucht, die optimale Menge H_2O_2 für die Umsetzung im Industriemassstab zu ermitteln (Abbildung 8-4). Es ist auffällig, dass sich der Flugasche-Mix von KW 2/2017 bezüglich Redoxpotential anders verhält als bei Serie 1, wo Flugasche aus KW 48/2016 ohne Beimischung von Fremdasche B verwendet wurde. Es wird generell mehr Oxidationsmittel benötigt um über den ganzen Extraktionsprozess oxidative Bedingungen zu halten. Das H_2O_2 wurde kontinuierlich während den ersten 15 Minuten der Extraktion zugegeben und bei allen getesteten Mengen (50, 60, 70 und 90 L H_2O_2/t FA) konnten in dieser Zeit positive Eh-Werte gehalten werden (Abbildung 8-4). Nach Beendigung der Zugabe sank das Redoxpotential der Asche-Suspension je nach eingesetzter Menge H_2O_2 und somit vorhandenem Überschuss in der Lösung schnell in Richtung negative Werte.

Zink ist nicht redox-sensitiv und lässt sich deshalb unter oxidativen Bedingungen nicht besser mobilisieren. Die Extraktionsausbeute für Zn bleibt auf konstanten ca. 45%, was mit dem tiefen Flüssig-Fest-Verhältnis von 2.5 erklärt werden kann. Für Cd ist der Einfluss des H_2O_2 erkennbar und bereits beim Einsatz von 50 L H_2O_2/t FA wird eine Ausbeute von 88% erreicht, die sich mit zunehmender Menge H_2O_2 nicht mehr signifikant steigern lässt.

Grössere Mengen H_2O_2 führen zu steigenden Extraktionsausbeuten für Pb mit einer maximalen Mobilisierung von 41%. Cu hingegen lässt sich auch beim Einsatz grosser Mengen H_2O_2 nicht mobilisieren. Am Ende der Extraktion wird ein pH-Wert von ~5.5 (Abbildung 8-7) in der Aschesuspension gemessen und der pH-Wert des Filtrats liegt im Bereich von pH 5.8-6.1. Kupfer beginnt bei einem pH-Wert um 4.0-4.5 als Kupferhydroxid auszufallen, wie das auch im Industriemassstab gezeigt werden kann (Kapitel 8.5.4). Die Hydroxidausfällung von Cu und anteilsweise auch Pb führt zu den tiefen Extraktionsausbeuten (Gleichung 8-8). Für eine Steigerung der Extraktionsausbeuten dieser Elemente muss die FLUWA zwingend mit tieferem pH-Wert so betrieben werden, dass der pH-Wert im letzten Extraktionsbehälter eine Hydroxidausfällung der entsprechenden Metalle verhindert (Abbildung 8-7). Des Weiteren verbessert ein grösseres Flüssig-Fest-Verhältnis die Metallausbetuen aller Elemente.

Da bei der KVA Linth batchweise Flugasche Linth und Fremdasche mittels FLUWA-Verfahren behandelt wird, ist die optimale Dosierung von H_2O_2 schwierig. Mit einer Dosierung gesteuert über das Redoxpotential könnte man dieses Problem umgehen und Schwankungen der Flugaschezusammensetzung und des Quenchwasser wären einfach zu handhaben. Aus diesem Grund wurde in diversen Laborversuchen versucht, das Redoxpotential auf bestimmte Werte einzustellen (Abbildung 8-6). Kurz nach der Zugabe der Flugasche zum Quenchwasser sinkt das Redoxpotential rasant von >300 mV auf -500 mV (Oxidation metallischer Anteile in der Flugasche). Um über den ganzen Extraktionsprozess Redoxbedingungen >300 mV zu halten, werden 90 L H_2O_2/t FA benötigt. Für die Ansteuerung tieferer Eh-Werte (100 mV, 0 mV und -200 mV) wird nur eine Menge von ca. 30 L H_2O_2/t FA benötigt. Beginnt das Redoxpotential zu sinken, wird beim Erreichen des gewünschten Wertes mit der Peroxidzugabe begonnen. Um den Wert stabil zu halten

wird während dem ganzen Extraktionsprozess konstant eine gewisse Menge zugegeben. Dabei wird nur gerade die Menge H_2O_2 zugegeben die gerade verbraucht wird und deshalb verbleibt der Eh-Wert auf dem vorgegebenen Wert.

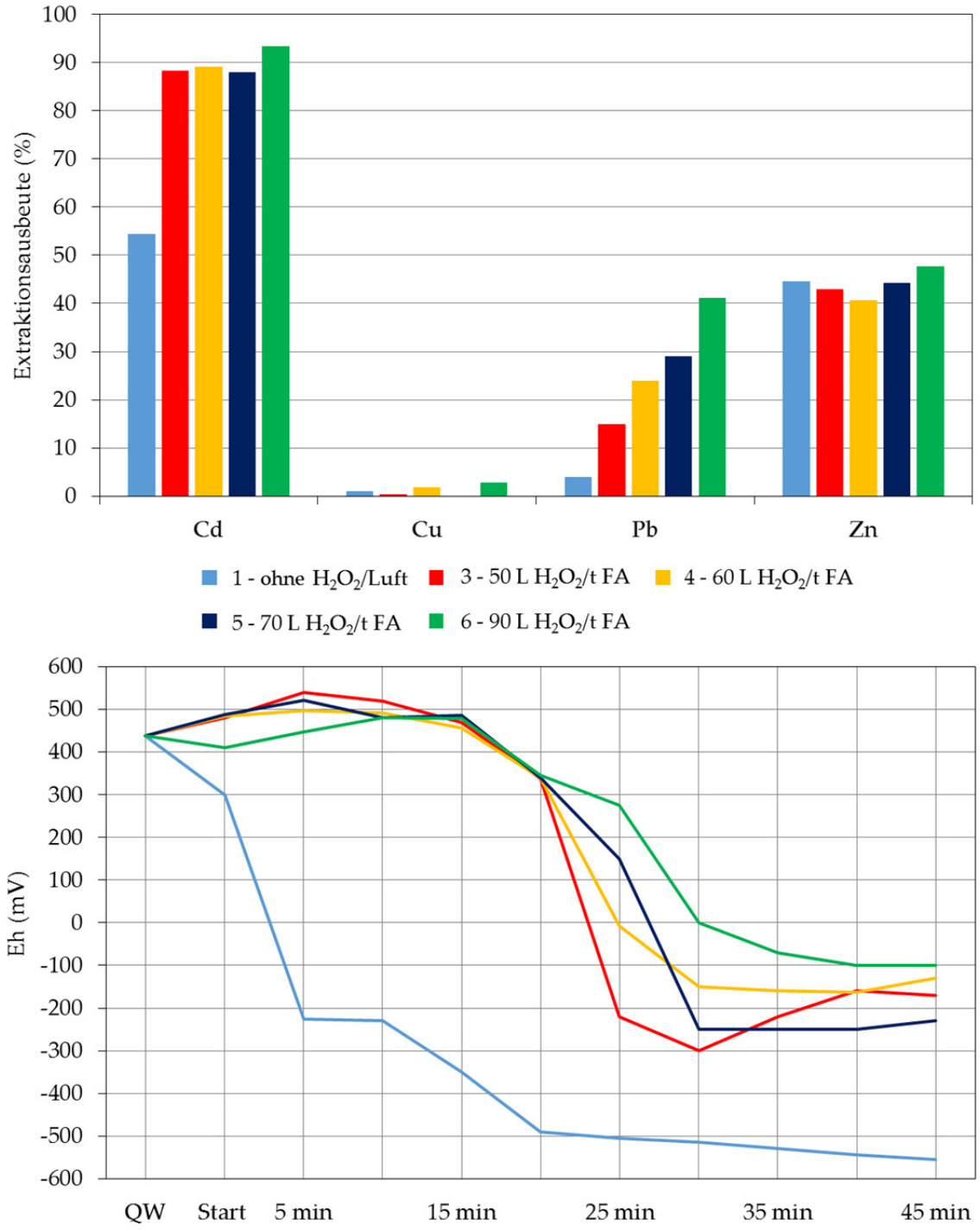

Abbildung 8-4: *(oben) Extraktionsausbeuten (%) für Cd, Cu, Pb und Zn für Laborversuche mit unterschiedlichen Mengen H_2O_2. (unten) Verlauf des Eh-Wertes während den Extraktionsversuchen.*

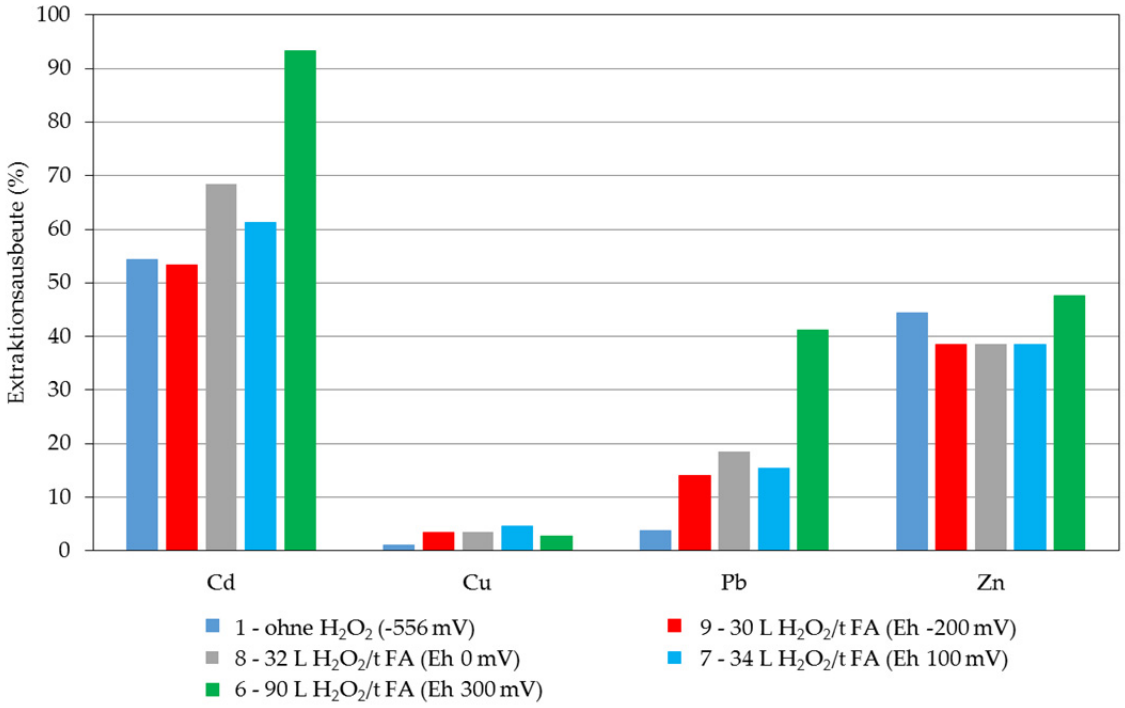

Abbildung 8-5: *Extraktionsausbeuten (%) für Cd, Cu, Pb und Zn bei Laborversuchen mit fixem Eh-Wert.*

Der zwingende Einsatz eines Oxidationsmittels für die Optimierung der Extraktionsausbeuten für redox-sensitive Elemente ist bekannt. Aus ökonomischer und ökologischer Sicht wäre es vorteilhaft, einen gewissen Teil des H_2O_2 durch die Eindüsung von Luft in die Extraktionsbehälter einsparen zu können. Im der ersten Versuchsserie konnte gezeigt werden, dass der Einsatz von Luft nur in Kombination mit H_2O_2 sinnvoll ist. Versuche der Serie 2 zeigen, dass Luft alleine die Eh-Werte der Aschesuspension von -500 mV auf -200 mV zu erhöhen vermag, was sich jedoch nicht positiv auf die Metallextraktionsausbeuten auswirkt (Abbildung 8-6). Die Extraktionsversuche ohne Zugabe von H_2O_2 und Luft, nur mit Luftzugabe sowie mit der Zugabe der gesamten Menge H_2O_2 zu Beginn der Extraktion führten bei allen Versuchen innerhalb von 5 Minuten zu stark negativen Eh-Potentialen (Abbildung 8-6). Der Einsatz von 50 L H_2O_2/t FA mit und ohne zusätzliche Unterstützung von Luft in Behälter 1 führte einer starken Abnahme des Redoxpotentials nach dem Ende der Peroxidzugabe. Die Extraktionsausbeuten mit Luft sind für Pb jedoch deutlich höher (15% ohne Luft, 28% mit Luft). Mit der Eindüsung von Luft während 30 Minuten (Simulation erster und zweiter Behälter) können nachhaltig oxidative Bedingungen geschaffen werden, was sich auch positiv auf die Abreicherung von Pb auswirkt. Es scheint sich v.a. zu lohnen im zweiten Behälter Luft einzudüsen, da dadurch das Ausgasen des Peroxids durch die Luft im ersten Behälter verhindert werden kann. Der exotherme Prozess der Flugascheextraktion führt dazu, dass grosstechnisch während dem ganzen Prozess Temperaturen von 60°C vorherrschen. Bei den Laborversuchen muss dazu aktiv auf 60°C geheizt werden. Wird die Heizplatte nach 15 Minuten entfernt,

kühlt die einströmende Luft die Lösung bis auf 30°C. Die tiefere Temperatur erlaubt eine bessere Aufnahme des Sauerstoffs der einströmenden Luft, was zu erhöhten Extraktionsausbeuten für Pb und teilweise Cu führt. Die Wirkung der Luft ist abhängig von der Aufnahmefähigkeit der Lösung und es scheint wichtig zu sein, eine möglichst optimale Einströmung zu gewährleisten (kleine Blasenbildung etc.).

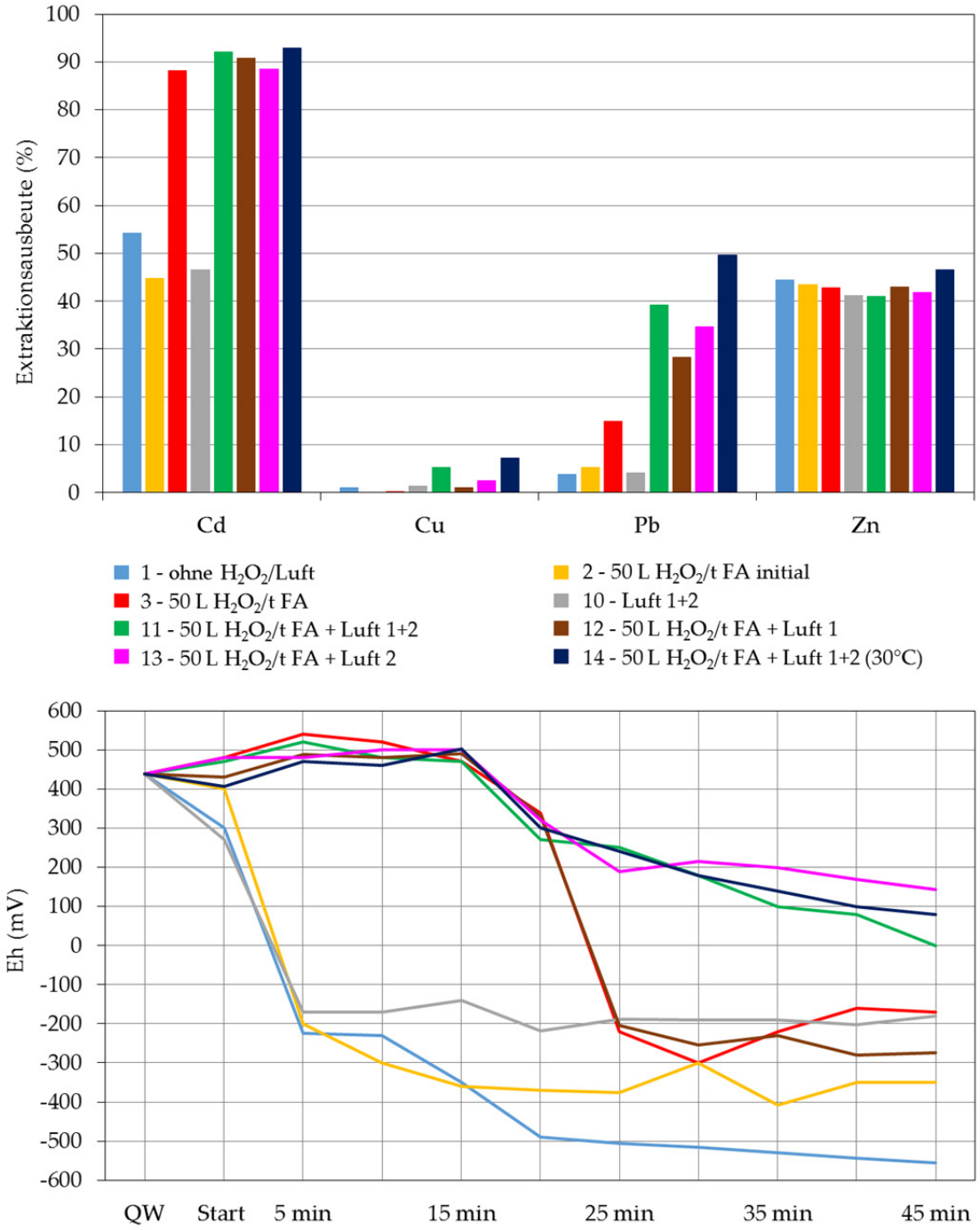

Abbildung 8-6: *(oben) Extraktionsausbeuten (%) für Cd, Cu, Pb und Zn für Laborversuche mit und ohne Lufteindüsung. (unten) Verlauf des Eh-Wertes während den Extraktionsversuchen.*

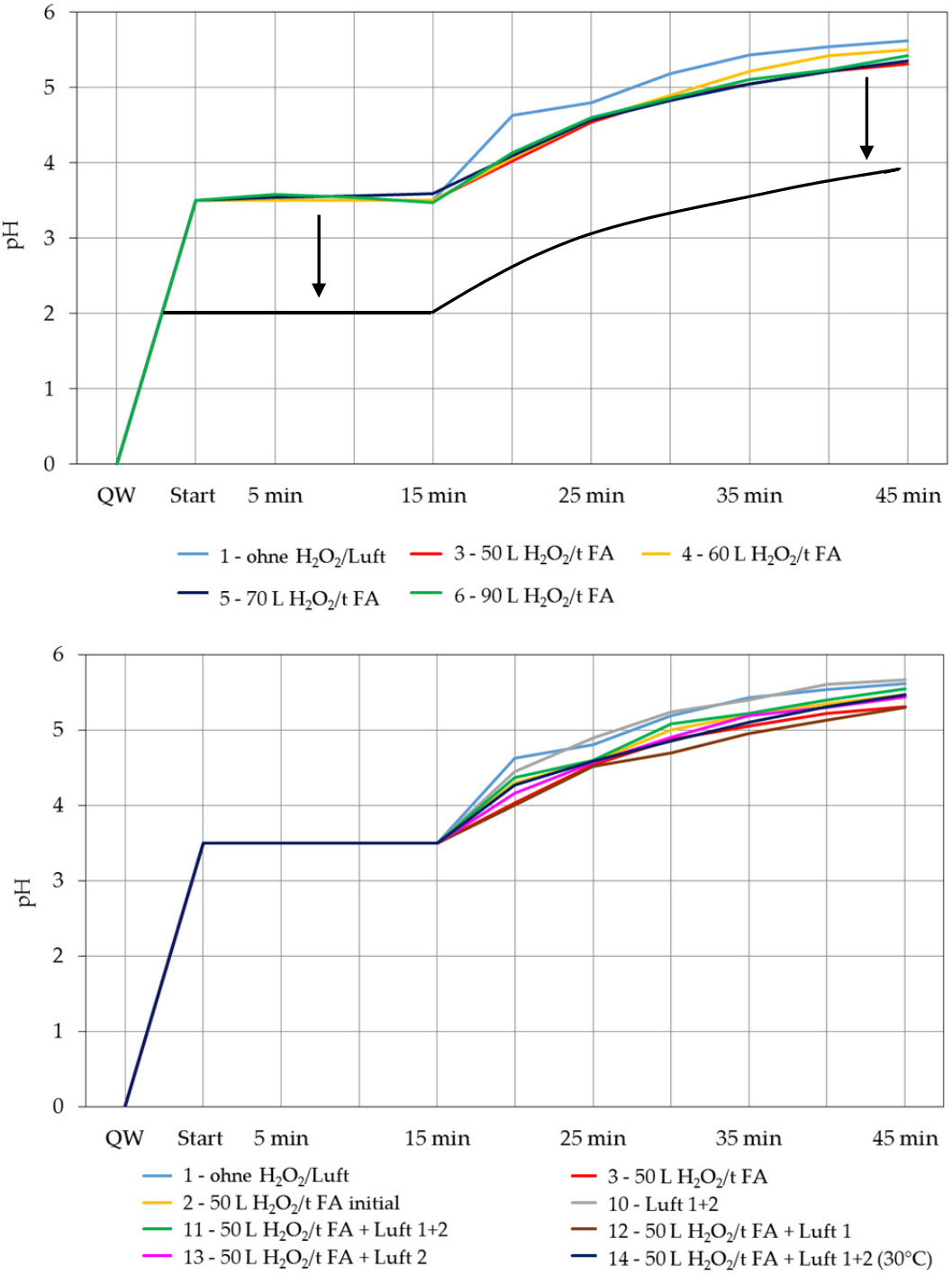

Abbildung 8-7: *Verlauf des pH-Wertes während den Extraktionsversuchen der Serie 2 mit einer pH-Wert Anpassung von 3.5 während den ersten 15 Minuten der Extraktion (Behälter 1). In schwarz wird der mögliche Verlauf des pH-Wertes bei einer Anpassung auf pH-Wert 2 gezeigt.*

Der pH-Wert wurde für alle Laborversuche während den ersten 15 Minuten mit HCl 32% auf pH 3.5 eingestellt (Abbildung 8-7). Im weiteren Verlauf der Extraktion pufferte die Flugasche den pH-Wert auf >5.0. Eine Anpassung auf pH-Wert 2.0 während den ersten

15 Minuten der Extraktion würde in einem End-pH-Wert von <4.0 resultieren, was die Metallhydroxidausfällung verringert (Abbildung 8-7). Ein Filtrations-pH-Wert von 4 erlaubt zudem eine effiziente Filtration, welche bei tieferem pH-Wert (pH 2.0) durch die Bildung von Kieselsäure stark eingeschränkt ist. Durch die Zugabe von H_2O_2 musste durchschnittlich 30-40% mehr HCl 32% zur Extraktion zugegeben werden, da aufgrund der Metalloxidation von (Fe^{2+} oder Al^{3+}), H^+-Ionen verbraucht werden (Gleichung 8-2).

$$H_2O_2 + 2\ H^+ + 2\ Fe^{2+} \rightarrow 2\ H_2O + 2\ Fe^{3+} \qquad (8\text{-}2)$$

Die grössere Menge zugegebene Säure führt dazu, dass mehr Karbonatpuffer zerstört wurde und der pH-Wert bei den Versuchen mit Einsatz von H_2O_2 dadurch etwas weniger stark gepuffert wird, verglichen zum Versuch ohne H_2O_2 (Abbildung 8-7).

8.6.3 Erkenntnisse aus den Laborversuchen

Die Laborversuche mit Flugasche und Quenchwasser der KVA Linth dienten dazu, Anhaltspunkte für die grosstechnische Optimierung des FLUWA-Prozesses zu erhalten. Es wurde u.a. getestet welche Mengen an H_2O_2 und/oder Luft in welchem Behälter am effektivsten wirken. Da im Labor der kontinuierliche Extraktionsprozess, wie er beim FLUWA-Verfahren angewendet wird, nur schwer abbildbar ist, basieren die Erkenntnisse ausschliesslich auf Batch-Versuchen. Es zeigte sich, dass eine minimale Menge von 30 L H_2O_2/t Flugasche benötigt wird um die Extraktionsausbeuten von Pb und Cu zu verbessern. Weiter wurde deutlich, dass der Betrieb einer Lufteindüsung im zweiten Behälter effizienter ist als im ersten Behälter. Die Lufteindüsung in Behälter 1 vermag das zugegebene H_2O_2 teilweise auszutreiben.

Basierend auf den Erkenntnissen der Laborversuche wurde ein dreistufiger Versuchsablauf im Industriemassstab geplant:

- FLUWA-Betrieb ohne die Zugabe von Oxidationsmittel.
- Dosierung von 34 L H_2O_2/t Flugasche Wasserstoffperoxid 30% in Behälter 1 (entspricht 120 L/h H_2O_2).
- Lufteindüsung in Behälter 2.

8.7 Optimierung FLUWA Teil 2: Industriemassstab

Basierend auf den Erkenntnissen der Laborversuche aus Kapitel 8.6, wurde am 31. März 2017 ein Werkversuch bei der KVA Linth durchgeführt. Ziel des Versuchs war das Schaffen oxidativer Extraktionsbedingungen durch die Zugabe von H_2O_2 und Luft während dem FLUWA-Prozess. Wie im Labor gezeigt werden konnte, werden unter oxidativen Bedingungen höhere Extraktionsausbeuten für die redox-sensitiven Elemente Pb, Cu und Cd erreicht.

8.7.1 Bauliche Massnahmen

Vom Anlagenbetreiber wurden folgende bauliche Massnahmen vorgenommen:

- Leitungsbau zu Extraktionsbehälter 1 zur Förderung von 1 m^3 technischem H_2O_2 (30%) (Abbildung 8-8).

- Bau des Zugangs für die Lufteindüsung in Behälter 1 und 2. PVC-Rohr mit feinen Öffnungen am Ende zum Einströmen der Luft, welches durch ein fixes Führungsrohr während dem Betrieb in den Behälter eingeführt werden kann (Abbildung 8-9).

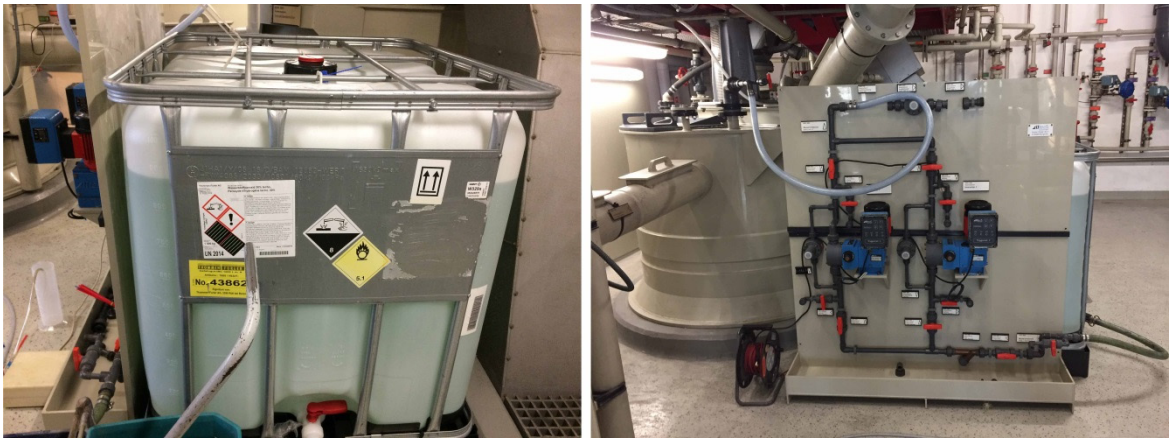

Abbildung 8-8: *Versuchseinrichtung der H_2O_2-Zugabe während dem FLUWA-Betrieb bei der KVA Linth.*

Abbildung 8-9: *Versuchseinrichtung der Lufteindüsung während dem FLUWA-Betrieb der KVA Linth.*

8.7.2 Betriebsbedingungen

Die FLUWA am 31. März 2017 wurden gemäss den Optimierungen des ersten Teils (Kapitel 8.5) betrieben. Dabei wurde Quenchwasser mit HCl 32% Zusatz und alle drei Extraktionsbehälter benutzt (Tabelle 8-7). Da der Versuch an einem Freitag stattfand, konnte die FLUWA mit einem erhöhten Flüssig-Fest-Verhältnis von 3 betrieben werden, da über das Wochenende genügend Zeit für die Leerung des limitierenden Filtrat-Sedimentationsbehälters zur Verfügung stand. Nach 4 Stunden (11.30 Uhr) musste aus Kapazitätsgründen die Flugaschedosierung von Silo 1 (Fremdasche A) auf Silo 2 (Flugasche Linth) gewechselt werden.

Tabelle 8-7: *Betriebsbedingungen FLUWA der KVA Linth bei den Optimierungsversuchen.*

Parameter	Versuchsbedingungen
Datum	31.03.2017
FLUWA-Betrieb	06.30-15.00 Uhr
Art der Flugasche	06.30-11.30: Fremdasche A 11.30-15.00: Flugasche Linth
Menge Flugasche	3.5t/h
Menge Quenchwasser	Quenchwasser sauer : 5.74 m^3/h Quenchwasser basisch: 4.68 m^3/h
Waschwassermengen Vakuumbandfilter	Deion. Wasser: ca. 2.5 m^3/h
FF-Verhältnis	3.0
Extraktionsbehälter	3 (je 3 m^3)
Verweilzeit	15 Minuten pro Tank
Zugabe H_2O_2 (30%)	Behälter 1
Zugabe Luft	Behälter 2

8.7.3 Versuchsablauf

Der Versuchsablauf mit Monitoring der Extraktionsbedingungen und Zeitpunkt der Probenahme sind in Tabelle 8-8 bis Tabelle 8-10 aufgelistet.

Tabelle 8-8: *Ablauf der Optimierungen des FLUWA-Prozesses am 31. 03. 2017 bei der KVA Linth.*

Zeit	Aktion
06.30	Start FLUWA-Betrieb mit Fremdasche A
11.05	Start Peroxidzugabe 34 L/t Flugasche
11.30	Menge H_2O_2 auf 17 L/t Flugasche reduzieren, Silowechsel auf Flugasche Linth
12.50	Start Luftzugabe
13.40	H_2O_2 auf 8.5 L/t Flugasche reduzieren, Lufteindüsung auf Maximum
14.25	Lufteindüsung abschalten
15.00	Stopp FLUWA-Betrieb

Während des FLUWA-Betriebs wurde in regelmässigen Abständen die Parameter pH-Wert, Redoxpotential und Temperatur in allen drei Extraktionsbehältern gemessen. Dabei wurde mit einem Becherglas ein möglichst repräsentatives Aliquot der Aschesuspension entnommen und die Parameter erfasst. Durch die erschwerten Messbedingungen mussten die pH-Elektrode im Verlauf des Tages mehrfach nachkalibriert werden (pH 4, 7, 9). Aufgrund eines Defekts des Luftdurchflussmessers kurz nach Beginn des Versuchs, konnte die Lufteindüsung nich überprüft werden. Es wurde entschieden, den Versuch mit einer maximalen und einer reduzierten Lufteindüsung (Hahn halb zu) durchzuführen (Abbildung 8-11).

Tabelle 8-9: *Monitoring der Versuchsbedingungen während dem FLUWA-Prozess am 31. 03. 2017 bei der KVA Linth. (xx) Maximale Lufteindüsung, (x) reduzierte Lufteindüsung.*

Extraktionsbehälter 1					
Zeit	**pH-Wert**	**Eh-Wert (mV)**	**Temp. (°C)**	**H_2O_2 (L/t FA)**	**Luft**
Fremdasche A					
10.00	2.4	-450	63	-	-
11.00	2.4	-400	63	-	-
11.15	3.5	625	65	34	-
11.30	2.0	560	65	34	-
Flugasche Linth					
12.45	2.9	508	61	17	-
13.35	2.4	630	59	17	-
13.45	2.8	500	62	8.5	-
14.20	2.9	520	61	8.5	-
14.35	3.1	400	59	8.5	-

Extraktionsbehälter 2					
Fremdasche A					
10.00	3.1	-560	64	-	-
11.00	3.2	-550	63	-	-
11.15	3.3	665	62	-	-
11.30	3.3	400	65	-	-
Flugasche Linth					
12.45	3.9	370	64	-	-
13.35	4.0	420	63	-	x
13.45	4.3	400	65	-	xx
14.20	4.4	430	64	-	xx
14.35	3.1	400	60	-	-

Extraktionsbehälter 3					
Fremdasche A					
10.00	3.6	-513	64	-	-
11.00	3.5	-510	64	-	-
11.15	4.0	106	60	-	-
11.30	4.0	-210	63	-	-
Flugasche Linth					
12.45	5.1	-200	68	-	-
13.35	-	-	-	-	-
13.45	5.3	-200	65	-	-
14.20	5.2	-180	64	-	-
14.35	4.9	-270	60	-	-

Beim kontinuierlichen Extraktionsbetrieb ist es schwierig einen stabilen Betrieb einzustellen. Es ist jedoch bekannt, dass die Flugasche im Durchschnitt ca. 15 Minuten im Extraktionsbehälter verweilt und nach 45 Minuten auf das Vakuumband kommt. Nach dem Anpassen eines Parameters (Tabelle 8-8) wurde deshalb jeweils eine Stunde bis zur Probenahme des gewaschenen Filterkuchens abgewartet.

Tabelle 8-10: *Probenahmen von Flugasche und gewaschenem Filterkuchen während dem FLUWA-Prozesse am 31. 03. 2017 bei der KVA Linth. (xx) Maximale Lufteindüsung, (x) reduzierte Lufteindüsung.*

Zeit	**Probentyp**	**H_2O_2 (L/t FA)**	**Luft**	**Bemerkungen**	**Probe-bezeichnung**
10.00	Fremdasche A			Probenahme Silo	FA 1a
11.45	Fremdasche A			Probenahme Silo	FA 1b
13.00	Flugasche Linth			Probenahme Eintritt Behälter 1	FA 2
10.00	Filterkuchen 1	-	-		FK 1-1
11.00	Filterkuchen 1	-	-		FK 1-2
11.45	Filterkuchen 1	34	-	Filtrationsleistung eingeschränkt	FK 1-3
13.00	Filterkuchen 2	17	-	Filtrationsleistung eingeschränkt	FK 2-1
14.00	Filterkuchen 2	17	x	Filtrationsleistung eingeschränkt	FK 2-2
14.45	Filterkuchen 2	8.5	xx	Filtrationsleistung eingeschränkt	FK 2-3

8.7.4 Beobachtungen und Interpretation

Die Zugabe von 34 L H_2O_2/t Flugasche führte innerhalb der ersten 15 Minuten zu positiven Eh-Werten in allen drei Extraktionsbehältern (Tabelle 8-9). Nicht verbrauchtes H_2O_2 gelangte via Überfluss in die weiteren Behälter und trieb das Redoxpotential in die Höhe. Nach weiteren 15 Minuten sank der Eh-Wert in Behälter 2 von 665 mV auf 400 mV, wo er die restliche Zeit des Versuchs blieb. In Behälter 3 stellten sich nach 30 Minuten negative Eh-Werte um die -200 mV ein. Es wurden in Behälter 1 und 2 bei der Zugabe von 34 L H_2O_2/t Flugasche stark oxidative Bedingungen gemessen (>500 mV), weshalb nach 30 Minuten die Dosierung auf 17 L H_2O_2/t Flugasche reduziert wurde.

Generell wurde eine starke Gasentwicklung und eine Temperaturerhöhung von 60°C bis auf 68°C während der Peroxiddosierung in den Extraktionsbehältern festgestellt (Tabelle 8-9). Dies ist mit der stark exothermen Zersetzung von Wasserstoffperoxid (30%) unter Licht- und Wärmeeinwirkung in Gegenwart von Katalysatoren wie Staub oder Schwermetallsalzen, zu Wasser und Sauerstoff zu erklären (Holleman and Wiberg, 2007).

$$2\ H_2O_2 \rightarrow 2\ H_2O + O_2 \qquad \Delta H° = -98.3\ kJ/mol \tag{8-3}$$

Die katalytische Zersetzung (Gleichung 8-3) findet in Konkurrenz zur Redoxreaktion statt, wo H_2O_2 in der Umgebung der Flugaschesuspension als Oxidationsmittel wirkt. Ohne den Einsatz von H_2O_2 liegt Fe im Filtrat weitestgehend zweiwertig vor. Durch die Zugabe von H_2O_2 kommt es zur Eisenoxidation (Gleichung 8-4).

$$H_2O_2 + 2\ H^+ + 2\ Fe^{2+} \rightarrow 2\ H_2O + 2\ Fe^{3+} \tag{8-4}$$

Zudem werden durch die Zugabe von H_2O_2 metallische Anteile wie Al^0 oder Fe^0 in der Flugasche oxidiert (Gleichung 8-5), was dazu führt, dass edlere Metalle wie Pb und Cu während der Extraktion nicht reduktiv abgeschieden werden.

$$2\ Al^0 + 3\ H_2O_2 + 6H^+ \rightarrow 2\ Al^{3+} + 6\ H_2O \tag{8-5}$$

Der Wechsel von Fremdasche A zu Flugasche Linth um 11.30 Uhr führte zu keinen signifikanten Veränderungen beim Redoxpotential, jedoch zu erhöhten pH-Werten im dritten Behälter (Fremdasche A: pH 4.0, Flugasche Linth: pH 5.3). Weiter wurde festgestellt, dass sich die Vakuumbandfiltration durch die Peroxidzugabe veränderte (Abbildung 8-10). Die Eisenoxidation ($Fe^{2+} \rightarrow Fe^{3+}$), aufgrund der H_2O_2-Zugabe, führt zur Ausfällung von Fe^{3+}-Hydroxid bei den vorliegenden pH-Werten von >4.0 und in Anwesenheit von OH^- in der Aschesuspension (Gleichung 8-6, Hartinger 1991).

$$Fe^{3+} + 3\ OH^- \rightarrow Fe(OH)_3\downarrow \tag{8-6}$$

Aluminium bildet ebenfalls ein schwerlösliches dreiwertiges Hydroxid, das bereits bei pH-Werten >2.5 auszufallen beginnt (Gleichung 8-7).

$$Al^{3+} + 3\ OH^- \rightarrow Al(OH)_3\downarrow \tag{8-7}$$

Die beobachtete, feinkörnige Schicht auf der Oberfläche des gewaschenen Filterkuchens (Abbildung 8-10) entspricht mit grosser Wahrscheinlichkeit ausgefällten Metallhydroxiden, welche beim Einsatz von H_2O_2 zu einer veränderten Filtrationsleistung führten (Abbildung 8-10).

Abbildung 8-10: *(links) Veränderte Filtrationsleistung beim Einsatz von H_2O_2. (rechts) Feinkörnige Schicht (Metallhydroxide) auf der Oberfläche des Filterkuchens, welche die Filtration beeinflussen.*

Mit dem Start der Lufteindüsung in Behälter 2 konnte keine Veränderung des Redoxpotentials festgestellt werden. Der Einfluss der Luft über Eh-Messung ist schwer abzuschätzen, jedoch führte die Luft zu einer zusätzlichen Durchmischung der Aschesuspension (Abbildung 8-11). Aufgrund der stark exothermen, katalytischen Zersetzung des H_2O_2 konnte trotz der einströmenden Luft keine Abkühlung der Suspension festgestellt werden. Messungen mittels Sauerstoffgerät auf der Oberfläche der Suspension ergaben 15 vol.% O_2, was einen Verbrauch von 6% (Luft 21 vol.% O_2) während dem Durchströmen im Extraktionsbehälter entspricht.

Abbildung 8-11: *Durchmischung der Aschesuspension bei maximaler Lufteindüsung (links) und reduzierter Lufteindüsung (rechts) in Behälter 2.*

8.7.5 Extraktionsausbeuten

Die Extraktionsausbeuten für die redox-sensitiven Elemente Cd, Cu und Pb für Fremdasche A (FLUWA-Betrieb am Vormittag) haben sich durch den Einsatz von 34 L H_2O_2/t Flugasche nicht verbessert (Tabelle 8-11). Trotz den stark oxidativen Bedingungen (Eh-Werte >500 mV bei 34 L H_2O_2/t Flugasche) ist eine höhere Peroxiddosierung erforderlich. Dies deckt sich mit den Werten aus den Laborexperimenten, wo höhere Extraktionsausbeuten für Pb (>20%) erst beim Einsatz von >60 L H_2O_2/t FA erreicht wurden (Abbildung 8-4).

Die Metallgehalte der Flugasche Linth liegen in einem ähnlichen Bereich wie die der Fremdasche A (siehe Anhang 8). Die Extraktionsausbeuten für Flugasche Linth sind jedoch v.a. für Cd und Pb signifikant höher verglichen zu Fremdasche A, obwohl nur noch 17 L H_2O_2/t Flugasche eingesetzt wurde und der pH-Wert am Ende der Extraktion höhere Werte erreichte (Fremdasche A: pH 4.0, Flugasche Linth: pH 5.3).

Kupfer beginnt bei einem pH-Wert um 4.0-4.5 als Kupferhydroxid auszufallen (Gleichung 8-8) und reichert sich im gewaschenen Filterkuchen an (Hartinger 1991).

$$Cu^{2+} + 2\ OH^- \rightarrow Cu(OH)_2\downarrow \qquad (8\text{-}8)$$

Mobilisiertes Pb^{2+} und Cu^{2+} wird zusätzlich reduktiv auf der Oberfläche weniger edler Metalle wie Al^0, Fe^0 oder Zn^0 abgeschieden (siehe Beschreibung der Zementierungsphasen in Kapitel 3). Die Schwankung der Extraktionsausbeute des Zn bei Fremdasche A muss auf Konzentrationsschwankungen der Ausgangsflugasche zurückzuführen sein. Faktoren wie das Flüssig-Fest-Verhältnis oder der pH-Wert, welche die Zn-Mobilisierung massgeblich beeinflussen, waren während des ganzen FLUWA-Betriebs am Vormittag stabil.

Der Einfluss der Lufteindüsung ist weder in den Eh-Werten noch den Extraktionsausbeuten deutlich erkennbar und es werden sehr ähnliche spezifische Extraktionsausbeuten erreicht wie ohne Luftzugabe (Tabelle 8-11). Die letzte Probenahme (FK 2-3) zeigt tiefere Ausbeuten für die redox-sensitiven Elemente Pb, Cu und Cd aufgrund der geringeren H_2O_2-Zugabe (8.5 L H_2O_2/t Flugasche). Die erhöhte Ausbeute für Zn von 79% bei FK 2-3 hingegen, muss durch eine veränderte Zusammensetzung der Ausgangsflugasche zu erklären sein. Allgemein war die verwendete Menge H_2O_2 deutlich zu gering und die Art und Menge der Lufteindüsung nicht optimal.

Verglichen zu den Extraktionsausbeuten der KVA Linth von 2013 (Kapitel 3) mit einem Flüssig-Fest-Verhältnis von 1.4 und ohne den Einsatz von H_2O_2 (Zn 40%, Pb 8%, Cu 6% und Cd 53%) werden für Cd (80%), Pb (40%) und Zn (65%) deutlich höhere Extraktionsausbeuten erreicht (Tabelle 8-11). Dies ist nebst dem Einfluss des H_2O_2 auf das erhöhte Flüssig-Fest-Verhältnis von 3.0 und einer besseren Spülung des Filterkuchens nach der Vakuumbandfiltration zurückzuführen.

Tabelle 8-11: *Extraktionsausbeuten (%) für Cd, Cu, Pb und Zn des FLUWA-Verfahrens während den jeweiligen Optimierungsschritten am 31.03.2017.*

Bezeichnung	Optimierung	Cd	Cu	Pb	Zn
Fremdasche A					
FK 1-1	-	59	8	13	54
FK 1-2	-	50	17	26	67
FK 1-3	34 L H_2O_2/t FA	62	8	16	67
Flugasche Linth					
FK 2-1	17 L H_2O_2/t FA	83	0	42	65
FK 2-2	17 L H_2O_2/t FA, Luft	82	10	36	66
FK 2-3	8.5 L H_2O_2/t FA, Luft (Durchfluss erhöht)	75	0	15	79

8.8 Fazit und Ausblick

Die Umsetzung der Erkenntnisse vom Labor in den Industriemassstab erwies sich unter den gegebenen Umständen als schwierig.

- Mechanische und chemische Optimierungen im Industriemassstab setzen vernünftige verfahrenstechnische Anordnungen voraus. Die Durchführung des dreistufigen Tests (konventioneller Betrieb – Peroxiddosierung - Lufteindüsung) innerhalb eines Tages (9h FLUWA-Betriebszeit) erwies sich als zu kurz. Es braucht deutlich längere Betriebszeiten unter den gleichen Extraktionsbedingungen um einen stabilen Betrieb zu garantieren. Dies würde das Monitoring der Leitparameter (pH, Eh, Temperatur) vereinfachen und eine repräsentativere Beprobung der gewaschenen Filterkuchen ermöglichen. Für weitere Tests wird vorgeschlagen, über einen längeren Zeitraum die Optimierungsschritte mit Flugasche vergleichbarer Zusammensetzung vorzunehmen und mehrmals täglich die Flugasche und den Filterkuchen zu beproben.

- Mechanische Optimierungen wie die Inbetriebnahme des dritten Extraktionsbehälters führte zu höheren Metallausbeuten aufgrund der längeren Interaktionszeit von Flugasche und Quenchwasser. Das tiefe Flüssig-Fest-Verhältnis ist v.a. für die tiefen Extraktionsausbeuten der meisten Metalle verantwortlich. Pro Flugascheäquivalent muss mehr Flüssigkeit zur Verfügung gestellt werden. Dies kann einerseits durch eine reduzierte Leitfähigkeit des Quenchwassers oder andererseits durch die Zugabe von zusätzlichem Quenchwasser oder Wasser erreicht werden. Eine erhöhte Menge Spülwasser nach der Vakuumbandfiltration trägt weiter dazu bei, die Metallausbeuten zu erhöhen.

- Chemische Optimierungen wie die Anpassung des pH-Wertes und Redoxpotentials während dem FLUWA-Prozess zeigen im Labor grosses Potential. Im Vergleich zu den Laborversuchen gestaltet sich das Monitoring des pH-Wertes und Redoxpo-

tentials unter den gegebenen Werkbedingungen als schwierig. Ohne ein kontinuierliches Monitoring über längere Zeiträume mit fest eingebauten Elektroden sind die benötigen Mengen HCl 32% und H_2O_2 30% schwierig zu bestimmen. Testläufe über eine längere Zeit sollten das vorhandene Potential aufzeigen. Ob eine gekoppelte Zugabe der Chemikalien grosstechnisch möglich ist oder ob die benötigte Menge (L/h H_2O_2) über Laborversuche bestimmt werden muss, gilt es abzuklären. Für eine Steigerung der Extraktionsausbeuten von Pb und Cu muss die FLUWA zwingend mit tiefem pH-Wert so betrieben werden, dass der pH-Wert im letzten Extraktionsbehälter eine Hydroxidausfällung der entsprechenden Metalle verhindert (idealer pH-Wert ~4.0). Tiefere pH-Werte führen zu schlechteren Filtrationsleistungen aufgrund von Kieselsäurebildung im Filterkuchen. Der Einfluss des pH-Wertes und Oxidationsmittels auf die Metallhydroxidausfällung und somit die Extraktionsausbeuten, sollten in weiteren, systematischen Versuchen detailliert untersucht werden. Dazu müsste man u.a. die Schichtung des Filterkuchens beim Einsatz von H_2O_2 chemisch und mineralogisch charakterisieren.

- Die abgeschätzte Menge an verbrauchtem Sauerstoff beträgt 30% vom verfügbaren Luftsauerstoff (21 vol.%). In den Laborexperimenten wurde deutlich, dass die Art der Eindüsung entscheidend für den Übergang des Sauerstoffs aus der Luft in die Lösung ist. Um die Effizienz der Lufteindüsung zu beurteilen und allenfalls zu optimieren, sollte dies vorgängig auf der Anlage gemessen werden.

- In einem eintägigen Werkversuch wurde versucht, möglichst viele Erkenntnisse aus dem Labor in den Industriemassstab zu übertragen. Es ist zu erkennen, dass die Tendenzen grosstechnisch in die richtige Richtung führen. Jedoch können die Resultate im Industriemassstab nur in der Tendenz, nicht aber quantitativ beurteilt werden. Um aussagekräftige elementspezifische Extraktionsausbeuten zu erheben, muss die ganze Systemtechnik (Verfahrenstechnik - Chemie) vorgängig optimal abgestimmt und während der gesamten Versuchsdauer begleitet werden.

Referenzen

AWEL, Amt für Abfall, Wasser, Energie und Luft des Kantons Zürich, 2013. Stand der Technik für die Aufbereitung von Rauchgasreinigungsrückständen (RGRR) aus Kehrichtverbrennungsanlagen.

Bühler, A., Schlumberger, S., 2010. Schwermetalle aus der Flugasche zurückgewinnen « Saure Flugaschewäsche – FLUWA-Verfahren » ein zukunftsweisendes Verfahren in der Abfallverbrennung. KVA-Rückstände in der Schweiz - Der Rohstoff mit Mehrwert (Federal Office for the Environment, FOEN), 185-192.

Bundesamt für Umwelt, 2016. Verordnung über die Vermeidung und die Entsorgung von Abfällen (VVEA). 1-46.

Hartinger, L., 1991. Handbuch der Abwasser- und Recyclingtechnik. Fachbuchverlag Leipzig.

Holleman, A.F., Wiberg, E., 2007. Lehrbuch der Anorganischen Chemie, 102 ed.

Schlumberger, S., Schuster, M., Ringmann, S., Koralewska, R., 2007. Recovery of high purity zinc from filter ash produced during the thermal treatment of waste and inerting of residual materials. Waste Management & Research 25, 547-555.

Anhang 8

Rohdaten Betriebsstand 2016 und Optimierung Teil 1

Tabelle A8-1: *Chemische Zusammensetzung (mg/kg) der Flugasche in den beprobten Kalenderwochen (KW), gemessen mit ED-XRF.*

	Ausgangslage 2016		**Optimierung Teil 1**				
Element	**KW 45/46/ 2016**	**KW 48/ 2016**	**KW 2/ 2017**	**KW 7/ 2017**	**KW 8/ 2017**	**KW 9/ 2017**	**KW 10/ 2017**
Al	32'997	27'650	30'730	27'570	32'760	27'600	26'890
Ba	2'149	2'449	1'967	1'959	2'259	2'072	2'018
Ca	148'533	140'000	164'500	158'900	163'700	147'800	141'300
Cd	309	380	304	223	246	292	340
Cl	87'353	113'600	128'200	160'100	124'600	108'700	110'600
Cr	601	572	556	411	446	557	595
Cu	2'857	2'839	1'990	1'853	2'113	2'003	2'181
Fe	24'147	21'050	15'920	12'790	16'640	15'770	16'460
K	47'240	54'430	52'820	43'290	49'300	61'320	62'630
Mn	804	888	894	721	772	1'007	1'019
P	3'502	3'779	4'081	3'583	3'875	3'994	3'806
Pb	11'040	11'120	7'352	7'543	7'031	10'470	11'540
S	52'617	62'630	49'060	58'190	47'330	74'560	69'780
Sb	3'469	2'632	1'968	2'365	2'854	2'297	2'004
Si	73'947	67'540	69'150	61'900	68'670	60'410	60'000
Sn	1'484	1'622	1'253	1'319	1'384	1'248	1'296
Ti	9'415	8'475	9'480	8'176	9'739	8'572	8'268
Zn	55'323	49'980	37'610	32'830	40'840	37'210	39'800

Tabelle A8-2: *Chemische Zusammensetzung (mg/kg) der gewaschenen Filterkuchen in den beprobten Kalenderwochen (KW), gemessen mit ED-XRF.*

	Ausgangslage 2016		Optimierung Teil 1				
Element	**KW 45/46/ 2016**	**KW 48/ 2016**	**KW 2/ 2017**	**KW 7/ 2017**	**KW 8/ 2017**	**KW 9/ 2017**	**KW 10/ 2017**
Wassergehalt (%)	-	40.3	36.6	36.0	33.3	35.7	34.0
Massenverlust (%)	30	20	30	40	20	30	30
Al	32'113	26'340	31'810	29'630	31'600	30'430	29'270
Ba	2'581	2'800	2'426	2'512	2'708	2'391	2'551
Ca	184'067	195'800	198'000	196'400	201'900	184'000	188'200
Cd	149	135	175	147	148	184	178
Cl	5'237	6'087	11'290	10'050	10'190	8'372	9'173
Cr	744	679	710	586	593	755	736
Cu	3'108	3'054	2'628	2'355	2'509	2'059	2'392
Fe	27'740	21'820	20'500	17'810	19'990	16'840	18'850
K	6'454	6'276	9'264	8'186	7'922	15'310	11'910
Mn	804	846	973	852	957	996	944
P	5'148	4'779	5'908	5'619	5'273	6'202	5'540
Pb	10'948	11'460	8'667	9'058	7'865	12'510	12'770
S	87'350	94'080	86'020	102'800	90'500	106'600	99'260
Sb	4'362	3'491	2'488	3'241	2'955	3'275	3'015
Si	78'353	67'040	73'770	70'980	70'730	75'610	70'930
Sn	1'902	1'762	1'510	1'595	1'502	1'619	1'534
Ti	11'457	10'630	11'390	10'800	10'650	10'780	11'190
Zn	31'900	32'820	29'740	22'760	27'320	20'000	24'020

Tabelle A8-3: *Chemische Zusammensetzung (mg/kg) der Flugasche und gewaschener Filterkuchen der KW 48 2016 und KW 2 2017, gemessen mit Totalaufschluss/ICP-OES (TA-ICP-OES).*

	Flugaschen		Filterkuchen	
Element	**KW 48/2016**	**KW/2 2017**	**KW 48/2016**	**KW 2/2017**
Al	34'632	33'711	42'045	45'301
Ba	2'552	2'120	3'267	2'799
Ca	176'601	189'912	217'811	209'183
Cd	393	344	136	166
Cr	689	708	894	893
Cu	2'735	2'159	3'468	3'058
Fe	21'529	18'496	27'071	23'532
K	45'273	42'063	12'219	12'273
Mg	14410	13'170	13'827	13'368
Na	52857	46'144	8'705	9'240
Ni	200	136	231	196
P	4'846	6'242	6'283	8'074
Pb	10'667	7'692	12'562	10'210
S	63'065	49'971	84'081	74'409
Sb	2'892	2'316	3'877	2'948
Si	69'829	60'628	87'138	79'359
Ti	10'454	12'042	14'675	15'650
Zn	45'428	32'509	31'065	26'796

Tabelle A8-4: *Chemische Zusammensetzung (mg/L) des sauren (QWs) und basischen (QWb) Quenchwasser aus KW 48/49/2016 sowie KW 2/2017 gemessen mit ICP-OES und IC.*

Element	QWs KW 48	QWs KW 49	QWb KW 49	QWs KW 2	QWb KW 2
Al	<25	<25	<25	<25	<25
Ba	<0.5	<0.5	<0.5	<0.5	<0.5
Ca	305	319	<25	312	<25
Cd	<0.25	<0.25	<0.25	<0.25	<0.25
Co	<5	<5	<5	<5	<5
Cr	<0.5	<0.5	<0.5	<0.5	<0.5
Cu	<0.5	<0.5	<0.5	<0.5	<0.5
Fe	<5	<5	<5	<5	<5
K	<25	<25	<25	<25	<25
Mg	45	46	4.6	34	2.5
Mn	<0.5	<0.5	<0.5	<0.5	<0.5
Na	142	133	31'512	70	11'687
Ni	<0.25	<0.25	<0.25	<0.25	<0.25
P	<5	<5	<5	<5	<5
Pb	<5	<5	<5	<5	<5
S	491	446	18'556	338	6'303
Sb	<5	<5	<5	<5	<5
Si	16	10	4.8	13	4.8
Ti	<0.25	<0.25	<0.25	<0.25	<0.25
Zn	<5	<5	5.9	<5	<5
F	<500	<500	<500	<500	<500
Cl	56'401	54'026	10'913	83'084	5'232
Br	1'245	745	<500	581	<500
NO_3^-	<500	<500	<500	<500	<500
PO_4^{3-}	<500	<500	<500	<500	<500
SO_4^{2-}	1'521	1'359	62'144	1'008	19'262

Rohdaten Optimierung Teil 2: Laborversuche

Tabelle A8-5: *Chemische Analysen der Filtrate (ICP-OES) und Filterkuchen (ED-XRF).*

ICP-OES/IC	Einwaage FA	Volumen Filtrat	Al	Ba	Ca	Cd	Co	Cr	Cu	Fe	K	Mg	Mn	Na	Ni	P	Pb	S	Sb	Si	Ti	Zn
	g	mL	mg/L	mg/L	mg/L	mg/L	mg/L	mg/L	mg/L	mg/L	mg/L	mg/L	mg/L	mg/L	mg/L	mg/L	mg/L	mg/L	mg/L	mg/L	mg/L	mg/L
Serie 1																						
1 ohne H_2O_2/Luft		15	3	1'165	106	3	<0.1	1	81	18'984	2'064	76	38'158	0	<1	22	3'242	4	30	<0.05	11'386
2 25 L H_2O_2/t FA		28	2	1'749	172	3	<0.1	1	2	18'635	2'147	84	36'313	6	1	1'442	2'100	5	23	0	11'511
3 40 L H_2O_2/t FA		18	1	1'512	156	3	<0.1	62	1	14'946	1'697	71	29'844	6	<1	1'672	2'211	4	21	<0.05	9'160
4 50 L H_2O_2/t FA		24	2	1'892	161	3	<0.1	370	3	17'587	2'062	78	34'612	7	3	2'261	2'220	5	31	1	10'599
5 25 L H_2O_2/t FA + Luft		14	2	1'586	154	3	<0.1	6	<1	17'987	2'043	79	35'366	4	<1	763	2'521	4	20	<0.05	10'786
7 40 L H_2O_2/t FA + Luft		28	1	1'385	154	3	<0.1	24	1	16'571	1'912	76	33'532	5	<1	1'623	2'789	5	30	0	10'339
8 25 L H_2O_2 + O_2		8	2	3'152	187	3	<0.1	360	<1	19'649	2'375	93	37'348	6	2	2'637	1'507	4	13	<0.05	11'501
Serie 2																						
1 ohne H_2O_2/Luft	100.03	295	<5	17	17'652	63	2	<0.1	1	<1	13'362	1'846	72	19'192	0	<1	34	596	5	10	<0.05	5'205
2 50 L H_2O_2/t FA initial	100.05	285	<5	13	18'412	54	2	<0.1	1	<1	13'413	1'910	74	19'227	0	<1	23	631	5	9	<0.05	5'206
3 50 L H_2O_2/t FA	100.01	300	<5	12	17'547	94	2	<0.1	4	<1	13'096	1'829	79	18'703	2	<1	336	597	5	7	<0.05	4'926
4 60 L H_2O_2/t FA	100.01	295	<5	11	16'654	96	2	<0.1	6	<1	12'243	1'722	80	17'517	2	<1	509	573	4	6	<0.05	4'534
5 70 L H_2O_2/t FA	100.00	300	<5	11	18'099	95	2	<0.1	5	<1	12'947	1'870	78	18'572	3	<1	659	611	5	7	<0.05	5'193
6 90 L H_2O_2/t FA (Eh 300 mV)	100.00	290	<5	11	20'378	100	2	<0.1	21	<1	14'780	2'087	80	21'264	4	<1	1'140	680	5	7	<0.05	5'855
7 34 L H_2O_2/t FA (Eh 100 mV)	100.00	295	<5	13	17'461	69	2	<0.1	28	<1	13'018	1'812	74	18'699	1	<1	356	610	3	4	<0.05	4'536
8 32 L H_2O_2/t FA (Eh 0 mV)	100.02	295	<5	13	17'009	75	2	<0.1	35	<1	12'753	1'757	72	18'284	1	<1	440	602	3	4	<0.05	4'466
9 30 L H_2O_2/t FA (Eh -200 mV)	100.01	295	<5	14	17'241	62	2	<0.1	19	<1	13'060	1'795	74	18'693	1	<1	255	603	4	5	<0.05	4'438
10 Luft 1+2	100.03	280	<5	16	16'346	56	2	<0.1	1	<1	12'350	1'728	73	17'681	0	<1	33	559	5	6	<0.05	4'698
11 50 L H_2O_2/t FA + Luft 1+2	100.09	282	<5	12	19'087	105	2	<0.1	33	<1	13'628	1'946	83	19'357	3	<1	925	631	5	6	<0.05	4'927
12 50 L H_2O_2/t FA + Luft 1	100.02	292	<5	12	17'424	100	2	<0.1	10	<1	12'537	1'780	83	17'789	3	<1	651	569	5	7	<0.05	4'858
13 50 L H_2O_2/t FA + Luft 2	100.02	287	<5	11	17'645	97	2	<0.1	23	<1	12'596	1'818	80	18'007	3	<1	859	579	5	6	<0.05	4'836
14 50 L H_2O_2/t FA + Luft 1+2 (30°C	100.03	312	<5	7	16'817	95	3	<0.1	49	<1	12'321	1'745	81	17'401	4	<1	1'109	615	3	7	<0.05	5'019

ED-XRF	Einwaage FA	Gewicht FK	Wassergehalt	Massenverlust	Massenverlust	Al	Ba	Ca	Cd	Cr	Cu	Fe	K	Mg	Mn	Na	Ni	P	Pb	S	Sb	Si	Ti	Zn
Serie 2	g	g	%	über Gewicht %	inerte Elemente %	mg/kg	mg/kg	mg/kg	mg/kg	mg/kg	mg/kg	mg/kg	mg/kg	mg/kg	mg/kg	mg/kg	mg/kg	mg/kg	mg/kg	mg/kg	mg/kg	mg/kg	mg/kg	mg/kg
Flugasche																								
KW 2 2017 (TA-ICP-OES)						33'711	2'120	189'912	344	708	2'159	18'496	42'063	136	6'242	7'692	49'971	2'316	60'628	12'042	32'509
KW 2 2017 (ED-XRF)						30'730	1'967	164'500	304	556	1'990	15'920	52'820	110	4'081	7'352	49'060	1'968	69'150	9'480	37'610
Filterkuchen																								
1 ohne H_2O_2/Luft	100.03	71.71	49	28	42	32'580	2'558	180'200	223	847	2'723	21'510	12'860	147	7'154	9'609	89'770	2'854	90'970	13'210	27'200
2 50 L H_2O_2/t FA initial	100.05	72.64	56	27	39	41'300	2'467	176'600	69	829	2'791	21'890	11'640	135	6'910	8'643	86'680	2'792	89'430	13'200	28'270
3 50 L H_2O_2/t FA	100.01	71.40	50	29	41	36'940	2'519	177'600	254	846	2'774	21'660	13'430	151	7'063	9'144	88'670	2'773	89'870	13'360	27'190
4 60 L H_2O_2/t FA	100.01	72.17	50	28	39	41'390	2'555	174'800	64	823	2'680	20'860	12'700	139	6'958	7'393	86'870	2'717	86'660	13'310	28'330
5 70 L H_2O_2/t FA	100.00	71.72	52	28	40	41'300	2'572	175'000	75	833	2'801	21'470	12'130	144	7'012	7'076	86'530	2'751	88'100	13'360	27'870
6 90 L H_2O_2/t FA (Eh 300 mV)	100.00	72.30	52	29	41	42'970	2'587	176'700	52	837	2'729	23'250	12'440	139	7'152	6'628	88'330	2'728	92'580	13'670	27'220
7 34 L H_2O_2/t FA (Eh 100 mV)	100.00	72.36	56	28	42	41'870	2'595	178'100	187	855	2'612	22'690	12'920	153	7'230	8'491	88'410	2'812	93'450	13'390	30'460
8 32 L H_2O_2/t FA (Eh 0 mV)	100.02	72.31	54	28	37	41'350	2'540	178'200	150	810	2'704	22'450	12'570	148	7'020	8'206	87'040	2'683	91'910	13'100	30'070
9 30 L H_2O_2/t FA (Eh -200 mV)	100.01	72.90	55	27	37	39'460	2'485	176'800	222	820	2'615	22'960	12'880	137	6'941	8'267	87'270	2'700	88'830	12'950	29'890
10 Luft 1+2	100.03	72.79	52	27	40	34'460	2'497	176'900	245	847	2'667	22'680	13'760	150	6'919	9'406	87'530	2'822	89'730	12'970	27'140
11 50 L H_2O_2/t FA + Luft 1+2	100.09	71.77	54	28	37	40'780	2'491	174'000	55	833	2'616	20'740	12'310	145	6'784	5'862	85'810	2'615	86'250	13'210	28'820
12 50 L H_2O_2/t FA + Luft 1	100.02	71.56	53	29	43	42'750	2'573	176'400	62	875	2'765	23'070	12'220	134	7'027	7'118	87'480	2'741	90'630	13'750	27'130
13 50 L H_2O_2/t FA + Luft 2	100.02	71.72	57	28	39	41'220	2'540	173'200	64	821	2'723	21'640	13'740	163	7'011	6'580	87'350	2'695	88'810	13'490	27'910
14 50 L H_2O_2/t FA + Luft 1+2 (30°C)	100.03	70.77	46	29	42	42'580	2'543	176'700	50	866	2'619	21'550	11'380	128	6'598	4'956	88'340	2'669	91'830	13'790	25'700

Tabelle A8-6: *Extraktionsausbeuten (Mittelwert gerechnet aus Filtrat und Filterkuchen).*

	Extraktionsausbeuten	Al %	Ba %	Ca %	Cd %	Cr %	Cu %	Fe %	K %	Ni %	P %	Pb %	S %	Sb %	Si %	Ti %	Zn %
1	ohne H_2O_2/Luft	12	5	27	54	0	1	2	79	2	0	4	0	0	3	0	44
2	50 L H_2O_2/t FA initial	6	4	27	45	0	0	1	77	0	0	5	0	0	3	0	43
3	50 L H_2O_2/t FA	2	6	28	88	0	0	1	79	9	0	15	0	0	4	0	43
4	60 L H_2O_2/t FA	1	4	27	89	0	2	3	76	7	0	24	0	1	5	0	41
5	70 L H_2O_2/t FA	2	4	28	88	0	0	2	79	7	0	29	0	0	4	0	44
6	90 L H_2O_2/t FA (Eh +300 m V)	0	4	30	93	0	3	0	84	10	0	41	0	1	2	0	48
7	34 L H_2O_2/t FA (Eh +100 m V)	1	3	26	61	0	5	0	78	1	0	15	0	0	1	0	38
8	32 L H_2O_2/t FA (Eh 0 m V)	1	4	26	68	0	4	0	77	3	0	18	0	1	2	0	39
9	30 L H_2O_2/t FA (Eh -200 m V)	3	5	26	53	0	4	0	78	6	0	14	0	0	3	0	38
10	Luft 1+2	9	5	25	46	0	1	0	73	0	0	4	0	0	3	0	41
11	50 L H_2O_2/t FA + Luft 1+2	2	5	28	92	0	5	3	78	6	0	39	0	3	5	0	41
12	50 L H_2O_2/t FA + Luft 1	0	4	27	91	0	1	0	76	11	0	28	0	1	3	0	43
13	50 L H_2O_2/t FA + Luft 2	2	5	28	89	0	3	1	75	1	0	35	0	1	4	0	42
14	50 L H_2O_2/t FA + Luft 1+2 (30°C)	1	5	28	93	0	7	2	79	15	0	50	0	2	3	0	47

Rohdaten Optimierung Teil 2: Industriemassstab

Tabelle A8-7: *Chemische Zusammensetzung (mg/kg) der Flugaschen beim Werkversuch vom 31.03.2017, gemessen mit ED-XRF. Für Probe FA 2 wurde eine Dreifachbestimmung durchgeführt.*

	FA-1a	**FA 1b**	**FA 2**	**FA 2**	**FA 2**
Asche-Typ	Fremdasche A		Flugasche Linth		
Al	33'970	31'660	34'270	34'410	35'640
Ba	2'083	2'170	2'822	2'777	2'803
Br	3'467	2'980	4'005	4'008	4'001
Ca	151'400	145'400	149'000	147'700	149'300
Cd	352	347	261	261	256
Cl	144'000	144'700	138'200	139'900	133'200
Cr	823	783	554	524	537
Cu	2'837	3'063	2'846	2'843	2'866
Fe	17'400	15'640	16'270	16'240	15'660
K	58'210	58'000	46'780	47'270	45'690
Mn	1'104	1'075	683	704	685
Ni	164	127	158	149	153
P	4'381	4'318	3'542	3'503	3'683
Pb	8'738	10'080	10'980	10'980	10'890
S	61'150	64'270	50'490	49'800	50'620
Sb	2'021	2'148	2'828	2'839	2'812
Si	77'310	71'680	92'160	91'070	94'550
Sn	1'296	1'423	1'337	1'352	1'352
Ti	9'653	9'453	9'994	9'756	10'070
Zn	39'960	40'500	67'660	67'620	67'540

Tabelle A8-8: *Chemische Zusammensetzung (mg/kg) der gewaschenen Filterkuchen des Werkversuchs vom 31.03.2017, gemessen mit ED-XRF. Für Probe FK 2-2 wurde eine Dreifachbestimmung durchgeführt.*

	FK 1-1	**FK 1-2**	**FK 1-3**	**FK 2-1**	**FK 2-2**	**FK 2-2**	**FK 2-2**	**FK 2-3**
Asche-Typ	Filterkuchen Fremdasche A			Filterkuchen Linth				
Massenverlust (%)	30	50	40	40	50	50	50	60
Al	37'190	39'700	45'180	41'380	43'940	44'380	43'510	43'700
Ba	2'597	2'716	2'782	3'345	3'471	3'569	3'535	3'789
Br	238	105	179	435	321	319	323	167
Ca	189'800	178'600	177'400	169'500	166'000	166'700	166'500	169'200
Cd	185	255	188	59	70	68	68	102
Cl	8'127	3'887	7'296	14'270	10'930	10'600	10'550	4'507
Cr	1'069	1'211	1'159	808	843	805	770	831
Cu	3'642	3'762	3'964	3'965	3'718	3'804	3'842	4'754
Fe	21'400	20'590	24'670	22'280	22'830	23'740	23'010	25'250
K	10'230	9'114	10'220	10'120	9'249	9'268	9'193	7'031
Mn	1'202	1'151	1'223	840	754	764	746	767
Ni	177	176	178	163	172	185	167	203
P	6'539	7'382	7'210	5'833	6'106	6'057	5'851	6'433
Pb	11'320	11'020	11'900	8'685	10'500	10'670	10'790	14'700
S	102'900	108'600	101'000	94'370	92'870	93'670	93'420	94'830
Sb	2'652	3'293	3'000	3'411	4'271	4'362	4'433	4'601
Si	93'210	108'700	107'700	110'500	119'700	121'200	120'100	122'700
Sn	1'558	1'866	1'612	1'727	2'122	2'122	2'127	2'190
Ti	12'740	14'520	14'350	13'370	13'800	13'790	13'790	15'600
Zn	23'950	19'830	18'830	32'080	34'250	34'530	34'900	22'750

Tabelle A8-9: *Chemische Zusammensetzung (mg/L) des sauren (QWs) und basischen (QWb) Quenchwasser beim Werkversuch am 31.3.2017, gemessen mit IC.*

Element	**QWs**	**QWb**
F	121	690
Cl	56'425	19'098
Br	608	1'354
NO_3^-	<50	<50
PO_4^{3-}	<50	<50
SO_4^{2-}	748	36'147

Monitoring Leitparameter FLUWA

KW	Tag	Datum	Betriebszeit	Probenahme	Flugasche	Saures Quenchwasser	Basisches Quenchwasser	LS	Extraktionsbehälter 1 (3m³)				Extraktionsbehälter 2 (3m³)				Extraktionsbehälter 3 (3m³)			
									pH-Wert	Eh-Wert (mV)	Temp. (°C)	Verweildauer (min)	pH-Wert	Eh-Wert (mV)	Temp. (°C)	Verweildauer (min)	pH-Wert	Eh-Wert (mV)	Temp. (°C)	Verweildauer (min)
				ja/nein	(t/h)	(m^3/h)	(m^3/h)													
48	Mo	28.11.2016	5.50-14.30	Ja	3.5	5.69	4.61	2.9	4.6	-	-	14.3	-	-	-	14.5	-	-	-	-
	Di	29.11.2016	5.45-12.45	Ja	3.5	5.59	4.61	2.9	4.6	-	57.1	15	-	-542	57.1	15	-	-	-	-
	Mi	30.11.2016	kein FLUWA-Betrieb	-	-	-	-	-	-	-	-	-	-	-	-	-	-	-	-	-
	Do	01.12.2016	5.45-13.15	Ja	3.5	5.36	4.62	2.9	4.8	-	56.4	15.3	-	-565	56.4	15.3	-	-	-	-
	Fr	02.12.2016	5.45-13.30	Ja	3.5	5.54	4.61	2.9	4.8	-	56.9	15.1	-	-551	56.9	15.1	-	-	-	-
49	Mo	05.12.2016	5.30-13.00	Nein	5	5.53	4.65	2.0	5	-509	57.5	14.2	5.1	-514	58.5	14.2	-	-	-	-
	Di	06.12.2016	5.30-12.45	Nein	5	5.96	3.94	2.0	3.7	-524	56.6	14.7	4.6	-561	56.4	14.7	-	-	-	-
	Mi	07.12.2016	5.30-12.30	Nein	5	6.1	3.9	2.0	4.4	-510	58.4	14.4	5.3	-532	59.2	14.4	-	-	-	-
	Do	08.12.2016	5.30-13.30	Nein	4	6.22	3.91	2.5	4	-447	58.4	14.8	5	-482	59.2	14.8	-	-	-	-
	Fr	09.12.2016	5.30-13.00	Nein	5	6.07	4.01	2.0	3.8	-525	57.3	14.3	5	-547	58.4	14.3	-	-	-	-
50	Mo	12.12.2016	5.30-13.00	Nein	4	6.01	3.94	2.5	3.6	-385	59.2	15.1	4.4	-405	59.6	15.1	-	-	-	-
	Di	13.12.2016	5.30-14.00	Nein	5	6.08	3.94	2.0	3.8	-410	59.5	14.3	5	-451	59.9	14.3	-	-	-	-
	Mi	14.12.2016	5.45-12.15	Nein	5	5.99	3.9	2.0	4.2	-532	61.1	14.5	5.3	-554	62.2	14.5	-	-	-	-
	Do	15.12.2016	kein FLUWA-Betrieb	-	-	-	-	-	-	-	-	-	-	-	-	-	-	-	-	-
	Fr	16.12.2016	5.30-	Nein	5	6.06	3.9	2.0	4	-536	59.4	14.4	5.2	-581	59.7	14.4	-	-	-	-
51	Mo	19.12.2016	5.30-13.00	Nein	5	6.03	3.98	2.0	3.3	-515	59.8	14.3	4.7	-553	61.5	14.3	-	-	-	-
	Di	20.12.2016	5.30-14.00	Nein	5	6.03	3.96	2.0	3	-495	59	14.4	3.6	-541	60.2	14.4	-	-	-	-
	Mi	21.12.2016	5.30-14.15	Nein	5	6.04	3.92	2.0	3.2	-511	59.3	14.4	4.4	-541	61.1	14.4	-	-	-	-
	Do	22.12.2016	5.30-12.30	Nein	5	5.98	3.87	2.0	3.6	-505	59.9	14.5	5.4	-532	63	14.5	-	-	-	-
	Fr	23.12.2016	5.30-13.00	Nein	5	6.19	3.85	2.0	3.5	-532	58.1	14.3	5	-583	60	14.3	-	-	-	-
52	Mo	26.12.2016	-	-	-	-	-	-	-	-	-	-	-	-	-	-	-	-	-	-
	Di	27.12.2016	5.15-12.45	Nein	5	6.24	3.98	2.0	3.2	-524	61.1	14.1	4.3	-572	62.2	14.1	-	-	-	-
	Mi	28.12.2016	5.15-12.15	Nein	5	6.09	3.92	2.0	4.4	-464	62.2	14.3	5.6	-537	64.1	14.3	-	-	-	-
	Do	29.12.2016	4.15-12.45	Nein	5	6.14	3.9	2.0	3.6	-483	61.9	14.3	4.8	-541	62.4	14.3	-	-	-	-
	Fr	30.12.2016	5.15-14.00	Nein	5	6.03	3.85	2.0	3.3	-467	62	14.5	4.4	-513	63.2	14.5	-	-	-	-

KW	Tag	Datum	Betriebszeit	Probenahme	Flugasche	Saures Quenchwasser	Basisches Quenchwasser	LS	Extraktionsbehälter 1 (3m³)				Extraktionsbehälter 2 (3m³)				Extraktionsbehälter 3 (3m³)			
				ja/nein	(t/h)	(m^3/h)	(m^3/h)		pH-Wert	Eh-Wert (mV)	Temp. (°C)	Verweildauer (min)	pH-Wert	Eh-Wert (mV)	Temp. (°C)	Verweildauer (min)	pH-Wert	Eh-Wert (mV)	Temp. (°C)	Verweildauer (min)
1	Mo	02.01.2017	4.00-11.30	Nein	5	6.13	3.93	2.0	3.4	-490	58.9	14.3	4.4	-577	59.8	14.3	-	-	-	-
	Di	03.01.2017	5.30-13.15	Nein	5	6.23	3.9	2.0	3.6	-483	59.1	14.2	4.9	-532	60.2	14.2	-	-	-	-
	Mi	04.01.2017	5.30-13.30	Nein	5	6.05	3.85	2.0	4	-495	57.7	14.5	5.6	-563	59.3	14.5	-	-	-	-
	Do	05.01.2017	5.30-12.15	Nein	5	6.16	3.9	2.0	3.8	-476	58.5	14.3	4.8	-522	60.3	14.3	-	-	-	-
	Fr	06.01.2017	5.30-15.30	Nein	5	6.08	3.92	2.0	3.8	-473	61.4	14.4	5.2	-553	64.1	14.4	-	-	-	-
2	Mo	09.01.2017	5.15-13.30	Ja	5	5.07	5.11	2.0	3.2	-519	59.3	14.2	4.4	-546	62.7	14.2	-	-	-	-
	Di	10.01.2017	5.15-13.30	Ja	5	5.06	5.14	2.0	3.4	-533	58.5	14.2	4.8	-587	61.9	14.2	-	-	-	-
	Mi	11.01.2017	4.45-13.45	Ja	5	5.06	5.1	2.0	3.3	-542	58.4	14.2	4.7	-589	61	14.2	-	-	-	-
	Do	12.01.2017	5.00-12.30	Ja	5	5.09	5.06	2.0	3.7	-527	59.4	14.2	5.1	-596	61.5	14.2	-	-	-	-
	Fr	13.01.2017	5.00-13.00	Ja	5	5.08	5.06	2.0	3.5	-507	60.2	14.2	4.9	-553	62.3	14.2	-	-	-	-
3	Mo	16.01.2017	5.30-14.00	Nein	5	5.06	5.08	2.0	-	-	-	14.2	-	-	-	14.2	-	-	-	-
	Di	17.01.2017	5.30-14.00	Nein	5	5.03	5	2.0	3.1	-421	59.4	14.3	3.8	-482	60.6	14.3	-	-	-	-
	Mi	18.01.2017	4.50-13.30	Nein	5	5.03	5.06	2.0	4	-442	59.2	14.3	5.5	-495	61.3	14.3	-	-	-	-
	Do	19.01.2017	5.30-14.00	Nein	5	5.16	5.08	2.0	3.6	-412	59.1	14.1	4.4	-576	61	14.1	-	-	-	-
	Fr	20.01.2017	5.30-16.15	Nein	5	5	5.06	2.0	4.4	-476	51.1	14.3	5.2	-553	52.3	14.3	-	-	-	-
4	Mo	23.01.2017	4.50-13.45	Nein	5	5.06	5.06	2.0	3.8	-531	59.3	14.2	4.9	-575	61.2	14.2	-	-	-	-
	Di	24.01.2017	4.45-13.15	Nein	5	5.08	5.02	2.0	3.6	-543	58.7	14.3	5	-586	60.1	14.3	-	-	-	-
	Mi	25.01.2017	5.00-13.00	Nein	5	5.07	5.07	2.0	3.6	-522	59.4	14.2	4.8	-556	61.5	14.2	-	-	-	-
	Do	26.01.2017	5.45-12.45	Nein	5	5.08	5.11	2.0	3.5	-536	59.1	14.1	4.6	-583	61.7	14.1	-	-	-	-
	Fr	27.01.2017	5.30-16.00	Nein	5	5.1	5.1	2.0	3.7	-544	58.6	14.2	4.8	-591	60.5	14.2	-	-	-	-
5	Mo	30.01.2017	5.15-13.15	Nein	5	5.06	5.03	2.0	2.6	-446	56.7	14.2	3.4	-558	58.1	14.2	-	-	-	-
	Di	31.01.2017	5.15-13.30	Nein	5	5.1	5.1	2.0	2.4	-426	56.2	14.1	3	-568	58.2	14.1	-	-	-	-
	Mi	01.02.2017	5.15-15.00	Nein	5	5.07	5.04	2.0	2.5	-458	57.2	14.2	3.2	-572	59	14.2	-	-	-	-
	Do	02.02.2017	5.15-14.00	Nein	5	5.12	5.1	2.0	2.7	-445	56.6	14.1	3.9	-536	58.2	14.1	-	-	-	-
	Fr	03.02.2017	4.45-13.00	Nein	5	5.12	5.11	2.0	-	-	-	14.1	-	-	-	14.1	-	-	-	-

KW	Tag	Datum	Betriebszeit	Probenahme	Flugasche	Saures Quenchwasser	Basisches Quenchwasser	LS	Extraktionsbehälter 1 (3m³)				Extraktionsbehälter 2 (3m³)				Extraktionsbehälter 3 (3m³)			
				ja/nein	(t/h)	(m^3/h)	(m^3/h)		pH-Wert	Eh-Wert (mV)	Temp. (°C)	Verweildauer (min)	pH-Wert	Eh-Wert (mV)	Temp. (°C)	Verweildauer (min)	pH-Wert	Eh-Wert (mV)	Temp. (°C)	Verweildauer (min)
6	Mo	06.02.2017	5.40-13.45	Nein	5	5.01	5.14	2.0	2.8	-405	58.2	14.2	4	-515	59.8	14.2	-	-	-	-
	Di	07.02.2017	5.00-11.45	Nein	5	5.12	5.06	2.0	2.6	-504	57.6	14.1	3.8	-586	59.2	14.1	-	-	-	-
	Mi	08.02.2017	5.00-13.30	Nein	5	5.13	5.08	2.0	2.5	-443	59.1	14.1	3.5	-527	60.6	14.1	-	-	-	-
	Do	09.02.2017	5.15-13.15	Nein	5	5.11	5.06	2.0	2.7	-517	58.4	14.2	4	-623	60.2	14.2	-	-	-	-
	Fr	10.02.2017	4.45-16.00	Nein	3.5	5.08	5.02	2.9	2.5	-506	58.1	15.2	3.6	-589	59.5	15.2	-	-	-	-
7	Mo	13.02.2017	4.45-12.30	Ja	3.5	5.09	5.12	2.9	2.4	-443	58.3	15	3.5	-516	60.2	15	-	-	-	-
	Di	14.02.2017	5.50-12.15	Ja	5	5.12	5.08	2.0	2.6	-529	58.8	14.2	3.6	-597	60.1	14.2	-	-	-	-
	Mi	15.02.2017	4.45-15.30	Ja	5	5.08	5.08	2.0	2.4	-447	59.3	14.2	3.4	-523	61	14.2	-	-	-	-
	Do	16.02.2017	4.45-12.00	Ja	5	5.19	5.06	2.1	2.8	-436	58.6	14.2	4.1	-552	60.3	14.2	-	-	-	-
	Fr	17.02.2017	-	Ja	5	5.14	5.09	2.0	2.8	-512	59.8	14.1	4.2	-589	61.3.	14.1	-	-	-	-
8	Mo	20.02.2017	5.30-13.30	Ja	5	5.14	5.17	2.1	2.9	-427	58.7	14	4	-485	60.2	14	-	-	-	-
	Di	21.02.2017	5.30-12.00	Ja	5	5.13	5	2.0	2.4	-547	59.2	14.2	3.5	-598	60.6	14.2	-	-	-	-
	Mi	22.02.2017	5.30-13.30	Ja	5	5.13	5.06	2.0	2.6	-556	58.5	14.2	3.8	-621	59.4	14.2	-	-	-	-
	Do	23.02.2017	5.30-13.45	Ja	5	5.16	5	2.0	2.5	-432	58.3	14.2	3.8	-496	59.8	14.2	-	-	-	-
	Fr	24.02.2017	5.30-16.00	Ja	5	5.12	5	2.0	2.7	-512	59.6	14.2	3.8	-564	61	14.2	-	-	-	-
9	Mo	27.02.2017	4.45-13.30	Nein	5	5.17	5.04	2.0	2.7	-512	58.3	14.2	3.8	-567	59.7	14.2	-	-	-	-
	Di	28.02.2017	4.45-12.00	Nein	5	5.19	4.9	2.0	2.4	-478	59.3	14.3	3.4	-548	60.6	14.3	-	-	-	-
	Mi	01.03.2017	4.45-14.00	Nein	5	5.19	4.8	2.0	2.4	-482	58.6	14.4	3.6	-562	59.9	14.4	-	-	60	14.4
	Do	02.03.2017	4.45-13.15	Nein	5	5.2	4.8	2.0	2.5	-521	60.1	14.4	3.5	-587	61.3	14.4	3.7	-599	61.4	14.4
	Fr	03.03.2017	4.45-15.00	Nein	5	5.3	4.7	2.0	2.4	-501	58.8	14.4	3.5	-561	59.4	14.4	3.6	-589	59.6	14.4
10	Mo	06.03.2017	-	-	-	-	-	-	-	-	-	-	-	-	-	-	-	-	-	-
	Di	07.03.2017	5.30-13.00	Ja	5	5.36	4.77	2.0	2.6	-487	59.6	14.2	3.6	-561	60.2	14.2	3.8	-584	60.4	14.2
	Mi	08.03.2017	5.30-12.45	Ja	5	5.34	4.78	2.0	2.7	-491	58.2	14.2	3.7	-546	59.4	14.2	3.9	-573	59.6	14.2
	Do	09.03.2017	5.30-13.30	Ja	5	5.33	4.73	2.0	2.4	-523	58.6	14.3	3.5	-587	59.5	14.3	3.6	-596	59.6	14.3
	Fr	10.03.2017	5.30-13.00	Ja	5	5.25	5.04	2.1	2.6	-517	59.4	14.1	3.6	-576	60.3	14.1	3.8	-596	60.5	14.1

Part D: Summary and Outlook

Chapter 9

Summary

In the following, the main findings of this thesis of almost 4 years research focusing on chemical associations, recovery of heavy metals from fly ash and finally the optimization of acidic fly ash leaching (FLUWA process) are presented.

9.1 Chemical associations of heavy metals in fly ash and leached filter cake

The findings of a detailed characterization contribute significantly to a better description of the morphological occurrence of phases and the chemical associations of heavy metals contained in fly ash and in leached residues (filter cake). The successful identification of these metal associations allows a more detailed understanding of the relevant processes taking place during fly ash leaching.

- The composition of fly ash from individual plants varies significantly, mainly depending on waste input and season. Fly ash from the incineration of household-dominated waste is characterized by high concentration of lime (CaO) and carbonate ($CaCO_3$) and thus by high buffering capacity. Such alkaline fly ash shows elevated concentration of metallic Al^0 but lower concentration of heavy metals such as Zn (20'000 mg/kg), Pb (3'000 mg/kg), Cu (1'000 mg/kg) and Cd (200 mg/kg) compared to other fly ash. Fly ash from the incineration of more industrial-dominated waste shows elevated Cl and S concentration and is strongly enriched in heavy metals such as Zn (60'000 mg/kg), Pb (12'000 mg/kg), Cu (2'500 mg/kg) and Cd (400 mg/kg). These differences have significant effects on the efficiency for the fly ash leaching process.

- Focussing on particle formation, single and multi-component particles are observed. Residual carbon particles, quartz fragments and hollow glassy cenospheres account for the major part of the larger-size particles in fly ash. Fly ash consists of a remarkable content of crystalline phases (ca. 40 wt.%) when considering the rapid formation and cooling processes taking place during incineration and transport in the flue gas. Refractory particles (Al-foil, unburnt carbon, quartz, feldspar) and

newly formed high-temperature phases (silicate glass, gehlenite, wollastonite) surrounded by a dust rim are characteristic for fly ash.

- The formation of fly ash and the incorporation of metals is a complex multi-stage process. Metals are either carried along with the flue gas as particles (Fe-oxides, brass), forming enriched mineral aggregates (quartz, feldspar, wollastonite, glass) or vaporize and condense as complex chlorides (K_2ZnCl_4) or sulphates ($PbSO_4$) in fly ash. Reaction products such as wollastonite ($CaSiO_3$) and glasses are generally found in contact with core grains such as quartz and feldspars. In most cases, larger metallic Fe-fragments and finely distributed brass ($Cu_{0.6}Zn_{0.4}$) are incorporated within wollastonite and glassy matrix.

- Acidic leached filter cake from the FLUWA process still show residual metal contents. Predominantly Zn and Cu are still incorporated in small, only few µm-sized Ca-Al-Si particles such as aluminosilicates or bound in the glassy matrix. The exposure and dissolution of these residual metals is therefore limited because the dissolution rate of a Ca-Si matrix is comparatively slow at the leaching conditions used.

9.2 Heavy metal separation and recovery from fly ash

Selected leaching procedures in combination with mechanical separation experiments were the key for a better understanding of the complex phase associations and processes influencing metal mobilization.

- Leaching experiments with two different fly ashes using various agents and conditions show that the efficiency of the heavy metal leaching is dependent on the binding environment of the metals, pH-value of ash slurry, redox conditions, liquid to solid ratio (LS), temperature and leaching time. High buffer capacity and high amount of metallic components in fly ash have a negative influence on pH-values and redox conditions during fly ash leaching. Elevated pH-values in the ash slurry (precipitation of metal hydroxides) and reducing leaching conditions forced by the oxidation of the metallic components negatively influence heavy metal depletion.

- The pH-value is a key parameter for fly ash leaching. The carbonate system buffers the pH of the ash slurry up to pH >12 using pure water as a reagent. It has been shown that at pH-values around 2.5 the mobilization of heavy metals is most effective, independent of the type of acid used for fly ash leaching. The leaching with HCl, H_2SO_4 and H_3PO_4 shows very similar results for the same acid strength. The use of H_2SO_4 produces large amounts of gypsum accumulated in the filter cake. This results in elevated costs for landfilling of the filter cake due to the mass increase of gypsum formation. Gypsum recycling would hardly be practical and

therefore most often HCl 32% is used to acidify the scrub water when performing the FLUWA process.

- The redox conditions present during fly ash leaching significantly influence the mobility of redox-sensitive elements such as Pb, Cu and partially Cd. The oxidation of metallic components in fly ash leads to reducing conditions already within the first 5 minutes of leaching. If the leaching conditions allow the dissolution of Pb- and Cu containing phases from fly ash, the extraction of Pb and Cu are limited because reductive separation (cementation) produces the formation of a $PbCu^0$-alloy-phase. The addition of an oxidizing agent such as hydrogen peroxide (H_2O_2) in combination with air injection prevents the reductive separation by complete oxidation of metallic components in the fly ash and thus leads to significantly higher metal depletion factors.

- To optimize the metal recovery, the subsequent leaching of the filter cake from the FLUWA process with concentrated NaCl-solution was investigated and has shown great potential. This additional step using NaCl-solution (300 g/L) is especially efficient for Pb and Cu depletion. In the highly concentrated NaCl-solution metal-chloride-complexes are formed whereby the dissolved Pb forms complexes with increased chloride content ($PbCl_3^-$, $PbCl_4^{2-}$), which significantly increases the solubility of the metal.

- Mechanical separation steps were also tested and were found to have almost no potential. Grains size fractionation and sophisticated magnetic separation tests in fly ash slurries had very small throughput and only a minor concentration effect. Milling of the fly ash resulted in only a small increase of the surface area (4-6%) and identical metal recovery as in the case of non-ground fly ash for leaching are achieved. The milling resulted in smaller grain sizes, but not in a larger surface area accessible to the extracting agent possibly due to porous particles.

- Inert elements which are hardly dissolved from fly ash, such as Ba, Ti, Cr, Sb, P or Sn, provide a robust tracer for determination of the metal depletion factors. These elements are relatively enriched in the residual filter cake due to the mobilization of readily soluble components from fly ash. The calculation of metal depletion factors using inert elements is especially useful at industrial scale, where calculation of mass balance is otherwise difficult due to the complex mass flows.

Depending on the leaching parameters and type of fly ash, 60-80% Zn, 60-85% Cd and 0-30% Pb and Cu can be extracted by the FLUWA process. Metal recovery is positively influenced by increasing LS ratio and by a stronger acid attack that results in a lower equilibrium pH-value of the fly ash slurry. The mobilization of Zn in fly ash is limited by the binding form (incorporation of Zn in Ca-Al-Si matrix) and a maximum recovery of 80% Zn can be achieved. The addition of an oxidizing agent such as H_2O_2 during fly ash leaching keeps the redox-sensitive metals (Pb, Cu and Cd) in solution, leading to significantly higher depletion factors (Pb 50-90%, Cu 40-80%, Cd 85-95%). A low pH-value of the fly ash slurry (pH <4) at the end of the leaching process, prevents metal hydroxide precipitation (e.g. $Cu(OH)_2$) and results in elevated metal depletion factors. The recovery of Pb and Cu is additionally increased by metal-chloride-complex formation using concentrated NaCl-solution. The combined use of acidic fly ash leaching and NaCl-leaching leads to an increase in mobilization of 85-100% Pb, 60-80% Cu and 90-100% Cd.

9.3 Implications for the optimization of the FLUWA process

Based on findings at laboratory scale, the following implications are supported for the optimization of the acidic fly ash leaching process (FLUWA).

- The treatment of fly ash mixtures from different MSWI plants brings several benefits. Temporal variability in composition is averaged and can be adjusted. This allows the formation of an optimal mixture for acidic leaching and more stable process conditions for a more constant metal recovery. Material characteristics of single fly ash such as high buffer capacity or high metallic content that negatively influence the FLUWA process can be attenuated with the use of fly ash mixtures. With the revised Swiss Waste Ordinance and the prescribed treatment of fly ash with metal recovery by 2021, regional FLUWA treatment centres present an efficient option. This enables the centralization of technical installations and know-how and allows a more powerful and economic operation of the fly ash leaching process.

- Performing the FLUWA process at elevated LS ratio (3-4) increases the metal recovery significantly. The high LS ratio allows a more intensive contact of the extraction agent with the metal-bearing particles and a reduced carryover of dissolved metals in the filter cake after filtration. The FLUWA process must be operated at low pH-value (pH ~2.0) in the first extraction tank, so that the pH-value in the last extraction tank is in the range of 4.0-4.5 to prevent precipitation of metal hydroxides. Lower pH-values at the end of the process favour the formation of silica-gel that complicates the vacuum belt filtration.

- Oxidative conditions during the FLUWA process are essential for mobilization of redox-sensitive elements Pb, Cu and Cd. The combination of the addition of H_2O_2

30% supported by air injection into the fly ash slurry lead to increasing depletion factors for Pb, Cu and Cd. The continuous addition of H_2O_2 in the first extraction tank in combination with air injection in the second extraction tank seems to be most efficient. The addition of air starting in the second tank avoids driving out the H_2O_2 by the inflowing air in the first tank. Performing the FLUWA process under oxidizing conditions is more cost intensive but may be justified not only by reducing metal loads to the environment but also by reduced deposition costs.

- An additional option to the available technology is a secondary leaching step of the filter cake before deposition. The use of concentrated NaCl-solution shows promising results for enhanced mobilization of Pb (>85%) and Cu (>60%). At industrial scale chloride-containing water from waste water treatment could be used by recirculation to the FLUWA process.

- Tests at industrial scale at MSWI plant Linth/Niederurnen between November 2016 and March 2017 show that the trends of the chemical processes and metal recovery pointing in the right direction. Difficulties have been experienced in keeping and monitoring stable leaching conditions during the addition of H_2O_2 and air injection. Additional investigations are proposed, where an ideal coordination of the system technology (process engineering – chemistry) and stable process conditions over several weeks are necessary.

Chapter 10

Outlook

The revised Swiss Waste Ordinance prescribes fly ash treatment with metal recovery by 2021. With the present thesis, additional contributions to the characterization and leaching behaviour of fly ash are presented and a better understanding in numerous aspects is achieved. For a final implementation, great efforts and innovations are needed in the next few years. In an upcoming implementation aid the "state-of-the-art" has to be determined either by definition for fly ash depletion factors or by the description of a methodology for the determination of the required metal recovery efficiency.

In this context and from a geochemical point of view, further attention could be focused on two aspects.

- Extending the chemical and mineralogical characterization of the fly ash to all MSWI plants in Switzerland allows a better estimation of the overall situation with respect to parameters important for fly ash leaching. The extended knowledge serves as a basis for the estimation of metal recovery potentials and strategic considerations for implementation.

- An acidic leaching of all MSWI fly ash will result in less harmful residues for deposition. The addition of HCl 32% (lower pH-value of ash slurry) and H_2O_2 30% (oxidative leaching conditions) during the FLUWA process results again in more metal-depleted residues. However, the accumulation of such reagents in the leached filter cake and their environmental impact has not been studied in detail. Geochemical modelling would allow the assessment of long-term behaviour of differently leached filter cakes over mid- to long-term periods (100-10'000 years). The thermodynamic database has been extended by the species important for fly ash and filter cake composition and implemented in the geochemical code GEM-Selektor during this thesis.

Erklärung

gemäss Art. 28 Abs. 2 RSL 05

Name/Vorname:	*Weibel Gisela*
Matrikelnummer:	*08-123-606*
Studiengang:	*MSc Phil-nat. (Erdwissenschaften)*

Bachelor ☐ Master ☐ Dissertation ☒

Titel der Arbeit: *Optimized Metal Recovery from Fly Ash from Municipal Solid Waste Incineration*

Leiter der Arbeit: *PD. Dr. U. Mäder*
Dr. U. Eggenberger
Dr. S. Schlumberger

Ich erkläre hiermit, dass ich diese Arbeit selbstständig verfasst und keine anderen als die angegebenen Quellen benutzt habe. Alle Stellen, die wörtlich oder sinngemäss aus Quellen entnommen wurden, habe ich als solche gekennzeichnet. Mir ist bekannt, dass andernfalls der Senat gemäss Artikel 36 Absatz 1 Buchstabe o des Gesetzes vom 5. September 1996 über die Universität zum Entzug des auf Grund dieser Arbeit verliehenen Titels berechtigt ist.

Bern, 09.05.2017